STUDIES ON CONTROLLABILITY ANALYSIS AND CONTROL STRUCTURE DESIGN

by

Kjetil Havre

A Thesis Submitted for the Degree of Dr. Ing.

Department of Chemical Engineering
Norwegian University of Science and Technology

Submitted January 1998

ABSTRACT

As chemical processes tend to become more tightly integrated, the control structure design becomes more important and a more difficult task. Most (if not all) available control theories and design methods assume that the control structure is given prior to the design. That is, they do not explicitly address the structural decisions involved in the control structure design. This has resulted in a *gap* between control theory and chemical process control applications. The *main objective* of this thesis is to provide new theory and tools in order to reduce this gap. The approach taken has been to derive and apply tools which address the inherent controllability of the plant. It is important that these tools are independent of the controller in order to reflect the performance limitations of the plant. In this thesis, existing controllability measures are used and new controllability measures are introduced to:

- *Obtain insights into the directionality of zeros and poles*. The Popov-Belevitch-Hautus eigenvector tests for state controllability and observability have been restated in terms of the pole directions. These restatements make the concepts state controllability and observability more useful in the task of control structure design.

- *Quantify performance limitations imposed by instability and non-minimum phase behavior (poles and zeros in the right half plane) in the plant*. These quantifications are given as controller independent lower bounds on the $\mathcal{H}_\infty$-norm of various closed-loop transfer functions. Analytical $\mathcal{H}_\infty$-optimal controllers which prove that the lower bounds are tight (in many cases), are given.

- *Quantify the minimum input usage needed to stabilize a plant with one unstable mode in the presence of measurement noise or disturbances, and to find the best input–output pairing to stabilize a plant with one unstable mode*. The quantifications of the input usage, are made both in terms of the $\mathcal{H}_2$-norm (energy) and the $\mathcal{H}_\infty$-norm. The results show that the best input and the best output for stabilization of an unstable mode using a SISO controller are independent of the norm, and that the two norms are closely related in this particular problem.

- *Quantify the effect of disturbances, measurement noise and reference changes in partially controlled systems*. Partial control is introduced, its relation to indirect and cascade control, and implications on control structure design on the regulatory control layer, are considered.

- *Quantify the effect of input and output uncertainty on the performance at the output of the plant*. New results that link the relative gain array and the condition number to control performance, measured in terms of the output sensitivity function with input and output uncertainty, are given.

- Throughout the thesis, several realistic case studies demonstrating the topics considered, are given.

ACKNOWLEDGEMENTS

---

[1] Skogestad, S. and Postlethwaite, I. (1996). *Multivariable Feedback Control, Analysis and Design*, John Wiley & Sons, Chichester.

Contents

Notation and nomenclature

There is no standard notation to cover all the topics in this thesis. Attempts have been made to use the most familiar notation from the literature. The most important nomenclature used in this thesis is summarized in the following lists:

- Main notation, contains all symbols except: Greek letters, symbols used to denote zero and pole directions and vectors, and all-pass factorizations of RHP zeros and poles.
- Greek letters.
- Indices and subscripts.
- Vectors and directions of zeros and poles in multivariable systems.
- All-pass factorizations of RHP zeros and poles.
- Norms.
- Abbreviations.

These lists are not complete, and additional notation is introduced in the text. For further details see also Sections 1.4 and 2.2. Note, in the text it is often omitted to show the dependence on the complex variable s for rational transfer functions and transfer function matrices. The hat $(\hat{\cdot})$ is used to denote unscaled transfer function models, i.e. $\widehat{G}$, $\widehat{G}_d$, and unscaled signals, i.e. $\hat{y}$, $\hat{u}$, $\hat{d}$, $\hat{n}$ and $\hat{r}$. It is also used in some few cases to denote estimated variables.

Main notation

$\times$ – symbol used to denote sizes of matrices.

$\times$ – element-by-element multiplication (Hadamard or Schur product).

$\overline{\cdot}$ – complex conjugate.

$(\dot{\cdot})$ – time derivative, i.e. $\dot{x} = \frac{dx}{dt}$.

$(\cdot)^T$ – transposed.

$(\cdot)^H$ – complex conjugate transposed, i.e. the hermitian.

$\angle(\cdot, \cdot)$ – angle between two vectors.

A – $n \times n$ state-space matrix in the state-space realization of G.

B – $n \times m$ input matrix in the state-space realization of G.

C – $l \times n$ output matrix in the state-space realization of G.

$\mathbb{C}$ – field of complex numbers.

$\mathbb{C}_+$, $\overline{\mathbb{C}}_+$ – open, closed right half plane.

D – $l \times m$ matrix with the direct effect from u to y in the state-space realization of G.

D_I, D_O – diagonal scaling matrices.

D_d – diagonal scaling matrix for disturbances.

D_e – diagonal scaling matrix for control error.

D_n – diagonal scaling matrix for measurement noise.

D_r – diagonal scaling matrix for references.

D_u – diagonal scaling matrix for inputs.

$E\{\cdot\}$ – expectation operator.

E_I, E_O – input, output uncertainties.

$G(s)$ – $l \times m$ rational transfer function matrix describing the plant (process). We sometimes write

$$G(s) \stackrel{s}{=} \left[\begin{array}{c|c} A & B \\ \hline C & D \end{array} \right]$$

to mean that the transfer function $G(s)$ has a state-space realization given by the quadruple (A, B, C, D).

$G_d(s)$ – $l \times n_d$ rational transfer function matrix describing the disturbance plant (process).

$G_{ij}(s)$ – denotes the element in row i and column j in G.

$\mathcal{G}_p$, $\mathcal{G}_z$ – geometric multiplicity of a given pole, zero.

I, (I_n) – identity matrix (size $n \times n$).

$\mathbb{I}$ – field of integers.

$\mathrm{Im}(\cdot)$ – imaginary part of complex numbers.

J – matrix in Jordan form.

J – performance objective in linear quadratic Gaussian control of all outputs using all inputs.

$J(i,j)$ – performance objective in linear quadratic Gaussian control of output i using input j.

$J_{\mathrm{LQR}}(j)$ – performance objective used in linear quadratic regulator, using input j.

K – state feedback gain matrix in linear quadratic Gaussian control.

$K(s)$ – controller, K is used to denote both the one degree-of-freedom feedback controller and the two degrees-of-freedom controller.

$K_1(s)$ – feed forward part from the references in the two degrees-of-freedom controller.

$K_2(s)$ – feedback part from measurements in the two degrees-of-freedom controller.

$K_{\mathrm{LQG}}(s)$ – linear quadratic Gaussian controller controlling all outputs using all inputs.

K_f – constant feedback gain from measurement of the outputs to the states.

$K_{f,i}$ – constant feedback gain from measurement of output i to the states.

K_j – constant state feedback gain to input j.

$K_{ji}(s)$ – SISO controller linking output i to input j.

$L(s)$ – loop transfer function $L \triangleq GK$, where K is the feedback controller.

$L_I(s)$ – input loop transfer function $L_I \triangleq KG$, where K is the feedback controller.

M_L, M_R – matrices containing the left, right generalized vectors from the Jordan form.

$N(s)$ – noise model, most often used to scale the measurement noise relative to the maximum allowed control error in the outputs.

$\mathcal{N}_p$, $\mathcal{N}_z$ – multiplicity of a given pole, zero.

N_u, N_y – selection matrices for inputs, outputs.

$P(s)$ – rational transfer function matrix used in the controllers proving tightness of the lower bounds (see Chapters 4 and 5).

P_d – partial disturbance gain.

P_n – partial gain for measurement noise.

P_r – partial reference gain.

P_y – partial gain from secondary outputs y_2 to primary outputs y_1.

Q – positive semidefinite ($Q \geq 0$) weighting matrix in the linear quadratic regulator problem.

$Q(s)$ – rational transfer function matrix used in the controllers proving tightness of the lower bounds (see Chapters 4 and 5).

$\mathbb{R}$ – field of real numbers.

$R(s)$ – reference model, most often used to scale the references relative to the maximum allowed control error in the outputs.

$\mathrm{Re}(\cdot)$ – real part of complex numbers.

S – diagonal scaling matrix in Jordan form. Note that the main use of S is sensitivity.

$S(s)$ – sensitivity, i.e. $S \triangleq (I + L)^{-1}$.

$S_I(s)$ – input sensitivity, i.e. $S_I \triangleq (I + L_I)^{-1}$.

$S_{\mathrm{LQG}}(s)$ – sensitivity when the feedback controller is K_{LQG}, i.e. $S \triangleq (I + GK_{\mathrm{LQG}})^{-1}$.

$S_{ii}(s)$ – sensitivity in output i, i.e. $S_{ii} \triangleq (I + G_{ij}K_{ji})^{-1}$.

$S_x(s)$ – $S_x \triangleq (I + K(sI - A)^{-1}B)^{-1}$, where K is the constant state feedback gain.

T – similarity transformation. Note that the main use of T is complementary sensitivity.

T – time horizon in linear quadratic Gaussian control. Note that the main use of T is complementary sensitivity.

$T(s)$ – complementary sensitivity, i.e. $T \triangleq L(I + L)^{-1} = I - S$.

$T_I(s)$ – input complementary sensitivity, i.e. $T_I \triangleq L_I(I + L_I)^{-1} = I - S_I$.

U – matrix containing the output singular directions.

U_0 – constant matrix used in the controllers proving tightness of the lower bounds (see Chapters 4 and 5).

U_r – matrix containing the output singular directions corresponding to nonzero singular values (economy sized singular value decomposition).

V – matrix containing the eigenvectors.

V – matrix containing the input singular directions.

V_0 – constant matrix used in the controllers proving tightness of the lower bounds (see Chapters 4 and 5).

V_r – matrix containing the input singular directions corresponding to nonzero singular values (economy sized singular value decomposition).

$V(s)$ – "weight" used in the lower bounds.

W – power spectral density matrix of the disturbance w, in linear quadratic Gaussian control. Note, $W(s)$ is also used to denote the "weight" in the lower bounds.

$W(s)$ – "weight" used in the lower bounds.

$W_I(s)$ – diagonal rational transfer function matrix with bounds on the input uncertainty in the different channels.

$W_P(s)$ – performance weight on the sensitivity.

$W_T(s)$ – performance weight on the complementary sensitivity.

$W_u(s)$ – performance weight on the input usage KS.

X – solution to the algebraic Riccati equation in the linear quadratic regulator problem.

X_L, X_R – matrices containing the left, right eigenvectors.

Y – solution to the algebraic Riccati equation in the linear quadratic estimator problem.

$\cos(\cdot)$ – cosine.

d – disturbances.

$\det(\cdot)$ – determinant.

e – control error $e \triangleq y - r$.

e_i, e_j – unit vector of length l, m with zeros in all positions except position i, j, which contains 1. Note that e_i is also used to denote the control error in output i.

i – used to denote a particular output.

i – index.

j – the complex number $\sqrt{-1}$.

j – used to denote a particular input.

j – index.

k – used to denote a particular disturbance.

l – number of outputs.

ℓ_p, ℓ_z – number of linearly independent eigenvectors corresponding to a given pole, zero.

m – number of inputs.

$\max(\cdot)$ – maximum.

$\min(\cdot)$ – minimum.

n – denotes both measurement noise in the outputs y scaled relative to the control error, and the number of states.

$\tilde{n}$ – normalized measurement noise.

n_d – number of disturbances.

p – pole.

r – normal rank of $G(s)$. Note that r is also used to denote references.

r – references to outputs y, scaled relative to the control error e.

$\tilde{r}$ – normalized references.

r_z – rank of $G(z)$.

$\text{rk}(\cdot)$ – rank.

s – complex number.

$s(s)$ – sensitivity, scalar case.

$\sin(\cdot)$ – sine.

$\sup(\cdot)$ – supremum, least upper bound.

t – time.

$t(s)$ – complementary sensitivity, scalar case.

$\text{tr}(\cdot)$ – trace, i.e. the sum of the diagonal elements.

u – inputs, u_i is also used to denote the i'th output singular direction.

u_i – used to denote the i'th output singular direction.

$v(s)$ – scalar "weight" used in the lower bounds,

v_i – used to denote the i'th input singular direction.

v_k – right eigenvector of the A matrix in the state-space description, corresponding to the eigenvalue λ_k.

w – random measurement noise used in linear quadratic Gaussian control problem.

$w(s)$ – scalar "weight" used in the lower bounds,

$w_I(s)$ – bound on input uncertainty.

$w_O(s)$ – bound on output uncertainty.

$w_P(s)$ – scalar performance weight on the sensitivity.

$w_T(s)$ – scalar performance weight on the complementary sensitivity.

w_k – left eigenvector of the A matrix in the state-space description, corresponding to the eigenvalue λ_k.

$w_u(s)$ – scalar performance weight on the input usage KS.

$w_{\text{unc}}(s)$ – scalar uncertainty weight.

x – states.

$\hat{x}$ – estimated states.

x_0 – initial state at time $t = t_0$, i.e. $x_0 = x(t_0)$.

y – outputs.

y_m – measured outputs, i.e. $y_m = y + n$, scaled relative to the control error e.

z – zero.

Greek letters

Λ – diagonal matrix containing the eigenvalues.

Λ – relative gain array $\Lambda(G) = G \times G^{-T}$.

Σ – matrix containing the singular values on the diagonal.

Σ_r – matrix containing the nonzero singular values on the diagonal (economy sized singular value decomposition).

β_{jk} – relative (open-loop/closed-loop) disturbance gain for input j and disturbance k.

γ – free variable used in the convex optimization when searching for the $\mathcal{H}_\infty$-optimal controller using γ-iteration (state-space methods). It is equal to the $\mathcal{H}_\infty$-norm or the inverse of the $\mathcal{H}_\infty$-norm of the closed-loop transfer function.

$\gamma(\cdot)$ – condition number, $\gamma(G) \triangleq \frac{\bar{\sigma}(G)}{\underline{\sigma}(G)}$.

$\gamma^*(\cdot)$ – minimized condition number, $\gamma^*(G) \triangleq \min\limits_{D_I, D_O} \gamma(D_O G D_I)$.

$\gamma_I^*(\cdot)$ – input minimized condition number, $\gamma_I^*(G) \triangleq \min\limits_{D_I} \gamma(G D_I)$.

$\gamma_O^*(\cdot)$ – output minimized condition number, $\gamma_O^*(G) \triangleq \min\limits_{D_O} \gamma(D_O G)$.

λ – eigenvalue.

λ_{ij} – relative (open-loop/closed-loop) gain between input j and output i.

$\varrho_2(i,j)$ – performance degradation due to SISO control quantified in terms of $\mathcal{H}_2$-norm.

$\varrho_\infty(i,j)$ – performance degradation due to SISO control quantified in terms of $\mathcal{H}_\infty$-norm.

$\bar{\sigma}(\cdot)$ – largest singular value.

$\underline{\sigma}(\cdot)$ – smallest singular value.

$\sigma_i(\cdot)$ – i'th singular value.

ω – frequency.

ω_B, ω_{B2} – bandwidth of primary, secondary (outer, inner) loop.

Indices and subscripts

i – output i (y_i): control error e_i measurement noise n_i, measured output $y_{m,i}$.

i – pole i (p_i).

j – input j (u_j).

j – zero j (z_j).

k – disturbance k (d_k).

Vectors and directions of zeros and poles in multivariable systems

Note that **bold** font is used to denote the vectors (zero and pole vectors), whereas the normal font is used to denote directions (zero and pole directions).

$\boldsymbol{U}_p$ – matrix containing the input pole vectors.

U_p – matrix containing the input pole directions.

$\boldsymbol{U}_\infty$ – matrix containing the input vectors with infinite gain.

U_∞ – matrix containing the input directions with infinite gain.

$\boldsymbol{X}_{pi}$ – matrix containing the state input pole vectors.

X_{pi} – matrix containing the state input pole directions.

$\boldsymbol{X}_{po}$ – matrix containing the state output pole vectors.

X_{po} – matrix containing the state output pole directions.

$\boldsymbol{X}_{zi}$ – matrix containing the state input zero vectors.

$\bar{X}_{zi}$ – matrix containing the state input zero directions.

$\boldsymbol{X}_{zo}$ – matrix containing the state output zero vectors.

X_{zo} – matrix containing the state output zero directions.

$\boldsymbol{Y}_p$ – matrix containing the output pole vectors.

Y_p – matrix containing the output pole directions.

$\boldsymbol{Y}_\infty$ – matrix containing the output vectors with infinite gain.

Y_∞ – matrix containing the output directions with infinite gain.

$\boldsymbol{u}_p$ – input pole vector.

u_p – input pole direction, i.e. $u_p = \boldsymbol{u}_p / \left\| \boldsymbol{u}_p \right\|_2$.

$\boldsymbol{u}_\infty$ – input vector with infinite gain.

u_∞ – input direction with infinite gain.

$\boldsymbol{u}_z$ – input zero vector.

u_z – input zero direction, i.e. $u_z = \boldsymbol{u}_z / \left\| \boldsymbol{u}_z \right\|_2$.

$\boldsymbol{x}_{pi}$ – state input pole vector.

x_{pi} – state input pole direction, i.e. $x_{pi} = \boldsymbol{x}_{pi} / \left\| \boldsymbol{x}_{pi} \right\|_2$.

$\boldsymbol{x}_{po}$ – state output pole vector.

x_{po} – state output pole direction, i.e. $x_{po} = \boldsymbol{x}_{po} / \left\| \boldsymbol{x}_{po} \right\|_2$.

$\boldsymbol{x}_{zi}$ – state input zero vector.

x_{zi} – state input zero direction, i.e. $x_{zi} = \boldsymbol{x}_{zi} / \left\| \boldsymbol{x}_{zi} \right\|_2$.

$\boldsymbol{x}_{zo}$ – state output zero vector.

x_{zo} – state output zero direction, i.e. $x_{zo} = \boldsymbol{x}_{zo} / \left\| \boldsymbol{x}_{zo} \right\|_2$.

$\boldsymbol{y}_p$ – output pole vector.

y_p – output pole direction, i.e. $y_p = \boldsymbol{y}_p / \left\| \boldsymbol{y}_p \right\|_2$.

$\boldsymbol{y}_\infty$ – output vector with infinite gain.

y_∞ – output direction with infinite gain.

$\boldsymbol{y}_z$ – output zero vector.

y_z – output zero direction, i.e. $y_z = \boldsymbol{y}_z / \left\| \boldsymbol{y}_z \right\|_2$.

All-pass factorizations of RHP zeros and poles

In the notation given here, the factorizations are viewed as operators which return and take as an argument a rational transfer function matrix:

$(\cdot)_m$ – minimum phase representation of SISO transfer functions.

$(\cdot)_{ms}$ – minimum phase stable representation of SISO transfer functions.

$(\cdot)_{mi}$ – input minimum phase representation of MIMO transfer function matrices.

$(\cdot)_{mo}$ – output minimum phase representation of MIMO transfer function matrices.

$(\cdot)_s$ – stable representation of SISO transfer functions.

$(\cdot)_{si}$ – input stable representation of MIMO transfer function matrices.

$(\cdot)_{so}$ – output stable representation of MIMO transfer function matrices.

$(\cdot)_{xx}^{-1}$ – means $((\cdot)_{xx})^{-1}$ where $xx \in \{m, mi, mo, s, si, so\}$.

$(\cdot)_{xxyy}$ – means $((\cdot)_{xx})_{yy}$ where $yy, xx \in \{m, mi, mo, s, si, so\}$.

$(\cdot)_{xxyy}^{-1}$ – means $(((\cdot)_{xx})_{yy})^{-1}$ where $yy, xx \in \{m, mi, mo, s, si, so\}$.

$\mathcal{B}_p(\cdot)$ – all-pass filter defined by the SISO factorization of RHP-poles.

$\mathcal{B}_{pi}(\cdot)$ – all-pass filter defined by the input factorization of RHP-poles.

$\mathcal{B}_{po}(\cdot)$ – all-pass filter defined by the output factorization of RHP-poles.

$\mathcal{B}_z(\cdot)$ – all-pass filter defined by the SISO factorization of RHP-zeros.

$\mathcal{B}_{zi}(\cdot)$ – all-pass filter defined by the input factorization of Rhp-zeros.
$\mathcal{B}_{zo}(\cdot)$ – all-pass filter defined by the output factorization of Rhp-zeros.
$\mathcal{B}_{xx}^{-1}(\cdot)$ – means $(\mathcal{B}_{xx}(\cdot))^{-1}$ where $xx \in \{m, mi, mo, s, si, so\}$

The following all-pass filters are special:

$\mathcal{B}(s)$ – general all-pass filter (see Appendix A).
$\mathcal{B}_p(s)$ – simplified notation for $\mathcal{B}_p(G(s))$.
$\mathcal{B}_z(s)$ – simplified notation for $\mathcal{B}_z(G(s))$.

Norms

$\|\cdot\|_\infty$ – Systems: $\mathcal{H}_\infty$-norm of stable rational transfer function matrix $M(s)$, i.e.

$$\|M(s)\|_\infty \triangleq \sup_\omega \bar{\sigma}(M(j\omega))$$

Signal: peak value in time, i.e.

$$\|e(t)\|_\infty \triangleq \max_\tau \left(\max_i |e_i(\tau)| \right)$$

$\|\cdot\|_2$ – Systems: $\mathcal{H}_2$-norm of a strictly proper stable rational transfer function matrix $M(s)$, i.e.

$$\|M(s)\|_2 \triangleq \sqrt{\frac{1}{2\pi} \int_{-\infty}^{\infty} \mathrm{tr}\left(M^H(j\omega)M(j\omega)\right) d\omega}$$

Signal: integral square error ISE (signal energy), i.e.

$$\|e(t)\|_2 \triangleq \sqrt{\int_{-\infty}^{\infty} \sum_i |e_i(\tau)|^2 d\tau}$$

Vector: Euclidean norm, i.e.

$$\|a\|_2 \triangleq \sqrt{\sum_i |a_i|^2}$$

$\|\cdot\|_{i\infty}$ – (matrices) induced infinity norm – maximum row sum (sum of element magnitudes), i.e.

$$\|A\|_{i\infty} \triangleq \max_i \sum_j |a_{ij}|$$

l_1 – induced max norm, i.e.

$$\|g(t)\|_1 = \max_{d(t)} \frac{\|e(t)\|_\infty}{\|d(t)\|_\infty}$$

where $g(t)$ is the system impulse response.

Abbreviations

1-DoF – one degree-of-freedom.

2-DoF – two degrees-of-freedom.

ARE – algebraic Riccati equation.

BRGA – block relative gain array.

CLDG – closed loop disturbance gain.

DoF – degree(s)-of-freedom.

IMC – internal model control.

ISE – integral square error.

LQE – linear quadratic estimator.

LQG – linear quadratic Gaussian.

LQR – linear quadratic regulator.

Mimo – multiple input multiple output or multivariable.

PBH – Popov-Belevitch-Hautus.

PDG – partial disturbance gain.

PID – proportional integral derivative.

PRGA – performance relative gain array.

RDG – relative disturbance gain.

RGA – relative gain array.

Rhp – right half plane, may denote both the open and the closed right half plane.

RPDG – relative partial disturbance gain.

Siso – single input single output.

SSE – sum of squared errors.

SVD – singular value decomposition.

Chapter 1

Introduction

The title of this thesis is "Studies on controllability analysis and control structure design". At this point it seems appropriate to define the terms *controllability* and *control structure* (Skogestad and Postlethwaite, 1996):

Controllability (input-output) *is the ability to achieve acceptable control performance; that is, to keep the outputs (y) within specified bounds or displacements from their references (r), in spite of unknown but bounded variations, such as disturbances (d) and plant changes, using available inputs (u) and available measurements $(y_m$ or $d_m)$.*

A plant is controllable if and only if there *exists* a controller, interconnecting the measurements and the manipulated variables, that yields acceptable performance for all expected plant variations. The *controllability* of a plant *is independent of the controller, and is a property of the plant*. It follows that the controllability only can be affected by changing the plant, i.e. design changes.

Control structure (control strategy) design *refers to all structural decisions included in the design of a control system.*

For further details on control structure design see Section 1.3.

1.1   Motivation

Increasing demands to efficient operation and utilization of energy and raw materials in chemical processes result in more integrated processes. Unreacted raw materials are recycled and hot process streams are heat exchanged against cold process streams. The increasing integration has a pronounced effect on the dynamics, control and operation of chemical process plants. The impacts on the control structure design are that better knowledge and understanding of the complex dynamic and steady-state behavior of these processes are necessary in order to design control systems which result in efficient and reliable operation. In addition, there is a need to use more sophisticated controller design procedures to operate the process closer to the optimal operating point in spite of disturbances and environmental changes.

Indeed, the modern control theory has provided more sophisticated controller design

methods, i.e. with the introduction of: optimal control theory in the 1960's, $\mathcal{H}_{\infty}$-optimal control and model predictive control in the 1980's. However, most (if not all) available control theories and design methods assume that a control structure is given prior to the design. That is, they do not consider the structural decisions involved in the control structure design in an explicit manner. They therefore fail to answer some of the following basic questions which a control engineer regularly meets in practice: which variables should be controlled, which variables should be measured, which inputs should be manipulated, and which links should be made between them?

Control structure design was (among others) considered by Foss (1973) in his paper entitled "Critique of chemical process control theory". Foss concluded by challenging the control theoreticians to close the gap between control theory and applications. Later Morari, Arkun and Stephanopoulos (1980) presented an overview of control structure design, hierarchical control and multilevel optimization in the series of papers entitled "Studies in the synthesis of control structures for chemical processes". Skogestad and Postlethwaite (1996) note that the gap still remains to some extent today.

The *main objective* of this thesis is to try to close some of the gap between control theory and applications. The approach taken in this thesis is to develop and apply tools which address the controllability of the plant. It is important that these tools are independent of the controller in order to reflect the performance limitations of the plant. In this thesis, existing controllability measures are used and new controllability measures are introduced, with the objective to:

- Obtain insights into the directionality of zeros and poles, and state controllability and observability of poles (Chapter 2).
- Quantify performance limitations imposed by instabilities and right half plane zeros in the plant (Chapters 3–5).
- Quantify the minimum input usage needed to stabilize an unstable plant with one unstable mode, and to find the best (in terms of minimum input usage) input and output to stabilize a plant with one unstable mode using a SISO controller (Chapter 6).
- Quantify the effect of disturbances, measurement noise and reference changes in partially controlled systems (Chapter 7).
- Address the input/output selection for partial control, and in particular look at the selection of secondary measurements in indirect and cascade control (Chapters 6–9).
- Quantify the effect of input and output uncertainty on the performance at the output of the plant (Chapter 10).

1.2   Relations to previous work

The book by Skogestad and Postlethwaite (1996) gives a good overview of the main issues which form the basis for this thesis. Actually, some of the main topics of this thesis were initiated during the time of writing the book, and some of the earlier results from this thesis also made its way into the book. Although, Skogestad and Postlethwaite (1996) give a quite throughout review of previous work, some of it is repeated here for completeness.

Ziegler and Nichols (1943) defined *controllability* as *"the ability of the process to achieve and maintain the desired equilibrium value"*. However, in the 1960's "controllability" became synonymous with "state controllability" introduced by Kalman, and the term is still used in this manner in system theory. State controllability is the ability to bring a system from a given initial state to an arbitrary final state within finite time. As noted by Skogestad and Postlethwaite, state controllability does not address the quality of the response between and after these two states, and the required inputs may be excessive. Later Morari (1983) introduced the term *dynamic resilience* to address the input-output controllability of the plant, and to avoid any confusion with state controllability. In a series of articles Morari and coworkers have studied: the effect of RHP zeros on dynamic resilience (Holt and Morari, 1985b; Morari, Zafiriou and Holt, 1987), the effect of dead time on dynamic resilience (Holt and Morari, 1985a), the effect of model uncertainty on dynamic resilience (Skogestad and Morari, 1987). In the work (Morari, 1983), he made use of the concept of "perfect control". A drawback with the name "dynamic resilience" is that it does not reflect its relation to control. This thesis follows Skogestad and Postlethwaite (1996), and use the term "input-output controllability" or simply "controllability" when it is clear that the text does not refer to state controllability. New controllability measures which can be used to quantify the control performance both at the input and at the output of the plant and to address the structural issues in control structure design, are introduced. In addition, pole directions are introduced and their relations to state controllability and observability, are given.

Bode (1945), in his book on network analysis and feedback amplifiers, was probably the first to study a priori constraints on the achievable performance of SISO-systems. His analysis focused on gain-phase relationships in the frequency domain which resulted in many useful interpretations applicable to feedback control. Horowitz (1963) summarizes and generalizes Bode's work to control systems. The well-known *Bode sensitivity integral* (Bode, 1945) states that for stable SISO-systems with pole-zero excess of two or larger, the integral of the logarithmic magnitude of the sensitivity function over all frequencies must equal zero. This implies that a peak in $|S|$ larger than 1 is unavoidable. Later Bode's criterion has been extended to plants with RHP zeros and poles by Freudenberg and Looze (1985; 1988).

With the introduction of modern control in the beginning of the 1960's, the *poles* in multivariable systems gained much focus, which resulted in several useful results on state controllability, observability and modal control. Although the poles can be moved with state feedback, it became pretty clear that the open-loop zeros can not be moved by state-feedback. About the same time, optimal control theory in terms of Linear Quadratic Gaussian (LQG) control, reached maturity. From these studies it became clear that the open-loop transfer function from the inputs to the states contains no zeros. This may have had a misleading role in multivariable feedback design, which resulted in that very little attention was given to multivariable zeros during the 1960's and 70's. In the 1970's multivariable zeros started to gain focus. Rosenbrock (1966; 1970) defined zeros in multivariable systems using the Smith-McMillan form. For multivariable systems Kwakernaak and Sivan (1972, pages 306–307) state that perfect tracking with state feedback can be achieved if and only if the rational transfer function matrix from the inputs to the outputs has no RHP-zeros.

The *important* work by Zames (1981), introduced the $\mathcal{H}_\infty$-norm into the control litera-

ture, and in particular it focuses on the engineering implications of the $\mathcal{H}_\infty$-norm. That is, the work emphasizes the use of the $\mathcal{H}_\infty$-norm from an analysis point of view. Zames (1981) derived a lower bound on the weighted sensitivity function which is based on the interpolation constraint on the sensitivity function valid for RHP-zeros in G. Later most of the work on $\mathcal{H}_\infty$-control theory have focused on finding the $\mathcal{H}_\infty$-optimal controller minimizing the $\mathcal{H}_\infty$-norm of general closed-loop transfer functions. This includes (among others) the early work of Doyle (1984) and the work by Doyle, Glover, Khargonekar and Francis (1989), the latter contains the state-space solution to the $\mathcal{H}_\infty$-problem.

Boyd and Desoer (1985), Freudenberg and Looze (1988), Boyd and Barratt (1991) and Chen (1993; 1995) have studied the limitations imposed by RHP zeros and poles in terms of *sensitivity integral formulas* for multivariable systems. A breakthrough was made by Boyd and Desoer who obtained inequality versions of the sensitivity and Poisson integral formulas. The work by Chen differs from the work by Boyd and Desoer in that Chen seeks equality versions of the sensitivity and Poisson integral formulas. Based on the results by Boyd and Desoer, Freudenberg and Looze, and Boyd and Barratt generalize the integral constraints on the sensitivity (like Bode's sensitivity integral) to multivariable systems. In this thesis controller independent lower bounds on the $\mathcal{H}_\infty$-norm of closed-loop transfer functions are derived, using algebraic rather than integral constraints. These bounds are based on interpolation constraints imposed by RHP zeros and poles and the approach taken is similar to the approach used by Zames (1981) in the derivation of the lower bound on the weighted sensitivity function when the plant has a RHP-zero. A further objective is to prove that (and in which cases) the lower bounds are tight, i.e. to find analytical controllers which achieve an $\mathcal{H}_\infty$-norm of the closed-loop transfer function equal to the lower bounds. The approach taken to derive these controllers, is similar to the early interpolation theoretic methods (Doyle, 1984) and it is also related to the polynomial approach of Kwakernaak (1986; 1993).

The latter part of this thesis deals with control structure selection and introduces controllability measures to address the structural issues in control structure design. In Chapter 6 the pole vectors are used to find the best input and the best output to stabilize a plant with one unstable mode with minimum input usage. Related work on this topic are the theories within optimal and the modal control. In addition, this work is also related to the work in the earlier chapters, since when quantifying the minimum input usage in terms of the $\mathcal{H}_\infty$-norm the results derived in Chapters 4 and 5, are used. Partial control is also used to address the control structure design. Related work on partial control includes: Manousiouthakis, Savage and Arkun (1986), Skogestad and Wolff (1992), and Häggblom (1994). For further details see Chapters 7–9.

1.3   Control structure design

One important task in the design of a control system is the specification of the control structure. Skogestad and Postlethwaite (1996) summarize the steps in control structure design to be:

1) The selection of controlled outputs (a set of variables which are to be controlled to achieve a set of specific objectives).
2) The selection of manipulations and measurements (sets of variables which can be manipulated and measured for control purposes).
3) The selection of a *control configuration* (a structure interconnecting measurements, references (commands) and manipulated variables).
4) The selection of a *controller type* (control law specification, e.g. PID-controller, decoupler, LQG, etc.).

One may easily recognize that the design of a control structure is more complex than the task of synthesizing a controller for given sets of measurements and actuators. With a large number of candidate measurements and/or manipulations, the number of possible combinations of inputs and outputs have a combinatorial growth, so an approach consisting of performing a controllability analysis and/or controller design for each possible combination becomes time consuming. The work in this thesis on control structure design mainly considers steps 1), 2) and 3) and introduces controllability measures to address the input/output selection problem (see Chapters 6–9).

1.4 Scaling

Proper scaling of the variables is important in order to apply the results in this thesis. In addition, proper scaling makes the model analysis and the controller design (selection of weights) much easier. Considering the scaling of variables early in the control system design forces the control engineer to make a judgement about: the required performance of the system, the maximum allowed change in the inputs (input constraints), and the influence of external signals like disturbances and measurement noise.

The variables involved are: outputs y, inputs u, disturbances d, measurement noise n, measured outputs $y_m = y + n$ and references r. Let the unscaled linear model of the process be

$$\hat{y} = \widehat{G}\hat{u} + \widehat{G}_d\hat{d}; \qquad \hat{e} = \hat{y} - \hat{r}; \qquad \hat{y}_m = \hat{y} + \hat{n} \tag{1.1}$$

where the hat $(\hat{\ })$ is used to show that the variables are in their original unscaled units. As a basic rule, the variables are scaled by *dividing each variable by its maximum expected or allowed change (variation)*. Let $\hat{u}_{j,\max}$, $\hat{d}_{k,\max}$, $\hat{r}_{i,\max}$, $\hat{n}_{i,\max}$ and $\hat{e}_{i,\max}$ denote the maximum allowed change in input $\hat{u}_j$, disturbance $\hat{d}_k$, reference $\hat{r}_i$, measurement noise $\hat{n}_i$ and control error $\hat{e}_i$ in output $\hat{y}_i$. Note that the variables $\hat{y}_i$, $\hat{e}_i$, $\hat{r}_i$, $\hat{y}_{m,i}$ and $\hat{n}_i$ are in the same units, so the same scaling factor should be applied to each. We scale the output $\hat{y}_i$ relative to the maximum allowed control error $\hat{e}_{i,\max}$. By introducing the scaling matrix for the control error $D_e = \text{diag}\{\hat{e}_{i,\max}\}$, we obtain

$$y = D_e^{-1}\hat{y}, \quad e = D_e^{-1}\hat{e}, \quad r = D_e^{-1}\hat{r}, \quad y_m = D_e^{-1}\hat{y}_m \quad \text{and} \quad n = D_e^{-1}\hat{n} \tag{1.2}$$

We also introduce the scaling matrices for inputs $D_u = \text{diag}\{\hat{u}_{j,\max}\}$, disturbances $D_d = \text{diag}\{\hat{d}_{k,\max}\}$, references $D_r = \text{diag}\{\hat{r}_{i,\max}\}$ and measurement noise $D_n = \text{diag}\{\hat{n}_{i,\max}\}$.

We obtain

$$\hat{u} = D_u u, \qquad \hat{d} = D_d d, \qquad \hat{r} = D_r \tilde{r} \quad \text{and} \quad \hat{n} = D_n \tilde{n} \tag{1.3}$$

Introducing the scaled variables into (1.1) gives

$$y = \underbrace{D_e^{-1} \widehat{G} D_u}_{G} u + \underbrace{D_e^{-1} \widehat{G}_d D_d}_{G_d} d; \quad e = y - \underbrace{D_e^{-1} D_r}_{R} \tilde{r}; \quad y_m = y + \underbrace{D_e^{-1} D_n}_{N} \tilde{n} \tag{1.4}$$

where $R = \operatorname{diag}\left\{\frac{\hat{r}_{i,\max}}{\hat{e}_{i,\max}}\right\}$, $N = \operatorname{diag}\left\{\frac{\hat{n}_{i,\max}}{\hat{e}_{i,\max}}\right\}$ and we note that $r = R\tilde{r}$ and $n = N\tilde{n}$. By introducing the scaled transfer functions in the model (1.4), we obtain the scaled model

$$y = Gu + G_d d; \qquad e = y - r = y - R\tilde{r}; \qquad y_m = y + n = y + N\tilde{n} \tag{1.5}$$

Here each input u_j, control error e_i, disturbance d_k, reference $\tilde{r}_i$ and measurement noise $\tilde{n}_i$ should be less than one in magnitude. The diagonal elements of R are typically greater or equal to one, i.e. $R_{ii} = \frac{\hat{r}_{i,\max}}{\hat{e}_{i,\max}} \geq 1$, and represent the largest expected change in the reference for output i relative to the allowed control error in output i. The diagonal elements of N are typically less or equal to one, i.e. $N_{ii} = \frac{\hat{n}_{i,\max}}{\hat{e}_{i,\max}} \leq 1$, and represent the largest expected change in measurement noise for output i relative to the allowed control error in output i (inverse of signal to noise ratio). The block diagram representing the scaled model is given
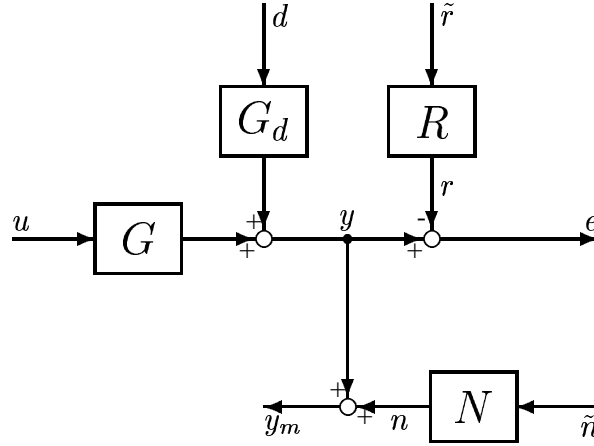
Figure 1.1: Model in terms of scaled variables

in Figure 1.1, for which following control objective is relevant:

- In terms of scaled variables we have that $|d_k(t)| \leq 1$, $\forall t$, $\forall k$, $|\tilde{n}_i(t)| \leq 1$, $\forall t$, $\forall i$ and $|\tilde{r}_i(t)| \leq 1$, $\forall t$, $\forall i$, and the control objective is to manipulate u with $|u_j(t)| \leq 1$, $\forall t$, $\forall j$ such that $|e_i(t)| = |y_i(t) - r_i(t)| \leq 1$, $\forall t$, $\forall i$.

REMARK 1. A number of the interpretations used in this thesis depend on correct scaling. For example, for MIMO-systems one cannot correctly make use of the sensitivity function $S = (I + GK)^{-1}$ unless the control errors are of comparable magnitude.

REMARK 2. With the above scalings, the worst-case behavior of a system is analyzed by considering disturbances d_k, references $\tilde{r}_i$ and measurement noise $\tilde{n}_i$ of magnitude 1.

REMARK 3. The control error is

$$e = y - r = Gu + G_d d - R\tilde{r} \tag{1.6}$$

and we see that a normalized reference change $\tilde{r}$ can be viewed as a special case of a disturbance with $G_d = -R$, where R usually is a constant diagonal matrix.

REMARK 4. The scaling of each output relative to the control error is used when analyzing a given plant. However, if the issue is to *select* the best output to stabilize an unstable mode, see Chapter 6, then one should scale each output relative to the best (minimum) achievable control error, which at steady-state is similar to the expected variation in the measurement noise.

REMARK 5. If the expected or allowed variation of a variable about 0 (its nominal value) is not symmetric, then the largest variation should be used for $\hat{d}_{k,\max}$ and $\hat{n}_{i,\max}$, and the smallest variation for $\hat{u}_{j,\max}$ and $\hat{e}_{i,\max}$.

A further brief discussion of scaling is given in each of the chapters, and in some of the results special scalings are required.

1.5   Thesis overview

The results in this thesis can be divided into the following two main topics (parts):

1) Limitations imposed by RHP zeros and poles on performance in (multivariable) feedback systems. This first part involves Chapters 3–5. Chapter 2 and Appendix A provide the necessary technical background for these chapters.

2) Control structure selection which involves Chapters 6–9. Chapter 2 provides the necessary technical background for Chapter 6.

Chapter 10 is to some degree disconnected from the rest of the thesis, however, the effect of input uncertainty is similar to the effect of RHP-zeros on performance in multivariable systems. The main chapters are written as self contained papers, so it is not necessary to read the background material before reading the main chapters. Some more information on each of the chapters follows:

Chapter 2 contains a review of zeros, poles and their directions in multivariable systems. In particular, it shows how to compute the zero and pole directions in multivariable systems in terms of eigenvalue computations. The second part of the chapter deals with state-controllability and observability in terms of pole directions.

Parts of this chapter were presented at: AIChE annual meeting, 10-15 November, Chicago, USA, 1996. The results on computing the pole directions in terms of eigenvalue computations are also included in (Skogestad and Postlethwaite, 1996).

Chapter 3 can be viewed as an introduction to the effect of RHP zeros and poles in multivariable systems. The results quantify the fundamental limitations imposed by RHP zeros and poles in terms of lower bounds on the peaks in the weighted sensitivity and complementary sensitivity functions. This work was carried out in collaboration with Sigurd Skogestad, during a visit to University of California, Berkeley, in the spring of 1995.

This paper is accepted for publication in Journal of Process Control. It was first presented at: UKACC, Control'96, 2-5 September, Exeter, UK, 1996, and the results are also included in (Skogestad and Postlethwaite, 1996).

Chapter 4 is the second chapter which deals with the effect of RHP zeros and poles, however, this chapter only considers SISO-systems. The results in this chapter generalize the results of Chapter 3 to also consider other closed-loop transfer functions than sensitivity and complementary sensitivity. This means that lower bounds on the $\mathcal{H}_\infty$-norm of two general classes of closed-loop transfer functions when the plant has RHP-zeros and/or RHP-poles, are given. Furthermore, *analytical* $\mathcal{H}_\infty$-optimal controllers which show that the lower bounds are *tight* in a large number of cases, are given. Instabilities in the plant require active use of the plant inputs. An application of the lower bounds which gets much focus, is to *quantify* the input magnitudes required for disturbance and measurement noise rejection in unstable SISO systems.

Parts of this paper together with the MIMO generalization in Chapter 5, were first presented at: European Control Conference, ECC97, 1-4 July, Brussels, Belgium, 1997.

Chapter 5 is the third chapter studying the effect of RHP zeros and poles in multivariable systems. It generalizes the results of Chapter 4 to MIMO-systems. That is, it provides lower bounds on the $\mathcal{H}_\infty$-norm of general closed-loop transfer functions. It is proved that the lower bounds are *tight* by giving *analytical* controllers, which achieve the lower bounds in a large number of cases. Previously derived lower bounds on weighted sensitivity and complementary sensitivity (Chapter 3) are generalized to the case with matrix valued weights. Furthermore, new bounds which quantify the minimum input usage needed for stabilization in the presence of measurement noise and disturbances, are derived. A separate bound applicable to two degrees-of-freedom control, is also derived. Controllers which prove that this bound is tight when the plant has one RHP-zeros, are also given.

The author notes that this chapter is theoretical and the notation is complicated. However, the bounds can easily be computed using MATLAB. The controllers minimizing the $\mathcal{H}_\infty$-norm of a particular closed-loop transfer function, can in many cases be found by using MATLAB with state-space computations. In particular, this is the case when minimizing the $\mathcal{H}_\infty$-norm of the input usage (i.e. minimizing $\|K_2S(s)\|_\infty$), since the feedback controller K_2 minimizing the $\mathcal{H}_\infty$-norm of K_2S is semi-proper and can be represented on state-space form. The main reason for writing the SISO paper (Chapter 4) is to show the implications of the lower bounds and to simplify the notation so that the engineering usefulness becomes more visible. These implications and the usefulness of the lower bounds carry over to MIMO systems considered in Chapter 5. The author therefore advices the reader to read Chapter 4 before reading Chapter 5 and to look at the example given in Section 5.7.

Furthermore, the theorems which give the lower bounds and the controllers which achieve these lower bounds, are similar. All these theorems are stated and all the proofs are given, mainly for completeness. So, the reader may at least skip reading some of the proofs.

Parts of this paper were first presented at: European Control Conference, ECC97, 1-4 July, Brussels, Belgium, 1997.

Chapter 6 considers control structure design using the information given in the pole vectors. It is shown how the input and output pole vectors are related to the minimum input usage needed to stabilize a plant with one unstable mode using a Siso controller. The input usage due to measurement noise is quantified both in terms of the $\mathcal{H}_2$-norm (input energy) and the $\mathcal{H}_\infty$-norm. The best choice of one input and one output for Siso stabilizing control is the same for both norms and corresponds to the elements in the pole vectors with largest magnitude. Stable but slow modes which need to be shifted further into the Left Half Plane (Lhp) using feedback control, are also considered. Moving stable slow modes are accomplished with modal control, and the results are interpreted in terms of Linear Quadratic Gaussian (LQG) control.

With this chapter the focus (in the thesis) moves from control theory over to control structure design (although control theory is still present in the later chapters). The case study concerning the Tennessee Eastman problem, shows that the results given in this chapter can easily be applied (provided that one has a model of the plant) to obtain a stabilizing control structure for a relatively complex plant using limited physical process knowledge. The main advantage of selecting the inputs and outputs according to the results in this chapter, is that the approach taken can be justified from a control theoretical point of view.

The reader may skip reading some of the material on modal control given in Appendix A in this chapter, since this material is not too important (the reason for including this is that it can be useful for later work).

Parts of this paper were first presented at: AIChE annual meeting, 10-15 November, Chicago, USA, 1996.

Chapter 7 gives an introduction to control structure design, and in particular it addresses the issue of selecting measurements and manipulations for partial control. Partial control at a given level involves controlling a subset of the outputs with an associated control objective. The relative gain array (RGA) and singular value decomposition (SVD) are useful measures for selecting inputs and outputs.

This paper was first presented at: 13th IFAC World Congress, 30 June - 5 July, San Francisco, USA, 1996.

Chapter 8. Integrated chemical process plants are in practice controlled using a hierarchy of control loops. The basis is to implement inner control loops, resulting in a partially controlled system. The idea is that the primary outputs, with these inner control loops closed should be less sensitive to disturbances. In addition, it is desirable that the control error in the primary outputs should not be sensitive to control errors in the inner control loops. Two simple tools for efficiently analyzing such problems are presented in this chapter. These tools are applicable to input/output selection for indirect and cascade control.

Parts of this paper were first presented at: UKACC, Control'96, 2-5 September, Exeter, UK, 1996. However, the content is completely rewritten.

Chapter 9 considers indirect control of product compositions by controlling the temperature at two selected stages in a binary distillation column. The two approaches derived in Chapter 8, are applied in order to find the best stages to measure the temperatures. The most

obvious (direct) approach is to minimize the combined effect of (temperature) measurement noise and disturbances (changes in feed rate and feed composition) on the product compositions. The second (indirect) approach is to maximize the gain in the weak direction of the selected subsystem to be controlled.

This case study was first presented at: UKACC, Control'96, 2-5 September, Exeter, UK, 1996.

Chapter 10. The relative gain array (RGA) and condition number are commonly used tools in controllability analysis. New results that link these measures to control performance, measured in terms of the output sensitivity function with input and output uncertainty, are given in this chapter.

This paper was first presented at ESCAPE-6, 26-29 May, Rhodes, Greece, 1996.

Chapter 11. Conclusions and suggestions for future work are given in this chapter.

Appendix A. Analytical state-space realizations for factorizations of zeros and poles in multivariable systems into *Blaschke* products are given in this appendix. Some useful properties of these factorizations are also considered. These factorizations are used in Chapters 3–5.

Appendix B considers the left and the right eigenvalue problems and the left and the right Jordan form. These are used to compute the pole directions and the directions with infinite gains in Chapter 2.

References

Bode, H. W. (1945). *Network Analysis and Feedback Amplifier Design*, D. Van Nostrand Co., New York.

Boyd, S. and Barratt, C. (1991). *Linear Controller Design — Limits of Performance*, Prentice-Hall, Englewood Cliffs.

Boyd, S. and Desoer, C. A. (1985). Subharmonic functions and performance bounds in linear time-invariant feedback systems, *IMA J. Math. Contr. and Info.* **2**: 153–170.

Chen, J. (1993). Sensitivity integral relations and design trade-offs in linear multivariable feedback systems, *Proc. American Control Conference*, San Francisco, CA, pp. 3160–3164.

Chen, J. (1995). Sensitivity integral relations and design trade-offs in linear multivariable feedback systems, *IEEE Transactions on Automatic Control* **AC-40**(10): 1700–1716.

Doyle, J. C. (1984). *Lecture Notes on Advances in Multivariable Control*, ONR/Honeywell Workshop, Minneapolis, October.

Doyle, J. C., Glover, K., Khargonekar, P. P. and Francis, B. A. (1989). State-space solutions to standard $\mathcal{H}_2$ and $\mathcal{H}_\infty$ control problems, *IEEE Transactions on Automatic Control* **AC-34**(8): 831–847.

Foss, A. S. (1973). Critique of chemical process control theory, *AIChE Journal* **19**: 209–214.

Freudenberg, J. S. and Looze, D. P. (1985). Right half plane poles and zeros and design tradeoffs in feedback systems, *IEEE Transactions on Automatic Control* **AC-30**(6): 555–565.

Freudenberg, J. S. and Looze, D. P. (1988). *Frequency Domain Properties of Scalar and Multivariable Feedback Systems*, Vol. 104 of *Lecture Notes in Control and Information Sciences*, Springer-Verlag, Berlin.

Häggblom, K. (1994). Modelling of control structures for partially controlled plants, *IFAC Workshop on Intergration of Process Design & Control'94, Baltimore, MD, June 27-28, 1994,* pp. 183–188.

Holt, B. R. and Morari, M. (1985a). Design of resilient processing plants V — The effect of deadtime on dynamic resilience, *Chemical Engineering Science* **40**: 1229–1237.

Holt, B. R. and Morari, M. (1985b). Design of resilient processing plants VI — The effect of right plane zeros on dynamic resilience, *Chemical Engineering Science* **40**: 59–74.

Horowitz, I. M. (1963). *Synthesis of Feedback Systems*, Academic Press, London.

Kwakernaak, H. (1986). A polynomial approach to minimax frequency domain optimization of multivariable feedback systems, *Int. J. Control* **44**(1): 117–156.

Kwakernaak, H. (1993). Robust control and $\mathcal{H}_\infty$-optimization — Tutorial paper, *Automatica* **29**: 255–273.

Kwakernaak, H. and Sivan, R. (1972). *Linear Optimal Control Systems*, Wiley Interscience, New York.

Manousiouthakis, V., Savage, R. and Arkun, Y. (1986). Synthesis of decentralized process control structures using the concept of block relative gain, *AIChE Journal* **32**(6): 991–1003.

Morari, M. (1983). Design of resilient processing plants III – a general framework for the assessment of dynamic resilience, *Chemical Engineering Science* **38**: 1881–1891.

Morari, M., Arkun, Y. and Stephanopoulos, G. (1980). Studies in the synthesis of control structures for chemical process, Part I: Formulation of the problem. Process decomposition and the classification of the control tasks. Analysis of the optimizing control structures, *AIChE Journal* **26**(2): 220–232.

Morari, M., Zafiriou, E. and Holt, B. R. (1987). Design of resilient processing plants. new characterization of the effect of rhp zeros, *Chem. Eng. Science* pp. 2425–2428.

Rosenbrock, H. H. (1966). On the design of linear multivariable systems, *Third IFAC World Congress*. Paper 1A.

Rosenbrock, H. H. (1970). *State-space and Multivariable Theory*, Nelson, London.

Skogestad, S. and Morari, M. (1987). Design of resilient processing plants - IX. effect of model uncertainty on dynamic resilience, *Chem. Eng. Sci.* pp. 1765–1780.

Skogestad, S. and Postlethwaite, I. (1996). *Multivariable Feedback Control, Analysis and Design*, John Wiley & Sons, Chichester.

Skogestad, S. and Wolff, E. A. (1992). Controllability measures for disturbance rejection, *IFAC Workshop on Interactions between Process Design and Process Control*, London, UK, pp. 23–29.

Zames, G. (1981). Feedback and optimal sensitivity: model reference transformations, multiplicative seminorms, and approximate inverses, *IEEE Transactions on Automatic Control* **AC-26**(2): 301–320.

Ziegler, J. G. and Nichols, N. B. (1943). Process lags in automatic-control circuits, *Transactions of the A.S.M.E.* **65**: 433–444.

Chapter 2

Directions of zeros and poles in multivariable systems

2.1 Introduction

With the introduction of modern control in the beginning of the 1960's, the *poles* in multivariable systems gained much focus, which resulted in several useful results on state controllability, observability and modal control. The main focus of the work in modal control is to find a state feedback gain matrix which result in some desired prespecified closed-loop poles. Although the poles can be moved with state feedback, it became pretty clear that the open-loop zeros can not be moved by state-feedback. That is, the closed-loop transfer function from the references to the outputs contains the open-loop zeros. About the same time, optimal control theory in terms of Linear Quadratic Gaussian (LQG) control reached maturity and was successfully applied to aerospace applications such as rocket maneuvering with minimum fuel consumption. It is well known that the Separation Theorem splits the LQG problem into the deterministic Linear Quadratic Regulator (LQR) problem and the stochastic Linear Quadratic Estimation (LQE) problem. The constant state feedback solution to the LQR problem and the fact that the rational transfer function matrix from the inputs to the states contains no zeros, may have had a misleading role in multivariable system theory, with result that very little attention was given to *multivariable zeros* during the 1960's.

In the 1970's multivariable zeros started to gain focus. Rosenbrock (1966; 1970) introduced the following definitions of zeros and poles in multivariable systems using the Smith-McMillan form: "The zeros of G are the roots of the non-zero numerator polynomials in the Smith-McMillan form of G" and "The poles of G are the roots of the denominator polynomials in the Smith-McMillan form of G". These definitions of zeros and poles in multivariable systems are commonly used and they are also adopted (among many others) by Kailath (1980) and more recently by Zhou, Doyle and Glover (1996). However, in this paper we will make use of the following definitions of zeros and poles.

DEFINITION (ZEROS, MacFarlane and Karcanias, 1976). *$z_i \in \mathbb{C}$ is a zero of $G(s)$ if the rank of $G(z_i)$ is less than the normal rank of $G(s)$.*

DEFINITION (POLES, Bode, 1945). *The poles $p_i \in \mathbb{C}$ of a rational transfer function matrix $G(s)$ are the points in the complex plane where one or more elements of $G(s)$ becomes infinite.*

We will return to these definitions later, but for now note that they generalizes Rosenbrock's definitions to also include non-rational systems, e.g. system with time-delays.

There are several other definitions of zeros in multivariable systems, the most important one is due to Desoer and Schulman (1974) which define the zeros from coprime polynomial matrix factorization of G.

A second step on the way towards the definition and computation of zeros and their directions, is to recognize that computing the zeros is numerically equivalent to solve the generalized eigenvalue problem on the form $z\hat{A}\hat{x} = \hat{B}\hat{x}$ where $\hat{A} = \begin{bmatrix} I_n & 0 \\ 0 & 0 \end{bmatrix}$ and $\hat{B} = \begin{bmatrix} A & -B \\ C & -D \end{bmatrix}$. This fact was first pointed out by Kaufman (1973) for Single Input Single Output (SISO) systems. Kaufman also present an algorithm to compute the zeros. This algorithm is extended to multivariable systems in (Patel, 1976). Today, a reliable numerical computational scheme for solving generalized eigenvalue problems exist in terms of the QZ-algorithm. MacFarlane and Karcanias (1976) point out that the zeros computed from generalized eigenvalue problem corresponds to the transmission zeros if the state-space realization is minimal. Having realized that the zeros can be computed from generalized eigenvalue problem, the directionality of the zero follows as the generalized eigenvectors and the implications of zeros in terms of the well known transmission blocking properties follows (see, MacFarlane and Karcanias, 1976). One could argue that the definitions and the computations of zeros and their directions in multivariable system has been established for some time now. However, the same is *not* true for the *pole directions*.

It is easy to recognize the "symmetric" definitions of zeros and poles of G, i.e. the zeros of G are the poles of G^{-1} and the poles of G are the zeros of G^{-1}. Indeed, there are some authors who define the pole directions in terms of the zero directions of G^{-1} (see, Zhou et al., 1996; Chen, 1993; Chen, 1995). In this paper we show how to compute the pole directions and pole *vectors* in terms of standard eigenvalue problems, thereby avoiding the inversion of G. Surprisingly, the computation of pole directions in terms of standard eigenvalue problems seems to be new, or at least it has not been clearly stated. More importantly, many of the previous results on controllability and observability can be restated in a natural way in terms of the pole vectors. Our conclusion is that these restatements also provides more insight to controllability and observability, and that the pole directions are tools which can successfully be applied to the task of control structure selection. These restatements are also equivalent with modal controllability and observability.

The intention with this paper is therefore to give an introduction to multivariable zeros and poles, with particular emphasize on the directionality and computations.

Finally, we make some remarks on the use of the terms *vector* and *direction* in this paper. We use the term *direction* in connection with zeros or poles we generally mean a *normalized* basis vector for the zero or pole spaces[1]. When we use the term *vector* in connection with zeros or poles we also mean basis vectors for the zeros or pole spaces, however, the vector is

---

[1]We shall see that the zero and pole directions can in certain special cases be of zero length.

not forced to be of unit length. In particular we find the pole vectors to be important tools in the task of input/output selection (see, Chapter 6), whereas the zero and pole directions play important roles when studying the effect of RHP zeros and poles on closed-loop performance (see Chapters 3 to 5). We therefore choose to distinguish between zero/pole directions and zero/pole vectors.

2.2 Basics from linear control theory

The most common way to describe a continuous linear time-invariant dynamical systems is the state-space description

$$\dot{x} = Ax + Bu \tag{2.1}$$

$$y = Cx + Du \tag{2.2}$$

In (2.1)–(2.2), u are the external inputs x are the states and y are the outputs. A, B, C and D are real matrices of dimensions $n \times n$, $n \times m$, $l \times n$ and $l \times m$ where n is the number of states, m is the number of inputs and l is the number of outputs. The time domain solution to (2.1)–(2.2) for a given initial state $x_0 = x(t_0)$ and a given trajectory of the external input $u(t)$ is

$$x(t) = e^{At}x_0 + \int_{t_0}^{t} e^{A(t-\tau)} Bu(\tau)d\tau \tag{2.3}$$

$$y(t) = Cx(t) + Du(t) \tag{2.4}$$

By inserting $x(t)$ from (2.3) into (2.4) we obtain

$$y(t) = Ce^{At}x_0 + \int_{t_0}^{t} Ce^{A(t-\tau)} Bu(\tau)d\tau + Du(t) \tag{2.5}$$

Applying the Laplace transform to (2.1)–(2.2) with initial state x_0 yields

$$(sI - A)x(s) = Bu(s) + x_0 \tag{2.6}$$

$$y(s) = Cx(s) + Du(s) \tag{2.7}$$

By inserting $x(s)$ from (2.6) into (2.7) we get the rational transfer function description of a LTI dynamical system

$$\begin{aligned} y(s) &= C(sI - A)^{-1}Bu(s) + Du(s) + C(sI - A)^{-1}x_0 \\ &= C(sI - A)^{-1}\{x_0 + Bu(s)\} + Du(s) \end{aligned} \tag{2.8}$$

With zero initial state we obtain

$$G(s) = C(sI - A)^{-1}B + D \tag{2.9}$$

where the rational transfer function matrix G (of size $l \times m$) given by (2.9) can be evaluated as a function of the complex variable s. The input/output behavior of the system system G in the frequency domain is then described by

$$y(s) = G(s)u(s) \tag{2.10}$$

The short-hand notations

$$G \overset{s}{=} \left[\begin{array}{c|c} A & B \\ \hline C & D \end{array}\right] \quad \text{and} \quad (A,\, B,\, C,\, D) \tag{2.11}$$

are frequently used to describe a linear state-space model of a continuos system G given by (2.1)–(2.2).

Given a system G with state-space realization $(A,\, B,\, C,\, D)$ where A can be diagonalized (A has n linearly eigenvectors). Then $G(s)$ can be written in the following partial fraction expansion

$$G(s) = \sum_{k=1}^{n} C v_k \frac{1}{s - p_k} w_k^H B + D \tag{2.12}$$

In (2.12) w_k and v_k are left and right eigenvectors corresponding to the pole p_k, where w_k and v_k are scaled such that $w_k^H v_k = 1$. There are several ways to prove this result, one way is given in (Douglas and Athans, 1995).

REMARK 1. $C v_k$ is a vector of dimension $l \times 1$, Douglas and Athans (1995) note that $C v_k$ indicates how much the k'th mode is observed in the outputs.

REMARK 2. $w_k^H B$ is a vector of dimension $1 \times m$, and Douglas and Athans (1995) note similarly that $w_k^H B$ indicates how much the k'th mode is exited by the inputs. One problem with this view on controllability and observability, is that we are free to scale w_k and v_k arbitrarily, so the length of the vector $w_k^H B$ can be made as large as one wants by multiplying w_k with a non-zero constant c. However, then the length of the vector $C v_k$ becomes correspondingly small, since $w_k^H v_k = 1$ is required.

The following result is stated in several books (see for example; Zhou et al., 1996), it concerns the dynamic response due to certain type of input signals.

LEMMA 2.1. *Let $G(s)$ be a strictly or semi-proper rational transfer function matrix of size $l \times m$, and let $(A,\, B,\, C,\, D)$ be a minimal state-space realization of G. Consider the dynamic response at the output of G due to the initial state $x(t_0) = x_0$ and the following input*

$$u(t) = \begin{cases} u_0 e^{s_0 t} & t \geq t_0, \\ 0 & t < t_0 \end{cases} \tag{2.13}$$

where $u_0 \in \mathbb{C}^m$ and $s_0 \in \mathbb{C} - \{\lambda_i(A)\}$. Then

$$y(t) = e^{At}\{x_0 - (s_0 I - A)^{-1} B u_0\} + G(s_0) u_0 e^{s_0 t} \tag{2.14}$$

and for the special initial state $x_0 = (s_0 I - A)^{-1} B u_0$, the only visible mode at the output $y(t)$ is s_0, resulting in

$$y(t) = G(s_0) u_0 e^{s_0 t} \tag{2.15}$$

2.3   Zeros and zero directions in multivariable systems

Zeros of a system may arise when competing internal effects are such that the output is zero even when the inputs (and the states) are not themselves identically zero. For Single Input Single Output (SISO) systems, the zeros are the solutions $s = z$ to $G(s) = 0$, and thus it could be argued that they are values of s at which $G(s)$ looses rank (from rank 1 to rank 0). From the Smith-McMillan form $G(s) = L(s)M(s)R(s)$ (see Kailath, 1980), the zero $s = z$ is a root in one of the numerator polynomials $\epsilon_i(s)$, then M (and thereby also G) looses rank due to the zero $s = z$. This decrease in rank for the complex number $s = z$ is the basis for the definition of zeros given by Desoer and Schulman (1974), who consider a left coprime polynomial matrix factorization of $G(s)$, $G(s) = D_l^{-1}(s)N_l(s)$ and defines the zeros as the complex numbers z where the rank of $N_l(z)$ is less than the normal rank of $N_l(s)$. This is similar to the definition of zeros used in this paper, given in the introduction and repeated here.

DEFINITION 2.1 (ZEROS, MacFarlane and Karcanias, 1976). *$z_i \in \mathbb{C}$ is a zero of $G(s)$ if the rank of $G(z_i)$ is less than the normal rank of $G(s)$. The zero polynomial is defined as $z(s) = \prod_{i=1}^{N_z}(s - z_i)$ where N_z is the number of finite zeros of $G(s)$.*

The normal rank of $G(s)$ is defined as the rank of $G(s)$ at all s except a finite number of singularities (which are the zeros). This definition of zeros is based on the transfer function matrix, corresponding to a minimal state-space realization. These zeros are sometimes called "transmission zeros" (see MacFarlane and Karcanias, 1976), but we shall simply call them "zeros".

If $G(s)$ has a zero for $s = z$, then there exist non-zero vectors labeled the input zero direction u_z and the output zero direction y_z, such that $u_z^H u_z = 1$, $y_z^H y_z = 1$ and

$$G(z)u_z = 0, \qquad G(s)u_z \neq 0 \quad \forall s \neq z \tag{2.16}$$

$$y_z^H G(z) = 0, \qquad y_z^H G(s) \neq 0 \quad \forall s \neq z \tag{2.17}$$

Kaufman (1973) was first to point out that zeros (of SISO systems) can be computed using the generalized eigenvalue problem. For a plant G with a given minimal state-space realization, the input and output zero directions can be supplemented with the state input and output zero vectors through the use of generalized eigenvalues. For a system G, the zeros z of the system, the input zero directions u_z and the state input zero vectors $\boldsymbol{x}_{zi}$ can all be computed from the generalized eigenvalue problem

$$\begin{bmatrix} A - zI & B \\ C & D \end{bmatrix} \begin{bmatrix} \boldsymbol{x}_{zi} \\ u_z \end{bmatrix} = \begin{bmatrix} 0 \\ 0 \end{bmatrix} \tag{2.18}$$

In this setup we normalize the length of u_z, i.e. $u_z^H u_z = 1$. This imply that the length of $\boldsymbol{x}_{zi}$ is different from one. Note that if z is not an eigenvalue of the A matrix then $(zI - A)^{-1}$ exists, and from the first equation in (2.18) we have that

$$\boldsymbol{x}_{zi} = (zI - A)^{-1}Bu_z \tag{2.19}$$

This is exactly the initial state at $t = t_0$ which makes the different modes of the system G to disappear in (2.14) so that the system response is (2.15). By inserting $\boldsymbol{x}_{zi}$ from (2.19) into the second equation in (2.18) we obtain

$$0 = C\boldsymbol{x}_{zi} + Du_z = \underbrace{\{C(zI - A)^{-1}B + D\}}_{G(z)}u_z \quad \Leftrightarrow \quad G(z)u_z = 0 \qquad (2.20)$$

Since u_z is in the right nullspace of $G(z)$, eq. (2.20), the response due to

$$u(t) = \begin{cases} u_z e^{zt} & t \geq t_0, \\ 0 & t < t_0 \end{cases}$$

and the initial state $x_0 = \boldsymbol{x}_{zi}$, is identically equal to zero for $t \geq 0$.

Similarly, one can compute the zeros z, the output zero direction y_z and the state output zero vectors $\boldsymbol{x}_{zo} \in \mathbb{C}^n$ through the generalized eigenvalue problem

$$\begin{bmatrix} \boldsymbol{x}_{zo}^H & y_z^H \end{bmatrix} \begin{bmatrix} A - zI & B \\ C & D \end{bmatrix} = \begin{bmatrix} 0 & 0 \end{bmatrix} \qquad (2.21)$$

Where again the length of y_z is normalized, so that $y_z^H y_z = 1$. By combining the two equations in (2.21), one can easily obtain

$$0 = \boldsymbol{x}_{zo}^H B + y_z^H D = y_z^H \underbrace{\{C(zI - A)^{-1}B + D\}}_{G(z)} \quad \Leftrightarrow \quad y_z^H G(z) = 0 \qquad (2.22)$$

and it follows that y_z is in the left nullspace of $G(z)$.

REMARK 1. By taking the transpose of (2.21) one obtains

$$\begin{bmatrix} A^T - zI & C^T \\ B^T & D^T \end{bmatrix} \begin{bmatrix} \bar{\boldsymbol{x}}_{zo} \\ \bar{y}_z \end{bmatrix} = \begin{bmatrix} 0 \\ 0 \end{bmatrix} \qquad (2.23)$$

From this we see that the input directions of the transposed system G^T is equal to the conjugate of the output directions of G. In MATLAB the generalized eigenvalue problem (2.21) can therefore be solved via the transposed problem.

REMARK 2. Let (A, B, C, D) be a minimal realization of $G(s)$, computing the zeros from the eigenvalue problems (2.18) and (2.21) yields the "transmission zeros" (MacFarlane and Karcanias, 1976).

When computing the input and output directions we have normalized u_z and y_z. Thus, the length of the input and output state vectors are generally different from one. Note, we use the term "vectors" to indicate that these state vectors are not normalized. Instead of normalizing the input and output directions, we could have normalized the state vectors to obtain the input and output zero vectors, $\boldsymbol{u}_z$ and $\boldsymbol{y}_z$, since any eigenvector multiplied by a non-zero constant is still an eigenvector.

A zero with numerical value z may appear more than once. We define the *multiplicity*[2] $(\mathcal{N}_z)$ of a zero z as the number of times the zero appears in a minimal state-space realization

---

[2]The multiplicity of a zero defined here is similar to the definition of *algebraic multiplicity* defined in (MacFarlane and Karcanias, 1976) and is equal to the number of zeros with numerical value z computed from the Smith-McMillan form.

of G. This implies that the gain of $G(z)$ can be zero in more than one direction at the input and the output. Let G (with minimal state-space realization) have normal rank r and let $G(z)$ have rank r_z, then we define the *geometric multiplicity*[3] of the zero z as the integer $\mathcal{G}_z \triangleq r - r_z$. We define the input and output zero spaces as the additional left and right nullspaces of $G(z)$ due to $s = z$. It follows that we need $\mathcal{G}_z$ linearly independent directions to describe the input and output zero spaces. A third important property connected to the zero z, with multiplicity $\mathcal{N}_z$, is the number of linearly independent eigenvectors (ℓ_z) in the eigenvalue problems (2.18) and (2.21). For a system G with minimal state-space realization we have $\ell_z \leq \mathcal{G}_z \leq \mathcal{N}_z$. Zeros where $\ell_z = \mathcal{N}_z$ are said to have a *simple structure*, while zeros where $\ell_z < \mathcal{N}_z$ are said to have a *non-simple* structure. Systems where all the zeros have a simple structure are said to have a *simple zero structure*. Systems where the zeros are distinct has a simple zero structure. From the eigenvalue computations (2.18) and (2.21) we compute ℓ_z linearly independent zero directions. In this paper we consider zeros with simple structure. For a further treatment of zeros with non-simple structure refer to MacFarlane and Karcanias (1976). The transmission blocking properties can be extended for systems with non-simple zero structure, see MacFarlane and Karcanias (1976). To do this, they expand the generalized eigenvalue problem into generalized Jordan chains in a similar manner as for the Jordan form. In Section 2.7.1, we use the Jordan form of the state-space matrix A in a similar manner to find all directions with infinite gains. However, the additional directions obtained using the Jordan form are not of such fundamental importance as the directions obtained from eigenvectors.

2.3.1   Zero directions from singular value decomposition of $G(z)$

The zero directions can also be calculated from the singular value decomposition of $G(z)$. Let G have normal rank r, then

$$G(z) = U_z \Sigma_z V_z^H = \sum_{i=1}^{r} u_i \sigma_i v_i^H = u_1 \sigma_1 v_1^H + u_2 \sigma_2 v_2^H + \cdots + u_r \sigma_r v_r^H$$

When the system has normal rank r and geometric multiplicity $\mathcal{G}_z$, the last $\min(l, m) - r + \mathcal{G}_z$ singular values are zero. The task is to sort out which of the last $m - r + \mathcal{G}_z$ columns in V_z and $l - r + \mathcal{G}_z$ columns in U_z that span the left and right nullspaces due to the zero $s = z$. If G is square and has full normal rank, then there are only $\mathcal{G}_z$ zero singular values, and the $\mathcal{G}_z$ zero directions follows easily.

2.4   Poles and pole directions in multivariable systems

Rosenbrock (1970), MacFarlane and Karcanias (1976), Callier and Desoer (1982) and Zhou et al. (1996) all define the poles as the roots of the denominator polynomials in the Smith-McMillan form. Bode (1945) states that *the poles are the singular points at which the transfer function fails to be analytic*. The partial fraction expansion (2.12), where the A matrix in the

---

[3]This definition of multiplicity is identical to the definition given by MacFarlane and Karcanias (1976).

state-space realization has n linearly independent eigenvectors, shows that G can be written as a sum of n first order rank one systems. For SISO systems, the terms Cv_k and $w_k^H B$ are scalars. When we consider the partial fraction expansion of $G(s)$ for the complex numbers p_k, we see that the singularities occurs in the denominator, and the function $G(s)$ is not analytic at $s = p_k$. The value of $G(s)$ as s approaches p_k becomes infinite. In this work we therefore replace "fails to be analytic" with "is infinite", which certainly implies that the transfer function is *not analytic*. Multivariable systems represented by rational transfer function matrices also fail to be analytic in the poles, in the sense that one or more elements becomes infinite for the complex values $s = p$.

DEFINITION 2.2 (POLES, Bode, 1945). *The poles $p_i \in \mathbb{C}$ of a rational transfer function matrix $G(s)$ are the points in the complex plane where one or more elements of $G(s)$ becomes infinite. The pole polynomial is defined as $\phi(s) \triangleq \prod_{i=1}^{N_p}(s - p_i)$ where N_p is the number of poles of $G(s)$.*

This definition of poles corresponds to the roots in the denominator polynomials in the Smith-McMillan form. For a rational transfer function matrix G with a minimal state-space realization (A, B, C, D) the poles are the eigenvalues of the A matrix, i.e. the roots in the characteristic equation $\phi(s) \triangleq \det(sI - A)$, for a proof refer to (Callier and Desoer, 1982, pages 75–78).

Since one or more elements becomes infinite for $s = p$ (or as s approaches p), it appears that the gain in certain linear combinations of the inputs and the outputs become infinite. This can also be seen from the partial fraction expansion (2.12) of $G(s)$ where the gain in the input direction $B^H w_k$ and the output direction Cv_k become infinite.

For a system on state-space form with a pole located at $s = p$, we define (compute) the input and output *pole vectors* as

$$\boldsymbol{u}_p = B^H x_{pi}; \qquad \boldsymbol{y}_p = C x_{po} \tag{2.24}$$

where $x_{pi}, x_{po} \in \mathbb{C}^n$ are *normalized* eigenvectors corresponding to the two eigenvalue problems

$$x_{pi}^H A = p x_{pi}^H \quad \text{and} \quad A x_{po} = p x_{po} \tag{2.25}$$

In the eigenvalue computations (2.25) the length of x_{pi} and x_{po} are normalized, we therefore use the terms input and output pole state directions for these vectors. This implies that the length of the input and output pole vectors are generally different from one, i.e. $\|\boldsymbol{u}_p\|_2 \neq 1$ and $\|\boldsymbol{y}_p\|_2 \neq 1$. Theorem 2.2 in Section 2.6 states that the mode p is uncontrollable if and only if $\boldsymbol{u}_p = 0$ and unobservable if and only if $\boldsymbol{y}_p = 0$. A minimal state-space realization will not contain uncontrollable and/or unobservable modes. The corresponding *pole directions* are obtained by normalizing the pole vectors (if one or more modes are uncontrollable we set the corresponding input pole directions equal to zero, and if one or more modes are unobservable we set the corresponding output pole directions to zero):

$$u_p = \begin{cases} \boldsymbol{u}_p / \|\boldsymbol{u}_p\|_2 & \text{if } \|\boldsymbol{u}_p\|_2 \neq 0 \\ 0 & \text{if } \|\boldsymbol{u}_p\|_2 = 0 \end{cases} \tag{2.26}$$

$$y_p = \begin{cases} \boldsymbol{y}_p / \left\| \boldsymbol{y}_p \right\|_2 & \text{if } \left\| \boldsymbol{y}_p \right\|_2 \neq 0 \\ 0 & \text{if } \left\| \boldsymbol{y}_p \right\|_2 = 0 \end{cases} \tag{2.27}$$

A pole p may appear more than once. We define the multiplicity $(\mathcal{N}_p)$ of the pole p as the number of times the pole p appears in the minimal state-space realization of G. When the multiplicity of the pole p is larger than one, more than one direction at the input and the output may get infinite gain. For a system G with a minimal state space realization, we define the input and output pole spaces as the spaces in $\mathbb{C}^m$ and $\mathbb{C}^l$ which gets infinite gain for $s = p$. We define the *geometric multiplicity* $(\mathcal{G}_p)$ of the pole p as the number of linearly independent vectors in $\mathbb{C}^m$ and $\mathbb{C}^l$ required to describe the input and output pole spaces. A third parameter connected to the pole p is the number of linearly independent eigenvectors (ℓ_p) in the state-space matrix A corresponding to the pole p. It follows that $\ell_p \leq \mathcal{G}_p \leq \mathcal{N}_p$. If $\ell_p = \mathcal{N}_p$ then the pole is said to have a *simple structure*, while poles where $\ell_p < \mathcal{N}_p$ are said to have a *non-simple* structure. Systems where all the poles have a simple structure are said to have a *simple pole structure*. Systems where all the poles are distinct has a simple pole structure. It follows that we compute ℓ_p linearly independent directions with infinite gain using (2.26) and (2.27). In Section 2.7 we treat the case where the state-space matrix A is defective (the state-space matrix A does not contain n linearly independent eigenvectors) and we show how to compute the remaining $\mathcal{G}_p - \ell_p$ directions with infinite gain.

2.4.1 Partial fraction expansion of $G(s)$ in terms of the pole vectors

System with simple pole structure (systems where the state-space matrix A has n linearly independent eigenvectors) can be expressed as a sum of n rank one systems in terms of the input and output pole vectors and the corresponding state directions

$$G(s) = \sum_{k=1}^{n} C x_{po,k} \frac{\left(x_{pi,k}^H x_{po,k} \right)^{-1}}{s - p_k} x_{pi,k}^H B + D = \sum_{k=1}^{n} \boldsymbol{y}_{p_k} \frac{\left(x_{pi,k}^H x_{po,k} \right)^{-1}}{s - p_k} \boldsymbol{u}_{p_k}^H + D \tag{2.28}$$

where $x_{pi,k}$ and $x_{po,k}$ are the *normalized* (i.e. $\left\| x_{pi,k} \right\|_2 = 1$ and $\left\| x_{po,k} \right\|_2 = 1$) left and the right eigenvectors, $\boldsymbol{y}_{p_k}$ is the output pole vector and $\boldsymbol{u}_{p_k}$ is the input pole vector corresponding to the mode p_k.

Proof of (2.28). Both v_k in (2.12) and $x_{po,k}$ are right eigenvectors of the A matrix corresponding to the eigenvalue p_k. Similarly, w_k in (2.12) and $x_{pi,k}$ are left eigenvectors of the A matrix corresponding to the eigenvalue p_k. Assume that v_k is normalized, i.e. $v_k = x_{po,k}$, then the length of w_k is generally not equal to one and we have that $w_k = c x_{pi,k}$ for some constant $c \in \mathbb{C}$. Since $w_k^H v_k = 1$ is required in (2.12) and the eigenvectors $x_{pi,k}$ and $x_{po,k}$ are normalized, we get the additional factor $c = (x_{pi,k}^H x_{po,k})^{-1}$ in (2.28) compared to (2.12). $\qquad\square$

2.4.2 Relation between the pole-directions of G and G^T

The state input and output pole directions x_{pi} and x_{po} of G corresponding to the pole p are given by

$$x_{pi}^H (A - pI) = 0 \quad \text{and} \quad (A - pI) x_{po} = 0$$

Similarly, for the transposed system

$$G^T \overset{s}{=} \left[\begin{array}{c|c} A^T & C^T \\ \hline B^T & D^T \end{array} \right]$$

the state input and output pole directions x'_{pi} and x'_{po} corresponding to the pole p are given by

$$x'^{H}_{pi}(A^T - pI) = 0 \quad \text{and} \quad (A^T - pI)x'_{po} = 0$$

which implies

$$(A - pI)\bar{x}'_{pi} = 0 \quad \text{and} \quad x'^{T}_{po}(A - pI) = 0$$

The relations between pole directions $(u_p, y_p, x_{pi}, x_{po})$, for G and the pole directions $(u'_p, y'_p, x'_{ip}, x'_{op})$ for G^T become:

$$\begin{align} x_{pi} = \bar{x}'_{po} \quad &\Leftrightarrow \quad \boldsymbol{x}_{pi} = \bar{\boldsymbol{x}}'_{po} \tag{2.29}\\ x_{po} = \bar{x}'_{pi} \quad &\Leftrightarrow \quad \boldsymbol{x}_{po} = \bar{\boldsymbol{x}}'_{i} \tag{2.30}\\ \boldsymbol{u}_p = B^H x_{pi} = \bar{B}^T \bar{x}'_{po} = \bar{\boldsymbol{y}}'_p \quad &\Leftrightarrow \quad u_p = \bar{y}'_p \tag{2.31}\\ \boldsymbol{y}_p = C x_{po} = (\bar{C}^T)^H \bar{x}'_{pi} = \bar{\boldsymbol{u}}'_p \quad &\Leftrightarrow \quad y_p = \bar{u}'_p \tag{2.32} \end{align}$$

2.4.3 Pole directions from singular value decomposition of $G(p)$

Let $G(s)$ have normal rank r. From the singular value decomposition of $G(p)$ we have

$$G(p) = U_p \Sigma_p V_p^H = \sum_{i=1}^{r} u_i \sigma_i v_i^H = u_1 \sigma_1 v_1^H + u_2 \sigma_2 v_2^H + \cdots + u_r \sigma_r v_r^H$$

The directions with largest gain are associated with σ_1, the input direction u_p is v_1 and the output direction y_p is u_1. However, since $G(p)u_p = \infty$ and $y_p^H G(p) = \infty$ we can not evaluate $G(p)$. Instead, we can consider $G(p + \epsilon)$ when $\epsilon \to 0$, but this is more difficult numerically.

For a square system, G, with minimal state-space realization (A, B, C, D) where D is nonsingular, the inverse is given by (Zhou et al., 1996, p. 67)

$$G^{-1} \overset{s}{=} \left[\begin{array}{c|c} A - BD^{-1}C & -BD^{-1} \\ \hline D^{-1}C & D^{-1} \end{array} \right] \tag{2.33}$$

The output pole direction is then given by $G^{-1}(p)y_p = 0$, similarly the input pole direction is given by $u_p^H G^{-1}(p) = 0$. The pole directions can therefore be found as the the zero directions of $G^{-1}(p)$, $G^{-1}(p) = U\Sigma V^H$, with y_p as the zero direction in V and u_p as the zero direction in U. However, to calculate the pole directions from SVD of $G(p)$ or $G^{-1}(p)$ has rather poor numerical properties. So, the computation of pole directions from SVD is not recommended.

2.4.4 Relations between zero and pole directions for G and G^{-1}

To find a relationship between pole directions for G (output pole direction y_p and output state vector $\boldsymbol{x}_{po}$) and zero directions for G^{-1} (input zero direction u_z and input zero state vector $\boldsymbol{x}_{zi}$), assume that G is square with a non-singular D matrix. The input zero directions of G^{-1} are given through the use of (2.33).

$$\begin{bmatrix} A - BD^{-1}C - pI & -BD^{-1} \\ D^{-1}C & D^{-1} \end{bmatrix} \begin{bmatrix} \boldsymbol{x}_{zi} \\ u_z \end{bmatrix} = \begin{bmatrix} 0 \\ 0 \end{bmatrix} \tag{2.34}$$

From (2.34) we have

$$(A - pI)\boldsymbol{x}_{zi} - BD^{-1}(C\boldsymbol{x}_{zi} + u_z) = 0 \tag{2.35}$$

$$D^{-1}(C\boldsymbol{x}_{zi} + u_z) = 0 \tag{2.36}$$

Clearly,

$$\boldsymbol{x}_{zi} = -x_{po}/\|Cx_{po}\|_2 = -\boldsymbol{x}_{po} \qquad \text{and} \qquad u_z = y_p \tag{2.37}$$

is a solution to (2.34).

Next, assume that G^{-1} exists with D square and non-singular. It is the easy to prove that the zeros of G can be computed from the poles of G^{-1}. For the zeros z we have (2.18)

$$\begin{bmatrix} A - zI & B \\ C & D \end{bmatrix} \begin{bmatrix} \boldsymbol{x}_{zi} \\ u_z \end{bmatrix} = \begin{bmatrix} 0 \\ 0 \end{bmatrix}$$

From the bottom equation we obtain

$$u_z = -D^{-1}C\boldsymbol{x}_{zi} \tag{2.38}$$

Inserting (2.38) in the upper equation in (2.18) gives

$$(A - BD^{-1}C - zI)\boldsymbol{x}_{zi} = 0 \tag{2.39}$$

The matrix $A - BD^{-1}C$ is the state-matrix in G^{-1} given in (2.33). So, the zeros of G can be computed from the eigenvalue problem (2.39) when D is non-singular.

2.5 Uniqueness of input/output zero and pole directions

It follows that zero and pole directions generally are non-unique, i.e. any zero/pole direction multiplied by a complex number with magnitude one and any phase is also a zero/pole direction. However, the directionality of the input and output pole directions are independent of the state-space realization, see Remark 3 on page 28. The same applies for input and output zero directions, since they can be calculated as the pole directions of G^{-1}.

If the dimensions of the zero/pole spaces are greater than one, i.e. the geometric multiplicity is greater than one, any normalized linear combination of a set of input and output directions corresponding to a zero/pole are zero/pole directions. However, we note that the order of the zero/pole is generally different in the different directions.

The input/output zero and pole directions are dependent on the input/output scaling, which is reasonable. In general, we prefer to scale the inputs so that maximum allowed change for each input stays between ± 1 and the outputs so that the maximum allowed control error corresponds to ± 1. However, some special applications may require different scalings to be applied.

2.6 Controllability and observability from pole directions

The criteria for state controllability and observability discussed in this section were introduced independently by several people, among them: Popov (1973), Belevitch (1968), Hautus (1969), Rosenbrock (1970). The tests were first given by Gilbert (1963) for the special case when the state-space matrix A is diagonalizable. Due to the generalization provided by Popov and Belevitch and the fact that Hautus was the first to note their wide applicability, it is common to refer to these tests for state controllability and observability as Popov-Belevitch-Hautus (PBH) tests (Kailath, 1980).

THEOREM 2.1 (PBH EIGENVECTOR TESTS). *Given a* LTI-*system G with state-space realization* (A, B, C, D), *then the following is true:*

1) The pair (A, B) *is controllable if and only if for all poles* p

$$B^H x_{pi} = 0 \quad \Rightarrow \quad x_{pi} = 0 \quad where \quad x_{pi}^H A = p x_{pi}^H \tag{2.40}$$

2) The pair (C, A) *is observable if and only if for all poles* p

$$C x_{po} = 0 \quad \Rightarrow \quad x_{po} = 0 \quad where \quad A x_{po} = p x_{po}, \tag{2.41}$$

REMARK 1. Condition (2.40) says that the pair (A, B) is controllable if and only if no left eigenvector of the A matrix is completely in the left nullspace of the B matrix. That is, no left eigenvector of the A matrix is orthogonal to all the columns of the B matrix.

REMARK 2. Condition (2.41) says that the pair (C, A) is observable if and only if no right eigenvector of the A matrix is completely in the right nullspace of the C matrix. That is, no right eigenvector of the A matrix is orthogonal to all the rows of the C matrix.

REMARK 3. If the condition (2.40) is not fulfilled for some mode p, then it is common to say that the mode p is not controllable (uncontrollable), and if the condition (2.41) is not fulfilled for some mode p, then it is common to say that the mode p is not observable (unobservable). For a definition of modal controllability and observability refer to (Zhou et al., 1996).

Next, we will state PBH eigenvector tests in terms of pole directions. This application of the pole directions turns out to be useful.

THEOREM 2.2 (PBH EIGENVECTOR TESTS IN TERMS OF POLE DIRECTIONS). *Given a* LTI-*system G with state-space realization* (A, B, C, D), *then the following is true:*

1) The pair (A, B) *is controllable if and only if all input pole vectors (directions) are different from zero, i.e.*

$$\boldsymbol{u}_p \neq 0 \quad (u_p \neq 0), \quad \forall p \tag{2.42}$$

2) The pair $(C,\, A)$ is observable if and only if all output pole vectors (directions) are different from zero, i.e.

$$\boldsymbol{y}_p \neq 0 \quad (y_p \neq 0), \quad \forall p \tag{2.43}$$

Proof of Theorem 2.2. The statement (A $\Rightarrow$ B) is equivalent to (not B $\Rightarrow$ not A), so the first part of Theorem 2.1 can be restated as: "The pair $(A,\, B)$ is controllable if and only if for all p

$$x_{pi} \neq 0 \quad \Rightarrow \quad B^H x_{pi} \neq 0 \quad \text{where} \quad x_{pi}^H A = p x_{pi}^H.\text{"}$$

When we introduce the pole vector $\boldsymbol{u}_p = B^H x_{pi}$ we implicitly assume that $x_{pi} \neq 0$ and that it satisfies $x_{pi}^H A = p x_{pi}^H$, so these assumptions do not need to be stated. The first part of Theorem 2.2 then follows. The second part is derived in an analogous manner. □

From Theorem 2.2, the mode p is uncontrollable if and only if $\boldsymbol{u}_p = 0$ and unobservable if and only if $\boldsymbol{y}_p = 0$. Theorem 2.2 is just a restatement of PBH eigenvector tests. However, it is much easier to understand and remember since the eigenvalue problems are hidden. So, our conclusion is that it is a useful restatement.

The pole vectors contain a lot of information about the structure. Consider selecting the transfer function element G_{ij} corresponding to output i and and input j. We can do this in terms of multiplying G with e_i^T on the left and e_j on the right, where

e_i is a vector of length l with zeros in all positions except position i which contains 1.

e_j is a vector of length m with zeros in all positions except position j which contains 1.

We obtain

$$G_{ij}(s) = e_i^T G(s) e_j \stackrel{s}{=} \left[\begin{array}{c|c} A & B e_j \\ \hline e_i^T C & e_i^T D e_j \end{array} \right] \tag{2.44}$$

The input $(\tilde{\boldsymbol{u}}_p)$ and the output $(\tilde{\boldsymbol{y}}_p)$ pole vectors of G_{ij} corresponding to the pole p become

$$\tilde{\boldsymbol{u}}_p = (B e_j)^H x_{pi} = e_j^T B^H x_{pi} = e_j^T \boldsymbol{u}_p = \boldsymbol{u}_{p,j} \tag{2.45}$$

$$\tilde{\boldsymbol{y}}_p = e_i^T C x_{po} = e_i^T \boldsymbol{y}_p = \boldsymbol{y}_{p,i} \tag{2.46}$$

where $\boldsymbol{u}_{p,j}$ denotes the j'th element of input pole vector $\boldsymbol{u}_p$ and $\boldsymbol{y}_{p,i}$ denotes the i'th element of output pole vector $\boldsymbol{y}_p$ of G corresponding to the mode p. By using Theorem 2.2 we may conclude:

COROLLARY 2.1. *For a plant G with pole p, input pole vector $\boldsymbol{u}_p$ (input pole direction u_p) and output pole vector $\boldsymbol{y}_p$ (output pole direction y_p), the following is true:*

1) The mode p is uncontrollable in input j if and only if the j'th element of $\boldsymbol{u}_p$ (u_p) is zero

$$\boldsymbol{u}_{p,j} = 0 \quad (u_{p,j} = 0)$$

2) The mode p is unobservable in output i if and only if the i'th element of $\boldsymbol{y}_p$ (y_p) is zero

$$\boldsymbol{y}_{p,i} = 0 \quad (y_{p,i} = 0)$$

Proof of Corollary 2.1. Replace the B matrix with $B e_j$ and C with $e_i^T C$ and apply Theorem 2.2. □

2.6.1   Decoupling zeros and uncontrollable/unobservable modes

There is a link between poles and a class of zeros defined by Rosenbrock (1970; 1973; 1974). Rosenbrock (1970) defines[4] input and output decoupling zeros as follows

$$\text{Input decoupling zeros } z_i: \qquad \text{rk} \begin{bmatrix} z_iI - A & B \end{bmatrix} < n$$

$$\text{Output decoupling zeros } z_o: \qquad \text{rk} \begin{bmatrix} z_oI - A \\ -C \end{bmatrix} < n$$

The input decoupling zeros concern the situation where some free modal motion of the system state is uncoupled from the input. Similarly, the output decoupling zeros concern the situation where some free modal motion of the system state is uncoupled from the outputs. It follows that the only potential candidate values for input or output decoupling zeros are the eigenvalues of the state-space matrix A, since these are the points where $sI - A$ becomes singular. In addition for input decoupling zeros the left nullspace $z_iI - A$ must overlap with the left nullspace of B. For output decoupling zeros it follows similarly that z_o must be an eigenvalue of the A matrix and the nullspace of $z_oI - A$ must overlap with the nullspace of C. Note that these conditions are exactly the conditions under which the mode p (equal to z_i or z_o) is uncontrollable or unobservable. The similarities become even more obvious in the PBH rank tests (Kailath, 1980).

THEOREM 2.3 (PBH RANK TESTS). *Given a* LTI-*system G with state-space realization* $(A,\ B,\ C,\ D)$*, then the following is true:*

1) The pair $(A,\ B)$ *is controllable if and only if*

$$\text{rk} \begin{bmatrix} sI - A & B \end{bmatrix} = n \quad \forall s \tag{2.47}$$

2) The pair $(C,\ A)$ *is observable if and only if*

$$\text{rk} \begin{bmatrix} sI - A \\ -C \end{bmatrix} = n \quad \forall s \tag{2.48}$$

REMARK 1. Condition 1) and (2.47) says that $(A,\ B)$ is controllable if and only if there are no input decoupling zeros.

REMARK 2. Condition 2) and (2.48) says that $(C,\ A)$ is observable if and only if there are no output decoupling zeros.

The conclusions are:

- *Input decoupling zeros are uncontrollable poles.*
- *Output decoupling zeros are unobservable poles.*

---

[4]Obtained by setting $T(s) = sI - A, U(s) = B, V(s) = -C$ and $W(s) = D$ in Rosenbrock's system matrix.

2.7 Repeated poles

2.7.1 All directions with infinite gains

In Section 2.4 we defined the pole directions from the left and right eigenvectors, and showed that the gains in these directions become infinite for $s = p$. For systems with simple pole structure these directions are sufficient to describe the input and output pole spaces. The pole spaces have dimension $\mathcal{G}_p \leq \mathcal{N}_p$ and in the general case we only have $\ell_p \leq \mathcal{G}_p$ pole directions. This suggests that more than ℓ_p directions with infinite gains exist. The question is then:

- Where do the additional $\mathcal{G}_p - \ell_p$ directions come from, and which role do they play?

It turns out that when a system G has poles p with multiplicity $\mathcal{N}_p$, geometric multiplicity $\mathcal{G}_p$ and $\ell_p < \mathcal{G}_p$ linearly independent eigenvectors, then the state-space matrix A is defective and can not be diagonalized. We are able to compute the additional $\mathcal{G}_p - \ell_p$ directions with infinite gains by using the Jordan form. The additional "pseudo" state vectors obtained from the Jordan form are linearly independent of the eigenvectors. Before using the Jordan form to compute all directions with infinite gains, some warning remarks are appropriate:

- The notation becomes messy, mainly because we need to combine two Jordan forms, the left and the right Jordan form.
- As we have seen, many useful interpretations can be made in terms of the pole vectors and directions. However, the same is not true for the generalized vectors obtained from the Jordan form, so one may conclude that these directions are not of fundamental importance as is the case with the pole directions.

The most useful result obtained by considering all directions with infinite gains is that we can prove that the input and output pole directions corresponds to the directions with maximum order[5] of the pole.

Section B.2 in Appendix B defines and shows how the left and the right Jordan forms can be combined into

$$M_L^H A M_R S^{-H} = S^{-H} M_L^H A M_R = J \tag{2.49}$$

where M_R and M_L are the non-singular similarity transformations which gives

$$M_R^{-1} A M_R = J, \qquad M_L^H A M_L^{-H} = J$$

and the columns in M_R and M_L which are eigenvectors are scaled such that their norms are equal to one. Furthermore, S has the structure given in (B.15) and

$$M_L = M_R^{-H} S$$

Note, both the left and the right Jordan form has the ones in the J matrix above the diagonal as defined in Section B.2, Appendix B. This is the normal definition of the right Jordan form. For the left Jordan form one could argue that the ones should be below the main diagonal

---

[5]The order of a pole in the input and output directions u and y is defined as the order of the pole in the scalar function $y^H G(s) u$.

in J. However, then it is not possible to combine the left and the right Jordan form into the equation (2.49). Defining the left Jordan form with the ones above the main diagonal in J implies that the ordering of the vectors in the matrix M_L corresponding to Jordan block J_ℓ is opposite of the normal ordering. This means that the last vector in $M_{L,\ell}$ (where $M_{L,\ell}$ contains the vectors corresponding to Jordan block J_ℓ as columns) is the eigenvector and the other vectors are the generalized vectors. For further details see Section B.2 in Appendix B.

LEMMA 2.2 (POLE DIRECTIONS AND DIRECTIONS WITH INFINITE GAINS). *Let $G(s)$ be a rational transfer function matrix, with minimal state-space realization (A, B, C, D). Let p be a pole of $G(s)$ with multiplicity $\mathcal{N}_p$ and geometric multiplicity $\mathcal{G}_p$. Then there exist $\mathcal{N}_p$ input and output directions, $u_{\infty,j}$ and $y_{\infty,j}$, which approaches infinity as s approaches p. These directions are given by*

$$u_{\infty,j} = B^H m_{L,j} / \|B^H m_{L,j}\|_2 \, ; \qquad y_{\infty,j} = C m_{R,j} / \|C m_{R,j}\|_2 \qquad (2.50)$$

where $m_{L,j}$ and $m_{R,j}$ corresponds to the columns in M_L and M_R associated with the pole p. $\mathcal{G}_p$ of these directions are linearly independent and the ℓ_p directions corresponding to the eigenvectors are the pole directions.

REMARK 1. If A has n linearly independent eigenvectors, each Jordan block is of size 1×1, $M_L = X_L$, $M_R = X_R$, $J = \Lambda$, the matrix A is diagonalizable and all directions are pole directions.
REMARK 2. If A has distinct eigenvalues, then A has n linearly independent eigenvectors and A can be diagonalized.
REMARK 3. The *directionality* of the pole vectors, pole directions and the vectors with infinite gains are *independent* of the state-space realization. To prove this define a new state vector with the non-singular similarity transformation T

$$z = Tx$$

The new state-space realization becomes

$$\dot{z} = \underbrace{TAT^{-1}}_{A'} z + \underbrace{TB}_{B'} u; \quad y = \underbrace{CT^{-1}}_{C'} z + Du$$

From the the construction of the Jordan form we have $M_R^{-1} A M_R = J$. Inserting $A = T^{-1} A' T$ gives

$$M_R^{-1} T^{-1} A' \underbrace{T M_R}_{M_R'} = J$$

and we have $M_L' = M_R'^{-H} = T^{-H} M_R^{-H} = T^{-H} M_L$ or

$$m_{R,i}' = T m_{R,i}; \quad m_{L,i}' = T^{-H} m_{L,i}$$

The new output vector with infinite gain becomes

$$y_\infty' = C' m_{R,i}' = CT^{-1} T m_{R,i} = C m_{R,i} = y_\infty$$

and the new input vector with infinite gain becomes

$$u_\infty' = B'^H m_{L,i}' = B^H T^H T^{-H} m_{L,i} = B^H m_{L,i} = u_\infty$$

REMARK 4. The *length* of the pole vectors and the vectors with infinite gains *depend* on the state-space realization. This follows since multiplying the C matrix with a non-zero constant k and multiplying the B matrix with $1/k$ yields the same rational transfer function, but the input and output vectors with infinite gains of the modified system G' with state-space realization $(A, \frac{1}{k}B, kC, D)$ become

$$\boldsymbol{u}'_\infty = \frac{1}{k}B^H m_{L,i} = \frac{1}{k}\boldsymbol{u}_\infty, \quad \text{and} \quad \boldsymbol{y}'_\infty = kC m_{R,i} = k\boldsymbol{y}_\infty$$

EXAMPLE 2.1 SYSTEMS IN SERIES AND PARALLEL. This example illustrate the difference in structure involved when system has a repeated pole p with two linearly independent eigenvectors, and only one eigenvector. We consider the following two structures:

Systems in parallel.   Systems in series.
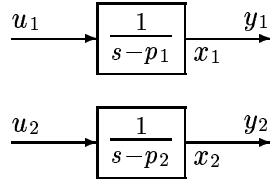
$$G(s) = \begin{bmatrix} \frac{1}{s-p_1} & 0 \\ 0 & \frac{1}{s-p_2} \end{bmatrix} \qquad\qquad G(s) = \begin{bmatrix} \frac{1}{s-p_1} & \frac{1}{(s-p_1)(s-p_2)} \\ 0 & \frac{1}{s-p_2} \end{bmatrix}$$

$$G(s) \overset{s}{=} \left[\begin{array}{cc|cc} p_1 & 0 & 1 & 0 \\ 0 & p_2 & 0 & 1 \\ \hline 1 & 0 & 0 & 0 \\ 0 & 1 & 0 & 0 \end{array}\right] \qquad\qquad G(s) \overset{s}{=} \left[\begin{array}{cc|cc} p_1 & 1 & 1 & 0 \\ 0 & p_2 & 0 & 1 \\ \hline 1 & 0 & 0 & 0 \\ 0 & 1 & 0 & 0 \end{array}\right]$$

When $p_1 = 1$ and $p_2 = 2$ we get pole directions:

$$U_p = \begin{bmatrix} 1 & 0 \\ 0 & 1 \end{bmatrix}, \quad Y_p = \begin{bmatrix} 1 & 0 \\ 0 & 1 \end{bmatrix} \qquad U_p = \begin{bmatrix} \frac{\sqrt{2}}{2} & 0 \\ -\frac{\sqrt{2}}{2} & 1 \end{bmatrix}, \quad Y_p = \begin{bmatrix} 1 & \frac{\sqrt{2}}{2} \\ 0 & \frac{\sqrt{2}}{2} \end{bmatrix}$$

When $p_1 = 1$ and $p_2 = 1.1$ we get pole directions:

$$U_p = \begin{bmatrix} 1 & 0 \\ 0 & 1 \end{bmatrix}, \quad Y_p = \begin{bmatrix} 1 & 0 \\ 0 & 1 \end{bmatrix} \qquad U_p = \begin{bmatrix} 0.0995 & 0 \\ -0.995 & 1 \end{bmatrix}, \quad Y_p = \begin{bmatrix} 1 & 0.995 \\ 0 & 0.0995 \end{bmatrix}$$

When $p_1 = p = 1$ and $p_2 = p = 1$ we get pole directions:

$$U_p = \begin{bmatrix} 1 & 0 \\ 0 & 1 \end{bmatrix}, \quad Y_p = \begin{bmatrix} 1 & 0 \\ 0 & 1 \end{bmatrix} \qquad U_p = \begin{bmatrix} 0 & 0 \\ -1 & 1 \end{bmatrix}, \quad Y_p = \begin{bmatrix} 1 & 1 \\ 0 & 0 \end{bmatrix}$$

For the systems in parallel, the A matrix in the state-space description has two linearly independent eigenvectors for all values of p_1 and p_2. So, for the case when $p_1 = p_2 = p$ the geometric multiplicity of the pole p for the system in parallel is two.

For the systems in series, the A matrix has two linearly independent eigenvectors whenever $p_1 \neq p_2$. For the special case $p_1 = p_2 = p$ the A matrix only has one linearly independent eigenvector. In this case G is

$$G(s) = \begin{bmatrix} \frac{1}{s-p} & \frac{1}{(s-p)^2} \\ 0 & \frac{1}{s-p} \end{bmatrix}$$

It is interesting to see how element $g_{12}(s)$ in $G(s)$ dominates over the diagonal elements when $p_1 = p_2 = p$ and $|s - p| < 1$ for the systems in series. The reason is of course that element g_{12} has a pole of order two and therefore approaches infinity much faster than the diagonal elements as s approaches p. The main point here is that this is reflected in the eigenvalue computation and therefore also in the pole directions. It is also interesting to note that element g_{12} represents the only possible pairing which can stabilize the plant $G(s)$ with one SISO control loop, and that the pole directions identify this control loop in this case. However, the pole directions fail to identify all directions with infinite gain (they only identify the linear combination of inputs and outputs where the pole appears in the order two). To get all directions with infinite gains for $s = p$ we need to use the Jordan form. We then get the directions

$$U_\infty = \begin{bmatrix} 1 & 0 \\ 0 & 1 \end{bmatrix} \quad \text{and} \quad Y_\infty = \begin{bmatrix} 1 & 0 \\ 0 & 1 \end{bmatrix}$$

2.7.2   Controllability and observability of repeated poles

The following result follows easily from the PBH rank test.

COROLLARY 2.2 (CONTROLLABILITY AND OBSERVABILITY OF REPEATED MODES). *Given a* LTI-*system G with state-space realization (A, B, C, D), a repeated pole p, multiplicity $\mathcal{N}_p$ and ℓ_p linearly independent eigenvectors. Then the following is true:*

  1) *The pole p is controllable if and only if*

$$\text{rk} \begin{bmatrix} pI - A & B \end{bmatrix} = n$$

  2) *The pole p is controllable only if B contains ℓ_p or more linearly independent columns.*
  3) *If B has less than ℓ_p linearly independent columns then the pole p and the pair (A, B) is uncontrollable.*
  4) *The pole p is observable if and only if*

$$\text{rk} \begin{bmatrix} pI - A \\ -C \end{bmatrix} = n$$

  5) *The pole p is observable only if C contains ℓ_p or more linearly independent rows.*
  6) *If C has less than ℓ_p linearly independent rows then the pole p and the pair (C, A) is unobservable.*

Proof. The proof is given in Section A.

Some useful insights on controllability and observability of repeated poles can be obtained by looking at pole/zero cancellations when reducing the size of G.

PROBLEM 2.1 POLE/ZERO CANCELLATIONS WHEN REDUCING SIZE TO LESS THAN ℓ_p. *Consider the plant G of size $l \times m$ with state-space realization (A, B, C, D), a repeated pole p, multiplicity $\mathcal{N}_p$ and $\ell_p > 1$ linearly independent eigenvectors. We want to predict when pole/zero cancellations occur so that when a pole which appears in a minimal realization of G does not appear in a minimal realization of a selected subsystem $G_{\gamma,\beta}$ of G, where the integer multiples β and γ describes the inputs and the outputs of G which are preserved in $G_{\gamma,\beta}$.*

To illustrate the use of the integer multiples γ and β let us consider the 2×2 subsystem of G, consisting of the inputs 1 and 3 and the outputs 2 and 4. We get $\beta = (1,3)$ and $\gamma = (2,4)$.

We need to introduce some more notation:

- Let n_γ and n_β denote the number of elements in the integer multiples γ and β.
- Define the matrix N_β of size $m \times n_\beta$ where column i in N_β corresponds to element i in β, and is equal to the unit vector e_j of size l, with zeros in all positions except for position j which contains 1 and where j is the value of the i'th element in γ.
- Define the matrix N_γ of size $l \times n_\gamma$, where column i in N_γ corresponds to element i in γ, and is equal to the unit vector e_j of size l, with zeros in all positions except for position j which contains 1 and where j is the value of the i'th element in γ.

With the use of N_γ and N_β we get

$$G_{\gamma,\beta}(s) \triangleq N_\gamma^T G N_\beta \stackrel{s}{=} \left[\begin{array}{c|c} A & B_\beta \\ \hline C_\gamma & D_{\gamma,\beta} \end{array} \right] \qquad (2.51)$$

where $B_\beta = BN_\beta$, $C_\gamma = N_\gamma^T C$ and $D_{\gamma,\beta} = N_\gamma^T D N_\beta$.

To illustrate the use of N_β, N_γ and (2.51) let $\gamma = (2,4)$, $\beta = (1,3)$ and let the size of G be 4×3 then

$$N_\beta = \begin{bmatrix} 1 & 0 \\ 0 & 0 \\ 0 & 1 \end{bmatrix}, \quad N_\gamma = \begin{bmatrix} 0 & 0 \\ 1 & 0 \\ 0 & 0 \\ 0 & 1 \end{bmatrix}$$

and

$$G_{\gamma,\beta}(s) = \begin{bmatrix} 0 & 1 & 0 & 0 \\ 0 & 0 & 0 & 1 \end{bmatrix} \begin{bmatrix} g_{11} & g_{12} & g_{13} \\ g_{21} & g_{22} & g_{23} \\ g_{31} & g_{32} & g_{33} \\ g_{41} & g_{42} & g_{43} \end{bmatrix} \begin{bmatrix} 1 & 0 \\ 0 & 0 \\ 0 & 1 \end{bmatrix} = \begin{bmatrix} g_{21} & g_{23} \\ g_{41} & g_{43} \end{bmatrix}$$

With the notation introduced we have the following result.

LEMMA 2.3 (POLE/ZERO CANCELLATIONS WHEN REDUCING SIZE TO LESS THAN ℓ_p). *Let the system G of size $l \times m$ with minimal state-space realization (A, B, C, D), have a pole p with multiplicity $\mathcal{N}_p$ and ℓ_p linearly independent eigenvectors ($\ell_p \leq m$ and $\ell_p \leq l$). Consider a subsystem $G_{\gamma,\beta}$ of G, defined by (2.51), where $\min(n_\beta, n_\gamma) < \ell_p$, i.e. $G_{\gamma,\beta}$ contains less inputs or less outputs than ℓ_p. Then at least $\ell_p - \min(n_\beta, n_\gamma)$ pole/zero cancellations occur in $G_{\gamma,\beta}$.*
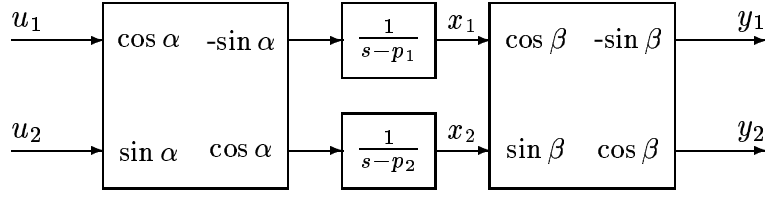
Figure 2.1: Systems in parallel with input and output rotations

Proof. The proof is given in Section A.

Note, additional pole/zero cancellations occur if the selected subsystem $G_{\gamma,\beta}$ contains less than $\mathcal{N}_p - \ell_p + \min(n_\beta, n_\gamma)$ at $s = p$. If for example a minimal realization of $G_{\gamma,\beta}$ contains no poles at $s = p$, we get $\mathcal{N}_p$ pole/zero cancellations. By studying the pole directions it is possible to predict the number of these additional pole/zero cancellations in $G_{\gamma,\beta}$.

The implications for control and input/output selection is summarized in the following theorem.

THEOREM 2.4. *Consider a system G with state-space realization (A, B, C, D), a repeated pole p, multiplicity $\mathcal{N}_p$ and ℓ_p linearly independent eigenvectors. In order to affect the pole p in all ℓ_p directions one need to control at least ℓ_p outputs using ℓ_p inputs.*

Proof. The proof is given in Section A.

EXAMPLE 2.2 IDENTICAL SYSTEMS IN PARALLEL. Consider the system shown in Figure 2.1, with $p_1 = p_2 = p = 1$ we have

$$G(s) \overset{s}{=} \left[\begin{array}{cc|cc} p & 0 & \cos\alpha & -\sin\alpha \\ 0 & p & \sin\alpha & \cos\alpha \\ \hline \cos\beta & -\sin\beta & 0 & 0 \\ \sin\beta & \cos\beta & 0 & 0 \end{array} \right]$$

The state-space matrix A has two linearly independent left and right eigenvectors for the pole $p = 1$

$$X_{pi} = X_{po} = \begin{bmatrix} 1 & 0 \\ 0 & 1 \end{bmatrix}$$

Input and output pole directions are

$$U_p = \begin{bmatrix} \cos\alpha & \sin\alpha \\ -\sin\alpha & \cos\alpha \end{bmatrix} \quad \text{and} \quad Y_p = \begin{bmatrix} \cos\beta & -\sin\beta \\ \sin\beta & \cos\beta \end{bmatrix}$$

The two input and output pole directions are orthogonal. The transfer function $G(s)$ is given by

$$G(s) = \begin{bmatrix} \frac{\cos(\alpha+\beta)(s-p)}{(s-p)^2} & -\frac{\sin(\alpha+\beta)(s-p)}{(s-p)^2} \\ \frac{\sin(\alpha+\beta)(s-p)}{(s-p)^2} & \frac{\cos(\alpha+\beta)(s-p)}{(s-p)^2} \end{bmatrix} = \begin{bmatrix} \frac{\cos(\alpha+\beta)}{s-p} & -\frac{\sin(\alpha+\beta)}{s-p} \\ \frac{\sin(\alpha+\beta)}{s-p} & \frac{\cos(\alpha+\beta)}{s-p} \end{bmatrix}$$

We have two linearly independent eigenvectors corresponding to $p = 1$. Lemma 2.3 then predicts that one pole/zero cancellation occurs within any subsystem of G, so that no elements contain the term $(s - 1)^2$ in the denominator. In order to control the pole p we need to use both inputs and both outputs to affect the pole p in both directions.

2.7.3 Limitations on the use of pole directions

We have already seen one limitation in the use of pole directions to select inputs and outputs. This limitation is demonstrated in Example 2.2 where the system $G(s)$ has a repeated pole p, multiplicity two, and two linearly independent eigenvectors. As stated in Example 2.2 this system can not be stabilized by controlling one output and using one input. This is the case despite the fact that both input pole directions has a component in one of the inputs for all $\alpha \neq k \cdot 90°$, $k \in \mathbb{N}$ and both output pole directions has a component in one of the outputs for all $\beta \neq k \cdot 90°$, $k \in \mathbb{N}$. This problem is caused by one pole/zero cancellation in each of the elements in G. However, the situation can be identified by the fact that the system has a repeated pole p, multiplicity two, and two linearly independent eigenvectors.

EXAMPLE 2.3 ALMOST IDENTICAL SYSTEMS IN PARALLEL. In this example we consider again two systems in parallel but in this case we have $p_1 \neq p_2$ so no pole/zero cancellation occurs for values of α and β between $0°$ and $90°$. Thus, in theory the plant can be stabilized using one input and one output. However, in practice this may be impossible with a stable controller, due to the presence of a RHP-zero in $G_{ij}(s)$ which is close to the two RHP-poles (see Chapter 3). We have

$$G(s) \overset{s}{=} \left[\begin{array}{cc|cc} p_1 & 0 & \cos\alpha & -\sin\alpha \\ 0 & p_2 & \sin\alpha & \cos\alpha \\ \hline \cos\beta & -\sin\beta & 0 & 0 \\ \sin\beta & \cos\beta & 0 & 0 \end{array} \right]$$

The left and right eigenvectors corresponding to the poles p_1 and p_2 are

$$X_{pi} = X_{po} = \begin{bmatrix} 1 & 0 \\ 0 & 1 \end{bmatrix}$$

Input and output pole directions corresponding to the modes $\{p_1,\ p_2\}$ are

$$U_p = \begin{bmatrix} \cos\alpha & \sin\alpha \\ -\sin\alpha & \cos\alpha \end{bmatrix}; \quad Y_p = \begin{bmatrix} \cos\beta & -\sin\beta \\ \sin\beta & \cos\beta \end{bmatrix}$$

The transfer function $G(s)$ is given by

$$G(s) = \begin{bmatrix} \frac{n_{11}(s)}{(s-p_1)(s-p_2)} & \frac{n_{12}(s)}{(s-p_1)(s-p_2)} \\ \frac{n_{21}(s)}{(s-p_1)(s-p_2)} & \frac{n_{22}(s)}{(s-p_1)(s-p_2)} \end{bmatrix}$$

where

$$\begin{aligned} n_{11}(s) &= (s-p_2)\cos(\alpha)\cos(\beta) - (s-p_1)\sin(\alpha)\sin(\beta) \\ &= \cos(\alpha+\beta)s - p_2\cos(\alpha)\cos(\beta) + p_1\sin(\alpha)\sin(\beta) \\ n_{12}(s) &= -(s-p_2)\sin(\alpha)\cos(\beta) - (s-p_1)\cos(\alpha)\sin(\beta) \\ &= -\sin(\alpha+\beta)s + p_2\sin(\alpha)\cos(\beta) + p_1\cos(\alpha)\sin(\beta) \\ n_{21}(s) &= (s-p_2)\cos(\alpha)\sin(\beta) + (s-p_1)\sin(\alpha)\cos(\beta) \\ &= \sin(\alpha+\beta)s - p_2\cos(\alpha)\sin(\beta) - p_1\sin(\alpha)\cos(\beta) \\ n_{22}(s) &= -(s-p_2)\sin(\alpha)\sin(\beta) + (s-p_1)\cos(\alpha)\cos(\beta) \\ &= \cos(\alpha+\beta)s + p_2\sin(\alpha)\sin(\beta) - p_1\cos(\alpha)\cos(\beta) \end{aligned}$$

Zeros in the individual transfer function elements are

$$z_{11} = p_1 \frac{p_2/p_1 \cos(\alpha)\cos(\beta) - \sin(\alpha)\sin(\beta)}{\cos(\alpha + \beta)}$$

$$z_{12} = p_1 \frac{p_2/p_1 \sin(\alpha)\cos(\beta) + \cos(\alpha)\sin(\beta)}{\sin(\alpha + \beta)}$$

$$z_{21} = p_1 \frac{p_2/p_1 \cos(\alpha)\sin(\beta) + \sin(\alpha)\cos(\beta)}{\sin(\alpha + \beta)}$$

$$z_{22} = p_1 \frac{\cos(\alpha)\cos(\beta) - p_2/p_1 \sin(\alpha)\sin(\beta)}{\cos(\alpha + \beta)}$$

When $p_1 = p_2 = p$ all elements of $G(s)$ has a RHP-zero for $s = p$ and we have pole/zero cancellation. Set $p_1 = 1$ and consider

$$p_2 \in \{1.1, \ 1.01, \ 1, \ 0.99, \ 0.9\}$$

The zeros of the transfer function elements for $\alpha = 30°$ and $\beta \in \{30°, \ 50°\}$ are given in Table 2.1. We

Table 2.1: Zeros of the transfer function elements.

α	β	p_2	z_{11}	z_{12}	z_{21}	z_{22}
		1.1	1.15	1.05	1.05	0.95
		1.01	1.015	1.005	1.005	0.995
30°	30°	1	1	1	1	1
		0.99	0.985	0.995	0.995	1.005
		0.9	0.85	0.95	0.95	1.05
		1.1	1.321	1.032	1.067	0.779
		1.01	1.032	1.003	1.007	0.978
30°	50°	1	1	1	1	1
		0.99	0.968	0.997	0.993	1.022
		0.9	0.679	0.967	0.933	1.221

observe that all elements has RHP-zeros. Table 2.2 summarizes the pole directions, and the controllability/observability results for the case with systems in parallel. Except for $\alpha, \beta = 0°$ and $\alpha, \beta = 90°$, there is no warning given in this table about the fact that stabilization using one input and one output may be difficult due to the presence of nearby RHP-zeros.

This example demonstrates one limitation on the use of pole directions for input/output selection. The reason for this is that the information about the zeros is not taken into account. The example can also be viewed as a counter example on the usefulness of the controllability and observability measures defined in Tarokh (1992), which also fails to signal the problems with SISO "controllability" for α, β different from 0° and 90°.

2.8 Discussion

We have defined and shown how to compute the zeros and pole directions in terms of eigenvalue problems. Many of the useful results on state controllability and observability can then

Table 2.2: Controllability, observability and pole directions.

	Observability				Controllability			
β	Y_p	y_1 [a]	y_2 [b]	α	U_p	u_1 [c]	u_2 [d]
$0°$	$\begin{bmatrix} 1 & 0 \\ 0 & -1 \end{bmatrix}$	No	No	$0°$	$\begin{bmatrix} 1 & 0 \\ 0 & 1 \end{bmatrix}$	No	No
$30°$	$\begin{bmatrix} \sqrt{3}/2 & 1/2 \\ -1/2 & \sqrt{3}/2 \end{bmatrix}$	Yes	Yes	$30°$	$\begin{bmatrix} \sqrt{3}/2 & 1/2 \\ -1/2 & \sqrt{3}/2 \end{bmatrix}$	Yes	Yes
$45°$	$\begin{bmatrix} \sqrt{2}/2 & -\sqrt{2}/2 \\ \sqrt{2}/2 & \sqrt{2}/2 \end{bmatrix}$	Yes	Yes	$45°$	$\begin{bmatrix} \sqrt{2}/2 & \sqrt{2}/2 \\ -\sqrt{2}/2 & \sqrt{2}/2 \end{bmatrix}$	Yes	Yes
$60°$	$\begin{bmatrix} 1/2 & -\sqrt{3}/2 \\ \sqrt{3}/2 & 1/2 \end{bmatrix}$	Yes	Yes	$60°$	$\begin{bmatrix} 1/2 & \sqrt{3}/2 \\ -\sqrt{3}/2 & 1/2 \end{bmatrix}$	Yes	Yes
$90°$	$\begin{bmatrix} 1 & 0 \\ 0 & 1 \end{bmatrix}$	No	No	$90°$	$\begin{bmatrix} 1 & 0 \\ 0 & 1 \end{bmatrix}$	No	No

[a]Observable with y_1 only.
[b]Observable with y_2 only.
[c]Controllable with u_1 only.
[d]Controllable with u_2 only.

be stated in terms of the pole directions. These restatements are pretty obvious, but they are still useful. From the pole directions we can give definite conclusions about state controllability and observability in the different inputs and outputs for *distinct* poles.

For repeated modes, there may exist more than ℓ_p linearly independent directions with infinite gain for $s = p$. It is shown that the input and output pole directions (u_p and y_p) corresponding to the mode p are the directions which maximizes the order of the scalar transfer function $y_p^H G(s) u_p$. Furthermore, the results on state controllability and observability (PBH eigenvector test) are still in terms of the eigenvectors of the A matrix and not in terms of the "pseudo" state vectors obtained from the Jordan form. This is the reason why we define (name) the directions with infinite gains corresponding to the eigenvectors as the pole directions.

The close relationship between input/output decoupling zeros (defined by Rosenbrock, 1970) and uncontrollable/unobservable modes in LTI multivariable systems, shows that the term "input and output decoupling zeros" is poorly chosen since uncontrollable and unobservable has nothing to do with what is usually ment by "decoupling". When there is a uncontrollable mode there is also an "input decoupling zero" which cancel the uncontrollable mode so that both the pole and the zero disappear in a minimal realization. The situation is similar with unobservable modes and "output decoupling zeros".

This could take us to the conclusion that uncontrollable/unobservable modes and input/output decoupling zeros do not play any role in control structure design and controllability analysis. In many cases this is true, and it suffice to make sure that the model is a minimal realization. However, as noted by Rosenbrock (also noted by Kalman, 1966) and stated in Corollary 2.1, there is information about the physical structure in uncontrollable/unobservable modes. To show what we mean, consider a large linear model of a chemical process plant. As control engineers we have got the job of designing a control structure

for the plant. That is, we are going to select outputs to be controlled, inputs to be used for control and make the desired links between the selected outputs and inputs. Let us assume that the overall linear model is a minimal realization of the whole plant. When we consider selecting some inputs and outputs to control some small part of the plant it appears that a lot of modes are not observable and controllable in the "smaller" model we are working with at the moment. This structural information is available in the pole directions but not in state controllability and observability in terms of some rank test. For example, consider the presence of an unstable mode which we want to stabilize. An important question is:

- *Does this unstable mode appear in the part of the plant we are looking at?*

The answer to this and similar questions lies in theoretical tools developed in system theory over several decades. Despite this, *it does not seem to be recognized.* Let us give an answer to the question. Look into the output pole direction for the unstable mode, if the pole direction has significant components in one or more of the outputs associated with the part of the plant under consideration, then the answer to the question above is: Yes. However, if the pole direction has zero elements in the outputs considered, we can conclude that the mode is unobservable in the part of the model we are working with. In a similar way we can answer if it is possible to affect (stabilize) the unstable mode by using some candidate inputs by looking into input pole direction. This and similar ideas are expressed in Chapter 6.

To conclude, we can significantly improve usefulness of concepts like state controllability and observability by introducing tools like the pole directions and pole vectors, rather than applying the rank tests. Unfortunately, the latter is the common way of viewing state controllability and observability.

References

Belevitch, V. (1968). *Classical Network Theory*, Holden-Day, San Francisco.

Bode, H. W. (1945). *Network Analysis and Feedback Amplifier Design*, D. Van Nostrand Co., New York.

Callier, F. M. and Desoer, C. A. (1982). *Multivariable Feedback Systems*, Springer-Verlag, Berlin.

Chen, J. (1993). Sensitivity integral relations and design trade-offs in linear multivariable feedback systems, *Proc. American Control Conference*, San Francisco, CA, pp. 3160–3164.

Chen, J. (1995). Sensitivity integral relations and design trade-offs in linear multivariable feedback systems, *IEEE Transactions on Automatic Control* **AC-40**(10): 1700–1716.

Desoer, C. and Schulman, J. (1974). Zeros and poles of matrix transfer functions and their interpretation, *IEEE Transactions on Circuits and Systems* **CAS-21**(1): 3–8.

Douglas, J. and Athans, M. (1995). *The Control Handbook*, 30 ed., CRC Press, chapter Multivariable Poles, Zeros, and Pole-Zero Cancellations, pp. 445–450.

Gilbert, E. G. (1963). Controllability and observability in multivariable control systems, *SIAM J. Control* **1**: 128–151.

Hautus, M. L. J. (1969). Controllability and observability conditions of linear autonomous systems, *Ned. Akad. Wetenshappen, Proc. Ser. A* **72**: 443–448.

Kailath, T. (1980). *Linear Systems*, Prentice-Hall, Englewood Cliffs.

Kalman, R. (1966). On the structural properties of linear constant multivariable systems, *Third IFAC World Congress*. Paper 6A.

Kaufman, I. (1973). On poles and zeros of linear systems, *IEEE Transactions on Circuit Theory* **CT-20**(2): 93–101.

MacFarlane, A. G. J. and Karcanias, N. (1976). Poles and zeros of linear multivariable systems: A survey of algebraic, geometric and complex variable theory, *International Journal of Control* **24**(1): 33–74.

Patel, R. V. (1976). On computing the invariant zeros of multivariable systems, *International Journal of Control* **24**(1): 145–146.

Popov, V. M. (1973). *Hyperstability of Control Systems*, Springer-Verlag (translation based on a revised text prepared shortly after the publication of the Romanian ed., 1966).

Rosenbrock, H. H. (1966). On the design of linear multivariable systems, *Third IFAC World Congress*. Paper 1A.

Rosenbrock, H. H. (1970). *State-space and Multivariable Theory*, Nelson, London.

Rosenbrock, H. H. (1973). The zeros of a system, *International Journal of Control* **18**(2): 297–299.

Rosenbrock, H. H. (1974). Correction to 'the zeros of a system', *International Journal of Control* **20**(3): 525–527.

Tarokh, M. (1992). Measures for controllability, observability, and fixed modes, *IEEE Transactions on Automatic Control* **37**(8): 1268–1273.

Zhou, K., Doyle, J. C. and Glover, K. (1996). *Robust and Optimal Control*, Prentice-Hall, Upper Saddle River.

Appendix A Proofs of the results

A.1 Proof of Lemma 2.1

Inserting $u(s) = u_0 \frac{1}{s - s_0}$ into (2.8) gives

$$y(s) = C(sI - A)^{-1}x_0 + C(sI - A)^{-1}Bu_0 \frac{1}{s - s_0} + Du_0 \frac{1}{s - s_0}$$

using

$$(sI - A)^{-1}(s - s_0) = I - (sI - A)^{-1}(s_0 I - A)$$

$$\Updownarrow$$

$$(sI - A)^{-1} = (s_0 I - A)^{-1} - (sI - A)^{-1}(s - s_0)(s_0 I - A)^{-1}$$

yields

$$
\begin{aligned}
y(s) &= C(sI - A)^{-1}x_0 - C(sI - A)^{-1}(s - s_0)(s_0 I - A)^{-1}Bu_0 \frac{1}{s - s_0} \\
&\quad + \{C(s_0 I - A)^{-1}B + D\}u_0 \frac{1}{s - s_0} \\
&= C(sI - A)^{-1}\{x_0 - (s_0 I - A)^{-1}Bu_0\} + G(s_0)u_0 \frac{1}{s - s_0}
\end{aligned}
$$

which yields the response given in (2.14), and for the initial state $x_0 = (s_0 I - A)^{-1}Bu_0$ we get

$$
y(s) = G(s_0)\frac{u_0}{s - s_0}
$$

$\square$

A.2   Lemma 2.2: Pole directions and directions with infinite gains

From (B.19), $A = M_L^{-H} S^H J M_R^{-1}$, then we have

$$
\begin{aligned}
(sI - A) &= (sI - M_L^{-H} S^H J M_R^{-1}) = (M_L^{-H} S^H M_R^{-1} s - M_L^{-H} S^H J M_R^{-1}) \\
&= M_L^{-H} S^H (sI - J) M_R^{-1} \tag{2.52}
\end{aligned}
$$

and $G(s)$ can be written

$$
\begin{aligned}
G(s) &= C(sI - A)^{-1}B + D = CM_R(sI - J)^{-1}S^{-H} M_L^H B + D \\
&= Y_\infty (sI - J)^{-1}S^{-H} U_\infty^H + D \tag{2.53}
\end{aligned}
$$

as an alternative we could extract the scalings on the other side of $(sI - J)^{-1}$

$$
G(s) = CM_R S^{-H}(sI - J)^{-1}M_L^H B + D = Y_\infty S^{-H}(sI - J)^{-1} U_\infty^H + D \tag{2.54}
$$

Consider $(sI - J)^{-1}$ for $s = p$

$$
(sI - J)^{-1} = \begin{bmatrix} (sI - J_1)^{-1} & & \\ & \ddots & \\ & & (sI - J_v)^{-1} \end{bmatrix}
$$

where v is the number of Jordan blocks. For the Jordan blocks involving p we get

$$
(sI_\ell - J_\ell)^{-1} = \begin{bmatrix} 1/(s-p) & -1/(s-p)^2 & \cdots & (-1)^{\nu-2}/(s-p)^{\nu-1} & (-1)^{\nu-1}/(s-p)^\nu \\ 0 & 1/(s-p) & \cdots & (-1)^{\nu-3}/(s-p)^{\nu-2} & (-1)^{\nu-2}/(s-p)^{\nu-1} \\ \vdots & \vdots & \ddots & \vdots & \vdots \\ 0 & 0 & \cdots & 1/(s-p) & -1/(s-p)^2 \\ 0 & 0 & \cdots & 0 & 1/(s-p) \end{bmatrix} \tag{2.55}
$$

where ν is the size of Jordan block ℓ. When inserting $s = p$ we see that the upper triangular part of $(sI_\ell - J_\ell)^{-1}$ becomes ∞. We partition M_R and M_L into blocks so that the columns in M_R and M_L corresponding to Jordan block number ℓ, are collected in $M_{R,\ell}$ and $M_{L,\ell}$. Then (2.53) can be rewritten

$$
G(s) = C[\, M_{R,1} \quad \cdots \quad M_{R,v} \,] \begin{bmatrix} (sI_1 - J_1)^{-1}\bar{s}_1 & & \\ & \ddots & \\ & & (sI_v - J_v)^{-1}\bar{s}_v \end{bmatrix} \begin{bmatrix} M_{L,1}^H \\ \vdots \\ M_{L,v}^H \end{bmatrix} B + D
$$

Assume that block number one is the only block involving p, inserting $s = p$ in $G(s)$ gives

$$G(s = p) = C \begin{bmatrix} M_{R,1} & \cdots & M_{R,v} \end{bmatrix} \begin{bmatrix} \infty \cdot T_1 \bar{s}_1 & & \\ & \ddots & \\ & & O \cdot T_v \bar{s}_v \end{bmatrix} \begin{bmatrix} M_{L,1}^H \\ \vdots \\ M_{L,v}^H \end{bmatrix} B + D$$

where T_ℓ is used to signal an upper triangular matrix compatible in size with J_ℓ, ∞ is used to signal infinite gain and O is used to signal finite gain. The directions associated with infinite gain at the output are those contained in $M_{R,1}$, or if Jordan block ℓ is involved, the directions are contained in $M_{R,\ell}$. The output vectors become

$$\boldsymbol{Y}_\infty = CM_{R,\ell}, \quad \forall \ell \text{ whose Jordan block involves } p.$$

and the input vectors become

$$\boldsymbol{U}_\infty = B^H M_{L,\ell}, \quad \forall \ell \text{ whose Jordan block involves } p.$$

From the construction of the Jordan forms it follows that the columns of M_L and M_R are linear independent, i.e. n linearly independent directions in the state-space. The Jordan chains for the left and the right Jordan form are

$$m_{L,i-1}^H (A - pI) = m_{L,i}^H \quad \text{and} \quad (A - pI)m_{R,i} = m_{R,i-1}$$

where the left Jordan chain ends with the left eigenvector and the right Jordan chain starts with the right eigenvector. This implies that the first column in $M_{R,\ell}$ is the right eigenvector for Jordan block J_ℓ and that the last column in $M_{L,\ell}$ is the left eigenvector for Jordan block J_ℓ. From (2.55) we see that the input and output pole vectors with largest order for Jordan block ℓ, J_ℓ, corresponds to $B^H M_{L,\ell} e_\nu$ and $CM_{R,\ell} e_1$, i.e. the input and output pole directions. $\qquad\square$

A.3   Corollary 2.2: Controllability and observability of repeated modes

If the pole p has ℓ_p linearly independent eigenvectors, then $pI - A$ has rank $n - \ell_p$. A necessary condition for the pole p to be controllable is that the matrix B has at least ℓ_p linearly independent columns. A sufficient condition for controllability of the mode p is that there are n linearly independent columns in the matrix $\begin{bmatrix} pI - A & B \end{bmatrix}$. Sufficient condition for the mode p being uncontrollable is that B has less than ℓ_p linearly independent columns. The proof of observability is similar. $\qquad\square$

A.4   Lemma 2.3: Pole/zero cancellations when reducing size...

The subsystem $G_{\gamma,\beta}$ of G, with state-space realization

$$G_{\gamma,\beta}(s) \stackrel{s}{=} \left[\begin{array}{c|c} A & B_\beta \\ \hline C_\gamma & D_{\gamma,\beta} \end{array} \right]$$

can be written as a rational transfer function matrix

$$G_{\gamma,\beta}(s) = C_\gamma (sI - A)^{-1} B_\beta + D_{\gamma,\beta} = \frac{C_\gamma \mathrm{adj}(sI - A)B_\beta + D_{\gamma,\beta}\,\phi(s)}{\phi(s)} \qquad (2.56)$$

where $\phi(s) \triangleq \det(sI - A)$. Since $\phi(p) = 0$, it is sufficient to show that the system described by

$$G'_{\gamma,\beta}(s) \stackrel{s}{=} \left[\begin{array}{c|c} A & B_\beta \\ \hline C_\gamma & 0 \end{array} \right] \tag{2.57}$$

at least has $\ell_p - \min(n_\beta, n_\gamma)$ zeros for $s = p$ and that these zeros cancel with the corresponding poles, i.e. the poles are either uncontrollable, unobservable or both at the same time. The zeros z of $G'_{\gamma,\beta}(s)$ are the values of s where the matrix

$$\begin{bmatrix} sI - A & B_\beta \\ C_\gamma & 0 \end{bmatrix} \quad \text{is singular, i.e.} \quad \det \begin{bmatrix} zI - A & B_\beta \\ C_\gamma & 0 \end{bmatrix} = 0$$

The zeros and the directionality of the input/output zero directions are independent of the state-space realization so let us define a new state vector $z = M_R^{-1} x$ where M_R is the matrix which brings A to Jordan form, i.e. $M_R^{-1} A M_R = J$. Consider

$$H(s) \triangleq \begin{bmatrix} M_R^{-1} & 0 \\ 0 & I_{n_\gamma} \end{bmatrix} \begin{bmatrix} (sI - A) & B_\beta^r \\ C_\gamma^r & 0 \end{bmatrix} \begin{bmatrix} M_R & 0 \\ 0 & I_{n_\beta} \end{bmatrix} = \begin{bmatrix} sI - J & M_R^{-1} B_\beta \\ C_\gamma M_R & 0 \end{bmatrix} \tag{2.58}$$

When inserting $s = p$ in (2.58), ℓ_p columns and ℓ_p rows in $pI - J$ become equal to zero since J has ℓ_p Jordan blocks with p on the main diagonal, so the rank of $pI - J$ is $n - \ell_p$. The matrices $M_R^{-1} B_\beta$ and $C M_R$ contains n_β linearly independent columns and n_γ linearly independent rows. An upper bound on the rank of $H(p)$ when $\min(n_\beta, n_\gamma) \leq \ell_p$ is

$$n - \ell_p + 2 \min(n_\beta, n_\gamma) \leq n + \min(n_\beta, n_\gamma) = \text{Normal rank of } H(s)$$

which leaves us with a zero at least of multiplicity $\ell_p - \min(n_\beta, n_\gamma)$.

We need to show that the mode p is uncontrollable, unobservable or both at the same time.

1. $n_\beta < \ell_p$, then

$$\text{rk} \begin{bmatrix} pI - A & B_\beta \end{bmatrix} < n \quad \Rightarrow \quad \text{the mode } p \text{ is uncontrollable.}$$

2. $n_\gamma < \ell_p$, then

$$\text{rk} \begin{bmatrix} pI - A \\ -C_\gamma \end{bmatrix} < n \quad \Rightarrow \quad \text{the mode } p \text{ is unobservable.}$$

3. $n_\beta < \ell_p$ *and* $n_\gamma < \ell_p$ then the mode p is both uncontrollable and unobservable. $\square$

A.5 Proof of Theorem 2.4

From Corollary 2.2, in any subsystem $G_{\gamma,\beta}$ of G with size less than $\ell_p \times \ell_p$ there are one or more modes for $s = p$ which are uncontrollable, unobservable or both uncontrollable and unobservable at the same time. $\square$

Chapter 3

Effect of RHP zeros and poles on the sensitivity functions in multivariable systems

Kjetil Havre[*] and Sigurd Skogestad[†]

Chemical Engineering,
Norwegian University of Science and Technology
N-7034 Trondheim, Norway.

Abstract

This paper examines the implications of Right Half Plane (RHP) zeros and poles on performance of multivariable feedback systems. The results quantify the fundamental limitations imposed by RHP zeros and poles in terms of lower bounds on the peaks in the weighted sensitivity and complementary sensitivity functions.

[*]Also affiliated with: Institute for energy technology, P.O.Box 40, N-2007 Kjeller, Norway, Fax: (+47) 63 81 11 68, E-mail: Kjetil.Havre@ife.no.
[†]Fax: (+47) 73 59 40 80, E-mail: skoge@chembio.ntnu.no.

3.1   Introduction

It is well known that the presence of RHP ("unstable") zeros and poles pose fundamental limitations on the achievable control performance. This was quantified for SISO-systems by Bode (1945) more than 50 years ago, and most control engineers have an intuitive feeling of the limitations for scalar systems. Rosenbrock (1966; 1970) pointed out that multivariable RHP-zeros pose similar limitations. Nevertheless, the quantification of the effect of RHP zeros and poles on closed-loop performance has been much more difficult for MIMO than for SISO systems. Important reasons are:

1) The definition of phase is difficult to generalize to MIMO-systems.
2) The directionality of zeros and poles in multivariable systems has not been well understood.

The goal of this paper is therefore to address the following questions:

1) How is closed-loop performance influenced by the location of the RHP zeros and poles in MIMO-systems?
2) How is closed-loop performance influenced by the directionality of the RHP zeros and poles in MIMO-systems?
3) How is closed-loop performance influenced by the combined effect of RHP zeros and poles and their directions?

We will mainly quantify the fundamental limitations imposed by RHP zeros and poles in terms of lower bounds on the peaks ($\mathcal{H}_\infty$-norm) in the closed-loop transfer functions S (sensitivity) and T (complementary sensitivity).

3.1.1   Why consider peaks in S and T?
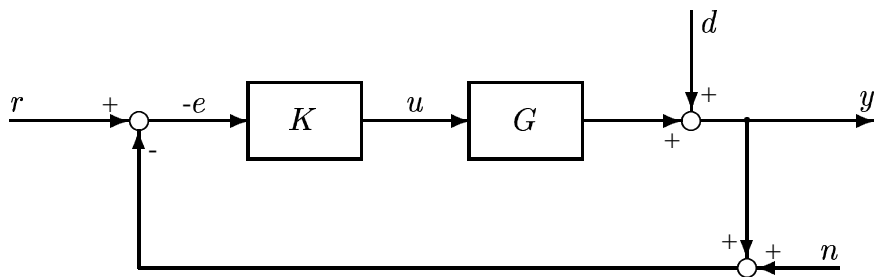
Figure 3.1: One degree-of-freedom feedback control configuration

Figure 3.1 shows a one degree-of-freedom (1-DOF) feedback control configuration. The closed-loop system is driven by the reference commands r, disturbances d and measurement noise n. The outputs to be controlled are y, and u are the manipulated variables. We assume that the performance is measured at the output of the plant G in terms of the error signal $e \triangleq y - r$. For the closed-loop system we have the following important relationships:

$$y(s) \quad = \quad T(s)r(s) + S(s)d(s) - T(s)n(s) \tag{3.1}$$

$$
\begin{aligned}
e(s) &= -S(s)r(s) + S(s)d(s) - T(s)n(s) & (3.2)\\
u(s) &= K(s)S(s)\left(r(s) - n(s) - d(s)\right) & (3.3)
\end{aligned}
$$

where sensitivity and complementary sensitivity functions are defined by

$$
S(s) \triangleq (I + L(s))^{-1} \tag{3.4}
$$

$$
T(s) \triangleq L(s)\left(I + L(s)\right)^{-1} = L(s)S(s) = I - S(s) \tag{3.5}
$$

and $L \triangleq GK$ is the loop transfer function. The relationships (3.1)–(3.3) imply several closed-loop objectives, in addition to the requirement that K should stabilize G (e.g. Doyle and Stein, 1981):

1) For *disturbance rejection* make $\bar{\sigma}(S)$ small.
2) For *noise attenuation* make $\bar{\sigma}(T)$ small.
3) For *reference tracking* make $\bar{\sigma}(T) \approx \underline{\sigma}(T) \approx 1$.
4) For *control energy reduction* make $\bar{\sigma}(KS)$ small.

If the unstructured uncertainty in the plant model G is represented by an additive perturbation, i.e. $G_p = G + \Delta$, then a further closed-loop objective is

5) For *robust stability* in the presence of an additive perturbation make $\bar{\sigma}(KS)$ small.

Alternatively, if the uncertainty is modeled by a multiplicative output perturbation such that $G_p = (I + \Delta)G$, then we have:

6) For *robust stability* in the presence of a multiplicative output perturbation make $\bar{\sigma}(T)$ small.

The condition $S + T = I$ holds for MIMO-systems, and it then follows that we cannot have both S and T small simultaneously, and that $\bar{\sigma}(S)$ is large if and only if $\bar{\sigma}(T)$ is large.

Typical plots of the maximum singular values $\bar{\sigma}(S(j\omega))$ and $\bar{\sigma}(T(j\omega))$ are shown in Figure 3.2. For those frequencies where $\bar{\sigma}(S(j\omega)) > 2$, we have more than 100% control
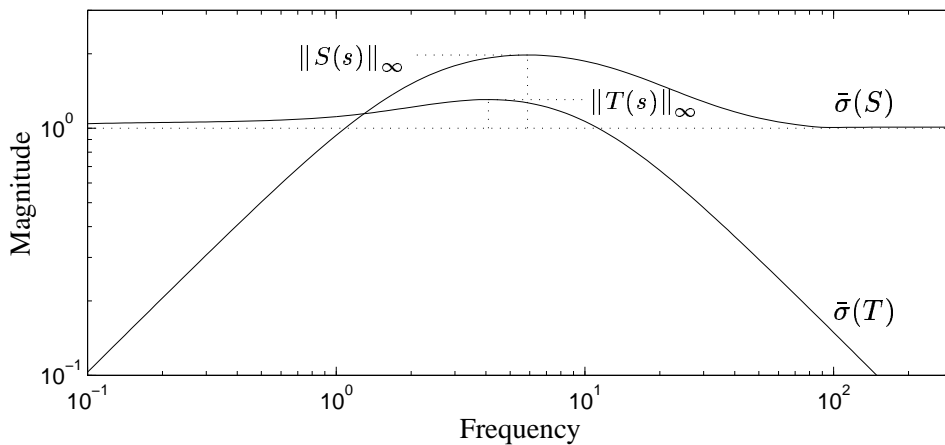
Figure 3.2: Typical plots of $\bar{\sigma}(S(j\omega))$ and $\bar{\sigma}(T(j\omega))$

error and for those frequencies where $\bar{\sigma}(T(j\omega)) > 2$, we have more than 100% amplification

of the noise. The peaks $\|S(s)\|_\infty$ and $\|T(s)\|_\infty$ therefore tell us a great deal about the performance of the feedback system for the worst case direction and the worst case frequency. Although, S and T depend on the controller K, the lower bounds on $\|S(s)\|_\infty$ and $\|T(s)\|_\infty$ derived in this paper, are independent of K. If the lower bounds are large (typically larger than 4) then the plant G is fundamentally difficult to control, i.e. the "controllability"[1] of the plant G is poor. In this paper we look at the combined effect of RHP zeros and poles, and we show that the lower bounds on $\|S(s)\|_\infty$ and $\|T(s)\|_\infty$ can become quite large when the plant contains both RHP zeros and poles. Finally, it should be noted that there are also other fundamental limitations on performance than those imposed by RHP zeros and poles. In Chapter 10 we look at the effect of uncertainty, in particular at input uncertainty, on the peak in the sensitivity function.

3.1.2   Notation and outline

Notation. We consider linear time invariant dynamical systems on state-space form

$$\dot{x} = Ax + Bu \tag{3.6}$$

$$y = Cx + Du \tag{3.7}$$

In (3.6)–(3.7), u are the external inputs, x are the states and y are the outputs. A, B, C and D are real matrices of dimensions $n \times n$, $n \times m$, $l \times n$ and $l \times m$ where n is the number of states, m is the number of inputs and l is the number of outputs. The short-hand notations

$$G \overset{s}{=} \left[\begin{array}{c|c} A & B \\ \hline C & D \end{array} \right] \quad \text{and} \quad (A,\, B,\, C,\, D) \tag{3.8}$$

are frequently used to describe a linear state-space model of the continuos system G given by (3.6)–(3.7). The rational transfer function matrix $G(s)$ (of size $l \times m$) defined by (3.8), can be evaluated as a function of the complex variable s

$$G(s) = C(sI - A)^{-1}B + D \tag{3.9}$$

We often omit to show the dependence on the complex variable s for transfer functions. We consider the feedback control configuration shown in Figure 3.1 with the closed-loop transfer functions given in (3.1)–(3.3), where the sensitivity and the complementary sensitivity functions (S and T) are defined by (3.4) and (3.5). With the term "peak of a rational transfer function matrix" we mean its $\mathcal{H}_\infty$-norm, defined as (see also Figure 3.2)

$$\|M(s)\|_\infty \triangleq \sup_\omega \bar{\sigma}(M(j\omega)) \tag{3.10}$$

RHP zeros z and poles p are in this paper defined to be in the closed RHP, denoted $\overline{\mathbb{C}}_+$, i.e. $z \in \overline{\mathbb{C}}_+$ implies $\operatorname{Re} z \geq 0$, and $p \in \overline{\mathbb{C}}_+$ implies $\operatorname{Re} p \geq 0$. However, for some of the results in this paper the locations of some RHP-zeros or RHP-poles are restricted to be within the open RHP, denoted $\mathbb{C}_+$, i.e. $z \in \mathbb{C}_+$ implies $\operatorname{Re} z > 0$, and $p \in \mathbb{C}_+$ implies $\operatorname{Re} p > 0$.

---

[1]The term "controllability" is here used in a wider sense than the meaning of state-controllability, see Skogestad and Postlethwaite (1996, Definition 5.1 page 160 and the discussion on page 123).

Outline. The outline of the paper is as follows. First we give a literature overview, and then we discuss zeros and poles of multivariable systems and their directions. We then derive constraints on the sensitivity and the complementary sensitivity functions imposed by RHP zeros and poles. Next, we consider the lower bounds on the peak in the weighted sensitivity and complementary sensitivity functions. At the end we give two examples and a conclusion. All proofs are given in Section A.

3.2 Previous work

Bode (1945), in his book on network analysis and feedback amplifiers, was probably the first to study a priori constraints on the achievable performance of SISO-systems. His analysis focused on gain-phase relationships in the frequency domain which resulted in many useful interpretations applicable to feedback control. Horowitz (1963) summarizes and generalizes Bode's work to control systems. The well-known *Bode sensitivity integral* (Bode, 1945) states that for stable SISO-systems with pole-zero excess of two or larger, the integral of the logarithmic magnitude of the sensitivity function over all frequencies must equal zero

$$\int_0^\infty \ln |S(j\omega)| \, d\omega = 0 \qquad (3.11)$$

This implies that a peak in $|S|$ larger than 1 is unavoidable. Later Bode's criterion has been extended to plants with RHP zeros and poles by Freudenberg and Looze (1985; 1988). From these results it is clear that even larger peaks are expected when the plant contains RHP-zeros and/or RHP-poles.

A related result from optimal control theory is the *Kalman inequality* (Kalman, 1964)

$$\bar{\sigma}(S_x(j\omega)) \leq 1, \quad \forall \omega \qquad (3.12)$$

where $S_x \triangleq (I + K(sI - A)^{-1}B)^{-1}$ and K is the optimal state feedback gain matrix. The Kalman inequality is valid for both stable and unstable MIMO-systems under optimal state feedback control with diagonal weight on the manipulated variables in the performance objective (Skogestad and Postlethwaite, 1996, pages 357–358). This inequality is neither in conflict with the Bode's sensitivity integral nor with the extended version valid for RHP-zeros. The reason for this is that optimal control with state feedback yields a loop transfer function with a pole-zero excess of one, so Bode's sensitivity integral does not apply. Secondly, there are *no* zeros when all the states are measured so the extended Bode's sensitivity integral can not be applied.

The combination of no zeros when all the states are measured and the results from optimal control theory (i.e. the Kalman inequality), may have had a misleading role in multivariable feedback design, which resulted in that very little attention was given to multivariable zeros during the 1960's and 70's. As one example, in their book Anderson and Moore (1971) do not mention the effect of zeros on closed-loop performance for multivariable system at all. However, some quantification of the effect of RHP-zeros has been made during the 1970's. For MIMO-systems Kwakernaak and Sivan (1972, pages 306–307) state that perfect tracking

with state feedback can be achieved if and only if the rational transfer function matrix from the inputs to the outputs has no RHP-zeros.

Zames and coworkers (Zames, 1981; Zames and Francis, 1983; Zames and Bensoussan, 1983; Francis and Zames, 1984; O'Young and Francis, 1985) consider minimizing the $\mathcal{H}_\infty$-norm of the sensitivity matrix multiplied by suitable weighting matrices. In (Zames, 1981) it is shown how feedback can reduce the weighted sensitivity and in particular how the weighted sensitivity can be made arbitrarily small whenever the plant has no RHP-zeros. In (Zames and Bensoussan, 1983) an alternative approach is developed which is not dependent on *a priori* parameterization, but specialized to diagonal feedback. Zames (1981) derives a lower bound on the weighted sensitivity function (see Theorem 3.1 below), which is based on the interpolation constraint on the sensitivity function valid for RHP-zeros in G. The results in this paper are based on this and a similar interpolation constraint on the complementary sensitivity function valid for RHP-poles in G. We then follow much of the same approach as Zames to derive the lower bounds.

Boyd and Desoer (1985), Freudenberg and Looze (1988), Boyd and Barratt (1991) and Chen (1995) have studied the limitations imposed by RHP zeros and poles in terms of *sensitivity integral formulas* for MIMO-systems. A breakthrough was made by Boyd and Desoer who obtained inequality versions of the sensitivity and Poisson integral formulas, based on the recognition that the logarithm of the largest singular value of an analytic transfer function matrix is a subharmonic function. The work by Chen differs from the work by Boyd and Desoer in that Chen seeks equality versions of the sensitivity and Poisson integral formulas. Based on the results by Boyd and Desoer, Freudenberg and Looze, and Boyd and Barratt generalize the integral constraints on the sensitivity (like Bode's sensitivity integral) to MIMO-systems. Although these integral relationships are interesting, it seems difficult to derive any concrete bounds on achievable performance from them. However, for the case when G has one RHP-zero z with output direction y_z and one RHP-pole p with output direction y_p, the following bound is given by Boyd and Desoer (1985):

$$\| S(s) \|_\infty \;\geq\; \frac{|z + \bar{p}|}{|z - p|} \, \cos \angle(y_p, y_z) \tag{3.13}$$

The following similar but improved bound for the same case (one RHP-zero and one RHP-pole), is given in (Chen, 1993; Chen, 1995):

$$\| S(s) \|_\infty \;\geq\; e^{Q(z)/\pi} \sqrt{\sin^2 \angle(y_p, y_z) \;+\; \frac{|z + \bar{p}|^2}{|z - p|^2} \, \cos^2 \angle(y_p, y_z)} \tag{3.14}$$

where

$$Q(z) \triangleq \frac{1}{2} \iint\limits_{\overline{\mathbb{C}}_+} \log \left| \frac{x + jy + \bar{z}}{x + jy - z} \right| \nabla^2 \log \bar{\sigma}(S_m(x + jy)) dx dy \tag{3.15}$$

and $Q(z) \geq 0$ (see the text following proof of Corollary 5.1 on page 1712 in Chen, 1995). Note that the factor $Q(z)$ can not be evaluated without knowledge about the controller K, and even when K is known it is hard to evaluate $Q(z)$. In any case, it appears from the results

in Chapter 5 that $Q(z) = 0$ for the optimal controller minimizing $\|S(s)\|_\infty$. Using algebraic rather than integral constraints, we derive in this paper a tight bound which is similar to (3.14) with $Q(z) = 0$. However, the bounds presented here extend (3.14) to the case where the plant G has more than one RHP-pole (Theorem 3.3). Furthermore, we derive similar results in terms of the weighted complementary sensitivity $\|w_T T(s)\|_\infty$ for the case where the plant G has one or more RHP-poles and any number of RHP-zeros (Theorem 3.4).

3.3 Zeros and poles of multivariable systems

3.3.1 Zeros

Rosenbrock (1970), Kailath (1980) and Zhou et al. (1996) all define the zeros as the roots of the non-zero numerator polynomials in the Smith-McMillan form. A slightly different approach which yield the same set of zeros, is taken by Desoer and Schulman (1974). They consider a left coprime polynomial matrix factorization of $G(s)$, $G(s) = D_l^{-1}(s)N_l(s)$ and define the zeros as the complex numbers z where the rank of $N_l(z)$ is less than the normal rank of $N_l(s)$. This is similar to the definition we use, which is taken from MacFarlane and Karcanias (1976):

DEFINITION 3.1 (ZEROS). *$z_i \in \mathbb{C}$ is a zero of $G(s)$ if the rank of $G(z_i)$ is less than the normal rank of $G(s)$.*

The normal rank of $G(s)$ is defined as the rank of $G(s)$ at all s except a finite number of singularities (which are the zeros). This definition of zeros is based on the transfer function matrix, corresponding to a minimal realization of a system. These zeros are sometimes called "transmission zeros" (MacFarlane and Karcanias, 1976), but we shall simply call them "zeros".

DEFINITION 3.2 (ZERO DIRECTIONS). *If $G(s)$ has a zero for $s = z \in \mathbb{C}$ then there exist non-zero vectors labeled the output zero direction $y_z \in \mathbb{C}^l$ and the input zero direction $u_z \in \mathbb{C}^m$, such that $y_z^H y_z = 1$, $u_z^H u_z = 1$ and*

$$G(z)u_z = 0; \qquad y_z^H G(z) = 0 \tag{3.16}$$

The definitions of input and output zero directions can further be extended with the state input and output zero vectors through the use of generalized eigenvalues. For a system $G(s)$, the zeros z of the system, the input zero directions u_z and the state input zero vectors $\boldsymbol{x}_{zi} \in \mathbb{C}^n$ can all be computed from the generalized eigenvalue problem

$$\begin{bmatrix} A - zI & B \\ C & D \end{bmatrix} \begin{bmatrix} \boldsymbol{x}_{zi} \\ u_z \end{bmatrix} = \begin{bmatrix} 0 \\ 0 \end{bmatrix} \tag{3.17}$$

In this setup we normalize the length of u_z, i.e. $u_z^H u_z = 1$. This implies that the length of $\boldsymbol{x}_{zi}$ is different from one[2].

---

[2]That $\|\boldsymbol{x}_{zi}\|_2$ is generally different from 1 is the primary reason for denoting $\boldsymbol{x}_{zi}$ vector and not a direction.

Similarly, one can compute the zeros z, the output zero directions y_z and the state output zero vectors $\boldsymbol{x}_{zo} \in \mathbb{C}^n$ through the generalized eigenvalue problem

$$
\begin{bmatrix} \boldsymbol{x}_{zo}^H & y_z^H \end{bmatrix} \begin{bmatrix} A - zI & B \\ C & D \end{bmatrix} = \begin{bmatrix} 0 & 0 \end{bmatrix} \tag{3.18}
$$

with the length of y_z is normalized, so that $y_z^H y_z = 1$. Let (A, B, C, D) be a minimal realization of $G(s)$, computing the zeros from the eigenvalue problems (3.17) and (3.18) yields the "transmission zeros" (MacFarlane and Karcanias, 1976).

3.3.2 Poles

Rosenbrock (1970), MacFarlane and Karcanias (1976), Callier and Desoer (1982) and Zhou et al. (1996) all define the poles as the roots of the denominator polynomials in the Smith-McMillan form of $G(s)$. For a linear time invariant system with minimal state-space description (3.6)–(3.7), these roots correspond to the eigenvalues of the A matrix (Callier and Desoer, 1982, pages 75–78). Thus, the poles are the roots of the characteristic equation

$$
\phi(s) = \det(sI - A) = \prod_{i=1}^{n}(s - p_i) = 0 \tag{3.19}
$$

Bode (1945) states that the poles are the singular points at which the transfer function fails to be analytic. The singularities appear in the denominator so when the system G is evaluated[3] at $s = p$, $G(p)$ is infinite in some directions at the input and the output. This is the basis for the following definition of input and output pole directions.

DEFINITION 3.3 (POLE DIRECTIONS). *Let $s = p \in \mathbb{C}$ be a distinct pole of $G(s)$, then there exist unique input and output directions $u_p \in \mathbb{C}^m$ and $y_p \in \mathbb{C}^l$ such that*

$$
G(p)u_p = \infty; \qquad y_p^H G(p) = \infty \tag{3.20}
$$

More precisely $G(p)u_p = y_p \cdot \infty$ and $y_p^H G(p) = u_p^H \cdot \infty$.

The following result shows how to compute the pole directions for a system with state-space realization.

LEMMA 3.1 (POLE DIRECTIONS). *For a system G with a minimal state-space realization (A, B, C, D), the pole directions associated with the distinct pole $p \in \mathbb{C}$ can be computed from*

$$
u_p = B^H x_{pi} / \left\| B^H x_{pi} \right\|_2 ; \qquad y_p = C x_{po} / \left\| C x_{po} \right\|_2 \tag{3.21}
$$

where $x_{pi} \in \mathbb{C}^n$ and $x_{po} \in \mathbb{C}^n$ are the eigenvectors corresponding to the two eigenvalue problems

$$
x_{pi}^H A = x_{pi}^H p; \qquad A x_{po} = p x_{po}
$$

---

[3]Strictly speaking, the transfer function $G(s)$ can *not* be evaluated at $s = p$, since $G(s)$ is not analytic at $s = p$.

3.3.3   Constraints on S and T

To have internal stability, we cannot allow right half plane pole-zero cancellations between the plant and the controller. This may be formulated as "interpolation constraints" on closed-loop transfer functions, such as S and T. For MIMO-systems these interpolation constraints have directions.

CONSTRAINT 3.1 (RHP-ZERO). *If $G(s)$ has a* RHP-*zero at $s = z$ with output zero direction y_z, then for internal stability of the feedback system, the following interpolation constraints must apply*

$$y_z^H T(z) = 0; \qquad y_z^H S(z) = y_z^H \tag{3.22}$$

In words, (3.22) says that T must have a RHP-zero in the same direction as G and that $S(z)$ has an eigenvalue of 1 with corresponding left eigenvector y_z.

CONSTRAINT 3.2 (RHP-POLE). *If $G(s)$ has a* RHP-*pole at $s = p$ with output direction y_p, then for internal stability of the feedback system, the following interpolation constraints must apply*

$$S(p)y_p = 0; \qquad T(p)y_p = y_p \tag{3.23}$$

Similar constraints apply to the input sensitivity S_I and the input complementary sensitivity T_I, but these are in terms of *input* zero and pole directions, u_z and u_p.

3.3.4   All-pass factorizations of RHP zeros and poles

A transfer function matrix $B(s)$ is all-pass if $B(-s)^T B(s) = I$, which implies that all singular values of $B(j\omega)$ are equal to one.

A plant $G(s)$ with RHP-poles $p_i \in \mathbb{C}_+$ and RHP-zeros $z_j \in \mathbb{C}_+$, can be factorized at the *output* as follows[4]

$$G(s) = \mathcal{B}_{po}^{-1}(G(s)) \, G_{so}(s); \qquad G(s) = \mathcal{B}_{zo}(G(s)) \, G_{mo}(s) \tag{3.24}$$

where G_{mo} is minimum phase, G_{so} is stable, and $\mathcal{B}_{po}(G)$ and $\mathcal{B}_{zo}(G)$ are stable all-pass rational transfer function matrices. $\mathcal{B}_{po}(G)$ contains the RHP-poles of G as RHP-zeros and $\mathcal{B}_{zo}(G)$ contains the RHP-zeros of G. $\mathcal{B}_{po}(G)$ is obtained by factorizing at the output one RHP-pole at a time, starting with $G(s) = \mathcal{B}_{p_1}^{-1}(G) \, G_{p_1}(s)$ where

$$\mathcal{B}_{p_1}^{-1}(G) = I + \frac{2\mathrm{Re}(p_1)}{s - p_1} \hat{y}_{p_1} \hat{y}_{p_1}^H$$

and $\hat{y}_{p_1} = y_{p_1}$ is the output pole direction for p_1. This procedure may be continued to factor out p_2 from $G_{p_1}(s)$ where $\hat{y}_{p_2}$ is the output pole direction of G_{p_1} (which need not coincide

---

[4]Note that the notation on the all-pass factorizations of RHP-zeros and poles used in this paper are reversed compared to the notation used in (Green and Limebeer, 1995; Skogestad and Postlethwaite, 1996; Havre and Skogestad, 1996). The reason for this change of notation is to get consistent with what the literature generally defines as an all-pass filter.

with y_{p_2}, the pole direction of G), and so on. A similar procedure may be used for the RHP-zeros. We get (Appendix A):

$$\mathcal{B}_{po}(G) = \prod_{i=N_p}^{1} (I - \frac{2\mathrm{Re}(p_i)}{s + \bar{p}_i} \hat{y}_{p_i} \hat{y}_{p_i}^H); \qquad \mathcal{B}_{po}^{-1}(G) = \prod_{i=1}^{N_p} (I + \frac{2\mathrm{Re}(p_i)}{s - p_i} \hat{y}_{p_i} \hat{y}_{p_i}^H) \qquad (3.25)$$

$$\mathcal{B}_{zo}(G) = \prod_{j=1}^{N_z} (I - \frac{2\mathrm{Re}(z_j)}{s + \bar{z}_j} \hat{y}_{z_j} \hat{y}_{z_j}^H); \qquad \mathcal{B}_{zo}^{-1}(G) = \prod_{j=N_z}^{1} (I + \frac{2\mathrm{Re}(z_j)}{s - z_j} \hat{y}_{z_j} \hat{y}_{z_j}^H) \qquad (3.26)$$

If $N_z = 0$ we define $\mathcal{B}_{zo}(G) = I$ and if $N_p = 0$ define $\mathcal{B}_{po}(G) = I$. For further details regarding the state-space realizations of the factorizations and properties of the all-pass filters, see Appendix A. The output factorization of RHP-zeros is also given in (Zhou et al., 1996, p.145) and in (Chen, 1993; Chen, 1995). It can be traced back to Wall, Doyle and Harvey (1980). We note that similar factorizations of RHP-zeros and poles apply at the plant input.

   Alternative all-pass factorizations are in use, e.g. the inner-outer factorization used in (Morari and Zafiriou, 1989) which is the same as (3.26) except for the multiplication of a constant unitary matrix. Reasons for using the factorizations (3.25) and (3.26) are:

   1) The factorization of RHP-zeros given here is analytic and in terms of the zeros and the zero directions, whereas the inner-outer factorization in (Morari and Zafiriou, 1989) is given in terms of the solution to an algebraic Riccati equation.

   2) To factorize RHP-poles using the inner-outer factorization, one needs to assume that G^{-1} exist.

3.4 Lower bounds on $\|w_P S(s)\|_\infty$ and $\|w_T T(s)\|_\infty$

3.4.1 Limitations imposed by RHP-zeros

The following result is originally from Zames (1981), and it is based on the interpolation constraints imposed by RHP-zeros in G.

THEOREM 3.1 (RHP-ZERO AND $\|w_P S(s)\|_\infty$). *Suppose the plant $G(s)$ has a RHP-zero at $s = z$. Let $w_P(s)$ be a scalar stable transfer function. Then for closed-loop stability the weighted sensitivity function must satisfy*

$$\|w_P S(s)\|_\infty \geq |w_P(z)| \qquad (3.27)$$

Condition (3.27) shows that there are inherent performance limitations imposed by RHP-zeros. It involves the maximum singular value, $\|w_P S(s)\|_\infty = \sup_\omega \bar{\sigma}(w_P(S(j\omega)))$, which is the "worst" direction, and the RHP-zero may therefore not be a limitation in the other directions.

3.4.2 Limitations imposed by RHP-poles

The following "symmetric" result is based on the interpolation constraints imposed by RHP-poles in G. It extends the SISO result given in (Doyle, Francis and Tannenbaum, 1992).

THEOREM 3.2 (RHP-POLE AND $\|w_T T(s)\|_\infty$). *Suppose the plant* $G(s)$ *has a* RHP-*pole at* $s = p$. *Let* $w_T(s)$ *be a scalar stable transfer function. Then for closed-loop stability the weighted complementary sensitivity function must satisfy*

$$\|w_T T(s)\|_\infty \geq |w_T(p)| \tag{3.28}$$

3.4.3 RHP-zeros combined with RHP-poles

By considering the effect of one RHP-zero and one RHP-pole separately, we derived in (3.27) and (3.28) the conditions

$$\|w_P S(s)\|_\infty \geq c_1 |w_P(z)| \tag{3.29}$$

$$\|w_T T(s)\|_\infty \geq c_2 |w_T(p)| \tag{3.30}$$

with $c_1 = c_2 = 1$. These conditions may be optimistic in that the lower bound may be too small, and indeed we show below that $c_1 > 1$ and $c_2 > 1$ for the case when we have both a RHP-zero and a RHP-pole with some alignment in the same direction.

THEOREM 3.3 (MIMO SENSITIVITY PEAK). *Suppose the plant* $G(s)$ *has* $N_z \geq 1$ RHP-*zeros* z_j *with output directions* y_{z_j} *and* $N_p \geq 0$ RHP-*poles* $p_i \in \mathbb{C}_+$ *with output directions* y_{p_i}. *Let the performance weight* w_P *be a scalar stable minimum phase transfer function. Define the all-pass transfer function matrix in (3.25). Then for closed-loop stability the weighted sensitivity function must satisfy*

$$\|w_P S(s)\|_\infty \geq \max_{z_j} c_{1,j} \cdot |w_p(z_j)| \quad where \quad c_{1,j} = \|y_{z_j}^H \mathcal{B}_{po}^{-1}(G)|_{s=z_j}\|_2 \geq 1 \tag{3.31}$$

THEOREM 3.4 (MIMO COMPLEMENTARY SENSITIVITY PEAK). *Suppose the plant* $G(s)$ *has* $N_z \geq 0$ RHP-*zeros* $z_j \in \mathbb{C}_+$ *with output directions* y_{z_j} *and* $N_p \geq 1$ RHP-*poles* p_i *with output directions* y_{p_i}. *Let the performance weight* w_T *be a scalar stable minimum phase transfer function. Define the all-pass transfer function matrix in (3.26). Then for closed-loop stability the weighted complementary sensitivity function must satisfy*

$$\|w_T T(s)\|_\infty \geq \max_{p_i} c_{2,i} \cdot |w_T(p_i)| \quad where \quad c_{2,i} = \|\mathcal{B}_{zo}^{-1}(G)|_{s=p_i} y_{p_i}\|_2 \geq 1 \tag{3.32}$$

Note that $c_{1,j}$ and $c_{2,i}$ are independent of the feedback controller K and only depend on the location of RHP-zeros, poles and their directions. As we shall see in the examples, the values of $c_{1,j}$ and $c_{2,i}$ can be much larger than one when the plant has both a RHP-zero and a RHP-pole located close to each other and with some alignment in their directions.

One RHP-zero and one RHP-pole.

COROLLARY 3.1 (ONE RHP-ZERO AND ONE RHP-POLE). *Given the system* $G(s)$ *with one* RHP-*pole and one* RHP-*zero. In this case the constants* c_1 *and* c_2 *in (3.31) and (3.32) are given by the equation*

$$c = c_1 = c_2 = \sqrt{\sin^2(\phi) + \frac{|z+p|^2}{|z-p|^2} \cos^2(\phi)} \geq 1 \tag{3.33}$$

where $\phi = \cos^{-1}(|y_z^H y_p|)$.

From the condition (3.33) we clearly get a large value of $c = c_1 = c_2$ if the zero and the pole are aligned in the same direction $\phi \approx 0$, and if the zero is located close to the pole. Conversely, if the zero and the pole are aligned orthogonally to each other, then $\phi = 90°$ and $c = c_1 = c_2 = 1$, and there is no additional penalty for having both a RHP-zero and a RHP-pole.

Siso-systems. Theorems 3.3 and 3.4 become:

COROLLARY 3.2 (SISO SENSITIVITY PEAK). *Let the plant $G(s)$ be a* SISO-*system with $N_z \geq 1$* RHP-*zeros z_j and $N_p \geq 0$* RHP-*poles $p_i \in \mathbb{C}_+$. Let the performance weight w_P be a stable minimum phase transfer function. Then for closed-loop stability the weighted sensitivity function must satisfy*

$$\|w_P S(s)\|_\infty \geq \max_{z_j} c_{1,j} |w_P(z_j)| \quad where \quad c_{1,j} = \prod_{i=1}^{N_p} \frac{|z_j + \bar{p}_i|}{|z_j - p_i|} \geq 1 \qquad (3.34)$$

COROLLARY 3.3 (SISO COMPLEMENTARY SENSITIVITY PEAK). *Let the plant $G(s)$ be a* SISO-*system with $N_z \geq 0$* RHP-*zeros $z_j \in \mathbb{C}_+$ and $N_p \geq 1$* RHP-*poles p_i. Let the performance weight w_T be a stable minimum phase transfer function. Then for closed-loop stability the weighted complementary sensitivity function must satisfy*

$$\|w_T T(s)\|_\infty \geq \max_{p_i} c_{2,i} |w_T(p_i)| \quad where \quad c_{2,i} = \prod_{j=1}^{N_z} \frac{|\bar{z}_j + p_i|}{|z_j - p_i|} \geq 1 \qquad (3.35)$$

Equations (3.34) and (3.35) follow easily from Theorems 3.3 and 3.4 by setting the zero and pole directions equal to 1 and assuming that all RHP-poles are observable and all RHP-zeros are "transmission zeros".

Peaks in S and T. From Theorem 3.3 we get by selecting $w_P(s) = 1$

$$\|S(s)\|_\infty \geq \max_{\text{RHP-zeros, } z_j} c_{1,j} \qquad (3.36)$$

and from Theorem 3.4 we get by selecting $w_T(s) = 1$

$$\|T(s)\|_\infty \geq \max_{\text{RHP-poles, } p_i} c_{2,i} \qquad (3.37)$$

Thus, a peak for $\bar{\sigma}(S(j\omega))$ and $\bar{\sigma}(T(j\omega))$ larger than 1 is unavoidable if the plant has both a RHP-zero and a RHP-pole (unless their relative angle ϕ is 90°).
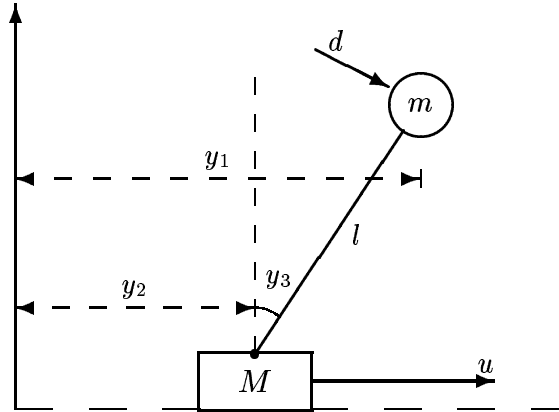
Figure 3.3: Balancing a rod in upright position

3.5 Examples

EXAMPLE 3.1 BALANCING A ROD. This example is taken from Doyle et al. (1992), and considers the problem of balancing a rod in the palm of one's hand (one dimension). The objective is to keep the rod upright, by small hand movements, based on observing the rod either at its far end (output y_1, case A) or the end in one's hand (output y_2, case B), see Figure 3.3. A linearized model of the system is given by

$$\dot{x} = Ax + Bu + B_d d; \qquad y = Cx$$

where

$$A = \begin{bmatrix} 0 & 1 & 0 & 0 \\ 0 & 0 & -gm/M & 0 \\ 0 & 0 & 0 & 1 \\ 0 & 0 & (M+m)\frac{g}{Ml} & 0 \end{bmatrix}, \quad B = \begin{bmatrix} 0 \\ 1/M \\ 0 \\ \frac{-1}{Ml} \end{bmatrix}, \quad B_d = \begin{bmatrix} 0 \\ 1/M \\ 0 \\ \frac{M+m}{Mml} \end{bmatrix} \quad \text{and} \quad C = \begin{bmatrix} 1 & 0 & l & 0 \\ 1 & 0 & 0 & 0 \\ 0 & 0 & 1 & 0 \end{bmatrix}$$

The transfer function from u to y_1 (case A) is

$$G_A(s) = \frac{-g}{s^2 \left(Mls^2 - (M+m)g \right)}$$

and from u to y_2 (case B) is

$$G_B(s) = \frac{ls^2 - g}{s^2 \left(Mls^2 - (M+m)g \right)}$$

where

- l [m] is the length of the rod,
- m [kg] is the mass of the rod,
- M [kg] is the mass of the hand and
- g [≈ 10 m/s^2] is the acceleration due to gravity.

In both cases, the plant has three unstable poles: two at the origin and one at $p = \sqrt{\frac{(M+m)g}{Ml}}$. A short rod with a large mass gives a large value of p, (the pole is far from the imaginary axis in the RHP), and this in turn means that the system is more difficult to stabilize. For example, with $M = m$ and $l = 1$ [m] we get $p = 4.5$ [rad/s], and we desire a bandwidth of about 9 [rad/s], corresponding to a response time of about 0.1 [s]. In general, to stabilize an unstable plant with the pole $p > 0$ and to get good performance, we desire a closed-loop bandwidth of approximately $2p$ (e.g. Skogestad and

Postlethwaite, 1996, eq. (5.46) page 185). If one is measuring y_1 (looking at the far end of the rod, case A), then achieving this bandwidth is the main requirement. However, if one tries to balance the rod by looking at one's hand (y_2, case B) there is also a RHP-zero at $z = \sqrt{\frac{g}{l}}$. If the mass of the rod is small (m/M is small), then p is close to z and stabilization is in practice impossible with any controller. However, even with a large mass, stabilization is very difficult because $p > z$ whereas we would normally prefer to have the RHP-zero far from the origin and the RHP-pole close to the origin ($z > p$). So, although in theory, the rod can be stabilized by looking at one's hand (case B), it seems doubtful that this is possible for a human. To quantify these problems use (3.34) or (3.35), we get

$$c_1 = c_2 = \frac{|z + p|}{|z - p|} = \frac{|1 + \gamma|}{|1 - \gamma|}, \ \gamma = \sqrt{\frac{M + m}{M}}$$

Let $g/l = 9.8$ [s^2] and consider a light weight rod with $m/M = 0.1$, for which we expect stabilization to be difficult. We obtain $c_1 = c_2 = 42$, and we must have

$$\|S_B(s)\|_\infty \geq 42 \quad \text{and} \quad \|T_B(s)\|_\infty \geq 42$$

so poor control performance is inevitable if we try to balance the rod by looking at our hand (y_2). To illustrate the difficulties with stabilization of case B compared to case A, we design $\mathcal{H}_\infty$-optimal controllers for the two cases by solving

$$\min_K \left\| \begin{bmatrix} w_P S(s) \\ w_u K S(s) \end{bmatrix} \right\|_\infty \quad \text{with} \quad w_u = 10^{-3}; \quad w_P = \frac{s/M + w_B^*}{s} \tag{3.38}$$

where $M = 1$ and $w_B^* = 1$. The weight w_P for the weighted sensitivity means that we require $\|S(s)\|_\infty$ less than one, and require tight control up to a frequency of $w_B^* = 1$ [rad/s]. Also notice the small weight on the control usage, $w_u = 10^{-3}$, which in practice means that we are minimizing $\|w_P S(s)\|_\infty$. Table 3.1 summarizes the results from the $\mathcal{H}_\infty$-designs. In Figure 3.4 the sensitivity

Table 3.1: Results for Example 3.1.

		Case A	Case B
p		3.28	3.28
z		-	3.13
$c_1 = c_2$		1	42
$\mathcal{H}_\infty$-designs using (3.38)	$\|S(s)\|_\infty$	2.55	63.41
	$\|T(s)\|_\infty$	3.16	64.35
	Stable K?	Yes	No
	$\gamma(S/KS)$	2.61	64.02

functions for both cases are plotted together with the inverse of the performance weight w_P. Notice the large peak value in $|S|$, of 63.41 in case B. An unstable controller is needed to stabilize the plant in case B, which has a RHP-zero at $z = \sqrt{g/l} \approx 3.13$. In Figure 3.5 we also consider the response to a unit impulse in d of size 0.01, which corresponds to a small push in the top end of the rod. From the impulse response we see that controller K_B fails to keep the rod in upright position when also taking into account constraints (the minimum and maximum values of the angle y_3 in case B are $y_3 = -450°$ and $y_3 = 180°$). Even when ignoring the constraints on the angle y_3, the movements are very large;
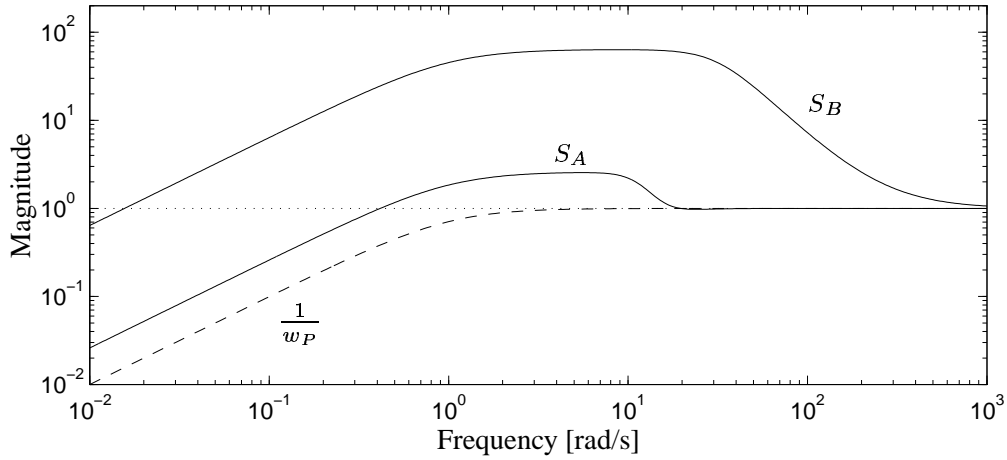
Figure 3.4: Sensitivity functions and performance weight $w_P(s)$

(a) Hand displacement y_2, [m] (b) Angle y_3, [°]
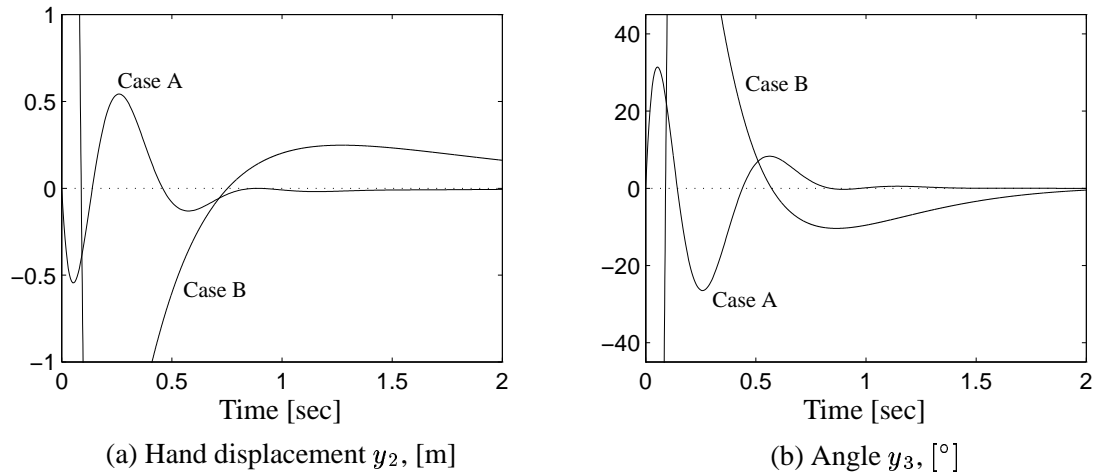
Figure 3.5: Response to impulse of size 0.01 in d

within 0.03 [sec] we need to move pretty near 8 [m] forward and then during the next 0.12 [sec] we need to move backwards about 12 [m] (ending at -4 [m]). However, by looking at the top end (case A), we see from the simulations that it is possible to balance the rod in upright position.

By increasing the weight w_u at high frequencies, we have verified that we can obtain smaller hand movements y_2, but at the cost of more oscillatory responses and larger peaks in S for both cases. By setting the weight $w_u = \frac{0.1s+1}{10s+1}10^{-4}$ and $w_P = 1$, we have managed to get the peak in S_B down to 42.26 which shows that the lower bound 42 is pretty close (remember that there are two poles at the origin in this case, so the lower bound $\|S(s)\|_\infty$ does not really apply. To avoid the poles at origin, we moved them slightly into the RHP, i.e. at $s = 10^{-4}$).

The difference between the two cases, measuring y_1 (the top end, case A) and measuring y_2 (position of the hand, case B), highlights the importance of sensor location on the achievable control performance.

EXAMPLE 3.2 RHP ZERO AND POLE WITH ALIGNMENT. We consider the following plant

$$G(s) = \begin{bmatrix} \frac{1}{s-p} & 0 \\ 0 & \frac{1}{s+p} \end{bmatrix} \underbrace{\begin{bmatrix} \cos\alpha & -\sin\alpha \\ \sin\alpha & \cos\alpha \end{bmatrix}}_{U_\alpha} \begin{bmatrix} \frac{s-z}{0.1s+1} & 0 \\ 0 & \frac{s+z}{0.1s+1} \end{bmatrix}; \quad z=2, \ p=3$$

which has a RHP-zero at $z = 2$ and a RHP-pole at $p = 3$. For $\alpha = 0°$ the rotation matrix $U_\alpha = I$, and the plant consists of two decoupled subsystems

$$G_{0°}(s) = \begin{bmatrix} \frac{s-z}{(0.1s+1)(s-p)} & 0 \\ 0 & \frac{s+z}{(0.1s+1)(s+p)} \end{bmatrix}$$

The subsystem g_{11} has both a RHP-zero and a RHP-pole, and closed-loop performance is expected to be poor. On the other hand, there are no particular control problems related to subsystem g_{22}. With $\alpha = 90°$, $U_\alpha = \begin{bmatrix} 0 & -1 \\ 1 & 0 \end{bmatrix}$, which gives

$$G_{90°}(s) = \begin{bmatrix} 0 & -\frac{s+z}{(0.1s+1)(s-p)} \\ \frac{s-z}{(0.1s+1)(s+p)} & 0 \end{bmatrix}$$

We have again two decoupled subsystems, but this time in the off-diagonal elements. The main difference is that there is no interaction between the RHP-zero and the RHP-pole in this case, so we expect this plant to be easier to control. For other values of α we do not have decoupled subsystems, and there will be some interaction between the RHP-zero and the RHP-pole. Since the pole is located at the output of the plant, its output direction is fixed, and we find $y_p = \begin{bmatrix} 1 & 0 \end{bmatrix}^T$ for all values of α. On the other hand, the zero direction changes from $\begin{bmatrix} 1 & 0 \end{bmatrix}^T$ for $\alpha = 0°$ to $\begin{bmatrix} 0 & 1 \end{bmatrix}^T$ for $\alpha = 90°$. Thus, the angle between the pole and zero direction, ϕ, will also vary between $0°$ and $90°$ as α varies from $0°$ to $90°$, as seen from Table 3.2, where we also give c_1 and c_2 for four rotation angles, $\alpha = 0°, 30°, 60°$ and $90°$. The table also shows the values of $\|S(s)\|_\infty$ and $\|T(s)\|_\infty$ using $\mathcal{H}_\infty$-optimal controllers minimizing

Table 3.2: Results for Example.

|	α	$0°$	$30°$	$60°$	$90°$
	y_z	$\begin{bmatrix} 1 \\ 0 \end{bmatrix}$	$\begin{bmatrix} 0.33 \\ -0.94 \end{bmatrix}$	$\begin{bmatrix} 0.11 \\ -0.99 \end{bmatrix}$	$\begin{bmatrix} 0 \\ 1 \end{bmatrix}$
	$\phi = \cos^{-1} |y_z^H y_p|$	$0°$	$70.9°$	$83.4°$	$90°$
	$c = c_1 = c_2$	5.0	1.89	1.15	1.0
$\mathcal{H}_\infty$-	$\|S(s)\|_\infty$	7.00	2.60	1.59	1.98
designs	$\|T(s)\|_\infty$	7.40	2.76	1.60	1.31
using	Stable K?	No	No	Yes	Yes
(3.39)	$\gamma(S/KS)$	9.55	3.53	2.01	1.59

$$\min_K \left\| \begin{bmatrix} w_P S \\ w_u KS \end{bmatrix} \right\|_\infty \quad \text{with} \quad w_u = 1; \quad w_P = (\frac{s/M + \omega_B^*}{s}) \tag{3.39}$$

where $M = 2$ and $\omega_B^* = 0.5$. The weight w_P for the weighted sensitivity means that we require $\|S(s)\|_\infty$ less than 2, and require tight control up to a frequency of about $\omega_B^* = 0.5$ [rad/s]. The

(a) Sensitivity S (b) Complementary sensitivity T
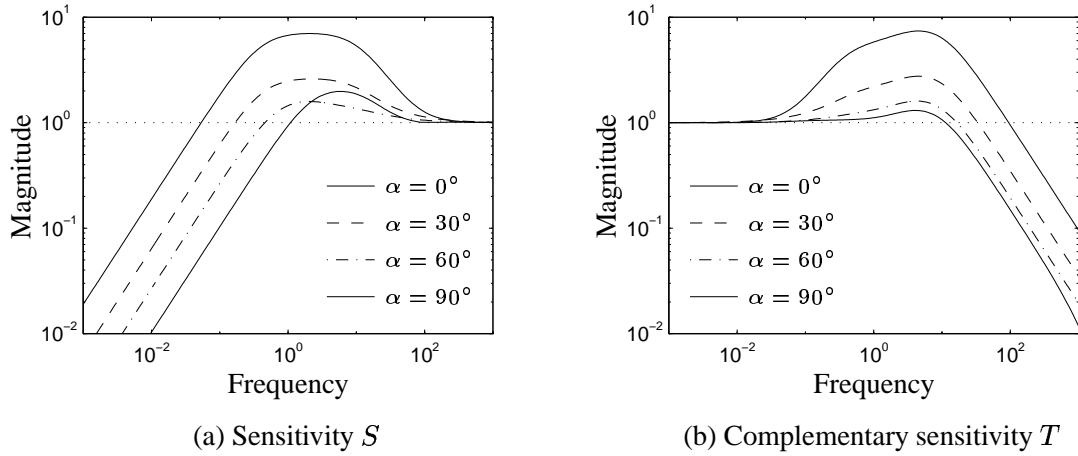
Figure 3.6: Sensitivity and complementary sensitivity functions for four angles α

minimum $\mathcal{H}_\infty$-norm for the stacked S/KS problem (3.39), is given by the value of γ in Table 3.2. Plots of the sensitivity S and the complementary sensitivity T are given in Figure 3.6. The responses to the step change in the reference $r = \begin{bmatrix} 1 & -1 \end{bmatrix}^T$ are shown in Figure 3.7. Several things are worth noting:

1) We see from the simulation for $\phi = 0°$ in Figure 3.7 that the response for y_1 is very poor. This is as expected because of the closeness of the RHP zero and pole ($z = 2, p = 3$).

2) The bound c_1 on $\|S(s)\|_\infty$ in (3.36) is tight in this case. This can be shown numerically by selecting $w_u = 0.01$, $\omega_B = 0.01$ and $M_s = 1$ (w_u and ω_B are small so the main objective is to minimize the peak of S). We find that the $\mathcal{H}_\infty$-designs for the four angles yield

α	$0°$	$30°$	$60°$	$90°$
$\|S(s)\|_\infty$	5.04	1.905	1.155	1.005
c_1	5.0	1.89	1.15	1.0

3) The angle ϕ between the zero and the pole directions, is quite different from the rotation angle α at intermediate values between $0°$ and $90°$. The reason for this is the influence of the RHP-pole in output 1, which yields a strong gain in this direction and thus tends to push the zero direction toward output 2.

4) For $\alpha = 0°$ we have $c_1 = c_2 = 5$ so $\|S(s)\|_\infty \geq 5$ and $\|T(s)\|_\infty \geq 5$, so it is clearly impossible to get $\|S(s)\|_\infty$ less than 2, as required by the performance weight w_P.

5) The $\mathcal{H}_\infty$-optimal controller is unstable for $\alpha = 0°$ and $30°$. This is not surprising because for $\alpha = 0°$, the plant is two SISO-systems, where g_{11} needs an unstable controller to stabilize it, since $p > z$.

3.6 Conclusion

We have presented lower bounds on the peak in weighted sensitivity and complementary sensitivity functions for systems with RHP zeros and poles. Peaks in the sensitivity and complementary sensitivity functions are unavoidable if the plant has both a RHP-zero and a RHP-pole with some alignment. These lower bounds on the sensitivity functions demonstrate
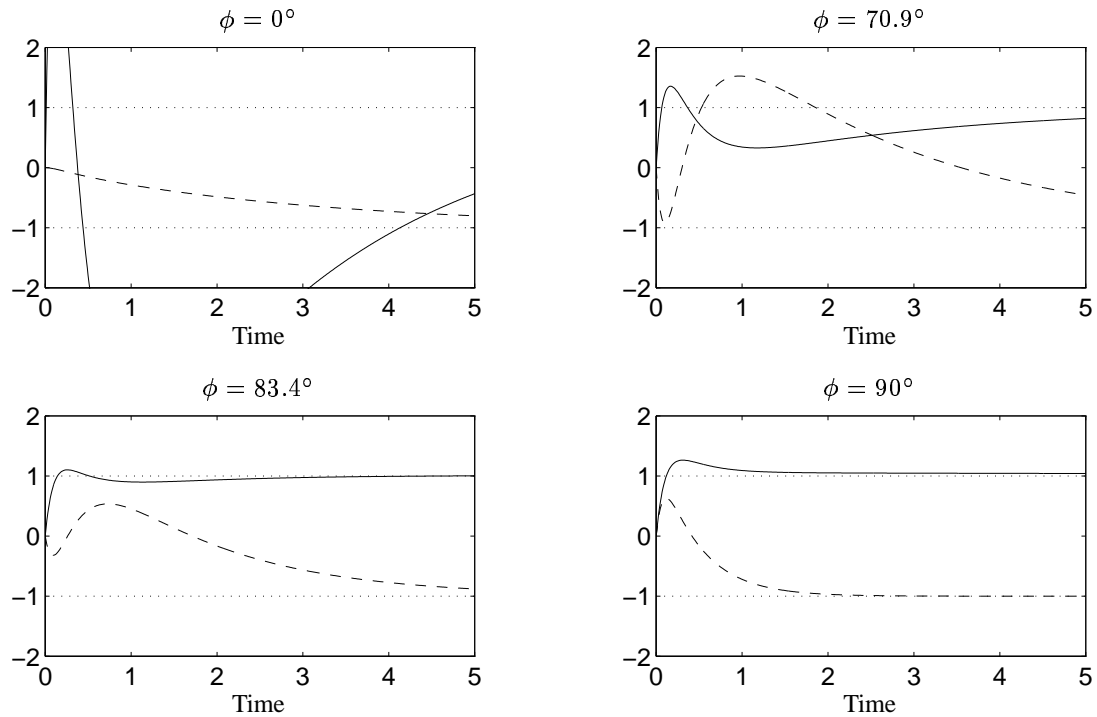
Figure 3.7: MIMO-plant with angle ϕ between the RHP-zero and the RHP-pole directions. Response to step in reference with $\mathcal{H}_\infty$-controller for four different values of ϕ. Solid line: y_1; Dashed line: y_2

the fundamental limitations imposed by open-loop characteristics as RHP zeros and poles. The intentions with the derivation of these lower bounds are:

- To derive measures which quantify the effect of open-loop RHP zeros and poles on closed-loop performance. These measures are independent of the feedback controller and the control configuration, and they therefore reflect the controllability of the plant.
- To get better understanding of the directionality of RHP zeros and poles.

We also expect that the derived bounds will be useful when selecting performance weights for controller design and analysis.

References

Anderson, B. D. O. and Moore, J. B. (1971). *Linear Optimal Control*, Prentice-Hall, Englewood Cliffs, New Jersey.

Bode, H. W. (1945). *Network Analysis and Feedback Amplifier Design*, D. Van Nostrand Co., New York.

Boyd, S. and Barratt, C. (1991). *Linear Controller Design — Limits of Performance*, Prentice-Hall, Englewood Cliffs.

Boyd, S. and Desoer, C. A. (1985). Subharmonic functions and performance bounds in linear time-invariant feedback systems, *IMA J. Math. Contr. and Info.* **2**: 153–170.

Callier, F. M. and Desoer, C. A. (1982). *Multivariable Feedback Systems*, Springer-Verlag, Berlin.

Chen, J. (1993). Sensitivity integral relations and design trade-offs in linear multivariable feedback systems, *Proc. American Control Conference*, San Francisco, CA, pp. 3160–3164.

Chen, J. (1995). Sensitivity integral relations and design trade-offs in linear multivariable feedback systems, *IEEE Transactions on Automatic Control* **AC-40**(10): 1700–1716.

Desoer, C. and Schulman, J. (1974). Zeros and poles of matrix transfer functions and their interpretation, *IEEE Transactions on Circuits and Systems* **CAS-21**(1): 3–8.

Doyle, J. C., Francis, B. and Tannenbaum, A. (1992). *Feedback Control Theory*, Macmillan Publishing Company.

Doyle, J. C. and Stein, G. (1981). Multivariable feedback design: Concepts for a classical/modern synthesis, *IEEE Transactions on Automatic Control* **AC-26**(1): 4–16.

Francis, B. A. and Zames, G. (1984). On $\mathcal{H}_\infty$ optimal sensitivity theory for SISO feedback systems, *IEEE Transactions on Automatic Control* **AC-29**(1): 9–16.

Freudenberg, J. S. and Looze, D. P. (1985). Right half plane poles and zeros and design tradeoffs in feedback systems, *IEEE Transactions on Automatic Control* **AC-30**(6): 555–565.

Freudenberg, J. S. and Looze, D. P. (1988). *Frequency Domain Properties of Scalar and Multivariable Feedback Systems*, Vol. 104 of *Lecture Notes in Control and Information Sciences*, Springer-Verlag, Berlin.

Green, M. and Limebeer, D. J. N. (1995). *Linear Robust Control*, Prentice-Hall, Englewood Cliffs.

Havre, K. and Skogestad, S. (1996). Effect of RHP zeros and poles on performance in multivariable systems, *Proc. from Control'96*, Institution of Electrical Engineers, Savoy Place, London, UK, University of Exeter, UK, pp. 930–935.

Horowitz, I. M. (1963). *Synthesis of Feedback Systems*, Academic Press, London.

Kailath, T. (1980). *Linear Systems*, Prentice-Hall, Englewood Cliffs.

Kalman, R. (1964). When is a linear control system optimal?, *Journal of Basic Engineering — Transaction on ASME — Series D* **86**: 51–60.

Kwakernaak, H. and Sivan, R. (1972). *Linear Optimal Control Systems*, Wiley Interscience, New York.

MacFarlane, A. G. J. and Karcanias, N. (1976). Poles and zeros of linear multivariable systems: A survey of algebraic, geometric and complex variable theory, *International Journal of Control* **24**(1): 33–74.

Morari, M. and Zafiriou, E. (1989). *Robust Process Control*, Prentice-Hall, Englewood Cliffs.

O'Young, S. D. and Francis, B. A. (1985). Sensitivity tradeoffs for multivariable plants, *IEEE Transactions on Automatic Control* **AC-30**(7): 625–632.

Rosenbrock, H. H. (1966). On the design of linear multivariable systems, *Third IFAC World Congress*. Paper 1A.

Rosenbrock, H. H. (1970). *State-space and Multivariable Theory*, Nelson, London.

Skogestad, S. and Postlethwaite, I. (1996). *Multivariable Feedback Control, Analysis and Design*, John Wiley & Sons, Chichester.

Wall, J. E., Doyle, J. C. and Harvey, C. A. (1980). Tradeoffs in the design of multivariable feedback systems, *Proceedings of 18th Allerton Conference*, pp. 715–725.

Zames, G. (1981). Feedback and optimal sensitivity: model reference transformations, multiplicative seminorms, and approximate inverses, *IEEE Transactions on Automatic Control* **AC-26**(2): 301–320.

Zames, G. and Bensoussan, D. (1983). Multivariable feedback, sensitivity, and decentralized control, *IEEE Transactions on Automatic Control* **AC-28**(11): 1030–1035.

Zames, G. and Francis, B. A. (1983). Feedback, minimax sensitivity, and optimal robustness, *IEEE Transactions on Automatic Control* **AC-28**(5): 585–600.

Zhou, K., Doyle, J. C. and Glover, K. (1996). *Robust and Optimal Control*, Prentice-Hall, Upper Saddle River.

Appendix A Proofs of the results

Proof of Lemma 3.1. For $s = p$ we have, $G(p) = C(pI - A)^{-1}B + D$. Since p is an eigenvalue of A and x_{po} is the eigenvector corresponding to the pole p, $(pI - A)x_{po} = 0$. Therefore x_{po} is the output state direction with infinite gain for $(pI - A)^{-1}$. The normalized output pole direction becomes $y_p = Cx_{po}/\|Cx_{po}\|_2$ as long as $\|D\|$ is finite. The input pole direction u_p follows similarly as the conjugate of the output direction of the transposed system G^T.   □

Proof of (3.22). The output direction is given by $y_z^H G(z) = 0$. For internal stability the controller cannot cancel the RHP-zero and it follows that $L = GK$ has a RHP-zero in the same direction, i.e. $y_z^H L(z) = 0$. Then, we have that $S = (I + L)^{-1}$ is stable and thus has no RHP-pole at $s = z$. It then follows from $T = LS$ that $y_z^H T(z) = 0$ and $y_z^H(I - S(z)) = 0 \iff y_z^H = y_z^H S(z)$.   □

Proof of (3.23). The square matrix $L(s) = GK(s)$ has a RHP-pole at $s = p$, and if we assume that $L(s)$ has no RHP-zero at $s = p$, then $L^{-1}(p)$ exists, and the output pole direction y_p is given by $L^{-1}(p)y_p = 0$. Since T is stable, it has no RHP-pole at $s = p$, so $T(p)$ is finite. It then follows from $S = TL^{-1}$ that $S(p)y_p = T(p)L^{-1}(p)y_p = 0$ and that $T(p)y_p = (I - S(p))y_p = y_p$.   □

Proof of Theorem 3.1. Introduce the scalar function

$$f(s) = y_z^H w_P(s)S(s)y_z$$

which is analytic in the RHP. We then have

$$\|w_P S(s)\|_\infty \geq \|f(s)\|_\infty \geq |f(z)| = |w_P(z)| \tag{3.40}$$

The first inequality follows since the singular value measures the maximum gain of a matrix and is independent of direction, so $\bar{\sigma}(A) \geq \|Aw\|_2$ and $\bar{\sigma}(A) \geq \|wA\|_2$ for any vector w with $\|w\|_2 = 1$. The second inequality follows from the maximum modulus theorem. The final equality follows since $w_P(s)$ is a scalar and from the interpolation constraint $y_z^H S(z) = y_z^H$ we get $y_z^H S(z)y_z = y_z^H y_z = 1$.
□

Proof of Theorem 3.2. Introduce the scalar function

$$f(s) = y_p^H w_T(s) T(s) y_p$$

which is analytic in the RHP since $w_T T(s)$ is stable. We then have

$$\|w_T T(s)\|_\infty \geq \|f(s)\|_\infty \geq |f(p)| = |w_T(p)| \tag{3.41}$$

The first inequality follows since the singular value measures the maximum gain of a matrix independent of direction and $\|y_p\|_2 = 1$. The second inequality follows from the maximum modulus theorem. The final equality follows since $w_T(s)$ is a scalar and from the interpolation constraint $T(p)y_p = y_p$ we get $y_p^H T(p) y_p = y_p^H y_p = 1$. $\qquad\square$

Proof of Theorem 3.3. We consider one RHP-zero z with output direction y_z at a time (the subscript j is omitted). Factorize the N_p RHP-poles p_i in $G(s) = \mathcal{B}_{po}^{-1}(G) G_{so}(s)$, where $\mathcal{B}_{po}^{-1}(G)$ is given by (3.25). It follows that $G_{so}(s)$ is stable, $\mathcal{B}_{po}(G)$ has all singular values and absolute value of all eigenvalues equal to one for $s = j\omega$ and $\bar\sigma(\mathcal{B}_{po}^{-1}(G(s))) \geq 1$ whenever $\text{Re}(s) \geq 0$, see Lemma A.1 in Appendix A. The loop transfer function can then be written

$$L(s) = GK(s) = \mathcal{B}_{po}^{-1} G_{so} K(s) \triangleq \mathcal{B}_{po}^{-1}(G) L_m(s)$$

then

$$S = TL^{-1} = TL_m^{-1}(s)\mathcal{B}_{po}(G(s)) \triangleq S_m \mathcal{B}_{po}(G(s))$$

Introduce the scalar function $f(s) = y_z^H w_P(s) S_m(s) y$ which is analytic (stable) in RHP. We want to choose y so that $|f(s)|$ obtains maximum

$$J(s) = \max_{\|y\|_2 = 1} |f(s)| = \max_{\|y\|_2 = 1} |y_z^H w_P(s) S_m(s) y|$$

We get

$$\|w_P S(s)\|_\infty = \|w_P S_m(s)\|_\infty \geq \|J(s)\|_\infty \geq |J(z)| = \max_{\|y\|_2=1} |w_P(z)| \cdot |y_z^H \mathcal{B}_{po}^{-1}(G)|_{s=z} y|$$

$$= |w_P(z)| \cdot \|y_z^H \mathcal{B}_{po}^{-1}(G)|_{s=z}\|_2 \tag{3.42}$$

The first equality follows since $\mathcal{B}_{po}^{-1}(G(s))$ is all-pass for $s = j\omega$. The first inequality follows since the singular value measures the maximum gain of a matrix independent of direction, so $\bar\sigma(A) \geq \|Aw\|_2$ and $\bar\sigma(A) \geq \|wA\|_2$ for any vector w with $\|w\|_2 = 1$. The second inequality follows from the maximum modulus theorem. The second equality follows from

$$y_z^H S_m(z) = y_z^H S(z)\mathcal{B}_{po}^{-1}(G)|_{s=z} = y_z^H \mathcal{B}_{po}^{-1}(G)|_{s=z}$$

and the fact that $w_P(s)$ is a scalar. The last equality follows from the fact that the largest singular value measures the largest gain and is equivalent to the two-norm. The fact that $c_{1,j} \geq 1$ follows from $\sigma_i(\mathcal{B}_{po}^{-1}(G(s))) \geq 1 \; \forall i$ when $\text{Re}(s) \geq 0$, Lemma A.1 in Appendix A. $\qquad\square$

Proof of Theorem 3.4. We consider one RHP-pole p with output direction y_p at a time (the subscript i is omitted). Factorize the N_z RHP-zeros z_i in $G(s) = \mathcal{B}_{zo}(G) G_{mo}(s)$, where $\mathcal{B}_{zo}(G)$ is given by (3.26). It follows that $G_{mo}(s)$ is minimum phase, $\mathcal{B}_{zo}(G)$ has all singular values and absolute value of all eigenvalues equal to one for $s = j\omega$, see Lemma A.1 in Appendix A. The loop transfer function becomes

$$L(s) = GK(s) = \mathcal{B}_{zo}(G) G_{mo} K(s) \triangleq \mathcal{B}_{zo}(G) L_m(s)$$

then

$$T = LS = \mathcal{B}_{zo}(G)\, L_m S \triangleq \mathcal{B}_{zo}(G)\, T_m$$

Introduce the scalar function $f(s) = y^H w_T T_m(s) y_p$ which is analytic in RHP. We want to choose y so that $|f(s)|$ obtains maximum

$$J(s) = \max_{\|y\|_2=1} |f(s)| = \max_{\|y\|_2=1} |y^H w_T(s) T_m(s) y_p|$$

We get

$$\|w_T T(s)\|_\infty = \|w_T T_m(s)\|_\infty \geq \|J(s)\|_\infty \geq |J(p)| = \max_{\|y\|_2=1} |w_T(p)| \cdot |y^H \mathcal{B}_{zo}^{-1}(G)|_{s=p} y_p|$$

$$= |w_T(p)| \cdot \|\mathcal{B}_{zo}^{-1}(G)|_{s=p} y_p\|_2 \tag{3.43}$$

The first equality follows since $\mathcal{B}_{zo}(G(s))$ is all-pass for $s = j\omega$. The first inequality follows since the singular value measures the maximum gain of a matrix and is independent of direction, so $\bar{\sigma}(A) \geq \|Aw\|_2$ and $\bar{\sigma}(A) \geq \|wA\|_2$ for any vector w with $\|w\|_2 = 1$. The second inequality follows from the maximum modulus theorem. The second equality follows from $T_m(p) y_p = \mathcal{B}_{zo}^{-1}(G)|_{s=p} T(p) y_p = \mathcal{B}_{zo}^{-1}(G)|_{s=p} y_p$. The last equality follows from the fact that the largest singular value measures the largest gain and is equivalent to the two-norm. The fact that $c_{2,i} \geq 1$ follows from $\sigma_j(\mathcal{B}_{zo}^{-1}(G(s))) \geq 1\ \forall j$ when $\mathrm{Re}(s) \geq 0$. $\square$

Proof of $c = c_1 = c_2$ in Corollary 3.1. Note that when $N_z = N_p = 1$ both z and p are real and positive, so $\bar{z} = z$ and $\bar{p} = p$. Consider c_2

$$c_2 = \left\|(I + \frac{2\mathrm{Re}(z)}{p-z} y_z y_z^H) y_p\right\|_2 = \left\|[\,U \quad y_z\,] \begin{bmatrix} I & 0 \\ 0 & \frac{p+\bar{z}}{p-z} \end{bmatrix} \begin{bmatrix} U^H \\ y_z^H \end{bmatrix} y_p \right\|_2$$

$$= \left\|UU^H y_p + \frac{p+\bar{z}}{p-z} y_z y_z^H y_p\right\|_2 = \sqrt{\sin^2(\phi) + \frac{|\bar{z}+p|^2}{|z-p|^2}\cos^2(\phi)} \tag{3.44}$$

The matrix U contains a basis for the orthogonal subspace to y_z, $y_z^\perp$. The angle between y_p and $y_z^\perp$ is $90 - \phi$, $\cos(90 - \phi) = \sin(\phi)$ and (3.44) follows. We can interpret (3.44) as a weighted projection of y_p on the subspaces $y_z^\perp$, with weight 1, and y_z, with weight $\frac{|\bar{z}+p|^2}{|z-p|^2}$. In (Boyd and Desoer, 1985, eq. (3.15) on p. 164) it is the projection on the orthogonal subspace $y_z^\perp$ which lacks.

The constant c_1 can be written in a similar way

$$c_1 = \left\|y_z^H (I + \frac{2\mathrm{Re}(p)}{z-p} y_p y_p^H)\right\|_2 = \left\|y_z^H [\,V \quad y_p\,] \begin{bmatrix} I & 0 \\ 0 & \frac{z+\bar{p}}{z-p} \end{bmatrix} \begin{bmatrix} V^H \\ y_p^H \end{bmatrix}\right\|_2$$

$$= \left\|y_z^H VV^H + \frac{z+\bar{p}}{z-p} y_z^H y_p y_p^H\right\|_2 = \sqrt{\sin^2(\phi) + \frac{|z+\bar{p}|^2}{|z-p|^2}\cos^2(\phi)} \tag{3.45}$$

$$\square$$

Chapter 4

Performance limitations for unstable SISO plants

Kjetil Havre* and Sigurd Skogestad†

Chemical Engineering,
Norwegian University of Science and Technology
N-7034 Trondheim, Norway.

*Also affiliated with: Institute for energy technology, P.O.Box 40, N-2007 Kjeller, Norway, Fax: (+47) 63 81 11 68, E-mail: Kjetil.Havre@ife.no.
†Fax: (+47) 73 59 40 80, E-mail: skoge@chembio.ntnu.no.

Abstract

This paper examines the fundamental limitations on closed-loop performance imposed by instability in the plant (Right Half Plane (RHP) poles). The main limitation is that instability requires active use of plant inputs, and we quantify this in terms of tight lower bounds on the input magnitudes required for disturbance and measurement noise rejection. These new bounds involve the $\mathcal{H}_\infty$-norm, which has direct engineering significance. The output performance in terms of disturbance rejection or reference tracking is *only* limited if the plant has RHP-zeros, and for a one degree-of-freedom controller the presence of RHP-poles further deteriorate the response, whereas there is no additional penalty for having RHP-poles if we use a two degrees-of-freedom controller. It is important to stress that the derived bounds are controller independent and that they are tight, meaning that there exist controllers which achieve the lower bounds.

4.1 Introduction

An unstable plant can only be stabilized by use of feedback control which implies active use of the plant inputs. If measurement noise and/or disturbances are present (which is always the case in practical process control), then the input usage may become unacceptable.

In this paper, the above statements are quantified by deriving tight lower bounds on the $\mathcal{H}_\infty$-norm of the closed-loop transfer functions SV and TV, where S and T are the sensitivity and complementary sensitivity functions. The transfer function V can be viewed as a *generalized* "weight", which for our purpose should be independent of the feedback controller K.

Some reasons for deriving such bounds are:

1) The lower bounds provide direct insights to the limitations imposed by RHP zeros and poles in Single Input Single Output (SISO) systems.
2) The lower bounds derived are independent of the controller, so they can be used as controllability measures.
3) In some cases we can show that the bounds are tight. This implies that we in these cases can find a controller K, analytically, which achieves an $\mathcal{H}_\infty$-norm of the closed-loop transfer function equal to the lower bound.
4) We can *quantify*, in terms of the $\mathcal{H}_\infty$-norm, the "best achievable" closed-loop effect of the worst case disturbance, measurement noise and references both at the input and at the output of the plant.

One important application is that we can quantify the minimum input usage for stabilization in the presence of worst case measurement noise and disturbances. Even for SISO-systems this has been a difficult task, which has not been solved analytically until now.

To give the reader some appreciation of the basis of the bounds and their usefulness, we consider as a motivating example, an unstable plant with a RHP-pole p. We want to obtain a lower bound on the $\mathcal{H}_\infty$-norm of the closed-loop transfer function KS from measurement noise n to plant input u. We first rewrite $KS = G^{-1}T$, which is on the form TV with $V = G^{-1}$. The basis of our bound is the use of the maximum modulus principle and the "interpolation constraint" $T(p) = 1$, which must apply to achieve internal stability. We obtain (see Theorem 4.1 for details)

$$\left\| KS(s) \right\|_\infty = \left\| G^{-1}T(s) \right\|_\infty \geq |G_s^{-1}(p)|$$

where G_s is the "stable" version of G (with the RHP-poles mirrored into the LHP). As an example, consider the plant $G(s) = \frac{1}{s-10}$, which has an unstable pole $p = 10$. We obtain $G_s(s) = \frac{1}{s+10}$. For *any* linear feedback controller K, we find that the lower bound

$$\left\| KS(s) \right\|_\infty \geq |G_s^{-1}(p)| = 2p = 20$$

must be satisfied. Thus, if we require that the plant inputs are bounded with $\|u\|_\infty \leq 1$, then we cannot allow the magnitude of measurement noise to exceed $\|n\|_\infty = 1/20 = 0.05$.

The basis for our results is the *important* work by Zames (1981), who made use of the interpolation constraint $S(z) = 1$ and the maximum modulus theorem to derive bounds on

the $\mathcal{H}_\infty$-norm of S for plants with one RHP-zero. Subsequently, these results were extended to unstable plants with one RHP-pole and then to plants with combined RHP zeros and poles, e.g. (Doyle et al., 1992, pp. 93–95) and (Skogestad and Postlethwaite, 1996).

However, these generalizations to unstable plants did *not* consider the input usage which involves the closed-loop transfer function KS. An important contribution of this paper is therefore to use the "trick" $KS = G^{-1}T$, which enables us to derive lower bounds on input usage, by using the general lower bound on $\|TV(s)\|_\infty$ with $V = G^{-1}$. But when G is unstable (with RHP-pole p), then $V = G^{-1}$ has a RHP-zero for $s = p$. A second important contribution compared to earlier work, is the ability to include RHP zeros and poles in the "weight" V (under the assumption that SV and TV are stable).

A third important contribution is that we show that the lower bounds are *tight*. That is, we give analytical expressions for controllers which *achieve* an $\mathcal{H}_\infty$-norm of the closed-loop transfer function which is equal to the lower bound.

Several authors, among them Kwakernaak (1995), have noted the symmetries between sensitivity and complementary sensitivity and the roles of RHP zeros and poles of G. In this paper, the symmetries are also reflected in where performance is measured. We find that RHP-zeros of G pose limitations on performance measured at the *output* of the plant, whereas RHP-poles of G pose limitations on performance measured at the *input* of the plant (input usage).

The bounds on $\|S(s)\|_\infty$ for plants with RHP-zero derived by Zames (1981) are also valid for multivariable systems. It is important to note that all the results given in this paper have been generalized to multivariable systems (see Chapter 5). However, the notation becomes complicated in the multivariable case, with the result that it is difficult to understand the implications of the bounds. In the SISO case, the bounds may easily be derived by hand for a particular plant. However, in the multivariable case, we must in general evaluate the bounds numerically.

The paper is organized as follows: First we introduce the notation and present some basics from linear control theory. In Section 4.3 we derive the general lower bounds on $\|SV(s)\|_\infty$ and $\|TV(s)\|_\infty$, and in Section 4.4 we prove the tightness of the lower bounds. In Section 4.5 we show some applications and implications of the lower bounds both on output performance, input usage, peaks in sensitivity and complementary sensitivity, and we give some simple examples to illustrate the applications and the implications. In Section 4.6 we discuss briefly the relationship to stabilization with input constraints. In Section 4.7 we derive a lower bound applicable to two degrees-of-freedom (2-DOF) control. The proofs of the results which are not given in the main text, are given in Section A.

4.2   Basics from linear control theory

We consider linear time invariant transfer function models on the form

$$y(s) = G(s)u(s) + G_d(s)d(s) \tag{4.1}$$

where u is the manipulated input, d is the disturbance, y is the output, G is the SISO plant model and G_d is the SISO disturbance plant model. The measured output is $y_m = y + n$

where n is the measurement noise.

The $\mathcal{H}_\infty$-norm of a stable rational transfer function $M(s)$ is defined as the peak value in the magnitude $|M(j\omega)|$ over all frequencies.

$$\|M(s)\|_\infty \triangleq \sup_\omega |M(j\omega)| \tag{4.2}$$

4.2.1 Zeros and poles

In a rational transfer function M the zeros and poles are the roots of the numerator and denominator polynomials. That is, the zeros z_j and the poles p_i are the solutions to the following equations

$$M(z_j) = 0 \quad \text{and} \quad M^{-1}(p_i) = 0 \tag{4.3}$$

When we refer to zeros and poles, we mean the zeros and poles of the plant G unless otherwise explicitly stated. The set of complex numbers s where $\text{Re}(s) > 0$ is denoted $\mathbb{C}_+$, and we refer to this set as the open right half plane (open RHP). Zeros and poles in the open RHP are zeros and poles with real part greater than zero, i.e. $\text{Re}(z) > 0$ and $\text{Re}(p) > 0$.

4.2.2 Factorizations of RHP zeros and poles

A rational transfer function $M(s)$ with zeros z_j and poles p_i in the open RHP, $\{z_j, p_i\} \in \mathbb{C}_+$, can be factorized in *Blaschke products* as follows[1]

$$M(s) = \mathcal{B}_z(M)\, M_m(s) \tag{4.4}$$
$$M(s) = \mathcal{B}_p^{-1}(M)\, M_s(s) \tag{4.5}$$
$$M(s) = \mathcal{B}_z(M)\, \mathcal{B}_p^{-1}(M)\, M_{ms}(s) \tag{4.6}$$

where

M_m – Minimum phase (subscript m) version of M with the RHP-zeros mirrored across the imaginary axis.

M_s – Stable (subscript s) version of M with the RHP-poles mirrored across the imaginary axis.

M_{ms} – Minimum phase, stable (subscript ms) version of M with the RHP zeros and poles mirrored across the imaginary axis.

$\mathcal{B}_z(M)$ – Stable all-pass rational transfer function $\left(|\mathcal{B}_z(M)|_{s=j\omega} = 1, \forall\omega\right)$ containing the RHP-zeros (subscript z) of M.

$\mathcal{B}_p(M)$ – Stable all-pass rational transfer function $\left(|\mathcal{B}_p(M)|_{s=j\omega} = 1, \forall\omega\right)$ containing the RHP-poles (subscript p) of M as RHP-zeros.

---

[1]Note that the notation on the all-pass factorizations of RHP zeros and poles used in this paper is reversed compared to the notation used in (Skogestad and Postlethwaite, 1996; Havre and Skogestad, 1997a). The reason for this change of notation is to get consistent with what the literature generally defines as an all-pass filter.

(a) on RHP-zeros z (b) on RHP-poles p (c) on RHP zeros and poles
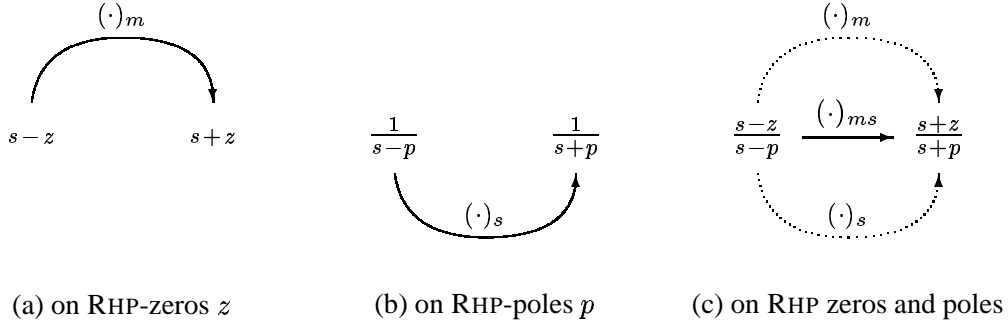
Figure 4.1: Operations on RHP zeros and poles for scalar transfer functions

The all-pass filters are

$$\mathcal{B}_z(M(s)) \quad = \quad \prod_{j=1}^{N_z} \frac{s - z_j}{s + \bar{z}_j} \tag{4.7}$$

$$\mathcal{B}_p(M(s)) \quad = \quad \prod_{i=1}^{N_p} \frac{s - p_i}{s + \bar{p}_i} \tag{4.8}$$

where N_z is the number of RHP-zeros $z_j \in \mathbb{C}_+$ and N_p is the number of RHP-poles $p_i \in \mathbb{C}_+$ in M. In most cases $M = G$ and to simplify the notation we often omit to show that the all-pass filters are dependent on G, i.e. we write $\mathcal{B}_p(s)$ and $\mathcal{B}_z(s)$ in the meaning of $\mathcal{B}_p(G(s))$ and $\mathcal{B}_z(G(s))$.

Figure 4.1 demonstrates the operations, $(\cdot)_m$ for RHP-zeros, $(\cdot)_s$ for RHP-poles and the combined operator $(\cdot)_{ms}$ of scalar transfer functions. The order of the two operations $(\cdot)_m$ and $(\cdot)_s$ in the combined operator $(\cdot)_{ms}$ is arbitrary. It also follows that

$$(M^{-1})_{ms} = (M_{ms})^{-1} = M_{ms}^{-1} \tag{4.9}$$

We use M_m^{-1} to denote $(M_m)^{-1}$, i.e. $M_m^{-1} = (M_m)^{-1}$. Similarly we use $M_s^{-1} = (M_s)^{-1}$. We note that

$$\|M(s)\|_\infty = \|M_m(s)\|_\infty = \|M_{ms}(s)\|_\infty \tag{4.10}$$

The first identity follows since $|\mathcal{B}_z(M)|_{s=j\omega} = 1$, $\forall \omega$, and the latter identity follows since M is stable, i.e. $M_{ms} = M_m$ and $\mathcal{B}_p(M_m) = \mathcal{B}_p(M) = 1$.

To prove the main results in this paper, we make use of the following Lemma.

LEMMA 4.1. *Consider a stable* SISO *transfer function AB which can be expressed by the product of the* SISO *transfer functions A and B, where both A and B may be unstable. Then*

$$\|AB\|_\infty = \|(AB)_m\|_\infty = \|A_{ms}B_{ms}\|_\infty \tag{4.11}$$

4.2.3   Closing the loop

A typical control problem is shown in Figure 4.2. In the figure possible performance weights
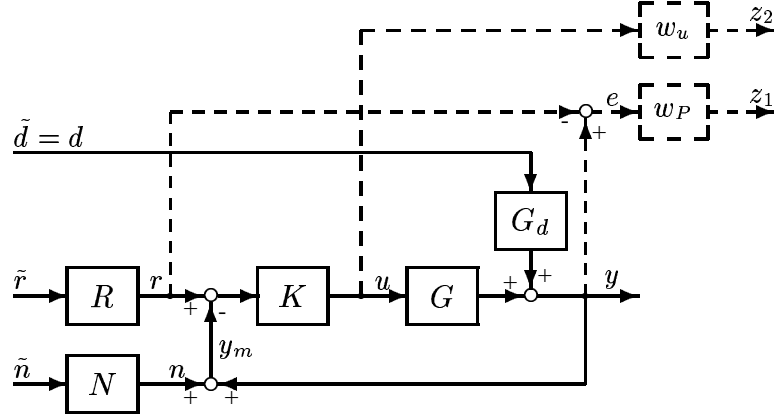
Figure 4.2: One degree-of-freedom control configuration

are given in dashed lines. Mainly for simplicity, but also because it is most practically relevant, we assume that the performance weights w_P and w_u have no zeros and poles in $\mathbb{C}_+$. If integrators (poles at $s = 0$) are present in w_P and w_u, then we need the same number of integrators in $L = GK$, to have a stable closed-loop transfer function. In Figure 4.2 we have included both the reference r and the measurement noise n, in addition to disturbances d as external inputs. The transfer functions, G_d, R and N can be viewed as weights on the inputs, and the inputs: $\tilde{d}$, $\tilde{r}$ and $\tilde{n}$ are normalized in magnitude. Normally, N is the inverse of signal to noise ratio. For most practical purposes, we can assume that R and N are stable. However, from the technical point of view it suffices that the unstable modes in N and R can be stabilized through the input u.

We apply negative feedback control

$$u = K(r - y_m) = K(r - y - n) \tag{4.12}$$

The closed-loop transfer function F from

$$v = \begin{bmatrix} \tilde{r} \\ \tilde{d} \\ \tilde{n} \end{bmatrix} \quad \text{to} \quad z = \begin{bmatrix} z_1 \\ z_2 \end{bmatrix} = \begin{bmatrix} w_P(y - r) \\ w_u u \end{bmatrix}$$

is

$$F(s) = \begin{bmatrix} -w_P SR & w_P SG_d & -w_P TN \\ w_u SKR & -w_u KSG_d & -w_u KSN \end{bmatrix} \tag{4.13}$$

where the sensitivity S and the complementary sensitivity T are defined as

$$S \triangleq (1 + GK)^{-1} = \frac{1}{1 + GK} \tag{4.14}$$

$$T \triangleq 1 - S = \frac{GK}{1 + GK} \tag{4.15}$$

To have good control performance (keep z_1 small) with a small input usage (keep z_2 small), we need to have $\|F(s)\|_\infty$ small. That is we want all the SISO transfer functions in (4.13)

small. In addition, there are robustness issues. For example, we wish to have $\|w_{\mathrm{unc}}T(s)\|_\infty$ small, where w_{unc} is the magnitude of the relative plant uncertainty.

The first requirement for being able to satisfy all these objectives (e.g. having all seven transfer functions mentioned above small), is that the weights w_P, w_u and w_{unc} are such that the objectives can be achieved. For example, since $S + T = 1$ we cannot have $w_P R$ and w_{unc} large *at the same frequency* if we want to have $\|w_P S R(s)\|_\infty$ (tight control of setpoint changes) and $\|w_{\mathrm{unc}}T(s)\|_\infty$ (the closed-loop response is insensitive to plant uncertainty) small. However, the presence of RHP zeros and poles in the plant G provide additional limitations, which are the focus of this paper.

4.2.4   Interpolation constraints

If G has a RHP-zero z or a RHP-pole p, then for internal stability of the feedback system the following interpolation constraints must apply (e.g. Skogestad and Postlethwaite, 1996):

$$T(z) = 0; \qquad S(z) = 1 \qquad\qquad (4.16)$$

$$S(p) = 0; \qquad T(p) = 1 \qquad\qquad (4.17)$$

Similar interpolation constraints apply to S and T if the feedback controller K has RHP zeros or poles.

4.3   Lower bounds on the $\mathcal{H}_\infty$-norm of closed-loop transfer functions

In this section we will give the main results, which are lower bounds on the $\mathcal{H}_\infty$-norm of closed-loop transfer functions which can be written on the forms TV or SV. The generalized "weight" V is assumed to be independent of the feedback controller K. V may be unstable but TV and SV must be stable. That is, it must be possible to stabilize all transfer functions by controlling the output y using the input u.

Some examples. Consider the six transfer functions in (4.13). The first two can be written on the form SV by selecting $V_{11} = w_P R$ and $V_{12} = w_P G_d$. The remaining four can be written on the form TV by selecting $V_{13} = w_P N$, $V_{21} = w_u G^{-1} R$, $V_{22} = w_u G^{-1} G_d$ and $V_{23} = w_u G^{-1} N$. From this we see that the "weight" V may be unstable (if one or both of G_d and G^{-1} are unstable) and may contain RHP-zeros (if one or both of G_d and G^{-1} contain RHP-zeros).

In the first result, which is the lower bound on $\|TV(s)\|_\infty$, we consider any number of RHP-zeros in the plant G and one RHP-pole at a time. Then, by maximizing over all RHP-poles in the plant G, we find the largest lower bound on $\|TV(s)\|_\infty$ which takes into account one RHP-pole and all RHP-zeros in the plant G.

THEOREM 4.1 (LOWER BOUND ON $\|TV(s)\|_\infty$). *Consider the* SISO *plant G with $N_z \geq 0$* RHP-*zeros $z_j \in \mathbb{C}_+$ and $N_p \geq 1$* RHP-*poles p_i. Let V be a rational transfer function,*

and assume that TV is (internally) stable. Then the following lower bound on $\|TV(s)\|_\infty$ applies:

$$\|TV(s)\|_\infty \geq \max_{\text{RHP-poles},\, p_i} |\mathcal{B}_z^{-1}(p_i)| \cdot |V_{ms}(p_i)| \tag{4.18}$$

where $\mathcal{B}_z(s)$ is the all-pass factor containing the RHP-zeros of $G(s)$.

Some remarks on Theorem 4.1 are given following Theorem 4.2.

Proof of Theorem 4.1.

1) **Factor out RHP zeros and poles in T and V.** Lemma 4.1 gives

$$\|TV(s)\|_\infty = \|T_{ms}V_{ms}(s)\|_\infty = \|T_m V_{ms}(s)\|_\infty$$

where the last equality holds since T is stable, i.e. $T_{ms} = T_m$.

2) **Introduce the stable scalar function $f(s) = T_m(s)V_{ms}(s)$.**

3) **Apply the maximum modulus theorem to $f(s)$ at the RHP-poles p_i of G.**

$$\|f(s)\|_\infty \geq |f(p_i)|$$

4) **Resubstitute the factorization of RHP-zeros in T**, i.e. use $T_m(s) = T(s)\mathcal{B}_z^{-1}(s)$, where $\mathcal{B}_z(s)$ contains the RHP-zeros of G, which due to internal stability also must be RHP-zeros of T. This gives

$$f(p_i) = T(p_i)\mathcal{B}_z^{-1}(p_i)V_{ms}(p_i)$$

5) **Use the interpolation constraint (4.17) for RHP-poles p_i in G**, i.e. use $T(p_i) = 1$.

6) **Evaluate the lower bound.**

$$|f(p_i)| = |\mathcal{B}_z^{-1}(p_i)| \cdot |V_{ms}(p_i)|$$

Note that $f(p_i)$ is independent of the controller K if V is independent of K.

Since these steps hold for all RHP-poles p_i, Theorem 4.1 follows. $\qquad\qquad\square$

In the next result, which is the lower bound on $\|SV(s)\|_\infty$, we consider any number of RHP-poles in the plant G and one RHP-zero at a time. Then, by maximizing over all RHP-zeros in the plant G, we find the largest lower bound on $\|SV(s)\|_\infty$ which takes into account one RHP-zero and all RHP-poles.

THEOREM 4.2 (LOWER BOUND ON $\|SV(s)\|_\infty$). *Consider the SISO plant G with $N_z \geq 1$ RHP-zeros z_j and $N_p \geq 0$ RHP-poles $p_i \in \mathbb{C}_+$. Let V be a rational transfer function, and assume that SV is (internally) stable. Then the following lower bound on $\|SV(s)\|_\infty$ applies:*

$$\|SV(s)\|_\infty \geq \max_{\text{RHP-zeros},\, z_j} |\mathcal{B}_p^{-1}(z_j)| \cdot |V_{ms}(z_j)| \tag{4.19}$$

where $\mathcal{B}_p(s)$ is the all-pass factor containing the RHP-poles of $G(s)$.

Remarks on Theorems 4.1 and 4.2:

1) The bound on $\|TV(s)\|_\infty$ is caused by the RHP-poles p_i in G, and the term

$$|\mathcal{B}_z^{-1}(p_i)| = \prod_{j=1}^{N_z} \frac{|p_i + \bar{z}_j|}{|p_i - z_j|} \geq 1 \qquad (4.20)$$

gives an additional penalty for plants which also have RHP-zeros. For the case when G has *no* RHP-zeros, then $\mathcal{B}_z^{-1}(p_i) = 1$. If one or more RHP-zeros are close to the RHP-pole p_i, then $|\mathcal{B}_z^{-1}(p_i)|$ is much larger than one.

2) The bound on $\|SV(s)\|_\infty$ is caused by the RHP-zeros z_j in G, and the term

$$|\mathcal{B}_p^{-1}(z_j)| = \prod_{i=1}^{N_p} \frac{|z_j + \bar{p}_i|}{|z_j - p_i|} \geq 1 \qquad (4.21)$$

gives an additional penalty for plants which also have RHP-poles. For the case when G has *no* RHP-poles, then $\mathcal{B}_p^{-1}(z_j) = 1$. If one or more RHP-poles are located close to the RHP-zero z_j, then $|\mathcal{B}_p^{-1}(z_j)|$ is much larger than one.

3) The bounds (4.18) and (4.19) are independent of the feedback controller K if the weight V is independent of K (we always assume that V is independent of K).

4) The assumptions that TV and SV are internally stable, means that TV and SV are stable, and we have no RHP pole/zero cancellations between G and K.

5) The lower bounds on $\|TV(s)\|_\infty$ and $\|SV(s)\|_\infty$ involve V_{ms}. Thus, we get the same result if the "weight" V is replaced by its stable minimum phase counterpart with the same magnitude V_{ms}. Note that for $V = V^1 V^2$ we have

$$\|TV(s)\|_\infty = \|T_m V_{ms}^1 V_{ms}^2\|_\infty \qquad (4.22)$$

Which means that we can treat the different factors of V independently.

4.4 Tightness of lower bounds

Theorems 4.1 and 4.2 provide lower bounds on $\|TV(s)\|_\infty$ and $\|SV(s)\|_\infty$. The question is whether these bounds are tight, meaning that there actually exist controllers which achieve the bounds? The answer is "yes" if there is only one RHP-zero or one RHP-pole. Specifically, we find that the bound on $\|TV(s)\|_\infty$ is tight if the plant G has one RHP-pole and any number of RHP-zeros, and that the bound on $\|SV(s)\|_\infty$ is tight if the plant G has one RHP-zero and any number of RHP-poles. First, we consider the controller which minimizes $\|TV(s)\|_\infty$.

THEOREM 4.3 (K WHICH MINIMIZES $\|TV(s)\|_\infty$). *Consider the SISO plant G with one RHP-pole p and $N_z \geq 0$ RHP-zeros $z_j \in \mathbb{C}_+$. Let V be a scalar rational transfer function where the RHP-poles of V in $\mathbb{C}_+$ also are RHP-zeros in G. A feedback controller K which stabilizes TV, is given by*

$$K(s) = G_{ms}^{-1}(s) P(s) Q^{-1}(s) \qquad (4.23)$$

where

$$P(s) = \mathcal{B}_z^{-1}(p)\, V_{ms}(p)\, V_{ms}^{-1}(s) \tag{4.24}$$

$$Q(s) = \mathcal{B}_p^{-1}(s)\, (1 - \mathcal{B}_z(s)\, P(s)) \tag{4.25}$$

$Q(s)$ *is stable since the* RHP-*zero for* $s = p$ *in* $1 - \mathcal{B}_z(s)P(s)$ *cancels the* RHP-*pole for* $s = p$ *in* $\mathcal{B}_p^{-1}(s)$, *in a minimal realization of* $Q(s)$. *With this controller we have*

$$\|TV(s)\|_\infty = |\mathcal{B}_z^{-1}(p)| \cdot |V_{ms}(p)| \tag{4.26}$$

which shows that the bound given in Theorem 4.1 is tight when the plant has one RHP-*pole.*

Some remarks are given following the next theorem, where we consider the controller which minimizes $\|SV(s)\|_\infty$.

THEOREM 4.4 (K WHICH MINIMIZES $\|SV(s)\|_\infty$). *Consider the* SISO *plant G with one* RHP-*zero z and* $N_p \geq 0$ RHP-*poles* $p_i \in \mathbb{C}_+$. *Let V be a scalar rational transfer function where the* RHP-*poles of V in* $\mathbb{C}_+$ *also are* RHP-*poles in G. A feedback controller K which stabilizes SV, is given by*

$$K(s) = G_{ms}^{-1}(s)\, P(s)\, Q^{-1}(s) \tag{4.27}$$

where

$$Q(s) = \mathcal{B}_p^{-1}(z)\, V_{ms}(z)\, V_{ms}^{-1}(s) \tag{4.28}$$

$$P(s) = \mathcal{B}_z^{-1}(s)\, (1 - \mathcal{B}_p(s)\, Q(s)) \tag{4.29}$$

$P(s)$ *is stable since the* RHP-*zero for* $s = z$ *in* $1 - \mathcal{B}_z(s)P(s)$ *cancels the* RHP-*pole for* $s = z$ *in* $\mathcal{B}_z^{-1}(s)$, *in a minimal realization of* $P(s)$. *With this controller we have*

$$\|SV(s)\|_\infty = |\mathcal{B}_p^{-1}(z)| \cdot |V_{ms}(z)| \tag{4.30}$$

which shows that the bound given in Theorem 4.2 is tight when the plant has one RHP-*zero.*

Some remarks on the controllers given in Theorems 4.3 and 4.4:

1) We stress that the bounds given in Theorems 4.1 and 4.2 are generally *not* tight if the plant has more than one RHP-pole and one RHP-zero respectively.
2) The controller $K(s)$ in Theorem 4.3 may be unstable since $Q(s)$ in (4.25) may contain RHP-zeros, but $K(s)$ contains no RHP-zeros in $\mathbb{C}_+$.
3) The controller $K(s)$ in Theorem 4.4 may contain RHP-zeros since $P(s)$ in (4.29) may contain RHP-zeros, but $K(s)$ contains no RHP-poles in $\mathbb{C}_+$. Note that $K(s)$ has a pole at $s = 0$ (integrator) if $GV(s)$ contains an integrator.
4) The controllers in Theorems 4.3 and 4.4 yield constant ("flat") frequency responses $|TV(j\omega)|$ and $|SV(j\omega)|$ for all ω. Kwakernaak (1986; 1993) names the fact that the $\mathcal{H}_\infty$-optimal closed-loop transfer function is constant (independent of frequency) for "equalizing property".

5) We note that no properness restriction has been imposed on the controllers, so the controllers given in Theorems 4.3 and 4.4 may be improper.

6) It may seem surprising that the controller $K(s)$ in Theorem 4.4 is strictly stable (no poles in $\mathbb{C}_+$) since it is known that some plants with RHP zeros and poles require an unstable controller to achieve closed-loop stability (Youla, Bongiorno and Lu, 1974), e.g. for the plant $G(s) = \frac{s-2}{(s-3)(0.1s+1)}$. However, this assumes that the loop transfer function GK is strictly proper, and do therefore not apply in our case where K may be improper. In practice, our controllers may be made proper by adding high-frequency dynamics, e.g. by multiplying with $\frac{1}{\prod \varepsilon_i s + 1}$ where $|\varepsilon_i|$ is small. A negative ε_i may be needed, e.g. for plants where an unstable controller is needed according to the theorem of Youla et al. (1974). A short (but not complete) explanation to this is as follows. It follows that RHP-poles in the feedback controller appears as zeros in S and increase the lower bound (4.19) on $\|SV(s)\|_\infty$. The extra factor in (4.19) becomes $|\mathcal{B}_p^{-1}(K)|_{s=z} \geq 1$. Assume that we need one RHP-pole p in the controller to make SV stable, then $|\mathcal{B}_p^{-1}(K)|_{s=z} = \frac{|z+p|}{|z-p|}$. In the design of the feedback controller we are free to move the RHP-pole. By maximizing the distance between the RHP-zero z of the plant G and the RHP-pole in the controller K, i.e. let $p \to \infty$, then $|\mathcal{B}_p^{-1}(K)|_{s=z} \to 1$. Indeed, this is confirmed by Example 4.1.

7) In Theorem 4.3 we assume that the RHP-poles of $V(s)$ also are RHP-zeros in $G(s)$. This is not a very restrictive assumption. First, it is satisfied in all the cases we have considered. Second, it may in fact easily be removed if we let $\mathcal{B}_z(s)$ in Theorems 4.1 and 4.3 contain, in addition to the RHP-zeros in $G(s)$, also the RHP-poles in $V(s)$ which are not RHP-zeros in $G(s)$. This follows by considering step 4 in the proof of Theorem 4.1 where we should include all RHP-zeros of T. That is, the RHP-zeros in G and the RHP-zeros in K. RHP-zeros in K are needed to cancel the RHP-poles of V, which are not canceled by RHP-zeros of G.

8) Similarly, in Theorem 4.4 we assume that the RHP-poles of $V(s)$ also are RHP-poles in $G(s)$. First, this assumption is satisfied in all the cases we have considered. Second, the assumption may easily be removed by adding to $\mathcal{B}_p(s)$, the RHP-poles in $V(s)$ which are not RHP-poles in $G(s)$. The additional RHP-poles will appear as RHP-poles in the controller $K(s)$ in Theorem 4.4.

EXAMPLE 4.1. The motivation for this example is to show how to use and the limitations of the results in Theorems 4.3 and 4.4. The example demonstrates the difference between stabilizing control using proper and improper controllers and stress the importance of the results by Youla et al. (1974). We consider the plant

$$G(s) = \frac{s-z}{(0.1s+1)(s-p)} \quad \text{with } z = 2 \text{ and } p = 3.$$

We find

$$\mathcal{B}_p(s) = \frac{s-3}{s+3}, \quad \mathcal{B}_z(s) = \frac{s-2}{s+2} \quad \text{and} \quad G_{ms}(s) = \frac{s+2}{(0.1s+1)(s+3)}$$

According to the results by Youla et al. (1974) the plant G needs an unstable feedback controller to yield a stable closed-loop system, since the unstable pole (odd number) is located to the right of the RHP-zero. We consider stabilizing this plant by deriving three different controllers.

1) **Minimizing the peak in the complementary sensitivity.** From the lower bound (4.18) in Theorem 4.1 with $V = 1$, we obtain

$$\|T(s)\|_\infty \geq |\mathcal{B}_z^{-1}(p)| = 5$$

By using Theorem 4.3 with $V = 1$ we find a feedback controller which minimizes $\|T(s)\|_\infty$. We obtain

$$P = \mathcal{B}_z^{-1}(p) = 5, \quad Q(s) = \mathcal{B}_p^{-1}(s)\left(1 - \mathcal{B}_z(s)P\right) = \frac{s+3}{s-3}\left(1 - 5\frac{s-2}{s+2}\right) = -4\frac{s+3}{s+2}$$

The feedback controller becomes

$$K(s) = G_{ms}^{-1}PQ^{-1}(s) = \frac{(0.1s+1)(s+3)}{s+2}\left(-\frac{5}{4}\right)\frac{s+2}{s+3} = -\frac{5}{4}(0.1s+1)$$

which is stable but improper. With this feedback controller we get

$$T(s) = \mathcal{B}_z(s)\,P = 5\frac{s-2}{s+2} \quad \text{which is stable, and} \quad \|T(s)\|_\infty = 5.$$

Making the controller $K(s)$ semi-proper by adding the first order lag $\frac{1}{\varepsilon s+1}$, where $\varepsilon = 0.001$, to $K(s)$ yields an unstable closed-loop system. However, when $\varepsilon < 0$ we obtain a semi-proper unstable controller K which makes the closed-loop transfer function T stable. For $\varepsilon = -0.001$ we obtain $\|T(s)\|_\infty = 5.095$ and by further decreasing the value of ε, $\|T(s)\|_\infty$ approaches the lower bound 5. At the same time the unstable pole moves to ∞.

By using state-space[2] $\mathcal{H}_\infty$-controller design methods, we design an $\mathcal{H}_\infty$-optimal controller K by solving

$$\min_K \left\| \begin{bmatrix} T(s) \\ w_u KS(s) \end{bmatrix} \right\|_\infty \quad \text{with} \quad w_u = 10^{-3}$$

Note the small weight $w_u = 10^{-3}$ on the input usage, which in practice means that we are minimizing $\|T(s)\|_\infty$. We obtain a strictly proper unstable controller, with: RHP-pole about $4.00 \cdot 10^4$, LHP-pole about $-4.64 \cdot 10^7$, LHP-zero at -10 and steady-state gain $-5/4$. This controller is very similar to the controller derived from Theorem 4.3. The closed-loop system is stable and $\|T(s)\|_\infty = 5.00$.

2) **Minimizing $\mathcal{H}_\infty$-norm of the input usage.** By rewriting $KS = TG^{-1}$ and setting $V = G^{-1}$ in Theorem 4.1 we obtain

$$\|KS(s)\|_\infty \geq |\mathcal{B}_z^{-1}(p)| \cdot |G_{ms}^{-1}(p)| = 5\frac{7.8}{5} = 7.8$$

By using Theorem 4.3 with $V = G^{-1}$ we find a feedback controller which minimizes $\|KS(s)\|_\infty$. We obtain

$$P(s) = 7.8\,G_{ms}(s), \quad Q(s) = \frac{0.1s - 6.2}{0.1s + 1}$$

The feedback controller becomes

$$K(s) = 7.8\frac{0.1s + 1}{0.1s - 6.2}$$

which is semi-proper and unstable. With this feedback controller we get

$$S(s) = \frac{(s-3)(0.1s - 6.2)}{(s+3)(0.1s + 1)}, \quad KS(s) = 7.8\frac{s-3}{s+3} \quad \text{and} \quad \|KS(s)\|_\infty = 7.8$$

---

[2]MATLAB-μ tools are used in this example.

By using state-space $\mathcal{H}_\infty$-controller design methods, we design an $\mathcal{H}_\infty$-optimal controller K by solving

$$\min_K \|KS(s)\|_\infty$$

The controller achieved is strictly proper and unstable, with: RHP-pole at 62, LHP-pole about $-5.55 \cdot 10^7$, LHP-zero at -10 and steady-state gain $K(j0) = -7.8/6.2$. The closed-loop system is stable and $\|KS(s)\|_\infty = 7.8$. This controller is a strictly proper version of the semi-proper controller derived by using Theorem 4.3.

3) **Minimizing the peak in the sensitivity.** From the lower bound (4.19) in Theorem 4.2 with $V = 1$, we obtain

$$\|S(s)\|_\infty \geq |\mathcal{B}_p^{-1}(z)| = 5$$

By using Theorem 4.4 with $V = 1$ we find a feedback controller which minimizes $\|S(s)\|_\infty$. We obtain

$$Q(s) = -5, \quad P(s) = 6\,\frac{s+2}{s+3}$$

The feedback controller becomes

$$K(s) = -\frac{6}{5}\,(0.1s + 1)$$

which is stable but improper. With this feedback controller we get

$$S(s) = -5\,\frac{s-3}{s+3}$$

which is stable and yields $\|S(s)\|_\infty = 5$. Making the controller $K(s)$ semi-proper by adding the first order lag $\frac{1}{\varepsilon s+1}$, where $\varepsilon = 0.001$, to $K(s)$ yields an unstable closed-loop system. However, when $\varepsilon < 0$ we obtain a semi-proper unstable controller K which makes the closed-loop transfer function S stable. For $\varepsilon = -0.001$ we obtain $\|S(s)\|_\infty = 5.138$ and by further decreasing the value of ε, $\|S(s)\|_\infty$ approaches the lower bound 5. At the same time the unstable pole moves to ∞.

By using state-space $\mathcal{H}_\infty$-controller design methods, we design an $\mathcal{H}_\infty$-optimal controller K by solving

$$\min_K \left\| \begin{bmatrix} S(s) \\ w_u KS(s) \end{bmatrix} \right\|_\infty \quad \text{with} \quad w_u = 10^{-3}$$

Note the small weight $w_u = 10^{-3}$ on the input usage, which in practice means that we are minimizing $\|S(s)\|_\infty$. We obtain a strictly proper and unstable controller, with: RHP-pole about $4.08 \cdot 10^4$, LHP-pole about $-4.59 \cdot 10^7$, LHP-zero -10 and steady-state gain -1.2. This controller is very similar to the controller derived from Theorem 4.4. The closed-loop system is stable and $\|S(s)\|_\infty = 5.00$.

We note that the results by Youla et al. (1974) do not apply to the improper controllers in 1) and 3) since the loop transfer function is not strictly proper. As predicted by the results in (Youla et al., 1974), the only way to obtain closed-loop stability with semi-proper controllers, is to add an unstable mode in the controllers. Furthermore, to get the $\mathcal{H}_\infty$-norm close to the lower bounds, we need to move instability far out in the RHP. In 2) the loop transfer function is strictly proper and the resulting optimal controller is unstable as predicted by Youla et al. (1974). We also note that the three controllers derived are very similar, they all have a LHP-zero for $s = -10$ (which comes from G_{ms}^{-1}) and a steady-state gain in the range from -1.2 to $-7.8/6.2 \approx -1.258$.

4.5 Applications of lower bounds

The lower bounds on $\|TV(s)\|_\infty$ and $\|SV(s)\|_\infty$ in Theorems 4.1 and 4.2 can be used to derive a large number of interesting and useful bounds.

4.5.1 Bounds on important closed-loop transfer functions

Consider again the six transfer functions in (4.13), and the weighted complementary sensitivity function $w_{\text{unc}}T$. For simplicity we assume that w_P, w_u, w_{unc}, R and N have no zeros and poles in $\mathbb{C}_+$ (or have been replaced by the stable minimum phase counterparts with same magnitude). From Theorems 4.1 and 4.2 we obtain:

Output performance, reference tracking:

$$\|w_P SR(s)\|_\infty \geq \max_{\text{RHP-zeros},\, z_j} |w_P(z_j)| \cdot |\mathcal{B}_p^{-1}(z_j)| \cdot |R(z_j)| \tag{4.31}$$

Output performance, disturbance rejection:

$$\|w_P SG_d(s)\|_\infty \geq \max_{\text{RHP-zeros},\, z_j} |w_P(z_j)| \cdot |\mathcal{B}_p^{-1}(z_j)| \cdot |(G_d)_{ms}(z_j)| \tag{4.32}$$

Output performance, measurement noise rejection:

$$\|w_P TN(s)\|_\infty \geq \max_{\text{RHP-poles},\, p_i} |w_P(p_i)| \cdot |\mathcal{B}_z^{-1}(p_i)| \cdot |N(p_i)| \tag{4.33}$$

Input usage, reference tracking:

$$
\begin{aligned}
\|w_u KSR(s)\|_\infty &= \|w_u TG^{-1}R(s)\|_\infty \\
&\geq \max_{\text{RHP-poles},\, p_i} |w_u(p_i)| \cdot |\mathcal{B}_z^{-1}(p_i)| \cdot |G_{ms}^{-1}(p_i)| \cdot |R(p_i)| \tag{4.34}
\end{aligned}
$$

Input usage, disturbance rejection:

$$
\begin{aligned}
\|w_u KSG_d(s)\|_\infty &= \|w_u TG^{-1}G_d(s)\|_\infty \\
&\geq \max_{\text{RHP-poles},\, p_i} |w_u(p_i)| \cdot |\mathcal{B}_z^{-1}(p_i)| \cdot |G_{ms}^{-1}(p_i)| \cdot |(G_d)_{ms}(p_i)| \tag{4.35}
\end{aligned}
$$

Input usage, measurement noise rejection:

$$
\begin{aligned}
\|w_u KSN(s)\|_\infty &= \|w_u TG^{-1}N(s)\|_\infty \\
&\geq \max_{\text{RHP-poles},\, p_i} |w_u(p_i)| \cdot |\mathcal{B}_z^{-1}(p_i)| \cdot |G_{ms}^{-1}(p_i)| \cdot |N(p_i)| \tag{4.36}
\end{aligned}
$$

REMARK. In the bounds (4.34)–(4.36) we can make use of the identity

$$|\mathcal{B}_z^{-1}(p_i)| \cdot |G_{ms}^{-1}(p_i)| = |G_s^{-1}(p_i)|$$

For example we get

$$\|KS(s)\|_\infty = \|TG^{-1}(s)\|_\infty \geq \max_{\text{RHP-poles},\, p_i} |G_s^{-1}(p_i)| \tag{4.37}$$

where G_s is the "stable" version of G (with the RHP-poles in $\mathbb{C}_+$ mirrored into LHP). We made use of this bound in the introduction and we will use it in Chapter 6.

Closed-loop sensitivity to plant uncertainty:

$$\|w_{\text{unc}}T(s)\|_\infty \geq \max_{\text{RHP-poles},\, p_i} |w_{\text{unc}}(p_i)| \cdot |\mathcal{B}_z^{-1}(p_i)| \tag{4.38}$$

Note that we mainly have inherent limitations on (output) performance when the plant has RHP-zeros. The exception is for measurement noise, where the requirement of stabilizing an unstable pole may give poor performance. On the other hand, all the bounds on input usage are caused by the presence of RHP-poles. This is reasonable since we need active use of the input in order to stabilize the plant. This is considered in more detail in the next section.

4.5.2   Implications for stabilization with bounded inputs

Our bounds involve the $\mathcal{H}_\infty$-norm, and their large engineering usefulness may not be immediate. In the following we will concentrate on the bounds involving input usage and we will use the lower bounds to derive and *quantify* the conclusion:

- *Bounded inputs combined with disturbances and noise may make stabilization impossible.*

The input signal for a one degree-of-freedom (1-DOF) controller due to disturbance d, measurement noise n of magnitude N and reference r of magnitude R, is

$$u = KS(R\tilde{r} - G_d d - N\tilde{n}) \tag{4.39}$$

Measurement noise. The transfer function from normalized measurement noise $\tilde{n}$ to the input u is KSN. Then from (4.36) with $w_u = 1$

$$\|u\|_\infty = \|KSN(s)\|_\infty \geq \max_{\text{RHP-poles},\, p_i} |\mathcal{B}_z^{-1}(p_i)| \cdot |G_{ms}^{-1}(p_i)| \cdot |N(p_i)| \tag{4.40}$$

Thus, to have $\|u\|_\infty \leq 1$ for $\|\tilde{n}\|_\infty = 1$, we must require

$$|G_{ms}(p_i)| \geq |\mathcal{B}_z^{-1}(p_i)| \cdot |N(p_i)| \quad \text{for the worst case pole } p_i \tag{4.41}$$

(we have here assumed that N is minimum phase). That is:

- *To keep the input magnitude less than one ($\|u\|_\infty \leq 1$) we must require that the plant gain is larger than the measurement noise at frequencies corresponding to the unstable poles.*

To better understand this statement, we will make use of the interpretation of the $\mathcal{H}_\infty$-norm in terms of steady-state sinusoids. Consider the case when $\|\tilde{n}\|_\infty = 1$ and assume that the lower bound in terms of $\|u\|_\infty = \|KSN(s)\|_\infty$ in (4.40) is larger than one (i.e. (4.41) is *not* satisfied). In this case, no matter what linear controller we design, there will always be a sinusoidal noise signal

$$n(t) = n_{\max}\sin(\omega_0 t), \quad n_{\max} = |N(j\omega_0)|$$

such that the resulting input signal

$$u(t) = u_{\max}\sin(\omega_0 t + \varphi)$$

has $u_{\max} > 1$ (the value of φ is not of interest here). For a given controller K, the worst case frequency ω_0 may be chosen as the frequency ω where $|KSN(j\omega)|$ has its peak value, i.e. $|KSN(j\omega_0)| = \|KSN(s)\|_\infty$.

Disturbances. Similar results as those for measurement noise apply to disturbances if we replace N by G_d. From (4.35) with $w_u = 1$ we obtain

$$\|u\|_\infty = \|KSG_d(s)\|_\infty \geq \max_{\text{RHP-poles, } p_i} |\mathcal{B}_z^{-1}(p_i)| \cdot |G_{ms}^{-1}(p_i)| \cdot |(G_d)_{ms}(p_i)| \qquad (4.42)$$

To have $\|u\|_\infty \leq 1$ for $\|d\|_\infty = 1$ we must require

$$|G_{ms}(p_i)| \geq |\mathcal{B}_z^{-1}(p_i)| \cdot |(G_d)_{ms}(p_i)| \quad \text{for the worst case pole } p_i \qquad (4.43)$$

That is:

- *To keep the input magnitude less than one* ($\|u\|_\infty \leq 1$) *we must require that the plant gain is larger than the gain of the disturbance plant at frequencies corresponding to the unstable poles.*

References. For reference changes with $\|\tilde{r}\|_\infty = 1$, we find the same bound (4.42), but with G_d replaced by R. However, the implications are less severe since we may choose *not* to follow the references (e.g. set $R = 0$). Also, in the case of reference changes we may use a 2-DOF controller, such that the "burden" on the feedback part of the controller K is less. This is discussed in Section 4.7.

4.5.3 Examples

EXAMPLE 4.2. The intention with this example is to show the engineering application of the lower bound on $\|KSN(s)\|_\infty$ and to demonstrate the use of Theorem 4.3 to find the feedback controller K which minimize $\|KSN(s)\|_\infty$. We consider the unstable plant

$$G(s) = \frac{1}{s-p}, \qquad p > 0$$

with RHP-pole at p. From (4.40) we have the following lower bound on the $\mathcal{H}_\infty$-norm of the transfer function from normalized measurement noise $\tilde{n}$ to input u (we assume that N is minimum phase)

$$\|KSN(s)\|_\infty \geq |G_{ms}^{-1}(p)| \cdot |N(p)|$$

In our case $G^{-1} = s - p$, $G_{ms}^{-1}(s) = s + p$, $G_{ms}^{-1}(p) = 2p$, and the lower bound becomes

$$\|KSN(s)\|_\infty \geq 2p \cdot |N(p)| \qquad (4.44)$$

The controller which minimizes $\|TV(s)\|_\infty$ and achieves the bound (4.44) is given in Theorem 4.3. Rewriting $KSN = TG^{-1}N$ and by using $V = G^{-1}N$ we obtain $V_{ms}(s) = (s+p)N(s)$, where we have assumed N to be stable minimum phase. Furthermore, $\mathcal{B}_z(s) = 1$, $\mathcal{B}_p(s) = \frac{s-p}{s+p}$. Thus, from Theorem 4.3 we obtain

$$P(s) = \frac{2p \cdot N(p)}{(s+p) \cdot N(s)} \quad \text{and} \quad Q(s) = \frac{s+p}{s-p} \cdot \left(1 - \frac{2p \cdot N(p)}{(s+p) \cdot N(s)}\right)$$

which gives

$$K(s) = \frac{2p \cdot N(p)\,(s - p)}{(s + p)N(s) - 2p \cdot N(p)}$$

Remark: It seems like this controller has a RHP-zero for $s = p$, but this is not the case for its minimal realization since

$$(s + p) \cdot N(s)|_{s=p} - 2p \cdot N(p) = 0$$

For the special case where $N(s)$ is a constant $N(s) = N$, we get the proportional feedback controller

$$K(s) = \frac{2p(s - p)}{s + p - 2p} = 2p$$

As a numerical example, let $p = 10$, then

$$G(s) = \frac{1}{s - 10}$$

and we must have for any stabilizing feedback controller K

$$\|KSN(s)\|_\infty \geq 20\,|N(p)|$$

Thus with $\|\tilde{n}\|_\infty = 1$ we will need excessive inputs ($\|u\|_\infty > 1$) if $|N(p)| \geq |G_{ms}(p)| = 0.05$. Assume that $N(s) = N(p) = 0.05$, then $K(s) = 2p = 20$. This controller gives a "flat" frequency response, i.e. $|KS(j\omega)| = 20$, $\forall\omega$. Thus, at any frequency ω_0 the closed-loop response in u due to

$$n(t) = 0.05\sin(\omega_0 t), \quad \text{is} \quad u(t) = \sin(\omega_0 t + \varphi) \quad \forall\omega$$

So, the input $u(t)$ oscillates between ± 1. The response in u and y due to $n(t) = 0.05\sin(4t)$ is shown in Figure 4.3.
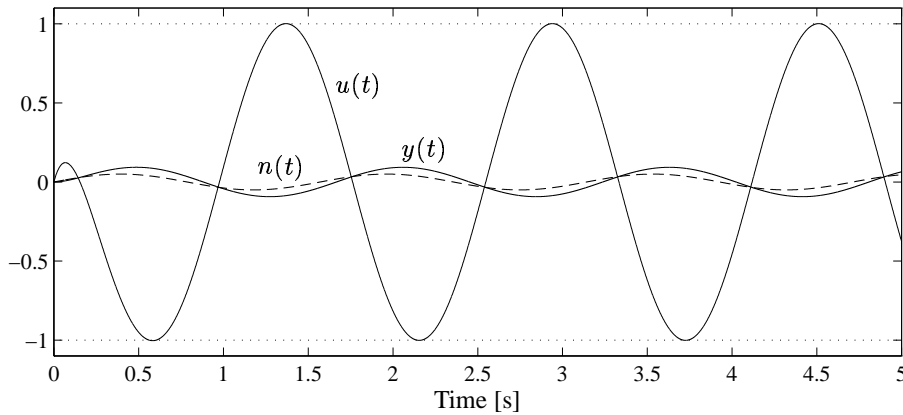
Figure 4.3: Closed-loop response at input u and output y of the plant G, due to $n(t) = 0.05\sin(4t)$ (dashed), with $K = 20$

EXAMPLE 4.3. In this example we consider disturbance rejection for a plant with one RHP zero and pole. Let

$$G(s) = \frac{k}{z}\frac{s - z}{s - p}, \quad G_d(s) = k_d G(s) \quad \text{with} \quad z = 2,\ p = 1$$

We see that the disturbance is of magnitude k_d and enters at the input of the plant. Note that

$$(G_d)_{ms} = \frac{k \cdot k_d}{z} \frac{s+z}{s+p} \quad \text{and} \quad G_{ms}^{-1} = \frac{z}{k} \frac{s+p}{s+z}$$

The factors involving the interactions between the RHP zero z and pole p become

$$|\mathcal{B}_p^{-1}(z)| = |\mathcal{B}_z^{-1}(p)| = \frac{|z+p|}{|z-p|} = 3$$

and we find that peaks in the sensitivity S and the complementary sensitivity T less than 3 are unavoidable since

$$\|S(s)\|_\infty \geq \frac{|z+p|}{|z-p|} = 3 \quad \text{and} \quad \|T(s)\|_\infty \geq \frac{|z+p|}{|z-p|} = 3$$

Since G has a RHP-zero, we have a bound on the $\mathcal{H}_\infty$-norm of the closed-loop transfer function from disturbance d to output $e = y - r$

$$\|SG_d(s)\|_\infty \geq |\mathcal{B}_p^{-1}(z)| \cdot |(G_d)_{ms}(z)| = \frac{|z+p|}{|z-p|} \cdot \frac{2|k \cdot k_d|}{|z+p|} = 2|k \cdot k_d|$$

and for $\|d\|_\infty = 1$, the output e will be unacceptable ($\|e\|_\infty > 1$) for $|k \cdot k_d| > 0.5$.
Similarly, since G has a RHP-pole p we have a bound on the $\mathcal{H}_\infty$-norm of the closed-loop transfer function from disturbance d to input u

$$\|KSG_d(s)\|_\infty \geq |\mathcal{B}_z^{-1}(p)| \cdot |G_{ms}^{-1}(p)| \cdot |(G_d)_{ms}(p)| = \frac{|z+p|}{|z-p|} \cdot |k_d| = 3|k_d|$$

and for $\|d\|_\infty = 1$ the input usage will be unacceptable ($\|u\|_\infty > 1$) when $|k_d| > 1/3$.

EXAMPLE 4.4. In this example we look at the effect of a RHP zero and pole in G_d. Let the plant be

$$G(s) = \frac{5}{(10s+1)(s-1)}$$

where $\mathcal{B}_z(s) = 1$ since there is no RHP-zeros in G. We consider the three disturbances

$$G_{d1}(s) = \frac{k_d}{(s-1)(0.2s+1)}, \quad G_{d2}(s) = \frac{k_d}{(s+1)(0.2s+1)}$$

$$\text{and} \quad G_{d3}(s) = \frac{k_d(s-2)}{(s+1)(0.2s+1)(s+2)}$$

For disturbance d_1 we must assume that the unstable pole at $p = 1$ is the same as the one in the plant G, such that it can be stabilized using feedback control. There is no RHP-zero in G, so we have no lower bound on $\|SG_{dk}(s)\|_\infty$. However, since G has a RHP-pole p there is a bound on $\|KSG_{dk}(s)\|_\infty$, and we find that the same lower bound applies to all three disturbances ($k \in \{1, 2, 3\}$), since

$$(G_{d1})_{ms} = (G_{d2})_{ms} = (G_{d3})_{ms} = \frac{k_d}{(s+1)(0.2s+1)}$$

We obtain

$$\|KSG_{dk}(s)\|_\infty \geq |G_{ms}^{-1}(p)| \cdot |(G_{dk})_{ms}(p)| = \left| \frac{(10s+1)(s+1)}{5} \frac{k_d}{(s+1)(0.2s+1)} \right|_{s=1} = \frac{11}{6} \cdot |k_d|$$

Thus, for $\|d\|_\infty = 1$ and if we require $\|u\|_\infty \leq 1$ we need to have $|k_d| \leq \frac{6}{11} \approx 0.55$. In other words, we may encounter excessive plant inputs (for all controllers) if $|k_d| > \frac{6}{11} \approx 0.55$.

4.6   Stabilization with input saturation

Our results provide tight lower bounds for the required input signals for an unstable plant. Can these bounds be used to say anything about the possibility of stabilizing a plant with constrained inputs (e.g. $|u(t)| \leq 1$, $\forall t$)? Assume that we have found, from one of these bounds, that we need $\|u\|_\infty > 1$. That is, at some frequency ω_0 we need $u(t) = u_{\max} \sin(\omega_0 t)$, with $u_{\max} > 1$. Will the system become unstable in the case where input is constrained such that $|u(t)| \leq 1$ ($\forall t$)?

Unfortunately, all our results are for linear systems, and we have not derived any results for this nonlinear effect of input saturation. Nevertheless, for simple low order systems we find as expected very good agreement between our lower bounds and the actual stability limit in systems with input saturation. Intuitively, this agreement should be good if the input remains saturated for a time which is longer than about $1/p$, where p is the RHP-pole.

4.6.1   Examples

EXAMPLE 4.2 CONTINUED. Consider again the plant

$$G(s) = \frac{1}{s - 10}$$

with the controller $K = 20$ which minimizes $\|KSN(s)\|_\infty$ when N is constant. With this controller we get $|KS(j\omega)| = 20$, $\forall \omega$, from which we know that sinusoidal measurement noise

$$n(t) = n_0 \sin(\omega_0 t)$$

cause the input to become

$$u(t) = 20 n_0 \sin(\omega_0 t + \varphi)$$

for any frequency ω_0. Thus, for $n_0 = f \cdot 0.05$ we have that $u(t) = f \sin(\omega_0 t + \varphi)$, and for $f > 1$ the plant input will exceed ± 1 in magnitude. The question is: what happens if the inputs are constrained to be within ± 1? Will the stability be maintained? We will investigate this numerically by considering three frequencies; $\omega_0 = 1$ [rad/s], $\omega_0 = 10$ [rad/s] and $\omega_0 = 100$ [rad/s].

First, Figure 4.4 shows the response to $n(t) = 1.01 \cdot 0.05 \sin(t)$ ($\omega_0 = 1$ [rad/s], $f = 1.01$). We see that the plant becomes unstable due to the input saturation. Next, we consider $\omega_0 = 10$ [rad/s]. In this case we do *not* get instability with $f = 1.01$ and $\omega_0 = 10$ [rad/s]. We find numerically that we need to increase the magnitude of the sinusoidal noise to about $f = 1.29$ to get instability for this frequency. Figure 4.5 shows the response to $n(t) = 1.29 \cdot 0.05 \sin(10t)$ ($\omega = 10$ [rad/s] and $f = 1.29$). Finally, as shown in Figure 4.6, we get instability with $n(t) = 1.6 \cdot 0.05 \sin(100t)$ ($\omega = 100$ [rad/s] and $f = 1.6$).

We experience that we have to increase the magnitude of the noise somewhat to get instability for sinusoidal measurement noise with frequency around the bandwidth and higher. However, we are still within a factor of two for a large frequency range for this particular plant. Measurement noise usually contains a large range of frequencies, which makes it even more probable that one loose stability of the plant if the lower bounds exceeds the allowable input range.

Note that the control system designer seldom wants the input to saturate when stabilizing an unstable plant due to the possibility of loosing stability. So our "engineering bounds" are really applicable in practical controller design.
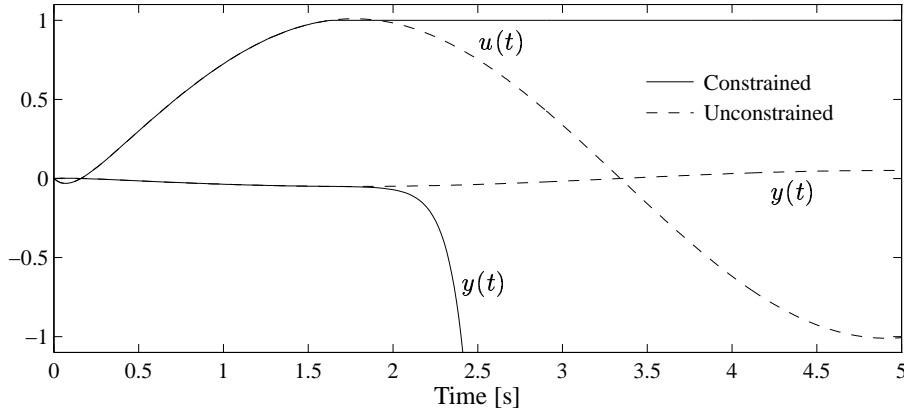
Figure 4.4: Closed-loop response at input u and output y of the plant G, due $n(t) = 1.01 \cdot 0.05 \sin(t)$
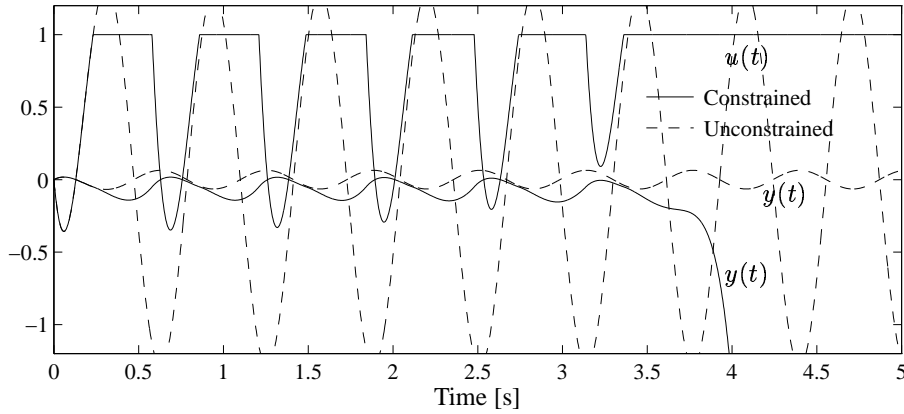
Figure 4.5: Closed-loop response at input u and output y of the plant G, due $n(t) = 1.29 \cdot 0.05 \sin(10t)$

As a final simulation, Figure 4.7 shows the closed-loop response due to a step of size $1.01 \cdot 0.05$ in n. (1% increase relative to the limit which cause u to exceed ± 1). This input signal can be viewed as consisting of infinite number of frequencies with decreasing magnitude, where the steady-state effect is the most important and can be viewed as a slowly varying sinusoid with $\omega_0 = 0$ [rad/s] and amplitude $1.01 \cdot 0.05$. As can be seen from the figure, the unconstrained input exceeds 1 slightly. When the input is constrained to be within ± 1, stability of the plant is lost.

EXAMPLE 4.4 CONTINUED. Consider again the plant

$$G(s) = \frac{5}{(10s + 1)(s - 1)}$$

In the simulations shown in this example, we have used the disturbance plant $G_d = G_{d3}$

$$G_d(s) = \frac{k_d(s - 2)}{(s + 1)(0.2s + 1)(s + 2)}$$

However, it does not really matter which G_{dk} one uses, except that the initial responses may be different.

By using Theorem 4.3 with $V = G^{-1}G_d$, we obtain:

$$\mathcal{B}_z(s) = 1, \quad \mathcal{B}_p(s) = \frac{s - 1}{s + 1}, \quad G_{ms}(s) = \frac{5}{(s + 1)(10s + 1)}, \quad (G_d)_{ms}(s) = \frac{k_d}{(s + 1)(0.2s + 1)},$$
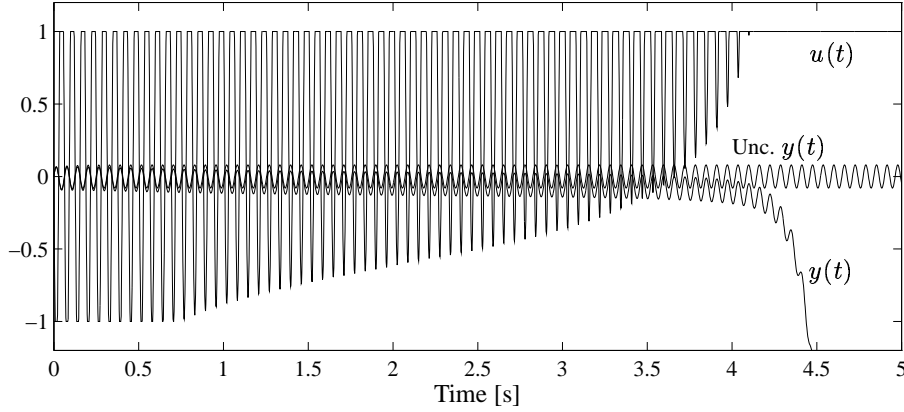
Figure 4.6: Closed-loop response at input u and output y of the plant G, due $n(t) = 1.6 \cdot 0.05 \sin(100t)$, (unconstrained input not shown)
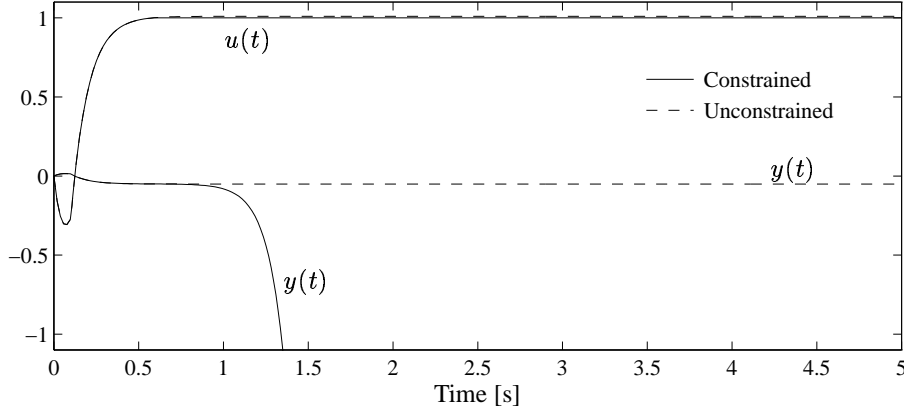
Figure 4.7: Closed-loop response at input u and output y of the plant G, due to step in measurement noise, $n(s) = 1.01 \cdot \frac{0.05}{s}$

$$V_{ms}(s) = \frac{k_d}{5}\frac{10s+1}{0.2s+1}, \quad V_{ms}(p) = \frac{11}{6} \cdot k_d, \quad P(s) = \frac{55}{6}\frac{0.2s+1}{10s+1} \quad \text{and} \quad Q(s) = \frac{49}{6}\frac{s+1}{10s+1}$$

The $\mathcal{H}_\infty$-optimal controller minimizing $\|KSG_d(s)\|_\infty$ becomes

$$K_\infty(s) = \frac{49}{11}(0.2s+1)(10s+1)$$

which is not proper. For $k_d = \frac{6}{11}$ the controller K_∞ results in $\|K_\infty SG_d(s)\|_\infty = 1$, and when $k_d = 0.55 > \frac{6}{11}$ (0.55 is the value of k_d used in the simulations) $\|K_\infty SG_d(s)\|_\infty = 1.008$. We note that the specter of $K_\infty SG_d(j\omega)$ is flat (constant). To get a realizable (proper) controller, we add second order dynamics at high frequency to obtain the $\mathcal{H}_\infty$-suboptimal controller

$$\widetilde{K}_\infty(s) = \frac{49}{11}\frac{(0.2s+1)(10s+1)}{(0.01s+1)^2} \tag{4.45}$$

The $\mathcal{H}_\infty$-norm of the closed-loop transfer function $\widetilde{K}_\infty SG_d$ with $k_d = 0.55$ is

$$\|\widetilde{K}_\infty SG_d(s)\|_\infty = 1.027, \quad \text{for } \omega = 1.35 \text{ [rad/s]}.$$

To compare with a more traditional controller, which emphasizes tight control at low frequencies, we also consider controlling the plant G using the feedback controller

$$K(s) = \frac{0.4 \cdot (10s + 1)^2}{s(0.1s + 1)^2} \tag{4.46}$$

With this K the $\mathcal{H}_\infty$-norm of the closed-loop transfer function KSG_d for $k_d = 0.55$ becomes

$$\|KSG_d(s)\|_\infty = 2.845, \quad \text{for } \omega = 2.056 \text{ [rad/s]}.$$

The magnitude of the closed-loop transfer functions $\widetilde{K}_\infty SG_d$ for $\widetilde{K}_\infty$ given by (4.45) is shown in Figure 4.8 together with the magnitude of KSG_d for K given in (4.46). From the figure we see that
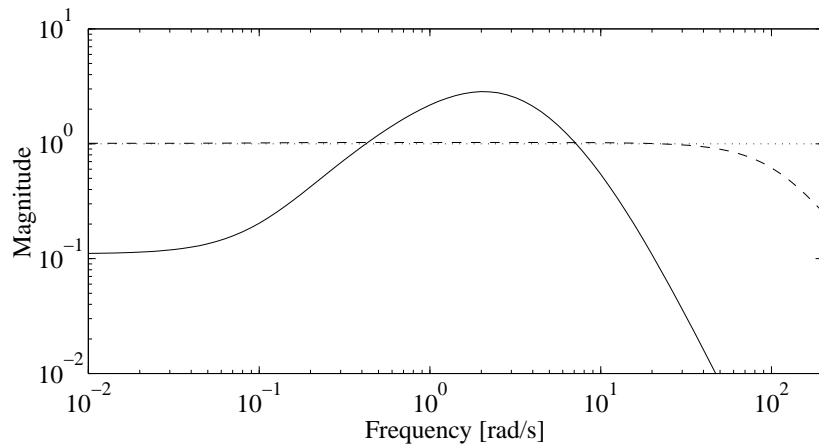
Figure 4.8: Closed-loop transfer functions KSG_d (solid) and $\widetilde{K}_\infty SG_d$ (dashed)

forcing $|KSG_d(j\omega)|$ to be small at low frequencies, results in a peak in the medium frequency range (compare $|KSG_d(j\omega)|$ with $|\widetilde{K}_\infty SG_d(j\omega)|$ in Figure 4.8).

The non-linear constrained and the linear unconstrained responses to the unit step in disturbance d using the suboptimal $\mathcal{H}_\infty$-controller $\widetilde{K}_\infty$ given by (4.45) and the controller K given by (4.46), are shown in Figures 4.9 and 4.10. From the simulations we see that the input saturates (it may be difficult to separate the unconstrained input from the constrained input in Figure 4.9, since the unconstrained input only slightly exceeds -1), with the consequence that we loose stability of the plant for both controllers.

4.7   Two degrees-of-freedom control

In this section we consider the 2-DoF controller where

$$u = K_1 r - K_2(y + n) \tag{4.47}$$

(the 1-DoF considered above follows by setting $K_1 = K_2 = K$). For a 2-DoF controller the closed-loop transfer function from references $\tilde{r}$ to outputs $z_1 = w_P(y - r)$ becomes

$$w_P(SGK_1 - 1)R \tag{4.48}$$

We then have the following "special" lower bound on this transfer function.
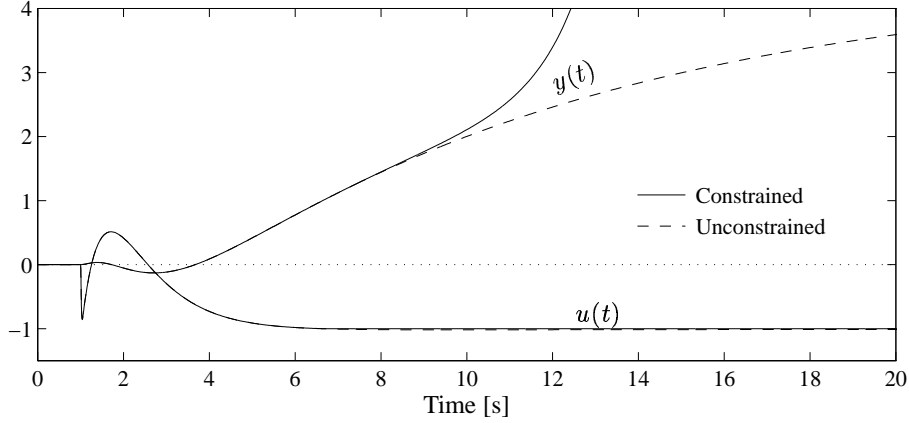
Figure 4.9: Responses in y and u due to unit step in disturbance d for constrained ($|u| \leq 1$) and unconstrained input with $\widetilde{K}_\infty$ given by (4.45)
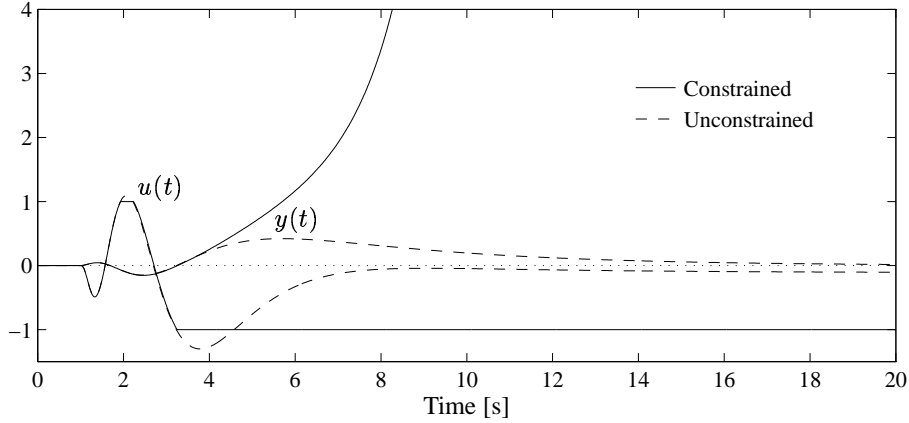
Figure 4.10: Responses in y and u due to unit step in disturbance d for constrained ($|u| \leq 1$) and unconstrained input with K given by (4.46)

THEOREM 4.5. *Consider the* SISO *plant G with $N_z \geq 1$* RHP-*zeros z_j and $N_p \geq 0$* RHP-*poles $p_i \in \mathbb{C}_+$. Let the performance weight w_P be minimum phase and let (for simplicity) R be stable. Assume that the closed-loop transfer function $w_P(SGK_1 - 1)R$ is stable. Then the following lower bound on $\|w_P(SGK_1 - 1)R(s)\|_\infty$ applies:*

$$\|w_P(SGK_1 - 1)R(s)\|_\infty \geq \max_{\text{RHP-zeros, } z_j} |w_P(z_j)| \cdot |R_m(z_j)| \tag{4.49}$$

The bound (4.49) is tight if the plant has one RHP-*zero z. Define*

$$P(s) = \mathcal{B}_z^{-1}(s)\left(1 - w_P^{-1}(s)R_m^{-1}(s)w_P(z)R_m(z)\right) \tag{4.50}$$

P is stable since the RHP-*zero for $s = z$ in $1 - w_P^{-1}(s)R_m^{-1}(s)w_P(z)R_m(z)$ cancels the* RHP-*pole for $s = z$ in $\mathcal{B}_z^{-1}(s)$, in a minimal realization of $P(s)$. One pair of controllers K_1 and K_2 which achieve the lower bound (4.49) are given by*

$$K_1 = \mathcal{B}_p(z)\, G_{ms}^{-1}(z)\, w_P^{-1}(z)\, w_P(s)\, P(s) \tag{4.51}$$

$$K_2 \quad = \quad \textit{The controller given in Theorem 4.4, minimizing } \|w_P SG(s)\|_\infty. \quad (4.52)$$

REMARK 1. The bound (4.49) is clearly a lower bound (both for 1-DOF and 2-DOF controllers). The important fact is that (4.49) provides a tight lower bound for a plant with one RHP-zero and with the 2-DOF controller given in Theorem 4.5.

REMARK 2. If w_P is unstable, then the unstable modes of w_P appears in K_1 and K_2.

REMARK 3. It is worth noting that we achieve the 2-DOF controller which minimize

$$\|w_P(SGK_1 - 1)R(s)\|_\infty$$

by first designing the feedback part K_2 and then designing the feed forward part K_1 taking into account K_2. In general, this kind of separation is not optimal, but since these controllers achieve the lower bound it follows that there is no "loss" in this case.

The bound in (4.49) should be compared to the corresponding bound for 1-DOF controller (4.31):

$$\|w_P SR(s)\|_\infty \geq \max_{\text{RHP-zeros, } z_j} |w_P(z_j)| \cdot |\mathcal{B}_p^{-1}(z_j)| \cdot |R_m(z_j)| \quad (4.53)$$

where it is assumed that R is stable. The fact that the lower bound (4.49) is tight when the plant has one RHP-zero and 2-DOF controller is applied, makes it possible to conclude that *only* the RHP-zero pose limitations in this case. Thus, with a 2-DOF controller there is no additional penalty for having RHP-poles in G when performance is measured as $z_1 = w_P(y - r)$. However, from (4.53) we see that the penalty for having both a RHP-zero z_j and RHP-poles is $|\mathcal{B}_p^{-1}(z_j)| \geq 1$ for a 1-DOF controller.

4.8 Discussion

From the lower bounds on input usage (see Section 4.5.2) we can easily *quantify* how much measurement noise and the magnitude of disturbance we can tolerate to avoid that the input exceeds some prespecified limits. We find this quantification appealing, and it should be useful for control engineers doing practical control design. We therefore used the term "engineering bounds" for this application of the lower bounds in the second part of Example 4.2. Here we will only stress that these bounds are of fundamental theoretical importance, and they are (in many cases) tight for the best possible controller. So the bounds are exact, i.e. these bounds are not rules of thumb.

In the $\mathcal{H}_\infty$-controller design procedure, the $\mathcal{H}_\infty$-norm of some weighted closed-loop transfer function is minimized. It has been shown that the resulting minimization problem is a convex problem, which can be solved numerically for example by introducing Linear Matrix Inequalities (LMI) or using γ-iteration.

In this paper we have looked at single closed-loop transfer functions which can be written as TV or SV. Practical $\mathcal{H}_\infty$-controller designs are usually set up as a stacked transfer function consisting of several closed-loop transfer functions. Usually the sensitivity appears as a factor in one or more of the closed-loop transfer functions, which is the origin to the name "mixed sensitivity". The controller designed will then reflect a trade-off between the different requirements expressed in each of the closed-loop transfer functions. For example, it is common to put weight on both the output performance and input usage. This can be expressed as

in the mixed S/KS $\mathcal{H}_\infty$ controller design where the problem is to find the controller K such that the $\mathcal{H}_\infty$-norm of $\begin{bmatrix} w_P S \\ w_u K S \end{bmatrix}$ is minimized, i.e.

$$\min_K \left\| \begin{bmatrix} w_P S(s) \\ w_u K S(s) \end{bmatrix} \right\|_\infty$$

Lower and upper bounds on the $\mathcal{H}_\infty$-norm of the mixed S/KS sensitivity are

$$
\begin{aligned}
\max\{\|w_P S(s)\|_\infty, \|w_u K S(s)\|_\infty\} &\leq \left\| \begin{bmatrix} w_P S(s) \\ w_u K S(s) \end{bmatrix} \right\|_\infty \\
&\leq \sqrt{2}\, \max\{\|w_P S(s)\|_\infty, \|w_u K S(s)\|_\infty\}
\end{aligned}
$$

which shows that our individual lower bounds on $\|w_P S(s)\|_\infty$ and $\|w_u K S(s)\|_\infty$ provide useful information also for practical $\mathcal{H}_\infty$-controller designs.

In the γ-iteration the $\mathcal{H}_\infty$-minimization over the controller K is transformed to a convex minimization problem in the free variable γ, defined as the $\mathcal{H}_\infty$-norm of the closed-loop transfer function[3]. Most packages[4] provides the γ-iteration using the bisection method. That is, given a high and a low value of γ (upper and lower bound) and a stabilizing controller, the bisection method is used to iterate on the value of γ. This "modern" controller synthesis shows one application of lower and upper bounds on the $\mathcal{H}_\infty$-norm of general closed-loop transfer functions. The lower bounds derived in this paper can be used as the low value of γ supplied to the γ-iteration. This follows since the largest singular value of a matrix is larger than the largest element in the matrix. So, the largest lower bound on the $\mathcal{H}_\infty$-norm of a SISO transfer function in a stacked multivariable transfer function matrix, still is a lower bound on the $\mathcal{H}_\infty$-norm of the stacked closed-loop transfer function matrix in question.

4.9   Conclusion

- We have derived tight lower bounds on closed-loop transfer functions. The bounds are independent of the controller and therefore reflects the controllability of the plant.
- The bounds extend and generalize the SISO results by Zames (1981), Doyle et al. (1992) and Skogestad and Postlethwaite (1996) to also handle non-minimum phase and unstable weights. This allows us to derive *new* lower bounds on input usage due to disturbances, measurement noise and reference changes.
- The new lower bounds on input usage make it possible to *quantify* the minimum input usage for stabilization of unstable plants in the presence of worst case disturbances, measurement noise and reference changes.
- It is proved that the lower bounds are *tight*, by deriving analytical expressions for controllers which achieve an $\mathcal{H}_\infty$-norm of the closed-loop transfer functions equal to the lower bound for large classes of systems.

---

[3]In MATLAB Robust Control Toolbox γ is the inverse of the $\mathcal{H}_\infty$-norm of the closed-loop transfer function.

[4]See MATLAB, μ-tools or Robust Control Toolbox.

- Theorem 4.5 expresses the benefit of applying a 2-DOF controller compared to a 1-DOF controller when the plant is unstable and has a RHP-zero.
- The applications of the lower bounds have been illustrated and the implications have been studied in several examples. Nonlinear simulations have been used to find the amount of noise and disturbances which, in combination with input constraints, cause loss of stability for unstable plants. The results show good agreement between this amount of noise/disturbances and the corresponding values predicted by the lower bounds, in the examples studied.

References

Doyle, J. C., Francis, B. and Tannenbaum, A. (1992). *Feedback Control Theory*, Macmillan Publishing Company.

Havre, K. and Skogestad, S. (1997a). Effect of RHP zeros and poles on performance in multivariable systems, *Accepted for publication in Journal of Process Control* .

Havre, K. and Skogestad, S. (1997b). Limitations imposed by RHP zeros/poles in multivariable systems, *Proc. from ECC97*, Brussels, Belgium.

Kwakernaak, H. (1986). A polynomial approach to minimax frequency domain optimization of multivariable feedback systems, *Int. J. Control* **44**(1): 117–156.

Kwakernaak, H. (1993). Robust control and $\mathcal{H}_\infty$-optimization — Tutorial paper, *Automatica* **29**: 255–273.

Kwakernaak, H. (1995). Symmetries in control system design, *Trends in Control - A European Perspective, Alberto Isidori (ed.)* pp. 17–51.

Skogestad, S. and Postlethwaite, I. (1996). *Multivariable Feedback Control, Analysis and Design*, John Wiley & Sons, Chichester.

Youla, D. C., Bongiorno, J. J. and Lu, C. N. (1974). Single-loop feedback stabilization of linear multivariable dynamical plants, *Automatica* **10**: 159–173.

Zames, G. (1981). Feedback and optimal sensitivity: model reference transformations, multiplicative seminorms, and approximate inverses, *IEEE Transactions on Automatic Control* **AC-26**(2): 301–320.

Appendix A Proofs of the results

A.1   Proof of Lemma 4.1

The first identity in (4.11) follows since extracting RHP-zeros in the product AB in terms of the all-pass filter $\mathcal{B}_z(AB)$, does not change the $\mathcal{H}_\infty$-norm. The reason is that $\mathcal{B}_z(AB)$ is all-pass for $s = j\omega$. To prove the latter identity, assume A has RHP-zeros which does not appear in the product AB, then B

has RHP-poles for those RHP-zeros, and these RHP-poles can be factorized as $\mathcal{B}_p^{-1}(B)$. Similarly, if B has RHP-zeros which does not appear in the product AB, then A has RHP-poles for those RHP-zeros, and these RHP-poles can be factorized as $\mathcal{B}_p^{-1}(A)$. We obtain

$$AB = \mathcal{B}_p^{-1}(A)\,\mathcal{B}_z(A)\,A_{ms}\,\mathcal{B}_p^{-1}(B)\,\mathcal{B}_z(B)\,B_{ms} = \underbrace{\mathcal{B}_p^{-1}(A)\,\mathcal{B}_z(A)\,\mathcal{B}_p^{-1}(B)\,\mathcal{B}_z(B)}_{=\mathcal{B}_z(AB)}\,\underbrace{A_{ms}\,B_{ms}}_{=(AB)_m}$$

Since, AB is stable then $(AB)_m = A_{ms}B_{ms}$, and it follows that

$$\mathcal{B}_p^{-1}(A)\,\mathcal{B}_z(A)\,\mathcal{B}_p^{-1}(B)\,\mathcal{B}_z(B) = \mathcal{B}_z(AB)$$

Note that, a minimal realization of $\mathcal{B}_p^{-1}(A)\,\mathcal{B}_z(B)$ contains the RHP-zeros of B which are *not* RHP-poles in A, and a minimal realization of $\mathcal{B}_z(A)\,\mathcal{B}_p^{-1}(B)$ contains the RHP-zeros of A which are *not* RHP-poles in B. □

A.2 Proof of lower bounds on the $\mathcal{H}_\infty$-norm of closed-loop transfer functions

Proof of Theorem 4.2.

1) **Factor out RHP zeros and poles in S and V.** Lemma 4.1 gives

$$\|SV(s)\|_\infty = \|S_{ms}V_{ms}(s)\|_\infty = \|S_m V_{ms}(s)\|_\infty$$

   where the last equality holds since S is stable, i.e. $S_{ms} = S_m$.

2) **Introduce the stable scalar function $f(s) = S_m(s)V_{ms}(s)$.**

3) **Apply the maximum modulus theorem to $f(s)$ at the RHP-zeros z_j of G.**

$$\|f(s)\|_\infty \geq |f(z_j)|$$

4) **Resubstitute the factorization of RHP-zeros in S**, i.e. use $S_m(s) = S(s)\mathcal{B}_p^{-1}(s)$, where $\mathcal{B}_p(s)$ contains the RHP-poles of G, which due to internal stability also must be RHP-zeros of S. This gives

$$f(z_j) = S(z_j)\mathcal{B}_p^{-1}(z_j)V_{ms}(z_j)$$

5) **Use the interpolation constraint (4.16) for RHP-zeros z_j in G**, i.e. use $S(z_j) = 1$.

6) **Evaluate the lower bound.**

$$|f(z_j)| = |\mathcal{B}_p^{-1}(z_j)| \cdot |V_{ms}(z_j)|$$

   Note that $f(z_j)$ is independent of the controller K if V is independent of K.

Since these steps hold for all RHP-zeros z_j, Theorem 4.2 follows. □

A.3 Proof of Theorems 4.3 and 4.4

Proof of Theorem 4.3. The transfer function P has no poles in $\mathbb{C}_+$, since $V_{ms}^{-1}(s)$ has no poles in $\mathbb{C}_+$ and the remaining matrices $\mathcal{B}_z^{-1}(p)$ and $V_{ms}(p)$ are finite constant matrices. Furthermore, $1 - \mathcal{B}_z(s)P(s)$ has a RHP-zero for $s = p$, since $P(p) = \mathcal{B}_z^{-1}(p)$ so that $1 - \mathcal{B}_z(p)P(p) = 0$. It follows that a minimal realization of Q has no poles in $\mathbb{C}_+$, no RHP-zero for $s = p$, but it might have RHP-zeros for other

values. Since Q and G_{ms} has no poles in $\mathbb{C}_+$, and P has no zeros in $\mathbb{C}_+$, it follows that K has no zeros in $\mathbb{C}_+$. We obtain

$$
\begin{aligned}
L(s) &= GK(s) = \mathcal{B}_z(s)\,\mathcal{B}_p^{-1}(s)\,G_{ms}(s)\,G_{ms}^{-1}(s)\,P(s)\,Q^{-1}(s) \\
T^{-1} &= 1 + L^{-1} = 1 + Q(s)\,P^{-1}(s)\,\mathcal{B}_p(s)\,\mathcal{B}_z^{-1}(s) \\
&= 1 + \mathcal{B}_p^{-1}(s)\,(1 - \mathcal{B}_z(s)P(s))\,P^{-1}(s)\,\mathcal{B}_p(s)\,\mathcal{B}_z^{-1}(s) = P^{-1}(s)\,\mathcal{B}_z^{-1}(s) \\
T(s) &= \mathcal{B}_z(s)\,P(s) = \mathcal{B}_z(s)\,\mathcal{B}_z^{-1}(p)\,V_{ms}(p)V_{ms}^{-1}(s) \\
TV(s) &= \mathcal{B}_z(s)\,\mathcal{B}_z^{-1}(p)\,V_{ms}(p)\,\mathcal{B}_z(V(s))\,\mathcal{B}_p^{-1}(V(s))
\end{aligned}
$$

It follows that both T and $S = 1 - T = 1 - \mathcal{B}_z(s)\,P(s) = \mathcal{B}_p(s)\,Q(s)$ has no poles in $\mathbb{C}_+$. We note that T has the same zeros as G and it has zeros for the poles in V with real part less or equal to 0. Since, the poles of V in $\mathbb{C}_+$, i.e. $\mathcal{B}_p^{-1}(V)$, cancel against zeros in G, i.e. $\mathcal{B}_z(s)$, it follows that TV is stable. The $\mathcal{H}_\infty$-norm of TV is

$$
\|TV(s)\|_\infty = |\mathcal{B}_z^{-1}(p)| \cdot |V_{ms}(p)|
$$

since $\mathcal{B}_z(s)\,\mathcal{B}_z(V(s))\,\mathcal{B}_p^{-1}(V(s))$ is all-pass for $s = j\omega$. Since the value of $\|TV(s)\|_\infty$ in (4.26) is the same as the lower bound (4.18), this controller minimize $\|TV(s)\|_\infty$. $\qquad\square$

Proof of Theorem 4.4. The transfer function Q has no poles in $\mathbb{C}_+$, since $V_{ms}^{-1}(s)$ has no poles in $\mathbb{C}_+$ and the remaining matrices $\mathcal{B}_p^{-1}(z)$ and $V_{ms}(z)$ are finite constant matrices. Furthermore, $1 - \mathcal{B}_p(s)Q(s)$ has a RHP-zero for $s = z$, since $Q(z) = \mathcal{B}_p^{-1}(z)$ so that $1 - \mathcal{B}_p(z)Q(z) = 0$. A minimal realization of P has no poles in $\mathbb{C}_+$, no RHP-zero for $s = z$, but might have RHP-zeros for other values. Since G_{ms}^{-1}, P and Q^{-1} all have no poles in $\mathbb{C}_+$ it follows that K has no poles in $\mathbb{C}_+$. We obtain

$$
\begin{aligned}
S^{-1}(s) &= 1 + GK(s) = 1 + \mathcal{B}_p^{-1}(s)\,\mathcal{B}_z(s)\,G_{ms}(s)G_{ms}^{-1}(s)P(s)\,Q^{-1}(s) \\
&= 1 + \mathcal{B}_p^{-1}(s)\,(1 - \mathcal{B}_p(s)\,Q(s))\,Q^{-1}(s) = \mathcal{B}_p^{-1}(s)\,Q^{-1}(s) \\
S(s) &= Q(s)\,\mathcal{B}_p(s) = \mathcal{B}_p^{-1}(z)\,V_{ms}(z)\,V_{ms}^{-1}(s)\,\mathcal{B}_p(s) \\
SV(s) &= \mathcal{B}_p^{-1}(z)\,V_{ms}(z)\,\mathcal{B}_z(V(s))\,\mathcal{B}_p^{-1}(V(s))\,\mathcal{B}_p(s) \tag{4.54}
\end{aligned}
$$

It follows that both S and $T = 1 - S = 1 - \mathcal{B}_p(s)\,Q(s) = \mathcal{B}_z(s)\,P(s)$ have no poles in $\mathbb{C}_+$. The zeros of S are the poles of G and the poles of V with real part less or equal to 0. SV is stable, since the poles of V in $\mathbb{C}_+$, i.e. $\mathcal{B}_p^{-1}(V)$, cancel against the zeros (poles of G in $\mathbb{C}_+$) in $\mathcal{B}_p(s)$. The $\mathcal{H}_\infty$-norm of SV is

$$
\|SV(s)\|_\infty = |\mathcal{B}_p^{-1}(z)| \cdot |V_{ms}(z)|
$$

since $\mathcal{B}_p(s)\,\mathcal{B}_z(V(s))\,\mathcal{B}_p^{-1}(V(s))$ is all-pass for $s = j\omega$. Since the value of $\|SV(s)\|_\infty$ in (4.30) is the same as the lower bound (4.19), this controller minimize $\|SV(s)\|_\infty$. $\qquad\square$

A.4   Proof of the results for 2-DOF control

Proof of Theorem 4.5. We first prove the lower bound (4.49). From Lemma 4.1 we have

$$
\|w_P(SGK_1 - 1)R(s)\|_\infty = \|w_P(SGK_1 - 1)_{ms}R_m(s)\|_\infty
$$

since w_P is stable and minimum phase and R is stable. Consider the scalar function $f(s) = w_P(SGK_1 - 1)_{ms}R_m$ which is analytic (stable) in RHP since the closed-loop system is stable. By applying the maximum modulus theorem to $f(s)$ we get

$$
\|w_P(SGK_1 - 1)_{ms}R_m(s)\|_\infty = \|f(s)\|_\infty \geq |f(z_j)|
$$

$$|f(z_j)| = |w_P(SGK_1 - 1)_m R_m|_{s=z_j} = |w_P(z_j)(-1)R_m(z_j)| = |w_P(z_j)| \cdot |R_m(z_j)|$$

The second equality follows since SGK_1 must have RHP-zeros for $s = z_j$, since G has RHP-zeros for $s = z_j$, and S and K_1 must be stable (no RHP-poles in S or K_1 to cancel the RHP-zeros in G). It then follows that $(SGK_1 - 1)$ has no RHP-zeros for $s = z_j$.

Next, we prove that the controllers K_1 (4.51) and K_2 (4.52) given in Theorem 4.5, achieves the lower bound for the case when the plant has one RHP-zero z. Consider the factor

$$1 - w_P^{-1}(s)R_m^{-1}(s)w_P(z)R_m(z)$$

which is stable and has a RHP-zero for $s = z$. It then follows that a minimal realization of $P(s)$ has no poles in $\mathbb{C}_+$ and no RHP-zero for $s = z$. From equation (4.54) in the proof of Theorem 4.4 we find that $w_P SG$ with $K = K_2$ (minimizing $\|w_P SG(s)\|_\infty$) and $V = w_P G$ becomes

$$w_P SG(s) = w_P(z)\,\mathcal{B}_p^{-1}(z)\,G_{ms}(z)\,\mathcal{B}_z(s)$$

With $K_1 = \mathcal{B}_p(z)\,G_{ms}^{-1}(z)\,w_P^{-1}(z)\,w_P(s)\,P(s)$ we obtain

$$
\begin{aligned}
SGK_1(s) - 1 &= \mathcal{B}_z(s)\,P(s) - 1 \\
&= \mathcal{B}_z(s)\mathcal{B}_z^{-1}(s)\left(1 - w_P^{-1}(s)R_m^{-1}(s)w_P(z)R_m(z)\right) - 1 \\
&= -w_P^{-1}(s)R_m^{-1}(s)w_P(z)R_m(z) \\
w_P(SGK_1(s) - 1)R(s) &= -\mathcal{B}_z(R)\,w_P(z)R_m(z)
\end{aligned}
$$

$w_P(SGK_1(s) - 1)R(s)$ is stable, since $\mathcal{B}_z(R)$ is stable and the remaining matrices are constant. We obtain

$$\|w_P(SGK_1(s) - 1)R(s)\|_\infty = |w_P(z)| \cdot |R_m(z)|$$

Hence, K_1 and K_2 given in (4.51) and (4.52) minimizes the $\mathcal{H}_\infty$-norm of $w_p(SGK_1(s) - 1)R(s)$. $\square$

Chapter 5

Achievable $\mathcal{H}_\infty$-performance of multivariable systems with unstable zeros and poles

Kjetil Havre[*] and Sigurd Skogestad[†]

Chemical Engineering,
Norwegian University of Science and Technology
N-7034 Trondheim, Norway.

[*]Also affiliated with: Institute for energy technology, P.O.Box 40, N-2007 Kjeller, Norway, Fax: (+47) 63 81 11 68, E-mail: Kjetil.Havre@ife.no.

[†]Fax: (+47) 73 59 40 80, E-mail: skoge@chembio.ntnu.no.

Abstract

This paper examines the limitations imposed by Right Half Plane (RHP) zeros and poles in multivariable feedback systems. The main result is to provide lower bounds on $\|WXV(s)\|_\infty$ where X is S, S_I, T or T_I (sensitivity and complementary sensitivity). Previously derived lower bounds on the $\mathcal{H}_\infty$-norm of S and T are thus generalized to the case with matrix-valued weights, including bounds for reference tracking and disturbance rejection. Furthermore, new bounds which quantify the minimum *input* usage for stabilization in the presence of measurement noise and disturbances, are derived. We find that *output* performance is *only* limited if the plant has RHP-zeros. For a one degree-of-freedom (1-DOF) controller the presence of RHP-poles further deteriorate the response, whereas there is no additional penalty for having RHP-poles if we use a two degrees-of-freedom (2-DOF) controller (where the disturbance and/or reference signal is measured). For large classes of plants we *prove* that the lower bounds given are *tight* in the sense that there exist stable controllers which achieve these bounds.

5.1   Introduction

It is well known that the presence of RHP zeros and poles pose fundamental limitations on the achievable control performance. This was quantified for SISO systems by Bode (1945) more than 50 years ago, and most control engineers have an intuitive feeling of the limitations for scalar systems. Rosenbrock (1966; 1970) was one of the first to point out that multivariable RHP-zeros pose similar limitations.

In Chapter 4 we derived tight lower bounds on Single Input Single Output (SISO) closed-loop transfer functions on the forms SV and TV when the plant has RHP zeros and/or poles. Here S is the SISO sensitivity, T is the SISO complementary sensitivity and V may be any known rational transfer function. In this paper we extend these results to multivariable closed-loop transfer functions.

Two factors which complicate the MIMO results compared to the SISO results, are:

1) Zeros and poles in MIMO systems have directions.
2) The order of multiplication in multivariable transfer functions matter, i.e. two multi-variable transfer functions do not in general commute.

The main results in the paper are lower bounds on the $\mathcal{H}_\infty$-norm of closed-loop transfer functions on the four forms WSV, WS_IV, WTV and WT_IV, where S is the sensitivity, T is the complementary sensitivity, S_I is the input sensitivity, T_I is the input complementary sensitivity, W and V are general known multivariable transfer function matrices.

The basis of our results is the *important* work by Zames (1981), who made use of the interpolation constraint $y_z^H S(z) = y_z^H$ and the maximum modulus theorem to derive bounds on $\mathcal{H}_\infty$-norm of S for plants with one RHP-zero. The results by Zames were generalized to plants with RHP-poles by Doyle et al. (1992) in the SISO case, and by Skogestad and Postlethwaite (1996), Havre and Skogestad (Chapter 3) in the MIMO case.

In this paper we extend the work of Zames (1981) and the work given in Chapters 3 and 4, and quantify the fundamental limitations imposed by RHP zeros and poles in terms of lower bounds on the $\mathcal{H}_\infty$-norm of important closed-loop transfer functions. The main generalization of the previous result is that from the results in this paper we can derive lower bounds on $\mathcal{H}_\infty$-norm of other closed-loop transfer functions than sensitivity and complementary sensitivity. Further[1] generalizations include:

1) Multivariable weights.
2) Unstable and non-minimum phase weights.

A further motivation and the basis for deriving these results, are given in Chapter 4. One important application of the lower bounds, is that we can *quantify* the minimum usage needed to stabilize an unstable plant in the presence of the "worst case" disturbance, measurement noise and reference changes for the "best"[2] possible controller.

An additional important contribution of this paper is that we prove that the lower bounds are *tight* in a large number of cases. That is, we give analytical expressions for controllers

---

[1]In order to accomplish lower bounds on $\mathcal{H}_\infty$-norm of general closed-loop transfer functions, it was necessary to generalize the previous results to include multivariable, unstable and non-minimum phase weights.

[2]The best possible controller in the sense that the controller which minimizes the $\mathcal{H}_\infty$-norm of the closed-loop transfer function from the disturbances, measurement noise and reference changes to the inputs.

which *achieve* an $\mathcal{H}_\infty$-norm of the closed-loop transfer function which is equal to the lower bound.

The outline of the paper is as follows. First we give a brief introduction to zeros and poles of multivariable systems. We introduce factorizations of RHP zeros and poles, and we consider constraints imposed by RHP zeros and poles on sensitivity, complementary sensitivity, input sensitivity and input complementary sensitivity. Section 5.3 contains the main contribution of this paper, which are the lower bounds on the $\mathcal{H}_\infty$-norm of large classes of closed-loop transfer functions. In Section 5.4 we prove that the bounds involving the sensitivities are tight if the plant has one RHP-zero, and that the bounds involving the complementary sensitivities are tight if the plant has one RHP-pole. Some applications of the lower bounds are given in Section 5.5. Section 5.6 contains a "special" lower bound (which does not follow from the main results) on the closed-loop transfer function from references to outputs for the two degrees-of-freedom (2-DOF) control configuration. The proofs of the results are given in Section A.

The rest of this section we devote to a brief review of the solution to the $\mathcal{H}_\infty$-problem. The $\mathcal{H}_\infty$-norm was introduced into the control literature by Zames (1981), where he mainly focused on the use of this norm to obtain insight into the achievable performance. Our paper provides a continuation of this line of research. However, most of the research on $\mathcal{H}_\infty$-control has been focused on obtaining the optimal controller K which minimizes the $\mathcal{H}_\infty$-norm of a given transfer function. The early frequency-n approaches involved interpolation theoretic methods. A state-space version of this was the early work of Doyle (1984), which made use of the Youla parameterization of stabilizing controller, interpolation constraints and co-prime factorizations to reduce the problem to a best approximation Nehari problem. This approach is well described by Francis (1987). Unfortunately, it gives controllers of very high order, and explicit solutions to some $\mathcal{H}_\infty$-problems which gave controllers of much lower order (e.g. Kwakernaak, 1986), suggested that a more elegant solution to the general problem may exist. Indeed, a general state-space solution which gives optimal controllers with the same order as the plant including weights, was presented by Doyle et al. (1989). Today, the state-space solution to the $\mathcal{H}_\infty$-control problem can be found in many text books (e.g. Zhou et al., 1996; Green and Limebeer, 1995). With the aim to prove tightness of our bounds, we derive $\mathcal{H}_\infty$-optimal controllers for some special problems. These controllers are derived analytically by assuming that the optimal closed-loop transfer functions are constant[3] functions of frequency, i.e. they are all-pass transfer functions, which due to internal stability also must satisfy the interpolation constraints for RHP zeros and poles. The approach taken in this paper, is similar to the early interpolation theoretic methods, see the simple analytic examples presented in Chapter 1 of Green and Limebeer (1995), and it is also related to the polynomial approach of Kwakernaak (1986; 1993; 1996). We finally note that analytical solutions to $\mathcal{H}_\infty$-optimal controllers to some special problems appears in the control literature, see for example the robust stabilization of a plant with normalized left coprime factorization

---

[3]Kwakernaak (1986; 1993) names the fact that the largest singular value of the $\mathcal{H}_\infty$-optimal closed-loop transfer function is constant (independent of frequency) for "equalizing property" (the solutions which results in closed-loop transfer functions on the forms $\lambda^2 I$ are named "equalizing solutions"). Kwakernaak also proves in the SISO case that the $\mathcal{H}_\infty$-optimal controller results in a constant largest singular of the optimal closed-loop transfer function, when the $\mathcal{H}_\infty$-norm of mixed sensitivity is minimized.

(Skogestad and Postlethwaite, 1996, page 376). An analytical solution to the $\mathcal{H}_\infty$-optimal controller for this problem can be found using a descriptor system approach (Safonov, Limebeer and Chiang, 1989).

5.2   Elements from linear system theory

We consider linear time invariant transfer function models on the form

$$y(s) = G(s)u(s) + G_d(s)d(s) \tag{5.1}$$

where u is the vector of manipulated inputs, d is the vector of disturbances and y is the vector of outputs. We often omit to show the dependence on the complex variable s for transfer functions. When we refer to zeros and poles and their directions, we mean the zeros and poles of the plant G unless otherwise explicitly stated. In order to be able to stabilize the pair (G, G_d) we must require that all unstable poles in G_d also are poles in G.

The $\mathcal{H}_\infty$-norm of a stable rational transfer function matrix $M(s)$ is defined as the peak value overall frequencies of the largest singular value of $M(j\omega)$

$$\|M(s)\|_\infty \triangleq \sup_\omega \bar{\sigma}(M(j\omega)) \tag{5.2}$$

5.2.1   Zeros and poles in multivariable systems

Zeros and zero directions. Zeros of a system arise when competing effects, internal to the system, are such that the output is zero even when the inputs and the states are not identically zero. Here we apply the following definition of zeros (MacFarlane and Karcanias, 1976).

DEFINITION 5.1 (ZEROS). *$z_i \in \mathbb{C}$ is a zero of $G(s)$ if the rank of $G(z_i)$ is less than the normal rank of $G(s)$.*

The normal rank of $G(s)$ is defined as the rank of $G(s)$ at all s except a finite number of singularities (which are the zeros).

DEFINITION 5.2 (ZERO DIRECTIONS). *If $G(s)$ has a zero for $s = z \in \mathbb{C}$ then there exist non-zero vectors, denoted the input zero direction $u_z \in \mathbb{C}^m$ and the output zero direction $y_z \in \mathbb{C}^l$, such that $u_z^H u_z = 1$, $y_z^H y_z = 1$ and*

$$G(z)u_z = 0; \qquad y_z^H G(z) = 0 \tag{5.3}$$

For a system $G(s)$ with state-space realization $\left[\begin{array}{c|c} A & B \\ \hline C & D \end{array}\right]$, the zeros z of the system, the input zero directions u_z and the state input zero vectors $x_{zi} \in \mathbb{C}^n$ (n is the number of states) can all be computed from the generalized eigenvalue problem

$$\begin{bmatrix} A - sI & B \\ C & D \end{bmatrix} \begin{bmatrix} x_{zi} \\ u_z \end{bmatrix} = \begin{bmatrix} 0 \\ 0 \end{bmatrix} \tag{5.4}$$

Similarly one can compute the zeros z and the output zero directions y_z from G^T, see Section 2.3 for further details.

Poles and pole directions. Bode (1945) states that *the poles are the singular points at which the transfer function fails to be analytic*. In this work we replace "fails to be analytic" with "is infinite", which certainly implies that the transfer function is *not analytic*. When we evaluate[4] the transfer function $G(s)$ at $s = p$, $G(p)$ is infinite in some directions at the input and the output. This is the basis for the following definition of input and output pole directions.

DEFINITION 5.3 (POLE DIRECTIONS). *If $s = p \in \mathbb{C}$ is a distinct pole of $G(s)$ then there exist one input direction $u_p \in \mathbb{C}^m$ and one output direction $y_p \in \mathbb{C}^l$ with infinite gain for $s = p$.*

For a system $G(s)$ with minimal state-space realization $\left[\begin{array}{c|c} A & B \\ \hline C & D \end{array}\right]$ the pole directions u_p and y_p for a *distinct* pole p can be computed from (Section 2.4)

$$u_p = B^H x_{pi} / \left\| B^H x_{pi} \right\|_2 ; \qquad y_p = C x_{po} / \left\| C x_{po} \right\|_2 \qquad (5.5)$$

where $x_{pi} \in \mathbb{C}^n$ and $x_{po} \in \mathbb{C}^n$ are the eigenvectors corresponding to the two eigenvalue problems

$$x_{pi}^H A = p x_{pi}^H; \qquad A x_{po} = p x_{po}$$

Note, that the pole directions are normalized, i.e. $\|u_p\|_2 = 1$ and $\|y_p\|_2 = 1$. For the sake of simplicity we will only consider distinct poles in this paper, for computation and definition of pole directions in the case when the pole p is not distinct refer to Chapter 2.

5.2.2   All-pass factorizations of RHP zeros and poles

A transfer function matrix $B(s)$ is all-pass if $B^T(-s)B(s) = I$, which implies that all singular values of $B(j\omega)$ are equal to one.

A rational transfer function matrix $M(s)$ with RHP-poles $p_i \in \mathbb{C}_+$, can be factorized either at the input (subscript i) or at the output (subscript o) of $M(s)$ as follows[5]

$$M(s) = M_{si}\, \mathcal{B}_{pi}^{-1}(M(s)); \qquad M(s) = \mathcal{B}_{po}^{-1}(M)\, M_{so}(s) \qquad (5.6)$$

M_{si}, M_{so} – Stable (subscript s) versions of M with the RHP-poles mirrored across the imaginary axis.

$\mathcal{B}_{pi}(M), \mathcal{B}_{po}(M)$ – Stable all-pass rational transfer function matrices containing the RHP-poles (subscript p) of M as RHP-zeros.

The all-pass filters are (Appendix A)

$$\mathcal{B}_{pi}(M(s)) = \prod_{i=1}^{N_p} (I - \tfrac{2\mathrm{Re}(p_i)}{s+\bar{p}_i}\hat{u}_{p_i}\hat{u}_{p_i}^H); \quad \mathcal{B}_{pi}^{-1}(M(s)) = \prod_{i=N_p}^{1} (I + \tfrac{2\mathrm{Re}(p_i)}{s-p_i}\hat{u}_{p_i}\hat{u}_{p_i}^H) \quad (5.7)$$

$$\mathcal{B}_{po}(M(s)) = \prod_{i=N_p}^{1} (I - \tfrac{2\mathrm{Re}(p_i)}{s+\bar{p}_i}\hat{y}_{p_i}\hat{y}_{p_i}^H); \quad \mathcal{B}_{po}^{-1}(M(s)) = \prod_{i=1}^{N_p} (I + \tfrac{2\mathrm{Re}(p_i)}{s-p_i}\hat{y}_{p_i}\hat{y}_{p_i}^H) \quad (5.8)$$

---

[4]Strictly speaking, the transfer function $G(s)$ can *not* be evaluated at $s = p$, since $G(s)$ is not analytic at $s = p$.

[5]Note that the notation on the all-pass factorizations of RHP zeros and poles used in this paper is reversed compared to the notation used in (Green and Limebeer, 1995; Skogestad and Postlethwaite, 1996; Havre and Skogestad, 1996). The reason for this change of notation is to get consistent with what the literature generally defines as an all-pass filter.

$\mathcal{B}_{po}(M)$ is obtained by factorizing at the output one RHP-pole at a time, starting with

$$M = \mathcal{B}_{p_1 o}^{-1}(M) M_{p_1 o}$$

where

$$\mathcal{B}_{p_1 o}^{-1}(M(s)) = I + \frac{2\,\mathrm{Re}(p_1)}{s - p_1} \hat{y}_{p_1} \hat{y}_{p_1}^H$$

and $\hat{y}_{p_1} = y_{p_1}$ is the output pole direction of M for p_1. This procedure may be continued to factor out p_2 from $M_{p_1 o}$ where $\hat{y}_{p_2}$ is the output pole direction of $M_{p_1 o}$ (which need not coincide with y_{p_2}, the pole direction[6] of M) and so on. A similar procedure may be used to factorize the poles at the input of M. Note that the sequence get reversed in the input factorization compared to the output factorization.

In a similar sequential manner, the RHP-zeros can be factorized either at the input or at the output of M

$$M(s) = M_{mi} \mathcal{B}_{zi}(M(s)); \qquad M(s) = \mathcal{B}_{zo}(M) M_{mo}(s) \tag{5.9}$$

M_{mi}, M_{mo} – Minimum phase (subscript m) versions of M with the RHP-zeros mirrored across the imaginary axis.

$\mathcal{B}_{zi}(M), \mathcal{B}_{zo}(M)$ – Stable all-pass rational transfer function matrices containing the RHP-zeros (subscript z) of M.

We get (Appendix A)

$$\mathcal{B}_{zi}(M(s)) = \prod_{j=N_z}^{1} \left(I - \frac{2\,\mathrm{Re}(z_j)}{s + \bar{z}_j} \hat{u}_{z_j} \hat{u}_{z_j}^H\right); \quad \mathcal{B}_{zi}^{-1}(M(s)) = \prod_{j=1}^{N_z} \left(I + \frac{2\,\mathrm{Re}(z_j)}{s - z_j} \hat{u}_{z_j} \hat{u}_{z_j}^H\right) \tag{5.10}$$

$$\mathcal{B}_{zo}(M(s)) = \prod_{j=1}^{N_z} \left(I - \frac{2\,\mathrm{Re}(z_j)}{s + \bar{z}_j} \hat{y}_{z_j} \hat{y}_{z_j}^H\right); \quad \mathcal{B}_{zo}^{-1}(M(s)) = \prod_{j=N_z}^{1} \left(I + \frac{2\,\mathrm{Re}(z_j)}{s - z_j} \hat{y}_{z_j} \hat{y}_{z_j}^H\right) \tag{5.11}$$

Alternative all-pass factorizations are in use, e.g. the inner-outer factorizations used in (Morari and Zafiriou, 1989) which are the same as (5.10) and (5.11) except for the multiplication of a constant unitary matrix. Reasons for using the factorizations given here are:

1) The factorizations of RHP-zeros given here are analytic and in terms of the zeros and the zero directions, whereas the inner-outer factorizations in (Morari and Zafiriou, 1989) are given in terms of the solution to an algebraic Riccati equation.

2) To factorize RHP-poles using the inner-outer factorization one needs to assume that G^{-1} exist.

Some useful properties. Assume that M^{-1} exists, then (Appendix A):

$$\mathcal{B}_{zi}(M) = \mathcal{B}_{po}(M^{-1}); \qquad M_{mi} = (M^{-1})_{so}^{-1} \tag{5.12}$$

$$\mathcal{B}_{zo}(M) = \mathcal{B}_{pi}(M^{-1}); \qquad M_{mo} = (M^{-1})_{si}^{-1} \tag{5.13}$$

---

[6]In fact: $\hat{y}_{p_2} = \mathcal{B}_{p_1 o}^{-H}(M)|_{s=p_2} y_{p_2}$. Here $\mathcal{B}|_{s=s_0}$ means the rational transfer function matrix $\mathcal{B}(s)$ evaluated at the complex number $s = s_0$. Thus, it provides an alternative to $\mathcal{B}(s_0)$, and it will mainly be used to avoid double parenthesis.

Repeated factorization (Appendix A):

$$\mathcal{B}_{pi}(\mathcal{B}_{pi}^{-1}(M)) = \mathcal{B}_{pi}(M); \qquad \mathcal{B}_{po}(\mathcal{B}_{po}^{-1}(M)) = \mathcal{B}_{po}(M) \qquad (5.14)$$

$$\mathcal{B}_{zi}(\mathcal{B}_{zi}(M)) = \mathcal{B}_{zi}(M); \qquad \mathcal{B}_{zo}(\mathcal{B}_{zo}(M)) = \mathcal{B}_{zo}(M) \qquad (5.15)$$

$$\mathcal{B}_{zi}(\mathcal{B}_{po}(M)) = \mathcal{B}_{po}(M); \qquad \mathcal{B}_{zo}(\mathcal{B}_{pi}(M)) = \mathcal{B}_{pi}(M) \qquad (5.16)$$

$$\mathcal{B}_{pi}(\mathcal{B}_{zo}^{-1}(M)) = \mathcal{B}_{zo}(M); \qquad \mathcal{B}_{po}(\mathcal{B}_{zi}^{-1}(M)) = \mathcal{B}_{zi}(M) \qquad (5.17)$$

Factorization of SISO systems. Factorizations of RHP zeros and poles in SISO systems can be found from the previous expressions by setting the directions equal to 1. Since the order of multiplication does not matter in rational transfer functions, the input and output factorizations are identical. We therefore drop the subscript which distinguish the input factorization from the output factorization. We obtain the well known and widely used all-pass factors:

$$\mathcal{B}_p(M(s)) \quad = \quad \prod_{i=1}^{N_p} 1 - \frac{2\mathrm{Re}(p_i)}{s + \bar{p}_i} \quad = \quad \prod_{i=1}^{N_p} \frac{s - p_i}{s + \bar{p}_i} \qquad (5.18)$$

$$\mathcal{B}_z(M(s)) \quad = \quad \prod_{i=1}^{N_z} 1 - \frac{2\mathrm{Re}(z_i)}{s + \bar{z}_i} \quad = \quad \prod_{j=1}^{N_z} \frac{s - z_j}{s + \bar{z}_j} \qquad (5.19)$$

5.2.3 Closing the loop

In this paper we consider the general two degrees-of-freedom (2-DOF) control configuration shown in Figure 5.1. In the figure the performance weights are given in dashed lines. We
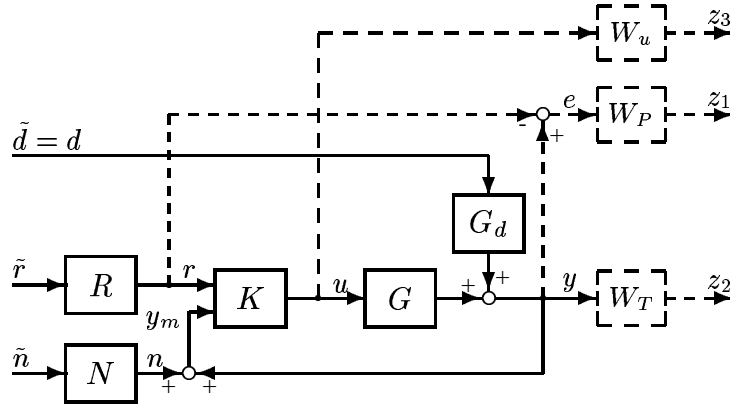
Figure 5.1: Two degrees-of-freedom control configuration

have included both references r and measurement noise n in addition to disturbances d as external inputs. The three matrices G_d, R and N can be viewed as weights on the inputs, and the inputs $\tilde{d}$, $\tilde{r}$ and $\tilde{n}$ are normalized in magnitude. Normally, N is diagonal and $[N]_{ii}$ is the inverse of signal to noise ratio. For most practical purposes, we can assume that R and N are stable. However, from a technical point of view it suffices that the unstable modes in N and R can be stabilized through the inputs u. For the disturbance plant G_d we assume that all the

unstable modes of G_d also appears in G (which is required if the unstable modes of G_d are state controllable in u).

The controller can be divided into a negative feedback part from y (K_2) and a feed forward part from r (K_1)

$$u = K_1 r - K_2 y_m = K_1 r - K_2 (y + n) \tag{5.20}$$

The closed-loop transfer function F from

$$v = \begin{bmatrix} \tilde{r} \\ \tilde{d} \\ \tilde{n} \end{bmatrix} \quad \text{to} \quad z = \begin{bmatrix} z_1 \\ z_2 \\ z_3 \end{bmatrix}^T = \begin{bmatrix} W_P(y - r) \\ W_T y \\ W_u u \end{bmatrix}$$

is

$$F(s) = \begin{bmatrix} W_P(SGK_1 - I)R & W_P SG_d & -W_P TN \\ W_T SGK_1 R & W_T SG_d & -W_T TN \\ W_u S_I K_1 R & -W_u K_2 SG_d & -W_u K_2 SN \end{bmatrix} \tag{5.21}$$

where the sensitivity S, the complementary sensitivity T and the input sensitivity S_I are defined by

$$S \triangleq (I + GK_2)^{-1} \tag{5.22}$$

$$T \triangleq I - S = GK_2(I + GK_2)^{-1} \tag{5.23}$$

$$S_I \triangleq (I + K_2 G)^{-1} \tag{5.24}$$

We also define the input complementary sensitivity

$$T_I \triangleq I - S_I = K_2 G(I + K_2 G)^{-1} \tag{5.25}$$

By setting $K_1 = K_2$ in the above equations, the one degree-of-freedom (1-DOF) control configuration can be analyzed.

5.2.4 Interpolation constraints on S, T, S_I and T_I

CONSTRAINT 5.1 (RHP-ZERO IN G). *If $G(s)$ has a* RHP*-zero at $s = z$ with output zero direction y_z, then for internal stability of the feedback system the following interpolation constraints must apply*

$$y_z^H T(z) = 0; \qquad y_z^H S(z) = y_z^H \tag{5.26}$$

$$T_I(z)u_z = 0; \qquad S_I(z)u_z = u_z \tag{5.27}$$

In words, (5.26) says that T must have a RHP-zero in the same output direction as G and that $S(z)$ has an eigenvalue of 1 with corresponding left eigenvector y_z. In a similar way T_I has RHP-zero with the same input direction as G.

CONSTRAINT 5.2 (RHP-POLE IN G). *If $G(s)$ has a* RHP*-pole at $s = p$ with output direction y_p, then for internal stability of the feedback system the following interpolation constraints must apply*

$$S(p)y_p = 0; \qquad T(p)y_p = y_p \tag{5.28}$$

$$u_p^H S_I(p) = 0; \qquad u_p^H T_I(p) = u_p^H \tag{5.29}$$

The constraint (5.26) was first proved by Zames (1981), the proof of (5.28) is given in (Skogestad and Postlethwaite, 1996). The proofs of (5.26) and (5.28) are given in Section A in Chapter 3. The proofs of (5.27) and (5.29) follow similarly and are given in Section A.

Similar constraints also apply to S, T, S_I and T_I when the feedback controller has RHP-zeros and RHP-poles.

5.3 Lower bounds on the $\mathcal{H}_\infty$-norm of closed-loop transfer functions

In this section we derive general lower bounds on the $\mathcal{H}_\infty$-norm of closed-loop transfer functions when the plant G has one or more RHP zeros and/or poles, by using the interpolation constraints and the maximum modulus principle. The bounds are applicable to closed-loop transfer functions on the form

$$W(s)X(s)V(s) \tag{5.30}$$

where X may be S, T, S_I or T_I. The idea is to derive lower bounds on $\|WXV(s)\|_\infty$ which are independent of the controller K. In general, we assume that WXV is stable. The "weights" W and V must be independent of K. They may be unstable, but it must be possible to stabilize all transfer functions through the outputs. This implies that the unstable modes of W and V also appear in $L = GK_2$. Otherwise, the system is not stabilizable. The results are stated in terms of four theorems.

Theorems 5.1 and 5.2 provide lower bounds on the $\mathcal{H}_\infty$-norm of closed-loop transfer functions on the forms WSV and WS_IV caused by one or more RHP-zeros in G. By maximizing over all RHP-zeros, we find the largest lower bounds on $\|WSV(s)\|_\infty$ and $\|WS_IV(s)\|_\infty$ which takes into account one RHP-zero and all RHP-poles in the plant.

THEOREM 5.1 (LOWER BOUND ON $\|WSV(s)\|_\infty$). *Consider a plant G with $N_z \geq 1$ RHP-zeros z_j, output directions y_{z_j} and $N_p \geq 0$ RHP-poles $p_i \in \mathbb{C}_+$. Let W and V be rational transfer function matrices, and assume that W has no RHP-poles at locations corresponding to RHP poles or zeros in G. Assume that the closed-loop transfer function WSV is (internally) stable. Then the following lower bound on $\|WSV(s)\|_\infty$ applies:*

$$\|WSV(s)\|_\infty \geq \max_{\text{RHP-zeros } z_j \text{ in } G} \|W_{mo}(z_j)\, y_{z_j}\|_2 \cdot \|y_{z_j}^H V \mathcal{B}_{zi}^{-1}(\mathcal{B}_{po}(G)\, V)|_{s=z_j}\|_2 \tag{5.31}$$

Proof. The main steps in the proof of (5.31) are given in Section 5.3.1. For a detailed proof see Section A.

THEOREM 5.2 (LOWER BOUND ON $\|WS_IV(s)\|_\infty$). *Consider a plant G with $N_z \geq 1$ RHP-zeros z_j, input directions u_{z_j} and $N_p \geq 0$ RHP-poles $p_i \in \mathbb{C}_+$. Let W and V be rational transfer function matrices, and assume that V has no RHP-poles at locations corresponding to RHP poles or zeros in G. Assume that the closed-loop transfer function WS_IV is (internally) stable. Then the following lower bound on $\|WS_IV(s)\|_\infty$ applies:*

$$\|WS_IV(s)\|_\infty \geq \max_{\text{RHP-zeros, } z_j \text{ in } G} \|\mathcal{B}_{zo}^{-1}(W\mathcal{B}_{pi}(G))\, W|_{s=z_j}\, u_{z_j}\|_2 \cdot \|u_{z_j}^H V_{mi}(z_j)\|_2$$

$$\tag{5.32}$$

Theorems 5.3 and 5.4 provide lower bounds on the $\mathcal{H}_\infty$-norm of closed-loop transfer functions on the forms WTV and WT_IV caused by one or more RHP-poles in G. Then by maximizing over all RHP-poles, we find the largest lower bounds on $\|WTV(s)\|_\infty$ and $\|WT_IV(s)\|_\infty$ which takes into account one RHP-pole and all RHP-zeros in the plant.

THEOREM 5.3 (LOWER BOUNDS ON $\|WTV(s)\|_\infty$). *Consider a plant G with $N_p \geq 1$ RHP-poles p_i, output directions y_{p_i} and $N_z \geq 0$ RHP-zeros $z_j \in \mathbb{C}_+$. Let W and V be rational transfer function matrices, and assume that V has no RHP-poles at locations corresponding to RHP zeros or poles in G. Assume that the closed-loop transfer function WTV is (internally) stable. Then the following lower bound on $\|WTV(s)\|_\infty$ applies:*

$$\|WTV(s)\|_\infty \geq \max_{\text{RHP-poles, } p_i \text{ in } G} \left\| \mathcal{B}_{zo}^{-1}(W\mathcal{B}_{zo}(G))\,W\big|_{s=p_i}\, y_{p_i} \right\|_2 \cdot \left\| y_{p_i}^H V_{mi}(p_i) \right\|_2$$

$$(5.33)$$

THEOREM 5.4 (LOWER BOUNDS ON $\|WT_IV(s)\|_\infty$). *Consider a plant G with $N_p \geq 1$ RHP-poles p_i, input directions u_{p_i} and $N_z \geq 0$ RHP-zeros $z_j \in \mathbb{C}_+$. Let W and V be rational transfer function matrices, and assume that W has no RHP-poles at locations corresponding to RHP zeros or poles in G. Assume that the closed-loop transfer function WT_IV is (internally) stable. Then the following lower bound on $\|WT_IV(s)\|_\infty$ applies:*

$$\|WT_IV(s)\|_\infty \geq \max_{\text{RHP-poles, } p_i \text{ in } G} \left\| W_{mo}(p_i)\,u_{p_i} \right\|_2 \cdot \left\| u_{p_i}^H V \mathcal{B}_{zi}^{-1}(\mathcal{B}_{zi}(G)\,V)\big|_{s=p_i} \right\|_2$$

$$(5.34)$$

Remarks on Theorems 5.1–5.4:

1) The somewhat messy notation can easily be interpreted. As an example take the last factor of (5.31): Factorize the RHP-poles at the output of G into an all-pass filter $\mathcal{B}_{po}(G)$ (yields RHP-zeros), multiply on the right with V (may add RHP-zeros if V is non-minimum phase), then factorize at the input the RHP-zeros of the product into an all-pass transfer function, take its inverse, multiply on the left with $y_{z_j}^H V$ and finally evaluate the result for $s = z_j$.

2) The lower bounds (5.31)–(5.34) are independent of the feedback controller K_2 if the weights W and V are independent of K_2.

3) The internal stability assumption on the closed-loop transfer functions WXV, where $X \in \{S, S_I, T, T_I\}$, means that WXV are stable, and we have no RHP pole/zero cancellations between the plant G and the feedback controller K_2.

4) For internal stability, the *only* way to stabilize unstable modes is to apply feedback control. For the closed-loop transfer functions WSV and WS_IV, this implies that all the unstable poles in W and V must appear as RHP-zeros in S and S_I (to cancel the unstable poles in W and V), which in turn implies that the loop transfer functions L and L_I have RHP-poles with corresponding directions. For the closed-loop transfer functions WTV and WT_IV, we need RHP-zeros in T and T_I to cancel the unstable modes in W and V, which in turn implies RHP-zeros in L and L_I with corresponding directions.

5) The following requirements on W and V follow from the requirement of internal stability (and are therefore not explicitly stated in the above theorems):

   a) Implicit requirements in Theorem 5.1. If the plant G has RHP-zeros z_j with output directions y_{z_j}, then internal stability of WSV implies:

      i) W can *not* have RHP-poles for $s = z_j$ with input directions y_{z_j}.
      ii) V can *not* have RHP-poles for $s = z_j$ with output directions y_{z_j}.

      Proof of ai). Assume that W has a RHP-pole for $s = z_j$ with input direction y_{z_j}. In order to cancel the pole in W, K_2 must have a RHP-pole for $s = z_j$ with input direction y_{z_j}, and for internal stability we can not allow G to have a zero $s = z_j$ with output direction y_{z_j}. The proof of aii) is similar.   □

   b) Implicit requirements in Theorem 5.2. If the plant G has RHP-zeros z_j with input directions u_{z_j}, then internal stability of WS_IV implies:

      i) W can *not* have RHP-poles for $s = z_j$ with input directions u_{z_j}.
      ii) V can *not* have RHP-poles for $s = z_j$ with output directions u_{z_j}.

   c) Implicit requirements in Theorem 5.3. If the plant G has RHP-poles p_i with output directions y_{p_i}, then internal stability of WTV implies:

      i) W can *not* have RHP-poles for $s = p_i$ with input directions y_{p_i}.
      ii) V can *not* have RHP-poles for $s = p_i$ with output directions y_{p_i}.

   d) Implicit requirements in Theorem 5.4. If the plant G has RHP-poles p_i with input directions u_{p_i}, then internal stability of WT_IV implies:

      i) W can *not* have RHP-poles for $s = p_i$ with input directions u_{p_i}.
      ii) V can *not* have RHP-poles for $s = p_i$ with output directions u_{p_i}.

6) In addition to the above implicit requirements on W and V, we have in each of the above theorems an additional assumption on the RHP-poles in W or V. This additional assumption is a result of splitting the transfer functions into two parts when deriving the bounds, e.g. WSV is split into W and SV etc. In any case, the additional assumption is in practice *not* restrictive, since when the assumption is *not* fulfilled we can generally rewrite the transfer function and apply another theorem instead.

EXAMPLE 5.1. Consider deriving a bound on $\mathcal{H}_\infty$-norm of the closed-loop transfer function K_2SG_d (input usage due to disturbances). We can use the relation $K_2SG_d = G^{-1}TG_d$ and apply Theorem 5.3 with $W = G^{-1}$ and $V = G_d$, but we must assume that G_d is *stable*. However, we can use the relation $K_2SG_d = T_IG^{-1}G_d$ and apply Theorem 5.4 with $W = I$ and $V = G^{-1}G_d$, and in this case we can also allow G_d to be *unstable*.

5.3.1 Main steps in the proof of Theorem 5.1

To provide some more insight to the results, we give the main steps in the proof of the lower bound (5.31) on $\|WSV(s)\|_\infty$. The main steps in the proof of the lower bounds (5.32)–(5.34) are similar.

   1) **Factor out RHP zeros in WSV to obtain $(WSV)_m$.**

   (a) Factor out RHP-zeros of S due to RHP-poles in G at the input of S.

   (b) Factor out RHP zeros of $\mathcal{B}_{pi}(G)V$ at the input of WSV.

   (c) Factor out RHP zeros of W at the output of WSV.

Note, make sure that no RHP-zeros in S due to poles in G, which cancel RHP-poles in V and W, are factorized:

   1) We avoid factorizing RHP-zeros in S which cancel poles in V, by factorizing the zeros of $\mathcal{B}_{po}(G)V$.

   2) With the assumption on the poles in Theorem 5.1 we avoid factorizing RHP-zeros in S which cancel poles in W.

2) **Introduce the stable scalar function $f(s)$ on the minimum phase version $(WSV)_m$ of WSV.**

3) **Apply the maximum modulus theorem to $f(s)$ at the RHP-zeros of G.**

4) **Resubstitute the factorization of RHP-zeros in S.**

5) **Use the interpolation constraint for RHP-zeros in G.**

6) **Evaluate the lower bound.**

5.3.2 Some important special cases

G has no RHP-poles. Then $\mathcal{B}_{po}(G) = I$, $\mathcal{B}_{pi}(G) = I$ and (5.31) and (5.32) become

$$\|WSV(s)\|_\infty \;\geq\; \max_{\text{RHP-zeros, } z_j \text{ in } G}\; \|W_{mo}(z_j)\,y_{z_j}\|_2 \cdot \|y_{z_j}^H V_{mi}(z_j)\|_2 \qquad (5.35)$$

$$\|WS_IV(s)\|_\infty \;\geq\; \max_{\text{RHP-zeros, } z_j \text{ in } G}\; \|W_{mo}(z_j)\,u_{z_j}\|_2 \cdot \|u_{z_j}^H V_{mi}(z_j)\|_2 \qquad (5.36)$$

These bounds quantify the effect of RHP-zeros in the plant G on the closed-loop performance. Note, if one or both of the weights W and V are unstable, then the feedback controller K_2 must be unstable to stabilize WSV and WS_IV.

G has no RHP-zeros. Then $\mathcal{B}_{zo}(G) = I$ and $\mathcal{B}_{zi}(G) = I$, and (5.33) and (5.34) become

$$\|WTV(s)\|_\infty \;\geq\; \max_{\text{RHP-poles, } p_i \text{ in } G}\; \|W_{mo}(p_i)\,y_{p_i}\|_2 \cdot \|y_{p_i}^H V_{mi}(p_i)\|_2 \qquad (5.37)$$

$$\|WT_IV(s)\|_\infty \;\geq\; \max_{\text{RHP-poles, } p_i \text{ in } G}\; \|W_{mo}(p_i)\,u_{p_i}\|_2 \cdot \|u_{p_i}^H V_{mi}(p_i)\|_2 \qquad (5.38)$$

These bounds quantify the effect of RHP-poles in the plant G on the performance. Note that the weights W and V may contain RHP-zeros. This is important when considering input usage since $KS = G^{-1}T = T_IG^{-1}$ where G^{-1} has one or more RHP-zeros when G is unstable. If the weights W and V are unstable, then the feedback controller K_2 must have RHP-zeros to stabilize WTV and WT_IV.

Scalar weights with no poles in $\mathbb{C}_+$. For the case with a scalar input weight $V(s) = v(s) \cdot I$ with no poles in $\mathbb{C}_+$, then the last terms in (5.31) and (5.34) become

$$V \mathcal{B}_{zi}^{-1}(\mathcal{B}_{po}(G)\,V) = v_m\,\mathcal{B}_{po}^{-1}(G) \tag{5.39}$$

$$V \mathcal{B}_{zi}^{-1}(\mathcal{B}_{zi}(G)\,V) = v_m\,\mathcal{B}_{zi}^{-1}(G) \tag{5.40}$$

Proof of (5.39)–(5.40). To prove (5.39) we look at

$$\mathcal{B}_{po}(G)V = v\mathcal{B}_{po}(G) = v_m \mathcal{B}_z(v)\mathcal{B}_{po}(G)$$

We obtain

$$\mathcal{B}_{zi}(\mathcal{B}_{po}(G)\,V) = \mathcal{B}_z(v)\mathcal{B}_{po}(G)$$

and

$$V\mathcal{B}_{zi}^{-1}(\mathcal{B}_{po}(G)\,V) = \underbrace{v\,\mathcal{B}_z^{-1}(v)}_{v_m}\,\mathcal{B}_{po}^{-1}(G) = v_m\,\mathcal{B}_{po}^{-1}(G)$$

The proof of (5.40) follows similarly.   □

Similarly, with a scalar output weight $W = w(s) \cdot I$ with no poles in $\mathbb{C}_+$, the two first terms of (5.32) and (5.33) become

$$\mathcal{B}_{zo}^{-1}(W\mathcal{B}_{pi}(G))\,W = w_m\mathcal{B}_{pi}^{-1}(G) \tag{5.41}$$

$$\mathcal{B}_{zo}^{-1}(W\mathcal{B}_{zo}(G))\,W = w_m\mathcal{B}_{zo}^{-1}(G) \tag{5.42}$$

Thus, for the case where both weights are scalar with no poles in $\mathbb{C}_+$, the bounds (5.31)–(5.34) become

$$\|wSv(s)\|_\infty \geq \max_{\text{RHP-zeros, } z_j \text{ in } G} |w_m(z_j)| \cdot |v_m(z_j)| \cdot \|y_{z_j}^H \mathcal{B}_{po}^{-1}(G)|_{s=z_j}\|_2 \tag{5.43}$$

$$\|wS_Iv(s)\|_\infty \geq \max_{\text{RHP-zeros, } z_j \text{ in } G} |w_m(z_j)| \cdot |v_m(z_j)| \cdot \|\mathcal{B}_{pi}^{-1}(G)|_{s=z_j}u_{z_j}\|_2 \tag{5.44}$$

$$\|wTv(s)\|_\infty \geq \max_{\text{RHP-poles, } p_i \text{ in } G} |w_m(p_i)| \cdot |v_m(p_i)| \cdot \|\mathcal{B}_{zo}^{-1}(G)|_{s=p_i}y_{p_i}\|_2 \tag{5.45}$$

$$\|wT_Iv(s)\|_\infty \geq \max_{\text{RHP-poles, } p_i \text{ in } G} |w_m(p_i)| \cdot |v_m(p_i)| \cdot \|u_{p_i}^H \mathcal{B}_{zi}^{-1}(G)|_{s=p_i}\|_2 \tag{5.46}$$

5.4   Tightness of lower bounds

Theorems 5.1 to 5.4 provide lower bounds on $\|WXV(s)\|_\infty$ where $X \in \{S, S_I, T, T_I\}$. The question is whether these bounds are tight, meaning that there exist controllers which achieve these bounds? The answer is "yes" if there is only one RHP-zero or one RHP-pole. Specifically, we find that the bounds on $\|WSV(s)\|_\infty$ and $\|WS_IV(s)\|_\infty$ are tight if the plant G has one RHP-zero and any number of RHP-poles. Similarly, we find that the bounds on $\|WTV(s)\|_\infty$ and $\|WT_IV(s)\|_\infty$ are tight if the plant G has one RHP-pole and any number of RHP-zeros. We prove tightness of the lower bounds by constructing controllers which achieve the bounds.

THEOREM 5.5 (CONTROLLER WHICH MINIMIZES $\|WSV(s)\|_\infty$). *Consider a plant G with one RHP-zero z, output direction y_z, and $N_p \geq 0$ RHP-poles $p_i \in \mathbb{C}_+$. Let W and V be rational transfer function matrices, and assume that W has no RHP-poles at locations corresponding to RHP poles or zeros in G. A feedback controller which stabilizes WSV, is given by*

$$K_2(s) = G_{smo}^{-1}(s)\,P(s)\,Q^{-1}(s) \tag{5.47}$$

where

$$Q(s) \;=\; W_{mo}^{-1}(s)\,W_{mo}(z)\,V_0\,\mathcal{B}_{po}^{-1}(G)|_{s=z}\,M_{mi}(z)\,M_{mi}^{-1}(s) \tag{5.48}$$

$$P(s) \;=\; \mathcal{B}_{zo}^{-1}(G_{so})\,(I - \mathcal{B}_{po}(G)\,Q) \tag{5.49}$$

$$V_0 \;=\; y_z y_z^H + k_0^2 U_0 U_0^H \quad and \quad M_{mi}(s) \;=\; (\mathcal{B}_{po}(G)\,V(s))_{mi}$$

where the columns of the matrix $U_0 \in \mathbb{R}^{l \times (l-1)}$ together with y_z forms an orthonormal basis for $\mathbb{R}^l$ and k_0 is any constant. $P(s)$ is stable since the RHP-zero for $s = z$ in $I - \mathcal{B}_{po}(G)\,Q$ cancels the RHP-pole for $s = z$ in $\mathcal{B}_{zo}^{-1}(G_{so})$, in a minimal realization of P. With this controller we have

$$\lim_{k_0 \to 0} \|WSV(s)\|_\infty = \|W_{mo}(z)\,y_z\|_2 \cdot \|y_z^H V \mathcal{B}_{zi}^{-1}(\mathcal{B}_{po}(G)\,V)|_{s=z}\|_2 \tag{5.50}$$

From Theorem 5.5 it follows that the bound (5.31) is tight when the plant has one RHP-zero.

In (Chen, 1993; Chen, 1995) the following lower bound on $\|S(s)\|_\infty$ for a plant G with one RHP-zero z and one RHP-pole p, is presented

$$\|S(s)\|_\infty \geq e^{Q(z)/\pi}\sqrt{\sin^2 \angle(y_p, y_z) + \frac{|z + \bar{p}|^2}{|z - p|^2}\cos^2 \angle(y_p, y_z)} \tag{5.51}$$

where

$$Q(z) \triangleq \frac{1}{2}\iint\limits_{\overline{\mathbb{C}}_+} \log\left|\frac{x + jy + \bar{z}}{x + jy - z}\right| \nabla^2 \log \bar{\sigma}(S_m(x + jy))dxdy \geq 0$$

This bound corresponds to the bound given in Corollary 3.1 and the bound (5.31) with $W = I$ and $V = I$, when the factor $e^{Q(z)/\pi} = 1$, i.e. $Q(z) = 0$. By applying Theorem 5.5 with $W = I$ and $V = I$, we can find a stable feedback controller K_2 which stabilizes G and achieves an $\mathcal{H}_\infty$-norm of S equal to the lower bound (5.51) with $Q(z) = 0$. We have hereby proved that $Q(z) = 0$ for the controller minimizing $\|S(s)\|_\infty$. That is, our lower bound on $\|S(s)\|_\infty$ presented in Chapter 3 and the bound (5.31) with $W = I$ and $V = I$, is tight. The factor $Q(z)$ takes into account the fact that the singular values of $S(j\omega)$ are subharmonic functions, i.e. they are in general not *analytic*. This follows since the singular values may cross each other. For the controller minimizing $\mathcal{H}_\infty$-norm of S, none of the singular values $\sigma_i(S(j\omega)) < \bar{\sigma}(S(j\omega))$ become the largest singular value for any frequency. Thus, $\bar{\sigma}(S(j\omega))$ is an analytic function (harmonic) and it follows that $Q(z) = 0$.

THEOREM 5.6 (CONTROLLER WHICH MINIMIZES $\|WS_IV(s)\|_\infty$). *Consider a plant G with one RHP-zero z, input direction u_z, and $N_p \geq 0$ RHP-poles $p_i \in \mathbb{C}_+$. Let W and*

V be rational transfer function matrices, and assume that V has no RHP*-poles at locations corresponding to* RHP *poles or zeros in G. A feedback controller which stabilizes WS_IV, is given by*

$$K_2(s) = Q^{-1}(s)\,P(s)\,G_{smi}^{-1}(s) \tag{5.52}$$

where

$$Q(s) = M_{mo}^{-1}(s)\,M_{mo}(z)\,\mathcal{B}_{pi}^{-1}(G)|_{s=z}\,V_0\,V_{mi}(z)\,V_{mi}^{-1}(s) \tag{5.53}$$

$$P(s) = (I - Q\mathcal{B}_{pi}(G))\,\mathcal{B}_{zi}^{-1}(G_{si}) \tag{5.54}$$

$$V_0 = u_z u_z^H + k_0^2 U_0 U_0^H \quad and \quad M_{mo}(s) = (W(s)\,\mathcal{B}_{pi}(G))_{mo}$$

where the columns of the matrix $U_0 \in \mathbb{R}^{m \times (m-1)}$ together with u_z forms an orthonormal basis for $\mathbb{R}^m$ and k_0 is any constant. $P(s)$ is stable since the RHP*-zero for $s = z$ in $I - Q\mathcal{B}_{pi}(G)$ cancels the* RHP*-pole for $s = z$ in $\mathcal{B}_{zi}^{-1}(G_{si})$, in a minimal realization of P. With this controller we have*

$$\lim_{k_0 \to 0} \|WS_IV(s)\|_\infty = \|\mathcal{B}_{zo}^{-1}(W\,\mathcal{B}_{pi}(G))\,W|_{s=z}\,u_z\|_2 \cdot \|u_z^H\,V_{mi}(z)\|_2 \tag{5.55}$$

From Theorem 5.6 it follows that the bound (5.32) is tight when the plant has one RHP-zero.

THEOREM 5.7 (CONTROLLER WHICH MINIMIZES $\|WTV(s)\|_\infty$). *Consider a plant G with one* RHP*-pole p, output direction y_p, and $N_z \geq 0$* RHP*-zeros $z_j \in \mathbb{C}_+$. Let W and V be rational transfer function matrices, and assume that V has no* RHP*-poles at locations corresponding to* RHP *zeros or poles in G. A feedback controller which stabilizes WTV, is given by*

$$K_2(s) = G_{mso}^{-1}(s)\,Q^{-1}(s)\,P(s) \tag{5.56}$$

where

$$P(s) = M_{mo}^{-1}(s)\,M_{mo}(p)\,\mathcal{B}_{zo}^{-1}(G)|_{s=p}\,V_0\,V_{mi}(p)\,V_{mi}^{-1}(s) \tag{5.57}$$

$$Q(s) = (I - P\mathcal{B}_{zo}(G))\,\mathcal{B}_{po}^{-1}(G_{mo}) \tag{5.58}$$

$$V_0 = y_p y_p^H + k_0^2 U_0 U_0^H \quad and \quad M_{mo}(s) = (W(s)\,\mathcal{B}_{zo}(G))_{mo}$$

where the columns of the matrix $U_0 \in \mathbb{R}^{l \times (l-1)}$ together with y_p forms an orthonormal basis for $\mathbb{R}^l$ and k_0 is any constant. $Q(s)$ is stable since the RHP*-zero for $s = p$ in $I - P\mathcal{B}_{zo}(G)$ cancels the* RHP*-pole for $s = p$ in $\mathcal{B}_{po}^{-1}(G_{mo})$, in a minimal realization of Q. With this controller we have*

$$\lim_{k_0 \to 0} \|WTV(s)\|_\infty = \|\mathcal{B}_{zo}^{-1}(W\,\mathcal{B}_{zo}(G))\,W|_{s=p}\,y_p\|_2 \cdot \|y_p^H\,V_{mi}(p)\|_2 \tag{5.59}$$

From Theorem 5.7 it follows that the bound (5.33) is tight when the plant has one RHP-pole.

THEOREM 5.8 (CONTROLLER WHICH MINIMIZES $\|WT_IV(s)\|_\infty$). *Consider a plant G with one* RHP*-pole p, input direction u_p, and $N_z \geq 0$* RHP*-zeros $z_j \in \mathbb{C}_+$. Let W and V be rational transfer function matrices, and assume that W has no* RHP*-poles at locations*

corresponding to RHP *zeros or poles in G. A feedback controller which stabilizes* WT_IV, *is given by*

$$K_2(s) = P(s)\, Q^{-1}(s)\, G_{msi}^{-1}(s) \tag{5.60}$$

where

$$
\begin{aligned}
P(s) &= W_{mo}^{-1}(s)\, W_{mo}(p)\, V_0\, \mathcal{B}_{zi}^{-1}(G)|_{s=p}\, M_{mi}(p)\, M_{mi}^{-1}(s) \tag{5.61}\\
Q(s) &= \mathcal{B}_{pi}^{-1}(G_{mi})\,(I - \mathcal{B}_{zi}(G)\, P) \tag{5.62}\\
V_0 &= u_p u_p^H + k_0^2 U_0 U_0^H \quad and \quad M_{mi}(s) = (\mathcal{B}_{zi}(G)\, V)_{mi}
\end{aligned}
$$

where the columns of the matrix $U_0 \in \mathbb{R}^{m \times (m-1)}$ *together with* u_p *forms an orthonormal basis for* $\mathbb{R}^m$ *and* k_0 *is any constant.* $Q(s)$ *is stable since the* RHP-*zero for* $s = p$ *in* $I - \mathcal{B}_{zi}(G)\, P$ *cancels the* RHP-*pole for* $s = p$ *in* $\mathcal{B}_{pi}^{-1}(G_{mi})$, *in a minimal realization of Q. With this controller we have*

$$\lim_{k_0 \to 0} \|WT_IV(s)\|_\infty = \|W_{mo}(p)\, u_p\|_2 \cdot \|u_p^H V \mathcal{B}_{zi}^{-1}(\mathcal{B}_{zi}(G)\, V)\|_2 \tag{5.63}$$

From Theorem 5.8 it follows that the bound (5.34) is tight when the plant has one RHP-pole.

5.5 Applications of lower bounds

The lower bounds on $\|W X V(s)\|_\infty$ in Theorems 5.1 and 5.4 can be used to derive a large number of interesting and useful bounds.

5.5.1 Output performance

The previously derived bounds in terms of the $\mathcal{H}_\infty$-norms of S and T given in (Zames, 1981; Skogestad and Postlethwaite, 1996) and in (Chapter 3) follow easily, and further generalizations involving output performance can be derived. Here we assume that the performance weights W_P and W_T are stable and minimum phase.

Weighted sensitivity, $W_P S$. Select $W = W_P$, $V = I$, and apply the bound (5.31) to obtain

$$\|W_P S(s)\|_\infty \geq \max_{\text{RHP-zeros, } z_j} \|W_P(z_j)\, y_{z_j}\|_2 \cdot \|y_{z_j}^H \mathcal{B}_{po}^{-1}(G)|_{s=z_j}\|_2 \tag{5.64}$$

Note, this generalizes the previously found bounds to the case with a matrix valued weight. For the special case $W_P = I$, we derive

$$\|S(s)\|_\infty \geq \max_{\text{RHP-zeros, } z_j} \|y_{z_j}^H \mathcal{B}_{po}^{-1}(G)|_{s=z_j}\|_2 \geq 1 \tag{5.65}$$

Weighted complementary sensitivity, $W_T T$. Select $W = W_T$, $V = I$, and apply the bound (5.33) to obtain

$$\|W_T T(s)\|_\infty \geq \max_{\text{RHP-poles, } p_i} \|\mathcal{B}_{zo}^{-1}(W_T \mathcal{B}_{zo}(G))\, W_T|_{s=p_i}\, y_{p_i}\|_2 \tag{5.66}$$

For the special case $W_T(s) = I$, we derive

$$\|T(s)\|_\infty \geq \max_{\text{RHP-poles, } p_i} \|\mathcal{B}_{zo}^{-1}(G)|_{s=p_i}\, y_{p_i}\|_2 \geq 1 \tag{5.67}$$

Disturbance rejection. Select $W = W_P$, $V = G_d$, and apply the bound (5.31) to obtain

$$\|W_P S G_d(s)\|_\infty \geq \max_{\text{RHP-zeros, } z_j} \|W_P(z_j) \, y_{z_j}\|_2 \cdot \|y_{z_j}^H G_d \, \mathcal{B}_{zi}^{-1}(\mathcal{B}_{po}(G) \, G_d)|_{s=z_j}\|_2 \quad (5.68)$$

Reference tracking. Select $W = W_P$, $V = R$, and apply the bound (5.31) to obtain

$$\|W_P S R(s)\|_\infty \geq \max_{\text{RHP-zeros, } z_j} \|W_P(z_j) \, y_{z_j}\|_2 \cdot \|y_{z_j}^H R \, \mathcal{B}_{zi}^{-1}(\mathcal{B}_{po}(G) \, R)|_{s=z_j}\|_2 \quad (5.69)$$

Note, we can also look at the combined effect of disturbances and references by selecting $V = [\, G_d \quad R \,]$.

Measurement noise rejection. Select $W = W_P$, $V = N$, and apply the bound (5.33) to obtain

$$\|W_P T N(s)\|_\infty \geq \max_{\text{RHP-poles, } p_i} \|\mathcal{B}_{zo}^{-1}(W_P \mathcal{B}_{zo}(G)) \, W_P|_{s=p_i} y_{p_i}\|_2 \cdot \|y_{p_i}^H N_{mi}(p_i)\|_2 \quad (5.70)$$

where we must assume that N has no RHP-poles corresponding to RHP zeros or poles in G. Normally N is stable.

5.5.2 Input usage

The above provide generalizations of previous results, but we can also derive some new bounds in terms of input usage from Theorems 5.3 and 5.4. These new bounds provide very interesting insights, for example, into the possibility of stabilizing an unstable plant with inputs of bounded magnitude.

The basis of these new bounds is to note that the transfer function from the outputs to the inputs, $K_2 S$, can be rewritten as $K_2 S = T_I G^{-1}$ or $K_2 S = G^{-1} T$. When G is unstable, G^{-1} has one or more RHP-zeros, so it is important that the bounds in Theorem 5.4 can handle the case when $V = G^{-1}$ has RHP-zeros. Otherwise, G^{-1} evaluated at the pole of G, would be zero in a certain direction, and we would not derive any useful bounds. Here we assume that the weight W_u on the input u is stable and minimum phase.

Some examples of bounds involving the input magnitude are (see Figure 5.1).

Disturbance rejection. Apply the equality $K_2 S = T_I G^{-1}$, select $W = W_u$, $V = G^{-1} G_d$, and use the bound (5.34) to obtain

$$\|W_u K_2 S G_d(s)\|_\infty \geq \max_{\text{RHP-poles, } p_i} \|W_u(p_i) \, u_{p_i}\|_2 \cdot \|u_{p_i}^H G^{-1} G_d \mathcal{B}_{zi}^{-1}(G_{mi}^{-1} G_d)|_{s=p_i}\|_2 \quad (5.71)$$

where we have used the identity $\mathcal{B}_{zi}(G) \, G^{-1} = G_{mi}^{-1}$.

Reference tracking. Apply the equality $K_2 S = T_I G^{-1}$, select $W = W_u$, $V = G^{-1} R$, and use the bound (5.34) to obtain

$$\|W_u K_2 S R(s)\|_\infty \geq \max_{\text{RHP-poles, } p_i} \|W_u(p_i) \, u_{p_i}\|_2 \cdot \|u_{p_i}^H G^{-1} R \mathcal{B}_{zi}^{-1}(G_{mi}^{-1} R)|_{s=p_i}\|_2 \quad (5.72)$$

Measurement noise rejection. Apply the equality $K_2 S = T_I G^{-1}$, select $W = W_u$, $V = G^{-1} N$, and use the bound (5.34) to obtain

$$\|W_u K_2 S N(s)\|_\infty \geq \max_{\text{RHP-poles, } p_i} \|W_u(p_i) u_{p_i}\|_2 \cdot \|u_{p_i}^H G^{-1} N \mathcal{B}_{zi}^{-1}(G_{mi}^{-1} N)|_{s=p_i}\|_2 \quad (5.73)$$

Note, we can also look at the combined effect of the three above by using (5.34) with $W = W_u$ and $V = G^{-1} \begin{bmatrix} G_d & R & N \end{bmatrix}$.

Simplified lower bound on $\|K_2 S(s)\|_\infty$. Two useful simplified lower bounds on $\|K_2 S(s)\|_\infty$ (which will be used in Chapter 6) can easily be derived. First, apply the equality $K_2 S = T_I G^{-1}$, select $W = I$, $V = G^{-1}$, and use the bound (5.34) to obtain

$$\|K_2 S(s)\|_\infty \geq \max_{\text{RHP-poles, } p_i} \|u_{p_i}^H G^{-1} \mathcal{B}_{zi}^{-1}(G_{mi}^{-1})|_{s=p_i}\|_2 = \|u_{p_i}^H G_{so}^{-1}|_{s=p_i}\|_2 \quad (5.74)$$

where the last identity follows from $\mathcal{B}_{zi}(G_{mi}^{-1}) = \mathcal{B}_{zi}(G^{-1}) = \mathcal{B}_{po}(G)$.

Similarly, we obtain from (5.33), with $W = G^{-1}$ and $V = I$

$$\|K_2 S(s)\|_\infty \geq \max_{\text{RHP-poles, } p_i} \|\mathcal{B}_{zo}^{-1}(G_{mo}^{-1}) G^{-1}|_{s=p_i} y_{p_i}\|_2 = \|G_{si}^{-1}|_{s=p_i} y_{p_i}\|_2 \quad (5.75)$$

where the last identity follows from $\mathcal{B}_{zo}(G_{mo}^{-1}) = \mathcal{B}_{zo}(G^{-1}) = \mathcal{B}_{pi}(G)$.

5.6 Two degrees-of-freedom control

For a 2-DOF controller the closed-loop transfer function from references $\tilde{r}$ to outputs $z_1 = W_p(y - r)$ becomes

$$W_P(SGK_1 - I)R \quad (5.76)$$

We then have the following "special" lower bound on this transfer function.

THEOREM 5.9. *Consider a plant G with $N_z \geq 1$ RHP-zeros z_j and $N_p \geq 0$ RHP-poles $p_i \in \mathbb{C}_+$. Let the performance weight W_P be minimum phase and let (for simplicity) R be stable. Assume that the closed-loop transfer function $W_P(SGK_1 - I)R$ is stable. Then the following lower bound on $\|W_P(SGK_1 - I)R(s)\|_\infty$ applies:*

$$\|W_P(SGK_1 - I)R(s)\|_\infty \geq \max_{\text{RHP-zeros } z_j \text{ in } G} \|W_P(z_j) y_{z_j}\|_2 \cdot \|y_{z_j}^H R_{mi}(z_j)\|_2 \quad (5.77)$$

The bound (5.77) is tight if the plant has one RHP-zero z. Define

$$P(s) = \mathcal{B}_{zo}^{-1}(G) \left(I - W_P^{-1}(s) W_P(z) y_z y_z^H R_{mi}(z) R_{mi}^{-1}(s) \right) \quad (5.78)$$

$P(s)$ is stable since the RHP-zero for $s = z$ in $I - W_P^{-1}(s) W_P(z) y_z y_z^H R_{mi}(z) R_{mi}^{-1}(s)$ cancels the RHP-pole for $s = z$ in $\mathcal{B}_{zo}^{-1}(G)$. One pair of controllers K_1 and K_2 which achieve the lower bound (5.77), are given by

$$K_1 = Q^{-1}(s) P(s) \quad \text{with} \quad (5.79)$$
$$Q(s) = \mathcal{B}_{zo}^{-1}(G) \left(W_P^{-1}(s) W_P(z) V_0 \mathcal{B}_{po}^{-1}(G)|_{s=z} G_{somi}(z) \mathcal{B}_{zi}(G_{so}) \right)$$
$$K_2 = \text{The controller given in Theorem 5.5, minimizing } \|W_P SG(s)\|_\infty \quad (5.80)$$

where $V_0 = y_z y_z^H + k_0^2 U_0 U_0^H$ *and* $k_0 \to 0$.

Note that this bound does not follow directly from Theorems 5.1–5.4. The bound in (5.77) should be compared to the following bound for a 1-DOF controller (which follows from Theorem 5.1, assuming that W_P is minimum phase).

$$\|W_P S R(s)\|_\infty \geq \max_{\text{RHP-zeros } z_j \text{ in } G} \|W_P(z_j) y_{z_j}\|_2 \cdot \|y_{z_j}^H R \mathcal{B}_{zi}^{-1} (\mathcal{B}_{po}(G)\,R)|_{s=z_j}\|_2 \quad (5.81)$$

We see that for the 2-DOF controller only the RHP-zeros pose limitations.

5.7 Example

In this section we consider the following multivariable plant G

$$G(s) = \begin{bmatrix} \frac{s-z}{s-p} & -\frac{0.1s+1}{s-p} \\ \frac{s-z}{0.1s+1} & 1 \end{bmatrix}, \quad \text{with} \quad z = 2.5 \quad \text{and} \quad p = 2$$

The plant G has one multivariable RHP-zero $z = 2.5$ and one RHP-pole $p = 2$. The input and output zero directions corresponding to the RHP-zero $z = 2.5$ are

$$u_z = \begin{bmatrix} 1 \\ 0 \end{bmatrix}, \qquad y_z = \begin{bmatrix} 0.371 \\ 0.928 \end{bmatrix}$$

and the input and output pole directions corresponding to the RHP-pole $p = 2$ are

$$u_p = \begin{bmatrix} 0.385 \\ 0.923 \end{bmatrix}, \qquad y_p = \begin{bmatrix} 1 \\ 0 \end{bmatrix}$$

We factorize the RHP-pole p at the output of the plant, i.e. $G(s) = \mathcal{B}_{po}^{-1}(G)G_{so}(s)$ where

$$\mathcal{B}_{po}(G) = \begin{bmatrix} \frac{s-p}{s+p} & 0 \\ 0 & 1 \end{bmatrix} \quad \text{and} \quad G_{so}(s) = \begin{bmatrix} \frac{s-z}{s+p} & -\frac{0.1s+1}{s+p} \\ \frac{s-z}{0.1s+1} & 1 \end{bmatrix}$$

First, we consider to find a controller which stabilizes the plant and minimizes the peak in the sensitivity function, i.e. minimizes $\|S(s)\|_\infty$. From the lower bound (5.31), with $W = I$ and $V = I$, we find

$$\|S(s)\|_\infty \geq \|y_z^H \mathcal{B}_{po}^{-1}(G)|_{s=z}\|_2 = \left\| \begin{bmatrix} 0.371 & 0.928 \end{bmatrix} \begin{bmatrix} 9 & 0 \\ 0 & 1 \end{bmatrix} \right\|_2 = 3.4691$$

Next, we use Theorem 5.5 (with $W = I$ and $V = I$) to find the controller which minimizes $\|S(s)\|_\infty$. We get

$$V_0 = y_z y_z^H + k_0^2 U_0 u_0^H \quad \text{with} \quad k_0 = 10^{-2}, \quad V_0 = \begin{bmatrix} 0.138 & 0.345 \\ 0.345 & 0.862 \end{bmatrix}$$

$$Q = V_0 \mathcal{B}_{po}^{-1}(G)|_{s=z} = \begin{bmatrix} 1.241 & 0.345 \\ 3.103 & 0.862 \end{bmatrix}$$

Factorizing the RHP-zero for $s = z$ in $I - \mathcal{B}_{po}(G)\,Q$ at the output yields

$$P(s) \overset{s}{=} \left[\begin{array}{c|cc} -2 & 1.175 & 0.326 \\ \hline -0.133 & -0.242 & -0.345 \\ -1.212 & -3.103 & 0.138 \end{array} \right]$$

One balanced minimal state-space realization of K_2 is

$$K_2(s) = G_{smo}^{-1} P Q^{-1}(s) \stackrel{s}{=} \left[\begin{array}{c|cc} -10 & 188.4 & -75.49 \\ \hline 0 & 306 & -122.6 \\ 203 & -6508 & 2605 \end{array} \right]$$

Note the large gain in the controller (large elements in the D matrix). The reason is the small value of $k_0 = 10^{-2}$, k_0 must be small to get the $\mathcal{H}_\infty$-norm of S close to the lower bound. With this controller we obtain

$$\|S(s)\|_\infty = 3.4691$$

Note, it is not surprising that we get large gains in the controller (and large input usage) since no weight has been put on the transfer function $K_2 S$.

Let us instead consider to minimize the input usage, i.e. to minimize the $\mathcal{H}_\infty$-norm of $K_2 S$. We have two lower bounds on $\|K_2 S(s)\|_\infty$, but they are identical since the bounds are tight. First we use the equality $K_2 S = T_I G^{-1}$ and the lower bound (5.34) with $W = I$ and $V = G^{-1}$, to obtain[7]

$$\|K_2 S(s)\|_\infty \geq \|u_p^H G^{-1} \mathcal{B}_{zi}^{-1}(G_{mi}^{-1})|_{s=p}\|_2 = \|u_p^H G_{so}^{-1}(p)\|_2 = 3.077$$

The second bound follows by using $K_2 S = G^{-1} T$, and the lower bound (5.33) with $W = G^{-1}$ and $V = I$. We obtain[8]

$$\|K_2 S(s)\|_\infty \geq \|\mathcal{B}_{zo}^{-1}(G_{mo}^{-1}) G^{-1}|_{s=p} y_p\|_2 = \|G_{si}^{-1}(p) y_p\|_2 = 3.077$$

By using Theorems 5.7 and 5.8 we can derive two controllers which minimizes $\|K_2 S(s)\|_\infty$. From Theorem 5.8 with $W = I$ and $V = G^{-1}$, we get

$$P(s) = V_0 \mathcal{B}_{zi}^{-1}(G)|_{s=p} M_{mi}(p) M_{mi}^{-1}(s), \quad \text{where } M = G_{mi}^{-1} \text{ and } V_0 = u_p u_p^H + k_0^2 U_0 U_0^H$$

With $k_0 = 10^{-3}$ we obtain one stable controller minimizing the $\mathcal{H}_\infty$-norm of $K_2 S$. A balanced minimal state-space realization of this controller is given by

$$K_2(s) \stackrel{s}{=} \left[\begin{array}{c|cc} -10 & 0.014 & 0 \\ \hline -0.002 & -0.623 & 0 \\ 0.013 & -1.495 & 0 \end{array} \right]$$

With this controller the $\mathcal{H}_\infty$-norm of $K_2 S$ becomes

$$\|K_2 S(s)\|_\infty = 3.077$$

It is worth noting that:

1) There is no feedback from y_2, and the reason is that the unstable mode p is *not* observable in y_2 (see the pole direction y_p).
2) The first column of the D matrix in the state-space realization of the controller is a constant scalar times the input pole direction u_p.

---

[7]We use the following relations: $\mathcal{B}_{zi}(G_{mi}^{-1}) = \mathcal{B}_{po}(G)$ and $G^{-1} \mathcal{B}_{po}^{-1}(G) = G_{so}^{-1}$. The first, follows since the input factorization of RHP-zeros in G does *not* change the output pole directions.

[8]We use the relations: $\mathcal{B}_{zo}(G_{mo}^{-1}) = \mathcal{B}_{pi}(G)$ and $\mathcal{B}_{pi}^{-1}(G) G^{-1} = G_{si}^{-1}$.

3) We have that

$$\left\| u_p^H K_2 S y_p(s) \right\|_\infty = \left\| K_2 S(s) \right\|_\infty$$

That is, the worst case input direction of $K_2 S$ is y_p, and the worst case output direction of $K_2 S$ is u_p. For all other combinations of directions the gain of $K_2 S$ is less than $\left\| K_2 S(s) \right\|_\infty$ for this particular K_2.

4) Since the lower bound is tight for the controller minimizing $K_2 S(s)$ and $\bar{\sigma}(K_2 S(j\omega)) = \left\| K_2 S(s) \right\|_\infty$, $\forall \omega$ we find that for sinusoidal measurement noise with direction y_p and magnitude larger than $1 / \left\| K_2 S(s) \right\|_\infty$ causes the input magnitude to exceed ± 1, i.e. $\left\| u \right\|_\infty > 1$ for $n(t) = y_p \, n_0 \, \sin(wt)$, $n_0 > 1 / \left\| K_2 S(s) \right\|_\infty = 1/3.077 = 0.3250$

5) The large gain in the controller which we obtained by minimizing $\left\| S(s) \right\|_\infty$, disappears when we minimize $\left\| K_2 S(s) \right\|_\infty$.

6) A minimal realization of the closed-loop transfer function $K_2 S$ contains only one state and the mode is $\lambda = -2$ (the mirror image of the unstable open-loop pole p). The closed-loop transfer function $K_2 S$ has a RHP-zero for $s = 2$ (at the location of the unstable open-loop pole $p = 2$).

7) As $k_0 \to 0$ we get the constant feedback

$$K_2 = \begin{bmatrix} -0.623 & 0 \\ -1.495 & 0 \end{bmatrix} = k u_p y_p^H, \quad \text{where} \quad k = 1.620$$

which yields $\left\| K_2 S(s) \right\|_\infty = 3.077$.

8) We can also use the relation $K_2 S = G^{-1} T$ and Theorem 5.7 to find an alternative controller. From Theorem 5.7 with $W = G^{-1}$, $V = I$ and $k_0 = 10^{-3}$ we get the controller

$$K_2(s) \stackrel{s}{=} \left[\begin{array}{c|cc} -10 & 0.01 & 0 \\ \hline -0.009 & -0.623 & 0 \\ 0.004 & -1.495 & 0 \end{array} \right] \quad \text{which yields} \quad \left\| K_2 S(s) \right\|_\infty = 3.077$$

By reducing k_0 we get the same constant feedback as above.

At the end we consider reference tracking, and apply Theorem 5.9 to illustrate the benefit of a 2-DOF controller when the plant is unstable. We assume $R = I$ and apply the following performance weight

$$W_P(s) = w_P(s) \cdot I, \quad \text{with} \quad w_P(s) = \frac{s/M + \omega_B^*}{s}, \quad M = 2 \quad \text{and} \quad \omega_B^* = 0.5$$

The weight w_P for the weighted sensitivity $W_P S$, means that we require $\left\| S(s) \right\|_\infty$ less than 2 (which we know can not be fulfilled), and we require tight control up to a frequency of about 0.5 [rad/s]. We first consider 1-DOF control and form the lower bound (5.69) with $R = I$. We get

$$\left\| W_P S(s) \right\|_\infty \geq \left\| W_P(z) y_z \right\|_2 \cdot \left\| y_z^H \mathcal{B}_{po}^{-1}(G) \big|_{s=z} \right\|_2 = 0.7 \cdot 3.4691 = 2.4284$$

From Theorem 5.5 with $k_0 = 10^{-2}$ we find the following controller which achieves the lower bound

$$K_2(s) \stackrel{s}{=} \left[\begin{array}{ccc|cc} 0 & 0 & 0 & -42.31 & 16.93 \\ 0 & 0 & 0 & 0.121 & 0.307 \\ 0 & 0 & -10 & -151 & 60.55 \\ \hline -5.174 & -0.328 & 0 & 218.5 & -87.58 \\ 45.28 & -0.038 & -162.7 & -4647 & 1861 \end{array} \right]$$

The three states in the controller are the two integrators in the performance weights and the stable mode in G_{smo}^{-1}. The $\mathcal{H}_\infty$-norm of the weighted sensitivity becomes

$$\|W_P S(s)\|_\infty = 2.4284$$

Next, we consider 2-DOF control and from Theorem 5.9 with $R = I$, we find

$$\|W_P(SGK_1 - I)\|_\infty \geq 0.7$$

First, we construct the controller K_2 which minimizes $\|W_P SG(s)\|_\infty$. From the lower bound (5.31) with $W = W_P$ and $V = G$, we obtain

$$\|W_P SG(s)\|_\infty \geq \|W_P(z)y_z\|_2 \cdot \|y_z^H G_{mi}(z)\|_2 = 0.7 \cdot 7.4278 = 5.1995$$

The controller which achieves this lower bound on $\|W_P SG(s)\|_\infty$, is given in Theorem 5.5. With $W = W_P$, $V = G$ and $k_0 = 10^{-2}$, we obtain: $M = \mathcal{B}_{po}(G)\,G = G_{so}$, $M_{mi} = G_{somi}$ and $Q = V_0\,\mathcal{B}_{po}^{-1}(G)|_{s=z}\,G_{somi}(z)\,G_{somi}^{-1}$. A balanced minimal state-space realization of the feedback controller K_2 (5.80) is given by

$$K_2(s) \overset{s}{=} \left[\begin{array}{ccc|cc} 0 & 0 & 0 & 48 & -19 \\ 0 & 0 & 0 & 0 & 0 \\ 0 & 0 & -10 & -8 & 0 \\ \hline 0 & 0 & 0 & 0 & 0 \\ -52 & 0 & 8 & -2458 & 985 \end{array}\right], \quad \text{which gives} \quad \|W_P SG(s)\|_\infty = 5.1995$$

A minimal state-space realization of the feed forward controller K_1 (5.79) from Theorem 5.9 with $R = I$, is given by

$$K_1(s) \overset{s}{=} \left[\begin{array}{cc|cc} 0 & 0 & 48 & -19 \\ 0 & 0 & 0 & 0 \\ \hline 0 & 0 & 0 & 0 \\ -52 & 0 & -2463 & 985 \end{array}\right]$$

The $\mathcal{H}_\infty$-norm of the closed-loop transfer function from references to the weighted outputs $W_P(y - r)$ with the 2-DOF controller $K = [\,K_1 \quad -K_2\,]$ is

$$\|W_P(SGK_1 - I)\|_\infty = 0.7$$

We have demonstrated the use of some of the lower bounds, and we have constructed controllers which achieve the lower bounds for the plant G. For further details regarding the usefulness of the lower bounds in engineering applications, the reader should consult Chapter 4.

5.8   Conclusion

- We have derived tight lower bounds on closed-loop transfer functions valid for multi-variable plants. The bounds are independent of the controller and therefore reflects the controllability of the plant.
- The bounds extend and generalize the results by Zames (1981), Doyle et al. (1992), Skogestad and Postlethwaite (1996) and the results given in Chapter 3, to also handle non-minimum phase and unstable weights. This allows us to derive *new* lower bounds on input usage due to disturbances, measurement noise and reference changes.

- The new lower bounds on input usage make it possible to *quantify* the minimum input usage for stabilization of unstable plants in the presence of worst case disturbances, measurement noise and reference changes.

- It is proved that the lower bounds are *tight*, by deriving analytical expressions for stable controllers which achieves an $\mathcal{H}_\infty$-norm of the closed-loop transfer functions equal to the lower bound for large classes of systems.

- Theorem 5.9 expresses the benefit of applying a 2-DOF controller compared to a 1-DOF controller when the plant is unstable and has a RHP-zero.

References

Bode, H. W. (1945). *Network Analysis and Feedback Amplifier Design*, D. Van Nostrand Co., New York.

Boyd, S. and Desoer, C. A. (1985). Subharmonic functions and performance bounds in linear time-invariant feedback systems, *IMA J. Math. Contr. and Info.* **2**: 153–170.

Chen, J. (1993). Sensitivity integral relations and design trade-offs in linear multivariable feedback systems, *Proc. American Control Conference*, San Francisco, CA, pp. 3160–3164.

Chen, J. (1995). Sensitivity integral relations and design trade-offs in linear multivariable feedback systems, *IEEE Transactions on Automatic Control* **AC-40**(10): 1700–1716.

Doyle, J. C. (1984). *Lecture Notes on Advances in Multivariable Control*, ONR/Honeywell Workshop, Minneapolis, October.

Doyle, J. C., Francis, B. and Tannenbaum, A. (1992). *Feedback Control Theory*, Macmillan Publishing Company.

Doyle, J. C., Glover, K., Khargonekar, P. P. and Francis, B. A. (1989). State-space solutions to standard $\mathcal{H}_2$ and $\mathcal{H}_\infty$ control problems, *IEEE Transactions on Automatic Control* **AC-34**(8): 831–847.

Francis, B. (1987). *A course in $\mathcal{H}_\infty$ control theory*, Lecture Notes in Control and Information Sciences, Springer-Verlag, Berlin.

Green, M. and Limebeer, D. J. N. (1995). *Linear Robust Control*, Prentice-Hall, Englewood Cliffs.

Havre, K. and Skogestad, S. (1996). Effect of RHP zeros and poles on performance in multivariable systems, *Proc. from Control'96*, Institution of Electrical Engineers, Savoy Place, London, UK, University of Exeter, UK, pp. 930–935.

Havre, K. and Skogestad, S. (1997a). Effect of RHP zeros and poles on performance in multivariable systems, *Accepted for publication in Journal of Process Control* .

Havre, K. and Skogestad, S. (1997b). Performance limitations for unstable SISO plants, *Submitted to Automatica* .

Kwakernaak, H. (1986). A polynomial approach to minimax frequency domain optimization of multivariable feedback systems, *Int. J. Control* **44**(1): 117–156.

Kwakernaak, H. (1993). Robust control and $\mathcal{H}_\infty$-optimization — Tutorial paper, *Automatica* **29**: 255–273.

Kwakernaak, H. (1996). *Frequency domain solution of the standard $\mathcal{H}_\infty$-problem*, In M.J. Grimble and V. Kucera's edition on: Polynomial Methods for Control System Design, Springer-Verlag, Heidelberg.

MacFarlane, A. G. J. and Karcanias, N. (1976). Poles and zeros of linear multivariable systems: A survey of algebraic, geometric and complex variable theory, *International Journal of Control* **24**(1): 33–74.

Morari, M. and Zafiriou, E. (1989). *Robust Process Control*, Prentice-Hall, Englewood Cliffs.

Rosenbrock, H. H. (1966). On the design of linear multivariable systems, *Third IFAC World Congress*. Paper 1A.

Rosenbrock, H. H. (1970). *State-space and Multivariable Theory*, Nelson, London.

Safonov, M. G., Limebeer, D. J. N. and Chiang, R. Y. (1989). Simplifying the $\mathcal{H}_\infty$ theory via loop-shifting, matrix-pencil and descriptor concepts, *International Journal of Control* **50**(6): 2467–2488.

Skogestad, S. and Postlethwaite, I. (1996). *Multivariable Feedback Control, Analysis and Design*, John Wiley & Sons, Chichester.

Zames, G. (1981). Feedback and optimal sensitivity: model reference transformations, multiplicative seminorms, and approximate inverses, *IEEE Transactions on Automatic Control* **AC-26**(2): 301–320.

Zhou, K., Doyle, J. C. and Glover, K. (1996). *Robust and Optimal Control*, Prentice-Hall, Upper Saddle River.

Internal reports and MATLAB-software to compute the bounds in Theorems 5.1 to 5.4 are available on the internet: `http://www.chembio.ntnu.no/users/skoge`.

Appendix A Proofs of the results

A.1   Proof of interpolation constraints on S_I and T_I

Proof of (5.27). From the definition of input zero direction we have $G(z)u_z = 0$. Consider

$$S_I^{-1}(z)u_z = (I + K_2 G(z))u_z = u_z + K_2 \underbrace{G(z)u_z}_{=0} = u_z$$

which implies $S_I(z)u_z = u_z$. From $T_I = I - S_I$ it follows that $T_I(z)u_z = u_z - S_I(z)u_z = 0$.   □

Proof of (5.29). Due to internal stability K_2 can not cancel the RHP-pole at $s = p$ in G, so the square matrix $L_I = K_2 G$ has a RHP-pole at $s = p$, and if we assume that L_I has no RHP-zero at $s = p$, then $L_I^{-1}(p)$ exists and the input pole direction is given by $u_p^H L_I^{-1}(p) = 0$. Since T_I is stable, it has no RHP-pole at $s = p$, so $T_I(p)$ is finite. It then follows from $S_I = L_I^{-1} T_I$ that

$$u_p^H S_I(p) = \underbrace{u_p^H L_I^{-1}(p)}_{=0} T_I(p) = 0$$

and from $T_I = I - S_I$ that $u_p^H T_I(p) = u_p^H - u_p^H S_I(p) = u_p^H$.   □

A.2   Proof of Theorems 5.1–5.4

Proof of Theorem 5.1. We prove (5.31) by applying the six steps given in Section 5.3.1.

1) Factor out RHP-zeros in WSV: RHP-poles in G appears as RHP-zeros in S (5.28). Factor out $S = \widetilde{S}\,\mathcal{B}_{po}(G)$ to obtain

$$
\begin{aligned}
WSV(s) &= \mathcal{B}_{zo}(W)\,W_{mo}\,\widetilde{S}\,\mathcal{B}_{po}(G)\,V \\
&= \mathcal{B}_{zo}(W)\,\underbrace{W_{mo}\,\widetilde{S}\,(\mathcal{B}_{po}(G)\,V)_{mi}}_{(WSV)_m}\,\mathcal{B}_{zi}(\mathcal{B}_{po}(G)\,V)
\end{aligned}
$$

WSV is stable by assumption. From the assumption on internal stability it follows that S is stable (if one closed-loop transfer function is stable then internal stability implies that all the other closed-loop transfer functions are stable). Then it is only the RHP-zeros in S which can cancel RHP-poles in V and W. So, factorizing the zeros in $\mathbb{C}_+$ of W does not introduce instability in $(WSV)_m$, since none of these cancel unstable modes in S or V. Similarly, we can factorize the zeros in $\mathbb{C}_+$ of V. However, when factorizing the zeros in S we must avoid factorizing the zeros which cancel poles in $\mathbb{C}_+$ of V. Otherwise, $(WSV)_m$ becomes unstable. By factorizing only the zeros in a minimal realization of $\mathcal{B}_{po}(G)\,V$ we accomplish this. By assumption none of the modes in $\mathbb{C}_+$ of W cancel against the zeros in S due to poles in G. It then follows that $(WSV)_m$ is stable.

2) Introduce $f(s) = \max\limits_{\|x_1\|_2 = 1,\ \|x_2\|_2 = 1} x_1^H (WSV)_m\,x_2$, then

$$
\|WSV(s)\|_\infty = \|(WSV(s))_m\|_\infty \geq \|f(s)\|_\infty
$$

3) Apply the maximum modulus theorem to $f(s)$ at the RHP-zeros z_j of G

$$
\|f(s)\|_\infty \geq |f(z_j)|
$$

4) Resubstitute the factorization of RHP-zeros in S, i.e. use $\widetilde{S} = S\,\mathcal{B}_{po}^{-1}(G)$

$$
\begin{aligned}
f(z_j) &= \max\limits_{\|x_1\|_2 = 1,\ \|x_2\|_2 = 1} x_1^H W_{mo}\,S\,\mathcal{B}_{po}^{-1}(G)\,(\mathcal{B}_{po}(G)\,V)_{mi}\big|_{s=z_j}\,x_2 \\
&= \max\limits_{\|x_1\|_2 = 1,\ \|x_2\|_2 = 1} x_1^H W_{mo}\,S\,V\,\mathcal{B}_{zi}^{-1}(\mathcal{B}_{po}(G)\,V)\big|_{s=z_j}\,x_2
\end{aligned}
$$

5) Use the interpolation constraint for RHP-zeros z_j in G, i.e. use $y_{z_j}^H S(z_j) = y_{z_j}^H$

$$
\begin{aligned}
f(z_j) &= \max\limits_{\|x_1\|_2 = 1,\ \|x_2\|_2 = 1} x_1^H W_{mo}\,S\,V\mathcal{B}_{zi}^{-1}(\mathcal{B}_{po}(G)\,V)\big|_{s=z_j}\,x_2 \\
&\geq \max\limits_{\|x_1\|_2 = 1,\ \|x_2\|_2 = 1} x_1^H W_{mo}\,y_{z_j}y_{z_j}^H S\,V\,\mathcal{B}_{zi}^{-1}(\mathcal{B}_{po}(G)\,V)\big|_{s=z_j}\,x_2 \\
&= \max\limits_{\|x_1\|_2 = 1,\ \|x_2\|_2 = 1} x_1^H W_{mo}\,y_{z_j}y_{z_j}^H V\,\mathcal{B}_{zi}^{-1}(\mathcal{B}_{po}(G)\,V)\big|_{s=z_j}\,x_2
\end{aligned}
$$

6) Evaluate the lower bound

$$
\|WSV(s)\|_\infty \geq |f(z_j)| \geq \|W_{mo}(z_j)y_{z_j}\|_2 \cdot \|y_{z_j}^H V\mathcal{B}_{zi}^{-1}(\mathcal{B}_{po}(G)\,V)\big|_{s=z_j}\|_2
$$

Since these steps apply to all RHP-zeros in G, the bound (5.31) follows. $\square$

Proof of Theorem 5.2.

1) Factor out RHP-zeros in WS_IV: RHP-poles in G appear as RHP-zeros in S_I (5.29). Factor out $S_I = \mathcal{B}_{pi}(G)\,\widetilde{S}_I$ to obtain

$$
\begin{aligned}
WS_IV(s) &= W\mathcal{B}_{pi}(G)\,\widetilde{S}_I\,V_{mi}\,\mathcal{B}_{zi}(V)\\
&= \mathcal{B}_{zo}(W\mathcal{B}_{pi}(G))\,\underbrace{(W\mathcal{B}_{pi}(G))_{mo}\,\widetilde{S}_I\,V_{mi}}_{(WS_IV)_m}\,\mathcal{B}_{zi}(V)
\end{aligned}
$$

WS_IV is stable by assumption, and from internal stability it follows that S_I is stable. Then we can factorize the zeros in $\mathbb{C}_+$ of V without introducing instability in $(WS_IV)_m$, and we avoid factorizing RHP-zeros in $\mathcal{B}_{pi}(G)$ which cancel RHP-poles in W by factorizing the zeros of $W\mathcal{B}_{pi}(G)$. By assumption, none of the modes in $\mathbb{C}_+$ of V cancel against the zeros in S_I due to poles in G. It then follows that $(WS_IV)_m$ is stable.

2) Introduce $f(s) = \max\limits_{\|x_1\|_2=1,\,\|x_2\|_2=1} x_1^H (WS_IV)_m\, x_2$, then

$$
\|WS_IV(s)\|_\infty = \|(WS_IV(s))_m\|_\infty \geq \|f(s)\|_\infty
$$

3) Apply the maximum modulus theorem to $f(s)$ at the RHP-zeros z_j of G

$$
\|f(s)\|_\infty \geq |f(z_j)|
$$

4) Resubstitute the factorization of RHP-zeros in S_I, i.e. use $\widetilde{S}_I = \mathcal{B}_{pi}^{-1}(G)\,S_I$

$$
\begin{aligned}
f(z_j) &= \max\limits_{\|x_1\|_2=1,\,\|x_2\|_2=1} x_1^H (W\mathcal{B}_{pi}(G))_{mo}\,\mathcal{B}_{pi}^{-1}(G)\,S_I\,V_{mi}\big|_{s=z_j}\,x_2\\
&= \max\limits_{\|x_1\|_2=1,\,\|x_2\|_2=1} x_1^H \mathcal{B}_{zo}^{-1}(W\mathcal{B}_{pi}(G))\,W\,S_I\,V_{mi}\big|_{s=z_j}\,x_2
\end{aligned}
$$

5) Use the interpolation constraint for RHP-zeros z_j in G, i.e. use $S_I(z_j)u_{z_j} = u_{z_j}$

$$
\begin{aligned}
f(z_j) &= \max\limits_{\|x_1\|_2=1,\,\|x_2\|_2=1} x_1^H \mathcal{B}_{zo}^{-1}(W\mathcal{B}_{pi}(G))\,W\,S_I\,V_{mi}\big|_{s=z_j}\,x_2\\
&\geq \max\limits_{\|x_1\|_2=1,\,\|x_2\|_2=1} x_1^H \mathcal{B}_{zo}^{-1}(W\mathcal{B}_{pi}(G))\,W\,S_I u_{z_j} u_{z_j}^H V_{mi}\big|_{s=z_j}\,x_2\\
&= \max\limits_{\|x_1\|_2=1,\,\|x_2\|_2=1} x_1^H \mathcal{B}_{zo}^{-1}(W\mathcal{B}_{pi}(G))\,W\, u_{z_j} u_{z_j}^H V_{mi}\big|_{s=z_j}\,x_2
\end{aligned}
$$

6) Evaluate the lower bound

$$
\|WS_IV(s)\|_\infty \geq |f(z_j)| \geq \|\mathcal{B}_{zo}^{-1}(W\mathcal{B}_{pi}(G))\,W\big|_{s=z_j} u_{z_j}\|_2 \cdot \|u_{z_j}^H V_{mi}(z_j)\|_2
$$

Since these steps apply to all RHP-zeros in G, the bound (5.32) follows. □

Proof of Theorem 5.3.

1) Factor out RHP-zeros in WTV: RHP-zeros in G appear as RHP-zeros in T (5.26). Factor out $T = \mathcal{B}_{zo}(G)\,\widetilde{T}$ to obtain

$$
\begin{aligned}
WTV(s) &= W\mathcal{B}_{zo}(G)\,\widetilde{T}\,V_{mi}\,\mathcal{B}_{zi}(V)\\
&= \mathcal{B}_{zo}(W\mathcal{B}_{zo}(G))\,\underbrace{(W\mathcal{B}_{zo}(G))_{mo}\,\widetilde{T}\,V_{mi}}_{(WTV)_m}\,\mathcal{B}_{zi}(V)
\end{aligned}
$$

WTV is stable by assumption, and from internal stability it follows that T is stable. Then we can factorize the zeros in $\mathbb{C}_+$ of V without introducing instability in $(WTV)_m$, and we avoid factorizing RHP-zeros in $\mathcal{B}_{zo}(G)$ which cancel RHP-poles in W by factorizing the zeros of $W\mathcal{B}_{zo}(G)$. By assumption, none of the modes in $\mathbb{C}_+$ of V cancel against the zeros in T due to zeros in G. It then follows that $(WTV)_m$ is stable.

2) Introduce $f(s) = \max\limits_{\|x_1\|_2 = 1,\, \|x_2\|_2 = 1} x_1^H (WTV)_m x_2$, then

$$\|WTV(s)\|_\infty = \|(WTV(s))_m\|_\infty \geq \|f(s)\|_\infty$$

3) Apply the maximum modulus theorem to $f(s)$ at the RHP-poles p_i of G

$$\|f(s)\|_\infty \geq |f(p_i)|$$

4) Resubstitute the factorization of RHP-zeros in T, i.e. use $\widetilde{T} = \mathcal{B}_{zo}^{-1}(G)\, T$

$$
\begin{aligned}
f(p_i) &= \max\limits_{\|x_1\|_2 = 1,\, \|x_2\|_2 = 1} x_1^H (W\mathcal{B}_{zo}(G))_{mo}\, \mathcal{B}_{zo}^{-1}(G)\, T\, V_{mi}\big|_{s=p_i} x_2 \\
&= \max\limits_{\|x_1\|_2 = 1,\, \|x_2\|_2 = 1} x_1^H \mathcal{B}_{zo}^{-1}(W\mathcal{B}_{zo}(G))\, W\, T\, V_{mi}\big|_{s=p_i} x_2
\end{aligned}
$$

5) Use the interpolation constraint for RHP-poles p_i in G, i.e. use $T(p_i)y_{p_i} = y_{p_i}$

$$
\begin{aligned}
f(p_i) &= \max\limits_{\|x_1\|_2 = 1,\, \|x_2\|_2 = 1} x_1^H \mathcal{B}_{zo}^{-1}(W\mathcal{B}_{zo}(G))\, W\, T\, V_{mi}\big|_{s=p_i} x_2 \\
&\geq \max\limits_{\|x_1\|_2 = 1,\, \|x_2\|_2 = 1} x_1^H \mathcal{B}_{zo}^{-1}(W\mathcal{B}_{zo}(G))\, W\, T y_{p_i} y_{p_i}^H V_{mi}\big|_{s=p_i} x_2 \\
&= \max\limits_{\|x_1\|_2 = 1,\, \|x_2\|_2 = 1} x_1^H \mathcal{B}_{zo}^{-1}(W\mathcal{B}_{zo}(G))\, W\, y_{p_i} y_{p_i}^H V_{mi}\big|_{s=p_i} x_2
\end{aligned}
$$

6) Evaluate the lower bound

$$\|WTV(s)\|_\infty \geq |f(p_i)| \geq \left\|\mathcal{B}_{zo}^{-1}(W\mathcal{B}_{zo}(G))\, W\big|_{s=p_i} y_{p_i}\right\|_2 \cdot \left\|y_{p_i}^H V_{mi}(p_i)\right\|_2$$

Since these steps apply to all RHP-poles in G, the bound (5.33) follows.　　　　□

Proof of Theorem 5.4.

1) Factor out RHP-zeros in WT_IV: RHP-zeros in G appear as RHP-zeros in T_I (5.27). Factor out $T_I = \widetilde{T}_I\, \mathcal{B}_{zi}(G)$ to obtain

$$
\begin{aligned}
WT_IV(s) &= \mathcal{B}_{zo}(W)\, W_{mo}\, \widetilde{T}_I\, \mathcal{B}_{zi}(G)\, V \\
&= \mathcal{B}_{zo}(W)\, \underbrace{W_{mo}\, \widetilde{T}_I(\mathcal{B}_{zi}(G)\, V)_{mi}}_{(WT_IV)_m}\, \mathcal{B}_{zi}(\mathcal{B}_{zi}(G)\, V)
\end{aligned}
$$

WT_IV is stable by assumption, and from internal stability it follows that T_I is stable. Then we can factorize the zeros in $\mathbb{C}_+$ of W without introducing instability in $(WT_IV)_m$, and we avoid factorizing RHP-zeros in $\mathcal{B}_{zi}(G)$ which cancel RHP-poles in V by factorizing the zeros of $\mathcal{B}_{zi}(G)\, V$. By assumption, none of the modes in $\mathbb{C}_+$ of W cancel against the zeros in T_I due to zeros in G. It then follows that $(WT_IV)_m$ is stable.

2) Introduce $f(s) = \max\limits_{\|x_1\|_2 = 1,\, \|x_2\|_2 = 1} x_1^H (WT_IV)_m x_2$, then

$$\|WT_IV(s)\|_\infty = \|(WT_IV(s))_m\|_\infty \geq \|f(s)\|_\infty$$

3) Apply the maximum modulus theorem to $f(s)$ at the RHP-poles p_i of G

$$\|f(s)\|_\infty \geq |f(p_i)|$$

4) Resubstitute the factorization of RHP-zeros in T_I, i.e. use $\widetilde{T}_I = T_I \mathcal{B}_{zi}^{-1}(G)$

$$
\begin{aligned}
f(p_i) &= \max_{\|x_1\|_2=1,\,\|x_2\|_2=1} x_1^H W_{mo} T_I \mathcal{B}_{zi}^{-1}(G)\,(\mathcal{B}_{zi}(G)\,V)_{mi}|_{s=p_i} x_2 \\
&= \max_{\|x_1\|_2=1,\,\|x_2\|_2=1} x_1^H W_{mo} T_I V \mathcal{B}_{zi}^{-1}(\mathcal{B}_{zi}(G)\,V)|_{s=p_i} x_2
\end{aligned}
$$

5) Use the interpolation constraint for RHP-poles p_i in G, i.e. use $u_{p_i}^H T_I(p_i) = u_{p_i}^H$

$$
\begin{aligned}
f(p_i) &= \max_{\|x_1\|_2=1,\,\|x_2\|_2=1} x_1^H W_{mo} T_I V \mathcal{B}_{zi}^{-1}(\mathcal{B}_{zi}(G)\,V)|_{s=p_i} x_2 \\
&\geq \max_{\|x_1\|_2=1,\,\|x_2\|_2=1} x_1^H W_{mo} u_{p_i} u_{p_i}^H T_I V \mathcal{B}_{zi}^{-1}(\mathcal{B}_{zi}(G)\,V)|_{s=p_i} x_2 \\
&= \max_{\|x_1\|_2=1,\,\|x_2\|_2=1} x_1^H W_{mo} u_{p_i} u_{p_i}^H V \mathcal{B}_{zi}^{-1}(\mathcal{B}_{zi}(G)\,V)|_{s=p_i} x_2
\end{aligned}
$$

6) Evaluate the lower bound

$$
\|WT_I V(s)\|_\infty \geq |f(p_i)| \geq \|W_{mo}(p_i) u_{p_i}\|_2 \cdot \|u_{p_i}^H V \mathcal{B}_{zi}^{-1}(\mathcal{B}_{zi}(G)\,V)|_{s=p_i}\|_2
$$

Since these steps apply to all RHP-poles in G, the bound (5.34) follows. $\qquad\square$

A.3 Proof of Theorems 5.5–5.8

Proof of Theorem 5.5. It follows that Q has no poles in $\mathbb{C}_+$, since W_{mo}^{-1} and M_{mi}^{-1} have no poles in $\mathbb{C}_+$, and the remaining matrices are constant and finite. Consider $I - \mathcal{B}_{po}(G)\,Q(s)$, at $s = z$ we have $Q(z) = V_0 \mathcal{B}_{po}^{-1}(G)|_{s=z}$

$$
\begin{aligned}
\tilde{y}_z^H (I - \mathcal{B}_{po}(G)|_{s=z} V_0 \mathcal{B}_{po}^{-1}(G)|_{s=z}) &= \tilde{y}_z^H \mathcal{B}_{po}(G)|_{s=z}(I - V_0)\mathcal{B}_{po}^{-1}(G)|_{s=z} \\
&= \tilde{y}_z^H \mathcal{B}_{po}(G)|_{s=z}(1 - k_0^2)\,U_0 U_0^H \mathcal{B}_{po}^{-1}(G)|_{s=z}
\end{aligned}
$$

Since $U_0 U_0^H$ has rank $l - 1$, and the singular directions both at the input and at the output of $U_0 U_0^H$ are y_z, it follows that $I - \mathcal{B}_{po}(G)\,Q(s)$ has a RHP-zero for $s = z$ with output direction

$$
\tilde{y}_z = \mathcal{B}_{po}^{-H}(G)|_{s=z}\,y_z\,/\,\|\mathcal{B}_{po}^{-H}(G)|_{s=z}\,y_z\|_2
$$

We find that this is the output direction of the RHP-zero z in G_{so} (that is the plant G with the RHP-poles factorized at the output). We can now write

$$
I - \mathcal{B}_{po}(G)\,Q(s) = \mathcal{B}_{zo}(G_{so})\,P(s)
$$

Since $I - \mathcal{B}_{po}(G)\,Q(s)$ has no poles in $\mathbb{C}_+$ and $\mathcal{B}_{zo}(G_{so})$ is stable, it follows that $P(s) = \mathcal{B}_{zo}^{-1}(G_{so})\,(I - \mathcal{B}_{po}(G)\,Q(s))$ has no poles in $\mathbb{C}_+$. That is, in a minimal state-space realization of P the RHP-pole for $s = z$ in $\mathcal{B}_{zo}^{-1}(G_{so})$ cancels the RHP-zero for $s = z$ in $I - \mathcal{B}_{po}(G)\,Q(s)$. We obtain

$$
\begin{aligned}
L &= GK_2 = \mathcal{B}_{po}^{-1}(G)\,\mathcal{B}_{zo}(G_{so})\,P\,Q^{-1}(s) \\
&= \mathcal{B}_{po}^{-1}(G)\,(I - \mathcal{B}_{po}(G)\,Q(s))\,Q^{-1}(s) = \mathcal{B}_{po}^{-1}(G)\,Q^{-1} - I \\
S &= (I + L)^{-1} = Q\,\mathcal{B}_{po}(G) = W_{mo}^{-1}(s)\,W_{mo}^{-1}(z)\,V_0 \mathcal{B}_{po}^{-1}(G)|_{s=z}\,M_{mi}(z)\,M_{mi}^{-1}(s)\,\mathcal{B}_{po}(G)
\end{aligned}
$$

It follows that S has no poles in $\mathbb{C}_+$ since Q has no poles in $\mathbb{C}_+$ and $\mathcal{B}_{po}(G)$ is stable. Consider

$$
\begin{aligned}
WSV(s) &= W(s)W_{mo}^{-1}(s)W_{mo}(z)V_0\mathcal{B}_{po}^{-1}(G)|_{s=z}M_{mi}(z)M_{mi}^{-1}(s)\overbrace{\mathcal{B}_{po}(G)\,V(s)}^{M(s)} \\
&= \mathcal{B}_{zo}(W)\underbrace{W_{mo}(z)\,V_0\,\mathcal{B}_{po}^{-1}(G)|_{s=z}\,M_{mi}(z)}_{(WSV)_m(z)}\,\mathcal{B}_{zi}(M) \qquad (5.82)
\end{aligned}
$$

We have that WSV is stable, since $\mathcal{B}_{zo}(W)$ and $\mathcal{B}_{zi}(M)$ are stable and $(WSV)_m(z)$ is constant (independent of s). We obtain

$$\|WSV(s)\|_\infty = \|(WSV)_m(z)\|_\infty = \|(WSV)_m(z)\|_2$$

where

$$
\begin{aligned}
(WSV)_m(z) &= W_{mo}(z)\, V_0\, \mathcal{B}_{po}^{-1}(G)|_{s=z}\, (\mathcal{B}_{po}(G)\,V)_{mi}|_{s=z} \\
&= W_{mo}(z)\, V_0\, \mathcal{B}_{po}^{-1}(G)|_{s=z}\, \mathcal{B}_{po}(G)|_{s=z}\, V \mathcal{B}_{zi}^{-1}(\mathcal{B}_{po}(G)\,V)|_{s=z} \\
&= W_{mo}(z)\, V_0\, V \mathcal{B}_{zi}^{-1}(\mathcal{B}_{po}(G)\,V)|_{s=z} \\
&= W_{mo}(z)\, (y_z y_z^H + k_0^2 U_0 U_0^H)\, V \mathcal{B}_{zi}^{-1}(\mathcal{B}_{po}(G)\,V)|_{s=z}
\end{aligned}
$$

and for $k_0 = 0$ we have

$$\|(WSV)_m(z)\|_2 = \|W_{mo}(z)\, y_z\|_2 \cdot \|y_z^H V \mathcal{B}_{zi}^{-1}(\mathcal{B}_{po}(G)\,V)|_{s=z}\|_2$$

and

$$\lim_{k_0 \to 0} \|VSW(s)\|_\infty = \|W_{mo}(z)\, y_z\|_2 \cdot \|y_z^H V \mathcal{B}_{zi}^{-1}(\mathcal{B}_{po}(G)\,V)|_{s=z}\|_2$$

$$\square$$

Proof of Theorem 5.6. It follows that Q has no poles in $\mathbb{C}_+$, since M_{mo}^{-1} and V_{mi}^{-1} has no poles in $\mathbb{C}_+$, and the remaining matrices are constant and finite. Consider $I - Q\mathcal{B}_{pi}(G)$, at $s = z$ we have $Q(z) = \mathcal{B}_{pi}^{-1}(G)|_{s=z} V_0$

$$
\begin{aligned}
(I - \mathcal{B}_{pi}^{-1}(G)|_{s=z} V_0 \mathcal{B}_{pi}(G)|_{s=z})\, \tilde{u}_z &= \mathcal{B}_{pi}^{-1}(G)|_{s=z}\, (I - V_0)\, \mathcal{B}_{pi}(G)|_{s=z}\, \tilde{u}_z \\
&= \mathcal{B}_{pi}^{-1}(G)|_{s=z}\, (1 - k_0^2) U_0 U_0^H \mathcal{B}_{pi}(G)|_{s=z}\, \tilde{u}_z
\end{aligned}
$$

Since $U_0 U_0^H$ has rank $m - 1$, and the singular directions both at the input and at the output of $U_0 U_0^H$ are u_z, it follows that $I - Q\mathcal{B}_{pi}(G)$ has a RHP-zero for $s = z$ with input direction

$$\tilde{u}_z = \mathcal{B}_{pi}^{-1}(G)|_{s=z}\, u_z\, /\, \|\mathcal{B}_{pi}^{-1}(G)|_{s=z}\, u_z\|_2$$

We find that this is the input direction of the RHP-zero z in G_{si} (that is the plant G with the RHP-poles factorized at the input). We can write

$$I - Q\mathcal{B}_{pi}(G) = P(s)\mathcal{B}_{zi}(G_{si})$$

Since $I - Q\mathcal{B}_{pi}(G)$ has no poles in $\mathbb{C}_+$ and $\mathcal{B}_{zi}(G_{si})$ is stable, it follows that $P(s) = (I - Q\mathcal{B}_{pi}(G))\mathcal{B}_{zi}^{-1}(G)$ has no poles in $\mathbb{C}_+$. That is, in a minimal state-space realization of P the RHP-pole for $s = z$ in $\mathcal{B}_{zi}^{-1}(G)$ cancels the RHP-zero for $s = z$ in $I - Q\mathcal{B}_{pi}(G)$. We obtain

$$
\begin{aligned}
L_I &= K_2 G = Q^{-1} P \, \mathcal{B}_{zi}(G_{si}) \mathcal{B}_{pi}^{-1}(G) = Q^{-1} (I - Q\mathcal{B}_{pi}(G))\, \mathcal{B}_{pi}^{-1}(G) = Q^{-1} \mathcal{B}_{pi}^{-1}(G) - I \\
S_I &= (I + L_I)^{-1} = \mathcal{B}_{pi}(G)\, Q(s) = \mathcal{B}_{pi}(G)\, M_{mo}^{-1}(s)\, M_{mo}(z)\, \mathcal{B}_{pi}^{-1}(G)|_{s=z} V_0\, V_{mi}(z)\, V_{mi}^{-1}(s)
\end{aligned}
$$

It follows that S_I has no poles in $\mathbb{C}_+$ since Q has no poles in $\mathbb{C}_+$ and $\mathcal{B}_{pi}(G)$ is stable. Consider

$$
\begin{aligned}
WS_I V(s) &= \overbrace{W(s)\, \mathcal{B}_{pi}(G)}^{M(s)}\, M_{mo}^{-1}(s)\, M_{mo}(z)\, \mathcal{B}_{pi}(G)|_{s=z} V_0\, V_{mi}(z)\, V_{mi}^{-1}(s)\, V(s) \\
&= \mathcal{B}_{zo}(M)\, \underbrace{M_{mo}(z)\, \mathcal{B}_{pi}^{-1}(G)|_{s=z} V_0\, V_{mi}(z)}_{(WS_I V)_m(z)}\, \mathcal{B}_{zi}(V)
\end{aligned}
$$

We have that $W S_I V$ is stable since $\mathcal{B}_{zo}(M)$ and $\mathcal{B}_{zi}(V)$ are stable and the matrix $(W S_I V)_m(z)$ is constant (independent of s). We obtain

$$\|V S_I W(s)\|_\infty = \|(W S_I V)_m(z)\|_\infty = \|(W S_I V)_m(z)\|_2$$

where

$$
\begin{aligned}
(W S_I V)_m(z) &= (W\,\mathcal{B}_{pi}(G))_{mo}\,\mathcal{B}_{pi}^{-1}(G)|_{s=z}\,V_0\,V_{mi}(z) \\
&= \mathcal{B}_{zo}^{-1}(W\,\mathcal{B}_{pi}(G))\,W|_{s=z}\,\mathcal{B}_{pi}(G)|_{s=z}\,\mathcal{B}_{pi}^{-1}(G)|_{s=z}\,V_0\,V_{mi}(z) \\
&= \mathcal{B}_{zo}^{-1}(W\,\mathcal{B}_{pi}(G))\,W|_{s=z}\,V_0\,V_{mi}(z) \\
&= \mathcal{B}_{zo}^{-1}(W\,\mathcal{B}_{pi}(G))\,W|_{s=z}(u_z u_z^H + k_0^2 U_0 U_0^H)\,V_{mi}(z)
\end{aligned}
$$

and for $k_0 = 0$ we have

$$\|(W S_I V)_m(z)\|_2 = \|\mathcal{B}_{zo}^{-1}(W\,\mathcal{B}_{pi}(G))\,W|_{s=z}\,u_z\|_2 \cdot \|u_z^H\,V_{mi}(z)\|_2$$

and

$$\lim_{k_0 \to 0} \|W S_I V(s)\|_\infty = \|\mathcal{B}_{zo}^{-1}(W\,\mathcal{B}_{pi}(G))\,W|_{s=z}\,u_z\|_2 \cdot \|u_z^H\,V_{mi}(z)\|_2$$

<div style="text-align:right">□</div>

Proof of Theorem 5.7. It follows that P has no poles in $\mathbb{C}_+$, since M_{mo}^{-1} and V_{mi}^{-1} have no poles in $\mathbb{C}_+$, and the remaining matrices are constant and finite. Consider $I - P\mathcal{B}_{zo}(G)$, at $s = p$ we have $P(z) = \mathcal{B}_{zo}^{-1}(G)|_{s=p} V_0$

$$
\begin{aligned}
(I - \mathcal{B}_{zo}^{-1}(G)|_{s=p} V_0 \mathcal{B}_{zo}(G))|_{s=p}\tilde{y}_p &= \mathcal{B}_{zo}^{-1}(G)|_{s=p}(I - V_0)\,\mathcal{B}_{zo}(G)|_{s=p}\tilde{y}_p \\
&= \mathcal{B}_{zo}^{-1}(G)|_{s=p}(1 - k_0^2)U_0 U_0^H \mathcal{B}_{zo}(G)|_{s=p}\tilde{y}_p
\end{aligned}
$$

Since $U_0 U_0^H$ has rank $l - 1$, and the singular directions both at the input and at the output of $U_0 U_0^H$ are y_p, it follows that $I - P\mathcal{B}_{zo}(G)$ has a RHP-zero for $s = p$ with input direction

$$\tilde{y}_p = \mathcal{B}_{zo}^{-1}(G)|_{s=p}\,y_p / \|\mathcal{B}_{zo}^{-1}(G)|_{s=p}\,y_p\|_2$$

We find that this is the output direction of the RHP-pole p in G_{mo} (that is the plant with the RHP-zeros factorized at the output). We can write

$$I - P\mathcal{B}_{zo}(G) = Q\,\mathcal{B}_{po}(G_{mo})$$

Since $I - P\mathcal{B}_{zo}(G)$ has no poles in $\mathbb{C}_+$ and $\mathcal{B}_{po}(G_{mo})$ is stable, it follows that Q has no poles in $\mathbb{C}_+$. That is, in a minimal state-space realization of Q the RHP-pole for $s = p$ in $\mathcal{B}_{po}^{-1}(G_{mo})$ cancels the RHP-zero for $s = z$ in $I - P\mathcal{B}_{zo}(G)$. We obtain

$$
\begin{aligned}
L &= GK_2 = \mathcal{B}_{zo}(G)\,\mathcal{B}_{po}^{-1}(G_{mo})\,Q^{-1}\,P \\
T^{-1} &= I + L^{-1} = I + P^{-1}(I - P\mathcal{B}_{zo}(G))\,\mathcal{B}_{zo}^{-1}(G) = P^{-1}\mathcal{B}_{zo}^{-1}(G) \\
T &= \mathcal{B}_{zo}(G)\,P = \mathcal{B}_{zo}(G)\,M_{mo}^{-1}(s)\,M_{mo}(p)\,\mathcal{B}_{zo}^{-1}(G)|_{s=p}\,V_0\,V_{mi}(p)\,V_{mi}^{-1}(s)
\end{aligned}
$$

It follows that T has no poles in $\mathbb{C}_+$, since P has no poles in $\mathbb{C}_+$ and $\mathcal{B}_{zo}(G)$ is stable. Consider

$$
\begin{aligned}
WTV(s) &= \overbrace{W(s)\mathcal{B}_{zo}(G)\,M_{mo}^{-1}(s)}^{M(s)}\,M_{mo}(p)\,\mathcal{B}_{zo}^{-1}(G)|_{s=p}\,V_0\,V_{mi}(p)\,V_{mi}^{-1}(s)V(s) \\
&= \mathcal{B}_{zo}(M)\,\underbrace{M_{mo}(p)\,\mathcal{B}_{zo}^{-1}(G)|_{s=p}\,V_0\,V_{mi}(p)}_{(WTV)_m(p)}\,\mathcal{B}_{zi}(V)
\end{aligned}
$$

We have that WTV is stable since $\mathcal{B}_{zo}(M)$ and $\mathcal{B}_{zi}(V)$ are stable and the matrix $(WTV)_m(p)$ is constant (independent of s). We obtain

$$\|WTV(s)\|_\infty = \|(WTV)_m(p)\|_\infty = \|(WTV)_m(p)\|_2$$

$$
\begin{aligned}
(WTV)_m(p) &= (W\,\mathcal{B}_{zo}(G))_{mo}\,\mathcal{B}_{zo}^{-1}(G)|_{s=p}\,V_0\,V_{mi}(p) \\
&= \mathcal{B}_{zo}^{-1}(W\,\mathcal{B}_{zo}(G))\,W|_{s=p}\mathcal{B}_{zo}(G)|_{s=p}\mathcal{B}_{zo}^{-1}(G)|_{s=p}\,V_0\,V_{mi}(p) \\
&= \mathcal{B}_{zo}^{-1}(W\,\mathcal{B}_{zo}(G))\,W|_{s=p}V_0\,V_{mi}(p) \\
&= \mathcal{B}_{zo}^{-1}(W\,\mathcal{B}_{zo}(G))\,W|_{s=p}(y_p y_p^H + k_0^2 U_0 U_0^H)\,V_{mi}(p)
\end{aligned}
$$

and for $k_0 = 0$ we have

$$\|(WTV)_m(p)\|_2 = \|\mathcal{B}_{zo}^{-1}(W\,\mathcal{B}_{zo}(G))\,W|_{s=p}y_p\|_2 \cdot \|y_p^H\,V_{mi}(p)\|_2$$

and

$$\lim_{k_0 \to 0}\|WTV(s)\|_\infty = \|\mathcal{B}_{zo}^{-1}(W\,\mathcal{B}_{zo}(G))\,W|_{s=p}y_p\|_2 \cdot \|y_p^H\,V_{mi}(p)\|_2$$

$\square$

Proof of Theorem 5.8. It follows that P has no poles in $\mathbb{C}_+$, since M_{mi}^{-1} and W_{mso}^{-1} have no poles in $\mathbb{C}_+$, and the remaining matrices are constant and finite. Consider $I - \mathcal{B}_{zi}(G)\,P$, at $s = p$ we have $P(p) = V_0\,\mathcal{B}_{zi}^{-1}(G)|_{s=p}$

$$
\begin{aligned}
\tilde{u}_p^H(I - \mathcal{B}_{zi}(G)|_{s=p}V_0\,\mathcal{B}_{zi}^{-1}(G)|_{s=p}) &= \tilde{u}_p^H\,\mathcal{B}_{zi}(G)|_{s=p}\,(I - V_0)\,\mathcal{B}_{zi}^{-1}(G)|_{s=p} \\
&= \tilde{u}_p^H\,\mathcal{B}_{zi}(G)|_{s=p}(1 - k_0^2)U_0 U_0^H\,\mathcal{B}_{zi}^{-1}(G)|_{s=p}
\end{aligned}
$$

Since $U_0 U_0^H$ has rank $m - 1$, and the singular directions both at the input and at the output of $U_0 U_0^H$ are u_p, it follows that $I - \mathcal{B}_{zi}(G)\,P$ has a RHP-zero for $s = p$ with output direction

$$\tilde{u}_p = \mathcal{B}_{zi}^{-H}(G)|_{s=p}\,u_p\,/\,\|\mathcal{B}_{zi}^{-H}(G)|_{s=p}\,u_p\|_2$$

We find that this is the input direction of the RHP-pole in G_{mi} (that is the plant with the RHP-zeros factorized at the input). We can write

$$I - \mathcal{B}_{zi}(G)\,P = \mathcal{B}_{pi}(G_{mi})\,Q$$

Since $I - \mathcal{B}_{zi}(G)\,P$ has no poles in $\mathbb{C}_+$ and $\mathcal{B}_{pi}(G_{mi})$ is stable, it follows that Q has no poles in $\mathbb{C}_+$. That is, in a minimal state-space realization of Q the RHP-pole for $s = p$ in $\mathcal{B}_{pi}^{-1}(G_{mi})$ cancels the RHP-zero for $s = z$ in $I - \mathcal{B}_{zi}(G)\,P$. We obtain

$$
\begin{aligned}
L_I &= K_2 G = PQ^{-1}\mathcal{B}_{pi}^{-1}(G_{mi})\,\mathcal{B}_{zi}(G) \\
T_I^{-1} &= I + L_I^{-1} = I + \mathcal{B}_{zi}^{-1}(G)\,(I - \mathcal{B}_{zi}(G)\,P)\,P^{-1} = \mathcal{B}_{zi}^{-1}(G)\,P^{-1} \\
T_I &= P\,\mathcal{B}_{zi}(G) = W_{mo}^{-1}(s)\,W_{mo}(p)\,V_0\,\mathcal{B}_{zi}^{-1}(G)|_{s=p}\,M_{mi}(p)\,M_{mi}^{-1}(s)\,\mathcal{B}_{zi}(G)
\end{aligned}
$$

It follows that T_I has no poles on $\mathbb{C}_+$, since P has no poles in $\mathbb{C}_+$ and $\mathcal{B}_{zi}(G)$ is stable. Consider

$$
\begin{aligned}
WT_IV(s) &= W(s)\,W_{mo}^{-1}(s)\,W_{mo}(p)\,V_0\,\mathcal{B}_{zi}^{-1}(G)|_{s=p}\,M_{mi}(p)\,M_{mi}^{-1}(s)\,\overbrace{\mathcal{B}_{zi}(G)\,V(s)}^{M(s)} \\
&= \mathcal{B}_{zo}(W)\,\underbrace{W_{mo}(p)\,V_0\,\mathcal{B}_{zi}^{-1}(G)|_{s=p}\,M_{mi}(p)}_{(WT_IV)_m(p)}\,\mathcal{B}_{zi}(M)
\end{aligned}
$$

We have that WT_IV is stable since $\mathcal{B}_{zo}(W)$ and $\mathcal{B}_{zi}(M)$ are stable and the matrix $(WT_IV)_m(p)$ is constant (independent of s). We obtain

$$\|WT_IV(s)\|_\infty = \|(WT_IV)_m(p)\|_\infty = \|(WT_IV)_m(p)\|_2$$

where

$$
\begin{aligned}
(WT_IV)_m(p) &= W_{mo}(p)\,V_0\,\mathcal{B}_{zi}^{-1}(G)|_{s=p}\,(\mathcal{B}_{zi}(G)\,V)_{mi}|_{s=p} \\
&= W_{mo}(p)\,V_0\,\mathcal{B}_{zi}^{-1}(G)|_{s=p}\,\mathcal{B}_{zi}(G)|_{s=p}\,V\mathcal{B}_{zi}^{-1}(\mathcal{B}_{zi}(G)\,V)|_{s=p} \\
&= W_{mo}(p)\,V_0\,V\mathcal{B}_{zi}^{-1}(\mathcal{B}_{zi}(G)\,V)|_{s=p} \\
&= W_{mo}(p)\,(u_p u_p^H + k_0^2 U_0 U_0^H)\,V\mathcal{B}_{zi}^{-1}(\mathcal{B}_{zi}(G)\,V)|_{s=p}
\end{aligned}
$$

and for $k_0 = 0$ we have

$$\|(WT_IV)_m(p)\|_2 = \|W_{mo}(p)\,u_p\|_2 \cdot \|u_p^H\,V\mathcal{B}_{zi}^{-1}(\mathcal{B}_{zi}(G)\,V)|_{s=p}\|_2$$

and

$$\lim_{k_0 \to 0}\|WT_IV(s)\|_\infty = \|W_{mo}(p)\,u_p\|_2 \cdot \|u_p^H\,V\mathcal{B}_{zi}^{-1}(\mathcal{B}_{zi}(G)\,V)|_{s=p}\|_2$$

$\square$

A.4 Proof of Theorem 5.9

Proof of (5.77). Factorize RHP zeros of R at the input, i.e. $R = R_{mi}\,\mathcal{B}_{zi}(R)$. Then

$$\|W_P(SGK_1 - I)R\|_\infty = \|W_P(SGK_1 - I)R_{mi}(s)\|_\infty$$

Introduce the scalar function $f(s) = x_1^H W_P(SGK_1 - I)R_{mi}x_2$ which is analytic (stable) in RHP since the closed-loop system is stable. We want to choose x_1 and x_2 so that $|f(s)|$ obtains maximum

$$J(s) = \max_{\|x_1\|_2=1,\,\|x_2\|_2=1}|f(s)|$$

We get

$$\|W_P(SGK_1 - I)R_{mi}\|_\infty \geq \|J(s)\|_\infty \geq J(z_j)$$

The first inequality follows since the largest singular value measures the maximum gain of a matrix independent of direction, i.e. $\bar{\sigma}(A) \geq \|Aw\|_2$ and $\bar{\sigma}(A) \geq \|w^H A\|_2$ for any vector w with $\|w\|_2 = 1$. The second inequality follows from the maximum modulus theorem. We get

$$
\begin{aligned}
J(z_j) &= \max_{\|x_1\|_2=1,\,\|x_2\|_2=1} x_1^H W_P(SGK_1 - I)R_{mi}(z_j)x_2 \\
&\geq \max_{\|x_1\|_2=1,\,\|x_2\|_2=1} x_1^H W_P y_{z_j} y_{z_j}^H(SGK_1 - I)R_{mi}(z_j)x_2 \\
&= \|W_P|_{s=z_j} y_{z_j}\|_2 \cdot \|(\underbrace{y_{z_j}^H G(z_j)}_{0} K_1(z_j) - y_{z_j}^H)R_{mi}(z_j)\|_2 \\
&= \|W_P|_{s=z_j} y_{z_j}\|_2 \cdot \|y_{z_j}^H R_{mi}(z_j)\|_2
\end{aligned}
$$

$\square$

Consider

$$I - W_P^{-1}(s)\, W_P(z)\, y_z y_z^H\, R_{mi}(z)\, R_{mi}^{-1}(s) = \mathcal{B}_{zo}(G)\, P(s)$$

Since $\left(I - W_P^{-1}(s)\, W_P(z)\, y_z y_z^H\, R_{mi}(z)\, R_{mi}^{-1}(s)\right)$ has no poles in $\mathbb{C}_+$ and $\mathcal{B}_{zo}(G)$ is stable it follows that $P(s)$ has no poles in $\mathbb{C}_+$. That is the unstable pole for $s = z$ in $\mathcal{B}_{zo}(G)$ cancels the RHP-zero for $s = z$ in a minimal realization of $P(s)$.

Proof of (5.79) and (5.80). The controller K_2 which minimizes $\|W_P SG(s)\|_\infty$ is given in Theorem 5.5, and from (5.82) with $W = W_P$, $V = G$, $M = \mathcal{B}_{po}(G)\, G = G_{so}$ we obtain

$$W_P SG(s) \quad = \quad W_P(z) V_0\, \mathcal{B}_{po}^{-1}(G)\big|_{s=z}\, G_{somi}(z)\, \mathcal{B}_{zi}(G_{so})$$

which has a RHP-zero (only one) for $s = z$, since $\mathcal{B}_{zi}(G_{zo})$ has a RHP-zero for $s = z$. By considering $y_z^H SG(z)$

$$y_z^H SG(z) = \underbrace{y_z^H W_P^{-1}(z) W_P(z) V_0}_{y_z^H}\, \underbrace{\mathcal{B}_{po}^{-1}(G)\big|_{s=z}\, \overbrace{G_{somi}(z)\, \mathcal{B}_{zi}(G_{so})\big|_{s=z}}^{G_{so}(z)}}_{G(z)} = y_z^H G(z)$$

which implies that the output zero direction of SG is y_z. We can then write

$$SG(s) = \mathcal{B}_{zo}(G)\, \left(W_P^{-1}(s) W_P(z) V_0\, \mathcal{B}_{po}^{-1}(G)\big|_{s=z}\, G_{somi}(z)\, \mathcal{B}_{zi}(G_{so})\right)_{mo} = \mathcal{B}_{zo}(G)\, Q(s)$$

With $K_1 = Q^{-1} P(s)$ we obtain

$$
\begin{aligned}
SGK_1 - I \quad &= \quad \mathcal{B}_{zo}(G)\, Q\, Q^{-1}\, P(s) - I \\
&= \quad -W_P^{-1}(s)\, W_P(z)\, y_z y_z^H\, R_{mi}(z) R_{mi}^{-1}(s) \\
W_P(SGK_1 - I)R \quad &= \quad -W_P(z)\, y_z y_z^H\, R_{mi}(z)\, \mathcal{B}_{zi}(R) \\
\|W_P(SGK_1 - I)R(s)\|_\infty \quad &= \quad \|W_P(z)\, y_z y_z^H\, R_{mi}(z)\|_\infty = \|W_P(z)\, y_z y_z^H\, R_{mi}(z)\|_2 \\
&= \quad \|W_P(z) y_z\|_2 \cdot \|y_z^H\, R_{mi}(z)\|_2
\end{aligned}
$$

$\square$

This completes the proof of Theorem 5.9. $\square$

Chapter 6

Selection of variables for regulatory control using pole vectors

Kjetil Havre[*] and Sigurd Skogestad[†]

Chemical Engineering,
Norwegian University of Science and Technology
N-7034 Trondheim, Norway.

Abstract

This paper considers control structure design using the information given in the pole vectors. It is shown how the input and output pole vectors are related to the minimum input usage needed to stabilize a plant with one unstable mode using a Single Input Single Output (SISO) controller. We quantify the input usage due to measurement noise both in terms of the $\mathcal{H}_2$-norm (input energy) and the $\mathcal{H}_\infty$-norm. We show that the best choice of one input and one output for SISO stabilizing control is the same for both norms, and corresponds to the elements in the pole vectors with largest magnitude. We also look at stable but slow modes which need to be shifted further into the Left Half Plane (LHP) using feedback control. Moving stable slow modes are accomplished with modal control and the results are interpreted in terms of Linear Quadratic Gaussian (LQG) control.

---

[*]Also affiliated with: Institute for energy technology, P.O.Box 40, N-2007 Kjeller, Norway, Fax: (+47) 63 81 11 68, E-mail: Kjetil.Havre@ife.no.

[†]Fax: (+47) 73 59 40 80, E-mail: skoge@chembio.ntnu.no.

6.1   Introduction

This paper considers the input/output selection for plants which need to be "stabilized" in an extended meaning. This includes plants which contain one or more unstable modes and therefore need to be stabilized in the mathematical sense, or plants which contain one or more stable slow modes which need to be "stabilized" form the operator's point of view. In order to provide this "stabilization" we need to move the modes (poles) in question by the use of a feedback controller. The *main* problem we will answer in this paper is:

- Given a plant G with one unstable mode p, where the measurements of the plant outputs are affected by noise. Which pair of one input j and one output i stabilize the unstable mode p with the minimum input usage?

In other words, we wish to find the controller K_{ji}, the best input j and the best output i such that the plant G is stabilized with minimum input usage

$$\min_{i,j} \min_{K_{ji}(s)} \|K_{ji}S_{ii}(s)\| \quad \text{where} \quad S_{ii}(s) = (1 + G_{ij}K_{ji}(s))^{-1}$$

We minimize the input usage, using two different norms:

1) $\mathcal{H}_2$-norm:

$$\min_{i,j} \min_{K_{ji}(s)} \|K_{ji}S_{ii}(s)\|_2$$

which corresponds to minimize the expected value of the input energy due to zero mean white measurement noise with unit intensity:

$$J(i,j) = E\left\{\lim_{T\to\infty} \frac{1}{T}\int_0^T u_j^2(t)dt\right\} \tag{6.1}$$

This is a special Linear Quadratic Gaussian (LQG) control problem with zero weight on the states, unity weight on the control u_j, no process noise and measurement noise unit intensity.

2) $\mathcal{H}_\infty$-norm:

$$\min_{i,j} \min_{K_{ji}(s)} \|K_{ji}S_{ii}(s)\|_\infty$$

which corresponds to minimize the input usage for the worst case sinusoidal measurement noise (worst case magnitude and frequency).

Both of these problems can be solved numerically for each possible pairing $u_j \leftrightarrow y_i$. We can then answer the input/output selection problem by choosing the pairing with the smallest norm of the closed-loop transfer function $K_{ji}S_{ii}$ (for the $\mathcal{H}_2$-case the norm is equivalent with the objective $J(i,j)$, i.e. $J(i,j) = \min_{K_{ji}(s)} \|K_{ji}S_{ii}(s)\|_2^2$). As we shall see in Section 6.3, we do *not* explicitly need to solve *any* minimum input LQG problem or any $\mathcal{H}_\infty$-control problem in order to find the best pairing when the plant has one unstable mode.

To emphasize the *practical application* of the results in this paper we provide the answer to the question above.

- Selecting the input j and output i corresponding to the element with largest magnitude in the pole vectors, minimize the best achievable input usage to stabilize a plant with one unstable mode using a SISO controller.

For the case when the plant G has no unstable modes, minimizing the input usage is meaningless since $u_j = 0$ gives $\|K_{ji}S_{ii}(s)\| = 0$. For a stable system a relevant problem is to move one slow open-loop mode further to the left in the complex plane using a single loop controller. That is, to speed up the open-loop response. To get a meaningful LQG control problem in this case, one needs to add some weight on the states. The interpretations of moving a stable pole is therefore clearly not in terms of minimum input usage. An alternative objective is to minimize the magnitude of the feedback controller gains. This problem is considered in Section 6.4 and some interpretations in terms of LQG control are given in Section 6.5.

An overview of zero and poles in multivariable system is given in (Douglas and Athans, 1995), where they also discuss controllability and observability. They mention: given a linear time invariant system, state-space realization (A, B, C, D), let λ_i be an eigenvalue of the A matrix with left and right eigenvectors w_i and v_i normalized so that $w_i^H v_i = 1$, then the product $w_i^H B$ is an indication of how much the i'th mode is exited by the inputs, and the product Cv_i is an indication of how much the i'th mode is observed in the outputs. This is similar to the ideas used in this paper, however, we emphasize that the two products above depend on the state-space realization.

Measures for state controllability and observability have been proposed by Tarokh (1992). However, we note that these measures do not reflect how easy it is to control or stabilize an unstable mode p. Based on the controllability measures proposed by Tarokh (1992), Li, Xi and Zhang (1994) suggest two approaches to select inputs to be used for control. However, their approaches have not been justified in terms of how easy it is to control or stabilize a given unstable mode.

The intention with this paper is to establish a direct link between the pole vectors and how easy it is to control or stabilize an unstable mode. This link will then serve as a justification for using the pole vectors to select one input and one output to control the mode.

6.1.1 Notation

We consider linear time invariant systems on state-space form

$$\dot{x} = Ax + Bu \tag{6.2}$$

$$y = Cx + Du \tag{6.3}$$

where A, B, C, and D are real matrices with dimensions $n \times n$, $n \times m$, $l \times n$ and $l \times m$, n is the number of states, l is the number of outputs and m is the number of inputs. The short-hand notations

$$G(s) \stackrel{s}{=} \left[\begin{array}{c|c} A & B \\ \hline C & D \end{array} \right] \quad \text{and} \quad (A, B, C, D) \tag{6.4}$$

are frequently used to describe a state-space model of a system G. The rational transfer function matrix G defined by (6.4) can be evaluated as a function of the complex variable s

$$G(s) = C(sI - A)^{-1}B + D$$

We often omit to show the dependence on the complex variable s for transfer functions.

For a strictly proper system $M(s)$ the $\mathcal{H}_2$-norm is defined as

$$\|M(s)\|_2 \triangleq \sqrt{\frac{1}{2\pi} \int_{-\infty}^{\infty} \mathrm{tr}\left(M^H(j\omega) M(j\omega)\right) d\omega} \tag{6.5}$$

By Parseval's theorem, (6.5) is equal to the $\mathcal{H}_2$-norm of the impulse response (time-domain). The $\mathcal{H}_\infty$-norm of a stable rational transfer function matrix $M(s)$ is defined as the peak value overall frequencies of the largest singular value of $M(j\omega)$

$$\|M(s)\|_\infty \triangleq \sup_\omega \bar{\sigma}(M(j\omega)) \tag{6.6}$$

The $\mathcal{H}_\infty$-norm has several time domain performance interpretations (see, Skogestad and Postlethwaite, 1996).

The results in this paper on the $\mathcal{H}_2$-norm have been derived from Single Input Single Output (SISO) Linear Quadratic Gaussian (LQG) control of output i using input j. We assume that the plant dynamics are linear and known, and that measurement noise n and disturbance signals (process noise) w are stochastic with known statistical properties. That is, we have the plant model

$$\dot{x} = Ax + Be_j u_j + w \tag{6.7}$$

$$y_i = e_i^T C x + e_i^T D e_j u_j + n_i \tag{6.8}$$

where e_j is a vector of length m with zeros in all elements except element j which contains 1, e_i is similarly a vector of length l with zeros in all elements except element i which contains 1. The disturbance w and measurement noise n are zero mean Gaussian stochastic processes with power spectral density matrices W and I. That is, w and n are white noise processes with covariances

$$E\{w(t)w^T(\tau)\} = W\,\delta(t-\tau) \tag{6.9}$$

$$E\{n(t)n^T(\tau)\} = I\,\delta(t-\tau) \tag{6.10}$$

and

$$E\{w(t)n^T(\tau)\} = 0, \quad E\{n(t)w^T(\tau)\} = 0 \tag{6.11}$$

In this case the LQG problem is to find the optimal control $u_j(t)$ which minimizes

$$J(i,j) = E\left\{ \lim_{T\to\infty} \frac{1}{T} \int_0^T x^T(t)Qx(t) + u_j^2(t)\, dt \right\} \tag{6.12}$$

where $Q \geq 0$ is a weighting matrix (design parameter). When we minimize the input energy we set $Q = 0$, we have that $\sqrt{J(i,j)}$ is equal to the $\mathcal{H}_2$-norm for measurement noise to plant inputs, i.e.

$$\|K_{ji}(1 + G_{ij}K_{ji})^{-1}\|_2^2 = J(i,j) \tag{6.13}$$

where $y_i = G_{ij}u_j$, $u_j = K_{ji}y_i$ and K_{ji} is the LQG controller (6.22) with zero weight on the states $(Q = 0)$, and no process noise $(W = 0)$.

6.1.2   Solution to the LQG problem

The solution to the LQG problem, known as the Separation Theorem or Certainty Equivalence Principle, is first to determine the optimal state feedback, Linear Quadratic Regulator (LQR), and then to design an optimal state observer, Linear Quadratic Estimator (LQE). The SISO LQG controller which minimizes (6.12) is the combined state-estimator and state feedback.

Optimal state feedback to input u_j. The single input LQR problem minimizes

$$J_{\text{LQR}}(j) = \int_0^\infty x^T(t)Qx(t) + u_j^2(t)dt \tag{6.14}$$

due to non-zero initial states x_0. The optimal solution (for any initial state x_0) is

$$u_j(t) = -K_j x(t) \tag{6.15}$$

where

$$K_j = \underbrace{e_j^T B^T} X = b_j^T X \tag{6.16}$$

and X is positive semidefinite solution to the algebraic Riccati equation (Skogestad and Postlethwaite, 1996)

$$A^T X + XA - XBe_j e_j^T B^T X + Q = 0 \tag{6.17}$$

The value of the objective $J_{\text{LQR}}(j)$ (6.14) due to the non-zero initial state x_0 becomes (Kwakernaak and Sivan, 1972)

$$J_{\text{LQR}}(j) = x_0^T X x_0 \tag{6.18}$$

Optimal state estimator based on y_i. The single output state-estimator (Kalman filter) is updated by only using the information in output y_i. The state equation describing the dynamics of the observer becomes

$$\dot{\hat{x}} = A\hat{x} + Be_j u_j + K_{f,i}(y_i - e_i^T C\hat{x} - e_i^T De_j u_j) \tag{6.19}$$

The optimal choice of $K_{f,i}$, which minimizes the mean square reconstruction error

$$E\left\{(x(t) - \hat{x}(t))^T(x(t) - \hat{x}(t))\right\}$$

due to measurement noise n_i, is given by

$$K_{f,i} = YC^T e_i \tag{6.20}$$

where $Y = Y^T \geq 0$ is the unique positive-semidefinite solution to the algebraic Riccati equation

$$YA^T + AY - YC^T e_i e_i^T CY + W = 0 \tag{6.21}$$

LQG: combined state estimation and state feedback. The transfer function from measurements y_i (including the noise n_i) to the inputs u_j (assuming positive feedback), is given by the state-space realization[1]

$$K_{ji}(s) \overset{s}{=} \left[\begin{array}{c|c} A - Be_jK_j - K_{f,i}e_i^TC + K_{f,i}e_i^TDe_jK_j & K_{f,i} \\ \hline -K_j & 0 \end{array} \right] \qquad (6.22)$$

The LQG controller K_{ji} has the same number of states as the plant.

Minimum value of objective. Two alternative expressions for the minimum value of the objective $J(i,j)$ are (Kwakernaak and Sivan, 1972, Theorem 5.4 part (d) pp. 394–395):

$$J(i,j) = \text{tr}\{XK_{f,i}K_{f,i}^T + YQ\} = \text{tr}\{XW + YK_j^TK_j\} \qquad (6.23)$$

6.1.3 Outline

The outline of the paper is a follows; Section 6.2 shows how to compute the input and output pole vectors and directions in terms of eigenvalue problems. This section also gives some examples on pole directions and the links between the pole directions and state controllability and observability. Section 6.3 contains the main result, which is to find one input and one output (and a SISO controller) which stabilize a given unstable mode with minimum input usage. In Section 6.4 we consider moving one or two poles from the open-loop locations to some desired closed-loop locations using a single control loop. We show that selecting the input corresponding to the element with largest magnitude in the input pole vector minimizes the norm of the feedback gain matrix from the states to the input. Similarly, selecting the output corresponding to the element with largest magnitude in the output pole vector minimizes the norm of the feedback gain matrix from the output to the states in the observer. In Section 6.5 we show when and how the results on pole placement can be interpreted in terms of LQG control. Section 6.6 discusses the implications of the results in terms of a procedure for input/output selection for plants which need "stabilization". Section 6.7 contains some relevant control engineering problems from chemical process plants which illustrates several of the results derived. A summary is given in Section 6.8. Section A contains brief treatment of modal control and estimation problems. Analytical formulas for the feedback gain matrices are given in terms of the pole vectors for the single input modal control problem and single output modal estimation problem. Section B contains the proofs of the results.

6.2 Pole vectors and directions

For a system on state-space form with a distinct[2] pole located at $s = p$, we compute the input and output *pole vectors* (non-normalized basis vectors for the input and output pole spaces)

---

[1] This state-space realization is not minimal if the plant G has modes which are uncontrollable in input u_j and/or unobservable in output y_i.

[2] For simplicity we assume in most of the paper that the poles are distinct. The results can be extended to the case with repeated poles, see Section A.3.

as

$$\boldsymbol{u}_p = B^H x_{pi}; \qquad \boldsymbol{y}_p = C x_{po} \qquad (6.24)$$

where $x_{pi}, x_{po} \in \mathbb{C}^n$ are *normalized* eigenvectors corresponding to the two eigenvalue problems

$$x_{pi}^H A = p x_{pi}^H \quad \text{and} \quad A x_{po} = p x_{po} \qquad (6.25)$$

Theorem 2.2 in Section 2.6 states that the mode p is uncontrollable if and only if $\boldsymbol{u}_p = 0$ and unobservable if and only if $\boldsymbol{y}_p = 0$. It follows that mode p is uncontrollable in input j if the j'th element in the input pole vector is equal to zero, i.e. $\boldsymbol{u}_{p,j} = 0$. Similarly, the mode p is unobservable in output i if the i'th element in the output pole vector is equal to zero, i.e. $\boldsymbol{y}_{p,i} = 0$.

A minimal state-space realization will not contain uncontrollable and/or unobservable modes. The corresponding *pole directions* are obtained by normalizing the pole vectors (if one or more modes are uncontrollable we set the corresponding input pole directions equal to zero, and if one or more modes are unobservable we set the corresponding output pole directions to zero):

$$u_p = \begin{cases} \boldsymbol{u}_p / \| \boldsymbol{u}_p \|_2 & \text{if } \| \boldsymbol{u}_p \|_2 \neq 0 \\ 0 & \text{if } \| \boldsymbol{u}_p \|_2 = 0 \end{cases} \qquad (6.26)$$

$$y_p = \begin{cases} \boldsymbol{y}_p / \| \boldsymbol{y}_p \|_2 & \text{if } \| \boldsymbol{y}_p \|_2 \neq 0 \\ 0 & \text{if } \| \boldsymbol{y}_p \|_2 = 0 \end{cases} \qquad (6.27)$$

The results in this paper are in terms of input and output pole vectors, however, the pole directions have turned out to be useful when studying the effect of zeros and poles on performance in multivariable systems, see Chapters 3 to 5 for further details.

EXAMPLE 6.1 SYSTEMS IN SERIES AND PARALLEL. We consider the following two structures:

Systems in parallel.

Systems in series.

$$G_A(s) = \begin{bmatrix} \frac{1}{s-p_1} & 0 \\ 0 & \frac{1}{s-p_2} \end{bmatrix}$$

$$G_B(s) = \begin{bmatrix} \frac{1}{s-p_1} & \frac{1}{(s-p_1)(s-p_2)} \\ 0 & \frac{1}{s-p_2} \end{bmatrix}$$

$$G_A(s) \overset{s}{=} \left[\begin{array}{cc|cc} p_1 & 0 & 1 & 0 \\ 0 & p_2 & 0 & 1 \\ \hline 1 & 0 & 0 & 0 \\ 0 & 1 & 0 & 0 \end{array} \right]$$

$$G_B(s) \overset{s}{=} \left[\begin{array}{cc|cc} p_1 & 1 & 1 & 0 \\ 0 & p_2 & 0 & 1 \\ \hline 1 & 0 & 0 & 0 \\ 0 & 1 & 0 & 0 \end{array} \right]$$
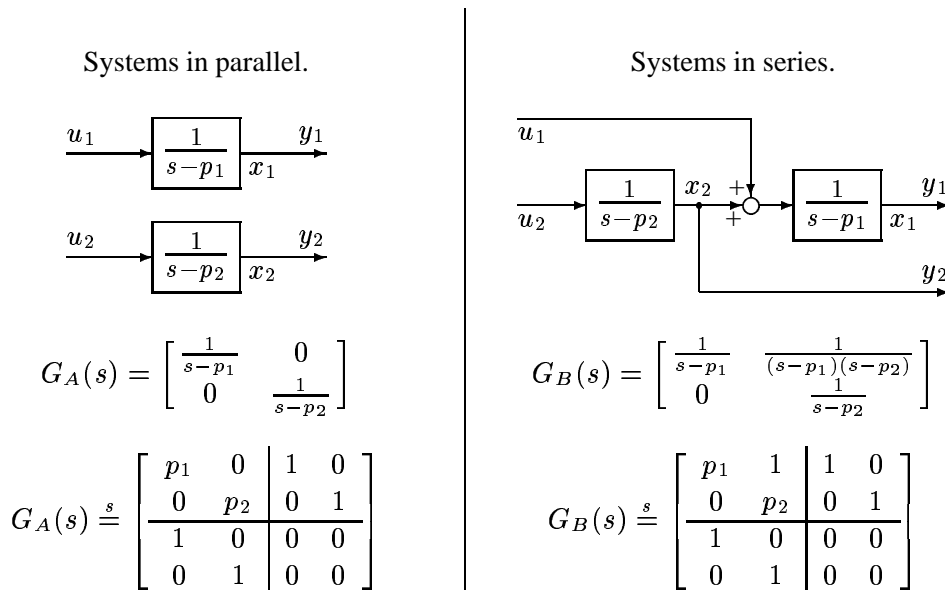
When $p_1 = 1$ and $p_2 = 2$ we get pole vectors (the first column corresponds to p_1 etc.):

$$\boldsymbol{U}_p = X_{pi} = \begin{bmatrix} 1 & 0 \\ 0 & 1 \end{bmatrix} \qquad \boldsymbol{U}_p = X_{pi} = \begin{bmatrix} -0.707 & 0 \\ 0.707 & -1 \end{bmatrix}$$

$$\boldsymbol{Y}_p = X_{po} = \begin{bmatrix} 1 & 0 \\ 0 & 1 \end{bmatrix} \qquad \boldsymbol{Y}_p = X_{po} = \begin{bmatrix} 1 & 0.707 \\ 0 & 0.707 \end{bmatrix}$$

When $p_1 = 1$ and $p_2 = 1.1$ we get pole vectors:

$$\boldsymbol{U}_p = X_{pi} = \begin{bmatrix} 1 & 0 \\ 0 & 1 \end{bmatrix} \qquad \boldsymbol{U}_p = X_{pi} = \begin{bmatrix} -0.1 & 0 \\ 0.995 & -1 \end{bmatrix}$$

$$\boldsymbol{Y}_p = X_{po} = \begin{bmatrix} 1 & 0 \\ 0 & 1 \end{bmatrix} \qquad \boldsymbol{Y}_p = X_{po} = \begin{bmatrix} 1 & 0.995 \\ 0 & 0.1 \end{bmatrix}$$

EXAMPLE 6.2. This example illustrates the influence of a zero close to the pole on the input and output pole "vectors"[3]. Consider the following SISO transfer function

$$G(s) = \frac{s - z}{s - p}, \quad z \geq p. \quad \text{One state-space realization is:} \quad G(s) \stackrel{s}{=} \left[\begin{array}{c|c} p & -\sqrt{z - p} \\ \hline \sqrt{z - p} & 1 \end{array} \right]$$

The state-space realization given is a balanced minimal realization when $z - p \neq 0$. The input and output pole vectors become

$$\boldsymbol{u}_p = -\sqrt{z - p} \quad \text{and} \quad \boldsymbol{y}_p = \sqrt{z - p}$$

Clearly, as the zero z approaches the pole p from above the input and output pole vectors approaches zero. When $z = p$, $G(s) = 1$ and the mode p is uncontrollable and unobservable, and both $\boldsymbol{u}_p$ and $\boldsymbol{y}_p$ are zero. The pole vectors are clearly influenced by the distance between the zero z and the pole p in this case.

6.3   Stabilizing control with minimum input usage

6.3.1   Single loop control minimizing the input energy ($\mathcal{H}_2$-norm)

In this section we consider the following problem, see also Figure 6.1.

PROBLEM 6.1. *Given a plant G with one unstable mode $p \in \mathbb{C}_+$ $(\operatorname{Re} p > 0)$ and white measurement noise n_i of unit intensity in each output y_i. Find the best pairing $u_j \leftrightarrow y_i$, such that the plant is stabilized with minimum achievable input energy*

$$J(i, j) = E \left\{ \lim_{T \to \infty} \frac{1}{T} \int_0^T u_j^2(t) dt \right\} \tag{6.28}$$

---

[3]The term vector is somewhat abused in this context since we consider a SISO transfer function, so the pole vectors are scalars.
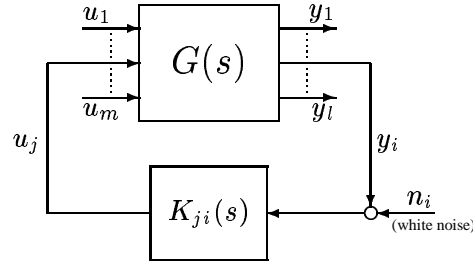
Figure 6.1: Plant G and stabilizing control loop with pairing $u_j \leftrightarrow y_i$
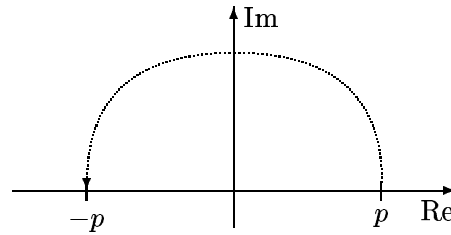
Figure 6.2: Mapping of pole from RHP to LHP with state feedback and minimum input usage

At first sight it is not clear that the output selection problem is included at all, since the outputs do not enter into the objective (6.28) explicitly. However, the output selection problem is included implicitly through the measurement noise and the expectation operator E. This problem can be cast into several LQG problems, one for each possible pairing, and solved numerically using a solver for Algebraic Riccati Equations (ARE) or some specialized functions for LQG, LQR or LQE problems (see the corresponding names in the Control System Toolbox in MATLAB). However, this problem is so "simple" that an analytical solution to the ARE's can be found in terms of the pole vectors.

THEOREM 6.1 (SOLUTION TO PROBLEM 6.1). *The minimum value of the objective $J(i,j)$, for a specified input j and a specified output i is*

$$J(i,j) = \frac{8p^3}{u_{p,j}^2 y_{p,i}^2}(x_{pi}^H x_{po})^2 \qquad (6.29)$$

where p is the pole, $u_{p,j}$ is the j'th element in the input pole vector, $y_{p,i}$ is the i'th element in the output pole vector, x_{pi} and x_{po} are the normalized left and right eigenvectors corresponding to the mode p. Hence, to stabilize the plant G with the unstable mode p using a SISO controller minimizing the input energy ($\mathcal{H}_2$-norm) due to measurement noise, one should:

- *Select input j corresponding to the largest entry $|u_{p,j}|$ in the input pole vector u_p.*
- *Select output i corresponding to the largest entry $|y_{p,i}|$ in the output pole vector y_p.*

The factor $\frac{(x_{pi}^T x_{po})^2}{u_{p,j}^2 y_{p,i}^2}$ can be used as a *controllability* measure for the effort required to stabilize the plant G with the unstable mode p, by controlling *output i* using *input j*. This follows since the objective $J(i,j)$ is directly related to $\frac{(x_{pi}^T x_{po})^2}{u_{p,j}^2 y_{p,i}^2}$.

REMARK 1. The directionality of the pole vectors are *not* dependent on the state-space realization. This implies that the ranking of the different inputs and outputs are independent of the state-space realization. However, the magnitude (length) of the pole vectors are[4] dependent on the state-space realization.

REMARK 2. Since the length of the pole vectors are dependent on the state-space realization, it can be an advantage to find a balanced realization of the plant G before computing the pole vectors. The disadvantage with a balanced realization is that any physical connection to the states are lost.

REMARK 3. We stress that it is *not* the size of the individual elements in the pole vectors that are important, but the relative sizes and the factor $\frac{(x_{pi}^T x_{po})^2}{u_{p,j}^2 y_{p,i}^2}$. The latter can be one reason for introducing (computing) the following scaled version of the pole vectors:

$$\tilde{u}_p = u_p / \sqrt{|x_{pi}^T x_{po}|} \quad \text{and} \quad \tilde{y}_p = y_p / \sqrt{|x_{pi}^T x_{po}|}$$

Then the value of the objective $J(i,j)$ becomes

$$J(i,j) = \frac{8p^3}{\tilde{u}_{p,j}^2 \, \tilde{y}_{p,i}^2}$$

Alternatively, one may use a state-space realization for which $x_{pi}^T x_{po} = 1$. For example if the A matrix has n linearly independent eigenvectors, one can use the realization where the A matrix is diagonal.

We prove (6.29) by using the Separation Theorem (Certainty Equivalence Principle) and find the best input using state feedback (LQR) under the assumption of perfect measurement of all states. The next step is to construct the optimal state observer (LQE) and find the best output so that mean square reconstruction error

$$E\left\{ (x(t) - \hat{x}(t))^T (x(t) - \hat{x}(t)) \right\} \tag{6.30}$$

is minimized using output y_i only.

It is well-known (Kwakernaak and Sivan, 1972) that minimum input to stabilize an unstable plant with state feedback $u = -Kx(t)$ mirrors the unstable poles across the imaginary axis, see Figure 6.2. Indeed, we find that this also happens in this case. The dual problem to state feedback which minimize the input usage, is the optimal state estimation problem with zero process noise and measurement noise of unit intensity. It follows that the unstable observer pole is mirrored across the imaginary axis by the use of the output to state estimate feedback.

Optimal state feedback to input u_j. In this case, the problem is to minimize the input usage due to non-zero initial states x_0, i.e. minimize the deterministic cost

$$J_{\text{LQR}}(j) = \int_0^\infty u_j^2(t) dt$$

That is, LQR problem with zero weight on the states $(Q = 0)$ and unity weight on the control u_j. The Riccati equation (6.17) with $Q = 0$ becomes

$$A^T X + XA - XBe_j e_j^T B^T X = 0 \tag{6.31}$$

---

[4]Consider multiplying the C matrix with the constant k_0 and B with $1/k_0$ then the pole vector changes as follows: $\tilde{u}_p = u_p / k_0$ and $\tilde{y}_p = y_p k_0$.

The solution to (6.31) is (for a proof refer to Section B.1)

$$X = \frac{2p}{\boldsymbol{u}_{p,j}^2} x_{pi} x_{pi}^T \geq 0 \tag{6.32}$$

where x_{pi} is the left eigenvector of A corresponding to the mode p. The state feedback gain K_j becomes

$$K_j = e_j^T B^T x_{pi} x_{pi}^T \frac{2p}{\boldsymbol{u}_{p,j}^2} = \underbrace{e_j^T \boldsymbol{u}_p}_{\boldsymbol{u}_{p,j}} x_{pi}^T \frac{2p}{\boldsymbol{u}_{p,j}^2} = \frac{2p}{\boldsymbol{u}_{p,j}} x_{pi}^T \tag{6.33}$$

Kalman filter based on y_i. In this case the Kalman filter is updated by only using the information in output y_i, and there is no process noise $(W = 0)$. The Riccati equation (6.21) with $W = 0$ becomes

$$Y A^T + A Y - Y C^T e_i e_i^T C Y = 0 \tag{6.34}$$

The solution to (6.34) is (for a proof refer to Section B.1)

$$Y = \frac{2p}{\boldsymbol{y}_{p,i}^2} x_{po} x_{po}^T \geq 0 \tag{6.35}$$

where x_{po} is the right eigenvector of A corresponding to the mode p. The feedback gain $K_{f,i}$ from output y_i to the state estimate becomes

$$K_{f,i} = \frac{2p}{\boldsymbol{y}_{p,i}^2} x_{po} x_{po}^T C^T e_i = \frac{2p}{\boldsymbol{y}_{p,i}} x_{po} \tag{6.36}$$

Minimum value of objective. To prove the minimum value of the objective $J(i,j)$ given in (6.28), we use the first equality in (6.23) with $Q = 0$, we obtain

$$J(i,j) = \text{tr}\left\{X K_{f,i} K_{f,i}^T\right\} = \text{tr}\left\{\frac{2p}{\boldsymbol{u}_{p,j}^2} x_{pi} x_{pi}^T \frac{2p}{\boldsymbol{y}_{p,i}} x_{po} \frac{2p}{\boldsymbol{y}_{p,i}} x_{po}^T\right\} = \frac{8p^3}{\boldsymbol{u}_{p,j}^2 \boldsymbol{y}_{p,i}^2} (x_{pi}^T x_{po})^2 \tag{6.37}$$

This completes the proof of (6.29). Finally, we note that the value of $J(i,j)$ is equal to the square of the $\mathcal{H}_2$-norm of the closed-loop transfer function from measurement noise n_i to input u_j, i.e.

$$J(i,j) = \|K_{ji} S_{ii}(s)\|_2^2 \quad \text{where} \quad S_{ii}(s) = (1 + G_{ij} K_{ji}(s))^{-1}$$

6.3.2 Multivariable control minimizing the input energy ($\mathcal{H}_2$-norm)

In this section we consider the following problem:

PROBLEM 6.2. *Given a plant G with one unstable mode $p \in \mathbb{C}_+$ (Re $p > 0$) and white measurement noise n_i of unit intensity in each output y_i. Consider full multivariable control of the plant G and find best achievable performance quantified as the minimum value of the objective*

$$J = E\left\{\lim_{T \to \infty} \frac{1}{T} \int_0^T u^T(t) u(t) dt\right\} \tag{6.38}$$

This is a LQG problem with zero weight on the states, unity weight on the inputs, no process noise and white measurement noise with unit intensity. By solving this problem and comparing the minimum value of the objective of this problem with the minimum value of the objective in Problem 6.1, we can quantify the extra input energy needed to stabilize the plant using SISO control compared to full multivariable control.

THEOREM 6.2 (SOLUTION TO PROBLEM 6.2). *The minimum value of the objective J is*

$$J = \frac{8p^3}{\|\boldsymbol{u}_p\|_2^2 \|\boldsymbol{y}_p\|_2^2} (x_{pi}^T x_{po})^2 \tag{6.39}$$

The factor $\frac{(x_{pi}^T x_{po})^2}{\|\boldsymbol{u}_p\|_2^2 \|\boldsymbol{y}_p\|_2^2}$ can be used as a *controllability* measure for the effort required to stabilize the plant G with the unstable mode p. This follows since the objective J is directly related to $\frac{(x_{pi}^T x_{po})^2}{\|\boldsymbol{u}_p\|_2^2 \|\boldsymbol{y}_p\|_2^2}$. Remarks 1 to 3 on scaling and balanced realization on page 135 applies also in this case.

To prove (6.39) we construct a state estimator using the information in all available outputs, and we apply state feedback from the estimated states using all inputs.

Optimal state feedback. The problem is to minimize the input usage due to non-zero initial state x_0, i.e. to minimize the deterministic cost

$$J_{\text{LQR}} = \int_0^T u^T(t)u(t)dt$$

The optimal solution (independent of x_0) is $u(t) = -Kx(t)$, where

$$K = B^T X$$

and $X = X^T \geq 0$ is the unique positive-semidefinite solution of the algebraic Riccati equation

$$A^T X + XA - XBB^T X = 0 \tag{6.40}$$

The solution to (6.40) is (for a proof refer to Section B.1)

$$X = \frac{2p}{\|\boldsymbol{u}_p\|_2^2} x_{pi} x_{pi}^T \geq 0 \tag{6.41}$$

The state feedback K becomes

$$K = B^T x_{pi} x_{pi}^T \frac{2p}{\|\boldsymbol{u}_p\|_2^2} = \frac{2p}{\|\boldsymbol{u}_p\|_2^2} \boldsymbol{u}_p x_{pi}^T \tag{6.42}$$

Kalman filter. In this case there is no process noise, the state equation of the observer becomes

$$\dot{\hat{x}} = A\hat{x} + Bu + K_f(y - C\hat{x} - Du) \tag{6.43}$$

The optimal choice of K_f, which minimizes the mean square reconstruction error

$$E\left\{(x(t) - \hat{x}(t))^T(x(t) - \hat{x}(t))\right\}$$

due to measurement noise n, is given by

$$K_f = YC^T$$

where $Y = Y^T \geq 0$ is the unique positive-semidefinite solution to the algebraic Riccati equation

$$YA^T + AY - YC^TCY = 0 \tag{6.44}$$

The solution to (6.44) is (for a proof refer to Section B.1)

$$Y = \frac{2p}{\|\boldsymbol{y}_p\|_2^2} x_{po} x_{po}^T \geq 0 \tag{6.45}$$

The feedback gain K_f from output y to the estimated states becomes

$$K_f = \frac{2p}{\|\boldsymbol{y}_p\|_2^2} x_{po} x_{po}^T C^T = \frac{2p}{\|\boldsymbol{y}_p\|_2^2} x_{po} \boldsymbol{y}_p^T \tag{6.46}$$

Minimum value of objective. We obtain (Kwakernaak and Sivan, 1972):

$$
\begin{aligned}
J &= \operatorname{tr}\{X K_f K_f^T\} = \operatorname{tr}\left\{ \frac{2p}{\|\boldsymbol{u}_p\|_2^2} x_{pi} x_{pi}^T \frac{2p}{\|\boldsymbol{y}_p\|_2^2} x_{po} \boldsymbol{y}_p^T \frac{2p}{\|\boldsymbol{y}_p\|_2^2} \boldsymbol{y}_p x_{po}^T \right\} \\
&= \frac{8p^3}{\|\boldsymbol{u}_p\|_2^2} \frac{\|\boldsymbol{y}_p\|_2^2 \, x_{pi}^T x_{po}}{\|\boldsymbol{y}_p\|_2^4} \operatorname{tr}\{x_{pi} x_{po}^T\} = \frac{8p^3}{\|\boldsymbol{u}_p\|_2^2 \|\boldsymbol{y}_p\|_2^2} (x_{pi}^T x_{po})^2
\end{aligned} \tag{6.47}
$$

This completes the proof of (6.39). Finally, we note that the value of J is equal to the square of the $\mathcal{H}_2$-norm of the closed-loop transfer function from the measurement noise n to the input u, i.e.

$$J = \|K_{\mathrm{LQG}} S_{\mathrm{LQG}}(s)\|_2^2 \quad \text{where} \quad S_{\mathrm{LQG}}(s) = (I + GK_{\mathrm{LQG}})^{-1}$$

and K_{LQG} is the full multivariable LQG controller minimizing the input energy.

6.3.3 Performance degradation due to SISO control

We are now in position to quantify the extra input usage needed to stabilize a plant G with one unstable mode p using a SISO controller linking output y_i to input u_j. We obtain

$$\varrho_2(i,j) = \frac{\|K_{ji} S_{ii}(s)\|_2}{\|K_{\mathrm{LQG}} S_{\mathrm{LQG}}(s)\|_2} = \frac{\sqrt{J(i,j)}}{\sqrt{J}} = \frac{\|\boldsymbol{u}_p\|_2 \|\boldsymbol{y}_p\|_2}{|u_{p,j}| \cdot |y_{p,i}|} \geq 1 \tag{6.48}$$

We find that SISO control is optimal if and only if $\boldsymbol{u}_p$ has zeros in all elements except element j and $\boldsymbol{y}_p$ has zeros in all elements except element i. That is, the pole p is only controllable in input j and only observable in output i. We have arrived at the conclusion:

- *If one element in $\boldsymbol{u}_p$ and one element in $\boldsymbol{y}_p$ has magnitude several times (three or more) larger than the second largest element, then the performance degradation due to SISO control may be acceptable.*

6.3.4 Corresponding results in terms of the $\mathcal{H}_\infty$-norm

We have seen that the results in the two previous sections can be interpreted in terms of minimizing the $\mathcal{H}_2$-norm from the measurement noise to the inputs. More precisely, the results in Section 6.3.1 solve the following problem

$$\min_{i,j} \min_{K_{ji}(s)} \|K_{ji}S_{ii}(s)\|_2 \quad \text{where} \quad S_{ii}(s) = (1 + G_{ij}K_{ji}(s))^{-1}$$

and the SISO controller K_{ji} is the LQG controller minimizing the input energy (6.1). Furthermore, the results in Section 6.3.2 solve the following problem

$$\min_{K(s)} \|KS(s)\|_2 \quad \text{where} \quad S(s) = (I + GK(s))^{-1}$$

and the controller K is the full multivariable LQG controller minimizing the input energy, i.e. $K = K_{\text{LQG}}$ with $Q = 0$, $R = I$, $W = 0$ and $V = I$ (see, Skogestad and Postlethwaite, 1996, for a state-space realization of K_{LQG}).

The most obvious question is:

- Why not choose a different norm, i.e. the $\mathcal{H}_\infty$-norm?

The fact is that we in Chapter 4 already have derived the tool to select the best input and the best output to stabilize the plant G with one unstable mode p and minimize the $\mathcal{H}_\infty$-norm of the input usage. Furthermore, from the results in Chapter 5, we can quantify the minimum achievable $\mathcal{H}_\infty$-norm of the input usage due to measurement noise for the full multivariable controller. That is, we are in a position to switch from the $\mathcal{H}_2$-norm to the $\mathcal{H}_\infty$-norm. The next theorem summarizes the results on minimizing the $\mathcal{H}_\infty$-norm of the input usage due to measurement noise for SISO control.

THEOREM 6.3 (STABILIZING SISO CONTROL MINIMIZING $\mathcal{H}_\infty$-NORM OF THE INPUT USAGE). *Consider a plant G with minimal state-space realization (A, B, C, D), one unstable mode p, input pole vector $\boldsymbol{u}_p$, output pole vector $\boldsymbol{y}_p$ and normalized additive measurement noise n_i, $|n_i| = 1$, in each output i. Assume that the mode p is controllable in input j and observable in output i. The minimum achievable $\mathcal{H}_\infty$-norm of the input usage due to measurement noise n_i, for SISO control of output i using input j is*

$$\min_{K_{ji}(s)} \|K_{ji}S_{ii}(s)\|_\infty = |(G_{ij})_s^{-1}(p)| = \frac{2p}{|\boldsymbol{u}_{p,j}| \cdot |\boldsymbol{y}_{p,i}|}|x_{pi}^H x_{po}| \qquad (6.49)$$

where $S_{ii}(s) = (1 + G_{ij}K_{ji}(s))^{-1}$, x_{pi} and x_{po} are normalized left and right eigenvectors of the A matrix corresponding to the mode p, and $(G_{ij})_s$ means the transfer function G_{ij} with the RHP-poles mirrored into LHP.

REMARK. The notation $(G_{ij})_s^{-1}(p)$ means:

1) Find the stabilized version of G_{ij}, i.e. $(G_{ij})_s$.
2) Take the inverse, i.e. $(G_{ij})_s^{-1} = ((G_{ij})_s)^{-1}$.
3) Evaluate $(G_{ij})_s^{-1}$ at $s = p$, i.e. $(G_{ij})_s^{-1}(p) = ((G_{ij})_s)^{-1}(p) = ((G_{ij})_s)^{-1}|_{s=p}$.

Proof. See Section B.1.

Importantly, by comparing (6.49) and (6.29) we see that the input usage in terms of the $\mathcal{H}_\infty$-norm is closely related to the $\mathcal{H}_2$-norm (white noise), we have

$$\min_{K_{ji}(s)} \|K_{ji}S_{ii}(s)\|_\infty = \frac{1}{\sqrt{2p}} \min_{K_{ji}(s)} \|K_{ji}S_{ii}(s)\|_2 = \sqrt{J(i,j)/2p} \qquad (6.50)$$

Thus, the two norms give the same choice for the best input-output pairing for stabilizing the plant G with the unstable mode p:

- Select input j corresponding to the largest entry $|\boldsymbol{u}_{p,j}|$ in the input pole vector $\boldsymbol{u}_p$.
- Select output i corresponding to the largest entry $|\boldsymbol{y}_{p,i}|$ in the output pole vector $\boldsymbol{y}_p$.

Several things are worth noting:

1) It is interesting that minimizing the input usage in terms of either the $\mathcal{H}_2$-norm or the $\mathcal{H}_\infty$-norm gives the same input j and output i for stabilization. This may be surprising, since the value of the two norms in general may be arbitrary far apart (e.g. see Table 6.1).

2) From (6.49) we see that the best input j and the best output i correspond to minimizing $|(G_{ij})_s^{-1}(p)|$, i.e. $\min_{i,j} |(G_{ij})_s^{-1}(p)| = \max_{i,j} |(G_{ij})_s(p)|$. An alternative to the pole vectors, is therefore to evaluate a minimal realization of the transfer function

$$\widehat{G}(s) = \frac{s-p}{s+p} G(s)$$

at $s = p$, and selecting the input/output combination (j/i) corresponding to the element with largest magnitude in $\widehat{G}(p)$.

3) Note that the effect of any RHP-zero in the element G_{ij} is taken into account, since $(G_{ij})_s(p)$ is small if there is a RHP-zero located close to p.

THEOREM 6.4 (STABILIZING CONTROL MINIMIZING $\mathcal{H}_\infty$-NORM OF THE INPUT USAGE). *Consider a plant G with one unstable mode p and normalized additive measurement noise n, $\|n\|_2 = 1$, at the output of the plant G. The minimum achievable $\mathcal{H}_\infty$-norm of the input usage due to the measurement noise n is*

$$\min_{K(s)} \|KS(s)\|_\infty = \|u_p^H G_{so}^{-1}(p)\|_2 = \|G_{si}^{-1}(p)y_p\|_2 \qquad (6.51)$$

where $S(s) = (I + GK(s))^{-1}$, G_{so} and G_{si} are the transfer function G with the RHP-poles factorized at the output and the input respectively (see Chapter 5).

REMARK 1. The notation G_{so}^{-1} means $G_{so}^{-1} = (G_{so})^{-1}$.
REMARK 2. Similarly, G_{si}^{-1} means $G_{si}^{-1} = (G_{si})^{-1}$.

The performance degradation due to SISO control of output i using input j relative to full multivariable control becomes

$$\varrho_\infty(i,j) = \frac{\min_{K_{ji}(s)} \|K_{ji}S_{ii}(s)\|_\infty}{\min_{K(s)} \|KS(s)\|_\infty} = \frac{|(G_{ij})_s^{-1}(p)|}{\|u_p^H G_{so}^{-1}(p)\|_2} \geq 1 \qquad (6.52)$$

6.3.5   Difference between the controllers minimizing the input usage in terms of the $\mathcal{H}_2$-norm and the $\mathcal{H}_\infty$-norm

When minimizing the input usage both in terms of the $\mathcal{H}_2$-norm and the $\mathcal{H}_\infty$-norm, the unstable open-loop pole p is mirrored into the LHP, that is, the closed-loop pole corresponding to the open-loop pole p is $\mu = -p$.

In general, when minimizing the $\mathcal{H}_2$-norm, the closed-loop transfer functions have $2n$ poles. However, from the expressions for the state feedback gain (6.33) and (6.42), we see that it is only the linear combination of the states corresponding to the pole p which affects the input (the linear combination x_{pi}). Similarly, from the expressions for the Kalman filter gain (6.36) and (6.46) we see that the states in the observer are updated by only adding the linear combination of the output corresponding to the pole p (the linear combination x_{po}). The result is that a minimal state-space realization of the closed-loop transfer functions from measurement noise to the inputs KS and $K_{ji}S_{ii}$ has 2 stable closed-loop poles located at $\mu = -p$. We note that the other closed-loop transfer functions may have more poles.

When minimizing the $\mathcal{H}_\infty$-norm, the only closed-loop pole of the transfer function from measurement noise to the input, i.e. KS and $K_{ji}S_{ii}$, is $\mu = -p$. The remaining $n-1$ poles in the plant G are not observable and/or controllable in the closed-loop transfer functions KS and $K_{ji}S_{ii}$. We note that the other closed-loop transfer functions may have more poles.

EXAMPLE 6.3. The purpose with this example is to illustrate the difference between minimizing the input usage in terms of the $\mathcal{H}_2$-norm and the $\mathcal{H}_\infty$-norm. We consider the following plant

$$G(s) \overset{s}{=} \left[\begin{array}{cc|c} -10 & 0 & \sqrt{120/11} \\ 0 & 1 & \sqrt{10/11} \\ \hline \sqrt{120/11} & -\sqrt{10/11} & 0 \end{array}\right] = \frac{s-2}{(0.1s+1)(s-1)}$$

which has one unstable mode $p = 1$ and a RHP-zero $z = 2$.

First, we consider minimizing the $\mathcal{H}_2$-norm. The input and output state directions and the pole vectors corresponding to the unstable mode $p = 1$ are

$$x_{pi} = x_{po} = \begin{bmatrix} 0 \\ 1 \end{bmatrix}, \quad u_p = \sqrt{10/11} \quad \text{and} \quad y_p = -\sqrt{10/11}$$

The state feedback gain K and the Kalman filter gain K_f becomes

$$K = \frac{2p}{u_p}x_{pi}^T = \begin{bmatrix} 0 & 2\sqrt{1.1} \end{bmatrix} \quad \text{and} \quad K_f = \frac{2p}{y_p}x_{po} = \begin{bmatrix} 0 \\ -2\sqrt{1.1} \end{bmatrix}$$

The LQG controller minimizing the input energy becomes

$$K_{\text{LQG}}(s) \overset{s}{=} \left[\begin{array}{cc|c} -10 & -2\sqrt{12} & 0 \\ 2\sqrt{12} & -3 & -2\sqrt{1.1} \\ \hline 0 & 2\sqrt{1.1} & 0 \end{array}\right] = -44\frac{0.1s+1}{s^2-13s+78}$$

The controller is strictly proper, has poles for $p_{1,2} = -6.5 \pm 5.98j$ and a zero for $z = -10$. The objective becomes $J = 9.68$, and the $\mathcal{H}_2$-norm of the closed-loop transfer function from n to u is

$$\|K_{\text{LQG}}S_{\text{LQG}}(s)\|_2 = \sqrt{9.68} = 3.11 \quad \text{where} \quad S_{\text{LQG}}(s) = (1 + GK_{\text{LQG}}(s))^{-1}$$

Table 6.1: Summary of results when minimizing the input usage, $\mathcal{H}_2$-norm and $\mathcal{H}_\infty$-norm.

	Zeros K	Poles K	Zeros KS	Poles KS	$\|KS(s)\|_2$	$\|KS(s)\|_\infty$
$\mathcal{H}_2$	-10	$-6.5 \pm 5.98j$	1	$\{-1,\,-1\}$	3.11	4.4
$\mathcal{H}_\infty$	-10	-34	1	-1	∞	2.2

The closed-loop poles in the minimal realization of $K_{\mathrm{LQG}}S_{\mathrm{LQG}}$ is $p_{1,2} = \{-1,\,-1\}$, and we see that the open-loop stable mode $p = -10$ of G cancel with the zero $z = -10$ in the controller. Table 6.1 summarizes some of the results for the LQG controller minimizing the input energy.

By using the identity $KS = TG^{-1}$ and applying Theorem 4.3 with $V = G^{-1}$ we obtain the controller minimizing the $\mathcal{H}_\infty$-norm of input usage due to measurement noise. The controller is

$$K_\infty(s) = -2.2\frac{0.1s + 1}{0.1s + 3.4}$$

The controller is semi-proper, has a pole $p = -34$ and a zero $z = -10$. The $\mathcal{H}_\infty$-norm of the closed-loop system is

$$\|K_\infty S_\infty(s)\|_\infty = 2.20 \quad \text{where} \quad S_\infty(s) = (1 + GK_\infty(s))^{-1}$$

The only pole of the closed-loop transfer function $K_\infty S_\infty$ is $p = -1$. Table 6.1 summarizes some of the results. The magnitude of closed-loop transfer functions S_{LQG}, $K_{\mathrm{LQG}}S_{\mathrm{LQG}}$, S_∞ and $K_\infty S_\infty$ are plotted as functions of frequency in Figure 6.3. We see that the $\mathcal{H}_\infty$-optimal controller results in a constant magnitude of the closed-loop transfer function $K_\infty S_\infty$.
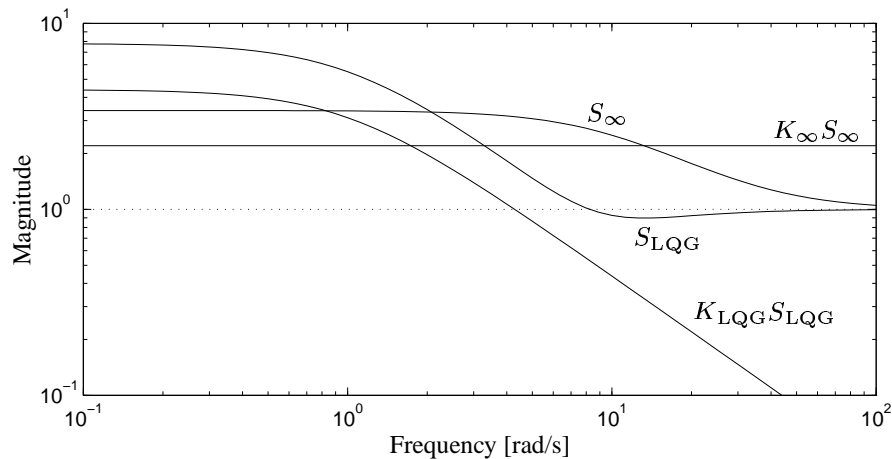
Figure 6.3: Frequency dependent plot of closed-loop transfer functions

6.3.6 Limitations in the use of the pole vectors

We have proved the usefulness of pole vectors for moving one pole with a single loop controller. But can we use the pole vectors to say anything about how easy it is to move two or

more poles using a single loop controller? The next two examples illustrate that the answer is generally *no*.

EXAMPLE 6.4. In this example we consider the effect of a zero on the pole vectors, where the zero is close to two poles at the same time. The example illustrates that we only can extract information about one pole at a time. We consider the following SISO transfer function

$$G(s) = \frac{2(s - p)}{(s - p + \varepsilon)(s - p - \varepsilon)} = \frac{1}{s - p - \varepsilon} + \frac{1}{s - p + \varepsilon}$$

where we note that the zero disappear in the individual terms in the partial fraction expansion of $G(s)$. So, the zero is obviously a combined effect of both poles. A balanced minimal state-space realization of G when $\varepsilon \neq 0$ is given by

$$G(s) \stackrel{s}{=} \left[\begin{array}{cc|c} p + \varepsilon & 0 & 1 \\ 0 & p - \varepsilon & 1 \\ \hline 1 & 1 & 0 \end{array} \right] \tag{6.53}$$

Both poles $p_{1,2} = p \pm \varepsilon$ are observable as long as $\varepsilon \neq 0$. We compute the input and output pole vectors corresponding to the poles $p_{1,2} = p \pm \varepsilon$ to be

$$\boldsymbol{U}_p = \begin{bmatrix} 1 & 1 \end{bmatrix} \quad \text{and} \quad \boldsymbol{Y}_p = \begin{bmatrix} 1 & 1 \end{bmatrix}$$

independent of the value of ε. From the pole vectors it seems like both poles can easily be moved. But as $\varepsilon \to 0$ we get $G(s) = \frac{2}{s-p}$, so this is incorrect for small values of ε. To verify, we construct an LQG controller minimizing the input energy

$$J = E \left\{ \lim_{T \to \infty} \frac{1}{T} \int_0^T u^T(t)u(t)dt \right\}$$

with measurement noise of unit intensity and no process noise. When $p = 2$, $\varepsilon = 0.1$ we obtain the state feedback gain to input u, K, and the feedback gain from the output y to the state estimate, K_f:

$$K = \begin{bmatrix} 84 & -76 \end{bmatrix} \quad \text{and} \quad K_f = \begin{bmatrix} 84 \\ -76 \end{bmatrix}$$

The closed-loop poles become $p_{1,2} = -p \pm \varepsilon$, and the objective becomes $J = 4.10 \cdot 10^7$, which is huge. The following table shows the value of the objective J for some different values of ε when $p = 2$.

ε	1.5	1	0.5	0.1	0.05	0.01
J	1164.6	4736	67712	$4.10 \cdot 10^7$	$6.56 \cdot 10^8$	$4.10 \cdot 10^{11}$

Similar results apply if the zero is located to the left or to the right of both poles. For example, consider

$$G(s) = \frac{s - p - \varepsilon}{(s - p)(s - p + \varepsilon)} = \frac{-1}{s - p} + \frac{2}{s - p + \varepsilon}$$

with balanced minimal state-space realization (when $\varepsilon \neq 0$)

$$G(s) \stackrel{s}{=} \left[\begin{array}{cc|c} p & 0 & -1 \\ 0 & p - \varepsilon & \sqrt{2} \\ \hline 1 & \sqrt{2} & 0 \end{array} \right] \tag{6.54}$$

The input and output pole vectors corresponding to the two poles $p_{1,2} = \{p, p - \varepsilon\}$ are

$$\boldsymbol{U}_p = \begin{bmatrix} -1 & \sqrt{2} \end{bmatrix} \quad \text{and} \quad \boldsymbol{Y}_p = \begin{bmatrix} 1 & \sqrt{2} \end{bmatrix}$$

independent of the value of ε. Again, from the pole vectors, it seems like both poles can easily be moved. But as $\varepsilon \to 0$ we get $G(s) = \frac{1}{s-p}$, so this is incorrect for small values of ε. To verify, we consider the controller minimizing the input energy required to stabilize the plant. With $p = 2$ and $\varepsilon = 0.1$ we obtain

$$K = [\,-156 \quad -104.8\,] \quad \text{and} \quad K_f = \begin{bmatrix} 156 \\ -104.8 \end{bmatrix}$$

The closed-loop poles become $p_{1,2} = \{-p+\varepsilon, -p\}$, and the objective becomes $J = 4.27 \cdot 10^7$, which is huge. The following table summarizes the value of the objective J for some different values of ε when $p = 2$.

ε	1.5	1	0.5	0.1	0.05	0.01
J	446.4	3618	71087	$4.27 \cdot 10^7$	$6.71 \cdot 10^8$	$4.12 \cdot 10^{11}$

We have seen that the pole vectors are unable to identify the difficulties with stabilizing these plants.

The two situations described in (6.53) and (6.54) are exactly what happens in the elements g_{ij} of the following 2×2 system

$$G(s) \overset{s}{=} \left[\begin{array}{cc|cc} p_1 & 0 & \cos\alpha & -\sin\alpha \\ 0 & p_2 & \sin\alpha & \cos\alpha \\ \hline \cos\beta & -\sin\beta & 0 & 0 \\ \sin\beta & \cos\beta & 0 & 0 \end{array} \right]$$

which was used to illustrate the limitations of pole directions in Example 2.3. This G corresponds to two subsystems in parallel with rotations at the input and the output, see Figure 2.1. The input and output pole vectors corresponding to the modes $\{p_1, p_2\}$ are

$$U_p = \begin{bmatrix} \cos\alpha & \sin\alpha \\ -\sin\alpha & \cos\alpha \end{bmatrix}; \qquad Y_p = \begin{bmatrix} \cos\beta & -\sin\beta \\ \sin\beta & \cos\beta \end{bmatrix}$$

In Example 2.3 it is shown that all transfer function elements have a zero close to one of the poles when p_1 and p_2 approaches each other. The diagonal elements in G have a zero to the left or to the right of the poles, and the off-diagonal elements in G have a zero between the poles. We note that G has no multivariable zeros. To control both modes in the 2×2 system G using one input and one output is difficult if the two modes are in RHP and located close to each other, due to the nearby zero in all transfer function elements. If the two modes are in LHP and located close to each other, large input usage is needed to move both poles. In the case when $p_1 = p_2$ we know that we need two inputs and two outputs to control both modes, see Theorem 2.4 on page 32 (we note that the pole vectors are orthogonal in this case).

A *practical* example containing the properties described here is the distillation column DB-configuration, see Example 6.8 in Section 6.7.

EXAMPLE 6.5. In Example 6.4 we considered two real poles with a nearby zero. We can still hope that complex conjugate poles are special, so that we can use the pole vectors to say something about how easy it is to move two complex conjugate poles. In this example therefore consider stabilizing a plant with two unstable complex conjugate poles and a nearby zero. We consider

$$G(s) \overset{s}{=} \left[\begin{array}{cc|c} p & -\varepsilon & 1 \\ \varepsilon & p & 0 \\ \hline 1 & 0 & 0 \end{array} \right] = \frac{s-p}{s^2 - 2ps + p^2 + \varepsilon^2}$$

The plant G has a RHP-zero for $s = p$ and two complex conjugate poles for $p_{1,2} = p \pm \varepsilon j$. We find (the left and the right eigenvector matrices)

$$X_{pi} = \begin{bmatrix} 0.707 & 0.707 \\ -0.707j & 0.707j \end{bmatrix} \quad \text{and} \quad X_{po} = \begin{bmatrix} -0.707 & -0.707 \\ 0.707j & -0.707j \end{bmatrix}$$

The pole "vectors" becomes

$$\boldsymbol{U}_p = \begin{bmatrix} 0.707 & 0.707 \end{bmatrix} \quad \text{and} \quad \boldsymbol{Y}_p = \begin{bmatrix} -0.707 & -0.707 \end{bmatrix}$$

Which is independent of the values in p and ε. When ε approaches zero we obtain $G(s) = \frac{1}{s-p}$ and we expect that we need large inputs to stabilize the plant for small values of ε. To verify our suspicion we construct an LQG controller minimizing the input usage

$$J = E \left\{ \lim_{T \to \infty} \frac{1}{T} \int_0^T u^T(t)u(t)dt \right\}$$

with measurement noise of unit intensity and no process noise. When $p = 2$, $\varepsilon = 0.1$ we obtain the state feedback gain K and the feedback gain from the outputs to the state estimate K_f

$$K = \begin{bmatrix} 8 & 160 \end{bmatrix} \quad \text{and} \quad K_f = \begin{bmatrix} 8 \\ -160 \end{bmatrix}$$

The closed-loop poles become $p_{1,2} = -p \pm \varepsilon j$, and the objective becomes $J = 1.64 \cdot 10^8$, which is huge. The following table summarizes the value of the objective J for some different values of ε when $p = 2$.

ε	1.5	1	0.5	0.1	0.05	0.01
J	2838.1	14848	$2.54 \cdot 10^5$	$1.64 \cdot 10^8$	$2.62 \cdot 10^9$	$1.64 \cdot 10^{12}$

Again, we have seen that the pole vectors are unable to identify the difficulties with stabilizing this plant.

6.4 Modal control with minimum feedback gains

In the previous section we showed that selecting input j and output i according to the largest elements in the pole vectors, corresponds to the best[5] input/output combination for stabilizing a plant with one unstable mode using a SISO controller. It is difficult to extend this result to the more general case of moving one stable pole or several poles at the same time.

However, an alternative interpretation to the minimum input usage is to select input u_j which minimizes the norm[6] of the state feedback gain K_j and to select output y_i which minimizes the norm of the Kalman filter gain $K_{f,i}$, see the expressions (6.33) and (6.36) for K_j and $K_{f,i}$.

In this section we consider moving one or two poles from their open-loop values to some desired closed-loop values, by constructing a state observer based on output y_i and using state feedback to input u_j.

---

[5] In terms of minimum input usage.

[6] Any matrix or vector norm applies. That is, the choice is independent of the particular norm chosen.

State feedback to input u_j. The state equation of the open-loop plant is

$$\dot{x} = Ax + Be_j u_j \tag{6.55}$$

We use feedback from states x to the input u_j

$$u_j = -K_j x \tag{6.56}$$

such that we move one or two poles from their open-loop values to some desired closed-loop values. That is, we find K_j such that the closed-loop state-space matrix

$$\widetilde{A} = A - Be_j K_j \tag{6.57}$$

has the desired closed-loop eigenvalues. General analytical formulas for the controller gain K_j which moves all the open-loop eigenvalues to some desired closed-loop values are given in Section A.1. Below we will use these formulas to move *one* or *two* open-loop eigenvalues to some desired closed-loop eigenvalues, and leaving the remaining ones unchanged.

State observer based on y_i. The dual problem to the state feedback problem, is to find the output to state feedback gain so that the observer has the desired closed-loop poles. That is, we consider

$$\dot{\hat{x}} = A\hat{x} + Be_j u_j; \qquad \hat{y}_i = e_i^T C\hat{x} + e_i^T De_j u_j \tag{6.58}$$

and by using feedback from $y_i - \hat{y}_i$ to the estimated states $\hat{x}$, i.e.

$$\dot{\hat{x}} = A\hat{x} + Be_j u_j + K_{f,i}(y_i - e_i^T C\hat{x} - e_i^T De_j u_j) \tag{6.59}$$

we move the closed-loop observer poles, i.e. the eigenvalues of

$$\widehat{A} = A - K_{f,i} e_i^T C \tag{6.60}$$

to the desired locations, which we will choose to be the *same* as those in $\widetilde{A}$ (for state feedback). Again, we will only consider moving one or two open-loop observer poles to some desired locations and leaving the remaining ones unchanged.

Combined state observer and state feedback. When we combine state feedback together with state estimation we get $2n$ closed-loop poles (the eigenvalues of $\widetilde{A}$ and $\widehat{A}$). The eigenvalues of $\widetilde{A}$ (regulator poles) and $\widehat{A}$ (observer poles) are generally different, but we choose here to move the regulator and the observer poles to the same locations.

6.4.1 Moving one pole

State feedback to input u_j. The problem is to move the distinct real open-loop pole p to μ by the use of state feedback (6.56) to input u_j. The solution is to use the state feedback gain vector

$$K_j = \frac{p - \mu}{u_{p,j}} x_{pi}^T \tag{6.61}$$

where $\boldsymbol{u}_{p,j}$ is the j'th element in the input pole vector corresponding to the pole p and x_{pi} is the corresponding state input pole direction, i.e. $x_{pi}^H A = p x_{pi}^H$. For a proof of (6.61) refer to Section B.2. Since *only* the constant $\frac{p-\mu}{\boldsymbol{u}_{p,j}}$ is dependent on the choice of input j, any matrix norm of K_j is minimized by selecting input j corresponding to the element with largest magnitude in the pole vector $\boldsymbol{u}_p$. Even though we are minimizing the state feedback gain vector, the choice j is independent of the state-space realization.

State observer based on y_i. In a similar way, we move the observer pole p to the desired location μ by adding feedback from $y_i - \hat{y}_i$ to the estimated state (6.59). The solution is

$$K_{f,i} = \frac{p - \mu}{\boldsymbol{y}_{p,i}} x_{po} \tag{6.62}$$

where $\boldsymbol{y}_{p,i}$ is the i'th element in the output pole vector corresponding to the pole p and x_{po} is the corresponding state output pole direction, i.e. $A x_{po} = p x_{po}$. For a proof of (6.62) refer to Section B.2. Any matrix norm of $K_{f,i}$ is minimized by selecting the output i corresponding to the element with largest magnitude in the pole vector $\boldsymbol{y}_p$. Again, the choice i is independent of the state-space realization.

6.4.2 Moving two distinct poles

By studying the SISO plants in Examples 6.4 and 6.5 it is shown that we generally can *not* say anything about how easy it is to stabilize a plant with two unstable modes from the pole vectors. This means that we can not use the pole vectors as controllability measures (which is the case when we consider moving one unstable mode). The pole vectors are unique up to a multiplum of a constant, so the relative influence of the different inputs and outputs on the pole is reflected in the relative magnitudes in the input and output pole vectors. We can then use the relative magnitudes to rank the different inputs and outputs. However, it is still an open issue (for research) what it means to rank candidate inputs and outputs using the pole vectors when one want to move two poles using one input and one output. It seems reasonable to do so, but it has been difficult to prove any concrete results.

One step on the way can be to find analytical expressions (in terms of the pole vectors) for the feedback gains K_j and $K_{f,i}$ which moves two open-loop poles to some desired closed-loop locations. In this section we therefore consider to move two distinct open-loop poles by using state feedback to input u_j and to move the corresponding observer poles by adding feedback from output y_i to the estimated states.

State feedback to input u_j. The feedback gain K_j to move the two poles p_1 and p_2, $p_1 \neq p_2$ to the desired locations μ_1 and μ_2 using state feedback (6.56) to input u_j is

$$K_j = k_1 x_{p_1 i}^H + k_2 x_{p_2 i}^H \tag{6.63}$$

where

$$k_1 = \frac{(p_1 - \mu_1)(p_1 - \mu_2)}{(p_1 - p_2)\bar{\boldsymbol{u}}_{p_1,j}}, \qquad k_2 = \frac{(p_2 - \mu_1)(p_2 - \mu_2)}{(p_2 - p_1)\bar{\boldsymbol{u}}_{p_2,j}} \tag{6.64}$$

$x_{p_1 i}$ and $x_{p_2 i}$ are the left eigenvectors corresponding to the poles p_1 and p_2, $\boldsymbol{u}_{p_1}$ and $\boldsymbol{u}_{p_2}$ are the corresponding input pole vectors, and finally $\boldsymbol{u}_{p_1,j}$ and $\boldsymbol{u}_{p_2,j}$ are the j'th element of the input pole vectors.

State observer based on $\boldsymbol{y}_i$. In a similar way, we can move the observer poles p_1 and p_2, $p_1 \neq p_2$ to the desired locations μ_1 and μ_2 by adding feedback from $y_i - \hat{y}_i$ to the estimated states (6.59). The solution is

$$K_{f,i} = k_1 x_{p_1 o} + k_2 x_{p_2 o} \tag{6.65}$$

where

$$k_1 = \frac{(p_1 - \mu_1)(p_1 - \mu_2)}{(p_1 - p_2)\,\bar{\boldsymbol{y}}_{p_1,i}}, \qquad k_2 = \frac{(p_2 - \mu_1)(p_2 - \mu_2)}{(p_2 - p_1)\,\bar{\boldsymbol{y}}_{p_2,i}} \tag{6.66}$$

$x_{p_1 o}$ and $x_{p_2 o}$ are the right eigenvectors corresponding to the poles p_1 and p_2, $\boldsymbol{y}_{p_1}$ and $\boldsymbol{y}_{p_2}$ are the corresponding input pole vectors and finally, $\boldsymbol{y}_{p_1,i}$ and $\boldsymbol{y}_{p_2,i}$ are the i'th element of the output pole vectors.

6.4.3 Moving complex conjugate poles

The case where we want to move two complex conjugate poles $(p, \bar{p})$ to some desired complex conjugate locations $(\mu, \bar{\mu})$ follows easily from the results in Section 6.4.2 by setting $p_1 = p$, $p_2 = \bar{p}$, $\mu_1 = \mu$, $\mu_2 = \bar{\mu}$, $x_{p_1 i} = x_{pi}$, $x_{p_2 i} = \bar{x}_{pi}$, $x_{p_1 o} = x_{po}$, $x_{p_2 o} = \bar{x}_{po}$, $\boldsymbol{u}_{p_1,j} = \boldsymbol{u}_{p,j}$, $\boldsymbol{u}_{p_2,j} = \bar{\boldsymbol{u}}_{p,j}$, $\boldsymbol{y}_{p_1,i} = \boldsymbol{y}_{p,i}$ and $\boldsymbol{y}_{p_2,i} = \bar{\boldsymbol{y}}_{p,i}$. Where x_{pi} and x_{po} are the left and the right eigenvectors corresponding to p, $\boldsymbol{u}_{p,j}$ is the j'th element of the pole vector $\boldsymbol{u}_p$ and $\boldsymbol{y}_{p,i}$ is the i'th element of the pole vector $\boldsymbol{y}_p$ for the pole p.

State feedback to input $\boldsymbol{u}_j$. From (6.63) we obtain

$$K_j = k_j x_{pi}^H + \bar{k}_j \bar{x}_{pi}^H, \quad \text{where} \quad k_j = \frac{(p-\mu)(p-\bar{\mu})}{(p-\bar{p})\,\bar{\boldsymbol{u}}_{p,j}} = \frac{m}{\bar{\boldsymbol{u}}_{p,j}} \tag{6.67}$$

$K_j = 2\mathrm{Re}(k_j x_{pi}^H)$ since $\bar{K}_j = K_j$. The 2-norm of K_j becomes[7]

$$\|K_j\|_2 = 2 \cdot \|\mathrm{Re}(k_j x_{pi}^H)\|_2 = 2 \cdot |k_j| \cdot \|\mathrm{Re}(e^{j\angle k_j} x_{pi}^H)\|_2 \tag{6.68}$$

which shows that we need to pay attention to $\angle u_{p,j}$ when selecting the single input j if we want to minimize $\|K_j\|_2$.

When $p > 0$ and $\mu = -p$, we get $m = \frac{2p\,\mathrm{Re}(p)}{j\,\mathrm{Im}(p)}$ (which is independent of the choice j)

$$k_j = \frac{2p(p+\bar{p})}{(p-\bar{p})\,\bar{\boldsymbol{u}}_{p,j}} = \frac{2p}{j}\frac{\mathrm{Re}(p)}{\mathrm{Im}(p)}\frac{1}{\bar{\boldsymbol{u}}_{p,j}} \tag{6.69}$$

The case when $\mu = -p$ corresponds to stabilizing control with minimum input usage for a plant with two complex conjugate unstable poles. This follows since the feedback gain

---

[7]When j is used as a subscript or together with the text "input" we mean input j, otherwise we mean the complex number $j = \sqrt{-1}$.

vector K_j in the SISO case is unique and the state feedback which minimizes the input usage mirrors the open-loop unstable poles into the LHP, i.e. the resulting closed-loop poles are $\mu = -p$ also for complex conjugate poles (Kwakernaak and Sivan, 1972, Theorem 3.11 on page 284). An alternative way to prove that the state feedback K_j (6.67) with k_j given by (6.69) minimizes the input usage, is to solve the Riccati equation (6.31) for the case when the state-space matrix A has two unstable complex eigenvalues. The solution is

$$X = \frac{|k_j|^2}{2\text{Re}(p)}(x_{pi}x_{pi}^H + \bar{x}_{pi}x_{pi}^T) + \frac{k_j^2}{2p}\bar{x}_{pi}x_{pi}^H + \frac{\bar{k}_j^2}{2\bar{p}}x_{pi}x_{pi}^T \tag{6.70}$$

State observer based on y_i. The estimator gain becomes

$$K_{f,i} = k_i x_{po} + \bar{k}_i \bar{x}_{po}, \quad \text{where} \quad k_i = \frac{(p-\mu)(p-\bar{\mu})}{(p-\bar{p})\bar{y}_{p,i}} = \frac{m}{\bar{y}_{p,i}} \tag{6.71}$$

$K_{f,i} = 2\text{Re}(k_i x_{po})$, since $\bar{K}_{f,i} = K_{f,i}$. The 2-norm of $K_{f,i}$ is

$$\|K_{f,i}\|_2 = 2 \cdot \|\text{Re}(k_i x_{po})\|_2 = 2 \cdot |k_i| \|\text{Re}(e^{j\angle k_i}x_{po})\|_2 \tag{6.72}$$

When $p > 0$ and $\mu = -p$ we obtain $m = \frac{2p\,\text{Re}(p)}{j\text{Im}(p)}$ (which is independent of the choice i)

$$k_i = \frac{2p(p+\bar{p})}{(p-\bar{p})\bar{y}_{p,i}} = \frac{2p}{j}\frac{\text{Re}(p)}{\text{Im}(p)}\frac{1}{\bar{y}_{p,i}} \tag{6.73}$$

The case with $\mu = -p$ corresponds to the feedback gain from the output y_i to the states which minimize the mean square reconstruction error when there is no process noise and measurement noise of unit intensity (follows from duality).

From the solution X (6.70) to the Riccati equation (6.31) and the expression for $K_{f,i}$ (6.71) with k_i given by (6.73) we can find the minimum value of the objective (6.1) for the case where the plant has two unstable complex poles. We obtain

$$J = \text{tr}\{XK_{f,i}K_{f,i}^T\}$$

However, we have not found any simple way (which may not be possible) to extract $\boldsymbol{u}_{p,j}$ and $\boldsymbol{y}_{p,i}$ from the expression for $XK_{f,i}K_{f,i}^T$. So, we can not prove any definite conclusion about the best input j and the best output i to stabilize a plant with two complex unstable modes. The reason is that the phase of $\boldsymbol{u}_{p,j}$ and $\boldsymbol{y}_{p,i}$ matter (as noted above). However, if the phase of the different elements in $\boldsymbol{u}_p$ are not too different[8] we are pretty safe selecting the input j with the largest magnitude in the pole vector $\boldsymbol{u}_p$. Similarly, when selecting the output i, if the phase of the elements with largest magnitudes in $\boldsymbol{y}_p$ are approximately the same, then we are pretty safe selecting the output i with largest magnitude in the output pole vector $\boldsymbol{y}_p$.

---

[8]In particular if the phase of the elements with largest magnitudes in $\boldsymbol{u}_p$ are approximately the same.

Im

$-p$ p Re
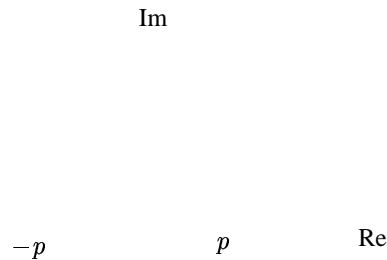
Figure 6.4: Attainable μ values in LQR and LQE problems

The attainable closed-loop poles μ are shown graphically in Figure 6.4. First, we need μ to be stable, i.e. $\operatorname{Re}\mu < 0$. Secondly, we need $\mu \leq p$ (not illustrated in the figure) otherwise the solution X to the Riccati equation is negative. Finally, if $\operatorname{Re}(p) > 0$, then it is required that $|\mu| \geq |p|$, otherwise Q in (6.75) is negative. The first requirement $p \geq \mu$, is equivalent to the second requirement when both p and μ are in LHP and it corresponds to positive semidefinite solutions to the ARE (6.17). The requirement expresses that positive effect of the control is to move the pole further into LHP, and that moving the pole p in the LHP closer to the imaginary axis (to the right) requires a negative solution to the ARE (6.17). The second requirement $|\mu| \geq |p|$ deals with the situation when p is in RHP, then any movement of the pole to the left satisfies a positive semidefinite solution to the ARE. However, traditional LQR requires Q to be positive semidefinite. For $\mu = -p$, we have $Q = 0$, and the objective J is to minimize the input usage. That is, stabilizing control with minimum input usage mirrors the unstable pole into the LHP. One might have thought that the unstable pole should have been moved as little as possible, namely just into the LHP, rather than being reflected about the imaginary axis. However, the need to *trade off* feedback gain vs. rate of decay in x dictates the latter requirement. It is interesting to see that in order to obtain a solution to the LQR problem with $-p < \mu < 0$ when $p \in \mathbb{C}_+$ requires a negative Q, which thereby also gives a

lower value of the objective J_{LQR} for the case when $-p < \mu < 0$ than $\mu = -p$. For example, $\mu = -0.5p$ gives (Kwakernaak and Sivan, 1972)

$$J_{\text{LQR}} = x_0^T X x_0 = \frac{1.5p}{\boldsymbol{u}_{p,j}^2}(x_0^T x_{pi})^2$$

whereas $\mu = -p$ gives

$$J_{\text{LQR}} = x_0^T X x_0 = \frac{2p}{\boldsymbol{u}_{p,j}^2}(x_0^T x_{pi})^2$$

State observer based on $\boldsymbol{y}_i$. We find that the pole placement can be interpreted in terms of LQE when $p \geq \mu$ and $|\mu| \geq |p|$, then the solution to the ARE (6.21) is

$$Y = \frac{p - \mu}{\boldsymbol{y}_{p,i}^2}x_{po}x_{po}^T \quad \text{when } p \geq \mu \tag{6.76}$$

with

$$W = \frac{\mu^2 - p^2}{\boldsymbol{y}_{p,i}^2}x_{po}x_{po}^T \quad \text{when } \mu^2 \geq p^2 \tag{6.77}$$

Minimum value of objective. The minimum value of the objective (6.12) becomes (6.23)

$$
\begin{aligned}
J(i,j) &= \text{tr}\{XK_{f,i}K_{f,i}^T + YQ\} \\
&= \text{tr}\left\{\frac{p - \mu}{\boldsymbol{u}_{p,j}^2}x_{pi}x_{pi}^T\frac{(p - \mu)^2}{\boldsymbol{y}_{p,i}^2}x_{po}x_{po}^T + \frac{p - \mu}{\boldsymbol{y}_{p,i}^2}x_{po}x_{po}^T\frac{\mu^2 - p^2}{\boldsymbol{u}_{p,j}^2}x_{pi}x_{pi}^T\right\} \\
&= \frac{(p - \mu)(x_{pi}x_{po}^T)}{\boldsymbol{u}_{p,j}^2\boldsymbol{y}_{p,i}^2}\text{tr}\{(\mu^2 - p^2)x_{pi}x_{po}^T + (p - \mu)^2 x_{po}x_{pi}^T\} \\
&= \frac{(p - \mu)(x_{pi}x_{po}^T)}{\boldsymbol{u}_{p,j}^2\boldsymbol{y}_{p,i}^2}2\mu(\mu - p)\text{tr}\{x_{pi}x_{po}^T\} = \frac{2\mu(p - \mu)(\mu - p)}{\boldsymbol{u}_{p,j}^2\boldsymbol{y}_{p,i}^2}(x_{pi}^T x_{po})^2 \ (6.78)
\end{aligned}
$$

6.5.2   Moving two or more poles

When we moved one open-loop pole by controlling one output using one input, we were able to deduce in which cases pole placement could be interpreted as LQG control, and from the feedback gains we were able to find positive semidefinite solutions (rank one matrices) to the algebraic Riccati equations. When moving two poles simultaneously the feedback gains are the sum of two vectors, and the solutions to the algebraic Riccati equations obtained from the feedback gains become more complicated. In this case it is the second order term in the algebraic Riccati equation causes cross coupling between the eigenvectors, and the solutions to the Riccati equations are weighted sums of four rank one matrices. This implies that we have not been able to find positive semidefinite weighting matrices (Q or W) in the general case. This may not be a big surprise since from root locus plot for the LQR problem as a function of different weighting between the states and the control input (see, Kwakernaak and Sivan, 1972, for further details) the closed-loop poles moves in certain patterns, for example the Butterworth pole configuration appears when we decrease the weight of the control usage

towards zero. The fact that the closed-loop poles move in certain patterns with varying weight on the control and the states, also appeared when moving a single pole. For example when we consider an open-loop pole $p > 0$, only closed-loop locations μ where $\mu \leq -p$ resulted in positive semidefinite Q. The point is that restrictions must be imposed on Q and W to ensure positive semidefiniteness, i.e. $Q \geq 0$ and $W \geq 0$. The analytical expressions for these restrictions can be hard (and impossible) to find.

6.6 Implications for input/output selection

The input/output pole vectors depend on scaling, so it is crucial to scale the inputs and outputs properly. One procedure for selecting inputs and outputs to stabilize a given unstable mode is:

1) Scale the inputs so that a change in each of the inputs are of equal importance in the objective.

2) Scale outputs relative to measurement noise.

3) Use input j for control, where j corresponds to a large element in the input pole vector $\boldsymbol{u}_p$

4) Control output i, where i corresponds to a large element in the output pole vector $\boldsymbol{y}_p$.

Strictly speaking, the results on stabilizing control with minimum input usage in Section 6.3 and the results on minimizing the norm of the feedback gains in modal control in Section 6.4, can *only* be applied to move *one* pole at a time. If the plant has several unstable modes which need to be stabilized, after stabilizing one mode using one loop, the poles and the pole vectors of the partially controlled system (closed-loop system with the SISO controller included) can be recomputed. However, we can clearly not interpret the results in terms of minimizing the input usage except for the last unstable mode which we stabilize. It may also be that the SISO controller has "stabilized" several unstable or slow modes. If there are remaining unstable poles then new control links can be identified from the recomputed pole directions and new controllers can be included, see the Tennessee Eastman example in Section 6.7 for an illustration of this procedure. We note that in the Tennessee Eastman example we identify two loops from the pole vectors of the open-loop plant before recomputing the pole vectors. Also note that in the distillation DB-configuration example (Example 6.8) we are able to deduce that it is impossible to move two modes which are close in the complex plane and where the pole vectors are orthogonal on each other. So, in some special cases (when the pole vectors are orthogonal) we are able to say something more also when there are more than one unstable pole.

We also note that the fractions $\frac{(x_{pi}^T x_{po})^2}{u_{p,j}^2 y_{p,i}^2}$ and $\frac{(x_{pi}^T x_{po})^2}{\|u_p\|_2^2 \|y_p\|_2^2}$ are controllability measures for how easy it is to stabilize a plant with one unstable mode p with SISO control of output i using input j and full multivariable control respectively. To extract further information from the pole vectors it is tempting to introduce special scalings of the input and the output pole vectors and/or make the definitions dependent on a special balanced state-space realization (see Remark 3 on page 136). However, then the physical connections (and the scalings applied based on physical considerations) to the states, inputs and outputs are lost. So if the

Figure 6.5: Tennessee Eastman test problem

EXAMPLE 6.6 TENNESSEE EASTMAN PROBLEM. In this example we consider the Tennessee East-
man problem, and we use the pole vectors to find a stabilizing control structure. The plant layout of the
Tennessee Eastman problem is shown in Figure 6.5. For details about the Tennessee Eastman problem
refer to (Downs and Vogel, 1993). In the figure both measurements y_i and manipulated variables u_j are
labeled. Also given in the figure are candidate outputs (y_i) for stabilizing control. A separate numbering
scheme is given for those outputs. Table 6.2 summarizes the selected candidate outputs for stabilizing
control and the corresponding variable number in the full model (referred to as PID No.). Also given in
the table is the scaling of the outputs used in this analysis. The manipulated variables are summarized
in Table 6.3, also given in the table is the scaling of the inputs used in this analysis. The linearized
model in the base case (mode 1, 50/50 G/H mass ratio) is used in this example.

The model has six unstable poles in the operating point considered

$$p_u = [\,0 \quad 0.001 \quad 0.023 \pm 0.156j \quad 3.066 \pm 5.079j\,]$$

Table 6.2: Candidate outputs for stabilizing control of the Tennessee Eastman problem.

Variable name	No.[a]	PID No.[b]	Scaling
Reactor pressure	y_1	y_7	54.1 [kPa]
Reactor level	y_2	y_8	1.5 %
Reactor temperature	y_3	y_9	1.2 [°C]
Separator temperature	y_4	y_{11}	1.0 [°C]
Separator level	y_5	y_{12}	1.0 %
Separator pressure	y_6	y_{13}	52.6 [kPa]
Stripper level	y_7	y_{15}	1.0 %
Stripper pressure	y_8	y_{16}	62.0 [kPa]
Stripper temperature	y_9	y_{18}	1.0 [°C]
Reactor cooling water outlet temperature	y_{10}	y_{21}	0.2 [°C]
Separator coolingwater outlet temperature	y_{11}	y_{22}	0.2 [°C]

[a] Variable number in the smaller model used in the analysis.
[b] Variable number in the full model provided by Downs and Vogel.

The inner products of the left and right eigenvectors corresponding to the unstable modes are

$$x_{pi}^H x_{po} = [\, 0.3209 \quad 0.0467 \quad 0.0210 \quad 0.0074 \,]$$

That is, $x_{pi}^H x_{po} = 0.3209$ for the mode $p = 0$, etc. The inner product of complex conjugate eigenvectors is equal, i.e. $x_{pi}^H x_{po} = \bar{x}_{pi}^H \bar{x}_{po}$, so we have only given the four values. The inner products enter into the expressions for the input usage, see (6.29) and (6.49), but have no influence on the relative order of the pairing alternatives.

The output pole vectors are

$$|Y_p| = \begin{bmatrix} 0.000 & 0.001 & 0.041 & 0.112 \\ 0.000 & 0.004 & 0.169 & 0.065 \\ 0.000 & 0.000 & 0.013 & 0.366 \\ 0.000 & 0.001 & 0.051 & 0.410 \\ 0.009 & 0.580 & 0.488 & 0.315 \\ 0.000 & 0.001 & 0.041 & 0.115 \\ 1.605 & 1.192 & 0.754 & 0.131 \\ 0.000 & 0.001 & 0.039 & 0.107 \\ 0.000 & 0.001 & 0.038 & 0.217 \\ 0.000 & 0.001 & 0.055 & 1.485 \\ 0.000 & 0.002 & 0.132 & 0.272 \end{bmatrix} \begin{matrix} \\ \\ \\ \\ \\ \\ \leftarrow y_{15} \\ \\ \\ \leftarrow y_{21} \\ \\ \end{matrix}$$

We have taken the absolute value to avoid complex numbers in the vectors. The first column corresponds to the pole $p_1 = 0$, the second column corresponds to the pole $p_2 = 0.001$, the third column corresponds to the complex conjugate pair $p_{3,4} = 0.023 \pm 0.156j$ and the fourth column corresponds to the complex conjugate pair $p_{5,6} = 3.066 \pm 5.079j$. We see that output y_{15} in the full model (row 7)

Table 6.3: Manipulated variables in the Tennessee Eastman problem.

Variable name	No.[a]	Stream no.	Scaling
D feed flow	u_1	2	10%
E feed flow	u_2	3	10%
A feed flow	u_3	3	10%
A and C feed flow	u_4	4	10%
Compressor recycle valve	u_5		10%
Purge valve	u_6	9	10%
Separator pot liquid flow	u_7	10	10%
Stripper liquid product flow	u_8	11	10%
Stripper steam valve	u_9	Stm	10%
Reactor cooling water flow	u_{10}	CWS	10%
Condenser cooling water flow	u_{11}	CWS	10%
Agitator speed	u_{12}		10%

[a]Variable number in both the full model and the model used in the analysis.

has the largest component in the output pole vector for the pole $p_1 = 0$, and none of the other outputs have significant components in this vector. In a similar way, output y_{21} (row 10) has a large component in the output pole vector corresponding to the complex conjugate pair $p_{5,6} = 3.066 \pm 5.079j$. The input pole vectors are

$$|U_p| = \begin{bmatrix} 6.815 & 6.909 & 2.573 & 0.964 \\ 6.906 & 7.197 & 2.636 & 0.246 \\ 0.148 & 1.485 & 0.768 & 0.044 \\ 3.973 & 11.550 & 5.096 & 0.470 \\ 0.012 & 0.369 & 0.519 & 0.356 \\ 0.597 & 0.077 & 0.066 & 0.033 \\ 0.132 & 1.850 & 1.682 & 0.110 \\ 22.006 & 0.049 & 0.000 & 0.000 \\ 0.007 & 0.054 & 0.009 & 0.013 \\ 0.247 & 0.708 & 1.501 & 2.020 \\ 0.109 & 0.976 & 1.446 & 0.753 \\ 0.033 & 0.094 & 0.201 & 0.302 \end{bmatrix} \begin{array}{l} \\ \\ \\ \\ \\ \\ \\ \leftarrow u_8 \\ \\ \leftarrow u_{10} \\ \\ \\ \end{array}$$

By considering both input and output pole vectors at the same time we arrive at the suggested pairings; $y_{15} \leftrightarrow u_8$ and $y_{21} \leftrightarrow u_{10}$ which corresponds to controlling the stripper level using the stripper liquid product flow and controlling reactor cooling water outlet temperature using the reactor cooling water flow. It can also be seen from the pole vectors that these two loops will interact very little since the common elements in the two vectors are almost zero. It is worth noting that both of these loops were also included by McAvoy and Ye (1994) in their study.

Using two PI-controllers with the tunings given in Table 6.4, we manage to stabilize all the unstable modes except the mode $p_2 = 0.001$. By recomputing the pole vectors with the controllers included we

Table 6.4: Tunings of PI-controllers.

Loop	k_p	T_i
$y_{15} \leftrightarrow u_8$	-0.1 [1/°C]	1 [min]
$y_{21} \leftrightarrow u_{10}$	-0.05 [m³/h]	300 [min]
$y_{12} \leftrightarrow u_7$	-0.0025 [m³/h]	200 [min]

get $x_{pi}^H x_{po} = 0.0787$, and

$$
Y_p = \begin{bmatrix} -0.001 \\ -0.005 \\ 0.000 \\ 0.001 \\ -0.867 \\ -0.001 \\ 0.000 \\ -0.001 \\ 0.001 \\ 0.000 \\ -0.002 \end{bmatrix} \leftarrow y_{12} \qquad \text{and} \qquad U_p = \begin{bmatrix} -7.363 \\ -7.536 \\ 1.410 \\ 11.515 \\ -0.346 \\ -0.065 \\ 2.465 \\ 0.000 \\ -0.062 \\ 0.008 \\ 0.901 \\ -0.078 \end{bmatrix} \leftarrow u_7
$$

We see that the output pole vector has a large element in y_{12} and only small elements in the other outputs. From the input direction we see that input u_4 is the best choice, however, this is a feed stream. We would like to avoid (if possible) to use the feed streams to stabilizing control and rather use these to set the production rate. The feed streams are all gas, so it makes sense from a physical point of view that these manipulated variables have large effect. Also u_1 and u_2 are feed streams so this leaves us with input u_7 which is the separator liquid flow. The pairing $y_{12} \leftrightarrow u_7$ corresponds to controlling the separator level using the separator liquid flow. The controller parameters are given in Table 6.4. After closing this loop the plant is stabilized. Figure 6.6 shows the Tennessee Eastman plant with the controllers included. The mode closest to the imaginary axis is about -0.07 which corresponds to a time constant about 14 hours, which from the operators point of view may seems like an unstable mode drifting away. Repeating the procedure for the slow modes identifies the next loop to be: $y_2 \leftrightarrow u_4$, that is, control reactor level using A and C feed flow.

The intention with this example was to demonstrate a systematic approach to the problem of control structure design and not to design a complete control structure for the Tennessee Eastman problem. Also note that no effort has been put into tuning of the controllers by us, we have used the tunings given in (McAvoy and Ye, 1994). However, we changed the controller gains of the first two loops to check the dependence of the pole directions of the partially controlled plant as a function of the controller gains. We found that the pole directions for the partially controlled plant corresponding to the remaining unstable poles was almost independent of the controller gains in this case. However, this may not be true in general.

EXAMPLE 6.7 UNSTABLE CSTR. In this example we consider a CSTR with two unstable modes. The relationships between modal state controllability and input pole vectors and modal observability and

output poles vectors are demonstrated. Furthermore, we use the pole vectors to identify one candidate pairing for stabilizing both unstable modes using a single loop controller.

We consider the CSTR with the chemical reaction; $A(l) \rightarrow B(l)$. We assume that: $\rho_A = \rho_B = \rho = $ constant, $C_{p,A} = C_{p,B} = C_p = $ constant, the flow out of the tank is independent of liquid height in the tank (the liquid is pumped out), and zero order reaction rate $r = k(T) = k_0\, e^{-\frac{E}{R}\left(\frac{1}{T} - \frac{1}{T_{\text{ref}}}\right)}$. The CSTR is shown in Figure 6.7. The material balances are
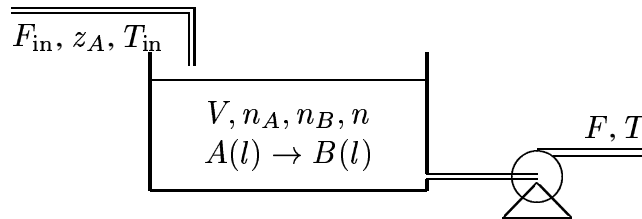
Figure 6.7: CSTR - liquid phase

$$\frac{dn}{dt} = F_{\text{in}} - F \tag{6.79}$$

$$\frac{dn_A}{dt} = F_{\text{in}} z_A - F\frac{n_A}{n} - k(T)n \tag{6.80}$$

where

n	[kmol]	total mass/mole in the CSTR,
n_A	[kmol]	mass/mole of component A,
F_{in}	[kmol/min]	flow into the CSTR,
F	[kmol/min]	flow out of the CSTR,
z_A	[-]	mole fraction of component A in F_{in},
$k(T)$	[1/min]	mole of component A reacted divided by total moles in reactor.

The energy balance becomes (assuming $C_v = C_p$)

$$\begin{aligned} \frac{dU}{dt} &= \frac{dn}{dt} C_p \left(T - T_{ref} \right) + n C_p \frac{dT}{dt} \\ &= F_{in} C_p \left(T_{in} - T_{ref} \right) - F C_p \left(T - T_{ref} \right) + k(T) n \left(\text{-}\Delta H_{rx} \right) \end{aligned}$$

Rearranging yields

$$\frac{dT}{dt} = \frac{F_{in}}{n} \left(T_{in} - T \right) + \frac{k(T)}{C_p} \left(\text{-}\Delta H_{rx} \right) \tag{6.81}$$

where the additional symbols are

T	[°K]	temperature in the CSTR,
T_{in}	[°K]	temperature of F_{in},
C_p	[kJ/kmol °K]	heat capacity of the mixture in the CSTR and
$\text{-}\Delta H_{rx}$	[kJ/kmol]	heat of reaction.

At steady-state we have

$$\frac{dn}{dt} = 0 \qquad \Leftrightarrow \qquad F = F_{in}$$

$$\frac{dT}{dt} = 0 \qquad \Leftrightarrow \qquad F_{in} C_p \left(T_{in} - T^* \right) + k_0 n^* \left(\text{-}\Delta H_{rx} \right) = 0$$

$$\frac{dn_A}{dt} = 0 \qquad \Leftrightarrow \qquad n_A^* = z_A n^* - \frac{k(T^*)}{F_{in}} n^{*2}$$

Linearizing the model around the operating point yields

$$\dot{x} = Ax + Bu + B_d d, \qquad y = Cx$$

where $x = \begin{bmatrix} \Delta n \\ \Delta n_A \\ \Delta T \end{bmatrix}, u = \begin{bmatrix} \Delta F \\ \Delta T_{in} \end{bmatrix}, d = \begin{bmatrix} \Delta F_{in} \\ \Delta z_A \end{bmatrix}, y = \begin{bmatrix} \Delta n \\ \Delta T \end{bmatrix},$

$$A = \begin{bmatrix} 0 & 0 & 0 \\ F \frac{n_A^*}{n^{*2}} - k_0 & -\frac{F}{n^*} & -\frac{Ek_0}{RT^{*2}} \\ \frac{F_{in}}{n^{*2}} (T_{in} - T^*) & 0 & -\frac{F_{in}}{n^*} + \frac{Ek_0}{RT^{*2}} \frac{\text{-}\Delta H_{rx}}{C_p} \end{bmatrix}, \quad B = \begin{bmatrix} -1 & 0 \\ -\frac{n_A^*}{n^*} & 0 \\ 0 & \frac{F_{in}}{n^*} \end{bmatrix},$$

$$B_d = \begin{bmatrix} 1 & 0 \\ z_A & F_{in} \\ \frac{T_{in} - T^*}{n^*} & 0 \end{bmatrix} \quad \text{and} \quad C = \begin{bmatrix} 1 & 0 & 0 \\ 0 & 0 & 1 \end{bmatrix}$$

The eigenvalues of A-matrix (poles of G) are

$$\lambda_1 = -\frac{F}{n^*}, \quad \lambda_2 = 0 \quad \text{and} \quad \lambda_3 = -\frac{F_{in}}{n^*} + \frac{Ek_0}{RT^{*2}} \frac{\text{-}\Delta H_{rx}}{C_p}$$

The operating point is specified in Table 6.5, and the physical process constants are given in Table 6.6.

Table 6.5: CSTR operating point.

Variable	Value	Unit	Variable	Value	Unit
n^*	1	[kmol]	T_{in}	300	[$^\circ$K]
n_A^*	0.2	[kmol]	z_A	1	[-]
T^*	370	[$^\circ$K]	F_{in}	1	[kmol/min]

Table 6.6: Physical constants for CSTR.

Variable	Value	Unit	Variable	Value	Unit
k_0	0.8	[min^{-1}]	E/R	8807	[$^\circ$K]
C_p	40	[kJ/kmol $^\circ$K]	$-\Delta H_{\text{rx}}$	3500	[kJ/kmol]
$T_{\text{ref}} = T^*$	370	[$^\circ$K]			

We scale the inputs using: $\Delta F = 1$ (100% variation), $\Delta T_{\text{in}} = 20\,^\circ$K, the outputs using: $\Delta n = 0.05$ (5% variation), $\Delta T = 1\,^\circ$K, and the disturbances using: $\Delta F_{\text{in}} = 0.5$ and $\Delta z_A = 1$. The full scaled linear state-space model becomes

$$
G_F(s) \overset{s}{=} \left[\begin{array}{c|cc} A & B & B_d \\ \hline C & 0 & 0 \end{array} \right] = \left[\begin{array}{ccc|cccc} 0 & 0 & 0 & -1 & 0 & 0.5 & 0 \\ -0.6 & -1 & -0.0514 & -0.2 & 0 & 0.5 & 1 \\ 70 & 0 & 3.5 & 0 & 20 & -35 & 0 \\ \hline 20 & 0 & 0 & 0 & 0 & 0 & 0 \\ 0 & 0 & 1 & 0 & 0 & 0 & 0 \end{array} \right]
$$

It should be obvious that the mode corresponding to the second state $x_2 = \Delta n_A$ is not observable. Let us check this by computing pole vectors. The inner products of the left and the right eigenvectors and pole vectors corresponding to the poles $\{-1,\ 0,\ 3.5\}$ are

$$
x_{pi}^H x_{po} = [\, 0.9805 \quad 0.0499 \quad 0.0499 \,],
$$

$$
U_p = \begin{bmatrix} 0 & 1 & -0.9988 \\ 0.2241 & 0 & 0.9988 \end{bmatrix} \quad \text{and} \quad Y_p = \begin{bmatrix} 0 & -0.9985 & 0 \\ 0 & 0.9985 & 1 \end{bmatrix}
$$

Where we see that the state corresponding to the mode $\lambda_1 = -1$ (i.e. $x_2 = \Delta n_A$) is not observable, which is reasonable from a physical point of view. A minimal state-space realization is

$$
G(s) \overset{s}{=} \left[\begin{array}{cc|cc} 0 & 0 & -1 & 0 \\ 70 & 3.5 & 0 & 20 \\ \hline 20 & 0 & 0 & 0 \\ 0 & 1 & 0 & 0 \end{array} \right] \quad \text{and} \quad G_d(s) \overset{s}{=} \left[\begin{array}{cc|cc} 0 & 0 & 0.5 & 0 \\ 70 & 3.5 & -35 & 0 \\ \hline 20 & 0 & 0 & 0 \\ 0 & 1 & 0 & 0 \end{array} \right]
$$

In the minimal realization, state $x_2 = \Delta n_A$ is removed and the new x_2 is the temperature $x_2 = \Delta T$. The inner products of the left and the right eigenvectors and pole vectors corresponding to the poles $p_{1,2} = \{0,\ 3.5\}$ are

$$
x_{pi}^H x_{po} = [\, 0.0499 \quad 0.0499 \,], \quad U_p = \begin{bmatrix} 1 & -0.9988 \\ 0 & 0.9988 \end{bmatrix} \quad \text{and} \quad Y_p = \begin{bmatrix} -0.9988 & 0 \\ 0.9988 & 1 \end{bmatrix}
$$
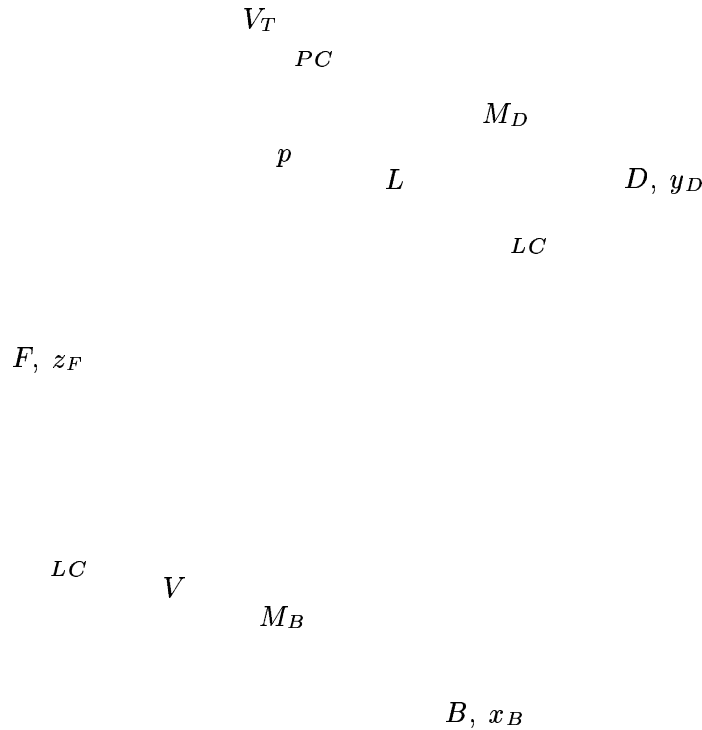
Figure 6.8: Distillation column DB-configuration

From the pole directions we consider to control the temperature (y_2) using the flow F (u_1). By using a LQG controller based on $g_{21}(s)$, it is verified that both modes can be stabilized with this control link. However, we did not manage to stabilize both modes using one PI-controller.

EXAMPLE 6.8 DISTILLATION COLUMN DB-CONFIGURATION. We consider the binary distillation column where the pressure and the liquid holdups in the condenser and reboiler are controlled using condenser cooling duty, reflux and boilup, respectively. This leaves the top D and the bottom B product flows left for product composition control, i.e. the DB-configuration. The distillation column DB-configuration is shown in Figure 6.8. The column data corresponds to column A studied by Skogestad and Morari (1988) and more recently by Skogestad (1997):

#Stages	y_D	$1 - x_B$	z_F	q_F	L/F	V/F	M_i/F^*	M_D/F^*	M_B/F^*
41	0.99	0.99	0.5	1.0	2.71	3.21	0.5	0.5	0.5

*[min]

Feed flowrate $F = 1$ [kmol/min] results in distillate D and bottom B product flows of 0.5 [kmol/min], and top and bottom product compositions $y_D = 0.99$ and $x_B = 0.99$.

The DB-configuration is stable except for two poles close[9] to zero. Experience shows that two control loops need to be included to "stabilize" these two modes. This is in contrast to the other distillation

---

[9]In this case we consider a pole p to be close to zero if $|p| < 0.01$.

column configurations, for example LV, LB, DV, and the configurations with single and double ratios, which have only one pole close to zero and therefore only need one "stabilizing" control loop.

In this example the objective is to predict the fact that the DB-configuration needs two control loops to be "stabilized", by looking at the poles, the pole directions/vectors and the zeros of the transfer function elements. The linearized model G of the distillation column contains the inputs u and outputs y

$$u = [\, D \quad B \,]^T \quad \text{and} \quad y = [\, y_D \quad x_B \,]^T$$

In addition we have the disturbance model G_d, where the disturbances are feed flowrate (F) and feed composition (z_F)

$$d = [\, F \quad z_F \,]^T$$

Scalings. The variables in the linear model have been scaled such that a magnitude of 1 corresponds to a change in F of 0.2 [kmol/min], a change in z_F of 0.2 mole fraction units, a change in x_B and y_D of 0.01 mole fraction units, and a change in D and B of 0.5 [kmol/min].

We compute the poles and find that the numerical values of the two poles close to zero are $p_{1,2} = \{-5.15 \cdot 10^{-3}, \, 0\}$. The corresponding input and output pole directions are

$$U_p = \begin{bmatrix} -0.718 & 0.707 \\ 0.696 & 0.707 \end{bmatrix} \quad \text{and} \quad Y_p = \begin{bmatrix} 0.627 & -0.707 \\ 0.779 & 0.707 \end{bmatrix}$$

The inner products between the normalized left and right eigenvectors are

$$x_{pi}^H x_{po} = [\, 0.7369 \quad 0.5907 \,]$$

and the corresponding input and output pole vectors are

$$U_p = \begin{bmatrix} -0.066 & 0.078 \\ 0.064 & 0.078 \end{bmatrix} \quad \text{and} \quad Y_p = \begin{bmatrix} 1.283 & -1.943 \\ 1.594 & 1.943 \end{bmatrix}$$

We see that the two input directions and the two output directions are nearly orthogonal. The relative angle between the two input directions is $89.1°$, and the relative angle between the two output pole directions is $83.8°$. In addition the two poles are very close so we may expect that all transfer function elements have a zero close to the poles. The transfer function G has several multivariable LHP zeros. The zeros closest to the imaginary axis are complex with real part less than -0.15. The real zero closest to origin is located at -0.252. The zeros closest to origin and RHP zeros of the transfer function elements are:

Element	G_{11}	G_{12}	G_{21}	G_{22}
min $|z|$	$-3.61 \cdot 10^{-3}$	$-8.57 \cdot 10^{-3}$	$-1.03 \cdot 10^{-2}$	$-3.38 \cdot 10^{-3}$
RHP-zero	-	0.568	0.211	-

We see that all elements have a zero close to origin (all of these are in LHP). In addition the off diagonal elements have one RHP-zero each. Since, each of the transfer function elements have one zero close to the poles we may conclude that it is in *practice* impossible to move both poles $p_{1,2}$ by controlling one output using one input.

To test this we decide to control bottom composition using bottom product flow B. That is, we pair[10] on G_{22}. We use proportional feedback control with $K_p = 2.5$. The closed-loop zeros $|z| < 0.01$ and poles $|p| < 0.01$, for the 2×2 closed-loop system with the full distillation column model in partial control

---

[10]We have no preferences for any of the two products, the products of the two elements in the pole vectors corresponding to G_{22} is slightly larger than G_{11} and we do not consider to pair on the off diagonal elements due to the RHP-zero.

with proportional control of x_B using B and where input u_2 is replaced by the reference r_2 to y_2, i.e. the closed-loop transfer function from the inputs $v = \begin{bmatrix} u_1 & r_2 \end{bmatrix}^T$ to the outputs $z = \begin{bmatrix} y_1 & y_2 \end{bmatrix}^T$, is given in Table 6.7. We see that we get a closed-loop pole at $p = -3.376 \cdot 10^{-3}$. Increasing the feedback gain up to $K_p = 100$, does not move the closed-loop pole significantly further to the left (yields $p = -3.382 \cdot 10^{-3}$). We also designed an $\mathcal{H}_\infty$-optimal controller to see if a more sophisticated

Table 6.7: Poles $|p| < 0.01$ for the distillation column DB-configuration.

	Open-loop G	One-point $y_2 \leftrightarrow u_2$ P-control	Two-point P-control K_p
Poles	0 $-5.16 \cdot 10^{-3}$	$-3.38 \cdot 10^{-3}$	-

controller was able to move the pole further to the left in the complex plane, but this is not the case. With two point proportional control of the distillation column using the controller

$$K_p = \begin{bmatrix} -1 & 0 \\ 0 & 0.5 \end{bmatrix} \tag{6.82}$$

In this case we are able to move both poles, so that there are no closed-loop poles $|p| < 0.01$, see Table 6.7. The closed-loop responses in the outputs y due to step changes in the disturbances F and z_F are shown in Figure 6.9. The figure clearly shows that the closed-loop system corresponding to one

(a) Step change in F

(b) Step change in z_F

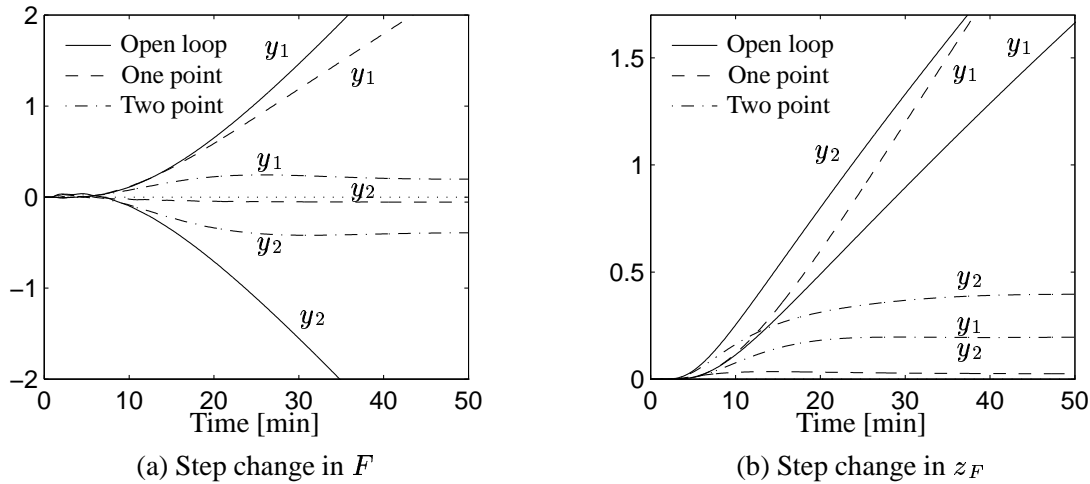Figure 6.9: Responses to steps in d for distillation column DB-configuration. Solid line: open-loop. Dashed line: One point control. Dash-dot line: Two point control

point control, contains closed-loop poles close to origin (the outputs drift).

6.8 Summary

- The input and output pole vectors are directly related to the minimum input energy needed to stabilize one unstable pole using a single loop controller. Due to this direct

relation we find that the best input and the best output to stabilize an unstable mode with a single SISO control loop, corresponds to the input and output with largest elements in the pole vectors. Here the term "best" is in the meaning of minimizing the input energy to stabilize the plant.

- By quantifying the input usage in terms of $\mathcal{H}_\infty$-norm instead of the $\mathcal{H}_2$-norm we find that the best input and the best output is the same as for the $\mathcal{H}_2$-norm. That is, the choices are independent of the norm.

- In a similar way, it is shown that the best input and the best output to move a pole from one location to a different location further to the left in the complex plane with single SISO control loop, corresponds to the input and output with the largest elements in the pole vectors. Here the term "best" is in the meaning of minimizing the gain form the outputs to the states in the observer and the gain from the states to the inputs.

- We have demonstrated the difficulty moving two poles located close together with a single loop controller. And we have shown that the reason for this difficulty is that all transfer function elements have a zero close to the poles. Furthermore, we have shown how to identify this situation by considering the location of the poles and looking for orthogonal pole directions.

- Finally, we have demonstrated the application of pole directions and vectors in the task of control structure design through several realistic process control examples.

References

Douglas, J. and Athans, M. (1995). *The Control Handbook*, 30 ed., CRC Press, chapter Multivariable Poles, Zeros, and Pole-Zero Cancellations, pp. 445–450.

Downs, J. J. and Vogel, E. F. (1993). A plant-wide industrial process control problem, *Computers Chem. Engng.* **17**(3): 245–255.

Gould, L. A., Murphy, A. T. and Berkman, E. F. (1970). On the Simon-Mitter pole allocation algorithm–Explicite gains for repeated eigenvalues, *IEEE Transactions on Automatic Control* **AC-15**: 259–260.

Kwakernaak, H. and Sivan, R. (1972). *Linear Optimal Control Systems*, Wiley Interscience, New York.

Li, K., Xi, Y. and Zhang, Z. (1994). A new method for selection of variables in industrial process control systems, *Proceedings of the Asian Control Conference*, Tokyo, pp. 219–222.

McAvoy, T. J. and Ye, N. (1994). Base control of Tennessee Eastman problem, *Computers Chem. Engng.* **18**(5): 383–413.

Rosenbrock, H. H. (1962). Distinctive problems of process control, *Chem. Eng. Progress* **58**(9): 43–50.

Skogestad, S. (1997). Dynamics and control of distillation columns – a tutorial introduction, *Plenary lecture at Distillation and Absorption '97, Maastricht, September 1997* .

Skogestad, S. and Morari, M. (1988). LV-control of a high-purity distillation column, *Chemical Engineering Science* **43**(1): 33–48.

Skogestad, S. and Postlethwaite, I. (1996). *Multivariable Feedback Control, Analysis and Design*, John Wiley & Sons, Chichester.

Tarokh, M. (1992). Measures for controllability, observability, and fixed modes, *IEEE Transactions on Automatic Control* **37**(8): 1268–1273.

Appendix A Modal control and estimation of SISO systems

We consider the n'th order linear constant system described by

$$\dot{x} = Ax + Bu \tag{6.83}$$

The modal control problem is to find a linear state variable feedback control law

$$u = -Kx + u_0 \tag{6.84}$$

such that the eigenvalues of the state matrix A denoted by the set $\{\lambda_i\}$, $i = 1, \cdots, n$, are moved to some desired locations specified by the set of closed-loop eigenvalues $\{\mu_i\}$ where complex eigenvalues appear in conjugate pairs. This problem was first discussed by Rosenbrock (1962) in connection with process control and it has since then gained a lot of attention, in particular in the late sixties and the beginning of the seventies.

For multiple input there are more degrees of freedom in terms of parameters k_{ij} in the feedback gain matrix K than specifications in terms of close-loop eigenvalues $\{\mu_i\}$. The algorithm implemented in MATLAB Control System Toolbox[11] utilizes these extra degrees of freedom to minimize the sensitivity of the poles to perturbations in the closed-loop system matrix $\widetilde{A} = A - BK$. For single input systems the number of gains matches the number of specifications (the closed-loop poles) so the feedback gain K is unique for a given state-space realization in this case.

In this paper we only consider single input and we calculate feedback gains as outlined in (Gould, Murphy and Berkman, 1970). Since we want to introduce the pole vectors into the equations, we repeat the main steps in the calculation here, but for a proof of the results the reader should refer to the original source.

Once the modal control problem is solved, then the modal estimation problem follows from duality.

A.1   Solution to the single input modal control problem

We map the system (6.83) to single input by only consider input u_j

$$\dot{x} = Ax + Be_j u_j \tag{6.85}$$

and we apply the feedback gain K_j from the states x to input u_j

$$u_j = -K_j x \tag{6.86}$$

---

[11]See the command place.

To simplify the problem we apply a non-singular similarity transformation on the states x to the new states z so that the new A matrix is in Jordan form J. There are two ways to do this, either the left or the right Jordan form, see Appendix B for further details. For the modal control problem we use the left Jordan form and for the modal estimation problem (introduced below) we use the right Jordan form. This is to get the desired links to the pole vectors. The relation between the original state x and the new state z is

$$z = M_L^H x \tag{6.87}$$

and the state equation becomes

$$\dot{z} = Jz + M_L^H B e_j u_j = Jz + \boldsymbol{U}_\infty^H e_j u_j \tag{6.88}$$

where M_L is the matrix consisting of the eigenvectors and generalized vectors for the left Jordan form, i.e. $M_L^H A = J M_L^H$, and $\boldsymbol{U}_\infty$ is the matrix containing all input directions with "infinite gains" as columns, see Chapter 2. We partition the states z, J and $\boldsymbol{U}_\infty$ according to the Jordan blocks

$$z = \begin{bmatrix} \boldsymbol{z}_1 \\ \vdots \\ \boldsymbol{z}_\ell \\ \vdots \\ \boldsymbol{z}_v \end{bmatrix}, \quad J = \begin{bmatrix} J_1 & & & & \\ & \ddots & & & \\ & & J_\ell & & \\ & & & \ddots & \\ & & & & J_v \end{bmatrix}$$

$$\text{and} \quad \boldsymbol{U}_\infty = [\, \boldsymbol{U}_{\infty,1} \quad \cdots \quad \boldsymbol{U}_{\infty,\ell} \quad \cdots \quad \boldsymbol{U}_{\infty,v} \,]$$

where v is the number of Jordan blocks. We have used bold font to emphasize that $\boldsymbol{z}_\ell$ is a vector and *not* the ℓ'th state in z. If A can be diagonalized then $J = \Lambda$ and $\boldsymbol{U}_\infty = \boldsymbol{U}_p$ where the latter is the matrix containing the pole vectors as columns. Note that a mode λ_i may only have one linearly independent eigenvector (geometric multiplicity one) in order to be controllable in one input, see Chapter 2. If this is not the case, it is necessary to use more inputs to control the mode. We therefore assume that the geometric multiplicity of all the poles which we might consider to move is one.

Each Jordan block J_ℓ with the corresponding pole p can now be treated separately. The size of the Jordan block is equal to the algebraic multiplicity of the pole p in the input and output pole directions which correspond to the left and the right eigenvectors in the Jordan block. To separate the equations involved in Jordan block J_ℓ from the other equations we multiply (6.88) on the left with the transposed of the selection matrix N_ℓ and introduce $z = N_\ell \boldsymbol{z}_\ell$ to obtain

$$\dot{\boldsymbol{z}}_\ell = N_\ell^T \dot{z} = N_\ell^T J N_\ell \boldsymbol{z}_\ell + N_\ell^T \boldsymbol{U}_\infty^H e_j u_j = J_\ell \boldsymbol{z}_\ell + \boldsymbol{U}_{\infty,\ell}^H e_j u_j \tag{6.89}$$

Now, assume that Jordan block J_ℓ starts with state z_k and has size ν. Then N_ℓ consists of ν columns with n elements, the first column being e_k, that is, a unit vector (size n) with zeros in all positions except position k which contains one. The second column is e_{k+1} etc. up to the last column which is $e_{k+\nu-1}$. Then $\boldsymbol{z}_\ell$ contains the ν states starting with z_k and ending with $z_{k+\nu-1}$, i.e. $\boldsymbol{z}_\ell = [\, z_k \quad \cdots \quad z_{k+\nu-1} \,]$. J_ℓ is ℓ'th Jordan block in J with the

eigenvalue $\lambda_\ell = p$ on the diagonal and $\boldsymbol{U}_{\infty,\ell}$ contains as columns the directions with infinite gains corresponding to p. The last column in $\boldsymbol{U}_{\infty,\ell}$ is the pole vector for the pole p. Let us denote the ν columns of M_L corresponding to p, the ν states in $\boldsymbol{z}_\ell$ and Jordan block J_ℓ, for $M_{L,\ell}$. That is,

$$M_{L,\ell} = M_L N_\ell = \begin{bmatrix} m_k & \cdots & m_{k+\nu-1} \end{bmatrix} \triangleq \begin{bmatrix} m_{\ell,1} & m_{\ell,2} & \cdots & m_{\ell,\nu-1} & x_{pi} \end{bmatrix}$$

and then we have that

$$\begin{aligned}
\boldsymbol{U}_{\infty,\ell} = B^H M_{L,\ell} &= \begin{bmatrix} B^H m_{\ell,1} & B^H m_{\ell,2} & \cdots & B^H m_{\ell,\nu-1} & B^H x_{pi} \end{bmatrix} \\
&= \begin{bmatrix} \boldsymbol{u}_{\infty,1} & \boldsymbol{u}_{\infty,2} & \cdots & \boldsymbol{u}_{\infty,\nu-1} & \boldsymbol{u}_p \end{bmatrix}
\end{aligned}$$

If the size of Jordan block J_ℓ is one then the pole vector $\boldsymbol{u}_p$ is the only column in $\boldsymbol{U}_{\infty,\ell}$, that is

$$\boldsymbol{U}_{\infty,\ell} = \boldsymbol{u}_p$$

The vector

$$\boldsymbol{U}_{\infty,\ell}^H e_j = \begin{bmatrix} \bar{\boldsymbol{u}}_{\infty,1,j} \\ \bar{\boldsymbol{u}}_{\infty,2,j} \\ \vdots \\ \bar{\boldsymbol{u}}_{\infty,\nu-1,j} \\ \bar{\boldsymbol{u}}_{p,j} \end{bmatrix}$$

first contains the j'th element of all the $\nu - 1$ input pole vectors with "infinite gains" and the last element is the j'th element of the pole vector.

The ν elements $\delta_{\ell,i}$ of the state feedback gain from $\boldsymbol{z}_\ell$ to u_j corresponding to the pole p are given by the relationship

$$\begin{bmatrix} \bar{\boldsymbol{u}}_{p,j} & 0 & 0 & \cdots & 0 \\ \bar{\boldsymbol{u}}_{\infty,\nu-1,j} & \bar{\boldsymbol{u}}_{p,j} & 0 & \cdots & 0 \\ \bar{\boldsymbol{u}}_{\infty,\nu-2,j} & \bar{\boldsymbol{u}}_{\infty,\nu-1,j} & \bar{\boldsymbol{u}}_{p,j} & \cdots & 0 \\ \vdots & \vdots & \vdots & \ddots & \vdots \\ \bar{\boldsymbol{u}}_{\infty,1,j} & \bar{\boldsymbol{u}}_{\infty,2,j} & \bar{\boldsymbol{u}}_{\infty,3,j} & \cdots & \bar{\boldsymbol{u}}_{p,j} \end{bmatrix} \begin{bmatrix} \delta_{\ell,1} \\ \delta_{\ell,2} \\ \delta_{\ell,3} \\ \vdots \\ \delta_{\ell,\nu} \end{bmatrix} = \begin{bmatrix} \xi_{\ell,1} \\ \xi_{\ell,2} \\ \xi_{\ell,3} \\ \vdots \\ \xi_{\ell,\nu} \end{bmatrix} \qquad (6.90)$$

where $\xi_{\ell,i}$ can be calculated from

$$\xi_{\ell,i} = \frac{1}{(i-1)!} \frac{d^{i-1}\{(s-p)^\nu g(s)\}}{ds^{i-1}} \Bigg|_{s=p} \qquad (6.91)$$

and $g(s)$ is defined as

$$g(s) = \frac{\prod_{i=1}^n (s - \mu_i)}{\prod_{i=1}^n (s - \lambda_i)}$$

The feedback gain from the states $\boldsymbol{z}_\ell$ to input u_j, $\Delta_{\ell,j}$, can be written

$$\Delta_{\ell,j} = \sum_{i=1}^\nu \delta_{\ell,i} e_{k+i-1}^T$$

and the feedback gain Δ_j from the states z to input u_j when taking into account all v Jordan blocks J_ℓ is

$$\Delta_j = \sum_{\ell=1}^{v} \Delta_{\ell,j}$$

The feedback gain K_j from x to u_j is given by

$$K_j = \Delta_j M_L^H = \sum_{\ell=1}^{v} K_{\ell,j} = \sum_{\ell=1}^{v} \Delta_{\ell,j} M_{L,\ell}^H \qquad (6.92)$$

A simple formula for $K_{\ell,j}$ in terms of the columns in $M_{L,\ell}$ is

$$K_{\ell,j} = \delta_{\ell,1} m_{\ell,1}^H + \delta_{\ell,2} m_{\ell,2}^H + \cdots + \delta_{\ell,\nu-1} m_{\ell,\nu-1}^H + \delta_{\ell,\nu} x_{pi}^H \qquad (6.93)$$

State to input feedback gains corresponding to Jordan blocks of size 1×1. If $\lambda_\ell = p$ is a simple pole, then $z_\ell = z_k$ and

$$K_{\ell,j} = \frac{\prod\limits_{i=1}^{n} (\lambda_\ell - \mu_i)}{\bar{u}_{p,j} \prod\limits_{\substack{i=1 \\ i \neq \ell}}^{n} (\lambda_\ell - \lambda_i)} x_{pi}^H \qquad (6.94)$$

A.2   Solution to the single output modal estimation problem

The dual problem to the single input modal control problem is the single output modal estimation problem. In this case we want to find an output to state feedback gain matrix L_i so that the modes of the observer are located at the specified closed-loop poles $\{\mu_i\}$. The state equation for the observer with feedback from the single output y_i becomes

$$\dot{\hat{x}} = A\hat{x} + Bu + L_i(y_i - e_i^T C\hat{x} - e_i^T Du) \qquad (6.95)$$

and the closed-loop state matrix for the observer is

$$\widehat{A} = A - L_i e_i^T C \qquad (6.96)$$

By taking the transposed of (6.96)

$$\widehat{A}^T = A^T - C^T e_i L_i^T \qquad (6.97)$$

and by comparing with the closed-loop state matrix in the single input modal control problem

$$\widetilde{A} = A - B e_j K_j \qquad (6.98)$$

It appears that we can solve the single output modal estimation problem by treating it as a single input modal control problem of the transposed system. The mapping between the matrices in the single input modal control problem of the systems

$$G(s) \overset{s}{=} \left[\begin{array}{c|c} A & B \\ \hline C & D \end{array} \right] \quad \text{and} \quad G^T(s) \overset{s}{=} \left[\begin{array}{c|c} A^T & B^T \\ \hline C^T & D^T \end{array} \right]$$

Table 6.8: Mapping between matrices for modal control of G and G^T and modal estimation of G

	Matrices								
	System	Specifications					Results		
Modal control	G	$\{\mu_i\}$	A	B	e_j	J	M_L	$\boldsymbol{U}_\infty$	K_j
Modal control	G^T	$\{\mu_i\}$	A^T	C^T	e_i	J^T	$\widetilde{M}_R$	$\widetilde{\boldsymbol{Y}}_\infty$	L_i^T
Modal estimation	G	$\{\mu_i\}$	A	C	e_i	J^T	$\widetilde{M}_R$	$\widetilde{\boldsymbol{Y}}_\infty$	L_i

and the single output modal estimation of G is given in Table 6.8. The setup and the matrices in Table 6.8 may need a little explanation. The solution to the single input modal control problem of system G (first row with data in Table 6.8) is derived in the previous section and it is known in terms of the matrices K_j, $\boldsymbol{U}_\infty$ and M_L which need to be calculated in terms of the specifications; the desired closed-loop poles $\{\mu_i\}$ and the matrices A, B, e_j and J. We note that we also have specified J which together with M_L tells us to compute the left Jordan form.

To solve the single input modal control of G^T (second row in Table 6.8) we insert the specifications in the second row into the first row, that is, replace A with A^T, B with C^T etc., and we must compute the left Jordan form of A^T

$$M_L^H A^T = J M_L^H \quad \Leftrightarrow \quad A \bar{M}_L = J^T \bar{M}_L$$

which is equivalent with computing the right Jordan form of A but with J replaced by J^T. The fact that J^T is involved rather than J, implies that the ordering of the vectors in M_R for each Jordan block is opposite than for the usual right Jordan form. However, the ordering is identical to the ordering in the left Jordan form, so the solution comes really easy. We signal the unusual ordering in M_R and $\boldsymbol{Y}_\infty$ by adding a tilde above M_R and $\boldsymbol{Y}_\infty$ in Table 6.8, i.e. $\widetilde{M}_r$ and $\widetilde{\boldsymbol{Y}}_\infty$. The solution of the single output estimation problem then follows easily. The output to state feedback gain L_i becomes

$$L_i = \sum_{\ell=1}^{\upsilon} L_{\ell,i} \quad \text{with} \quad L_{\ell,i} = \delta_{\ell,1} m_{\ell,1} + \delta_{\ell,1} m_{\ell,2} + \cdots + \delta_{\ell,\nu-1} m_{\ell,\nu-1} + \delta_{\ell,\nu} x_{po} \quad (6.99)$$

where

$$\widetilde{M}_{R,\ell} = [\, m_{\ell,1} \quad m_{\ell,2} \quad \cdots \quad m_{\ell,\nu-1} \quad x_{po} \,]$$

are the vectors in $\widetilde{M}_R$ which brings A to right Jordan form J^T and $\widetilde{M}_{R,\ell}$ are the columns of $\widetilde{M}_R$ which corresponds to Jordan block J_ℓ,

$$\widetilde{M}_R = [\, \widetilde{M}_{R,1} \quad \cdots \quad \widetilde{M}_{R,\ell} \quad \cdots \quad \widetilde{M}_{R,\upsilon} \,]$$

The vector of gains δ_ℓ is the solution to the following equations

$$
\begin{bmatrix}
\bar{y}_{p,i} & 0 & 0 & \cdots & 0 \\
\bar{y}_{\infty,\nu-1,i} & \bar{y}_{p,i} & 0 & \cdots & 0 \\
\bar{y}_{\infty,\nu-2,i} & \bar{y}_{\infty,\nu-1,i} & \bar{y}_{p,i} & \cdots & 0 \\
\vdots & \vdots & \vdots & \ddots & \vdots \\
\bar{y}_{\infty,1,i} & \bar{y}_{\infty,2,i} & \bar{y}_{\infty,3,i} & \cdots & \bar{y}_{p,i}
\end{bmatrix}
\begin{bmatrix}
\delta_{\ell,1} \\
\delta_{\ell,2} \\
\delta_{\ell,3} \\
\vdots \\
\delta_{\ell,\nu}
\end{bmatrix}
=
\begin{bmatrix}
\xi_{\ell,1} \\
\xi_{\ell,2} \\
\xi_{\ell,3} \\
\vdots \\
\xi_{\ell,\nu}
\end{bmatrix}
\tag{6.100}
$$

where $\xi_{\ell,i}$ can be found from (6.91), and the elements of the lower triangular matrix in (6.100) can be calculated using

$$
\widetilde{\boldsymbol{Y}}_\infty^H e_i =
\begin{bmatrix}
\bar{y}_{\infty,1,i} \\
\bar{y}_{\infty,2,i} \\
\vdots \\
\bar{y}_{\infty,\nu-1,i} \\
\bar{y}_{p,i}
\end{bmatrix}
$$

Output to state feedback gains corresponding to Jordan blocks of size 1×1. If $\lambda_\ell = p$ is a simple pole, then

$$
L_{\ell,i} = \frac{\displaystyle\prod_{j=1}^{n}(\lambda_\ell - \mu_i)}{\bar{y}_{p,i}\displaystyle\prod_{\substack{j=1 \\ j\neq \ell}}^{n}(\lambda_\ell - \lambda_i)}\, x_{po}
\tag{6.101}
$$

A.3 Moving repeated poles

We consider here the case when the multiplicity of the pole p is two. Note, a SISO system with repeated mode p can only have one linearly independent eigenvector for the mode p. That is, the geometric multiplicity of the pole p is one (otherwise the pole p is not observable and/or controllable). So, we need to consider the Jordan form in this case.

State feedback to input u_j. The feedback gain K_j to move the pole p with multiplicity two, to the desired locations μ_1 and μ_2 using state feedback (6.56) to input u_j becomes

$$
K_j = k_1 m_{pi}^H + k_2 x_{pi}^H
\tag{6.102}
$$

where

$$
k_1 = (p-\mu_1)(p-\mu_2)/\bar{u}_{p,j}, \quad k_2 = \{2p - \mu_1 - \mu_2 - \tfrac{\bar{u}_{\infty,j}}{\bar{u}_{p,j}}(p-\mu_1)(p-\mu_2)\}/\bar{u}_{p,j}
$$

$$
x_{pi}^H A = p x_{pi}^H, \quad m_{pi}^H A = p m_{pi}^H + x_{pi}^H, \quad \bar{u}_{p,j} = \boldsymbol{u}_p^H e_j \quad \text{and} \quad \bar{u}_{\infty,j} = m_{pi}^H B e_j
$$

State observer based on y_i. In a similar way, we can move the observer pole p with multiplicity two, to the desired locations μ_1 and μ_2 by adding feedback from $y_i - \hat{y}_i$ to the estimated states. The solution is

$$
K_{f,i} = k_1 m_{po} + k_2 x_{po}
\tag{6.103}
$$

where

$$k_1 = (p - \mu_1)(p - \mu_2)/\bar{y}_{p,i}, \quad k_2 = \{2p - \mu_1 - \mu_2 - \frac{\bar{y}_{\infty,i}}{\bar{y}_{p,i}}(p - \mu_1)(p - \mu_2)\}/\bar{y}_{p,i}$$

$$Ax_{po} = px_{po}, \quad Am_{po} = pm_{po} + x_{po}, \quad y_{p,i} = e_i^T y_p \quad \text{and} \quad y_{\infty,i} = e_i^T C m_{po}$$

Appendix B Proofs of the results

B.1 Proofs of the results on minimum input usage

Proof of (6.32). Since, p is real (only one unstable pole) $x_{pi} = \bar{x}_{pi}$, $u_p = \bar{u}_p$. x_{pi} is the left eigenvector of A corresponding to the mode p, i.e. $x_{pi}^H A = px_{pi}^H$. By taking the transposed we get $A^T x_{pi} = px_{pi}$. Inserting X into (6.31) we obtain

$$\underbrace{A^T x_{pi}}_{px_{pi}} x_{pi}^T \frac{2p}{u_{p,j}^2} + \frac{2p}{u_{p,j}^2} x_{pi} \underbrace{x_{pi}^T A}_{px_{pi}^T} - x_{pi} \underbrace{x_{pi}^T B e_j e_j^T B^T x_{pi}}_{u_{p,j}^2} x_{pi}^T \frac{4p^2}{u_{p,j}^4} = \frac{4p^2}{u_{p,j}^2}(x_{pi}x_{pi}^T - x_{pi}x_{pi}^T) = 0$$

$\square$

Proof of (6.35). Since, p is real (only one unstable pole) $x_{po} = \bar{x}_{po}$, $y_p = \bar{y}_p$. x_{po} is a right eigenvector of A corresponding to the mode p, i.e. $Ax_{po} = px_{po}$. By taking the transposed we get $x_{po}^T A^T = px_{po}^T$. Inserting Y into (6.34) we obtain

$$\frac{2p}{y_{p,i}^2} x_{po} \underbrace{x_{po}^T A^T}_{px_{po}^T} + \underbrace{Ax_{po}}_{px_{po}} x_{po}^T \frac{2p}{y_{p,i}^2} - x_{po} \underbrace{x_{po}^T C^T e_i e_i^T C x_{po}}_{y_{p,i}^2} x_{po}^T \frac{4p^2}{y_{p,i}^4} = \frac{4p^2}{y_{p,i}^2}(x_{po}x_{po}^T - x_{po}x_{po}^T) = 0$$

$\square$

Proof of (6.41). Note that $x_{pi}^T = x_{pi}^H$, $x_{po}^T = x_{po}^H$ since p is real. Inserting X into (6.40) gives

$$\underbrace{A^T x_{pi}}_{px_{pi}} x_{pi}^T \frac{2p}{\|u_p\|_2^2} + \frac{2p}{\|u_p\|_2^2} x_{pi} \underbrace{x_{pi}^T A}_{px_{pi}^T} - \frac{4p^2}{\|u_p\|_2^4} x_{pi} \underbrace{x_{pi}^T B B^T x_{pi}}_{u_p^T u_p} x_{pi}^T = \frac{4p^2}{\|u_p\|_2^2}(x_{pi}x_{pi}^T - x_{pi}x_{pi}^T) = 0$$

$\square$

Proof of (6.45). Note that $x_{pi}^T = x_{pi}^H$, $x_{po}^T = x_{po}^H$ since p is real. Inserting Y into (6.44) gives

$$\frac{2p}{\|y_p\|_2^2} x_{po} \underbrace{x_{po}^T A^T}_{px_{po}^T} + \underbrace{Ax_{po}}_{px_{po}} x_{po}^T \frac{2p}{\|y_p\|_2^2} - \frac{4p^2}{\|y_p\|_2^4} x_{po} \underbrace{x_{pi}^T C^T C x_{po}}_{y_p^T y_p} x_{po}^T = \frac{4p^2}{\|y_p\|_2^2}(x_{po}x_{po}^T - x_{po}x_{po}^T) = 0$$

$\square$

Proof of Theorem 6.3. From equation (4.37) with $G = G_{ij}$ in Chapter 4 and the fact that the lower bound is tight when the plant has one unstable pole p (Theorem 4.3) the first identity in (6.49) follows.

Since p is the only unstable mode, it follows that a partial fraction expansion of G contains the following two terms (2.28)

$$G(s) = \frac{(x_{pi}^H x_{po})^{-1}}{s - p} \boldsymbol{y}_p \boldsymbol{u}_p^H + G_{st}(s)$$

where G_{st} is stable. Then

$$
\begin{aligned}
G_{ij} &= e_i^T G e_j = \frac{(x_{pi}^H x_{po})^{-1}}{s - p} \boldsymbol{y}_{p,i} \boldsymbol{u}_{p,j} + e_i^T G_{st}(s) e_j \\
(G_{ij})_s &= \frac{s - p}{s + p} G_{ij}(s) = \frac{(x_{pi}^H x_{po})^{-1}}{s + p} \boldsymbol{y}_{p,i} \boldsymbol{u}_{p,j} + \frac{s - p}{s + p} e_i^T G_{st}(s) e_j \\
|(G_{ij})_s^{-1}(p)| &= \left| \left(\frac{(x_{pi}^H x_{po})^{-1}}{s + p} \boldsymbol{y}_{p,i} \boldsymbol{u}_{p,j} + \frac{s - p}{s + p} e_i^T G_{st}(s) e_j \right)^{-1} \right|_{s=p} \\
&= \frac{2p}{|\boldsymbol{y}_{p,i}| \cdot |\boldsymbol{u}_{p,j}|} |x_{pi}^H x_{po}|
\end{aligned}
$$

$\square$

Proof of Theorem 6.4. Equation (6.51) follows from the lower bounds (5.74) and (5.75) in Chapter 5 and the fact that the lower bounds are tight when the plant has one RHP-pole p (Theorems 5.7 and 5.8). $\square$

B.2 Proofs of the results on pole placement

Moving one pole.

Proof of (6.61). Since p is real, it follows that $x_{pi}^T = x_{pi}^H$ and $\bar{\boldsymbol{u}}_{p,j} = \boldsymbol{u}_{p,j}$. By inserting (6.56) and (6.61) into (6.55) we obtain the closed-loop state matrix

$$\widetilde{A} = A - B e_j x_{pi}^T \frac{p - \mu}{\boldsymbol{u}_{p,j}} = A - B e_j x_{pi}^H \frac{p - \mu}{\boldsymbol{u}_{p,j}}$$

and by multiplying $\widetilde{A}$ on the left by x_{pi}^H we obtain

$$x_{pi}^H \widetilde{A} = \underbrace{x_{pi}^H A}_{p x_{pi}^H} - \overbrace{\underbrace{x_{pi}^H B}_{} e_j}^{\boldsymbol{u}_p^H} x_{pi}^H \frac{p - \mu}{\boldsymbol{u}_{p,j}} = p x_{pi}^H - p x_{pi}^H + \mu x_{pi}^H = \mu x_{pi}^H$$

where the under-brace reads $\bar{\boldsymbol{u}}_{p,j}$.

$\square$

Proof of (6.62). By inserting (6.62) into (6.59) the modified state matrix of the observer becomes

$$\widehat{A} = A - K_{f,i} e_i^T C = A - \frac{p - \mu}{\boldsymbol{y}_{p,i}} x_{po} e_i^T C$$

Multiplying $\widehat{A}$ on the right with x_{po} gives

$$\widehat{A} x_{po} = A x_{po} - \frac{p - \mu}{\boldsymbol{y}_{p,i}} x_{po} \underbrace{e_i^T \overbrace{C x_{po}}^{\boldsymbol{y}_p}}_{\boldsymbol{y}_{p,i}} = p x_{po} - p x_{po} + \mu x_{po} = \mu x_{po}$$

$\square$

Moving two distinct poles.

Proof of (6.63). In this case we have two Jordan blocks of size 1×1 and the state feedback gain K_j follows from (6.92) and (6.94). $\square$

Proof of (6.65). In this case we have two Jordan blocks of size 1×1 and the state feedback gain L_i follows from (6.99) and (6.101). $\square$

Moving complex conjugate poles.

Proof of (6.67). Insert $p_1 = p$, $p_2 = \bar{p}$, $\mu_1 = -p$, $\mu_2 = -\bar{p}$, $x_{p1i} = x_{pi}$, $x_{p2i} = \bar{x}_{pi}$, $u_{p_1,j} = u_{p,j}$ and $u_{p_2,j} = \bar{u}_{p,j}$ in (6.63). $\square$

Proof of (6.70). It is easy to verify the X is real and symmetric, i.e. $X^H = X^T = X$. The Riccati equation (6.31) can be written

$$A^T X + X A - K_j^T K_j = 0 \tag{6.104}$$

Inserting X from (6.31) into (6.104) gives

$$
\begin{aligned}
A^T &\left(\frac{|k_j|^2}{2\text{Re}(p)} (x_{pi} x_{pi}^H + \bar{x}_{pi} x_{pi}^T) + \frac{k_j^2}{2p} \bar{x}_{pi} x_{pi}^H + \frac{\bar{k}_j^2}{2\bar{p}} x_{pi} x_{pi}^T \right) \\
&+ \left(\frac{|k_j|^2}{2\text{Re}(p)} (x_{pi} x_{pi}^H + \bar{x}_{pi} x_{pi}^T) + \frac{k_j^2}{2p} \bar{x}_{pi} x_{pi}^H + \frac{\bar{k}_j^2}{2\bar{p}} x_{pi} x_{pi}^T \right) A \\
&- |k_j|^2 (x_{pi} x_{pi}^H + \bar{x}_{pi} x_{pi}^T) - k_j^2 \bar{x}_{pi} x_{pi}^H - \bar{k}_j^2 x_{pi} x_{pi}^T \\
= & \frac{|k_j^2| \, 2\text{Re}(p)}{2\text{Re}(p)} (x_{pi} x_{pi}^H + \bar{x}_{pi} x_{pi}^T) + \frac{k_j^2 \, 2p}{2p} \bar{x}_{pi} x_{pi}^H + \frac{\bar{k}_j^2 \, 2\bar{p}}{2\bar{p}} x_{pi} x_{pi}^T \\
&- |k_j|^2 (x_{pi} x_{pi}^H + \bar{x}_{pi} x_{pi}^T) - k_j^2 \bar{x}_{pi} x_{pi}^H - \bar{k}_j^2 x_{pi} x_{pi}^T = 0
\end{aligned}
$$

$\square$

Proof of (6.71). Insert $p_1 = p$, $p_2 = \bar{p}$, $\mu_1 = -p$, $\mu_2 = -\bar{p}$, $x_{p1o} = x_{po}$, $x_{p2o} = \bar{x}_{po}$, $y_{p_1,i} = y_{p,i}$ and $y_{p_2,i} = \bar{y}_{p,i}$ in (6.65). $\square$

Moving repeated poles.

Proof of (6.102). In this case we have one Jordan block of size 2×2 and (6.93) gives

$$K_j = k_1 m_{pi}^H + k_2 x_{pi}^H$$

where k_1 and k_2 are given by the solution to the following equation (6.90):

$$
\begin{bmatrix} \bar{u}_{p,j} & 0 \\ \bar{u}_{\infty,j} & \bar{u}_{p,j} \end{bmatrix} \begin{bmatrix} k_1 \\ k_2 \end{bmatrix} = \begin{bmatrix} (p - \mu_1)(p - \mu_2) \\ 2p - \mu_1 - \mu_2 \end{bmatrix}
$$

which gives

$$k_1 = (p - \mu_1)(p - \mu_2)/\bar{u}_{p,j}, \quad k_2 = \left\{ 2p - \mu_1 - \mu_2 - \frac{\bar{u}_{\infty,j}}{\bar{u}_{p,j}} (p - \mu_1)(p - \mu_2) \right\} / \bar{u}_{p,j}$$

$\square$

Proof of (6.103). In this case we have one Jordan block of size 2×2 and (6.99) gives

$$L_j = k_1 m_{po} + k_2 x_{po}$$

where k_1 and k_2 are given by the solution to the following equation (6.100):

$$\begin{bmatrix} \bar{y}_{p,i} & 0 \\ \bar{y}_{\infty,i} & \bar{y}_{p,i} \end{bmatrix} \begin{bmatrix} k_1 \\ k_2 \end{bmatrix} = \begin{bmatrix} (p - \mu_1)(p - \mu_2) \\ 2p - \mu_1 - \mu_2 \end{bmatrix}$$

which gives

$$k_1 = (p - \mu_1)(p - \mu_2)/\bar{y}_{p,i}, \quad k_2 = \{2p - \mu_1 - \mu_2 - \frac{\bar{y}_{\infty,i}}{\bar{y}_{p,i}}(p - \mu_1)(p - \mu_2)\}/\bar{y}_{p,i}$$

$\square$

B.3 Proofs of interpretations in terms of LQG control

Proof of (6.74) and (6.75). By inserting for X from (6.74) into $K_j = e_j^T B^T X$ we obtain

$$K_j = e_j^T B^T X = e_j^T \underbrace{\overbrace{B^T x_{pi}}^{u_p} x_{pi}^T \frac{p - \mu}{u_{p,j}^2}}_{u_{p,j}} = \frac{p - \mu}{u_{p,j}} x_{pi}^T$$

and by inserting X from (6.74) and Q from (6.75) into (6.17) we obtain

$$\underbrace{A^T x_{pi}}_{p x_{pi}} x_{pi}^T \frac{p-\mu}{u_{p,j}^2} + x_{pi} \underbrace{x_{pi}^T A}_{p x_{pi}^T} \frac{p-\mu}{u_{p,j}^2} - \frac{p-\mu}{u_{p,j}^2} x_{pi} \underbrace{\overbrace{x_{pi}^T B}^{u_p^T} e_j}_{u_{p,j}} \underbrace{e_j^T \overbrace{B^T x_{pi}}^{u_p}}_{u_{p,j}} x_{pi}^T \frac{p-\mu}{u_{p,j}^2} + \frac{\mu^2 - p^2}{u_{p,j}^2} x_{pi} x_{pi}^T$$

$$= \frac{1}{u_{p,j}^2} x_{pi} x_{pi}^T \{2p(p - \mu) - (p - \mu)^2 + \mu^2 - p^2\} = 0$$

$\square$

Proof of (6.76) and (6.77). The measurement to state feedback gain is given in terms of Y as $K_{f,i} = Y C^T e_i$, inserting for Y from (6.76) gives

$$K_{f,i} = \frac{p - \mu}{y_{p,i}^2} x_{po} \underbrace{\overbrace{x_{po}^T C^T}^{y_p^T} e_i}_{y_{p,i}} = \frac{p - \mu}{y_{p,i}} x_{po}$$

and inserting for Y from (6.76) and Q from (6.77) into (6.21) gives

$$\frac{p-\mu}{y_{p,i}^2} x_{po} \underbrace{x_{po}^T A^T}_{p x_{po}} + \underbrace{A x_{po}}_{p x_{po}} x_{po}^T \frac{p-\mu}{y_{p,i}^2} - \frac{p-\mu}{y_{p,i}^2} x_{po} \underbrace{\overbrace{x_{po}^T C^T}^{y_p^T} e_i}_{y_{p,i}} \underbrace{e_i^T \overbrace{C x_{po}}^{y_p}}_{y_{p,i}} x_{po}^T \frac{p-\mu}{y_{p,i}^2} + \frac{\mu^2-p^2}{y_{p,i}^2} x_{po} x_{po}^T$$

$$= \frac{1}{y_{p,i}^2} x_{po} x_{po}^T \{2p(p - \mu) - (p - \mu)^2 + \mu^2 - p^2\} = 0$$

$\square$

Chapter 7

Input/output selection and partial control. Part I: Introduction and analysis of partial control

Kjetil Havre[*] and Sigurd Skogestad[†]

Chemical Engineering,
Norwegian University of Science and Technology
N-7034 Trondheim, Norway.

Abstract

This paper considers the process of control structure design, and in particular it addresses the issue of selecting measurements and manipulations for partial control. Partial control at a given level involves controlling a subset of the outputs with an associated control objective. The relative gain array (RGA) and singular value decomposition (SVD) are useful measures for selecting inputs and outputs.

---

[*]Also affiliated with: Institute for energy technology, P.O.Box 40, N-2007 Kjeller, Norway, Fax: (+47) 63 81 11 68, E-mail: Kjetil.Havre@ife.no.

[†]Fax: (+47) 73 59 40 80, E-mail: skoge@chembio.ntnu.no.

7.1   Introduction

One important task in the design of a control system is the specification of the control structure. Steps in the process of *control structure design* are (Skogestad and Postlethwaite, 1996):

1) Selection of controlled outputs.
2) Selection of manipulations and measurements.
3) Selection of control *configuration*.
4) Selection of controller type.

One may easily recognize that the design of a control structure is more complex than the task of synthesizing a controller for given sets of measurements and actuators. This paper mainly considers steps 1), 2) and 3) and introduces controllability measures to address the input/output selection problem. With a large number of candidate measurements and/or manipulations, the number of possible combinations of inputs and outputs have a combinatorial growth, so an approach consisting of performing a controllability analysis for each possible combination, becomes time consuming. In this paper we therefore suggest to use measures for non-square systems such as the relative gain array (RGA) and singular value decomposition (SVD) to select inputs and outputs.

7.1.1   Partial control

Partial control at a given level involves controlling only a subset of the outputs. A block diagram of a partially controlled system (G, G_d) is shown in Figure 7.1.
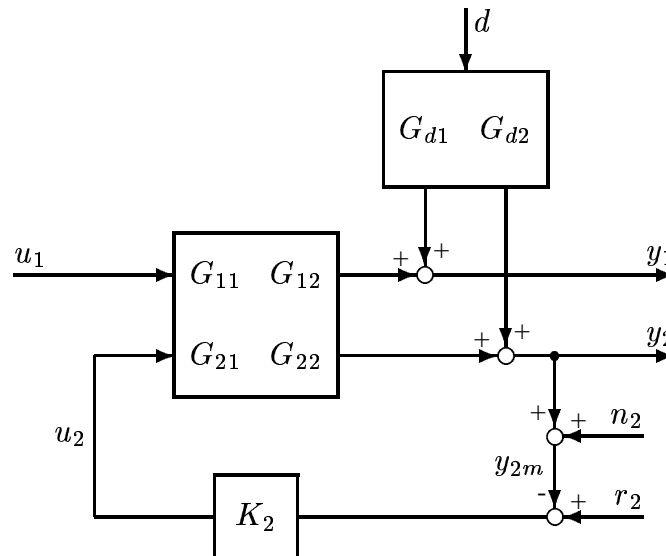

Figure 7.1: Block diagram of a partially controlled plant (G, G_d)

Divide the outputs and inputs into the sets:

- y_1 uncontrolled outputs at the present control layer.
- y_2 controlled outputs at the present control layer.

- u_1 inputs not used at the present control layer.
- u_2 inputs used to control y_2.

With this classification of inputs and outputs we can distinguish between the following four applications of partial control (Skogestad and Postlethwaite, 1996):

1) *Indirect control*. The outputs y_1 have an associated control objective, but they are not measured. Instead, we aim at indirectly controlling y_1 by controlling the "secondary" measured variables y_2 (which have no associated control objective). The references r_2 are used as degrees of freedom and the set u_1 is often empty.

2) *Cascade control*. Indirect control with outer loops adjusting the setpoints r_2 in the secondary loops.

3) *True partial control*. The outputs y (which include y_1 and y_2) all have an associated control objective, and we consider if acceptable control of y_1 can indirectly be achieved, by controlling the subset y_2. That is, the outputs y_1 remain uncontrolled and the set u_1 remains unused.

4) *Decentralized control (sequential-design)*. The outputs y (which include y_1 and y_2) all have an associated control objective, and we use a hierarchical control system. We first design a controller K_2 to control the subset y_2. With this controller K_2 in place (a partially controlled system), we may then design a controller K_1 for the remaining outputs.

Table 7.1 shows more clearly the difference between the four applications of partial control. In all cases there is a control objective associated with y_1 and a measurement of y_2. In all

Table 7.1: Control objectives and measurements in applications of partial control.

		Measurement of y_1?	Control objective for y_2?
1	Indirect control	No	No
2	Cascade control	Yes	No
3	True partial control	No	Yes
4	Decentralized control	Yes	Yes

four cases we want that:

A. It should be easy to control y_2 using u_2.

B. The effect of disturbances (including measurement noise) on the outputs y_1 should be reduced when y_2 is controlled.

To analyze the feasibility of partial control, one may consider the effect of the disturbances, reference changes and measurement noise in the controlled outputs, on the *uncontrolled* outputs.

7.1.2 Notation and scaling

Notation. We consider linear time invariant transfer function models on the form

$$y(s) = G(s)u(s) + G_d(s)d(s) \tag{7.1}$$

where u is the vector of manipulated inputs, d is the vector of disturbances and y is the vector of outputs. The objective is to keep the control error $e = y - r$ small, where r is the vector of reference signals. $G(s)$ and $G_d(s)$ are rational transfer function matrices of sizes $l \times m$ and $l \times n_d$. Throughout the paper subscripts i, j and k denote a particular output y_i, input u_j and disturbance d_k. The notations $y_{l \neq i}$ and $u_{m \neq j}$ mean all outputs and inputs except output number i and input number j. $[A]_{ij} = a_{ij}$ denotes the element in row i and column j of the matrix A, and $\tilde{A} = \text{diag}\{a_{ii}\}$ contains the diagonal elements of A. w_B and w_{B2} denote the bandwidth of primary and secondary control loops.

Scaling. The variables should be scaled to be within the interval -1 to 1, that is, their expected magnitudes should be normalized to be less than 1. This is done by dividing the unscaled signals by their *expected maximum allowed change* $u_{j,\max}$, $d_{k,\max}$, $r_{i,\max}$, $n_{i,\max}$ and $e_{i,\max}$. The scaled model can then be written

$$e = y - r = Gu + G_d d - R\tilde{r} \tag{7.2}$$

where $R = \text{diag}\{\frac{r_{i,\max}}{e_{i,\max}}\}$. In addition, we have noisy measurements y_m of the outputs y

$$y_m = y + n = y + N\tilde{n} \tag{7.3}$$

where n is the measurement noise (relative to y) and $N = \text{diag}\{\frac{n_{i,\max}}{e_{i,\max}}\}$.

At each frequency we assume $\|u\|_\infty < 1$, $\|d\|_\infty < 1$, $\|\tilde{r}\|_\infty < 1$, $\|\tilde{n}\|_\infty < 1$ and we want $\|e\|_\infty < 1$, where the vector ∞-norm (max-norm) is the largest element magnitude in the vector. That is, at each frequency we assume that the largest element magnitude is less than one.

7.2 Related and previous work

The relative gain array (RGA) was first introduced by Bristol (1966) at steady-state as the ratio of the "open-loop" and "closed-loop" gains between input j and output i when all other outputs $y_{l \neq i}$ are perfectly controlled using the inputs $u_{m \neq j}$

$$\lambda_{ij}(s) = \frac{\partial y_i / \partial u_j}{\partial y_i / \partial u_j|_{y_l \neq i}} = g_{ij} \left[G^{-1} \right]_{ji} \tag{7.4}$$

The RGA matrix can be computed at any frequency using the formula (Chang and Yu, 1990):

$$\Lambda(G(s)) = G(s) \times (G^\dagger(s))^T \tag{7.5}$$

where $G^\dagger$ is the pseudo-inverse of G. Interpreting the RGA in terms of perfect control at steady-state is only possible when $\text{rank}(G) = l$.

Stanley, Marino-Galarraga and McAvoy (1985) introduced the Relative Disturbance Gain (RDG) as the ratio between the input u_j needed when rejecting disturbance k in all outputs and the input u_j needed when rejecting disturbance k only in output j. Skogestad and Morari (1987) gave this measure a performance interpretation and found that it can be evaluated at any frequency using

$$\beta_{jk} = \frac{\partial u_j / \partial d_k|_{y_i=0,\ \forall i}}{\partial u_j / \partial d_k|_{y_i=0,\ (i=j)}} = \frac{g_{jj}[G^{-1}G_d]_{jk}}{[G_d]_{jk}} = \frac{[\tilde{G}G^{-1}G_d]_{jk}}{[G_d]_{jk}} \tag{7.6}$$

The following result is due to Grosdidier (Skogestad and Morari, 1987). It treats the necessary input in u_j for perfect control of one output y_j under influence of a single disturbance d_k

$$\left.\frac{\partial u_j}{\partial d_k}\right|_{y_j,u_{m\neq j}} = -[\tilde{G}^{-1}]_{jj}[G_d]_{jk} = -[\tilde{G}^{-1}[G_d]_k]^j \tag{7.7}$$

Similarly, the input for perfect control of all outputs under influence of a single disturbance d_k is

$$\left.\frac{\partial u_j}{\partial d_k}\right|_{y} = -[G^{-1}]^j[G_d]_k = -[G^{-1}G_d]_{jk} \tag{7.8}$$

Skogestad and Wolff (1992) introduced the Partial Disturbance Gain (PDG) as the effect of disturbance d_k on the uncontrolled output y_i when all other outputs $y_{l\neq i}$ are controlled by using the inputs $u_{m\neq j}$. For a square plant G they presented the following analytical expression for the PDG

$$PDG = \left.\frac{\partial y_i}{\partial d_k}\right|_{u_j,y_{l\neq i}} = \frac{[G^{-1}G_d]_{jk}}{[G^{-1}]_{ji}} \tag{7.9}$$

The Partial Disturbance Gain has been applied to a continuos bioreactor (Zhao and Skogestad, 1994) and to a FCC process (Wolff, Skogestad, Hovd and Mathisen, 1992). The partial disturbance gain can be generalized to a non-square and singular G using of the pseudo-inverse. However, the gains at steady-state can only be interpreted in terms of perfect control when $\text{rank}(G) = l$ ($G^\dagger$ is then a right-inverse of G). Otherwise, PDG can be interpreted in terms of *least square control*.

The Relative Partial Disturbance Gain (RPDG) was also introduced by Skogestad and Wolff (1992). It is defined as the ratio between the PDG and the open-loop disturbance gain for output i and disturbance k when input j is unused.

$$RPDG = \frac{\partial y_i / \partial d_k|_{u_j,y_{l\neq i}}}{\partial y_i / \partial d_k} = \frac{[G^{-1}G_d]_{jk}}{[G^{-1}]_{ji}[G_d]_{ik}} \tag{7.10}$$

For the case $i = j$ (a diagonal element in G is left uncontrolled), the RPDG is equal to the ratio between the RDG and RGA

$$RPDG = \frac{\delta_{ik}}{\lambda_{ii}[G_d]_{ik}} = \frac{\beta_{ik}}{\lambda_{ii}} \tag{7.11}$$

Chang and Yu (1990) define the Relative Gain Array for non-square multivariable systems with more outputs than inputs in terms of perfect control in the least square sense (minimize the sum of the squared errors, SSE) at steady-state. They show that for the case with more outputs than inputs, the sum of the elements in each row of the RGA matrix stays between zero and one. They also show that the steady-state error in output y_i due to a step change in one output $y_{l \neq i}$, is equal to $1 - \sum_{j=1}^{m} \lambda_{ij}$. For control structure selection for a $l \times m$ plant G (selecting m outputs to be controlled by the m inputs) they justify that selecting the m outputs with largest row sum in the RGA leads to small SSE at steady-state. They show this by considering the two cases: $m = 1$ (one manipulated input) and $l = m + 1$ (one more measurement than inputs). However, they fail to derive a general direct relationship between the row sums of RGA and the SSE. For the general case they have conducted a computer experiment to test the heuristic: "choosing the square subsystem by eliminating the $l - m$ outputs with smallest row sums leads to the minimum SSE". The computer experiment was based on ten thousand randomly generated matrices of a given dimension. The results show that the selection procedure based on the row sums of the RGA leads to the optimal subsystem in 77% of the cases tested. In this paper we justify why to select the outputs with largest row sum of the RGA, by proving that this particular set of m outputs contains more information about the non-singular directions than any other set of m outputs. Cao (1995) makes a similar justification involving the column sums of the RGA and the input selection problem for a non-square plant with more inputs than outputs.

Reeves and Arkun (1989) extend the block relative gain to non-square systems and give interpretation in terms of a performance-related tool for evaluating control structures prior to controller design.

However, neither Chang and Yu (1990) nor Reeves and Arkun (1989), consider the effect of disturbances on the performance when evaluating control structures prior to controller design.

Despite the fact that indirect and partial control has been studied in the literature and used extensively in industrial applications, the selection of secondary variables to be used for indirect control has *not* gained much focus in the literature except, for the rather rigorous approach taken by Lee and Morari (1991). Selection of inputs and outputs for regulatory control is discussed by Hovd and Skogestad (1993).

Related work on partial control include (Manousiouthakis et al., 1986; Skogestad and Wolff, 1992; Häggblom, 1994). Results on partial control directly applicable to distillation column control include (Waller, Häggblom, Sandelin and Finnerman, 1988; Häggblom and Waller, 1992; Häggblom, 1994). Indirect two-point control through one-point control of distillation is studied by Sandelin, Häggblom and Waller (1991). Related work on indirect control of product composition in distillation columns by controlling temperatures include (Tolliver and McCune, 1980; Yu and Luyben, 1984; Yu and Luyben, 1987; Moore, Hackney and Canter, 1987; Mejdell, 1990; Lee, Braatz, Morari and Packard, 1995; Lee and Morari, 1996; Wolff and Skogestad, 1996).

7.3 Transfer functions for partially controlled systems

By rearranging and partitioning the inputs and outputs as given above, the overall model $y = Gu + G_d d$, the error $e = y - R\tilde{r}$ and the measurement $y_m = y + N\tilde{n}$ can be written:

$$y_1 = G_{11}u_1 + G_{12}u_2 + G_{d1}d; \qquad e_1 = y_1 - R_1\tilde{r}_1; \qquad y_{1m} = y_1 + N_1\tilde{n}_1 \qquad (7.12)$$

$$y_2 = G_{21}u_1 + G_{22}u_2 + G_{d2}d; \qquad e_2 = y_2 - R_2\tilde{r}_2; \qquad y_{2m} = y_2 + N_2\tilde{n}_2 \qquad (7.13)$$

With feedback control of y_2 (measurements $y_{2m} = y_2 + n_2$, see Figure 7.1) using u_2,

$$u_2 = K_2(r_2 - y_2 - n_2) \qquad (7.14)$$

the partially controlled system becomes

$$
\begin{aligned}
y_1 &= (G_{11} - G_{12}K_2(I + G_{22}K_2)^{-1}G_{21})u_1 + (G_{d1} - G_{12}K_2(I + G_{22}K_2)^{-1}G_{d2})d \\
&\quad + G_{12}K_2(I + G_{22}K_2)^{-1}(r_2 - n_2) \qquad (7.15)
\end{aligned}
$$

REMARK. This may be rewritten in terms of linear fractional transformations with the generalized plant P and the controller K_2

$$y_1 = F_l(P, K_2)\begin{bmatrix} u_1 \\ d \\ r_2 \\ n_2 \end{bmatrix} \quad \text{where} \quad P = \begin{bmatrix} G_{11} & G_{d1} & 0 & 0 & G_{12} \\ -G_{12} & -G_{d2} & I & -I & -G_{22} \end{bmatrix} \qquad (7.16)$$

Perfect control of y_2. At some frequencies it may be reasonable to assume the measured y_2 perfectly controlled. We assume[1] that $G_{22}(s)$ is square and invertible (at a given value of s), we set $y_2 + n_2 = r_2$ ($e_2 = n_2$) and eliminate u_2 in (7.12) and (7.13) to get

$$
\begin{aligned}
y_1 &= \underbrace{\left(G_{11} - G_{12}G_{22}^{-1}G_{21}\right)}_{P_u} u_1 + \underbrace{\left(G_{d1} - G_{12}G_{22}^{-1}G_{d2}\right)}_{P_d} d \\
&\quad + \underbrace{G_{12}G_{22}^{-1}R_2}_{P_r}\tilde{r}_2 - \underbrace{G_{12}G_{22}^{-1}N_2}_{P_n}\tilde{n}_2 \qquad (7.17)
\end{aligned}
$$

where P_d is the *partial disturbance gain*.

P_r is the *partial reference gain*.

P_n is the gain for the measurement noise $\tilde{n}_2$ for a system under partial control.

P_u is the gain for the unused inputs u_1 for a system under partial control.

The advantage of the model (7.17) is that it is independent of K_2, but we stress that this only applies at frequencies where y_2 is tightly controlled.

REMARK 1. Eqs. (7.9) and (7.17) reflect two different ways of computing the PDG's which yield the same results. This follows from the definition. With one uncontrolled output and one unused input, (7.9) gives an efficient way of computing all combinations of PDG's for disturbance d_k. With more than one uncontrolled output and one unused input, it is easier to use (7.17).

---

[1]Strictly speaking, this is a frequency-by-frequency analysis, $s = j\omega$ (one particular frequency being the steady-state, $\omega = 0$).

REMARK 2. One advantage of (7.9) is that it provides direct insight into which uncontrolled output and unused input to select. We have:

1) Select u_j such that row j in $G^{-1}G_d$ has small elements (keep the input constant for which the desired change is small).

2) Select y_i corresponding to a large element in row j of G^{-1} (keep an output uncontrolled which is insensitive to u_j).

7.4 Uses of partial control

As mentioned in the introduction, four applications of partial control are:

1) *Indirect control* of y_1 by controlling y_2.

2) *Inner cascade loops* with extra measurements y_2.

3) *True partial control*.

4) *Sequential design* of decentralized controllers.

In the cases 3) and 4) there are performance objectives associated with the outputs y_2 (so $\tilde{r}_2$ is given). The four problems are closely related, and in all cases we want the effect of the disturbances on y_1 to be small when y_2 is controlled. In particular we want $\|P_d\| < \|G_{d1}\|$, compare eq. (7.12) and (7.17). With feedback control of y_2 using u_2, we introduce the measurement noise n_2 in the measurements of y_2 into the system. Then it is desirable that the effect of n_2 on y_1 is small, i.e. $\|P_n\|$ is small. In some cases there is a close relationship (correlation) between y_2 and y_1, in this case the measurement noise n_2 in y_2 can have large effect on y_1. The result is that a trade-off between measurement noise and disturbance rejection occurs. This is the case in Chapter 9, where we consider selecting temperature measurements for indirect two-point temperature control of a binary distillation column. An additional desirable property for all three cases is to achieve fast and acceptable control of y_2. A common controllability requirement is

- $\underline{\sigma}(G_{22}) > 1$, $\forall \omega < \omega_{B2}$ (ω_{B2} denotes the desired bandwidth of the secondary loop).

One justification of this requirement is to avoid input constraints in u_2.

7.4.1 Indirect control

In this case, y_2 are additional "secondary" measurements with *no associated performance objectives*. The control objective is to achieve satisfactory performance for the "primary" outputs y_1. However, in this case there is no measurements of y_1. So, in order to achieve acceptable control of y_1, we control some "secondary" variables y_2 which are closely related to y_1. This is similar to true partial control (see Section 7.4.3), however, there are no performance objectives associated with y_2.

Assume that the outputs have been scaled such that we can tolerate a control error of magnitude 1 in each of the primary outputs y_1, and that the maximum allowed variation in the disturbance d and measurement noise $\tilde{n}_2$ corresponds to magnitude 1. Let ω_B denote the desired bandwidth for the control loop. For combined disturbance and measurement noise rejection in y_1, the following requirement must be satisfied

- A set of outputs y_1 may be considered kept uncontrolled if $\left\| [\begin{array}{cc} P_d & P_n \end{array}] \right\|_{i\infty} < 1$, $\forall \omega < \omega_B$.

The induced infinity norm $\| \cdot \|_{i\infty}$ computes the maximum row sum (sum of element magnitudes) and reflects in this case the effect of d for the worst case output. Additional information can be obtained by also considering the other outputs by summing the element magnitudes in each rows.

7.4.2 Inner cascade loops

In this case we have additional measurements (which may not be reliable) of y_1. Due to properties of the plant like RHP-zeros, delays and input/output uncertainty, acceptable performance when controlling y_1 in a direct manner, may not be achievable. One way to improve the control of y_1 can be to control y_2. In particular, this may reduce the effect of the disturbances d on y_1, when d enters between the input of the plant and the measurements of "secondary" variables y_2. Note that with the inner loop closed, $\tilde{r}_2$ can be used to control y_1.

To have any benefit (measured in y_1) of controlling y_2 using u_2, we need to have:

$$\| [\begin{array}{cc} P_d & P_n \end{array}] \| < \| G_{d1} \|$$

for some frequencies within the bandwidth of the secondary loops ω_{B2}. Since the intention with secondary control loops is disturbance rejection for frequencies larger than the bandwidth ω_B of the outer control loop we require:

$$\| [\begin{array}{cc} P_d & P_n \end{array}] \|_{i\infty} < 1, \quad \forall \omega < \omega_B$$

The outer loops control the primary variables y_1 using $\tilde{r}_2$ and u_1. A common controllability requirement imposed on P_r and P_u is[2] then

- $\underline{\sigma}([\begin{array}{cc} P_r & P_u \end{array}]) > 1$, $\forall \omega < \omega_{G_{d1}}$.

This is to guarantee that u_1 and $\tilde{r}_2$ stay within the desired limits and applies irrespective of the controller type, provided that the secondary loops $y_2 \leftrightarrow u_2$ are intact.

Input/output selection for indirect and cascade control is treated separately in Chapter 8. This brief treatment is meant to be an introduction.

7.4.3 True partial control

In some cases, the outputs are correlated such that controlling the outputs y_2 indirectly gives acceptable control of some other outputs y_1. Two examples of "true" partial control from the chemical process industry are given in Examples 7.1 and 7.2.

Let ω_B denote the desired bandwidth of the control loop. For combined disturbance and measurement noise rejection in y_1, the following requirement must be satisfied:

- A set of outputs y_1 may be considered kept uncontrolled if $\left\| [\begin{array}{cc} P_d & P_n \end{array}] \right\|_{i\infty} < 1$, $\forall \omega < \omega_B$.

---

[2] Rescaling of P_r on the input is necessary to allow for some more variation in $\tilde{r}_2$.

Reference changes in $\tilde{r}_2$ may also be regarded as disturbances for the uncontrolled primary outputs y_1:

- For a change in a single reference $\tilde{r}_f$ separately, a set of outputs y_1 may be considered kept uncontrolled if $|[P_r]_{if}| < 1$, $\forall\, i \in \mathbf{1}$, $\forall \omega < \omega_B$.
- For combinations of reference changes, a set of outputs y_1 may be considered kept uncontrolled if $\|P_r\|_{i\infty} < 1$, $\forall \omega < \omega_B$.
- For combined reference changes, disturbances and measurement noise, a set of outputs y_1 may be considered kept uncontrolled if $\|[\,P_d \quad P_n \quad P_r\,]\|_{i\infty} < 1$, $\forall \omega < \omega_B$.

The induced infinity norm reflects the effect of the inputs (d, $\tilde{n}_2$ and $\tilde{r}_2$) on the worst case output. Additional information can be obtained by also considering the other outputs by summing the element magnitudes in each rows.

EXAMPLE 7.1 PARTIAL CONTROL OF DISTILLATION COLUMN. This example consider disturbance rejection in one-point partial control of a 2×2 distillation column. We use the reduced 5-state model of the distillation column given in (Hovd and Skogestad, 1992). The full 82-state model consists of 40 theoretical trays plus a total condenser and includes both liquid flow dynamics and composition dynamics. Disturbances in feed flowrate F (d_1) and feed composition z_F (d_2) are included. The LV configuration is used, that is, the manipulated inputs are reflux L (u_1) and boilup V (u_2). Outputs are product compositions y_D (y_1) and x_B (y_2). The disturbances and outputs have been scaled such that a magnitude of 1 corresponds to a change in F of 20%, a change in z_F of 20% and a change in x_B and y_D of 0.01 mole fraction units. One and two point control of binary distillation columns has also been studied by (Waller et al., 1988).

At steady-state the model and the RGA are

$$G = \begin{bmatrix} 88.23 & -86.77 \\ 108.82 & -110.07 \end{bmatrix}, \qquad G_d = \begin{bmatrix} 7.93 & 8.90 \\ 11.74 & 11.28 \end{bmatrix} \quad \text{and} \quad \Lambda = \begin{bmatrix} 36.1 & -35.1 \\ -35.1 & 36.1 \end{bmatrix}$$

The RGA-elements are much larger than 1 which indicates that the plant is fundamentally difficult to control. It also indicates that the two outputs are closely related. Consider the SVD at steady-state, $G(0) = USV^H$

$$U = \begin{bmatrix} 0.624 & -0.781 \\ 0.781 & 0.624 \end{bmatrix}, \qquad S = \begin{bmatrix} 198.2 & 0.0 \\ 0.0 & 1.36 \end{bmatrix} \quad \text{and} \quad V = \begin{bmatrix} 0.707 & -0.707 \\ -0.707 & -0.707 \end{bmatrix}$$

From U we see that the gain to the bottom composition is slightly larger than the top composition. This may indicate that it is best to control bottom composition and leave top composition uncontrolled.

The partial disturbance gain for the two disturbances for the four alternative partial control schemes are

$$P_{1,d}^{2,2} = [\,-1.32 \quad 0.013\,], \qquad P_{1,d}^{2,1} = [\,-1.59 \quad -0.24\,],$$

$$P_{2,d}^{1,2} = [\,1.68 \quad -0.016\,] \quad \text{and} \quad P_{2,d}^{1,1} = [\,1.95 \quad 0.297\,]$$

where we have introduced the notation $P_{i,d}^{l \neq i,j}$, for the partial disturbance gain (both disturbances) when output i is uncontrolled and the remaining output $l \neq i$ is controlled using input j. For example, the partial disturbance gain for the effect of disturbance 1 on output 1, with output 2 controlled using input 2, is

$$P_{1,d1}^{2,2} = G_{d11} - G_{12}G_{22}^{-1}G_{d21} = 7.9 - \frac{86.8}{110.1}11.7 = -1.32$$
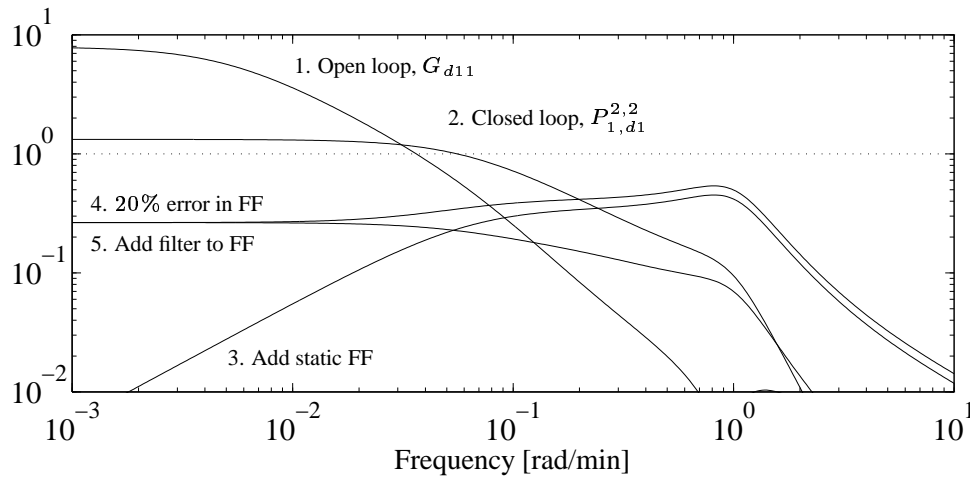
Figure 7.2: Effect of d_1 on y_1 for distillation column example

In all four cases we see that control of one output significantly reduces the effect of the disturbances on the uncontrolled output. In particular, this is the case for disturbance 2, for which the gain is reduced from about 10 to 0.30 and less. The best one-point control scheme is seen to be scheme 1 where the effect of disturbance 1 is -1.32, which is only slightly above one in magnitude. This scheme corresponds to controlling output y_2 (the bottom composition) with u_2 (the boilup V) while letting y_1 (the top composition) being uncontrolled, which also from a physical point of view, is a reasonable control scheme. Frequency-dependent plots for scheme 1 show that the same conclusion applies also at higher frequencies. This is seen in Figure 7.2 where we show for disturbance 1 both the open-loop disturbance gain (G_{d11}, Curve 1) and the partial disturbance gain ($P^{2,2}_{1,d1}$, Curve 2) as function of frequency.

Let us next consider how we may reduce the effect of disturbance 1 (the feed flowrate F) on y_1 (which is $P_d(0) = -1.32$ at steady-state) to be less than 1 by using a feed forward controller based on measuring d_1 (the feed flowrate F) and adjusting u_1 (the reflux L). In practice, this is easily implemented as a ratio controller which keeps L/F constant. This eliminates the steady-state effect of d_1 on y_1 (provided the other control loop is closed). With $P_u(0) = g_{11} - g_{12}g^{-1}_{22}g_{21} = -2.45$ we get $u_1 = -P^{-1}_u(0)P_d(0)d_1 = -1.32/2.45d_1 = -0.54d_1$. The resulting disturbance effect is shown in Figure 7.2 as curve 3. However, due to measurement error we cannot achieve perfect feed forward control, so let us assume the error is 20% and use $u_1 = -1.2 \cdot 0.54d_1$. The steady-state effect of the disturbance is then $P_d(0)(1 - 1.2) = 0.265$, which is still acceptable. However, as seen from the frequency-dependent plot (curve 4), the effect is above 0.5 at higher frequencies, which may not be desirable. The reason for the peak is that the feed forward controller, which is purely static, reacts too fast and in fact makes the response worse at higher frequencies (as seen when comparing curves 3 and 4 with curve 2). To avoid this we filter the feed forward action with a time constant of 3 min resulting in the following feed forward controller: $u_1 = -\frac{0.54}{3s+1}d_1$. To be realistic we again assume 20% error, and the resulting effect of the disturbance on the uncontrolled output is shown by curve 5. We see that the effect is now less than 0.265 at all frequencies.

7.4.4   Sequential controller design

One common way to implement a hierarchical control system, is to first implement a *lower-layer* control system for controlling the outputs y_2. With this lower-layer control system in place, one designs a controller K_1 for control of y_1. Some criteria for selecting u_2 and y_2 in this case, are given in (Hovd and Skogestad, 1993).

7.5   Partitioning tools

The subsets y_1, y_2, u_1 and u_2 can be expressed as:

$$y_1 = N_{y^\perp}^T y, \;\; y_2 = N_y^T y, \;\; u_1 = N_{u^\perp}^T u, \;\; u_2 = N_u^T u$$

where N is a selection (projection) matrix. For example, to select the two first outputs of a plant set $N_y = \begin{bmatrix} e_1 & e_2 \end{bmatrix}$ where e_i is a vector of size l with zeros in all elements except in position i which contains 1. With this notation the uncontrolled and controlled outputs can be written in terms of d, u_1 and u_2

$$y_1 = \overbrace{N_{y^\perp}^T G N_{u^\perp}}^{G_{11}} u_1 + \overbrace{N_{y^\perp}^T G N_u}^{G_{12}} u_2 + \overbrace{N_{y^\perp}^T G_d}^{G_{d1}} d \tag{7.18}$$

$$y_2 = \underbrace{N_y^T G N_{u^\perp}}_{G_{21}} u_1 + \underbrace{N_y^T G N_u}_{G_{22}} u_2 + \underbrace{N_y^T G_d}_{G_{d2}} d \tag{7.19}$$

7.5.1   RGA and the selection problem

Several authors have used the relative gain array (7.5) as a selection tool for control structure design and in particular in the pairing problem for decentralized control. Results which are connected to the row sums and column sums have also been suggested. Chang and Yu (1990) recognized that the row sums of the RGA stayed between zero and one for non-square plants with full column rank (more outputs than inputs). They used this to rank candidate outputs corresponding to the row sums of the RGA. Recently, Cao (1995) presented a similar suggestion for the input selection problem, involving the column sums of the RGA. Cao (1995) also derived the relation between input singular vectors and the column sums of the RGA. In Theorem 7.1 we generalize the result in (Cao, 1995) to the outputs (row sums of RGA) and also provide a simpler proof.

In the following, consider the model $y = Gu$ and write the singular value decomposition of G as

$$G = U\Sigma V^H = U_r \Sigma_r V_r^H \tag{7.20}$$

where Σ_r consists only of the $r = \text{rank}(G)$ nonzero singular values, U_r consists of the r first columns of U, and V_r consists of the r first columns of V.

Let e_j and e_i be defined as above ($u_j = e_j^T u$, $y_i = e_i^T y$). Then $e_j^T V_r$ yields the projection of a unit input u_j onto the non-zero input space of G, and $e_i^T U_r$ yields the projection of a unit

output y_i onto the non-zero output space of G. We follow (Cao, 1995) and define

Projection for input j onto the effective input space: $\quad \eta_{\mathrm{I},j} = \|e_j^T V_r\|_2 \quad$ (7.21)

Projection for output i onto the effective output space: $\quad \eta_{\mathrm{O},i} = \|e_i^T U_r\|_2 \quad$ (7.22)

The following theorem links the SVD to the RGA.

THEOREM 7.1 (RGA AND SVD).

$$\sum_{j=1}^m \lambda_{ij} = \|e_i^T U_r\|_2^2 \, ; \qquad \sum_{i=1}^l \lambda_{ij} = \|e_j^T V_r\|_2^2 \qquad (7.23)$$

The proof is given in Section A. Note that $\|e_i^T U_r\|_2$ is simply the 2-norm of row i in U_r. Essentially, for the case of extra measurements (outputs) one may consider eliminating measurements corresponding to rows in the RGA where the sum of the elements is much smaller than 1. Similarly, for the case of extra manipulations (inputs) one may consider eliminating manipulations corresponding to columns in the RGA where the sum of the elements is much smaller than 1. The RGA/SVD used in this way can be a useful tool for screening because a single computation includes all the alternative measurements and/or manipulations and thus avoids the combinatorial problem. However, we emphasize that there is no clear control engineering interpretations of this approach, as is the case with the pole vectors and minimum input usage for stabilization (see Chapter 6).

When G is square and non-singular, the input and output projections are equal to one (column and rows of RGA for a square non-singular G sums to one), and the RGA provides no ranking of inputs and outputs. We may then obtain more information by directly considering the SVD. We have

RESULT 7.1 (SVD FOR INPUT/OUTPUT SELECTION). *A ranking of potential inputs and outputs used in a control structure of dimension* $k_y \times k_u$ ($k_y < r$ *and* $k_u < r$, *where* $r = \mathrm{rank}(G)$), *can be obtained by considering the 2-norm of the rows in the matrices* U_{k_y} *and* V_{k_u} *where* U_{k_y} *consists of the first* k_y *columns of* U_r, *and* V_{k_u} *consists of the first* k_u *columns of* V_r.

This can be justified from the fact that the first k_y columns of U_r and the first k_u columns of V_r correspond to the most significant (largest gain) directions, and the 2-norms of the rows correspond to the input and output projections of the subsystem of dim $k_y \times k_u$. The singular value σ_{k+1} is a measure of the information disregarded in the partial control structure, i.e.

$$\|G - N_y G_{22} N_u^T\|_2 \geq \sigma_{k+1}$$

where $k = \max\{k_y, \, k_u\}$. See also example 7.2.

EXAMPLE 7.2 INPUT/OUTPUT SELECTION FOR FCC PROCESS. For the linear model of the FCC process considered by (Hovd and Skogestad, 1993; Wolff et al., 1992), we have at steady-state

$$G = \begin{bmatrix} 10.16 & 5.59 & 1.43 \\ 15.52 & -8.37 & -0.71 \\ 18.05 & 0.42 & 1.80 \end{bmatrix} ; \qquad G_d = \begin{bmatrix} 1.66 & 0.36 & -13.61 \\ 0.47 & 0.23 & -3.89 \\ 1.86 & 0.56 & -15.30 \end{bmatrix}$$

From a SVD of $G(j\omega)$ we find $\underline{\sigma}(G(j\omega)) < 1 \ \forall \omega$. Hence, it is likely to encounter input constraints for certain combinations of disturbances and reference changes. We therefore consider 2×2 control of the FCC process. With the two strongest input and output directions i.e. $U_2 = [\,u_1 \quad u_2\,]$, $V_2 = [\,v_1 \quad v_2\,]$, the 2-norms of the rows becomes

$$\eta_{\mathrm{I}} = [\,0.997 \quad 0.982 \quad 0.201\,]^T \quad \eta_{\mathrm{O}} = [\,0.774 \quad 0.927 \quad 0.736\,]^T$$

We clearly see that the input u_3 has little effect on G and that this input may be considered unused. For the outputs the situation is not so obvious, y_1 and y_3 seems to be of equal importance. However, for higher frequencies (not shown) $\eta_{\mathrm{O},1}$ and $\eta_{\mathrm{O},2}$ approaches 1, whereas $\eta_{\mathrm{O},3}$ approaches 0, so we select y_1 and y_2 together with u_1 and u_2 in a partial control structure of size 2×2. It is worth noting that this control structure (denoted Hicks) was considered by (Hovd and Skogestad, 1993) as the best one. They argued from a controllability point of view taking into account RHP-zeros, constraints and different operating modes.

EXAMPLE 7.1 CONTINUED. Instead of computing the partial disturbance gains to obtain the best output and the best input for one-point control of the distillation column, we use the input and output projections to screen the candidate inputs and outputs. We only consider the input and output directions corresponding to the largest singular value in U and V, i.e. use $U_1 = u_1$ and $V_1 = v_1$. This seems reasonable since $\underline{\sigma}(G) \ll \bar{\sigma}(G)$ at steady-state. We obtain

$$\eta_{\mathrm{O}} = \begin{bmatrix} 0.624 \\ 0.781 \end{bmatrix} \quad \text{and} \quad \eta_{\mathrm{I}} = \begin{bmatrix} 0.707 \\ 0.707 \end{bmatrix}$$

That is, we find that the best output is the bottom composition. However, it is not clear which input to use.

The criteria for selecting inputs and outputs through the use of RGA, considering all non-singular directions or only the k first non-singular directions, can be viewed in terms of maximizing the information contained in those directions on the selected inputs/outputs. It is not clear what this selection procedure implies in terms of measures like $\underline{\sigma}(G_{22})$, $\bar{\sigma}(G_{22})$, $\gamma(G_{22})$ and $\|G - N_y G_{22} N_u^T\|$. However, since there is a finite number of combinations, it is possible to find the projection matrices N_y and N_u which maximize $\underline{\sigma}(G_{22})$ or minimize $\|G - N_y G_{22} N_u^T\|$ for a given dimension $k_y \times k_u$ of G_{22}, simply by testing all possibilities.

The following example shows that although the RGA is an efficient screening tool, it must be used with some caution.

EXAMPLE 7.3. Consider a plant with 2 inputs and 4 candidate outputs of which we want to select 2. We have

$$G = \begin{bmatrix} 10 & 10 \\ 10 & 9 \\ 2 & 1 \\ 2 & 1 \end{bmatrix}, \quad \Lambda = \begin{bmatrix} -2.57 & 3.27 \\ 1.96 & -1.43 \\ 0.80 & -0.42 \\ 0.80 & -0.42 \end{bmatrix}$$

The four row sums of RGA are 0.70, 0.53, 0.38 and 0.38. To maximize the output projections we would select outputs 1 and 2. However, this yields a plant $G_1 = \begin{bmatrix} 10 & 10 \\ 10 & 9 \end{bmatrix}$ which is ill-conditioned with large RGA-elements, and most likely difficult to control. Selecting output 1 and 3 yields $G_2 = \begin{bmatrix} 10 & 10 \\ 2 & 1 \end{bmatrix}$ which is well conditioned. For comparison, the minimum singular values are $\underline{\sigma}(G) = 1.05$,

$\underline{\sigma}(G_1) = 0.51$, $\underline{\sigma}(G_2) = 0.70$. The minimized condition numbers ($\gamma^*(A) = \min_{D_1,D_2} \gamma(D_2 A D_1)$, where D_1 and D_1 are diagonal matrices) are $\gamma^*(G) = 11.69$, $\gamma^*(G_1) = 37.97$ and $\gamma^*(G_2) = 5.83$. This clearly shows that G_1 is the most ill-conditioned of all the matrices G, G_1 and G_2.

7.5.2 Least square and "true" partial control

In this section we view the rational transfer function $G(s)$ as a matrix function parameterized in the complex variable s. Then we can use the least square solution to the full (optimal) and the partial control problems, to quantify the imposed performance loss by partial control for a particular choice of N_y and N_u. To be able to compare the results in the full and the partial control problems, it only make sense to consider reference changes in the secondary outputs y_2, i.e. we consider the control error

$$\rho = y - \begin{bmatrix} 0 \\ r_2 \end{bmatrix} = y - \begin{bmatrix} 0 \\ R_2 \tilde{r}_2 \end{bmatrix} = y - N_y R_2 \tilde{r}_2$$

on a frequency-by-frequency basis. The least square control errors (ρ) for reference changes in $\tilde{r}_2$ and disturbance rejection for the full (ρ_f) and the partial (ρ_p) control problems, becomes

$$\rho_f = \begin{bmatrix} (GG^\dagger - I)N_y R_2 & -(GG^\dagger - I)G_d \end{bmatrix} \begin{bmatrix} \tilde{r}_2 \\ d \end{bmatrix} \tag{7.24}$$

$$\rho_p = \begin{bmatrix} G_{12}G_{22}^\dagger R_2 & G_{d1} - G_{12}G_{22}^\dagger G_{d2} \\ (G_{22}G_{22}^\dagger - I)R_2 & -(G_{22}G_{22}^\dagger - I)G_{d2} \end{bmatrix} \begin{bmatrix} \tilde{r}_2 \\ d \end{bmatrix} \tag{7.25}$$

The proofs of (7.24) and (7.25) are given in Section A. For the performance loss to be small, we want $\|\rho_p\|$ to be close to $\|\rho_f\|$. We note that the control errors can be interpreted on a frequency-by-frequency basis and represents a lower bound on the best achievable performance measured in the 2-norm. Thus, it is an induced two norm performance.

7.6 Summary

We have given a brief introduction to partial control. The partial disturbance, partial reference gains and the partial gain for measurement noise are introduced and the partial disturbance gain is related to the previouly defined partial disturbance gain (Skogestad and Wolff, 1992). We have shown how the partial disturbance gain, and the gain for the unused inputs can be used to find the best one-point control structure (including feed forward control) for a binary distillation column. It is important to note that we arrived at this control structure without designing any controllers.

  We have also established a direct relationship between the RGA and SVD which generalizes previous results (Cao, 1995; Chang and Yu, 1990). These tools, and the relationship between RGA and SVD, can be used to obtain a ranking of the possible inputs and outputs. However, they should be used with care since there are many other factors which determine controllability.

References

Bristol, E. H. (1966). On a new measure of interactions for multivariable process control, *IEEE Transactions on Automatic Control* **AC-11**: 133–134.

Cao, Y. (1995). *Control Structure Selection for Chemical Processes Using Input-output Controllability Analysis*, PhD thesis, University of Exeter.

Chang, J. and Yu, C. (1990). The relative gain for non-square multivariable systems, *Chem. Eng. Sci.,* **45**(5): 1309–1323.

Häggblom, K. (1994). Modelling of control structures for partially controlled plants, *IFAC Workshop on Intergration of Process Design & Control'94, Baltimore, MD, June 27-28, 1994,* pp. 183–188.

Häggblom, K. and Waller, K. (1992). Control structures, consistency, and transformations, *Practical Distillation Control, W. L. Luyben (ed.), Van Nostrand Reinhold, 1992,* pp. 192–228.

Havre, K. and Skogestad, S. (1996). Input/output selection and partial control, *Proc. from 13th IFAC World Congress*, San Francisco, USA, pp. 181–186.

Hovd, M. and Skogestad, S. (1992). Simple frequency-dependent tools for control system analysis, structure selection and design, *Automatica* **28**(5): 989–996.

Hovd, M. and Skogestad, S. (1993). Procedure for regulatory control structure selection with application to the FCC process, *AIChE Journal* **39**(12): 1938–1953.

Lee, J. H., Braatz, R. D., Morari, M. and Packard, A. (1995). Screening tools for robust control structure selection, *Automatica* **31**(2): 229–235.

Lee, J. H. and Morari, M. (1991). Robust measurement selection, *Automatica* **27**(3): 519–527.

Lee, J. H. and Morari, M. (1996). Control structure selection and robust control system design for a high-purity distillation column, *IEEE Trans. on Cont. Sys. Tech.,* In print .

Manousiouthakis, V., Savage, R. and Arkun, Y. (1986). Synthesis of decentralized process control structures using the concept of block relative gain, *AIChE Journal* **32**(6): 991–1003.

Mejdell, T. (1990). *Estimators for Product Composition in Distillation Columns*, PhD thesis, Norwegian University of Science and Technology, Trondheim.

Moore, C., Hackney, J. and Canter, D. (1987). Selecting sensor location and type for multivariable processes, *Shell Process Control Workshop (book), Butterworth* .

Reeves, D. and Arkun, Y. (1989). Interaction measures for nonsquare decentralized control structures, *AIChE J,* **35**(4): 603–613.

Sandelin, P., Häggblom, K. and Waller, K. (1991). Disturbance rejection properties of control structures at one-point control of a two-product distillation column., *Ind. Eng. Chem. Res.* pp. 1187–1193.

Skogestad, S. and Morari, M. (1987). The effect of disturbance directions on closed loop performance, *Ind. Eng. Chem. Res.,* **26**: 2029–2035.

Skogestad, S. and Postlethwaite, I. (1996). *Multivariable Feedback Control, Analysis and Design*, John Wiley & Sons, Chichester.

Skogestad, S. and Wolff, E. A. (1992). Controllability measures for disturbance rejection, *IFAC Workshop on Interactions between Process Design and Process Control*, London, UK, pp. 23–29.

Stanley, G., Marino-Galarraga, M. and McAvoy, T. J. (1985). Shortcut operability analysis. 1. The relative disturbance gain, *Industrial and Engineering Chemistry Process Design and Development* **24**: 1181–1188.

Tolliver, T. L. and McCune, L. C. (1980). Finding the optimum temperature control trays for distillation columns, *InTech* .

Waller, K. V., Häggblom, K. E., Sandelin, P. M. and Finnerman, D. H. (1988). Disturbance sensitivity of distillation control structures, *AIChE Journal* **34**(5): 853–858.

Wolff, E. A. and Skogestad, S. (1996). Temperature cascade control of distillation columns, *Ind. Eng. Chem. Res.* **35**(2): 475–484.

Wolff, E. A., Skogestad, S., Hovd, M. and Mathisen, K. (1992). A procedure for controllability analysis, *IFAC Workshop on Interactions between Process Design and Process Control*, London, UK, pp. 127–132.

Yu, C. C. and Luyben, W. L. (1984). Use of multiple temperatures for the control of multicomponent distillation columns, *Ind. Eng. Chem. Process Des. Dev.* pp. 590–597.

Yu, C. C. and Luyben, W. L. (1987). Control of multicomponent distillation columns using rigourous compositon estimators, *I. Cheme. E. Symp. Ser.* .

Zhao, Y. and Skogestad, S. (1994). A comparison of continuous various control schemes for continuous bioreactor, *Proc. IFAC-Symposium ADCHEM'94*, Kyoto, Japan, pp. 325–330.

Appendix A Proofs of the results

Proof of Theorem 7.1. The proof of the identities in (7.23) are given for the general case. Write the SVD of G as $G = U_r \Sigma_r V_r^H$ where Σ_r is invertible. We have that $g_{ij} = e_i^T U_r \Sigma_r V_r^H e_j$, $[G^\dagger]_{ji} = e_j^T V_r \Sigma_r^{-1} U_r^H e_i$, $U_r^H U_r = I_r$ and $V_r^H V_r = I_r$ where I_r denotes identity matrix of dim $r \times r$. The row sum becomes (sum of the elements in row i)

$$
\begin{aligned}
\sum_{j=1}^m \lambda_{ij} &= \sum_{j=1}^m e_i^T U_r \Sigma_r V_r^H e_j e_j^T V_r \Sigma_r^{-1} U_r^H e_i \\
&= e_i^T U_r \Sigma_r V_r^H \underbrace{\sum_{j=1}^m e_j e_j^T}_{I_m} V_r \Sigma_r^{-1} U_r^H e_i = \| e_i^T U_r \|_2^2
\end{aligned}
$$

and for the column sum (the sum of the elements in column j)

$$
\begin{aligned}
\sum_{i=1}^l \lambda_{ij} &= \sum_{i=1}^l e_j^H V_r \Sigma^{-1} U_r^H e_i e_i^H U_r \Sigma V_r^H e_j \\
&= e_j^H V_r \Sigma^{-1} U_r^H \underbrace{\sum_{i=1}^l e_i e_i^H}_{I_l} U_r \Sigma V_r^H e_j = \| V_r^H e_j \|_2^2 \quad (7.26)
\end{aligned}
$$

$\square$

Proof of (7.24). We set $y_1 = 0$, i.e. we want to reject disturbances and reference changes $\tilde{r}_2$ in y_1, and we set $y_2 = r_2 = R_2\tilde{r}_2$, i.e. track reference changes $\tilde{r}_2$ and reject disturbances d in y_2. The problem is to find the least square solution $u^\dagger$ to

$$\begin{bmatrix} 0 \\ r_2 \end{bmatrix} = \begin{bmatrix} 0 \\ R_2\tilde{r}_2 \end{bmatrix} = N_y R_2\tilde{r}_2 = Gu + G_d d \quad \Leftrightarrow \quad Gu = N_y R_2\tilde{r}_2 - G_d d \tag{7.27}$$

The least square solution $u^\dagger$ to (7.27) is

$$u^\dagger = G^\dagger(N_y R_2\tilde{r}_2 - G_d d) \tag{7.28}$$

By applying the control $u^\dagger$ in (7.28) the control error $\rho_f = y - \begin{bmatrix} 0 \\ R_2\tilde{r}_2 \end{bmatrix} = y - N_y R_2\tilde{r}_2$ becomes

$$\begin{aligned} \rho_f &= Gu^\dagger + G_d d - N_y R_2\tilde{r}_2 = GG^\dagger(N_y R_2\tilde{r}_2 - G_d d) + G_d d - N_y R_2\tilde{r}_2 \\ &= (GG^\dagger - I)\, N_y R_2\tilde{r}_2 - (GG^\dagger - I)\, G_d d \end{aligned}$$

$\square$

Proof of (7.25). We set $y_2 = r_2 = R_2\tilde{r}_2$ and $u_1 = 0$, i.e. track reference changes $\tilde{r}_2$ and reject disturbances d in y_2. The problem is to find the least square solution $u_2^\dagger$ to

$$r_2 = R_2\tilde{r}_2 = R_2\tilde{r}_2 = G_{22}u_2 + G_{d2}d \quad \Leftrightarrow \quad G_{22}u_2 = R_2\tilde{r}_2 - G_{d2}d \tag{7.29}$$

The least square solution $u_2^\dagger$ to (7.29) is

$$u_2^\dagger = G_{22}^\dagger(R_2\tilde{r}_2 - G_{d2}d) \tag{7.30}$$

By applying the control $u_2^\dagger$ in (7.30) the control error $\rho_p = y - \begin{bmatrix} 0 \\ R_2\tilde{r}_2 \end{bmatrix} = y - N_y R_2\tilde{r}_2$ becomes

$$\begin{aligned} \rho_p &= \begin{bmatrix} y_1 \\ y_2 - R_2\tilde{r}_2 \end{bmatrix} = \begin{bmatrix} G_{12}G_{22}^\dagger R_2\tilde{r}_2 + (G_{d1} - G_{22}G_{22}^\dagger G_{d2})d \\ (G_{22}G_{22}^\dagger - I)R_2\tilde{r}_2 - (G_{22}G_{22}^\dagger - I)G_{d2}d \end{bmatrix} \\ &= \begin{bmatrix} G_{12}G_{22}^\dagger R_2 & (G_{d1} - G_{22}G_{22}^\dagger G_{d2}) \\ (G_{22}G_{22}^\dagger - I)R_2 & -(G_{22}G_{22}^\dagger - I)G_{d2} \end{bmatrix} \begin{bmatrix} \tilde{r}_2 \\ d \end{bmatrix} \end{aligned}$$

$\square$

Chapter 8

Input/output selection and partial control. Part II: Tools for analyzing indirect and cascade control

Kjetil Havre[*] and Sigurd Skogestad[†]

Chemical Engineering,
Norwegian University of Science and Technology
N-7034 Trondheim, Norway.

Abstract

Integrated chemical process plants are in practice controlled using a hierarchy of control loops. The basis is to implement inner control loops, resulting in a partially controlled system. The idea is that the primary outputs, with these inner control loops closed should be less sensitive to disturbances. In addition it is desirable that the control error in the primary outputs should not be sensitive to control errors in the inner control loops. In this paper we present two simple tools for efficiently analyzing such problems.

---

[*] Also affiliated with: Institute for energy technology, P.O.Box 40, N-2007 Kjeller, Norway, Fax: (+47) 63 81 11 68, E-mail: Kjetil.Havre@ife.no.

[†] Fax: (+47) 73 59 40 80, E-mail: skoge@chembio.ntnu.no.

8.1   Introduction

Integrated chemical process plants are in practice controlled using a hierarchy of cascaded control loops. The reason for this is twofold: First, to allow for local disturbance rejection. Second, to make it possible to use simple process models, or to avoid the use of models all together, in the control system design.

The basis for cascade control is to implement inner control loops, resulting in a partially controlled system. The idea is that the primary outputs, with these inner loops closed, should be less sensitive to disturbances than the open-loop system. On the other hand, the control error in the primary outputs should not be sensitive to the control errors in the inner control loops.

To define the problem more carefully we rearrange and partition the outputs y and the inputs u into the following sets:

- y_1 – primary outputs (uncontrolled at the present control layer).
- y_2 – secondary outputs (controlled at the present control layer).
- u_1 – inputs not used (at the present control layer).
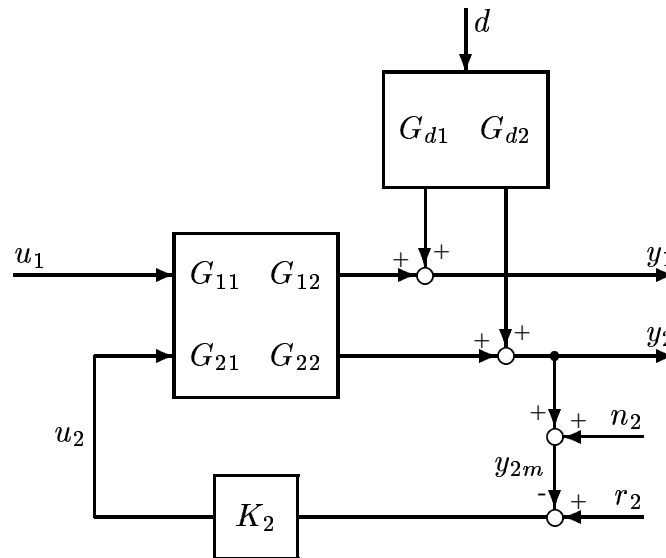- u_2 – inputs used to control y_2.

Figure 8.1: Block diagram of a partially controlled plant (G, G_d)

A block diagram of a partially controlled system (G, G_d) is shown in Figure 8.1. With this classification of inputs and outputs we can distinguish between the following four applications (see Chapter 7 for a discussion of the differences) of partial control.

1) *Indirect control.*
2) *Cascade control.*
3) *True partial control.*
4) *Decentralized control (sequential-design).*

In this paper the main focus is on *indirect control*, for which the control problem can be stated

as follows: We are given some "primary" variables y_1 with an associated control objective $y_1 \approx r_1$, where r_1 is the reference value for y_1. Assume that the primary variables y_1 are not measured, so the primary objective can not directly be measured. Instead, we have available some secondary outputs y_2, for which we have *no* control objective (so r_2 may be varied freely). In this case three approaches for controlling the primary variables are, see Figure 8.2:

1) **Centralized controller.** Design a centralized controller based on all available information about the process plant and all available measurements and known inputs (y_2 and r_1). This controller, which computes the optimal input u, combines estimation and control in a single "optimal" controller, see Figure 8.2(a).

2) **Inferential control.** Based on the known inputs (u) and measurements (y_2), inferential control estimates the primary variables ($\hat{y}_1$), and a separate controller manipulates u to achieve $\hat{y}_1 \approx r_1$, see Figure 8.2(b).

3) **Indirect control.** Only the secondary outputs are controlled, i.e. the controller manipulates u_2 to achieve $y_2 \approx r_2$ (where r_2 is a function of r_1). The aim is to indirectly achieve $y_1 \approx r_1$, see Figure 8.2(c).

With all relevant model information available, approach 1) will be the optimal and approach 3) will be the worst. On the other hand, the implementation of approach 3) requires only simple feedback control and no modeling effort. Therefore, if acceptable control of the primary variables (y_1) can be achieved with *indirect control*, this would generally be the preferred approach.
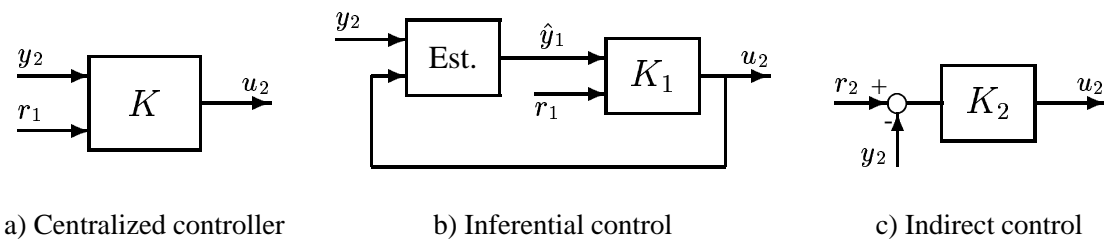

a) Centralized controller   b) Inferential control   c) Indirect control

Figure 8.2: Three approaches to indirect control of the primary variables y_1, using measurements of y_2

Cascade control is *indirect control* with an additional outer loop for adjusting r_2, see Figure 8.3. This is frequently used when additional measurements of the primary outputs y_1 are available, but fast control of y_1 by only measuring y_1 is not possible.

The differences between indirect and cascade control are mainly the frequency region of importance. In *indirect control* we want to keep $e_1 = y_1 - r_1$ small in spite of disturbances d and control errors in y_2. Since there is no measurement and feedback control of y_1, steady-state and low frequencies are most important in these cases. On the other hand, for *cascade control* the outer feedback loop takes care of the low frequencies, and in these cases the task of the inner control loops is disturbance rejection and to maintain good control at frequencies around and higher than the bandwidth ω_B of the outer control loops. Many of the same tools derived for indirect control therefore also applies to cascade control.
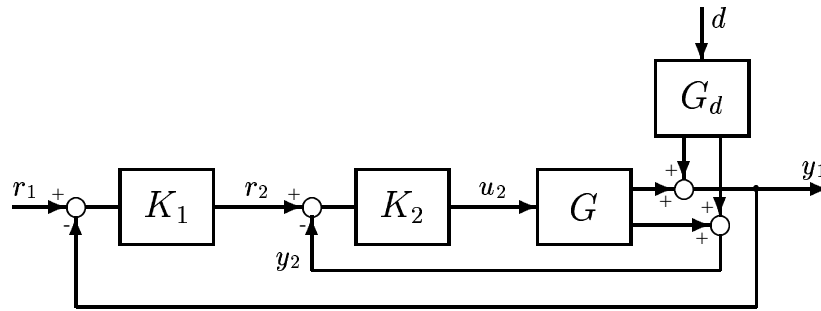
Figure 8.3: Cascade control

For *indirect* and *cascade control* we want to answer the following two questions:

1) Which variables should be selected as secondary measurements y_2?
2) How much can we improve the control of the primary variables y_1 by controlling the secondary variables y_2?

These two questions are closely related, in that a quantitative answer to the second question, gives a tool for answering the first one.

Indirect control of product compositions through two-point temperature control in a high-purity distillation column, studied in Chapter 9, fits this setup since frequent and reliable composition measurements are seldom available. So, instead of controlling the two product compositions (y_1), we control the temperatures (y_2) at two selected stages in the distillation column.

Sometimes there is a trade-off between the *sensitivity* to control errors in the secondary measurements and the *correlation* to the primary variables. If there is a control error $e_2 = y_2 - r_2$ in the secondary variables, then this results in a control error in the primary variables $e_1 = y_1 - r_1$. In a high-purity distillation column the gain from e_2 to e_1, and thus the sensitivity to measurement noise n_2, is very large for temperature measurements located close to the ends of the column. To reduce the *sensitivity* to the control errors e_2, the temperature measurements (y_2) should be placed towards the middle of the column. However, the *correlation* between secondary (y_2) and primary (y_1) variables is obviously better if the temperature measurements (y_2) are placed closer to the column ends.

In the paper we derive simple quantitative tools for addressing such issues. These tools are general controllability tools, i.e. they are *not* restricted to the high-purity distillation column application, and they are independent of the controller, i.e. design-independent controllability tools.

8.2   Previous work on measurement selection

When the primary control objective cannot be measured directly, one of the approaches is to use the *inferential control* scheme, e.g. see Stephanopoulos (1989). Different types of models can be used for estimation, which gives rise different types of inferential controllers with different properties. One class of estimators emphasize the importance of estimating the

effect of unknown disturbances on the primary variables. This includes Brosilow's inferential estimator (Weber and Brosilow, 1972; Joseph, Brosilow and Tong, 1978). Brosilow and co-workers suggest to select secondary measurements at steady-state according to the criteria:

1) Minimization of projection error, i.e. the nominal estimation error.
2) Minimization of the condition number for the steady-state model from the disturbances to the secondary outputs.

They indicate that the estimation error tends to decrease and the condition number tends to increase as the number of measurements increase. They leave the final decision in this trade-off to engineering judgement.

Morari and Stephanopoulos (1980) extend the work by Brosilow and co-workers to incorporate system dynamics based on the Kalman filter. They give several measurement selection criteria for secondary outputs, with the goal of minimizing the estimation error. They also assume that unmeasured process disturbances are of major importance, dominating the errors caused by measurement noise.

A procedure for sensor location to be used in inferential control is presented by Jørgensen, Goldschmidt and Clement (1984). The method distinguish between the purpose of surveillance and control. The selection of the secondary variables to be used in the estimation is based upon qualitative knowledge of process dynamics and open-loop stationary variances. Also this article emphasize the effect the unmeasured disturbances has on the primary variables by estimating the variances in the primary variables due to step changes in the unmeasured disturbances.

Mejdell and Skogestad (1993) performed a comparative study between the following three estimation methods:

1) Kalman-Bucy filter,
2) Brosilow's inferential estimator,
3) Static regression (PCR),

using as a case-study the estimation of product compositions in a high-purity distillation column. The performance of the estimators were compared using robust performance analysis (μ-analysis). Their conclusion is: For high-purity distillation, one can achieve remarkably good control performance with the static PCR estimator, which is almost as good as the dynamic Kalman filter. Furthermore, they conclude that a particular disadvantage of the Brosilow inferential estimator is that the estimate may not improve by adding measurements due to the sensitivity to modeling errors. For all estimators, they found that the use of input flow measurements does not improve the estimator performance, but does in fact damage the performance if a static estimator like Brosilow's inferential estimator and the PCR is used. This seems to contradict the importance of estimating the effect of the unknown disturbances (inputs) at least for the high-purity distillation example.

A different approach to the problem of measurement selection for linear multivariable control system is taken in (Ghosh and Knapp, 1989). They consider both deterministic and stochastic systems. The approach taken is to choose from all available measurements that subset which minimizes a criterion of performance subject to an investment cost constraint. The problem is formulated as an non-linear integer minimization problem. The control per-

formance criterion used, is the standard quadratic criterion from optimal control theory. Note that in this approach the number of measurements is traded-off against a maximum allowable investment cost in the measurements.

The three papers (Lee and Morari, 1991; Lee et al., 1995; Lee and Morari, 1996) consider robust control structure design through proper choice of measurements and manipulations. The paper (Lee and Morari, 1991) outline three approaches to secondary measurement selection. The first approach is to select the set of measurements which minimizes the robust performance specification (μ-analysis). It involves synthesizing a controller K for each candidate measurement set, and then compare the μ values for each set and choose the one with minimum μ. As they note, there are significant theoretical and practical drawbacks (in terms of computation) in this formulation. They conclude that in view of the combinatorial nature of the problem this first approach alone is clearly not a feasible solution to the measurement selection problem. In the second approach, necessary conditions for the existence of a controller achieving robust performance are used as screening tools to eliminate candidate measurement sets for which no controller exists that achieves robust performance. In approach three, sufficient conditions are used to locate measurement sets for which controllers achieving robust performance exists. The development of tight sufficient conditions useful for measurement selection and controller design is the focus of the paper. They derive design-dependent (assume Internal Model Control, IMC) measurement selection criteria for both indirect and inferential control.

In the second paper, Lee et al. (1995) introduces a set of design-independent screening tools that can be used to reduce the number of control structure candidates. Many of the same ideas in (Lee and Morari, 1991) carry over but they manage to make the tools independent of a particular controller design by dropping the causality requirement on the controller and using the Youla parameterization. The tools derived involves checking the spectral radius of convex matrix functions. Thus, the screening tools can be evaluated via convex optimization. The general approach taken in the paper is complicated both in terms of computation and in the effort required to define the robust performance objective. In the paper Lee et al. compares the two selection criteria:

1) Minimizing a weighted sum of the projection error and the condition number (as suggested Brosilow *et al.*).
2) Minimizing the worst-case closed-loop error.

Lee et al. shows that the first one corresponds to minimizing an upper bound on the worst-case closed-loop error. The results show that this selection criterion provides conservatism, and this conservativeness stems not only from the inequalities in the derivation but also from the fact that it assumes a least-squares type controller. From the results it is noted that this conservatism can cause the selection criterion to select measurement sets which are not physically intuitive.

In the third paper, Lee and Morari (1996) summarizes the results from the two first papers and discuss implementation of the controller, capable of handling hard constraints through the use of on-line optimization, i.e. a MPC implementation of the controller. In all papers they apply the results to the problem of selecting temperature measurements for indirect control of the product compositions in high-purity distillation columns. In the papers (Lee

and Morari, 1991; Lee and Morari, 1996) they use column A studied by Skogestad and Morari (1988) and in the paper (Lee et al., 1995) they use the column studied in (Joseph et al., 1978).

The approach taken in inferential control and the above mentioned articles, differ from the approach taken in this paper. We consider *indirect control* where the aim is to reduce the error in the primary variables by controlling the secondary variables. Indirect control as discussed in this paper is obviously related to inferential control and it is worth noting that Marlin (1995) uses the term inferential control to mean indirect control as discussed in this paper. So, there is no universal agreement on these terms.

8.3 Analysis of indirect control

We consider linear time invariant transfer function models on the form

$$y(s) = G(s)u(s) + G_d(s)d(s) \tag{8.1}$$

where u is the vector of manipulated inputs, d is the vector of disturbances and y is the vector of outputs. $G(s)$ and $G_d(s)$ are rational transfer function matrices of dimensions $l \times m$ and $l \times n_d$. To simplify the notation we omit to show the dependence on the complex number s for signals. However, to emphasize that the results are frequency dependent we explicitly show the dependency of the complex variable s for transfer functions in the main equations.

With the partitioning of the inputs and the outputs given in Section 8.1, the open-loop model (8.1) becomes

$$y_1 = G_{11}(s)u_1 + G_{12}(s)u_2 + G_{d1}(s)d \tag{8.2}$$
$$y_2 = G_{21}(s)u_1 + G_{22}(s)u_2 + G_{d2}(s)d \tag{8.3}$$

In this paper we do not consider the use of u_1, i.e. the set u_1 is empty, so u_2 can be regarded as the set consisting of all inputs, i.e. $u_2 = u$. Nevertheless, we will keep the variables u_1 for completeness.

We assume[1] that $G_{22}(s)$ is square and invertible (at a given value of s). We can use (8.3) to express u_2 as a function of y_2, u_1 and d

$$u_2 = G_{22}^{-1}(s)\left(y_2 - G_{21}(s)u_1 - G_{d2}(s)d\right) \tag{8.4}$$

Substituting (8.4) into (8.2) yields

$$\boxed{y_1 = P_u(s)u_1 + P_d(s)d + P_y(s)y_2} \tag{8.5}$$

where

$$P_u(s) \triangleq G_{11}(s) - G_{12}G_{22}^{-1}G_{21}(s) \tag{8.6}$$
$$P_d(s) \triangleq G_{d1}(s) - G_{12}G_{22}^{-1}G_{d2}(s) \tag{8.7}$$
$$P_y(s) \triangleq G_{12}G_{22}^{-1}(s) \tag{8.8}$$

---

[1]Strictly speaking, this is a frequency-by-frequency analysis, $s = j\omega$ (one particular frequency being the steady-state, $\omega = 0$).

Here P_d is the *partial disturbance gain*, P_y is the gain[2] from y_2 to y_1 and P_u is the partial input gain from the unused inputs u_1.

If we look more carefully at (8.5) then we see that the matrix P_d gives the effect of disturbances on the primary outputs y_1, when the manipulated inputs u_2 are adjusted to keep y_2 constant, which is consistent of the original definition of the partial disturbance gain given by Skogestad and Wolff (1992).

REMARK 1. Note that no approximation[3] has been made when deriving (8.5). Equation (8.5) applies on a frequency-by-frequency basis.

REMARK 2. Skogestad and Wolff (1992) considered the special case with one uncontrolled output (i) and one unused input (j) and derived in this special case the following expression for the partial disturbance gain

$$PDG = \frac{\partial y_i}{\partial d_k}\bigg|_{u_j, y_{l \neq j}} = \frac{[G^{-1}G_d]_{jk}}{[G^{-1}]_{ji}} \tag{8.9}$$

REMARK 3. The expression (8.9) was generalized by Zhao (1996) to the case with n uncontrolled outputs and n unused inputs

$$P_d = [G^{-1}]_{11}^{-1}[G^{-1}G_d]_1 \tag{8.10}$$

where G^{-1} are partioned according to the dimensions of y_1, y_2, u_1 and u_2 and $[G^{-1}]_{11}$ denotes the upper left block of G^{-1} and $[G^{-1}G_d]_1$ is the upper block of $G^{-1}G_d$.

REMARK 4. Similarly we have

$$P_y = -[G^{-1}]_{11}^{-1}[G^{-1}]_{12} \tag{8.11}$$

Proof of (8.11). Set $G_d = \begin{bmatrix} G_{d1} \\ G_{d2} \end{bmatrix} = \begin{bmatrix} 0 \\ -I \end{bmatrix}$ in (8.10).   □

For the case with one uncontrolled output i and one unused input j we obtain

$$P_y = \frac{\partial y_i}{\partial r_k}\bigg|_{u_j, y_{l \neq j}} = -\frac{[G^{-1}]_{jk}}{[G^{-1}]_{ji}} \tag{8.12}$$

In general, we want the effect of disturbances d on the error in the primary outputs y_1 to be small. To require $P_d = 0$ implies $G_{d1} = G_{12}G_{22}^{-1}G_{d2}$ or if G_{d2}^{-1} exists $G_{12}G_{22}^{-1} = G_{d1}G_{d2}^{-1}$, that is, the effect of d on $\|y_1\|/\|y_2\|$ is the same as the effect of u_2 on $\|y_1\|/\|y_2\|$. This can be achieved if $G_{12} \approx k \cdot G_{d1}$ and $G_{22} \approx k \cdot G_{d2}$ for any constant k. However, we also need to take into account how easy it is to control y_2, i.e. the control error $e_2 = y_2 - r_2$. So, *the selection of controlled outputs and inputs used for control should not be based on the expression for P_d alone.*

In the next two sections we apply (8.5) to indirect and cascade control.

8.3.1   Relating e_1 to the disturbances and control error

The first expression is just a slight variation of (8.5) where we introduce the control error for y_2, defined as

$$e_2 \triangleq y_2 - r_2 \tag{8.13}$$

---

[2]P_y is closely related to the partial reference gain P_r and the partial gain for measurements noise, defined in Chapter 7. More precisely we have $P_r = P_y R_2$ and $P_n = P_y N_2$.

[3]The assumption that G_{22}^{-1} exists for all frequencies can be relaxed by replacing the inverse with the pseudo-inverse.

where r_2 is the reference value for the secondary outputs y_2, see Figure 7.1. Substituting $y_2 = r_2 + e_2$ in (8.5) yields

$$y_1 = P_u(s)u_1 + P_d(s)d + P_y(s)r_2 + P_y(s)e_2 \qquad (8.14)$$

or

$$\boxed{e_1 = y_1 - r_1 = P_u(s)u_1 + P_d(s)d + P_y(s)r_2 + P_y(s)e_2 - r_1} \qquad (8.15)$$

Importantly, we assume that r_2 and e_2 are independent variables. There are two sources for the control error e_2:

1) The control of the secondary variables y_2 is not "tight".
2) Measurement noise n_2 in the secondary variables y_2.

8.3.2 Relating e_1 to the optimization and control error

For a short moment let us move one layer up in the control hierarchy and assume that the control loops at the regulatory control layer are closed, i.e. the secondary outputs y_2 are controlled using u_2. We assume that the references r_2 to the controlled variables y_2 can be used as degrees of freedom to improve control of the primary variables. We put ourselves in the position of an optimizer and consider the "optimal" values of y_2 for a given disturbance d and reference r_1. These are obtained by setting $y_1 = r_1$ in (8.5) and solving for y_2. We get (assuming that the appropriate inverse exists)

$$y_{2,\mathrm{opt}}(d, r_1) = P_y^{-1}(s)r_1 - P_y^{-1}P_u(s)u_1 - P_y^{-1}P_d(s)d \qquad (8.16)$$

where

$$P_y^{-1}(s) \quad = \quad G_{22}G_{12}^{-1}(s) \qquad (8.17)$$
$$P_y^{-1}P_u(s) \quad = \quad G_{22}G_{12}^{-1}G_{11}(s) - G_{21}(s) \qquad (8.18)$$
$$P_y^{-1}P_d(s) \quad = \quad G_{22}G_{12}^{-1}G_{d1}(s) - G_{d2}(s) \qquad (8.19)$$

We have assumed that the inverse G_{12}^{-1} exists for all $s = j\omega$.

To express the difference between the implemented value of r_2 and its "optimal" value $y_{2,\mathrm{opt}}(d, r_1)$, it is useful to introduce the "optimization error"

$$e_{2,\mathrm{opt}} = r_2 - y_{2,\mathrm{opt}} \qquad (8.20)$$

We then get

$$y_2 = \underbrace{y_{2,\mathrm{opt}} + e_{2,\mathrm{opt}}}_{r_2} + e_2 \qquad (8.21)$$

Substituting (8.21) and (8.16) into (8.5) yields

$$\boxed{e_1 = y_1 - r_1 = P_y(s)(e_2 + e_{2,\mathrm{opt}})} \qquad (8.22)$$

Equation (8.22) makes sense since we must have $y_1 = r_1$ if y_2 is at its "optimal" value such that $e_2 = 0$ and $e_{2,\mathrm{opt}} = 0$.

8.4   Measurement selection for indirect control

In this section we consider the following problem:

- Which variables should be selected as secondary measurements?

More specifically we want to answer the following question:

- How small can we keep e_1 by controlling the secondary variables y_2?

From (8.15) and (8.22) we get the following two approaches (see the derivation below):

1) Minimize the effect of disturbances and control error, i.e. minimize $\| [\, P_d \quad P_y \,] \|$.

2) Minimize the magnitude of $P_y = G_{12}G_{22}^{-1}$, which corresponds[4] to *maximize* the gain in the weak direction of the controlled subsystem G_{22}, i.e. maximize $\underline{\sigma}(G_{22})$.

The scaling of the variables are discussed in Section A, and a simple example to demonstrate the two approaches is given in Section 8.6.

For indirect control all frequencies should be considered and in particular steady-state. The results also apply to cascade control, but in these cases frequencies around and higher than the bandwidth ω_B of the outer loop are most important. Also, for cascade control we must consider the controllability of $P_u(s)$ and $P_r(s) = P_y R_2(s)$ at frequencies lower than ω_B.

8.4.1   Approach 1: Minimize $\| [\, P_d \quad P_y \,] \|$

The following additional assumptions are reasonable for indirect control:

1) u_1 is empty or u_1 is constant, i.e. we set $u_1 = 0$.
2) r_1 is constant, i.e. we set $r_1 = 0$.
3) r_2 is constant, i.e. we set $r_2 = 0$.

We then get from (8.15)

$$e_1 = P_d(s)d + P_y(s)e_2 \qquad (8.23)$$

First, we want P_d to be small such that, when the secondary variables y_2 are controlled, the effect of the disturbances d on the primary variables y_1 are small. Furthermore, we want P_y to be small, such that the effect of the control error (which is mainly caused by measurement noise) in the secondary variables y_2 on the primary variables y_1 are small. This can be summarized in the procedure given next.

Procedure for selecting controlled outputs for indirect control. Assume that the variables have been scaled as follows:

1) Disturbances: for each disturbance d_k the maximum allowed variation is of magnitude 1, i.e. $|d_k| \leq 1 \,\forall\, k$.

2) Secondary outputs y_2: the expected control error $e_{2,i}$ in each secondary output (which includes the measurement noise $n_{2,i}$) is of magnitude 1, i.e. $|e_{2,i}| \leq 1 \,\forall\, i$.

3) Primary outputs y_1: the expected control error $e_{1,i}$ in each primary output is of magnitude 1, i.e. $|e_{1,i}| \leq 1 \,\forall\, i$.

---

[4]Since G_{12} is independent of the choice of y_2.

For further information on the scalings applied, see Section A. To keep e_1 small we should then from (8.23) select sets of controlled secondary outputs y_2 which:

$$\text{Minimize:} \quad \| \, [\, P_d \quad P_y \,] \, \| \tag{8.24}$$

and we want this norm to be less than 1.

REMARK 1. When we scale the outputs y_2 relative to the measurement noise n_2, P_y in (8.24) is the same as the partial gain for measurement noise P_n introduced in Chapter 7 (page 181).

REMARK 2. The choice of norm in (8.24) depends on the scaling, but the choice is usually of secondary importance. The maximum singular value $\| \cdot \| = \bar{\sigma}(\cdot)$ arises if $\|d\|_2 \le 1$ and $\|e_2\|_2 \le 1$, and we want to minimize $\|e_1\|_2$.

8.4.2 Approach 2: Maximize the weak gain of G_{22}

The second approach is less exact, but provides more insight and is also applicable to other input/output selection problems than indirect control. Equation (8.22) forms the basis for this approach

$$e_1 = y_1 - r_1 = P_y(s)(e_2 + e_{2,\text{opt}})$$

Assume that $(e_2 + e_{2,\text{opt}})$ is of magnitude 1. Then from (8.22) we see that we should select secondary outputs y_2 such that $P_y = G_{12} G_{22}^{-1}$ is small, and since G_{12} is independent of the choice of y_2, this is the same as wanting G_{22}^{-1} small. Remember that $\bar{\sigma}(G_{22}^{-1}) = 1/\underline{\sigma}(G_{22})$, so we want the smallest singular value of G_{22} to be large and preferably as large as possible.

The criterion of maximizing $\underline{\sigma}(G_{22})$ assumes that the secondary outputs y_2 and the inputs u_2 has been scaled as follows:

1) Secondary outputs y_2: each of the candidate secondary outputs $y_{2,j}$ should be scaled such that the sum of the control error (e_2) and the optimization error $(e_{2,\text{opt}})$ is of magnitude 1, i.e. we want $|e_{2,j}| + |e_{2,j,\text{opt}}| \le 1 \,\forall\, j$.

2) Inputs u_2: we should scale the inputs u_2 such that they have similar effect on the primary outputs y_1.

Note that we use different scalings for y_2 in the two approaches. In approach 1 we scale y_2 based on the acceptable control error e_2 (which at steady-state is equal to the measurement noise), whereas in approach 2 the effect of the disturbances on the optimal value $y_{2,\text{opt}}$ is also included. For further information on the scalings applied, see Section A. Through (8.22) we have derived the following selection criterion

- Under the assumption of proper scaling of secondary outputs y_2 and inputs u_2 a useful criterion for selecting secondary outputs to be used for indirect control is to maximize $\underline{\sigma}(G_{22}(j\omega))$.

This criterion actually has a much wider applicability than for indirect control as considered here. Skogestad and Postlethwaite (1996) first derived this criterion for the general class of objectives $J(u, d)$, but they only considered steady-state.

The desire to have $\underline{\sigma}(G_{22})$ large is consistent with our intuition that we should ensure that the controlled outputs are independent of each other. Also note that the desire to have $\underline{\sigma}(G_{22})$ large (and preferably as large as possible) is here *not* related to the issue of input constraints.

Restrictions.

1) The selection criterion to maximize $\underline{\sigma}(G_{22})$ assumes that the "worst-case" combination of the outputs y_2 corresponding to the direction of $\underline{\sigma}(G_{22})$ for each frequency may occur in practice. From (8.22) we see that this assumes that the elements in the vectors e_2 and $e_{2,\text{opt}}$ are uncorrelated at each frequency. This may be reasonable for the contribution to the control error e_2 from the measurement noise. However, since $e_{2,\text{opt}}$ is a function of r_1 and d, i.e. $e_{2,\text{opt}}(r_1, d)$, it may be unrealistic to assume that the elements in the vector $e_{2,\text{opt}}$ are uncorrelated.

2) Another assumption for considering $\underline{\sigma}(G_{22})$ when selecting secondary outputs is that the "fixed" matrix G_{12} is such that maximizing $\underline{\sigma}(G_{22}) = \bar{\sigma}(G_{22}^{-1})$ also minimizes $\bar{\sigma}(P_y) = \bar{\sigma}(G_{12}G_{22}^{-1})$. For example, this will be case if one can choose the scaling of the inputs u_2 such that G_{12} is close to a unitary matrix times a scalar.

In summary, the method based on maximizing $\underline{\sigma}(G_{22})$ is less exact than minimizing $\|\, [\, P_d \quad P_y \,]\, \|$. On the other hand, $\underline{\sigma}(G_{22})$ is a well known tool for controllability analysis, with a wider applicability.

8.5 Partial control and model uncertainty

Model uncertainty is an important reason for applying feedback control instead of feed forward control. In particular, we can at steady-state with integral action in the control loop achieve perfect control of the measurements, in spite of uncertainty. However, uncertainty may cause poor performance at higher frequencies, and even lead to instability. The reason for these problems with uncertainty and feedback control is that the controller K is designed from the nominal plant model G, which may differ from the actual plant G_p. However, these arguments do not really apply to our analysis tools, such as P_d and P_y, as we do not perform any controller design. This may seem strange, taken into account that much of the previous work on measurement selection, such as the work of Brosilow and coworkers (Weber and Brosilow, 1972; Joseph et al., 1978) and the work by Morari and Stephanopoulos (1980), have put a large emphasis on the issue of model uncertainty. There are two reasons why uncertainty entered into their work:

1) They considered the problem of obtaining the best *estimate* of the primary variables, $\hat{y}_1$, rather than (as in our work) obtaining the best *indirect control* of y_1. Clearly, model uncertainty enters directly into the estimation problem, because here the real plant G_p will differ from the nominal model G used when designing the estimator.

2) In the work by Brosilow and co-workers, the importance of uncertainty was amplified by the particular method chosen. They suggested to use temperature measurements (y_2) to estimate the disturbances (d), and then use these estimates to compute the compositions ($\hat{y}_1$) in a feed forward fashion. As pointed out by Mejdell and Skogestad (1993), this idea is *not* very well suited to most distillation column problems because of its strong sensitivity to model uncertainty.

In our analysis the effect of uncertainty enters only indirectly through the magnitude of the control error $e_2 = y_2 - r_2$ and we have that e_2 will be large at frequencies where it is difficult

to achieve tight control of y_2 due to model uncertainty.

8.6 A simple example

The simplest example of output selection for indirect control contains three outputs (one primary output which we assume can not be measured, and two secondary outputs of which one shall be selected as the controlled output), one input and one disturbance. This example is mainly included to show better how the scaling of the variables enter into the procedure. The model in terms of the unscaled variables[5] in this case is (lower case letters are used to emphasize that the models are SISO transfer functions):

$$\hat{y}_1 = \hat{g}_{12}\hat{u}_2 + \hat{g}_{d1}\hat{d} \tag{8.25}$$

$$\text{Choice 1:} \quad \hat{y}_{2,1} = \hat{g}_{22,1}\hat{u}_2 + \hat{g}_{d1,1}\hat{d} \tag{8.26}$$

$$\text{Choice 2:} \quad \hat{y}_{2,2} = \hat{g}_{22,2}\hat{u}_2 + \hat{g}_{d1,2}\hat{d} \tag{8.27}$$

where $u_2 = u$ and $\hat{y}_{2,1}$ and $\hat{y}_{2,2}$ represents the two choices of the secondary variables. Let us consider steady-state and assume that the following model is given:

$$\hat{y}_1 = 2\hat{u}_2 + 2\hat{d} \tag{8.28}$$

$$\hat{y}_{2,1} = 3\hat{u}_2 + 2\hat{d} \tag{8.29}$$

$$\hat{y}_{2,2} = 2\hat{u}_2 + 3\hat{d} \tag{8.30}$$

where $|\hat{d}_{\max}| = 1$ and $|\hat{e}_{1,\max}| = |\hat{y}_1 - \hat{r}_1|_{\max} = 1$. The measurement error for the two secondary outputs are $|n_{2,1}| = 0.1$ and $|n_{2,2}| = 0.2$. The question is:

- Which of the two secondary variables ($y_{2,1}$ or $y_{2,2}$) should be controlled so that the primary variable y_1 can be kept close to some desired value for some non-zero disturbance and/or non-zero measurement error?

In the spirit of a true controllability measure we would like to answer this question without designing controllers for each of the two choices, otherwise the results would be biased by the controller type and the controller tunings applied.

The common scaling "matrices" used in both approaches are:

1) $|\hat{d}_{\max}| = 1 \Rightarrow D_d = 1$.
2) $|\hat{e}_{1,\max}| = |\hat{y}_1 - \hat{r}_1|_{\max} = 1 \Rightarrow D_{e_1} = 1$.
3) We assume integral action in the controllers so the control error in the secondary outputs at steady-state is equal to the measurement error, which implies

$$D_{e_2} = \text{diag}\{|n_{2,1}|, |n_{2,2}|\}, \quad \text{where } D_{e_{2,1}} = |n_{2,1}| = 0.1 \text{ and } D_{e_{2,2}} = |n_{2,2}| = 0.2.$$

---

[5]Here the hat ($\hat{\cdot}$) is used to denote unscaled variables (and not estimated variables).

8.6.1   Approach 1: minimizing $\|\begin{bmatrix} P_d & P_y \end{bmatrix}\|$

We have

$$P_d = D_{e_1}^{-1}(\hat{g}_{d1} - \hat{g}_{12}\hat{g}_{22}^{-1}\hat{g}_{d2})D_d \quad \text{and} \quad P_y = D_{e_1}^{-1}\hat{g}_{12}\hat{g}_{22}^{-1}D_{e_2}$$

Choice 1: $P_d = 1 \cdot (2 - 2 \cdot \frac{1}{3} \cdot 2) \cdot 1 = \frac{2}{3} \approx 0.67$ and $P_y = 1 \cdot 2 \cdot \frac{1}{3} \cdot 0.2 \approx 0.13$.

$$\|\begin{bmatrix} P_d & P_y \end{bmatrix}\|_2 \approx \sqrt{0.67^2 + 0.13^2} \approx 0.68$$

Choice 2: $P_d = 1 \cdot (2 - 2 \cdot \frac{1}{2} \cdot 3) \cdot 1 = -1$ and $P_y = 1 \cdot 2 \cdot \frac{1}{2} \cdot 0.1 = 0.1$.

$$\|\begin{bmatrix} P_d & P_y \end{bmatrix}\|_2 = \sqrt{1^2 + 0.1^2} \approx 1.00$$

The conclusion is to use the first of the two secondary outputs $y_{2,1}$. Note that in this case the measurement noise is of secondary importance, however, when the correlation between the primary and the secondary variables are good then the assumption about the measurement noise is of great importance. This is the case in the distillation column.

8.6.2   Approach 2: maximizing $\underline{\sigma}(G_{22})$

We have that

$$g_{22} = (D_{e_2} + D_{e_2,\text{opt}})^{-1}\hat{g}_{22}$$

where

$$D_{e_2,\text{opt}} = \|\hat{g}_{22}\hat{g}_{12}^{-1}\hat{g}_{d1} - \hat{g}_{d2}\|$$

Choice 1: $D_{e_2,\text{opt}} = |3 \cdot \frac{1}{2} \cdot 2 - 2| = 1$

$$g_{22} = (0.1 + 1)^{-1} \cdot 3 \approx 2.73$$

Choice 2: $D_{e_2,\text{opt}} = |2 \cdot \frac{1}{2} \cdot 2 - 3| = 1$

$$g_{22} = (0.2 + 1)^{-1} \cdot 2 \approx 1.67$$

Again, the conclusion is to use the first of the two secondary outputs since $\underline{\sigma}(g_{22}) = |g_{22}|$ is largest for choice 1.

8.7   Summary

In this paper we have looked at the selection of secondary variables to be used in *indirect* and *cascade control*. In either case we first close the loops involving the secondary outputs and consider the partially controlled system. The following two questions arise:

1) Which variables should be selected as secondary measurements?
2) How much can we improve the control of the primary outputs by controlling the secondary outputs?

By using the controllability measures introduced for partial control one may answer these questions. Based on these controllability measures the following two approaches for selection of secondary measurements are derived:

- Minimize the combined effect of disturbances and control error on the primary variables under feedback control of the secondary measurements.
- Maximize the smallest singular value of the selected subsystem to be controlled using feedback control.

The first approach is straightforward to apply, but it is restricted to the case of indirect control. The second approach is more difficult to apply (at least for indirect control), but it applies to a more general class of control problems than indirect control. Both approaches depend on proper scaling of the variables, but the scaling of the variables in the second approach may in some cases be more involved to find. The criteria derived do only depend on the characteristics of the plant (they are design-independent), so they do not suffer from bad choices in the controller design, and they can easily and efficiently be evaluated in a computer.

In Chapter 9 the two approaches described in this paper are applied to the problem of selecting secondary temperature measurements to be used in indirect control of product compositions in a high-purity distillation column. This case study clearly demonstrates the trade-off between disturbance rejection and rejection of measurement noise in the secondary variables.

References

Ghosh, D. and Knapp, C. H. (1989). Measurement selection for linear multivariable control systems, *Automatica* **25**(1): 55–63.

Havre, K., Morud, J. and Skogestad, S. (1996). Selection of feedback variables for implementing optimizing control schemes, *Proc. from Control'96*, University of Exeter, pp. 491–496.

Jørgensen, S., Goldschmidt, L. and Clement, K. (1984). A sensor location procedure for chemical processes, *Computers Chem. Engng.* **8**(3/4): 195–204.

Joseph, B., Brosilow, C. B. and Tong, M. (1978). Inferential control of processes: Part I. Steady state analysis and design, Joseph and Brosilow, 485-493. Part II. The structure and dynamics of inferential control systems, Brosilow and Tung, 492-500. Part III. Construction of optimal and suboptimal dynamic estimators, Joseph and Brosilow, 500-509, *AIChE Journal* **24**(3): 485–509.

Lee, J. H., Braatz, R. D., Morari, M. and Packard, A. (1995). Screening tools for robust control structure selection, *Automatica* **31**(2): 229–235.

Lee, J. H. and Morari, M. (1991). Robust measurement selection, *Automatica* **27**(3): 519–527.

Lee, J. H. and Morari, M. (1996). Control structure selection and robust control system design for a high-purity distillation column, *IEEE Trans. on Cont. Sys. Tech.,* In print .

Marlin, T. (1995). *Process Control*, Mc-Graw Hill.

Mejdell, T. and Skogestad, S. (1993). Output estimation using multiple secondary measurements: High-purity distillation, *AIChE Journal* **39**(10): 1641–1653.

Morari, M. and Stephanopoulos, G. (1980). Studies in the synthesis of control structures for chemical process, part III: Optimal selection of secondary measurements within the framework of state estimation in the presence of persistent unknown disturbances, *AIChE Journal* **26**(2): 247–259.

Skogestad, S. and Morari, M. (1988). LV-control of a high-purity distillation column, *Chemical Engineering Science* **43**(1): 33–48.

Skogestad, S. and Postlethwaite, I. (1996). *Multivariable Feedback Control, Analysis and Design*, John Wiley & Sons, Chichester.

Skogestad, S. and Wolff, E. A. (1992). Controllability measures for disturbance rejection, *IFAC Workshop on Interactions between Process Design and Process Control*, London, UK, pp. 23–29.

Stephanopoulos, G. (1989). *Chemical Process Control*, Prentice-Hall, Englewood Cliffs, New Jersey.

Weber, R. and Brosilow, C. (1972). The use of secondary measurements to improve control, *AIChE J.* **18**(3): 614–623.

Zhao, Y. (1996). *Studies on Modelling and Control of Continuos Biotechnical Processes*, PhD thesis, Norwegian University of Science and Technology, Trondheim.

Appendix A Scaling when selecting secondary outputs

In the study of control system with linearized models obtained from physical non-linear models in a selected operating point, all of the variables are deviation variables from the operating point. However, the units on the deviations are then given in the units in the original non-linear model, and may therefore *not* be suitable for the purpose of studying performance in control systems. In general we need to rescale all the variables of importance in the model. Also note that when applying the different techniques within linear control theory different scalings of the variables may be assumed. In our case the two approaches for selecting secondary measurements require different scalings of the variables to be used. The scaling to be applied in the two approaches for selecting secondary outputs are discussed in this appendix.

Let the unscaled linearized model based on the non-linear model be represented by

$$\hat{y}_1 = \hat{G}_{11}\hat{u}_1 + \hat{G}_{12}\hat{u}_2 + \hat{G}_{d1}\hat{d} \tag{8.31}$$

$$\hat{y}_2 = \hat{G}_{21}\hat{u}_1 + \hat{G}_{22}\hat{u}_2 + \hat{G}_{d2}\hat{d} \tag{8.32}$$

where ($\hat{\cdot}$) indicates that the model and the variables are unscaled, i.e. they are in their original physical units. Introduce the following scaling matrices:

$$D_d = \begin{bmatrix} \hat{d}_{1,\max} & & \\ & \ddots & \\ & & \hat{d}_{n_d,\max} \end{bmatrix}, \quad D_{e_2} = \begin{bmatrix} \hat{e}_{2,1,\max} & & \\ & \ddots & \\ & & \hat{e}_{2,n_{e2},\max} \end{bmatrix}$$

$$D_{e_2,\mathrm{opt}} = \begin{bmatrix} \hat{e}_{2,1,\mathrm{opt}} & & \\ & \ddots & \\ & & \hat{e}_{2,n_{e2},\mathrm{opt}} \end{bmatrix} \quad \text{and} \quad D_{e_1} = \begin{bmatrix} \hat{e}_{1,1,\max} & & \\ & \ddots & \\ & & \hat{e}_{1,n_{e1},\max} \end{bmatrix}$$

where

$\hat{d}_{k,\max}$ is the maximum expected change in disturbance d_k.

$\hat{e}_{2,i,\max}$ is the maximum allowed control error in secondary output $e_{2,i}$. This error can be split into the error caused by the imperfectness of the control algorithm and the error caused by measurement noise for the particular channel, i.e. $\hat{e}_{2,i,\max} = \hat{e}_{2,i,\max}(K_2) + \hat{n}_{2,i,\max}$ where:

$\hat{n}_{2,i,\max}$ is the maximum expected measurement noise in measurement of $y_{2,i}$.

$\hat{e}_{2,i,\max}(K_2)$ is the allowed control error in secondary output $e_{2,i}$ due to the imperfectness of K_2.

$\hat{e}_{2,i,\mathrm{opt}}$ is the maximum expected optimization error for secondary output $y_{2,i}$.

$\hat{e}_{1,i,\max}$ is the maximum allowed error in primary output $y_{1,i}$.

Let us also define $D_s \triangleq D_{e_2} + D_{e_2,\mathrm{opt}}$. In addition for method 2 we assume that the inputs u_2 are scaled such that each input has similar effect on the primary outputs y_1 (such that G_{12} is close to a unitary matrix times a scalar).

Note that if we where interested in input constraints then we would scale the inputs u such that $|u_{max}| < 1$ for each input. However, in this paper we assume that this is not the case, so that no particular scaling of the inputs are necessary.

REMARK. The reason we do not need to assume any particular scaling of the inputs is that for the closed-loop system (see Figure 8.1) with y_2 controlled using u_2, the variables u_2 are internal to the system, so the variables u_2 are not visible from the external inputs (d, n_2 and r_2) to the primary outputs y_1. If the inputs are constrained we need to take into account the magnitude of the inputs.

A.1 Approach 1: minimizing $\| [\, P_d \;\; P_y \,] \|$

Scalings applied:

$$d = D_d^{-1}\hat{d} \quad \Rightarrow \quad \hat{d} = D_d d \tag{8.33}$$

$$y_1 = D_{e_1}^{-1}\hat{y}_1 \quad \Rightarrow \quad \hat{y}_1 = D_{e_1} y_1 \tag{8.34}$$

$$y_2 = D_{e_2}^{-1}\hat{y}_2 \quad \Rightarrow \quad \hat{y}_2 = D_{e_2} y_2 \tag{8.35}$$

The scaled model becomes

$$y_1 = \overbrace{D_{e_1}^{-1}\hat{G}_{12}}^{G_{12}}\, \overbrace{\hat{u}_2}^{u_2} + \overbrace{D_{e_1}^{-1}\hat{G}_{d1}D_d}^{G_{d1}}\, d \tag{8.36}$$

$$y_2 = \underbrace{D_{e_2}^{-1}\hat{G}_{22}}_{G_{22}}\, \underbrace{\hat{u}_2}_{u_2} + \underbrace{D_{e_2}^{-1}\hat{G}_{d2}D_d}_{G_{d2}}\, d \tag{8.37}$$

The partial disturbance gain and the gain from y_2 to y_1, for the scaled model in terms of the unscaled model and the scaling matrices becomes

$$P_d = D_{e_1}^{-1}\overbrace{(\hat{G}_{d1} - \hat{G}_{12}\hat{G}_{22}^{-1}\hat{G}_{d2})}^{\hat{P}_d}D_d \tag{8.38}$$

$$P_y = G_{12}G_{22}^{-1} = D_{e_1}^{-1}\underbrace{\hat{G}_{12}\hat{G}_{22}^{-1}}_{\hat{P}_r}D_{e_2} \tag{8.39}$$

Only the scaling of the control error in the primary variables (y_1), the disturbances (d) and the control error (e_2) in the secondary variables (y_2) matters here. The last one includes the measurement noise. As predicted the scaling of u_2 does not matter.

A.2   Approach 2: maximizing $\underline{\sigma}(G_{22})$

Recall the matrix $D_s = D_{e_2} + D_{e_2,\mathrm{opt}}$. Scalings applied are:

1) $y_2 = D_s^{-1}\hat{y}_2$
2) Make sure that each u_2 has similar effect on the primary outputs y_1 (otherwise no particular scaling are needed).

Then

$$G_{22} = D_s^{-1}\hat{G}_{22} = (D_{e_2} + D_{e_2,\mathrm{opt}})^{-1}\hat{G}_{22} \tag{8.40}$$

We have that $e_{2,\mathrm{opt}} = r_2 - y_{2,\mathrm{opt}}$ where $y_{2,\mathrm{opt}}(d)$ depends on the disturbance. Whereas, we assume that r_2 is constant, i.e. $r_2 = 0$. From (8.16) the variation in $y_{2,\mathrm{opt}}$ due to variation in disturbances d is

$$y_{2,\mathrm{opt}}(d) = \underbrace{\{G_{22}G_{12}^{-1}G_{d1}(s) - G_{d2}(s)\}}_{P_{y_2,d}(s)=P_y^{-1}P_d(s)}d \tag{8.41}$$

This equation can be used to generate scalings for the candidate secondary variables y_2 by taking the norm of the rows in $P_{y_2,d}$. Denote row i in $P_{y_2,d}$ by $[P_{y_2,d}]_i$, then a reasonable scaling for the secondary output $y_{2,i}$ due to disturbances d is

$$[D_{e_2,\mathrm{opt}}]_{ii} = \|[\hat{G}_{22}\hat{G}_{12}^{-1}\hat{G}_{d1} - \hat{G}_{d2}]_i\| \quad \text{and} \quad [D_{e_2,\mathrm{opt}}]_{ij} = 0, \ \forall i \neq j \tag{8.42}$$

Note that the scaling of u_2 cancel out in (8.42), whereas the scaling of u_2 still applies in (8.40), this is the reason why we require that each candidate input should have similar effect on the primary variables.

Scalings of inputs u_2: $P_y = G_{12}G_{22}^{-1}$, to avoid taking into account the directions in G_{12} when considering G_{22}^{-1} we should scale the inputs such that G_{12} is close to a unitary matrix times a scalar, i.e. such that all the inputs u_2 have a similar effect on the primary outputs y_1. However, this may not be possible with a diagonal scaling matrix (too few degrees of freedom). This is a fundamental limitation of this approach.

Chapter 9

Input/output selection and partial control. Part III: Applied to selection of temperature locations in distillation columns

Kjetil Havre[*] and Sigurd Skogestad[†]

Chemical Engineering,
Norwegian University of Science and Technology
N-7034 Trondheim, Norway.

---

[*] Also affiliated with: Institute for energy technology, P.O.Box 40, N-2007 Kjeller, Norway, Fax: (+47) 63 81 11 68, E-mail: Kjetil.Havre@ife.no.

[†] Fax: (+47) 73 59 40 80, E-mail: skoge@chembio.ntnu.no.

Abstract

In this paper we consider indirect control of product compositions by controlling the temperature on two selected stages in a binary distillation column. We consider two approaches for selecting the best stages to measure the temperatures. The most obvious (direct) approach is to minimize the combined effect of (temperature) measurement noise and disturbances (changes in feedrate and feed composition) on the product compositions. That is, minimize $\left\| \begin{bmatrix} P_d & P_n \end{bmatrix} \right\|_2$, where P_d is the partial disturbance gain and P_n is the partial gain for measurement noise. The second (indirect) approach is to maximize the gain in the weak direction of the selected subsystem to be controlled. That is, select the stages for temperature measurements so that $\underline{\sigma}(G_{22})$ is maximized, where G_{22} is the subsystem linking the manipulated variables to the temperature measurements. Under the assumption of proper scaling we find that the two approaches yield the same "optimal" stage combination.

9.1   Introduction

The following two approaches for selection of secondary measurements to be used in indirect control are given in Chapter 8:

  1) Minimize the effect of disturbances and control error, i.e. minimize $\| [\, P_d \quad P_y \,] \|$.
  2) Maximize the gain in the weak direction of the controlled subsystem G_{22}, i.e. maximize $\underline{\sigma}(G_{22})$.

It is noted in Chapter 8 that the method based on maximizing $\underline{\sigma}(G_{22})$ is less exact than minimizing $\| [\, P_d \quad P_y \,] \|$. On the other hand, $\underline{\sigma}(G_{22})$ is a well known tool for controllability analysis.

In this chapter we apply these two methods to selection of temperature measurements for indirect two-point control of product compositions in a binary distillation column.

Since steady-state is of particular importance in indirect control, we apply the two ways of selecting the secondary measurements at steady-state. By including integral action in the secondary control loops, we can easily obtain perfect control of the measured temperatures (including the measurement noise). We therefore scale the control error e_2 in the secondary control loops relative to the measurement noise. Then the matrix P_y is identical to the partial gain for measurement noise P_n (see Chapter 7 for further details). We therefore replace P_y with P_n in the selection criterion $\| [\, P_d \quad P_y \,] \|$ in this paper.

9.2   Problem description

Indirect control of product compositions through temperature control on selected stages in distillation columns is widely used in practice. In this case study we will first focus on the selection of stages for temperature measurements. We will apply the two approaches for selecting controlled variables derived and described in Chapter 8. Then we show how the partially controlled plant can be analyzed using the tools described in Chapters 7 and 8. Related work on temperature control of distillation columns includes: Joseph and Brosilow (1978), Tolliver and McCune (1980), Yu and Luyben (1984; 1987), Moore et al. (1987), Mejdell (1990), Wolff and Skogestad (1996), Lee et al. (1995) and Lee and Morari (1996), see Chapter 8 for further details.

We consider a binary distillation column where the pressure in the column and the liquid holdups in the condenser and the reboiler are controlled using condenser cooling duty, top and bottom product flows, respectively. This leaves reflux L and boilup V left for product composition control, i.e. the LV-configuration. The distillation column with control loops is shown in Figure 9.1. The column data correspond to column A studied by Skogestad and Morari (1988):

#Stages	y_D	$1 - x_B$	z_F	q_F	L/F	M_i/F^*	M_D/F^*	M_B/F^*
41	0.99	0.99	0.5	1.0	2.71	0.5	32	11

* [min]

The temperature difference across the column is $13.5\,°C$. The model includes composition and liquid flow dynamics, resulting in a 82 order model which is linearized in the nominal

V_T

PC

M_D LC

p

L $D,\, y_D$

T_j TC S_p

$F,\, z_F$

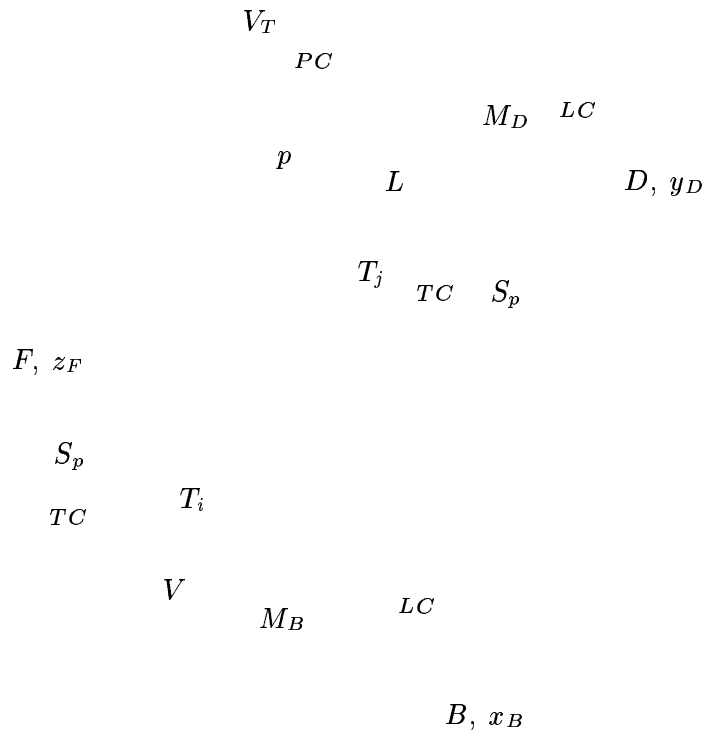S_p

T_i

TC

V

M_B LC

$B,\, x_B$

Figure 9.1: Distillation column with control loops

operating point[1]. The stages are numbered from the bottom to the top, i.e. stage 1 is the reboiler and stage 41 is the condenser. Stage 21 is the feed stage.

For a binary mixture with constant pressure there is a direct relationship between temperature (T) and composition (x). In terms of deviation variables we have $T(s) = K_T x(s)$, for simplicity we assume that K_T is independent of stage location. For ideal mixtures K_T is approximately equal to the difference in pure component boiling points, i.e. we use $K_T = -13.5\,^{\circ}\mathrm{C}$.

The control objective is to keep the primary outputs which are the product compositions

$$y_1 = \begin{bmatrix} y_D & x_B \end{bmatrix}^T$$

at their desired values. The candidate secondary outputs are the temperatures on all the stages, of which two shall be selected (see Figure 9.1)

$$y_2 = \begin{bmatrix} T_j & T_i \end{bmatrix}^T$$

This is a case of indirect control, see Section 8.4. We take into consideration measurement noise in the secondary outputs

$$n_2 = \begin{bmatrix} n_j & n_i \end{bmatrix}^T$$

---

[1] The non-linear model implemented in MATLAB is available on the internet:
`http://www.chembio.ntnu.no/users/skoge/book/matlab_m/cola/cola.html`

where n_j is the size of the temperature measurement noise in the upper stage (stage j) and n_i is the size of the temperature measurement in the lower stage (stage i). Inputs are reflux (L) and boilup (V)

$$u = \begin{bmatrix} L & V \end{bmatrix}^T$$

Disturbances are changes in feed flowrate (F) and feed composition (z_F)

$$d = \begin{bmatrix} F & z_F \end{bmatrix}^T$$

Scalings. The variables in the linear model have been scaled such that a magnitude of 1 corresponds to a change in F of 0.2 [kmol/min], a change in z_F of 0.2 mole fraction units, a change in x_B and y_D of 0.01 mole fraction units, and a change in L and V of 1 [kmol/min]. For simplicity, we assume that the measurement noise has the same magnitude $|n|$ on all stages, although in practical cases it is probably larger towards the middle of the column (see, Mejdell, 1990, Figure 7.5 on page 131 and Appendix A on pages 155–172). To study the effect of measurement noise on the measurement locations, we vary the magnitude of the measurement noise between $|n| = 0.1\,°C$ and $|n| = 1\,°C$.

9.3 Selection of stages for temperature control

We consider two approaches for selecting the stages (i/j) for the temperature measurements. In the first approach we minimize the norm $\left\| \begin{bmatrix} P_d & P_n \end{bmatrix} \right\|_2$ at steady-state. In the second approach we maximize the smallest singular value of the selected subsystem to be controlled at steady-state, i.e. maximize $\underline{\sigma}(G_{22}(j0))$, over all subsystems G_{22} of size 2×2. In the plots presented, we only consider combinations of two temperature measurements located symmetric around the feed stage. Indeed we find, for this "symmetric" column, that the optimal stage combination is nearly symmetric around the feed stage (e.g. see Table 9.1 below).

9.3.1 Two-point control, minimizing $\left\| \begin{bmatrix} P_d & P_n \end{bmatrix} \right\|_2$

To indirectly achieve tight control of y_1, we want to select the combination of two temperature measurements y_2 which minimizes $\left\| \begin{bmatrix} P_d & P_n \end{bmatrix} \right\|_2$. Both P_d and P_n depends on output scaling (y_1), P_d depends on input scaling (d) and P_n on the scaling of the measurement noise (n_2). To scale the variables we used the scalings outlined in Section 8.4.1 (also discussed in Section A.1 in Chapter 8).

Figure 9.2 shows the effect of the measurement locations on $P_d(j0)$, $P_n(j0)$ and the combined $\left\| \begin{bmatrix} P_d(j0) & P_n(j0) \end{bmatrix} \right\|_2$ for measurement noise n_2 of magnitude $|n| = 0.3\,°C$. The effect of disturbances on the compositions (y_1) with the temperatures (y_2) controlled, is given by $\|P_d\|_2$. $\|P_d\|_2$ approaches zero for measurements located close to the column ends, because at the column ends the temperature is a unique indicator of the product composition (for binary separation and with no measurement noise). For temperature measurements located away from the column ends, the correlation with the product composition is no longer

---

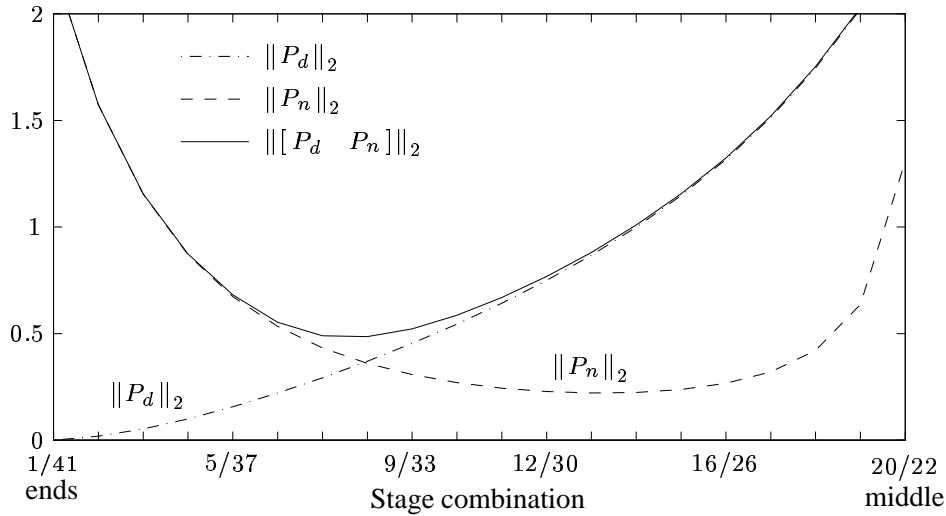[2]Only stage combinations symmetric around the feed stage are shown.

Figure 9.2: Effect of stage combination[2] i/j on $\|[\,P_d \quad P_n\,]\|_2$, $|n| = 0.3\,^\circ\mathrm{C}$

unique, and as expected the magnitude of $\|P_d\|_2$ increases towards the middle of the column. The reason why $\|P_d\|_2$ is large and approaches infinity when both measurements are located in the middle of the column, is because we cannot independently estimate two compositions (y_1) with both temperature measurements (y_2) at the same location.

In practice, the temperature measurements contains noise. The effect of temperature measurement noise on the primary outputs (see $\|P_n\|_2$ in Figure 9.2), is large at the ends of the column where the temperature profile (not shown) is almost constant.

The combined effect of the disturbance and measurement noise, is given by $\|[\,P_d \quad P_n\,]\|_2$ in Figure 9.2. The curve indicates that the optimal stage combination is 8/34. When considering all $\binom{41}{2} = 820$ possible combinations we find that stage combination 8/35 minimize $\|[\,P_d \quad P_n\,]\|_2$ when $|n| = 0.3\,^\circ\mathrm{C}$. The upper part of Table 9.1 gives the results for some other noise levels. From the table we find, as expected, that the optimal location for temperature

Table 9.1: Optimal stage combinations for different noise levels.

Measurement noise, n [°C]		0.1	0.3	0.7	1.0
$\|[\,P_d \quad P_n\,]\|_2$	Sym[a]	5/37	8/34	10/32	11/31
	All[b]	5/37	8/35	10/33	11/31
$\underline{\sigma}(G'_{22})$	Sym[a]	5/37	8/34	9/33	10/32
	All[b]	5/37	8/35	9/33	10/32

[a]Stage combinations symmetric around the feed location are considered.
[b]All 820 stage combinations are considered.

measurement is closer to the column ends with decreasing measurement noise.

9.3.2 Two-point control, maximizing $\underline{\sigma}(G_{22})$

We scale the variables as described in Section 8.4.2 (also discussed in Section A.2 in Chapter 8). That is, we compute the two scaling factors

$$s_j = \| [\, P_n^{-1} P_d(j0)\,]_j \|_2 + |n|, \quad s_i = \| [\, P_n^{-1} P_d(j0)\,]_i \|_2 + |n|$$

where $|n|$ is the magnitude of the measurement noise in the temperature measurements. The scalings of the outputs y_2 is then taken to be $D_s = \text{diag}\{1/s_j,\ 1/s_i\}$, i.e. we have $G'_{22} = D_s G_{22}$ where G_{22} is the lower part of the model and G'_{22} is the corresponding rescaled model using the scalers s_j and s_i.

Figure 9.3 shows $\underline{\sigma}(G_{22})$, $\underline{\sigma}(G'_{22})$, s_j and s_i when $|n| = 0.3\,^\circ\text{C}$ and with temperature measurements symmetricly located around the feed location. The curve $\underline{\sigma}(G'_{22})$ in Figure 9.3 indicates that the optimal stage combination is 8/34. Note that if rescaling is left out, curve $\underline{\sigma}(G_{22})$ in Figure 9.3, the result is far from the combination 8/34. It is therefore important to scale the secondary outputs y_2 properly when using this selection procedure. When we
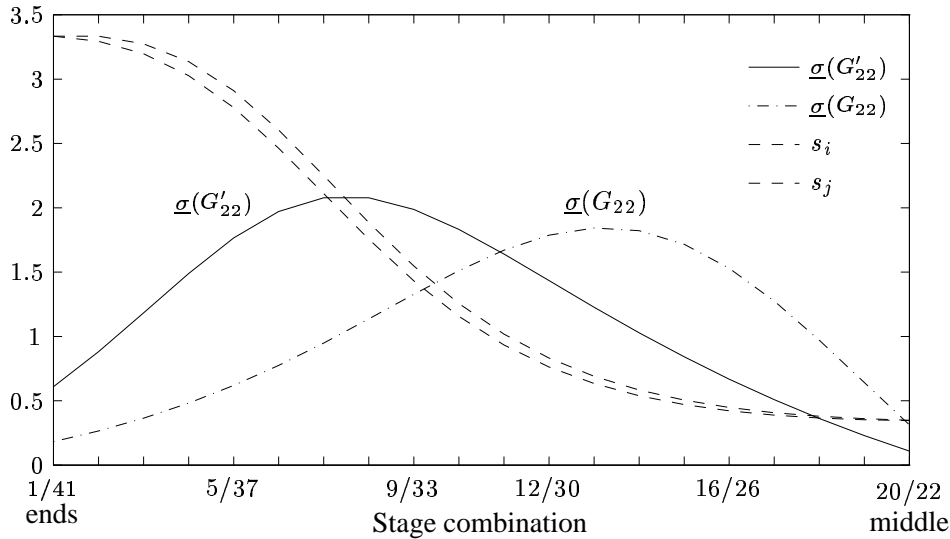

Figure 9.3: Effect of stage combination[3] i, j on $\underline{\sigma}(G'_{22})$, $|n| = 0.3\,^\circ\text{C}$

consider all $\binom{41}{2} = 820$ combinations, we find that the combination 8/35 maximizes $\underline{\sigma}(G'_{22})$, which is the same as we found when minimizing $\| [\, P_d \quad P_n\,] \|_2$. The lower part of Table 9.1 summarizes the results for the other noise levels.

9.3.3 One-point control, minimizing $\| [\, P_d \quad P_n\,] \|_2$

Figure 9.4 shows $\| [\, P_d \quad P_n\,] \|_2$, i.e. the combined effect of disturbances (d) and the measurement noise (n_2), for all possible stages using either L or V as the input for temperature control. As expected the values are higher than with two-point temperature control (see Figure 9.2). The "optimal" choice is to measure the temperature at stage number 12 (in the bottom section) and use the boilup V to control this temperature.

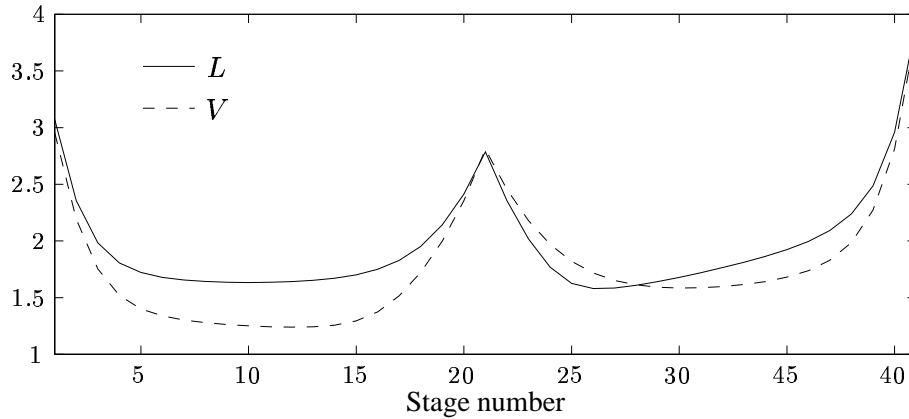[3]Only stage combinations symmetric around the feed stage are shown.

Figure 9.4: Effect of measurement location on $\left\|\left[\begin{array}{cc} P_d & P_n \end{array}\right]\right\|_2$, $|n| = 0.3\,^\circ$C, for one-point temperature control

9.4 Steady-state and dynamic analysis and simulation

In this section we examine more closely two-point temperature control on stage combinations 6/37, 8/35 and 10/33, respectively. We apply the same scalings as used in indirect control.

9.4.1 Steady-state analysis

For all combinations the open-loop effect of the manipulated variables u and disturbances d on the primary variables at steady-state are

$$G_{12}(j0) = \begin{bmatrix} 87.53 & -86.17 \\ 108.47 & -109.83 \end{bmatrix}; \quad G_{d1}(j0) = \begin{bmatrix} 7.88 & 17.62 \\ 11.72 & 22.38 \end{bmatrix}$$

The remaining steady-state matrices are given in Table 9.2, for the three different stage combinations. From G_{22} we see that the effect of the inputs u on the secondary measurements

Table 9.2: Steady-state results.

	Stage combination		
	6/37	8/35	10/33
G_{22}	$\begin{bmatrix} 145.2 & -143.0 \\ 215.6 & -218.1 \end{bmatrix}$	$\begin{bmatrix} 233.6 & -230.3 \\ 339.6 & -343.3 \end{bmatrix}$	$\begin{bmatrix} 347.0 & -342.5 \\ 493.2 & -498.3 \end{bmatrix}$
G_{d2}	$\begin{bmatrix} 13.1 & 29.4 \\ 23.2 & 44.8 \end{bmatrix}$	$\begin{bmatrix} 21.3 & 47.6 \\ 36.3 & 70.9 \end{bmatrix}$	$\begin{bmatrix} 31.8 & 71.2 \\ 52.6 & 103.4 \end{bmatrix}$
P_d	$\begin{bmatrix} 0 & -0.0861 \\ 0 & -0.1804 \end{bmatrix}$	$\begin{bmatrix} 0 & -0.1770 \\ 0 & -0.2912 \end{bmatrix}$	$\begin{bmatrix} 0 & -0.2862 \\ 0 & -0.4197 \end{bmatrix}$
P_n	$\begin{bmatrix} 0.6213 & -0.0123 \\ -0.0288 & 0.5225 \end{bmatrix}$	$\begin{bmatrix} 0.3994 & -0.0170 \\ -0.0305 & 0.3404 \end{bmatrix}$	$\begin{bmatrix} 0.2810 & -0.0203 \\ -0.0319 & 0.2424 \end{bmatrix}$

increases as we move closer to the middle of the column, but also the effect of the disturbances increases (G_{d2}).

From P_d we see that with perfect temperature control we get perfect steady-state rejection of disturbance 1, $d_1 = F$ (changes in feed flowrate), for all stage combinations. The reason is that all the intensive variables are unchanged. Also for disturbance 2, $d_2 = z_F$ (changes in feed composition) two-point temperature control improve disturbance rejection (compare P_d with open-loop G_{d1}) in the primary variables. The cost is that we introduce the measurement noise into the closed-loop system with feedback control. The sensitivity in the primary variables (product compositions) to the measurement noise is given by P_n, see Table 9.2. However, open-loop effect of the disturbances are clearly much larger than the combined effect of the disturbances and measurement noise for the closed-loop system (P_d and P_n). So, the benefit of controlling the temperatures compared to open-loop is large.

Table 9.3: RGA-element λ_{11} at steady-state.

	G_{12}	λ_{11} of G_{22} for		
		6/37	8/35	10/33
λ_{11}	35.94	38.37	40.60	43.61

It is interesting to look at the relative gain array (RGA). The RGA-element λ_{11} of G_{22} at steady-state for the three stage combinations are given in Table 9.3. From the table we see that the interactions in G_{22} at steady-state increase slightly as we move the temperature measurements closer to the feed location, which is reasonable.

Objective $J = \|y_1 - r_1\|_2^2$. Although the problem considered in this paper is a indirect control problem, we evaluate $J = \|y_1 - r_1\|_2^2$ at steady-state and in a neighborhood of the operating point. We assume perfect control of the temperatures (integral action in the secondary control loops easily achieve perfect control at steady-state), then the control error e_2 in the secondary control loop is equal to the measurement noise n_2. The steady-state control error $e_1 = y_1 - r_1$ in the primary variables (product compositions) due to measurement noise and disturbances d becomes (8.15)

$$y_1 - r_1 = P_d d + P_n n_2 = \begin{bmatrix} P_d & P_n \end{bmatrix} \begin{bmatrix} d \\ n_2 \end{bmatrix}$$

where P_d and P_n are the partial disturbance gain and the partial gain for measurement noise at steady-state. We evaluate J by varying d and n_2. From P_d in Table 9.2 we see that it is no reason for varying F, since F has no effect at steady-state. Denote the strong input direction (the input direction corresponding to the largest singular value) of P_n for v_1 (where $v_1^H v_1 = 1$). We only vary the magnitude of the measurement noise n_2 in this direction, i.e. we consider $n_2 = v_1 n$. We obtain

$$y_1 - r_1 = P_d \begin{bmatrix} 0 \\ 1 \end{bmatrix} z_F + P_n v_1 n = M \begin{bmatrix} z_F \\ n \end{bmatrix}$$
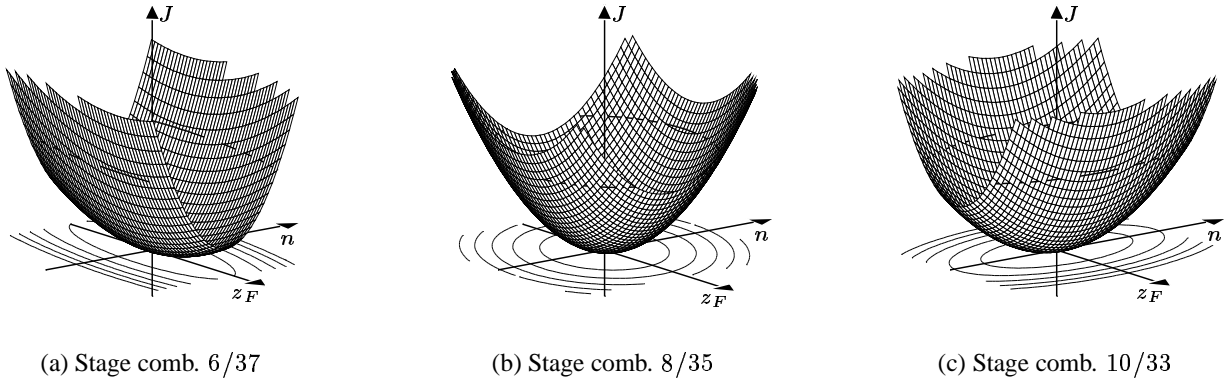
(a) Stage comb. 6/37   (b) Stage comb. 8/35   (c) Stage comb. 10/33

Figure 9.5: Objective $J = \|y_1 - r_1\|_2^2$ as function of z_F and n when controlling the temperature on stages i/j

$$J = \|y_1 - r_1\|_2^2 = [\, z_F \quad n \,] M^T M \begin{bmatrix} z_F \\ n \end{bmatrix}$$

Table 9.4 summarizes v_1 and M for the stage combinations 6/37, 8/35 and 10/33. The

Table 9.4: Steady-state results to obtain J.

	Stage combination		
	6/37	8/35	10/33
v_1[a]	$[\, 0.9821 \quad -0.1886 \,]^T$	$[\, 0.9461 \quad -0.3239 \,]^T$	$[\, 0.8981 \quad -0.4398 \,]^T$
M	$\begin{bmatrix} 0.0861 & 0.6125 \\ 0.1804 & -0.1268 \end{bmatrix}$	$\begin{bmatrix} 0.1770 & 0.3833 \\ 0.2912 & -0.1391 \end{bmatrix}$	$\begin{bmatrix} 0.2862 & 0.2613 \\ 0.4197 & -0.1352 \end{bmatrix}$
$\Lambda(M^T M)$[b]	$\begin{bmatrix} 0.3937 & 0 \\ 0 & 0.0374 \end{bmatrix}$	$\begin{bmatrix} 0.1783 & 0 \\ 0 & 0.1041 \end{bmatrix}$	$\begin{bmatrix} 0.2600 & 0 \\ 0 & 0.0847 \end{bmatrix}$
$V(M^T M)$[c]	$\begin{bmatrix} 0.0841 & 0.9965 \\ 0.9965 & -0.0841 \end{bmatrix}$	$\begin{bmatrix} 0.4024 & 0.9155 \\ 0.9155 & -0.4024 \end{bmatrix}$	$\begin{bmatrix} -0.9946 & 0.1034 \\ -0.1035 & -0.9946 \end{bmatrix}$

[a]Input direction of P_n with largest singular value.
[b]Eigenvalue matrix of $M^T M$.
[c]Eigenvector matrix of $M^T M$, so that $M^T M V = V \Lambda$.

matrix $M^T M$ is the Hessian of J with respect to z_F and n. The eigenvalues of $M^T M$ (see Table 9.4) gives the curvature in the two principal axis (the eigenvector directions). From the eigenvalues and eigenvectors of $M^T M$ we can see that n has largest influence on J for stage combination 6/37 and z_F has largest influence on J for stage combination 10/33.

To illustrate the effect of stage locations on the performance objective $J = \|y_1 - r_1\|_2^2$, we have plotted the objective J as a function of the disturbance z_F and the measurement noise n for the three stage combinations in Figure 9.5. Stage combination 8/35, which we have found to minimize $\|[\, P_d \quad P_n \,]\|_2^2$ and maximize $\underline{\sigma}(G'_{22})$ at steady-state, is shown in Figure 9.5(b). There is a good balance between rejecting the disturbance z_F (remember

that rejecting changes feed flowrate is perfect) and the sensitivity to measurement noise n. This can be seen from the circular shape of the objective J. For stage combination $6/37$, Figure 9.5(a), the temperature measurements are closer to the column ends and we get better disturbance rejection, but J becomes more sensitive to measurement noise. This can be seen from Figure 9.5(a), where the shape of J is formed more like a valley with the narrow direction pointing almost in the direction of n and the wider direction pointing almost in the direction of z_F. It is worth noting that the surface J becomes gradually more narrow in the direction of n as the measurements move towards the column ends. For stage combination $10/33$ (where the temperature measurements are closer to the feed stage than in the optimal case), the situation is opposite, i.e. J becomes less sensitive to measurement noise, but at the expense of less disturbance rejection, see Figure 9.5(c).

9.4.2 Dynamic analysis

Frequency dependent plots of the effect of disturbances in open-loop (upper curve) and closed-loop (lower curves; perfect temperature control) are given in Figure 9.6. We find
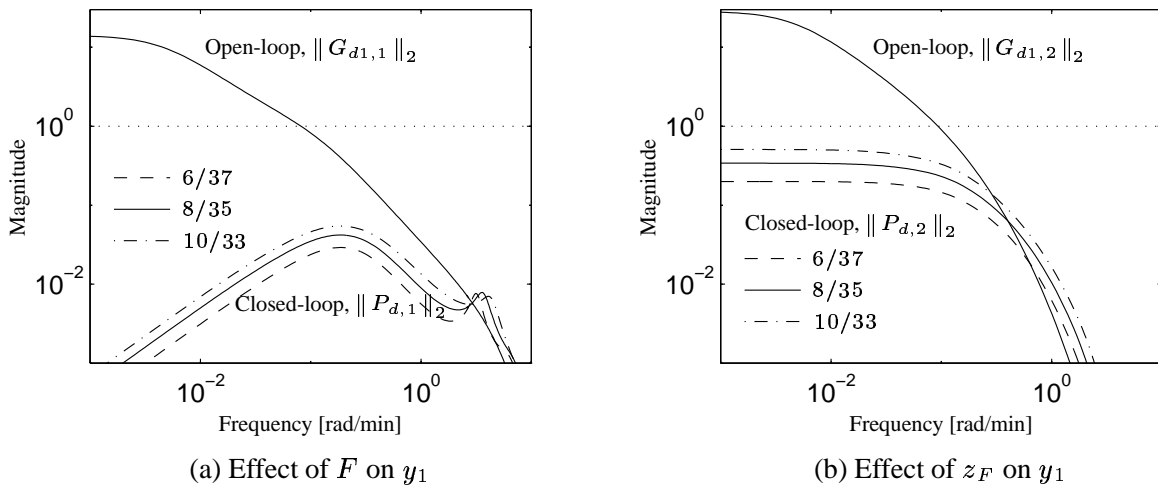

(a) Effect of F on y_1 (b) Effect of z_F on y_1

Figure 9.6: Improved disturbance rejection in $y_1 = \begin{bmatrix} y_D & x_B \end{bmatrix}^T$, for different stage combinations

that the disturbance rejection is improved also for frequencies $\omega > 0$ with two-point temperature control. The effect of the disturbances in the individual primary outputs $y_1 = \begin{bmatrix} y_D & x_B \end{bmatrix}$ are similar both for open and closed-loop.

Frequency dependent plots of $\|P_d\|_2$ (the combined effect of the two disturbances) and $\|P_n\|_2$ (the effect of measurement noise) are given in Figure 9.7(a) and (b) for the three stage combinations.

Frequency dependent plots of RGA-element λ_{11} of G_{12} and G_{22} for the three stage combinations are given in Figure 9.8. For frequencies in the bandwidth region we see that there is less interactions in G_{22} than in G_{12}, we also note that the peak of $\lambda_{11}(G_{22})$ in the bandwidth region is smaller than the corresponding peak of $\lambda_{11}(G_{12})$ and also that the peak of $\lambda_{11}(G_{22})$ decreases as the temperature measurements move closer to the feed location. Note

(a) $\|P_d(j\omega)\|_2$ (b) $\|P_n(j\omega)\|_2$
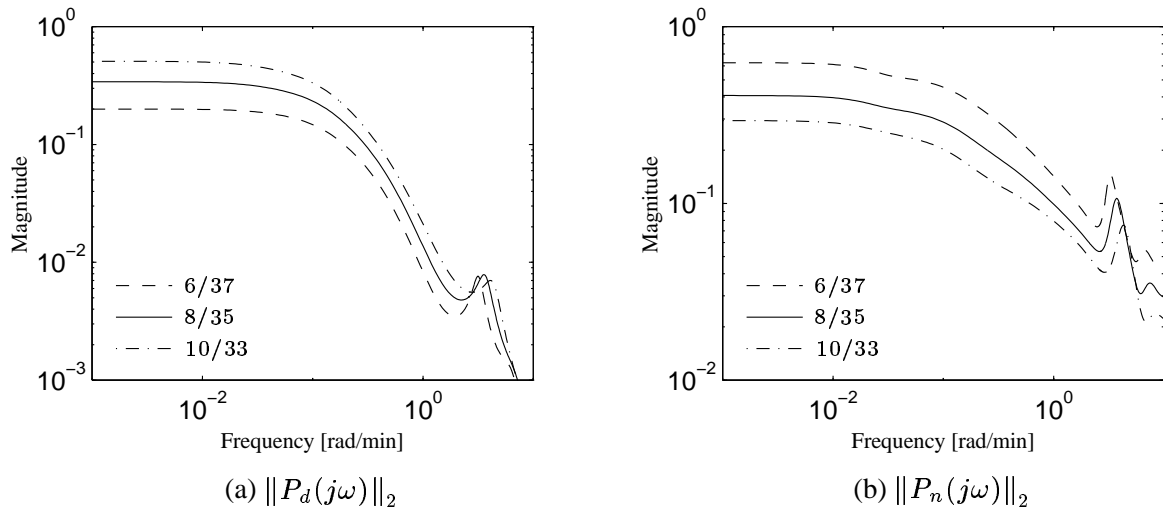
Figure 9.7: $\|P_d(j\omega)\|_2$ and $\|P_n(j\omega)\|_2$ for different stage combinations
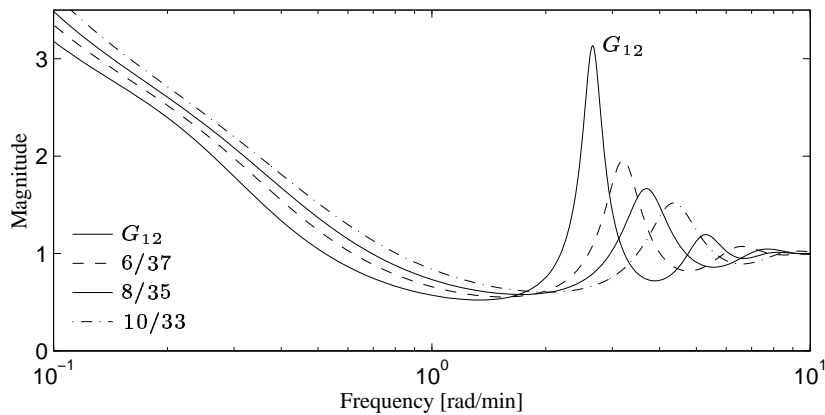
Figure 9.8: Frequency dependent plots of RGA-element λ_{11}

that the opposite is true for steady-state and low frequencies, see Table 9.3. The smaller RGA-elements in G_{22} than in G_{12} for frequencies around the bandwidth, indicates that it is easier to control the temperatures than the compositions directly[4].

9.4.3   Feedback control

To confirm the results above we consider simple decentralized PI-control of the temperatures on the three stage combinations. The controller tunings are given in Table 9.5. The tuning for tray combination $8/35$ was found by trial and error. The controller gains for the two other tray combinations are adjusted to take into account the non-linear gain variations in the

---

[4]This conclusion is solely based on RGA for frequencies around the bandwidth. For steady-state RGA the opposite conclusion is true. This example illustrates that RGA for frequencies in the bandwidth region are much more important than steady-state.

Table 9.5: PI-controller tunings.

| | Top, $T_j \leftrightarrow L$ | | Bottom, $T_i \leftrightarrow V$ | |
Stage comb.	$K_c{}^{\mathrm{a}}$	$\tau_I{}^{\mathrm{b}}$	$K_c{}^{\mathrm{a}}$	$\tau_I{}^{\mathrm{b}}$
6/37	3.26	10	-3.90	5
8/35	2	10	-2.5	5
10/33	1.32	10	-1.73	5

[a][mole/(min, °C)]
[b][min]

process given by the formula

$$L_T = \ln \frac{T - T_H}{T_L - T}$$

where T_H and T_L are the boiling points of the heavy and light components, see (Mejdell, 1990) for further details. The adjustment of the controller gains ensures that the loop gain and the resulting bandwidth is similar in the three cases.

Let us first consider the resulting closed-loop frequency response. The effect of d, r_2 and n_2 on y_1 for a partially controlled plant with controller K_2 is given by

$$
\begin{aligned}
y_1 &= \overbrace{\left(G_{d1}(s) - G_{12}K_2 S_2 G_{d2}(s)\right)}^{M(s)}d + \overbrace{G_{12}K_2 S_2(s)}^{N(s)}r_2 - \overbrace{G_{12}K_2 S_2(s)}^{N(s)}n_2 \\
&= M(s)d + N(s)r_2 - N(s)n_2
\end{aligned}
\tag{9.1}
$$

where $S_2 = (I + G_{22}K_2)^{-1}$. Figure 9.9 shows the effect of disturbances d and measurement noise n_2 on the primary variables y_1 in closed-loop, i.e. $\|M\|_2$. For frequencies where control is effective we see that there is excellent agreement between $\|P_d\|_2$ in Figure 9.7(a) and $\|M\|_2$ in Figure 9.9(a). There is also good agreement between $\|P_n\|_2$ in Figure 9.7(b) and $\|N\|_2$ in Figure 9.9(b) at frequencies where control is effective. For high frequencies we see that the closed-loop system with the PI-controllers actually has better properties when it comes to rejecting control errors e_2 (measurement noise n_2) (the reason for this is of course the inversion of G_{22} also for high frequencies, which is unrealistic).

Figure 9.10 shows the dynamic response to the following changes in the inputs:

1) Unit step (20% change) in $d_1 = F$ at time $t = 10$ [min].
2) Unit step (20% change) in $d_2 = z_F$ at $t = 100$ [min].
3) Step with size $[\,-0.3 \quad -0.3\,]^T$ in n_2 at time $t = 100$ [min].

Gaussian distributed measurement noise with zero mean and standard deviation 0.1 is included in the simulations. Several things are worth noting:

1) The effect of changes in F is minor in all cases. This agrees with the plot of P_{d1}, see Figure 9.6(a).
2) The effect of changes in z_F increase as the temperature measurements are moved closer to the feed stage. This agrees with the plot of P_{d2}, see Figure 9.6(b).
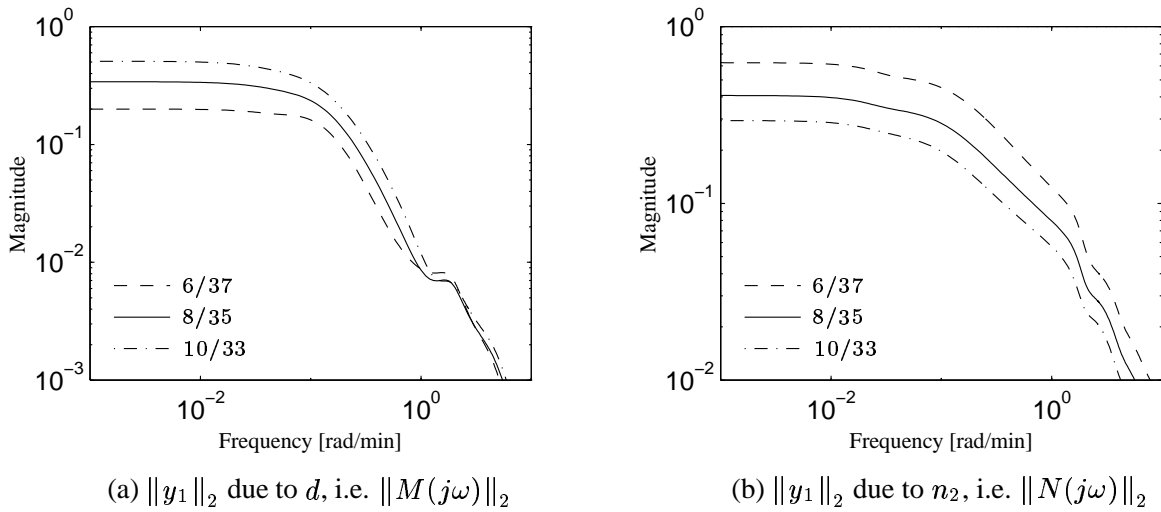
(a) $\|y_1\|_2$ due to d, i.e. $\|M(j\omega)\|_2$ (b) $\|y_1\|_2$ due to n_2, i.e. $\|N(j\omega)\|_2$

Figure 9.9: Frequency dependent plots of $\|y_1\|_2$ due to disturbances d and measurement noise n_2 for different stage combinations

3) The effect of the measurement noise decreases as the measurements are moved closer to the feed stage. This agrees with Figure 9.7(b).

4) The bottom composition x_B is more sensitive to high-frequency measurement noise than the top composition (less variation in y_D than in x_B).

5) A good trade-off between sensitivity to disturbance z_F and measurement noise appears to be with the temperature measurements located at stage combination $8/35$, Figure 9.10(b).

To summarize, we find that there is an excellent agreement between the controller independent controllability analysis based on P_d and P_n, and the closed-loop responses with PI-controllers.

9.4.4 One-point temperature control

In this section we analyze the controllability of one-point temperature control, and compare with the results from two-point temperature control. The effect of boilup V and the two disturbances d on top and bottom composition at steady-state are

$$G_{12}(j0) = \begin{bmatrix} -86.17 \\ -109.83 \end{bmatrix}, \quad G_{d1}(j0) = \begin{bmatrix} 7.88 & 17.62 \\ 11.72 & 22.38 \end{bmatrix}$$

and the effect of the same variables on the temperature at stage 12 at steady-state are

$$G_{22}(j0) = -652.97, \quad G_{d2}(j0) = \begin{bmatrix} 68.57 & 136.46 \end{bmatrix}$$

which gives

$$P_d(j0) = \begin{bmatrix} -1.1712 & -0.3841 \\ 0.1875 & -0.5763 \end{bmatrix} \quad \text{and} \quad P_n(j0) = \begin{bmatrix} 0.1320 \\ 0.1682 \end{bmatrix}$$
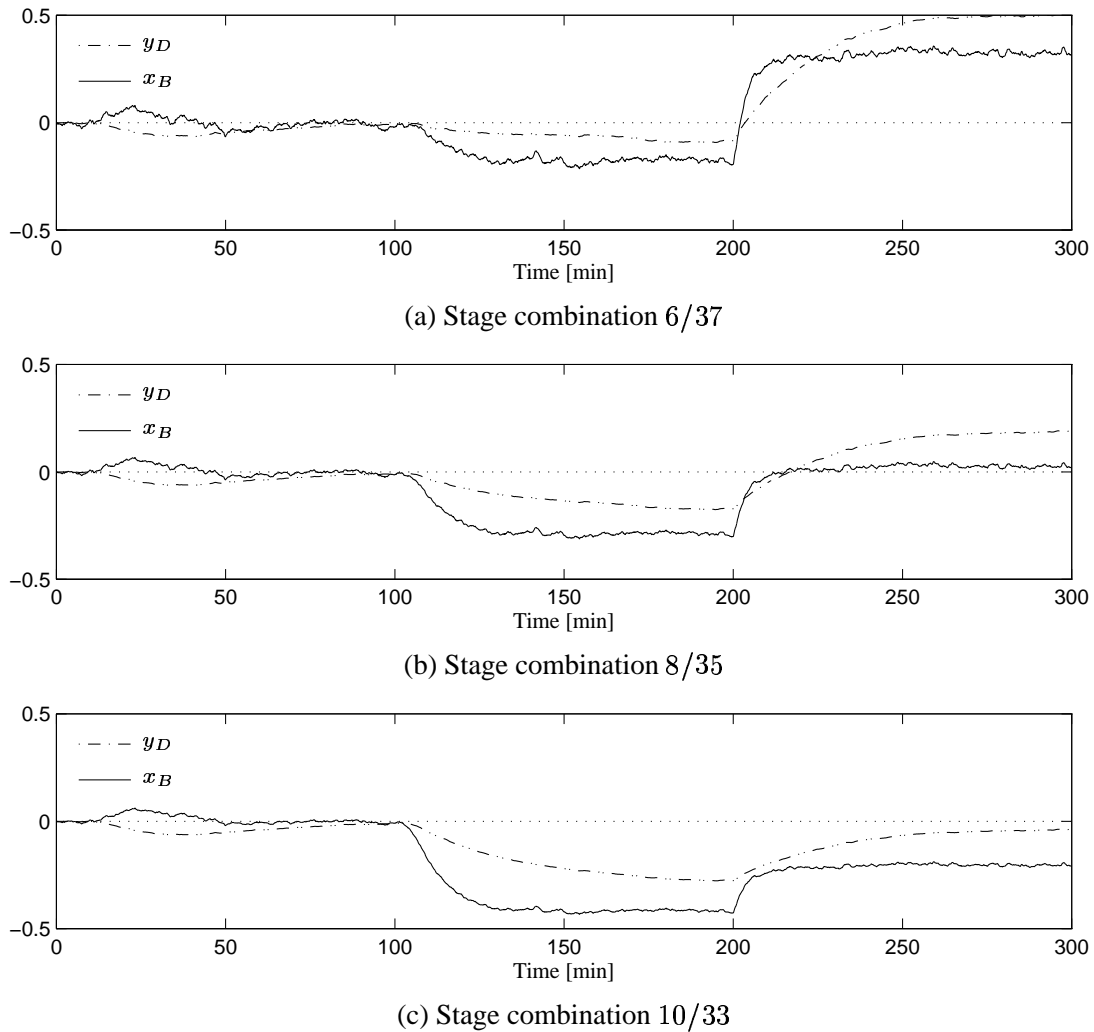
(a) Stage combination 6/37

(b) Stage combination 8/35

(c) Stage combination 10/33

Figure 9.10: Dynamic simulations with random measurement noise and step changes in F at $t = 10$ [min], z_F at $t = 100$ [min] and n_2 at $t = 200$ [min]

By comparing $G_{d1}(j0)$ with $P_d(j0)$ we see that the effect of the disturbances has been reduced significantly. However, the effect of feed rate disturbance $(d_1 = F)$ is still larger than one, which is undesirable. This is in contrast to two-point temperature control, see Table 9.2, where we have perfect rejection of the feed rate disturbance.

Frequency dependent plots which show the effect of F and z_F on y_1 (top and bottom compositions) are shown in Figure 9.11(a) and (b). These confirm the results from the steady-state analysis.

9.5 Summary

The two approaches for selecting the temperature measurements yield the same "optimal" stage combination. As expected, increasing the measurement noise (control error), moves
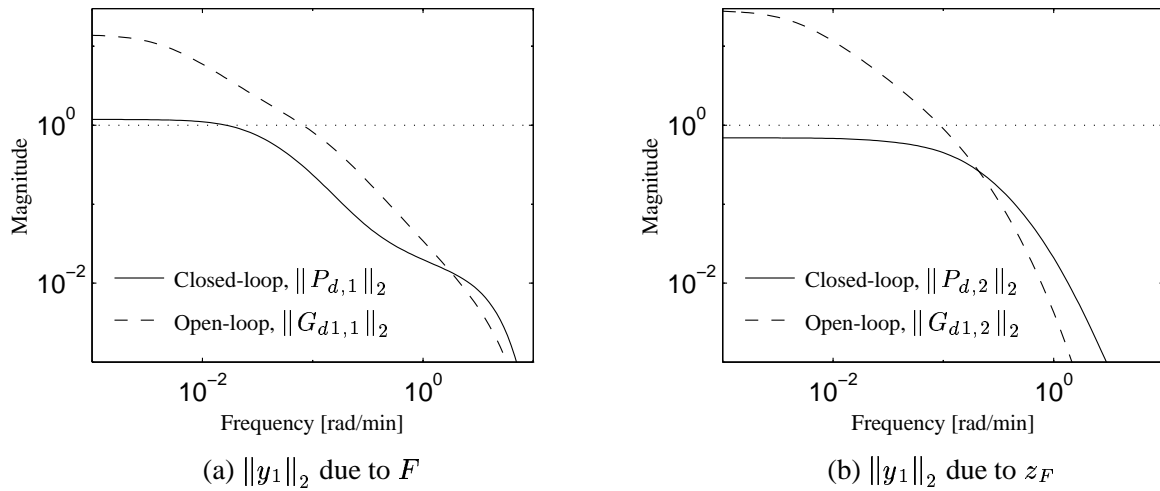
(a) $\|y_1\|_2$ due to F

(b) $\|y_1\|_2$ due to z_F

Figure 9.11: Improved disturbance rejection in $y_1 = \begin{bmatrix} y_D & x_B \end{bmatrix}^T$ when the temperature at stage 12 is controlled using boilup V

the optimal measurement locations towards the middle of the column. For our case study, the optimal locations for temperature measurements is almost symmetric around the feed location. This does not apply in general, but follows since we have equal product purities, and feed composition $z_F = 0.5$. Our conclusion, to select stage combination $8/35$ compares well with (Lee and Morari, 1996) who found the choice $7/35$ to be the best.

The results obtained from the controllability analysis using P_d and P_n also agrees very well with the closed-loop results obtained using PI-controllers. Some benefits and conclusions of two-point temperature control (LV-configuration) are:

1) Improved disturbance rejection and rejection of measurement noise, compared to open-loop and one-point temperature control.

2) For the column under consideration and with the assumption taken, sufficient performance can be achieved with two-point temperature control.

3) The large value of RGA-element $\lambda_{11}(G_{22})$ at steady-state does not imply difficulties for control, the main reason is that the same RGA-element is moderate in the bandwidth region.

4) When comparing the dynamic simulations shown in this paper with the one given in (Wolff and Skogestad, 1996) (who studied the same column) it is advisable to include two temperature loops. This contradicts point 2 in the discussion in (Wolff and Skogestad, 1996), where they state that a second temperature cascade in two-point distillation control is not advisable. They base their arguments on results obtained from dynamic closed-loop simulations.

An analysis similar to the one presented here is still applicable to cascaded control systems.

References

Havre, K., Morud, J. and Skogestad, S. (1996). Selection of feedback variables for implementing optimizing control schemes, *Proc. from Control'96*, University of Exeter, pp. 491–496.

Joseph, B. and Brosilow, C. B. (1978). Inferential control of processes: Part I. Steady state analysis and design, *AIChE Journal* **24**(3): 485–492.

Lee, J. H., Braatz, R. D., Morari, M. and Packard, A. (1995). Screening tools for robust control structure selection, *Automatica* **31**(2): 229–235.

Lee, J. H. and Morari, M. (1996). Control structure selection and robust control system design for a high-purity distillation column, *IEEE Trans. on Cont. Sys. Tech.,* In print .

Mejdell, T. (1990). *Estimators for Product Composition in Distillation Columns*, PhD thesis, Norwegian University of Science and Technology, Trondheim.

Moore, C., Hackney, J. and Canter, D. (1987). Selecting sensor location and type for multivariable processes, *Shell Process Control Workshop (book), Butterworth* .

Skogestad, S. and Morari, M. (1988). LV-control of a high-purity distillation column, *Chemical Engineering Science* **43**(1): 33–48.

Tolliver, T. L. and McCune, L. C. (1980). Finding the optimum temperature control trays for distillation columns, *InTech* .

Wolff, E. A. and Skogestad, S. (1996). Temperature cascade control of distillation columns, *Ind. Eng. Chem. Res.* **35**(2): 475–484.

Yu, C. C. and Luyben, W. L. (1984). Use of multiple temperatures for the control of multicomponent distillation columns, *Ind. Eng. Chem. Process Des. Dev.* pp. 590–597.

Yu, C. C. and Luyben, W. L. (1987). Control of multicomponent distillation columns using rigourous compositon estimators, *I. Cheme. E. Symp. Ser.* .

Chapter 10

The use of RGA and condition number as robustness measures

Sigurd Skogestad[*] and Kjetil Havre[†]

Chemical Engineering,
Norwegian University of Science and Technology
N-7034 Trondheim, Norway.

Abstract

The relative gain array (RGA) and condition number are commonly used tools in controllability analysis. In this paper we present new results that link these measures to control performance, measured in terms of the output sensitivity function with input and output uncertainty.

---

[*] Fax: (+47) 73 59 40 80, E-mail: skoge@chembio.ntnu.no.

[†] Also affiliated with: Institute for energy technology, P.O.Box 40, N-2007 Kjeller, Norway, Fax: (+47) 63 81 11 68, E-mail: Kjetil.Havre@ife.no.

10.1   Introduction

Diagonal input and output uncertainty are always present in any real system: diagonal input uncertainty in terms of unknown characteristics in the actuators and diagonal output uncertainty in terms of imperfect measurement devices. It is therefore reasonable to consider the effect of these two types of uncertainty on performance for a given control system. In particular, ill-conditioned plants with a large condition number are often believed to be sensitive to uncertainty, and the objective of the paper is to gain insight into this by answering the question:

- How can ill-conditioning which results in poor robust performance be identified?

In the paper we consider linear time invariant transfer function models on the form

$$y(s) = G(s)u(s)$$

For simplicity of the proofs we assume that G is stable. However, as noted in the conclusion the results are also valid for unstable plants. The results in the paper are stated in terms of the plant and controller condition numbers

$$\gamma(G) = \frac{\bar{\sigma}(G)}{\underline{\sigma}(G)}; \qquad \gamma(K) = \frac{\bar{\sigma}(K)}{\underline{\sigma}(K)} \tag{10.1}$$

and the following minimized condition numbers for the plant and the controller

$$\gamma_I^*(G) = \min_{D_I} \gamma(GD_I); \qquad \gamma_O^*(K) = \min_{D_O} \gamma(D_OK) \tag{10.2}$$

where D_I and D_O are diagonal scaling matrices. These minimized condition numbers can be computed as outlined by Braatz and Morari (1994). In the paper we also make use of the relative gain array (RGA) which was introduced by Bristol (1966). The RGA matrix can be computed at any frequency using the formula

$$\Lambda(s) = G(s) \times \left(G^{-1}(s)\right)^T \tag{10.3}$$

where the $\times$ symbol denotes element by element multiplication (Hadamard or Schur product). An important property of the RGA is that it is scaling independent.

The outline of the paper is as follows. In section 10.2 we introduce input and output multiplicative uncertainty. Section 10.3 discusses the implications of input and output uncertainty on feed forward control. Section 10.4 gives a similar discussion on feedback control. The results in this section are given as upper bounds on perturbed sensitivity function. Section 10.4.3 shows that for systems with large RGA elements in the bandwidth region and with input uncertainty there always exist a perturbation which results in poor performance. Section 10.5 gives examples on the results derived. Finally the paper ends with the conclusion. Section A provides proofs of the theorems, upper bounds and factorizations presented in the paper.

The rest of this section we devote to discuss some related work. Freudenberg and Saglik (1991) consider robust performance for 2×2 systems by using a integral relationship between
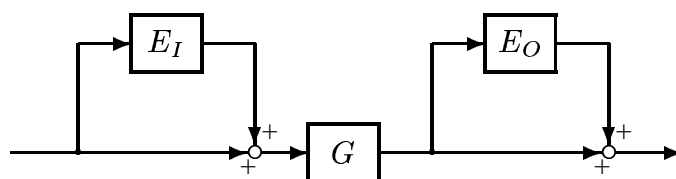
Figure 10.1: System with multiplicative input and output uncertainty

gain and phase. They use the classical sensitivity integral to derive an upper bound on the average value of the plant condition number at *low* frequencies. The results presented in this paper show that the frequencies in bandwidth region are more important than low frequencies.

Nett and Manousiouthakis (1987) give relationships between RGA, Block Relative Gain and the Euclidean condition number. The relationship between RGA and minimized condition number is also given in (Skogestad and Morari, 1987). Nett and Manousiouthakis proved the lower bound on the condition number. The upper bound was proven for 2×2 by Grosdidier, Morari and Holt (1985), but only conjectured for the general case. We note that these results have no direct connection to performance in terms of the sensitivity function.

Chen, Freudenberg and Nett (1994) consider the effect of modeling uncertainties on the open-loop properties. They mainly consider diagonal uncertainty, and give estimates for the worst case deviations in terms of structured singular values and minimized condition numbers. The main difference between their work and this work is that they consider open-loop and use the structured singular value, whereas we consider closed-loop and the largest singular value of the sensitivity function.

Waller, Sågfors and Waller (1994a; 1994b) consider nominal and robust stability of 2×2 systems and link the question of robust stability to minimized condition number of the plant and robust performance to the condition number of the plant. They argue that minimized condition number of the plant gives tight bounds for robust stability whereas the plant condition number gives conservative results. However, we will show that plant condition number also provides conservative results for performance, in particular if one use a diagonal controller we give an upper bound on the perturbed sensitivity which says that there is no problem with input uncertainty and robust performance as long as robust stability is provided.

10.2 Uncertainty

In practice, the true perturbed plant G' differs from that of the plant model G. This may be caused by a number of different sources, and in this paper we focus on input and output uncertainty. On multiplicative form the input and output uncertainties are (Figure 10.1)

$$\text{Output uncertainty:} \quad G' = (I + E_O)G \quad \text{or} \quad E_O = (G' - G)G^{-1} \tag{10.4}$$

$$\text{Input uncertainty:} \quad G' = G(I + E_I) \quad \text{or} \quad E_I = G^{-1}(G' - G) \tag{10.5}$$

These forms of uncertainty may seem similar, but we will show that their implications for control can be very different. In particular, note that for square plants $E_O = G E_I G^{-1}$. The main reason for writing the uncertainty in multiplicative (or relative) form is because this

makes it easier to quantify the uncertainty. In most cases we assume that the magnitude of the uncertainty at each frequency can be bounded in terms of its singular value

$$\bar{\sigma}(E_I) \leq |w_I|, \quad \bar{\sigma}(E_O) \leq |w_O| \tag{10.6}$$

where $w_I(s)$ and $w_O(s)$ are scalar weights. Typically the uncertainty bound, $|w_I|$ or $|w_O|$, is 0.2 at low frequencies and exceeds 1 at higher frequencies. If we allow E_I or E_O to be any uncertainty matrix satisfying the bound (10.6), then we have *full block* uncertainty. However, in many cases the source of uncertainty is in the individual input or output channels, and we have that E_I or E_O are diagonal matrices

$$E_I = \text{diag}\{\epsilon_{I1}, \epsilon_{I2}, \ldots\}, \quad E_O = \text{diag}\{\epsilon_{O1}, \epsilon_{O2}, \ldots\} \tag{10.7}$$

This is denoted *diagonal input uncertainty* and *diagonal output uncertainty*. We will assume that in each input channel j and in each output channel i the uncertainty is bounded as follows

$$|\epsilon_{Ij}| \leq |w_{Ij}|, \quad |\epsilon_{Oi}| \leq |w_{Oi}| \tag{10.8}$$

It is important to stress that diagonal input uncertainty is *always* present in real systems (whereas full block input uncertainty is present only in some cases).

10.3   Effect of uncertainty on feed forward control

For the nominal model with no disturbances we have $y = Gu$. The control error can be expressed as

$$e = y - r = Gu - r$$

Consider "perfect" feed forward control, $e = 0$, assuming an invertible plant G and solving for u gives the manipulated inputs $u = G^{-1}r$. However, for the actual plant G' we have $y' = G'u$ and the control error becomes

$$e' = y' - r = G'G^{-1}r - r$$

We get for the two sources of uncertainty

$$\text{Output uncertainty:} \qquad e' = E_O r \tag{10.9}$$
$$\text{Input uncertainty:} \qquad e' = GE_I G^{-1}r \tag{10.10}$$

From (10.9) we see that with output uncertainty the relative error $\frac{\|e'\|_2}{\|r\|_2}$ is equal to the relative uncertainty $\|E_O\|_2$. However, for input uncertainty the sensitivity may be much larger because the elements in the matrix $GE_I G^{-1}$ can be much larger than the elements in E_I. In particular for diagonal input uncertainty the elements of $GE_I G^{-1}$ are directly related to the RGA of G, Skogestad and Morari (1987)

$$\text{Diagonal uncertainty:} \quad [GE_I G^{-1}]_{ii} = \sum_{j=1}^{n} \lambda_{ij}(G)\epsilon_j \tag{10.11}$$

Since diagonal input uncertainty is *always* present we can conclude

- *If the plant has large RGA elements within the frequency range where effective control is desired, then it is* not *possible to achieve good reference tracking with feed forward control because of strong sensitivity to diagonal input uncertainty.*

We can quantify the result further by the following theorem.

THEOREM 10.1 (DIAGONAL INPUT UNCERTAINTY AND FEED FORWARD CONTROL). *Consider a plant G with diagonal input uncertainty of magnitude*

$$|W_I| = \text{diag}\{|w_{I1}|, |w_{I2}|, \ldots\}$$

Assume we apply a "perfect" feed forward controller $u = G^{-1}r$. Then there exists a combination of input uncertainties such that at each frequency

$$\frac{\|e'\|_2}{\|r\|_2} = \|GE_I G^{-1}\|_2 \geq \| \Lambda(G) |W_I| \|_{i\infty} \tag{10.12}$$

where $\| \Lambda(G) |W_I| \|_{i\infty}$ is the maximum row sum of the matrix $\Lambda(G) |W_I|$.

REMARK 1. If all input channels have the same relative uncertainty $|W_I| = |w_I|I$. Then we simply have

$$\frac{\|e'\|_2}{\|r\|_2} = \|GE_I G^{-1}\|_2 \geq |w_I| \|\Lambda(G)\|_{i\infty} \tag{10.13}$$

REMARK 2. Theorem 10.1 also applies to full-block uncertainty of the same magnitude since this also allows for diagonal uncertainty.

REMARK 3. The RGA-matrix is scaling independent, which makes the use of condition (10.11) and (10.12) attractive.

REMARK 4. We found that large RGA-elements imply difficulties for feed forward control. However, the reverse statement is not true, that is, if the RGA has *small* elements we can *not* conclude that the sensitivity to input uncertainty is *small*. This is seen from the following expression for the 2×2 case

$$GE_I G^{-1} = \begin{bmatrix} \lambda_{11}\epsilon_1 + \lambda_{12}\epsilon_2 & -\frac{g_{12}}{g_{22}}\lambda_{11}(\epsilon_1 - \epsilon_2) \\ \frac{g_{21}}{g_{11}}\lambda_{11}(\epsilon_1 - \epsilon_2) & \lambda_{21}\epsilon_1 + \lambda_{22}\epsilon_2 \end{bmatrix} \tag{10.14}$$

The results above are based on considering the diagonal elements in this matrix, but the off-diagonal elements can also be large. For example, consider a triangular plant with $g_{12} = 0$. In this case $\Lambda = I$ so the diagonal elements of $GE_I G^{-1}$ are ϵ_1 and ϵ_2. Still, the system may be sensitive to input uncertainty, since from (10.14) the $(2, 1)$-element of $GE_I G^{-1}$ may be large if g_{21}/g_{11} is large.

REMARK 5. Upper bounds for the effect of uncertainty on performance for feed forward control can be obtained form singular value inequalities. For full block and diagonal input uncertainty we have

$$\text{Full-block uncertainty:} \quad \|GE_I G^{-1}\|_2 \leq \gamma(G)\bar{\sigma}(E_I) \tag{10.15}$$

$$\text{Diagonal uncertainty:} \quad \|GE_I G^{-1}\|_2 \leq \gamma_I^*(G)\bar{\sigma}(E_I) \tag{10.16}$$

10.4 Effect of uncertainty on feedback control

One of the main reasons for applying feedback control rather than feed forward control is to reduce the effect of uncertainty. In particular, with integral action in the controller we can

achieve zero steady-state control error even with quite large model errors. Nevertheless, uncertainty poses limitations on the achievable feedback control performance, and the objective of this section is to show how the condition number and RGA can be used as tools to detect potential problems. We will base our arguments on the singular values of the perturbed sensitivity function

$$S' = (I + G'K)^{-1} \qquad (10.17)$$

which is directly related to performance measured at the output of the plant. For example, we have that

$$e' = -S'r, \qquad \text{and} \quad \max_r \frac{\|e'\|_2}{\|r\|_2} = \bar{\sigma}(S') \qquad (10.18)$$

We will derive upper bounds on $\bar{\sigma}(S')$ which involves the condition number and a lower bound on $\bar{\sigma}(S')$ which involves the RGA. The lower bound is useful for identifying plants which are difficult to control. Proofs of some of the results in this section are given in Section A.

10.4.1   Factorizations of the sensitivity function

The upper bounds are based on the following factorizations of the sensitivity function

Output uncertainty: $\qquad\qquad\qquad S' = S(I + E_O T)^{-1} \qquad (10.19)$

Input uncertainty: $\quad S' = S(I + GE_I G^{-1} T)^{-1} = SG(I + E_I T_I)^{-1} G^{-1} \quad (10.20)$

$$S' = (I + TK^{-1} E_I K)^{-1} S = K^{-1} (I + T_I E_I)^{-1} KS \quad (10.21)$$

We assume that the plants, G and G', are stable. We also assume closed-loop stability, so that both S and S' are stable. We then get that $(I + E_O T)^{-1}$ and $(I + E_I T_I)^{-1}$ are stable (equivalently $(I + TE_O)^{-1}$ and $(I + T_I E_I)^{-1}$ are stable). When deriving bounds we make use of properties like

$$\bar{\sigma}((I + E_I T_I)^{-1}) = \frac{1}{\underline{\sigma}(I + E_I T_I)} \le \frac{1}{1 - \bar{\sigma}(E_I T_I)} \le \frac{1}{1 - \bar{\sigma}(E_I)\bar{\sigma}(T_I)} \le \frac{1}{1 - |w_I|\bar{\sigma}(T_I)}$$

where we have made use of $\bar{\sigma}(E_I) \le |w_I|$. Of course these inequalities only apply if we assume $\bar{\sigma}(E_I T_I) < 1$, $\bar{\sigma}(E_I)\bar{\sigma}(T_I) < 1$ and $|w_I|\bar{\sigma}(T_I) < 1$. For simplicity, we will not state these assumptions each time.

10.4.2   Upper bounds on the sensitivity function

Output uncertainty.

$$\bar{\sigma}(S') \le \bar{\sigma}(S)\bar{\sigma}((I + E_O T)^{-1}) \le \frac{\bar{\sigma}(S)}{1 - \bar{\sigma}(E_O)\bar{\sigma}(T)} \le \frac{\bar{\sigma}(S)}{1 - |w_O|\bar{\sigma}(T)} \qquad (10.22)$$

From (10.22) we see that output uncertainty, be it diagonal or full block, poses no particular problem when performance is measured at the plant output. That is, if we have a reasonable margin to stability ($\|(I + E_O T)^{-1}\|_\infty$ is not to much larger than 1) then the nominal and perturbed sensitivity do not differ very much.

Input uncertainty. The sensitivity function can be much more sensitive to input uncertainty than output uncertainty.

1. *General case* (full block or diagonal input uncertainty and any controller).

$$\bar{\sigma}(S') \leq \gamma(G)\bar{\sigma}(S)\bar{\sigma}((I + E_I T_I)^{-1}) \leq \gamma(G)\frac{\bar{\sigma}(S)}{1-\bar{\sigma}(E_I)\bar{\sigma}(T_I)} \leq \gamma(G)\frac{\bar{\sigma}(S)}{1-|w_I|\bar{\sigma}(T_I)} \quad (10.23)$$

$$\bar{\sigma}(S') \leq \gamma(K)\bar{\sigma}(S)\bar{\sigma}((I + T_I E_I)^{-1}) \leq \gamma(K)\frac{\bar{\sigma}(S)}{1-\bar{\sigma}(T_I)\bar{\sigma}(E_I)} \leq \gamma(K)\frac{\bar{\sigma}(S)}{1-|w_I|\bar{\sigma}(T_I)} \quad (10.24)$$

From (10.24) we have the important result that if we use a "round" controller with $\gamma(K)$ close to 1, then the sensitivity function is *not* sensitive to input uncertainty. In many cases the bounds (10.23) and (10.24) are not very useful because they yield unnecessary large upper bounds. To improve on this, we present below bounds for some special cases, where we either restrict the uncertainty to be diagonal or restrict the controller to be of a particular form.

2. *Diagonal uncertainty* and *diagonal control.* In this case we have $K^{-1}E_I K = E_I$ and we get

$$\bar{\sigma}(S') \leq \bar{\sigma}(S)\bar{\sigma}((I + T E_I)^{-1}) \leq \frac{\bar{\sigma}(S)}{1-\bar{\sigma}(T)\bar{\sigma}(E_I)} \leq \frac{\bar{\sigma}(S)}{1-|w_I|\bar{\sigma}(T)} \quad (10.25)$$

Thus, in this important case S' is not sensitive to input uncertainty.

3. *Diagonal uncertainty* and *decoupling control.* Consider a decoupling controller on the form $K(s) = D(s)G^{-1}(s)$ where $D(s)$ is a diagonal matrix. In this case KG is diagonal so $T_I = KG(I + KG)^{-1}$ is diagonal (and we have that $E_I T_I = T_I E_I$). With diagonal uncertainty we get

$$\bar{\sigma}(S') \leq \gamma_I^*(G)\bar{\sigma}(S)\bar{\sigma}((I + E_I T_I)^{-1}) \leq \gamma_I^*(G)\frac{\bar{\sigma}(S)}{1-\bar{\sigma}(E_I)\bar{\sigma}(T_I)} \leq \gamma_I^*(G)\frac{\bar{\sigma}(S)}{1-|w_I|\bar{\sigma}(T_I)} \quad (10.26)$$

$$\bar{\sigma}(S') \leq \gamma_O^*(K)\bar{\sigma}(S)\bar{\sigma}((I + T_I E_I)^{-1}) \leq \gamma_O^*(K)\frac{\bar{\sigma}(S)}{1-\bar{\sigma}(T_I)\bar{\sigma}(E_I)} \leq \gamma_O^*(K)\frac{\bar{\sigma}(S)}{1-|w_I|\bar{\sigma}(T_I)} \quad (10.27)$$

The bounds (10.26) and (10.27) apply to any decoupling controller on the form $K = DG^{-1}$. In particular, they apply to inverse based control, $K = l(s)G^{-1}(s)$ which yields input-output decoupling with $T_I = T = t \cdot I$ where $t = \frac{l}{1+l}$. A diagonal controller has $\gamma_O^*(K) = 1$, so from (10.25) we see that (10.27) applies to both a diagonal and decoupling controller. Nevertheless, it does not seem like (10.27) applies generally for any controller. However, another bound which applies to any controller is given in (10.29).

4. *Diagonal uncertainty* (Any controller).

$$\bar{\sigma}(S') \leq \frac{\bar{\sigma}(S)}{1-\gamma_I^*(G)\bar{\sigma}(E_I)\bar{\sigma}(T)} \leq \frac{\bar{\sigma}(S)}{1-|w_I|\gamma_I^*(G)\bar{\sigma}(T)} \quad (10.28)$$

$$\bar{\sigma}(S') \leq \frac{\bar{\sigma}(S)}{1-\gamma_O^*(K)\bar{\sigma}(E_I)\bar{\sigma}(T)} \leq \frac{\bar{\sigma}(S)}{1-|w_I|\gamma_O^*(K)\bar{\sigma}(T)} \quad (10.29)$$

Again note that $\gamma_O^*(K) = 1$ for a diagonal controller so (10.29) confirms that diagonal uncertainty poses little problems when we use a diagonal controller.

10.4.3   Lower bound on the sensitivity function

Consider the special case of diagonal input uncertainty and inverse based control

$$K(s) = l(s)G^{-1}(s)$$

(which is a special case of decoupling control which yields $T = T_I = t \cdot I$ and $S = S_I = s \cdot I$). In this case we can generalize the *lower* bound on the sensitivity function for the 2×2 case given in Gjøsæter (1995).

THEOREM 10.2 (LOWER BOUND WITH INPUT UNCERTAINTY AND DECOUPLING CONTROL). *Consider a decoupling controller $K(s) = l(s)G^{-1}(s)$ which results in a nominally decoupled response with sensitivity $S = s \cdot I$ and complementary sensitivity $T = t \cdot I$ where $t(s) = 1 - s(s)$. Suppose the plant has diagonal input uncertainty of relative magnitude $|w_I(j\omega)|$ in each input channel. Then there exists a combination of input uncertainties such that at each frequency*

$$\bar{\sigma}(S') \; \geq \; \bar{\sigma}(S)\left(1 + \frac{|w_I t|}{1 + |w_I t|}\,\|\Lambda(G)\|_{i\infty}\right) \tag{10.30}$$

where $\|\Lambda(G)\|_{i\infty}$ is the maximum row sum of the RGA and $\bar{\sigma}(S) = |s|$.

It is important to notice that (10.30) provides a *lower* bound on $\bar{\sigma}(S')$, whereas our previous results discussed in Sec. 10.4.2 gave *upper* bounds. *A lower bound is more useful because it allows us to make definite conclusions about when the plant is not controllable.* Specifically, from (10.30) we see that with an inverse based controller the worst case sensitivity will be much larger than the nominal at frequencies where the plant has large RGA-elements. At frequencies where control is effective ($|s|$ is small and $|t| \approx 1$) this implies that control is not as good as expected, but it may still be acceptable. However, at crossover frequencies where $|s|$ and $|t| = |1 - s|$ are both close to 1, we find that $\bar{\sigma}(S')$ in (10.30) may become much larger than 1 if the plant has large RGA-elements at these frequencies.

By comparing the results for feedback control (10.30) and that of feed forward control (10.13) with same uncertainty in all channels, one may clearly see the benefits of feedback. For frequencies below the bandwidth we have that $\bar{\sigma}(S) < 1$. The effect of feedback is then to reduce the influence of uncertainty on the control error, remember that $|t| \approx 1$ for frequencies $\omega < \omega_B$, where ω_B is the bandwidth of the closed-loop system, i.e. $\bar{\sigma}(S(j\omega_B)) = 1/\sqrt{2}$. For feed forward control the effect of uncertainty on the control error is present for all frequencies. For frequencies $\omega > \omega_B$ we have $\bar{\sigma}(S) = 1$ and $|t| < 1$, so the result is similar, the effect of uncertainty for feedback control is reduced compared to feed forward control. For frequencies around the bandwidth we have that both $\bar{\sigma}(S)$ and $|t|$ can be much larger than one and the situation can be worse for feedback than feed forward control.

Worst-case errors. For simulations it is useful to know which combination of input errors gives poor performance. If all ϵ_k have the same magnitude, then the largest possible magnitude of any diagonal element in GE_IG^{-1} is given by $|w_I| \cdot \|\Lambda(G)\|_{i\infty}$. To obtain this value one may select the phase of each ϵ_k such that $\angle\epsilon_k = -\angle\lambda_{ik}$ where i denotes the row of $\Lambda(G)$ with the largest elements. In particular, if $\Lambda(G)$ is real (e.g., at steady-state), the signs of the ϵ_k's should be the same as those in the row of $\Lambda(G)$ with the largest elements.

Relationship to structured singular value, μ. The appropriate measure to analyze exactly the worst-case sensitivity under influence of input uncertainty $|w_I|$ is skewed-μ (μ^s). This involves computing $\mu_{\tilde{\Delta}}(N)$ with $\tilde{\Delta} = \text{diag}(\Delta_I, \Delta_p)$ where $N = \begin{bmatrix} w_I T_I & w_I KS \\ \frac{1}{\mu^s} SG & \frac{1}{\mu^s} S \end{bmatrix}$ and varying μ^s until $\mu(N) = 1$, where Δ_p is full block. The worst-case performance at a given frequency is then $\bar{\sigma}(S') = \mu^s$.

10.5 Examples

EXAMPLE 10.1 DISTILLATION COLUMN, LV-CONFIGURATION. In this example we consider the following model of an ill-conditioned distillation column, taken from Skogestad, Morari and Doyle (1988).

$$G = G_{LV}(s) = \frac{1}{\tau s + 1} \begin{bmatrix} 87.8 & -86.4 \\ 108.2 & -109.6 \end{bmatrix}, \quad \Lambda(G) = \begin{bmatrix} 35.1 & -34.1 \\ -34.1 & 35.1 \end{bmatrix} \tag{10.31}$$

We consider diagonal input uncertainty of magnitude $|w_I| = 0.2$ at all frequencies. We have that $\|\Lambda(G(j\omega))\|_{i\infty} = 69.14$, $\gamma^*(G) \approx \gamma_O^*(G) \approx 138.3$ and $\gamma(G) \approx \gamma_I^*(G) \approx 141.7$ at all frequencies. So, we may expect problems with input uncertainty for both feed forward and feedback control.

1. *Feed forward control.* For feed forward control we have from Theorem 10.1 the lower bound $|w_I| \cdot \|\lambda(G)\|_{i\infty} = 0.2 \cdot 69.14 = 13.83$. Theorem 10.1 says that there exists a combinations of input uncertainty where $\frac{\|e'\|_2}{\|r\|_2}$ is larger than the bound. By introducing input uncertainty in the same direction as the input direction corresponding to the largest singular value $\begin{bmatrix} 0.707 & -0.707 \end{bmatrix}^T$, with magnitude $|w_I(j\omega)| = 0.2$ in each channel E_I becomes, $E_I = \text{diag}\{0.2, -0.2\}$. With this input uncertainty one obtains $\|GE_I G^{-1}\|_2 = 28.35$. The difference between 13.83 form (10.13) and 28.35 which is the actual value for the worst input uncertainty, illustrates that the bound in terms of RGA is generally not tight, but it is nevertheless very useful.

2. *Inverse based feedback controller*:

$$K_{inv}(s) = \frac{k_1}{s} G^{-1}(s) = \frac{k_1(\tau s + 1)}{s} \begin{bmatrix} 0.3994 & -0.3149 \\ 0.3943 & -.3200 \end{bmatrix}, \quad k_1 = 0.7\,[\text{min}^{-1}]$$

The peak value for the lower bound in (10.30) is 6.81 for $\omega = 0.79$. As a comparison, the actual peak value with the inverse-based controller with 20% gain uncertainty is (Skogestad et al., 1988)

$$\|S'\|_\infty = \left\| \left(I + \frac{0.7}{s} G \begin{bmatrix} 1.2 & \\ & 0.8 \end{bmatrix} G^{-1} \right)^{-1} \right\|_\infty = 14.21$$

and occurs for $\omega = 0.69$. The difference between 6.76 and 14.2 illustrates that the bound in terms of the RGA is generally not tight, but it is nevertheless very useful.

Next we look at the upper bounds. Unfortunately, in this case $\gamma_I^*(G) = \gamma_O^*(K) \approx 141.7$, so the upper bound in (10.26) and (10.27) are not very useful (they are of magnitude 141.7, at high frequencies).
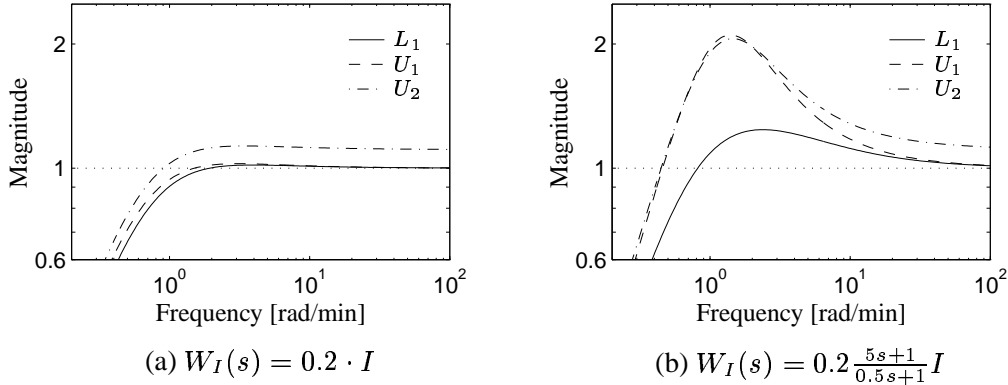
$$(a)\ W_I(s) = 0.2 \cdot I \qquad\qquad (b)\ W_I(s) = 0.2\frac{5s+1}{0.5s+1}I$$

Figure 10.2: Bounds on sensitivity function for distillation column with DV configuration, lower bound L_1 from (10.30), upper bounds U_1 from (10.28) and U_2 from (10.26)

3. *Diagonal feedback controller*:

$$K_{dia}(s) = \frac{k_2(\tau s + 1)}{s}\begin{bmatrix} 1 & 0 \\ 0 & -1 \end{bmatrix}, \qquad k_2 = 2.4 \cdot 10^{-2}\ [\text{min}^{-1}]$$

We have $\gamma(K_{dia}) = \gamma_O^*(K_{dia}) = 1$ since both loops are tuned equally. Tight upper bounds on perturbed sensitivity functions are therefore provided by (10.24), (10.25) and (10.29). We find that the actual peak in the perturbed sensitivity function is $\|S'\|_\infty = 1.05$ for $\omega = 1.30$ [rad/min] when $E_I = \text{diag}\{0.2, -0.2\}$, whereas the peaks in the upper bounds (10.24), (10.25) and (10.29) are all 1.26 for $\omega = 0.56$ [rad/min].

EXAMPLE 10.2 DISTILLATION COLUMN, DV-CONFIGURATION. In this example we consider the following model of a distillation column with DV configuration, also taken from Skogestad et al. (1988)

$$G = G_{DV}(s) = \frac{1}{\tau s + 1}\begin{bmatrix} -87.8 & 1.4 \\ -108.2 & -1.4 \end{bmatrix}, \qquad \Lambda(G) = \begin{bmatrix} 0.448 & 0.552 \\ 0.552 & 0.448 \end{bmatrix} \tag{10.32}$$

We have that $\|\Lambda(G(j\omega))\|_{i\infty} = 1$, $\gamma^*(G) \approx 1.00$ and $\gamma_I^*(G) \approx 1.11$ and $\gamma(G) \approx 70.76$ and $\gamma_O^*(G) \approx 69.24$ at all frequencies. We do not expect problems with input uncertainty and therefore design an inverse based controller, similar to the one considered by Skogestad et al. (1988). The controller is $K_{inv}(s) = \frac{k_1}{s}G^{-1}(s)$, $k_1 = 0.7$ [min^{-1}]. Since we use an inverse based controller we have $\gamma(K) = \gamma(G)$, and $\gamma_O^*(K) = \gamma_I^*(G)$. Also since $\gamma(G)$ is much larger than $\gamma_I^*(G)$ we find that the bounds in (10.23) and (10.24) are more conservative than the bounds in (10.26), (10.27), (10.28) and (10.29). In Figure 10.2 we show the lower bound given by (10.30) and the two upper bounds given by (10.26) and (10.28) for two different uncertainty weights. From these curves we see that the upper bounds (denoted U_1 and U_2) can be close in some cases, and conclude that the system is robust against input uncertainty.

10.6 Conclusions on robust performance with input uncertainty

The sensitivity to model uncertainty is reduced by applying feedback control rather than feed forward control. We find for feedback control that plants with large RGA-elements are diffi-

cult to control due to sensitivity to diagonal input uncertainty. The situation is not quite as bad as for feed forward control, because control problems are expected only if the RGA has large elements close to the crossover region (where $\sigma_i(L)$ is about 1 in magnitude). For example, with integral control, large RGA-elements in the plant at steady-state do not by themselves pose any limitation on performance for feedback control (but they do for feed forward control). Our conclusions on input minimized condition number, condition number and RGA are summarized below. The statements apply to the frequency-range around crossover. By "small', we mean about 2 or smaller. By "large" we mean about 10 or larger.

1) Condition number's $\gamma(G)$ or $\gamma(K)$ small: Robust to both diagonal and full-block input uncertainty.

2) Minimized condition number's $\gamma_I^*(G)$ or $\gamma_O^*(K)$ small: Robust to diagonal input uncertainty. Note that a diagonal controller has $\gamma_O^*(K) = 1$.

3) RGA(G) has large elements: Inverse-based controller is *not* robust to diagonal input uncertainty and should therefore *not* be used (since diagonal input uncertainty is unavoidable). Furthermore, a diagonal controller will most likely yield poor nominal performance for a plant with large RGA-elements, so we conclude that plants with large RGA-elements are fundamentally difficult to control.

4) $\gamma_I^*(G)$ is large while at the same time the RGA has small elements: Cannot make any definite conclusion about the sensitivity to input uncertainty based on the bounds in this paper.

The results also apply to unstable plants G, however, the proofs are then somewhat more complicated than shown in this paper.

Acknowledgement

References

Braatz, R. D. and Morari, M. (1994). Minimizing the Euclidean condition number, *SIAM Journal on Control and Optimization* **32**(6): 1763–1768.

Bristol, E. H. (1966). On a new measure of interactions for multivariable process control, *IEEE Transactions on Automatic Control* **AC-11**: 133–134.

Chen, J., Freudenberg, J. S. and Nett, C. N. (1994). The role of the condition number and the relative gain array in robustness analysis, *Automatica* **30**(6): 1029–1035.

Freudenberg, J. and Saglik, K. (1991). Ill-conditioned plants and integral relations, *Int. Workshop on Robust Control, San Antonio, TX, USA,* pp. 233–248.

Gjøsæter, O. B. (1995). *Structures for Multivariable Robust Process Control*, PhD thesis, Norwegian University of Science and Technology, Trondheim.

Grosdidier, P., Morari, M. and Holt, B. R. (1985). Closed-loop properties from steady-state gain information, *Industrial and Engineering Chemistry Process Design and Development* **24**: 221–235.

Nett, C. N. and Manousiouthakis, V. (1987). Euclidean condition and block relative gain - connections conjectures, and clarifications, *IEEE Transactions on Automatic Control* **AC-32**(5): 405–407.

Skogestad, S. and Morari, M. (1987). Effect of disturbance directions on closed-loop performance, *Industrial and Engineering Chemistry Research* **26**: 2029–2035.

Skogestad, S., Morari, M. and Doyle, J. C. (1988). Robust control of ill-conditioned plants: High-purity distillation, *IEEE Transactions on Automatic Control* **AC-33**(12): 1092–1105.

Waller, J., Sågfors, M. and Waller, K. (1994a). Ill-conditionedness and process directionality - the use of condition numbers in process control, *ADCHEM '94, Japan, May 25-27 1994*, pp. 465–470.

Waller, J., Sågfors, M. and Waller, K. (1994b). The robustness of ill-conditioned plants, *Proc. of PSE '94, Korea 30 May-3 June 1994*, pp. 1197–1201.

Appendix A Proofs of the results

Proof of Theorem 10.1. Since the two-norm is larger than the magnitude of any of the elements we have for any i,

$$\|GE_I G^{-1}\|_2 \geq |[GE_I G^{-1}]_{ii}|$$

To get the least conservative result we select element $[GE_I G^{-1}]_{ii}$ which has the largest magnitude. By using (10.11) and $\epsilon_j = |w_{I,j}|e^{j\angle \epsilon_j}$, we get

$$[GE_I G^{-1}]_{ii} = \sum_{j=1}^{n} \lambda_{ij}(G)|w_{I,j}|e^{j\angle \epsilon_j} = \sum_{j=1}^{n} |\lambda_{ij}(G)| \cdot |w_{I,j}|$$

The last equality follows since we are free to adjust the phase of ϵ_j ($\angle \epsilon_j$) to get the largest possible sum. Note that $|w_{I,j}|$ scales all elements in column j of Λ. When maximizing over all rows i, we get

$$\max_i \|[GE_I G^{-1}]_{ii}\|_2 = \max_i \sum_{j=1}^{n} |\lambda_{ij}(G)|\, |w_{I,j}| = \|\, \Lambda(G)\, |W_I|\, \|_{i\infty}$$

and the result follows.   □

Proof of (10.19). We have

$$I + G'K = I + (I + E_O)GK = (I + E_O GK(I + GK)^{-1})(I + GK) = (I + E_O T)(I + GK)$$

□

Proof of (10.20). We have

$$\begin{aligned} I + G'K &= I + G(I + E_I)K = G(I + (I + E_I)KG)G^{-1} \\ &= G(I + E_I T_I)\underbrace{(I + KG)\,G^{-1}}_{G^{-1}(I+GK)} = G(I + E_I T_I)G^{-1}(I + GK) \end{aligned}$$

□

Proof of (10.21). Start from $I + G'K = I + G(I + E_I)K$ and factor out $(I + GK)$ to the left to obtain

$$
\begin{aligned}
I + G'K &= (I + GK)(I + (I + GK)^{-1}GE_IK) \\
&= (I + GK)(I + \underbrace{GK(I + GK)^{-1}}_{T}K^{-1}E_IK) \\
&= (I + GK)K^{-1}(I + \underbrace{KG(I + KG)^{-1}}_{T_I}E_I)K
\end{aligned}
$$

$\square$

Proof of (10.22), (10.23) and (10.24). Apply singular value inequalities to (10.19) and to the last identity in (10.20) and (10.21). $\square$

Proof of (10.25). Set $KE_IK^{-1} = E_I$ in (10.21) first identity to obtain $S' = (I + TE_I)^{-1}S$ and apply singular value inequalities. $\square$

Proof of (10.26) and (10.27). Since E_I and T_I are diagonal, we have $E_I = DE_ID^{-1} = D^{-1}E_ID$ and $T_I = DT_ID^{-1} = D^{-1}T_ID$ for any diagonal matrix D. Then (10.20) first identity can be written

$$
\begin{aligned}
S' &= S(I + GE_IG^{-1}T)^{-1} = S(I + (GD_I)E_I(GD_I)^{-1}T)^{-1} \\
&= S(GD_I)(I + E_ID_I^{-1}T_ID_I)^{-1}(GD_I)^{-1} \\
&= S(GD_I)(I + E_IT_I)^{-1}(GD_I)^{-1}
\end{aligned}
\tag{10.33}
$$

Since (10.33) applies to any diagonal D_I, (10.26) follows by applying singular value inequalities to (10.33). Similarly (10.27) follows from (10.21). $\square$

Proof of (10.28) and (10.29). Apply singular value inequalities to second identity in (10.33), similar for (10.29) form equivalent equation with controller. $\square$

Proof of Proof of Theorem 10.2. Write the sensitivity function as

$$
S' = (I + G'K)^{-1} = SG(I + E_IT_I)^{-1}G^{-1} = SGDG^{-1}, \; E_I = \text{diag}\{\epsilon_k\}
$$

Since, D is a diagonal matrix, we have from (10.11) that the diagonal elements of S' are given in terms of the RGA of the plant G as

$$
s'_{ii} = s\sum_{k=1}^{n}\lambda_{ik}d_k; \quad d_k(s) = \frac{1}{1 + t(s)\epsilon_k(s)}; \quad \Lambda = G \times (G^{-1})^T
\tag{10.34}
$$

The singular value of a matrix is larger than any of its elements, so $\bar{\sigma}(S') \geq \max_i |s'_{ii}|$, and the objective in the following is to choose a combination of input errors ϵ_k such that the worst-case $|s'_{ii}|$ is as large (poor) as possible. Consider a given i and write each term in the sum in (10.34) as

$$
\lambda_{ik}d_k = \frac{\lambda_{ik}}{1 + t\epsilon_k} = \lambda_{ik} - \frac{\lambda_{ik}t\epsilon_k}{1 + t\epsilon_k}
\tag{10.35}
$$

We choose all ϵ_k to have the same magnitude $|w_I(j\omega)|$, so we have $\epsilon_k(j\omega) = |w_I|e^{j\angle\epsilon_k}$. We also assume that $|t\epsilon_k| < 1$ at all frequencies, such that the phase of $1 + t\epsilon_k$ lies between $-90°$ and $90°$.[1]

---

[1]The assumption $|t\epsilon_k| < 1$ is not included in the theorem since it is actually needed for robust stability, so if it does not hold we may have $\bar{\sigma}(S')$ infinite for some allowed uncertainty, and (10.30) clearly holds.

It is then always possible to select $\angle \epsilon_k$ (the phase of ϵ_k) such that the last term in (10.35) is real and negative, and we have at each frequency with these choices for ϵ_k

$$\frac{s'_{ii}}{s} = \sum_{k=1}^{n} \lambda_{ik} d_k = 1 + \sum_{k=1}^{n} \frac{|\lambda_{ik}| \cdot |t\epsilon_k|}{|1 + t\epsilon_k|} \geq 1 + \sum_{k=1}^{n} \frac{|\lambda_{ik}| \cdot |w_I t|}{1 + |w_I t|} = 1 + \frac{|w_I t|}{1 + |w_I t|} \sum_{k=1}^{n} |\lambda_{ik}| \quad (10.36)$$

where the first equality makes use of the fact that the row-elements of the RGA sum to 1, ($\sum_{k=1}^{n} \lambda_{ik} = 1$) and the inequality follows, since, $|\epsilon_k| = |w_I|$ and $|1 + t\epsilon_k| \leq 1 + |t\epsilon_k| = 1 + |w_I t|$. This derivation holds for any i (but only for one at a time), and (10.30) follows by selecting i to maximize $\sum_{k=1}^{n} |\lambda_{ik}|$ (the maximum row-sum of the RGA of G). $\qquad\Box$

Chapter 11

Conclusions and directions for future work

11.1 Discussion

The main objective with this work has been to provide new results and tools which can help to reduce the gap between control theory and process control applications. This has been and still is a challenging task. The approach taken is to obtain good insights into linear system and control theory, and to look for "relatively simple" but relevant practical process control problems which actually can be solved analytically by applying the insights obtained. Unfortunately, most engineers will regard this thesis as theoretical and many may have problems with seeing the practical implications of the results given in this thesis. Therefore, much work has been put into examples and case studies to exemplify and illustrate the use of the results, with the consequence that the thesis is rather long.

The directionalities of zeros and poles in multivariable systems are studied in Chapter 2. The chapter shows how the directionality of zeros and poles can be computed from eigenvalue problems. These directions are used in the factorizations of RHP zeros and poles in multivariable systems (Appendix A), to quantify the performance limitations imposed by RHP zeros and poles in multivariable systems (Chapters 3–5), and to quantify the minimum input energy ($\mathcal{H}_2$-norm) needed to stabilize a plant with one unstable mode. It is the authors opinion that these concepts have important roles to play both in linear system and control theory. Rosenbrock (1966; 1970) and Kalman (1966) both noted that state controllability and observability contain information about the physical structure. This structural information is also reflected in the directionality of the poles. However, the same is not true for the more commonly used rank tests for state controllability and observability. The usefulness of concepts like state controllability and observability in control structure design, is thus significantly improved when introducing the directionality of the poles. However, the author notes the similarities between the pole directions and the way of analytically solving linear time invariant dynamical initial value problems in terms of eigenvalue decomposition. Furthermore, new results on the controllability of repeated poles can be stated in terms of the pole directions, and the

practical significance of these are demonstrated in the distillation DB-configuration example
in Chapter 6.

Chapters 3–5 study the performance limitations imposed by RHP zeros and poles in mul-
tivariable systems by deriving lower bounds on the $\mathcal{H}_\infty$-norm of various closed-loop transfer
functions. Common to all the bounds is that they depend on interpolation constraints on the
sensitivities or complementary sensitivities, which must (for internal closed-loop stability)
apply if the plant has a RHP-zero or a RHP-pole. The use of interpolation constraint to derive
a lower bound on the $\mathcal{H}_\infty$-norm of a closed-loop transfer function was first considered by
Zames (1981), who derived a lower bound on the weighted sensitivity when the plant has a
RHP-zero.

In Chapter 3 the performance limitations are quantified in terms of peaks in the sensitivity
and complementary sensitivity functions. The advantages with the expressions presented in
this thesis compared to earlier work, are that they can easily be evaluated in a computer,
direct insights to the limitations can be obtained from the expressions and the directionality
of zeros and poles, and the expressions are given in terms of algebraic rather than integral
relations. One advantage with the earlier work involving sensitivity integral relations is that
they generalize the more classical Bode's sensitivity integral.

Chapters 4 and 5 present lower bounds on $\mathcal{H}_\infty$-norm of general closed-loop transfer func-
tions, when the plant has one or more RHP zeros or poles. The author has not seen any results
similar to these and with the same generality presented earlier in the control literature, and
it is believed that the derived bounds have large engineering implications. These implica-
tions involve quantifying the effect of disturbances and measurement noise on performance
measured both at the input and at the output of the plant. This means that one can say some-
thing about the achievable control performance without actually designing the controllers.
If the lower bounds are large then one can conclude that good control performance can not
be achieved, irrespective of the controller designed. One important application of the lower
bounds is that one can quantify the minimum input magnitudes required for stabilization in
the presence of disturbances and measurement noise. The controllers derived in these chap-
ters may not be applied in practical cases, however, the importance of these controllers is that
they prove that the lower bounds are tight. A consequence of the lower bounds being tight, is
that one can conclude that there are no other factors[1] than RHP zeros and poles which limit
the achievable control performance.

Most of the results in this thesis (except the results in Chapter 6 on stabilizing control with
minimum input energy) on performance limitations in multivariable systems, are quantified
using the $\mathcal{H}_\infty$-norm. Some results using the $\mathcal{H}_2$-norm rather than the $\mathcal{H}_\infty$-norm are given in
(Morari and Zafiriou, 1989). The author notes that the "advantage" with the $\mathcal{H}_\infty$-norm rather
than the $\mathcal{H}_2$-norm, is that the $\mathcal{H}_\infty$-norm only involves the worst case frequency, whereas the
$\mathcal{H}_2$-norm involves the integral overall frequencies. This advantage makes it easier to obtain
results using the $\mathcal{H}_\infty$-norm rather than the $\mathcal{H}_2$-norm. Of course, if the results using the $\mathcal{H}_\infty$-

---

[1]In this thesis we consider linear time invariant dynamical systems which can be described by rational transfer
function matrices (or by state-space description). This does not include time delays which also limit the achievable
control performance. However, by using the Padé approximation for the time delay, the performance limitations
imposed can be quantified using the results given here.

norm shall be applicable, they must allow weights to be included. In general, one could use any norm to quantify the performance limitations imposed by instability and non-minimum phase behavior.

In Chapter 6 the focus moves from the implications of RHP zeros and poles in multivariable systems over to the more practical problem of control structure design. In this chapter the minimum input usage needed for stabilization is quantified both in terms of the $\mathcal{H}_2$ and the $\mathcal{H}_\infty$ norms. The results involving the $\mathcal{H}_\infty$-norm relate nicely to the bounds in Chapters 4 and 5 on performance limitations imposed by RHP zeros and poles in multivariable systems. Results directly applicable to control structure design, are presented. The main advantages are that these results are based on theoretical considerations and can easily be quantified mathematically. In general, the difference between the $\mathcal{H}_2$ and the $\mathcal{H}_\infty$ norms can be infinite. However, for SISO control minimizing the input usage for a plant with one unstable mode, these norms are closely related. It also turns out that the best input and the best output are independent of the norm. This chapter also contains several realistic examples on the use of the pole vectors in control structure design. Among others, an unstable chemical reactor, the Tennessee Eastman problem and the distillation column DB-configuration, are considered.

Chapters 7–9 deal with partial control, its relation to indirect and cascade control, and implications on control structure design on the regulatory control layer. In particular, two approaches for selecting secondary measurements for indirect and cascade control, are given. Some new insights into the trade-off between rejecting measurement noise and disturbances, are obtained from these results. Chapter 9 contains a realistic case study, in which the tools (derived in Chapter 8) for selecting secondary measurements in indirect and cascade control, are applied to the problem of selecting secondary temperature measurements for indirect two-point control of product compositions in a binary distillation column. Furthermore, the tools (derived in Chapter 7) for addressing the controllability of partial control, are used to analyze indirect control of product compositions by controlling temperatures at two selected stages.

Chapter 10 presents results quantifying the effect of input and output uncertainty on performance in multivariable systems. For now it is just noted that the effect of input uncertainty on performance measured at the output of the plant is similar to the effect of RHP-zeros.

Mathematical descriptions of chemical process plants are in general nonlinear. In this thesis, nonlinearities are only taken into account in simulations and not in the analysis. The reason is that there is a need for conceptually and simple tools which can easily be applied in the analysis and to control structure design, and these tools exist so far only for linear systems.

11.2 Main contributions

The main contributions of this thesis are summarized below:

Chapter 2 shows how to compute the zero and pole directions in multivariable systems in terms of eigenvalue computations. The second part of the chapter deals with state controllability and observability in terms of pole directions. Restating the Popov-Belevitch-Hautus eigenvector tests in terms of the pole vectors (directions) make the results on state control-

lability and observability more useful in control structure design. If the plant has a repeated mode with linearly independent eigenvectors, the results in Chapter 2 can be used to identify the minimum number of inputs and outputs needed to control the mode. These results are also applicable to two closely located poles with (nearly) orthogonal pole directions.

Chapter 3. The results in Chapter 3 quantify the fundamental limitations imposed by RHP zeros and poles in terms of lower bounds on the peaks in the weighted sensitivity and complementary sensitivity functions. Previously derived lower bounds on the sensitivity function involves sensitivity integral relations. The results given in this chapter, are derived using algebraic rather than integral constraints. A tight lower bound on the $\mathcal{H}_\infty$-norm of the weighted sensitivity is derived. This bound is similar to the bounds presented in (Boyd and Desoer, 1985) and (Chen, 1993; Chen, 1995). However, the bounds presented in this chapter extend the bounds by Boyd and Desoer (1985) and Chen (1993; 1995) to the case where the plant G has more than one RHP-pole. A similar result in terms of the weighted complementary sensitivity $w_T T(s)$ for the case where the plant G has one or more RHP-poles and any number of RHP-zeros, are also given in this chapter.

Chapter 4. The basis for the results in this chapter is the *important* work by Zames (1981), who made use of the interpolation constraint $S(z) = 1$ and the maximum modulus theorem to derive bounds on the $\mathcal{H}_\infty$-norm of S for plants with one RHP-zero. Subsequently, these results were extended to unstable plants with one RHP-pole and then to plants with combined RHP zeros and poles (e.g. Doyle et al., 1992; Skogestad and Postlethwaite, 1996). However, these generalizations to unstable plants did *not* consider the input usage, which involves the closed-loop transfer function KS. In this chapter general lower bounds on $\mathcal{H}_\infty$-norm of SISO closed-loop transfer functions on the forms TV and SV are given. By applying the relation $KS = G^{-1}T$, it is possible to derive lower bounds on the input usage, by using the general lower bound on $\|TV(s)\|_\infty$ with $V = G^{-1}$. But when G is unstable (with RHP-pole p), then $V = G^{-1}$ has a RHP-zero for $s = p$. One contribution of this work, is the ability to include RHP zeros and poles in the "weight" V. An additional important contribution is the derivation of analytical $\mathcal{H}_\infty$-optimal controllers which *achieve* an $\mathcal{H}_\infty$-norm of the closed-loop transfer function equal to the lower bound. One important application of the lower bounds is to quantify the minimum input usage needed for stabilization in the presence of worst case measurement noise and disturbances.

Chapter 5 generalizes the results of Chapter 4 to MIMO-systems. This chapter extends the work of Zames (1981) and the work given in Chapters 3 and 4, and quantifies the fundamental limitations imposed by RHP zeros and poles in terms of lower bounds on the $\mathcal{H}_\infty$-norm of important closed-loop transfer functions. From the results in this chapter, lower bounds on $\mathcal{H}_\infty$-norm of other closed-loop transfer functions than sensitivity and complementary sensitivity can be derived. Further generalizations include:

1) Multivariable weights.
2) Unstable and non-minimum phase weights.

An additional important contribution of this paper is that the lower bounds are *tight* in a large number of cases. That is, analytical expressions for controllers which *achieve* an $\mathcal{H}_\infty$-norm

of the closed-loop transfer function (which is) equal to the lower bound, are given. Again, one important application of the lower bounds is to quantify the minimum input usage needed for stabilization in the presence of worst case measurement noise and disturbances.

Chapter 6 considers control structure design using the information given in the pole vectors. It is shown how the input and output pole vectors are related to the minimum input usage needed to stabilize a plant with one unstable mode using a SISO controller. The minimum input usage is quantified both in terms of the $\mathcal{H}_2$-norm (input energy) and the $\mathcal{H}_\infty$-norm. The best choice of one input and one output for SISO stabilizing control is the same for both norms and corresponds to the elements in the pole vectors with largest magnitude. Stable but slow modes which need to be shifted further into the Left Half Plane (LHP) using feedback control, are also considered. Moving stable slow modes are accomplished with modal control, and the results are interpreted in terms of Linear Quadratic Gaussian (LQG) control. The results given in this chapter are directly applicable to control structure design.

Chapter 7 introduces the controllability measures: partial disturbance gain, partial reference gain and the partial gain for measurement noise, to address the controllability of a partially controlled system. The partial disturbance gain is the same as the partial disturbance gain introduced by Skogestad and Wolff (1992). The relative gain array (RGA) and the singular value decomposition (SVD) are introduced as useful tools to assist when selecting inputs and outputs to be used in partial control.

Chapter 8 considers indirect control and cascade control. It is shown how the trade-off between measurement noise and disturbance rejection in indirect control can be analyzed using the tools derived for partial control. Two simple tools for selection of secondary measurement in indirect and cascade control are given in this chapter.

Chapter 9 exemplifies the use of the tools derived in Chapters 7 and 8. The problem considered is to select temperature measurements to be used in two-point indirect control of product compositions in a binary distillation column. The trade-off between measurement noise and disturbance rejection is demonstrated. Also one-point temperature control is considered.

Chapter 10. The relative gain array (RGA) and condition number are commonly used tools in controllability analysis. New results that link these measures to control performance, measured in terms of the output sensitivity function with input and output uncertainty, are given in this chapter.

11.3 Directions for future work

Some directions for future work include:

Chapter 2. The input and output zero and pole directions can easily be defined, and valuable insights into the geometrical interpretations of zeros and poles can be obtained by using the Smith-McMillan form. The author suggests to define the zero and pole directions for rational transfer function matrices using the Smith-McMillan form and to look into

the work by Kwakernaak (1995), on polynomial matrix methods in linear system and control theory.

Chapters 3–5. Extensions to the results on performance limitations imposed by RHP zeros and poles in linear systems, may include:

1) Improved bounds on $\|WSV(s)\|_\infty$ and $\|WS_IV(s)\|_\infty$ which takes into account more than one RHP-zero a time.

2) Improved bounds on $\|WTV(s)\|_\infty$ and $\|WT_IV(s)\|_\infty$ which takes into account more than one RHP-pole a time.

3) Find analytical expressions for the controllers which achieve these improved lower bounds.

At the moment, it seems difficult to provide these generalizations for multivariable systems. However, some results have been obtained on minimizing the $\mathcal{H}_\infty$-norm of the input usage (i.e. minimizing $\|KS(s)\|_\infty = \|G^{-1}T(s)\|_\infty$) for SISO systems, when the plant has more than one unstable mode. Although, these results are not reported in this thesis.

4) The controllers given in Chapters 4 and 5, which prove tightness of the lower bounds are similar to the controllers obtained by using the early interpolation theoretic methods (Doyle, 1984), and it is also related to the polynomial approach of Kwakernaak (1986; 1993; 1996). Mainly due to the lack of time, no attempts have been made in this thesis to compare and utilize the similarities in these approaches. It could therefore be wise to go through the earlier results to see if some benefit from these approaches can be applied in the approach given here.

5) Find analytical controllers which minimize the $\mathcal{H}_\infty$-norm of stacked closed-loop transfer functions, for example find $K(s)$ which solves:

$$\min_{K(s)} \left\| \begin{bmatrix} S(s) \\ KS(s) \end{bmatrix} \right\|_\infty$$

Chapter 6. Several attempts have been made to generalize and to interpret the results on moving (stabilizing) more than one unstable pole using SISO controller, however, these are still open issues for research.

Chapter 8. Relate the results in Chapter 8 to optimizing control using a standard quadratic criterion from optimal control theory.

Chapter 10. A straightforward extension of the work in Chapter 10, would be to consider output uncertainty and measure the performance at the input of the plant.

As noted in the discussion, this work quantifies the performance limitations imposed by instability and non-minimum phase behavior using the $\mathcal{H}_\infty$-norm. In general, one could use any norm for this quantification. One particular system norm which has gained some focus lately, is the l_1-norm (induced infinity norm). Further work can be to quantify the limitations imposed by instability and non-minimum phase behavior using the l_1-norm.

References

Boyd, S. and Desoer, C. A. (1985). Subharmonic functions and performance bounds in linear time-invariant feedback systems, *IMA J. Math. Contr. and Info.* **2**: 153–170.

Chen, J. (1993). Sensitivity integral relations and design trade-offs in linear multivariable feedback systems, *Proc. American Control Conference*, San Francisco, CA, pp. 3160–3164.

Chen, J. (1995). Sensitivity integral relations and design trade-offs in linear multivariable feedback systems, *IEEE Transactions on Automatic Control* **AC-40**(10): 1700–1716.

Doyle, J. C. (1984). *Lecture Notes on Advances in Multivariable Control*, ONR/Honeywell Workshop, Minneapolis, October.

Doyle, J. C., Francis, B. and Tannenbaum, A. (1992). *Feedback Control Theory*, Macmillan Publishing Company.

Kalman, R. (1966). On the structural properties of linear constant multivariable systems, *Third IFAC World Congress*. Paper 6A.

Kwakernaak, H. (1986). A polynomial approach to minimax frequency domain optimization of multivariable feedback systems, *Int. J. Control* **44**(1): 117–156.

Kwakernaak, H. (1993). Robust control and $\mathcal{H}_\infty$-optimization — Tutorial paper, *Automatica* **29**: 255–273.

Kwakernaak, H. (1995). State space algorithms for polynomial matrix computations, *Proc. from EURACO Workshop on Recent results in Robust and Adaptive Control*, Florence, Italy, pp. 133–170.

Kwakernaak, H. (1996). *Frequency domain solution of the standard $\mathcal{H}_\infty$-problem*, In M.J. Grimble and V. Kucera's edition on: Polynomial Methods for Control System Design, Springer-Verlag, Heidelberg.

Morari, M. and Zafiriou, E. (1989). *Robust Process Control*, Prentice-Hall, Englewood Cliffs.

Rosenbrock, H. H. (1966). On the design of linear multivariable systems, *Third IFAC World Congress*. Paper 1A.

Rosenbrock, H. H. (1970). *State-space and Multivariable Theory*, Nelson, London.

Skogestad, S. and Postlethwaite, I. (1996). *Multivariable Feedback Control, Analysis and Design*, John Wiley & Sons, Chichester.

Skogestad, S. and Wolff, E. A. (1992). Controllability measures for disturbance rejection, *IFAC Workshop on Interactions between Process Design and Process Control*, London, UK, pp. 23–29.

Zames, G. (1981). Feedback and optimal sensitivity: model reference transformations, multiplicative seminorms, and approximate inverses, *IEEE Transactions on Automatic Control* **AC-26**(2): 301–320.

Appendix A

Factorizations of zeros and poles in multivariable systems

Kjetil Havre[*] and Sigurd Skogestad[†]

Chemical Engineering,
Norwegian University of Science and Technology
N-7034 Trondheim, Norway.

Abstract

Analytical state-space realizations for factorizations of zeros and poles in multivariable systems into *Blaschke* products are given in this paper. Some useful properties of these factorizations are also considered.

---

[*]Also affiliated with: Institute for energy technology, P.O.Box 40, N-2007 Kjeller, Norway, Fax: (+47) 63 81 11 68, E-mail: Kjetil.Havre@ife.no.

[†]Fax: (+47) 73 59 40 80, E-mail: skoge@chembio.ntnu.no.

A.1   Introduction

The objective with this paper is to derive analytical state-space realizations for factorizations of zeros and poles in multivariable systems into *Blaschke* products. Factorizations of zeros and poles both on the input and the output are given. These factorizations can be used on any zeros and poles (both in the open Left Half Plane (LHP) and in the open Right Half Plane (RHP)) of a rational transfer function matrix (which can be non-square). However, the benefit of applying them to zeros and poles in the open LHP seems to be limited since the factorizations given then introduces zeros and poles in the open RHP in the representation of the factorized plant. So, our use have been restricted to factorize zeros and poles in the open RHP, see Chapters 3–5. We will therefore write this text assuming that the factorizations are applied to zeros and poles in the open RHP.

The main property of the factorizations is that the factor containing the singular points (the zeros or poles) has all except one singular value equal to one for all values of s in the complex plane, and for complex numbers on the imaginary axis ($s = j\omega$) the factor is all-pass (has all singular values equal to one). This property is used extensively in the Chapters 3–5, where the factorizations are used to derive lower bounds on the $\mathcal{H}_\infty$-norm of important closed-loop transfer functions. Some additional useful properties of the factorizations used in Chapter 5 are also given in this paper.

An alternative to the factorizations of RHP-zeros presented in this paper is the "inner-outer" factorization used in (Morari and Zafiriou, 1989, page 303 and given in Theorem 12.6.4 on page 309). However, this factorization is given in terms of a stabilizing solution to an algebraic Riccati equation, so the connection to the zero directions are not obvious. Also this factorization is all-pass for complex numbers on the imaginary axis, however, for complex numbers $s \in \mathbb{C}^+$ and $s \in \mathbb{C}^-$ more than one singular value is different from one. When using these factorizations in the derivation of the lower bounds on the $\mathcal{H}_\infty$-norm on closed-loop transfer functions, the bounds derived were generally not tight.

Factorizations of RHP-zeros/poles in Single Input Single Output (SISO) into *Blaschke* products have been used extensively in the control literature. Factorizations of RHP-zeros in Multiple Input Multiple Output (MIMO) have also been known for a period (Wall et al., 1980; Zhou et al., 1996), and factorizations of RHP-poles in MIMO-systems obtained from zero factorizations of the inverse plant G^{-1} have been used by Chen (1995). However, analytical state-space realizations of factorizations of RHP-poles in terms of the poles and pole directions have to our knowledge not been presented in the literature before. The main reason for this may be the lack of proper definitions of pole directions.

The main result in this paper is to provide these state-space realizations for factorization of RHP-poles into *Blaschke* products, and to prove some of the properties of the factorizations. All factorizations given in this paper are applicable to non-square systems.

The concepts of zeros and poles and their directions in multivariable systems are essential in this paper, and are therefore briefly reviewed in Section A.2. The zero-directions are well known from the control literature, but the definitions of pole-directions may be somewhat more obscure. Results regarding the definitions and computations of pole directions are given in Chapter 2. Section A.3 contains input and output factorizations of zeros and

poles. Section A.4 looks at the factorizations as operations which can be applied to a rational transfer function matrix, and reveal some of the properties of these operations.

For simplicity we will assume throughout the paper that the zeros and poles er distinct, i.e. multiplicity one. All the proofs are given in Section A at the end of the paper. This appendix contains the background material for Chapters 3–5.

Notation. We consider linear time invariant systems on state space form

$$\dot{x} = Ax + Bu \tag{A.1}$$

$$y = Cx + Du \tag{A.2}$$

where $A \in \mathbb{R}^{n \times n}$, $B \in \mathbb{R}^{n \times m}$, $C \in \mathbb{R}^{l \times n}$ and $D \in \mathbb{R}^{l \times m}$, n is the number of states, l is the number of outputs and m is the number of inputs. The short-hand notation

$$G = \left[\begin{array}{c|c} A & B \\ \hline C & D \end{array} \right] \tag{A.3}$$

for (A.1)–(A.2) is frequently used to describe a state-space model of a system G. The transfer function of G defined by (A.3) can be evaluated as a function of the complex variable $s \in \mathbb{C}$

$$G(s) = C(sI - A)^{-1}B + D \tag{A.4}$$

We often omit to show the dependence on the complex variable s for transfer functions.

We use the letter u to denote input directions and the letter y to denote output directions. The subscripts p and z are used to distinguish the pole direction from the zero direction. If there are more than one zero or one pole we use an additional subscript to denote the direction of that particular zero or pole. For the state directions the letter x is used with subscript z or p as above. To distinguish input state direction from the output state direction we use an additional subscript i for input or o for output.

With the term *direction* we mean a unit basis vector for the direction. When we use the term *vector* the length is generally *not* normalized. For example, the term "input pole vector" denotes a vector in $\mathbb{C}^m$ and the length of this vector is generally *not* equal to one. The term "input pole direction" (a vector) is used to denote the same direction as the input pole vector but the length of the vector is normalized.

A.2 Zeros and poles in multivariable systems

For a more detailed discussion of zeros and poles in multivariable systems refer to Chapter 2.

A.2.1 Zeros

For a system $G(s)$ with state-space realization $\left[\begin{array}{c|c} A & B \\ \hline C & D \end{array} \right]$, the zeros z of the system, the input zero directions u_z and the input zero state vectors $\boldsymbol{x}_{zi} \in \mathbb{C}^n$ can all be computed from the generalized eigenvalue problem

$$\begin{bmatrix} A - zI & B \\ C & D \end{bmatrix} \begin{bmatrix} \boldsymbol{x}_{zi} \\ u_z \end{bmatrix} = \begin{bmatrix} 0 \\ 0 \end{bmatrix} \tag{A.5}$$

The scaling of the vector $[\,\boldsymbol{x}_{zi}^T \quad u_z^T\,]$ in (A.5) is important for the expressions in the factorizations. The vector is scaled such that u_z is normalized, i.e. $u_z^H u_z = 1$.

Similarly, one can compute the zeros z, the output zero directions y_z and the output zero state vectors $\boldsymbol{x}_{zo} \in \mathbb{C}^n$ through the generalized eigenvalue problem

$$[\,\boldsymbol{x}_{zo}^H \quad y_z^H\,] \begin{bmatrix} A - zI & B \\ C & D \end{bmatrix} = [\,0 \quad 0\,] \tag{A.6}$$

where the vector $[\,\boldsymbol{x}_{zo}^H \quad y_z^H\,]$ is scaled such that $y_z^H y_z = 1$. By taking the transpose of (A.6) one obtains

$$\begin{bmatrix} A^T - zI & C^T \\ B^T & D^T \end{bmatrix} \begin{bmatrix} \bar{\boldsymbol{x}}_{zo} \\ \bar{y}_z \end{bmatrix} = \begin{bmatrix} 0 \\ 0 \end{bmatrix} \tag{A.7}$$

where the bar $\bar{\cdot}$ denotes the complex conjugate. From this we see that the input zero directions of the transposed system G^T are equal to the conjugate of the output zero directions of G. In MATLAB the generalized eigenvalue problem (A.6) can be solved via the transposed problem.

A.2.2   Poles

For a system $G(s)$ with minimal state-space realization $\left[\begin{array}{c|c} A & B \\ \hline C & D \end{array}\right]$ the input (u_p) and output (y_p) pole directions for a *distinct* pole p can be computed from[1] (see Chapter 2)

$$u_p = B^H x_{pi} / \, \|B^H x_{pi}\|_2 \, ; \qquad y_p = C x_{po} / \, \|C x_{po}\|_2 \tag{A.8}$$

where the input pole state direction $x_{pi} \in \mathbb{C}^n$ and the output pole state direction $x_{po} \in \mathbb{C}^n$ are the left and the right eigenvectors corresponding to the two eigenvalue problems

$$x_{pi}^H A = x_{pi}^H p; \qquad A x_{po} = p x_{po}$$

We also define the input and output state vectors for poles

$$\boldsymbol{x}_{pi} = x_{pi} / \, \|B^H x_{pi}\|_2 \, ; \qquad \boldsymbol{x}_{po} \triangleq x_{po} / \, \|C x_{po}\|_2 \tag{A.9}$$

Then we have that

$$u_p = B^H \boldsymbol{x}_{pi}; \qquad y_p = C \boldsymbol{x}_{po} \tag{A.10}$$

The input and output state vectors for the pole p are used in the factorizations of poles together with the input and output pole directions. For the case where the pole p is not distinct refer to Chapter 2.

A.3   All-pass factorizations of RHP-zeros and poles

A transfer function matrix $B(s)$ is all-pass if $B^T(-s)B(s) = I$, which implies that all singular values of $B(j\omega)$ are equal to one.

---

[1]It requires that the mode p is observable and controllable, which is the case for a minimal realization. If the mode p is not observable then $C x_{po} = 0$, i.e. $\|C x_{po}\|_2 = 0$, and if the mode p is not controllable then $B^H x_{pi} = 0$, i.e. $\|B^H x_{pi}\|_2 = 0$.

(a) Input factorization of RHP-zeros

(b) Output factorization of RHP-zeros

(c) Input factorization of RHP-poles
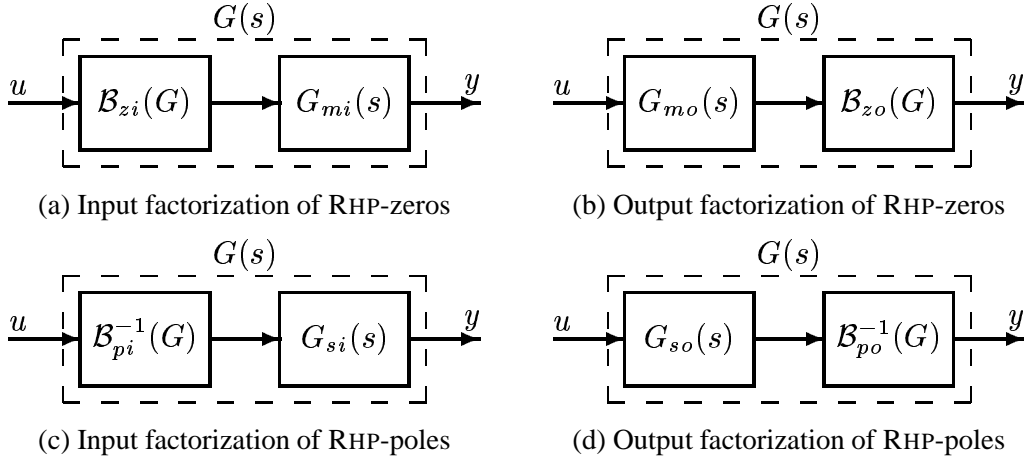
(d) Output factorization of RHP-poles

Figure A.1: Structure of input/output factorizations of RHP-zeros/poles

Right half plane zeros and poles (zeros/poles in the open right half plane, $\mathbb{C}^+$) of a rational transfer function $G(s)$ can be factorized in either of the two *Blaschke* products labeled "input factorization" (subscript i) or "output factorization" (subscript o) as follows (see Figure A.1)

	Input	Output	
RHP-zeros:	$G(s) = G_{mi}(s)\mathcal{B}_{zi}(G(s));$	$G(s) = \mathcal{B}_{zo}(G(s))\,G_{mo}(s)$	(A.11)
RHP-poles:	$G(s) = G_{si}(s)\mathcal{B}_{pi}^{-1}(G(s));$	$G(s) = \mathcal{B}_{po}^{-1}(G(s))\,G_{so}(s)$	(A.12)

where

G_{mi}, G_{mo} – Minimum phase versions of $G(s)$ with the RHP-zeros mirrored across the imaginary axis.

$\mathcal{B}_{zo}(G), \mathcal{B}_{zi}(G)$ – Stable all-pass rational transfer function matrices (all singular values are equal to 1 for $s = j\omega$) containing the RHP-zeros (subscript z) of $G(s)$.

G_{si}, G_{so} – Stable (subscript s) versions of $G(s)$ with the RHP-poles mirrored across the imaginary axis.

$\mathcal{B}_{po}(G), \mathcal{B}_{pi}(G)$ – Stable all-pass rational transfer function matrices (all singular values are equal to 1 for $s = j\omega$) containing the RHP-poles (subscript p) of $G(s)$ as RHP-zeros.

A REMARK ON NOTATION. The filters $\mathcal{B}_{zi}(G)$, $\mathcal{B}_{zo}(G)$, $\mathcal{B}_{pi}(G)$ and $\mathcal{B}_{po}(G)$ represent factorizations of all RHP-zeros/poles in the rational transfer function G. The filter is of course dependent on the RHP-zeros/poles and their input/output directions in G. This is reflected in the notation $\mathcal{B}_{xx}(G)$, where $xx \in \{zi,\ zo,\ pi,\ po\}$. On the other hand, the filters are rational transfer function matrices and are therefore function of the complex variable s. A strict notation would be $\mathcal{B}_{xx}(G, s)$, which we simplify to $\mathcal{B}_{xx}(G(s))$. As the reader may have noticed, we sometimes avoid to show the dependency of complex variable s, and write $\mathcal{B}_{xx}(G)$ instead. When we want to evaluate the rational transfer function at a complex number c for the complex variable s, i.e. $s = c$, we use the notation $\mathcal{B}_{xx}(G)|_{s=c}$. When the focus is on the rational transfer function containing the RHP-zeros/poles and some of its properties which are independent of the zeros/poles and their directions we write $\mathcal{B}(s)$. To summarize, the notation is twofold:

1) Operator: $\mathcal{B}_{xx}(G(s))$ is used to denote the factorization of RHP-zeros/poles in G. In these cases $\mathcal{B}_{xx}(\cdot)$ may be viewed as operators, and for example $\mathcal{B}_{zi}(G)$, means factorize the RHP-zeros

of G into the all-pass rational transfer function denoted $\mathcal{B}_{zi}(G)$. Some of the properties of the operators are summarized in Section A.4.

2) The rational transfer function matrix $\mathcal{B}_{xx}(G(s))$: Sometimes the singular points and the directions are of minor importance, in these cases we write $\mathcal{B}(s)$.

In a similar way $(\cdot)_{mi}$, $(\cdot)_{mo}$, $(\cdot)_{si}$ and $(\cdot)_{so}$ may both denote the operators which return "minimum phase" or "stable" versions of a rational transfer function, where the RHP-zeros or the RHP-poles are factorized either at the "input" or at the "output".

When factorizing RHP-zeros, the filters $\mathcal{B}_{zi}(G)$ and $\mathcal{B}_{zo}(G)$ consist of N_z (N_z is the number of RHP-zeros) series connected first order filters $\mathcal{B}_i(s)$ of size $k \times k$, each factorizing one RHP-zero z_i. If an output factorization is considered then $k = l$ and if an input factorization is considered then $k = m$. In a similar manner, when factorizing RHP-poles the filters $\mathcal{B}_{pi}(G)$ and $\mathcal{B}_{po}(G)$ consist of N_p (N_p is the number of RHP-poles) series connected first order filters $\mathcal{B}_i(s)$ of size $k \times k$ each factorizing one RHP-pole p_i.

A.3.1   All-pass filter $\mathcal{B}(s)$

The general filter $\mathcal{B}(s)$ describing $\mathcal{B}_{zi}(G)$, $\mathcal{B}_{zo}(G)$, $\mathcal{B}_{pi}(G)$ and $\mathcal{B}_{po}(G)$ and some of it's properties are summarized in Lemma A.1.
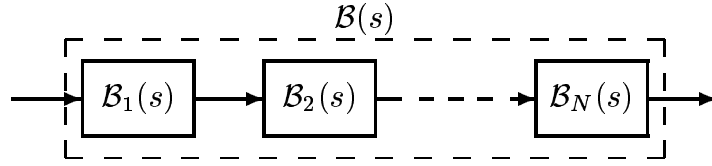

Figure A.2: All-pass filter

LEMMA A.1 (ALL-PASS FILTER). *Let $c_i \in \mathbb{C}^+$, $v_i \in \mathbb{C}^k$ with $v_i^H v_i = 1$, $\forall i \in 1, \dots, N$, and let the filter $\mathcal{B}(s)$ be defined as (see Figure A.2)*

$$\mathcal{B}(s) \quad = \quad \mathcal{B}_N(s)\mathcal{B}_{N-1}\cdots\mathcal{B}_1(s) = \prod_{i=0}^{N-1} \mathcal{B}_{N-i}(s) \quad where \tag{A.13}$$

$$\mathcal{B}_i(s) \quad = \quad I - \frac{2\mathrm{Re}(c_i)}{s + \bar{c}_i} v_i v_i^H \tag{A.14}$$

Consider the factor $\mathcal{B}_i(s)$ in $\mathcal{B}(s)$:

1) $\mathcal{B}_i(s)$ has $k - 1$ eigenvalues equal to one and the remaining eigenvalue is

$$\lambda_k(\mathcal{B}_i(s)) = \frac{s - c_i}{s + \bar{c}_i} \tag{A.15}$$

2) $\mathcal{B}_i(s)$ has $k - 1$ singular values equal to one and the remaining singular value is

$$\sigma_k(\mathcal{B}_i(s)) = |\lambda_k(\mathcal{B}_i(s))| = \frac{|s - c_i|}{|s + \bar{c}_i|} = \begin{cases} \underline{\sigma}(\mathcal{B}_i(s)) < 1 & for\ s \in \mathbb{C}^+ \\ \bar{\sigma}(\mathcal{B}_i(s)) > 1 & for\ s \in \mathbb{C}^- \\ 1 & for\ s = j\omega. \end{cases} \tag{A.16}$$

3) $\mathcal{B}_i(s)$ *has* RHP-*zero for* $s = c_i$ *with input and output zero directions* v_i.

4) $\mathcal{B}_i(s)$ *has* LHP-*pole for* $s = -\bar{c}_i$ *with input and output pole directions* v_i.

The inverse of $\mathcal{B}(s)$ *is given by*

$$\mathcal{B}^{-1}(s) \quad = \quad \mathcal{B}_1^{-1}(s)\mathcal{B}_2^{-1}(s)\cdots\mathcal{B}_N^{-1}(s) = \prod_{i=1}^{N}\mathcal{B}_i^{-1}(s) \quad where \tag{A.17}$$

$$\mathcal{B}_i^{-1}(s) \quad = \quad I + \frac{2\mathrm{Re}(c_i)}{s - c_i}v_i v_i^H \tag{A.18}$$

5) $\mathcal{B}_i^{-1}(s)$ *has* $k - 1$ *eigenvalues equal to one and the remaining eigenvalue is*

$$\lambda_k(\mathcal{B}_i^{-1}(s)) = \frac{s + \bar{c}_i}{s - c_i} \tag{A.19}$$

6) $\mathcal{B}_i^{-1}(s)$ *has* $k - 1$ *singular values equal to one and the remaining singular value is*

$$\sigma_k(\mathcal{B}_i^{-1}(s)) = |\lambda_k(\mathcal{B}_i^{-1}(s))| = \frac{|s + \bar{c}_i|}{|s - c_i|} = \begin{cases} \bar{\sigma}(\mathcal{B}_i^{-1}(s)) > 1 & for\ s \in \mathbb{C}^+ \\ \underline{\sigma}(\mathcal{B}_i^{-1}(s)) < 1 & for\ s \in \mathbb{C}^- \\ 1 & for\ s = j\omega. \end{cases} \tag{A.20}$$

7) $\mathcal{B}_i^{-1}(s)$ *has* RHP-*pole for* $s = c_i$ *with input and output pole directions* v_i.

8) $\mathcal{B}_i^{-1}(s)$ *has* LHP-*zero for* $s = -\bar{c}_i$ *with input and output zero directions* v_i.

Furthermore, a minimal realization of $\mathcal{B}(s)$ *has* N RHP-*zeros for* $s = c_i$ *and* N LHP-*poles for* $s = -\bar{c}_i$. *Define the two rational transfer functions*

$$\mathcal{B}_{N:j+1}(s) \quad = \quad \prod_{i=j+1}^{N}\mathcal{B}_{N+j+1-i}(s) = \mathcal{B}_N(s)\mathcal{B}_{N-1}(s)\cdots\mathcal{B}_{j+1}(s) \tag{A.21}$$

$$\mathcal{B}_{j-1:1}(s) \quad = \quad \prod_{i=1}^{j-1}\mathcal{B}_{j-i}(s) = \mathcal{B}_{j-1}(s)\mathcal{B}_{j-2}(s)\cdots\mathcal{B}_1(s) \tag{A.22}$$

so that

$$\mathcal{B}(s) = \mathcal{B}_{N:j+1}(s)\mathcal{B}_j(s)\mathcal{B}_{j-1:1}(s) \tag{A.23}$$

9) If $\mathcal{B}_{j-1:1}(s)$ *has no* RHP-*zeros for* $s = c_j$, *then the input zero direction of* $\mathcal{B}(s)$ *for the* RHP-*zero* $s = c_j$ *becomes*

$$u_{z=c_j} = \mathcal{B}_{j-1:1}^{-1}(c_j)\,v_j\,/\,\left\|\mathcal{B}_{j-1:1}^{-1}(c_j)\,v_j\right\|_2 \tag{A.24}$$

10) If $\mathcal{B}_{N:j+1}(s)$ *has no* RHP-*zeros for* $s = c_j$, *then the output zero direction of* $\mathcal{B}(s)$ *for the* RHP-*zero* c_j *becomes*

$$y_{z=c_j} = \mathcal{B}_{N:j+1}^{-H}(c_j)\,v_j\,/\,\left\|\mathcal{B}_{N:j+1}^{-H}(c_j)\,v_j\right\|_2 \tag{A.25}$$

11) If $\mathcal{B}_{j-1:1}(s)$ *has no* LHP-*poles for* $s = -\bar{c}_j$, *then the input pole direction of* $\mathcal{B}(s)$ *for the* LHP-*pole* $s = -\bar{c}_j$ *becomes*

$$u_{p=-\bar{c}_j} = \mathcal{B}_{j-1:1}^{H}(-\bar{c}_j)\,v_j\,/\,\left\|\mathcal{B}_{j-1:1}^{H}(-\bar{c}_j)\,v_j\right\|_2 \tag{A.26}$$

12) If $\mathcal{B}_{N:j+1}(s)$ has no LHP-poles for $s = -\bar{c}_j$, then the output pole direction of $\mathcal{B}(s)$ for the LHP-pole $s = -\bar{c}_j$ becomes

$$y_{p=-\bar{c}_j} = \mathcal{B}_{N:j+1}(-\bar{c}_j)\, v_j \, / \, \left\| \mathcal{B}_{N:j+1}(-\bar{c}_j)\, v_j \right\|_2 \tag{A.27}$$

REMARK 1. In Lemma A.1 it is assumed that $c_i \in \mathbb{C}^+$, however, most of the statements in Lemma A.1 still apply[2] for $c_i \in \mathbb{C}$. The main reason for the assumption $c_i \in \mathbb{C}^+$ is that our use of the results have been restricted to $c_i \in \mathbb{C}^+$. If the assumption is relaxed to $c_i \in \mathbb{C}$ then it is possible for the filter $\mathcal{B}(s)$ to have both a pole and a zero at the same location, for example let c_1 be a complex number with $\mathrm{Re}(c_1) > 1$ and $c_2 = -\bar{c}_1$ then the filter $\mathcal{B}(s)$ has zeros and poles for c_1 and $-\bar{c}_1$. If those zeros and poles cancel in a minimal realization or not, depends on the directions v_1 and v_2.

REMARK 2. The eigenvectors of $\mathcal{B}_i(s)$ equals the singular input vectors which again equals the singular output vectors. Also note that these vectors are independent of frequency.

REMARK 3. Since the input and output singular directions of $\mathcal{B}_i(s)$ are equal it follows that there is no rotation of the zero and pole directions from the input to the output in $\mathcal{B}_i(s)$.

A.3.2 Right half plane zeros
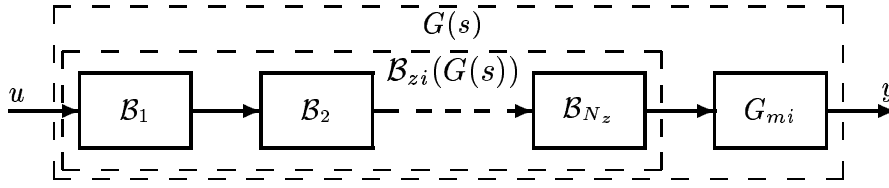
Input factorization of RHP-zeros.

Figure A.3: Input factorizations of RHP-zeros

THEOREM A.1 (INPUT FACTORIZATION OF RHP-ZEROS). *A system G with N_z RHP-zeros $z_i \in \mathbb{C}_+$, can be factorized in a minimum-phase system G_{mi} and an all-pass filter $\mathcal{B}_{zi}(G)$*

$$G(s) = G_{mi}(s)\mathcal{B}_{zi}(G(s)) \tag{A.28}$$

G_{mi} has all RHP-zeros of G mirrored into the LHP, and it is given by

$$G_{mi}(s) = \left[\begin{array}{c|c} A & B' \\ \hline C & D \end{array} \right] \tag{A.29}$$

---

[2]The statements which generally do not apply when $c_i \in \mathbb{C}$ are items 9)–12), in addition the following changes are needed:

1) In (A.16): $\bar{\sigma}(\mathcal{B}_i(s)) < 1$ if $\begin{cases} c_i, s \in \mathbb{C}^+ \\ \text{or} \\ c_i, s \in \mathbb{C}^- \end{cases}$ and $\bar{\sigma}(B_i(s)) > 1$ if $\begin{cases} c_i \in \mathbb{C}^+ \text{ and } s \in \mathbb{C}^- \\ \text{or} \\ c_i \in \mathbb{C}^- \text{ and } s \in \mathbb{C}^+ \end{cases}$

2) In (A.20): $\bar{\sigma}(\mathcal{B}_i^{-1}(s)) > 1$ if $\begin{cases} c_i, s \in \mathbb{C}^+ \\ \text{or} \\ c_i, s \in \mathbb{C}^- \end{cases}$ and $\bar{\sigma}(B_i^{-1}(s)) < 1$ if $\begin{cases} c_i \in \mathbb{C}^+ \text{ and } s \in \mathbb{C}^- \\ \text{or} \\ c_i \in \mathbb{C}^- \text{ and } s \in \mathbb{C}^+ \end{cases}$

3) $\mathcal{B}_i(s)$, $\mathcal{B}_i^{-1}(s)$ and $\mathcal{B}(s)$ may all have both LHP and RHP zeros and poles.

where B' can be calculated by applying the following two formulas repeatedly for $i = 1, \ldots, N_z$

$$
\begin{bmatrix} A - z_i I & B_{i-1} \\ C & D \end{bmatrix} \begin{bmatrix} \hat{\boldsymbol{x}}_{z_i} \\ \hat{u}_{z_i} \end{bmatrix} = \begin{bmatrix} 0 \\ 0 \end{bmatrix} \tag{A.30}
$$

$$
B_i = B_{i-1} - 2\mathrm{Re}(z_i)\hat{\boldsymbol{x}}_{z_i}\hat{u}_{z_i}^H \tag{A.31}
$$

with the vector $[\, \hat{\boldsymbol{x}}_{z_i}^T \quad \hat{u}_{z_i}^T \,]$ scaled such that $\hat{u}_{z_i}^H \hat{u}_{z_i} = 1$, $B_0 = B$ and $B' = B_{N_z}$.

The (all-pass) filter $\mathcal{B}_{zi}(G)$ contains the RHP-zeros of G with the same input zero directions as in G. It has all singular values $\sigma_i(s)$ and absolute value of all eigenvalues $\lambda_i(s)$ equal to one for $s = j\omega$. The filter has the same form as the general all-pass filter given in Lemma A.1, and it is given by

$$
\mathcal{B}_{zi}(G(s)) = \mathcal{B}_{N_z}(s)\mathcal{B}_{N_z-1}(s)\cdots\mathcal{B}_1(s) = \prod_{i=0}^{N_z-1} \mathcal{B}_{N_z-i}(s) \tag{A.32}
$$

where

$$
\mathcal{B}_i(s) = I - \frac{2\mathrm{Re}(z_i)}{s + \bar{z}_i}\hat{u}_{z_i}\hat{u}_{z_i}^H \tag{A.33}
$$

REMARK 1. The expressions above are valid for all $z \in \mathbb{C}$. For the case with $\mathrm{Im}(z) \neq 0$ the factorization yield complex realizations of $\mathcal{B}_{zi}(G)$.

REMARK 2. When G contains more than one RHP-zero, different sequences of factorizations yield the same overall $\mathcal{B}_{zi}(G)$ and G_{mi}, however, the individual filters $\mathcal{B}_i$ are different due to different directions. As an example, consider a system G with two RHP-zeros z_1 and z_2. Factorizing first z_1 and then z_2 yields $\mathcal{B}_{zi}(G) = \mathcal{B}_1(G)\mathcal{B}_2(G\mathcal{B}_1^{-1})$ and G_{mi}. Factorizing in the opposite sequence $\{z_2, z_1\}$ gives $\tilde{\mathcal{B}}_{zi}(G) = \tilde{\mathcal{B}}_2(G)\tilde{\mathcal{B}}_1(G\tilde{\mathcal{B}}_2^{-1})$ and $\tilde{G}_{mi}$ it then turns out that $G_{mi} = \tilde{G}_{mi}$ and $\mathcal{B}_{zi}(G) = \tilde{\mathcal{B}}_{zi}(G)$. However, $\mathcal{B}_1 \neq \tilde{\mathcal{B}}_1$ and $\mathcal{B}_2 \neq \tilde{\mathcal{B}}_2$.

Recursive formulas for the modified input zero directions and modified input zero state vectors for distinct zeros. The input zero directions $\hat{u}_{z_j}$ change as the factorization proceed. The input zero direction ($\hat{u}_{z_1}$) of the first RHP-zero (z_1) factorized, is equal to the input zero direction calculated from (A.5), i.e. $\hat{u}_{z_1} = u_{z_1}$. Let u_{z_2} denote the "original" input zero direction for the second RHP-zero to be factorized, and G_1 the system with the first RHP-zero factorized. We then have

$$
G_1(s)\mathcal{B}_1(G(s)) = G(s) \quad \Leftrightarrow \quad G_1(s) = G(s)\mathcal{B}_1^{-1}(G(s)) \tag{A.34}
$$

$\hat{u}_{z_2}$ is the input direction of the second RHP-zero to be factorized for the system with the first RHP-zero factorized, i.e. G_1. We then have

$$
G_1(z_2)\hat{u}_{z_2} = G \underbrace{\mathcal{B}_1^{-1}|_{s=z_2} \hat{u}_{z_2}}_{u_{z_2}} = 0 \tag{A.35}
$$

which gives the (normalized) modified input zero direction

$$
\hat{u}_{z_2} = \frac{\mathcal{B}_1|_{s=z_2} u_{z_2}}{\left\| \mathcal{B}_1|_{s=z_2} u_{z_2} \right\|_2} \tag{A.36}
$$

To generalize, the j'th (normalized) modified input zero direction $\hat{u}_{z_j}$ becomes

$$\hat{u}_{z_j} = \frac{\prod_{i=1}^{j-1} \mathcal{B}_{j-i}\big|_{s=z_j} u_{z_j}}{\left\| \prod_{i=1}^{j-1} \mathcal{B}_{j-i}\big|_{s=z_j} u_{z_j} \right\|_2} \tag{A.37}$$

Note, we must assume that the RHP-zeros z_j are distinct to use the formula (A.37).

The recursive formulas for the modified input zero state vectors follow from the first equation in (A.30) and by using the already calculated modified input zero direction $\hat{u}_{z_j}$ from (A.37). We get

$$\hat{x}_{z_j} = -(A - z_j I)^{-1} B_{j-1} \hat{u}_{z_j} \tag{A.38}$$

provided that z_j is *not* an eigenvalue of A.
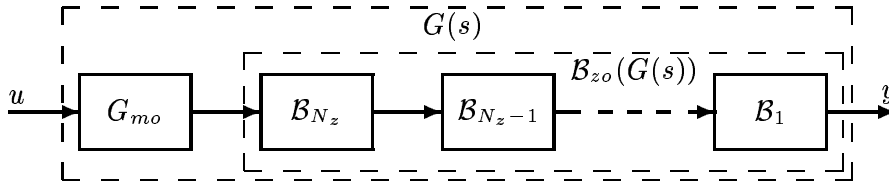
Output factorization of RHP-zeros.

Figure A.4: Output factorizations of RHP-zeros

THEOREM A.2 (OUTPUT FACTORIZATION OF RHP-ZEROS). *A system G with N_z RHP-zeros $z_i \in \mathbb{C}_+$, can be factorized into a minimum-phase system G_{mo} and an all-pass filter $\mathcal{B}_{zo}(G)$*

$$G(s) = \mathcal{B}_{zo}(G(s))\, G_{mo}(s) \tag{A.39}$$

G_{mo} has all RHP-zeros of G mirrored into the LHP, and it is given by

$$G_{mo}(s) = \left[\begin{array}{c|c} A & B \\ \hline C' & D \end{array} \right] \tag{A.40}$$

where C' can be calculated by applying the following two formulas repeatedly for $i = 1, \ldots, N_z$

$$\begin{bmatrix} \hat{x}_{z_i}^H & \hat{y}_{z_i}^H \end{bmatrix} \begin{bmatrix} A - z_i I & B \\ C_{i-1} & D \end{bmatrix} = \begin{bmatrix} 0 & 0 \end{bmatrix} \tag{A.41}$$

$$C_i = C_{i-1} - 2\mathrm{Re}(z_i)\hat{y}_{z_i}\hat{x}_{z_i}^H \tag{A.42}$$

with the vector $\begin{bmatrix} \hat{x}_{z_i}^H & \hat{y}_{z_i}^H \end{bmatrix}$ scaled such that $\hat{y}_{z_i}^H \hat{y}_{z_i} = 1$, $C_0 = C$ and $C' = C_{N_z}$.

The (all-pass) filter $\mathcal{B}_{zo}(G)$ contains the RHP-zeros of G with the same output zero directions as in G. It has all singular values $\sigma_i(s)$ and absolute value of all eigenvalues $\lambda_i(s)$

equal to one for $s = j\omega$. The filter has the same form as the general all-pass filter given in Lemma A.1, and it is given by

$$\mathcal{B}_{zo}(G(s)) = \mathcal{B}_1(s)\mathcal{B}_2(s)\cdots\mathcal{B}_{N_z}(s) = \prod_{i=1}^{N_z}\mathcal{B}_i(s) \tag{A.43}$$

where

$$\mathcal{B}_i(s) = I - \frac{2\mathrm{Re}(z_i)}{s + \bar{z}_i}\hat{y}_{z_i}\hat{y}_{z_i}^H \tag{A.44}$$

REMARK 1. The expressions above are valid for all $z \in \mathbb{C}$. For the case with $\mathrm{Im}(z) \neq 0$ the factorization yield complex realizations of $\mathcal{B}_{zo}(G)$.

Recursive formulas for the modified output zero directions and modified output zero state vectors for distinct zeros. The j'th (normalized) modified output zero direction becomes

$$\hat{y}_{z_j} = \frac{\left(\prod_{i=1}^{j-1}\mathcal{B}_i\big|_{s=z_j}\right)^H y_{z_j}}{\left\|\left(\prod_{i=1}^{j-1}\mathcal{B}_i\big|_{s=z_j}\right)^H y_{z_j}\right\|_2} \tag{A.45}$$

where y_{z_j} is the "original" output zero direction defined by (A.6). The modified output zero state vector becomes (from the upper equation in (A.41) and using the modified output direction given in (A.45))

$$\hat{x}_{z_j} = -(A - z_jI)^{-H}C_{j-1}^H\hat{y}_{z_j} \tag{A.46}$$

provided that z_j is *not* an eigenvalue of A.

A.3.3 Right half plane poles
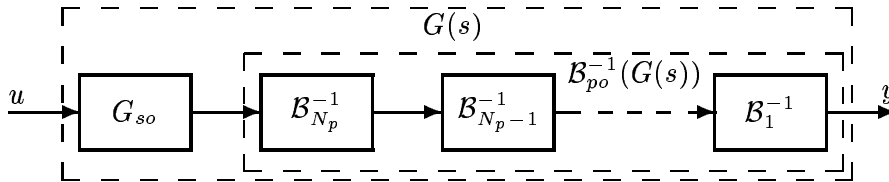
Output factorization of RHP-**poles.**

Figure A.5: Output factorizations of RHP-poles

THEOREM A.3 (OUTPUT FACTORIZATION OF RHP-POLES). *A system G with N_p* RHP-*poles $p_i \in \mathbb{C}_+$, can be factorized in a stable system G_{so} and an all-pass filter $\mathcal{B}_{po}(G)$ containing the* RHP-*poles of G as* RHP-*zeros*

$$G(s) = \mathcal{B}_{po}^{-1}(G(s))\,G_{so}(s) \tag{A.47}$$

G_{so} has all RHP-*poles of G mirrored into the* LHP, *and it is given by*

$$G_{so}(s) = \left[\begin{array}{c|c} A' & B' \\ \hline C & D \end{array} \right] \tag{A.48}$$

where A' and B' can be calculated by applying the following four formulas repeatedly for $i = 1, \ldots, N_p$

$$(A_{i-1} - p_i I)\hat{x}_{p_i} = 0; \quad \hat{y}_{p_i} = C\hat{x}_{p_i} \tag{A.49}$$

$$A_i = A_{i-1} - 2\mathrm{Re}(p_i)\hat{x}_{p_i}\hat{y}_{p_i}^H C \tag{A.50}$$

$$B_i = B_{i-1} - 2\mathrm{Re}(p_i)\hat{x}_{p_i}\hat{y}_{p_i}^H D \tag{A.51}$$

with the vector $[\, \hat{x}_{p_i}^T \quad \hat{y}_{p_i}^T \,]$ scaled such that $\hat{y}_{p_i}^H \hat{y}_{p_i} = 1$, $A_0 = A$, $B_0 = B$, $A' = A_{N_p}$ and $B' = B_{N_p}$.

The (all-pass) filter $\mathcal{B}_{po}(G)$ contains the RHP-poles of G as RHP-zeros, with input zero directions equal to the output pole directions for the RHP-poles of G. It has all singular values $\sigma_i(s)$ and absolute value of all eigenvalues $\lambda_i(s)$ equal to one for $s = j\omega$. The filter has the same form as the general all-pass filter given in Lemma A.1, and it is given by

$$\mathcal{B}_{po}(G) = \mathcal{B}_{N_p}(s)\mathcal{B}_{N_p-1}(s)\cdots\mathcal{B}_1(s) = \prod_{i=0}^{N_p-1} \mathcal{B}_{N_p-i}(s) \tag{A.52}$$

where

$$\mathcal{B}_i(s) = I - \frac{2\mathrm{Re}(p_i)}{s + \bar{p}_i}\hat{y}_{p_i}\hat{y}_{p_i}^H \tag{A.53}$$
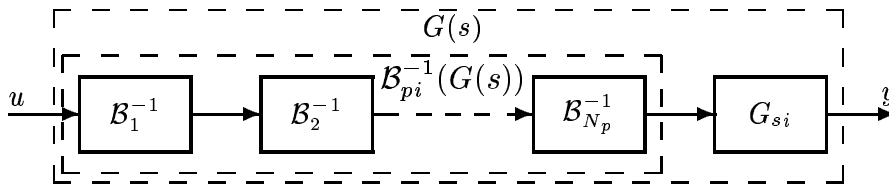
Input factorization of RHP-poles.

Figure A.6: Input factorizations of RHP-poles

THEOREM A.4 (INPUT FACTORIZATION OF RHP-POLES). *A system G with N_p RHP-poles $p_i \in \mathbb{C}_+$, can be factorized in a stable system G_{si} and an all-pass filter $\mathcal{B}_{pi}(G)$ containing the RHP-poles of G as RHP-zeros*

$$G(s) = G_{si}(s)\mathcal{B}_{pi}^{-1}(G(s)) \tag{A.54}$$

G_{si} has all RHP-*poles of G mirrored into the* LHP, *and it is given by*

$$G_{si}(s) = \left[\begin{array}{c|c} A' & B \\ \hline C' & D \end{array} \right] \tag{A.55}$$

where A' and C' can be calculated by applying the following four formulas repeatedly for $i = 1, \dots, N_p$

$$\hat{x}_{p_i}^H (A_{i-1} - p_i I) = 0; \quad \hat{u}_{p_i} = B^H \hat{x}_{p_i} \tag{A.56}$$

$$A_i = A_{i-1} - 2\mathrm{Re}(p_i) B \hat{u}_{p_i} \hat{x}_{p_i}^H \tag{A.57}$$

$$C_i = C_{i-1} - 2\mathrm{Re}(p_i) D \hat{u}_{p_i} \hat{x}_{p_i}^H \tag{A.58}$$

with the vector $[\, \hat{x}_{p_i}^H \quad \hat{u}_{p_i}^H \,]$ scaled such that $\hat{u}_{p_i}^H \hat{u}_{p_i} = 1$, $A_0 = A$, $C_0 = C$, $A' = A_{N_p}$ and $C' = C_{N_p}$.

The (all-pass) filter $\mathcal{B}_{pi}(G)$ contains the RHP-*poles of G as* RHP-*zeros, with output zero directions equal to the input pole directions for the* RHP-*poles of G. It has all singular values $\sigma_i(s)$ and absolute value of all eigenvalues $\lambda_i(s)$ equal to one for $s = j\omega$. The filter has the same form as the general all-pass filter given in Lemma A.1, and it is given by*

$$\mathcal{B}_{pi}(G(s)) = \mathcal{B}_1(s)\mathcal{B}_2(s)\cdots\mathcal{B}_{N_p}(s) = \prod_{i=1}^{N_p} \mathcal{B}_i(s) \tag{A.59}$$

where

$$\mathcal{B}_i(s) = I - \frac{2\mathrm{Re}(p_i)}{s + \bar{p}_i} \hat{u}_{p_i} \hat{u}_{p_i}^H \tag{A.60}$$

A.3.4 Single input single output systems

For SISO transfer functions the order in multiplication is irrelevant, so the all-pass filter containing the RHP-zeros or poles are identical for input and output factorizations.

RHP-zeros. By setting the zero directions to 1 in either Theorem A.1 or Theorem A.2 one gets the factorization of RHP-zeros $z_i \in \mathbb{C}_+$ for SISO-systems

$$G(s) = G_{mi}(s)\mathcal{B}_{zi}(G(s)) = \mathcal{B}_{zo}(G(s))\, G_{mo}(s) \triangleq G_m(s)\mathcal{B}_z(G(s)) \tag{A.61}$$

where

$$\mathcal{B}_z(G(s)) \triangleq \prod_{i=1}^{N_z} \frac{s - z_i}{s + \bar{z}_i} = \mathcal{B}_{zi}(G(s)) = \mathcal{B}_{zo}(G(s)) \tag{A.62}$$

If G is given in terms of the rational transfer function with polynomials α, β and $\tilde{\alpha}$ (where all roots of $\tilde{\alpha}$ have real part less than zero)

$$G(s) = \frac{\alpha(s)}{\beta(s)} = \frac{(s - z_1)(s - z_2)\cdots(s - z_{N_z})\tilde{\alpha}(s)}{\beta(s)} = \frac{\tilde{\alpha}(s)}{\beta(s)} \prod_{i=1}^{N_z} (s - z_i) \tag{A.63}$$

then G_m is given by

$$G_m(s) = \frac{(s + \bar{z}_1)(s + \bar{z}_2)\cdots(s + \bar{z}_{N_z})\tilde{\alpha}(s)}{\beta(s)} = \frac{\tilde{\alpha}(s)}{\beta(s)} \prod_{i=1}^{N_z} (s + \bar{z}_i) \tag{A.64}$$

If G is represented by the state-space realization (where $A \in \mathbb{R}^{n \times n}$, $b \in \mathbb{R}^{n \times 1}$, $c \in \mathbb{R}^{1 \times n}$ and $d \in \mathbb{R}^{1 \times 1}$)

$$G(s) = \left[\begin{array}{c|c} A & b \\ \hline c & d \end{array} \right] \tag{A.65}$$

Then one "input" realization G_{mi} of G_m is given by

$$G_{mi} = \left[\begin{array}{c|c} A & b' \\ \hline c & d \end{array} \right]$$

where b' can be calculated[3] by applying the following formula repeatedly for $i = 1, \ldots, N_z$

$$b_i = \left(I - 2\mathrm{Re}(z_i) \left(z_i I - A \right)^{-1} \right) b_{i-1}$$

with $b_0 = b$ and $b' = b_{N_z}$. Similarly, one "output" realization G_{mo} of G_m is given by

$$G_{mo} = \left[\begin{array}{c|c} A & b \\ \hline c' & d \end{array} \right]$$

where c' can be calculated[3] by applying the following formula repeatedly for $i = 1, \ldots, N_z$

$$c_i = c_{i-1} \left(I - 2\mathrm{Re}(z_i) \left(z_i I - A \right)^{-1} \right)$$

with $c_0 = c$ and $c' = c_{N_z}$.

RHP-poles. By setting the pole directions to 1 in either Theorem A.3 or Theorem A.4 one gets the factorization of RHP-poles p_i for SISO-systems

$$G(s) = G_{si}(s)\mathcal{B}_{pi}^{-1}(G(s)) = \mathcal{B}_{po}^{-1}(G(s)) \, G_{so}(s) \triangleq G_s(s)\mathcal{B}_p^{-1}(G(s)) \tag{A.66}$$

where

$$\mathcal{B}_p(G(s)) \triangleq \prod_{i=1}^{N_p} \frac{s - p_i}{s + \bar{p}_i} = \mathcal{B}_{pi}(G(s)) = \mathcal{B}_{po}(G(s)) \tag{A.67}$$

If $G(s)$ is given in terms of the rational transfer function with polynomials α, β and $\tilde{\beta}$ (where all roots of $\tilde{\beta}$ have real part less than zero)

$$G(s) = \frac{\alpha(s)}{\beta(s)} = \frac{\alpha(s)}{(s - p_1)(s - p_2) \cdots (s - p_{N_p})\tilde{\beta}(s)} = \frac{\alpha(s)}{\tilde{\beta}(s)} \prod_{i=1}^{N_p} \frac{1}{s - p_i} \tag{A.68}$$

then G_s is given by

$$G_s(s) = \frac{\alpha(s)}{(s + \bar{p}_1)(s + \bar{p}_2) \cdots (s + \bar{p}_{N_p})\tilde{\beta}(s)} = \frac{\alpha(s)}{\tilde{\beta}(s)} \prod_{i=1}^{N_p} \frac{1}{s + \bar{p}_i} \tag{A.69}$$

---

[3]We must assume that z_i is not an eigenvalue of the state-space matrix A. However, this assumption is fulfilled if we have an minimal state-space realization.

If G is represented by the state-space realization (A.65), one "input" realization G_{si} of G_s is given by

$$G_{si} = \left[\begin{array}{c|c} A' & b \\ \hline c' & d \end{array}\right]$$

where A' and c' can be calculated by applying the following formulas repeatedly for $i = 1, \ldots, N_p$

$$\hat{\boldsymbol{x}}_{p_i}^H (A_{i-1} - p_i I) = 0 \quad \text{with } \hat{\boldsymbol{x}}_{p_i} \text{ scaled such that}^4: b^H \hat{\boldsymbol{x}}_{p_i} = 1,$$

$$A_i = A_{i-1} - 2\text{Re}(p_i) b \hat{\boldsymbol{x}}_{p_i}^H \quad \text{and} \quad c_i = c_{i-1} - 2\text{Re}(p_i) d \hat{\boldsymbol{x}}_{p_i}^H$$

with $A_0 = A$, $c_0 = c$, $A' = A_{N_p}$ and $c' = c_{N_p}$. Similarly, one "output" realization G_{so} of G_s is given by

$$G_{so} = \left[\begin{array}{c|c} A' & b' \\ \hline c & d \end{array}\right]$$

where A' and b' can be calculated by applying the following formulas repeatedly for $i = 1, \ldots, N_p$

$$(A_{i-1} - p_i I) \hat{\boldsymbol{x}}_{p_i} = 0 \quad \text{with } \hat{\boldsymbol{x}}_{p_i} \text{ scaled such that}^5: c \hat{\boldsymbol{x}}_{p_i} = 1,$$

$$A_i = A_{i-1} - 2\text{Re}(p_i) \hat{\boldsymbol{x}}_{p_i} c \quad \text{and} \quad b_i = b_{i-1} - 2\text{Re}(p_i) \hat{\boldsymbol{x}}_{p_i} d$$

with $A_0 = A$, $c_0 = c$, $A' = A_{N_p}$ and $c' = c_{N_p}$.

A.3.5 Factorizations of rational transfer function vectors

As for rational transfer functions the factorizations of rational transfer function vectors can also be simplified. Consider the input factorization of RHP-zeros in W where W is of size $n_W \times 1$

$$W(s) = W_{mi} \mathcal{B}_{zi}(M(s))$$

Clearly, $\mathcal{B}_{zi}(W)$ is given by (5.19) for all *multivariable*[6] RHP-zeros of W, since W is single input. We use the notation

$$W(s) = W_m \mathcal{B}_z(W), \quad \text{for multivariable RHP-zeros of } W.$$

By changing the order[7] of W_m and $\mathcal{B}_z(W)$ we get

$$W(s) = \mathcal{B}_z(W) W_m(s)$$

And we obtain

$$W_{mo}(s) = W_m(s) = W_{mi}(s), \quad \mathcal{B}_{zo}(W) = \mathcal{B}_z(W) \cdot I_{n_W} \quad \text{and} \quad \mathcal{B}_{zi}(W) = \mathcal{B}_z(W)$$

---

[4]Requires that the mode p_i is controllable.

[5]Requires that the mode p_i is observable.

[6]Multivariable zeros of a rational transfer function vector must appear as a zero in all elements of the transfer function vector.

[7]Changing order of a scalar transfer function and a multivariable transfer function matrix is allowed.

In a similar way we can show that for the RHP-poles of W

$$W_{so}(s) = W_s(s) = W_{si}(s), \quad \mathcal{B}_{po}(W) = \mathcal{B}_p(W) \cdot I_{n_W} \quad \text{and} \quad \mathcal{B}_{pi}(W) = \mathcal{B}_p(W)$$

For V of size $1 \times n_V$ we obtain for the *multivariable* RHP-zeros of V

$$V_{mi}(s) = V_m(s) = V_{mo}(s), \quad \mathcal{B}_{zi}(V) = \mathcal{B}_z(V) \cdot I_{n_V} \quad \text{and} \quad \mathcal{B}_{zo}(V) = \mathcal{B}_z(V)$$

and for the RHP-poles of V

$$V_{si}(s) = V_s(s) = V_{so}(s), \quad \mathcal{B}_{pi}(V) = \mathcal{B}_p(V) \cdot I_{n_V} \quad \text{and} \quad \mathcal{B}_{po}(V) = \mathcal{B}_p(V)$$

A.4   Viewing the factorizations as operations

Define the following eight operators which returns and takes as an argument a rational transfer function matrix:

$\mathcal{B}_{zi}(\cdot)$ – Returns the all-pass filter defined by the input factorization of RHP-zeros.
$\mathcal{B}_{zo}(\cdot)$ – Returns the all-pass filter defined by the output factorization of RHP-zeros.
$\mathcal{B}_{pi}(\cdot)$ – Returns the all-pass filter defined by the input factorization of RHP-poles.
$\mathcal{B}_{po}(\cdot)$ – Returns the all-pass filter defined by the output factorization of RHP-poles.
$(\cdot)_{mi}$ – Returns the input minimum phase representation of the argument.
$(\cdot)_{mo}$ – Returns the output minimum phase representation of the argument.
$(\cdot)_{si}$ – Returns the input stable representation of the argument.
$(\cdot)_{so}$ – Returns the output stable representation of the argument.

A.4.1   Some properties

Operations applied to identity.

$$\mathcal{B}_{xx}(I) = I, \quad \text{where } xx \in \{zi, zo, pi, po\} \tag{A.70}$$

$$(I)_{yy} = I, \quad \text{where } yy \in \{mi, mo, si, so\} \tag{A.71}$$

Yields identity. If G has no RHP-zeros then

$$\mathcal{B}_{zi}(G) = I; \qquad \mathcal{B}_{zo}(G) = I \tag{A.72}$$

and if G has no RHP-poles then

$$\mathcal{B}_{pi}(G) = I; \qquad \mathcal{B}_{po}(G) = I \tag{A.73}$$

Repeated application.

$$\mathcal{B}_{zi}(\mathcal{B}_{zi}(G)) = \mathcal{B}_{zi}(G); \qquad \mathcal{B}_{zo}(\mathcal{B}_{zo}(G)) = \mathcal{B}_{zo}(G) \qquad \text{(A.74)}$$

$$\mathcal{B}_{zi}(\mathcal{B}_{zo}(G)) = \mathcal{B}_{zo}(G); \qquad \mathcal{B}_{zo}(\mathcal{B}_{zi}(G)) = \mathcal{B}_{zi}(G) \qquad \text{(A.75)}$$

$$\mathcal{B}_{pi}(\mathcal{B}_{pi}^{-1}(G)) = \mathcal{B}_{pi}(G); \qquad \mathcal{B}_{po}(\mathcal{B}_{po}^{-1}(G)) = \mathcal{B}_{po}(G) \qquad \text{(A.76)}$$

$$\mathcal{B}_{pi}(\mathcal{B}_{po}^{-1}(G)) = \mathcal{B}_{po}(G); \qquad \mathcal{B}_{po}(\mathcal{B}_{pi}^{-1}(G)) = \mathcal{B}_{pi}(G) \qquad \text{(A.77)}$$

$$\mathcal{B}_{zi}(\mathcal{B}_{po}(G)) = \mathcal{B}_{po}(G); \qquad \mathcal{B}_{zo}(\mathcal{B}_{pi}(G)) = \mathcal{B}_{pi}(G) \qquad \text{(A.78)}$$

$$\mathcal{B}_{pi}(\mathcal{B}_{zo}^{-1}(G)) = \mathcal{B}_{zo}(G); \qquad \mathcal{B}_{po}(\mathcal{B}_{zi}^{-1}(G)) = \mathcal{B}_{zi}(G) \qquad \text{(A.79)}$$

Note, all of these properties say: Repeating a factorization on a all-pass filter only gives back what is already obtained. Still it may be very useful to repeat a factorization as we shall see below.

Proof of (A.74)–(A.79). All of these properties follow easily from the state-space realization for the general all-pass filter, see Lemma A.1. $\square$

Similarly, we have

$$(G_{mi})_{mi} = G_{mi}; \qquad (G_{mo})_{mo} = G_{mo} \qquad \text{(A.80)}$$

$$(G_{mo})_{mi} = G_{mo}; \qquad (G_{mi})_{mo} = G_{mi} \qquad \text{(A.81)}$$

$$(G_{si})_{si} = G_{si}; \qquad (G_{so})_{so} = G_{so} \qquad \text{(A.82)}$$

$$(G_{so})_{si} = G_{si}; \qquad (G_{pi})_{po} = G_{pi} \qquad \text{(A.83)}$$

Proof of (A.80)–(A.83). Follows from (A.72) and (A.73). $\square$

Pole factorization of minimum phase representations. The following relationships are useful

$$\mathcal{B}_{po}(G_{mi}) = \mathcal{B}_{po}(G); \qquad \mathcal{B}_{pi}(G_{mo}) = \mathcal{B}_{pi}(G) \qquad \text{(A.84)}$$

$$G = \mathcal{B}_{po}(G)\, G_{miso}\, \mathcal{B}_{zi}(G); \qquad G = \mathcal{B}_{zo}(G)\, G_{mosi}\, \mathcal{B}_{pi}(G) \qquad \text{(A.85)}$$

A REMARK ON NOTATION. With G_{miso} we mean $(G_{mi})_{so}$. Similarly, $G_{mosi} = (G_{mo})_{si}$.

Proof of (A.84). When factorizing the RHP-zeros of G, only the input matrix B in the state-space description changes (A.29). The output factorization of RHP-poles in G depends on the poles and the output pole directions (A.52) and (A.53). Since the output pole directions only depend on the A and the C matrix in the state-space description it follows that the pole directions do not change when factorizing the zeros at the input, and the first part of (A.84) follows. The second part follows similarly, since only the output matrix C in the state-space description changes when factorizing the RHP-zero at the output, and the input factorization of RHP-poles only depends on the poles and the input pole directions, which do not change when factorizing the zeros. $\square$

Proof of (A.84).

$$G = G_{mi}\, \mathcal{B}_{zi}(G) = \mathcal{B}_{po}(G_{mi})\, G_{miso}\, \mathcal{B}_{zi}(G) = \mathcal{B}_{po}(G)\, G_{miso}\, \mathcal{B}_{zi}(G)$$

and

$$G = \mathcal{B}_{zo}(G)\, G_{mo} = \mathcal{B}_{zo}(G)\, G_{mosi}\, \mathcal{B}_{pi}(G_{mo}) = \mathcal{B}_{zo}(G)\, G_{mosi}\, \mathcal{B}_{pi}(G)$$

$$\square$$

Applied to the inverse. Assume that G^{-1} exists, then

$$\mathcal{B}_{zi}(G) = \mathcal{B}_{po}(G^{-1}); \qquad G_{mi} = (G^{-1})_{so}^{-1} \tag{A.86}$$

$$\mathcal{B}_{zo}(G) = \mathcal{B}_{pi}(G^{-1}); \qquad G_{mo} = (G^{-1})_{si}^{-1} \tag{A.87}$$

$$\mathcal{B}_{zi}(G^{-1}) = \mathcal{B}_{po}(G); \qquad (G^{-1})_{mi} = (G_{so})^{-1} \tag{A.88}$$

$$\mathcal{B}_{zo}(G^{-1}) = \mathcal{B}_{pi}(G); \qquad (G^{-1})_{mo} = (G_{so})^{-1} \tag{A.89}$$

$$\mathcal{B}_{zi}(G)\, G^{-1} = G_{mi}^{-1}; \qquad G^{-1}\mathcal{B}_{zo}(G) = G_{mo}^{-1} \tag{A.90}$$

$$\mathcal{B}_{pi}^{-1}(G)\, G^{-1} = G_{si}^{-1}; \qquad G^{-1}\mathcal{B}_{po}^{-1}(G) = G_{so}^{-1} \tag{A.91}$$

$$\mathcal{B}_{zi}(G_{mi}^{-1}) = \mathcal{B}_{po}(G); \qquad \mathcal{B}_{zo}(G_{mo}^{-1}) = \mathcal{B}_{pi}(G) \tag{A.92}$$

A REMARK ON NOTATION. With G_{mi}^{-1} we mean $(G_{mi})^{-1}$, i.e. $G_{mi}^{-1} = (G_{mi})^{-1}$. Similarly, $G_{mo}^{-1} = (G_{mo})^{-1}$, $G_{so}^{-1} = (G_{so})^{-1}$ and $G_{si}^{-1} = (G_{si})^{-1}$.

Proof of (A.86)–(A.92).

$$G = G_{mi}\mathcal{B}_{zi}(G) \quad \text{and} \quad G^{-1} = \mathcal{B}_{po}^{-1}(G^{-1})\,(G^{-1})_{so}$$

invert the latter to obtain $G = (G^{-1})_{so}^{-1}\,\mathcal{B}_{po}^{-1}(G^{-1})$, and (A.86) follows from inspection. Eq. (A.87) follows similarly from the output factorization of RHP-zeros and input factorization of RHP-poles for G^{-1}. Eq. (A.88) and (A.89) follow from (A.86) and (A.87) by replacing G with G^{-1}. Eq. (A.90) follows from $G = G_{mi}\mathcal{B}_{zi}(G)$ and the latter part from $G = \mathcal{B}_{zo}(G)G_{mo}$. Eq. (A.91) follows from $G = G_{si}\mathcal{B}_{pi}^{-1}(G)$ and the latter part from $G = \mathcal{B}_{po}^{-1}(G)G_{so}$. The first part of (A.92) follows from (A.88) by substituting G^{-1} with G_{mi}^{-1} and applying (A.84). The latter part follows similarly by substituting G^{-1} in (A.89) with G_{mo}^{-1} and using (A.84). $\qquad\square$

Applied to products. Consider the product NM between the two rational transfer function matrices N and M, see Figure A.7. Four additional rules for cases when there are no RHP-
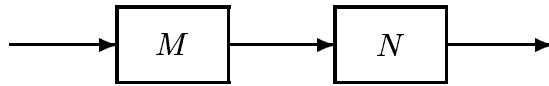

Figure A.7: Product NM of the two transfer functions N and M.

zero/pole cancellations between the two transfer functions M and N are:

$$\mathcal{B}_{zi}(NM) = \mathcal{B}_{zi}(\mathcal{B}_{zi}(N)M) \tag{A.93}$$

$$\mathcal{B}_{zo}(NM) = \mathcal{B}_{zo}(N\mathcal{B}_{zo}(M)) \tag{A.94}$$

$$\mathcal{B}_{pi}(NM) = \mathcal{B}_{pi}(\mathcal{B}_{pi}^{-1}(N)\,M) \tag{A.95}$$

$$\mathcal{B}_{po}(NM) = \mathcal{B}_{po}(N\mathcal{B}_{po}^{-1}(M)) \tag{A.96}$$

Proof of (A.93)–(A.96). Can easily be verified by drawing the corresponding block diagrams. Equation (A.93) can be proved by considering Figure A.8(a), we get

$$\mathcal{B}_{zi}(NM) = \mathcal{B}_{zi}(\mathcal{B}_{zi}(N)M)$$

since N_{mi} has no RHP-zeros. Equations (A.94)–(A.96) follow similarly by considering Figure A.8(b)–(d). $\qquad\square$

(a) $NM = N_{mi} \mathcal{B}_{zi}(N)\, M$ (b) $NM = N \mathcal{B}_{zo}(M)\, M_{mo}$

(c) $NM = N_{si} \mathcal{B}_{pi}^{-1}(N)\, M$ (d) $NM = N \mathcal{B}_{po}^{-1}(M)\, M_{so}$
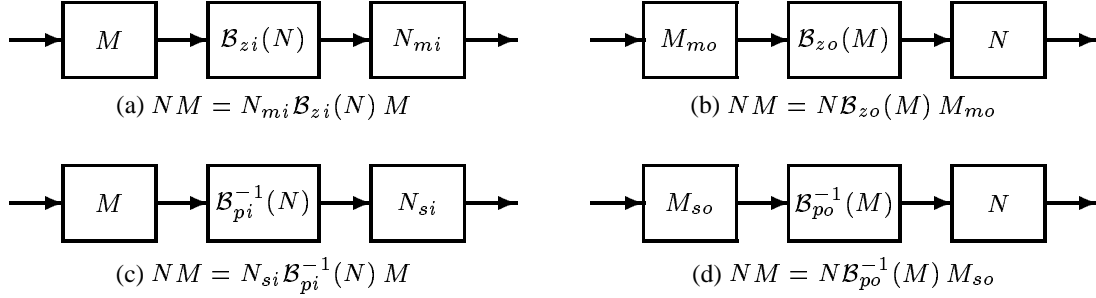
Figure A.8: Proof of (A.93)–(A.96)

Let N be unstable, a counter example on (A.93) could be

$$I = \mathcal{B}_{zi}(NN^{-1}) = \mathcal{B}_{zi}(\mathcal{B}_{zi}(N)\, N^{-1}) = \mathcal{B}_{zi}(N_{mi}^{-1}) = \mathcal{B}_{po}(N_{mi}) = \mathcal{B}_{po}(N) \neq I$$

So, we need the assumption of no RHP-pole/zero cancellation between N and M (i.e. we need to consider a minimal realization of the product NM).

Next, assume that M^{-1} exists and that $M(s)$ has minimal realization, then

$$\mathcal{B}_{zi}(\mathcal{B}_{zi}(M)\, M^{-1}N) = \mathcal{B}_{zi}(\mathcal{B}_{po}(M)\, N) \tag{A.97}$$

$$\mathcal{B}_{zo}(NM^{-1}\mathcal{B}_{zo}(M)) = \mathcal{B}_{zo}(N\mathcal{B}_{pi}(M)) \tag{A.98}$$

Proof of (A.97) and (A.98). Equation (A.97) follows from

$$\mathcal{B}_{zi}(\mathcal{B}_{zi}(M)\, M^{-1}N) = \mathcal{B}_{zi}(M_{mi}^{-1}N) = \mathcal{B}_{zi}(\mathcal{B}_{zi}(M_{mi}^{-1})\, N) = \mathcal{B}_{zi}(\mathcal{B}_{po}(M_{mi})\, N) = \mathcal{B}_{zi}(\mathcal{B}_{po}(M)\, N)$$

The first equality follows from first part of (A.90), the second equality follows from (A.93), the third equality follows from (A.86) and the fourth equality follows since the output pole directions of M do not change with input factorization of RHP-zeros. The proof of (A.98) follows similarly

$$\mathcal{B}_{zo}(NM^{-1}\mathcal{B}_{zo}(M)) = \mathcal{B}_{zo}(NM_{mo}^{-1}) = \mathcal{B}_{zo}(N\mathcal{B}_{zo}(M_{mo}^{-1})) = \mathcal{B}_{zo}(N\mathcal{B}_{pi}(M_{mo})) = \mathcal{B}_{zo}(N\mathcal{B}_{pi}(M))$$

by using (A.90), (A.94), (A.87) and that the fact that the input pole directions of M do not change with output factorization of RHP-zeros. $\qquad\square$

References

Chen, J. (1995). Sensitivity integral relations and design trade-offs in linear multivariable feedback systems, *IEEE Transactions on Automatic Control* **AC-40**(10): 1700–1716.

Morari, M. and Zafiriou, E. (1989). *Robust Process Control*, Prentice-Hall, Englewood Cliffs.

Wall, J. E., Doyle, J. C. and Harvey, C. A. (1980). Tradeoffs in the design of multivariable feedback systems, *Proceedings of 18th Allerton Conference*, pp. 715–725.

Zhou, K., Doyle, J. C. and Glover, K. (1996). *Robust and Optimal Control*, Prentice-Hall, Upper Saddle River.

Appendix A Proofs of the results

Proof of Lemma A.1. $\mathcal{B}_i(s)$ can be written

$$\mathcal{B}_i(s) = VD(s)V^H = \overbrace{\begin{bmatrix} u_1 & \cdots & u_{k-1} & v_i \end{bmatrix}}^{\triangleq V} \overbrace{\begin{bmatrix} 1 & \cdots & 0 & 0 \\ \vdots & \ddots & \vdots & \vdots \\ 0 & \cdots & 1 & 0 \\ 0 & \cdots & 0 & \frac{s-c_i}{s+\bar{c}_i} \end{bmatrix}}^{\triangleq D(s)} \overbrace{\begin{bmatrix} u_1^H \\ \vdots \\ u_{k-1}^H \\ v_i^H \end{bmatrix}}^{= V^H} \tag{A.99}$$

where we select the set of vectors $\{u_1,\ u_2,\ \cdots u_{k-1}\}$ such that they form an orthonormal basis for $\mathbb{C}^k$ together with v_i. Equation (A.99) gives

$$\mathcal{B}_i(s)V = VD(s)$$

consequently, $\mathcal{B}_i(s)$ has $k-1$ eigenvalues equal to 1 and one eigenvalue equal to

$$\lambda_k = \frac{s-c_i}{s+\bar{c}_i}$$

Furthermore, on a frequency-by-frequency basis

$$\mathcal{B}_i(s)\mathcal{B}_i^H(s) = VD(s)\underbrace{V^HV}_{=I}(D(s))^H V^H = VD(s)\overline{D}(s)V^H = V\begin{bmatrix} 1 & \cdots & 0 & 0 \\ \vdots & \ddots & \vdots & \vdots \\ 0 & \cdots & 1 & 0 \\ 0 & \cdots & 0 & \frac{|s-c_i|^2}{|s+\bar{c}_i|^2} \end{bmatrix}V^H$$

and it follows that $\mathcal{B}_i$ has $k-1$ singular values equal to 1 and one singular value equal to

$$\sigma_k(\mathcal{B}_i(s)) = \frac{|s-c_i|}{|s+\bar{c}_i|}$$

To prove

$$|\lambda_k(\mathcal{B}_i(s))| = \underline{\sigma}(\mathcal{B}_i(s)) = \frac{|s-c_i|}{|s+\bar{c}_i|} < 1 \quad \text{for } s, c_i \in \mathbb{C}^+ \text{ or } s, c_i \in \mathbb{C}^-$$

assume $|s+\bar{c}_i| < |s-c_i|$ and set $s = x_s + jy_s$ and $c_i = x_c + jy_c$. Then $|s+\bar{c}_i| < |s-c_i|$, implies $(x_s+x_c)^2 + (y_s-y_c)^2 < (x_s-x_c)^2 + (y_s-y_c)^2$ which gives $4x_cx_s < 0$. It follows that when s and c_i are in the same half plane then $\frac{|s-c_i|}{|s+\bar{c}_i|} < 1$, otherwise $\frac{|s-c_i|}{|s+\bar{c}_i|} \geq 1$. When either s or c_i is on the imaginary axis then $\frac{|s-c_i|}{|s+\bar{c}_i|} = 1$.

It follows from (A.99) that $\mathcal{B}_i$ has zero for $s = c_i$ with input and output direction v_i and that $\mathcal{B}_i$ has pole for $s = -\bar{c}_i$ with input and output directions v_i.

The inverse of $\mathcal{B}_i(s)$ is given by

$$\begin{aligned} \mathcal{B}_i^{-1}(s) &= VD^{-1}(s)V^H = \begin{bmatrix} u_1 & \ldots & u_{k-1} & v_i \end{bmatrix} \begin{bmatrix} 1 & \cdots & 0 & 0 \\ \vdots & \ddots & \vdots & \vdots \\ 0 & \cdots & 1 & 0 \\ 0 & \cdots & 0 & \frac{s+\bar{c}_i}{s-c_i} \end{bmatrix} \begin{bmatrix} u_1^H \\ \vdots \\ u_{k-1}^H \\ v_i^H \end{bmatrix} \\ &= VV^H + \frac{2\text{Re}(c_i)}{s-c_i}v_iv_i^H = I + \frac{2\text{Re}(c_i)}{s-c_i}v_iv_i^H \end{aligned} \tag{A.100}$$

It follows that $\mathcal{B}_i^{-1}(s)$ has $k - 1$ eigenvalues and singular values equal to 1,

$$\lambda_k(\mathcal{B}_i^{-1}(s)) = \frac{s + \bar{c}_i}{s - c_i}, \qquad \sigma_k(\mathcal{B}_i^{-1}(s)) = |\lambda_1(\mathcal{B}_i^{-1}(s))| = \frac{|s + \bar{c}_i|}{|s - c_i|}$$

and when $s, c_i \in \mathbb{C}^+$ or $s, c_i \in \mathbb{C}^-$ then $\bar{\sigma}(\mathcal{B}_i^{-1}(s)) = \frac{|s + \bar{c}_i|}{|s - c_i|} > 1$ and otherwise $\underline{\sigma}(\mathcal{B}_i^{-1}(s)) = \frac{|s + \bar{c}_i|}{|s - c_i|} \leq 1$.

It follows from (A.100) that $\mathcal{B}_i^{-1}$ has pole for $s = c_i$ with input and output direction v_i and that $\mathcal{B}_i^{-1}$ has zero for $s = -\bar{c}_i$ with input and output directions v_i.

By splitting up $\mathcal{B}(s)$ into three parts as given in (A.23)

$$\mathcal{B}(s) = \mathcal{B}_{N:j+1}(s)\mathcal{B}_j(s)\mathcal{B}_{j-1:1}(s)$$

where $\mathcal{B}_{N:j+1}(s)$ is given in (A.21), $\mathcal{B}_j(s)$ is given by (A.14) with $i = j$ and $\mathcal{B}_{j-1:1}(s)$ is given by (A.22). Since, $\mathcal{B}_j(s)$ has a zero for $s = c_j$ it follows that $\mathcal{B}(s)$ has a zero for $s = c_j$ since there is no pole to cancel this zero (no pole in $\mathbb{C}_+$). Since $s = c_j$ is a zero of $\mathcal{B}_j$ with input direction v_j, it follows that

$$\mathcal{B}(c_j)u = \mathcal{B}_{N:j+1}(c_j)\mathcal{B}_j(c_j)\underbrace{\mathcal{B}_{j-1:1}(c_j)u}_{=v_j} = 0$$

where $v_j = \mathcal{B}_{j-1:1}(c_j)u$ since $\mathcal{B}_{j-1:1}(c_j)$ is non-singular (by assumption) and v_j is the *only* singular direction for $\mathcal{B}_j(c_j)$. We get the *normalized* input zero direction for c_j

$$u_{z=c_j} = \mathcal{B}_{j-1:1}^{-1}(c_j)\,v_j \,/\, \|\mathcal{B}_{j-1:1}^{-1}(c_j)\,v_j\|_2$$

In a similar way we have $y^H \mathcal{B}_{N:j+1}(c_j) = v_j^H$ for the output direction, and we get *normalized* output zero direction for c_j

$$y_{z=c_j} = \mathcal{B}_{N:j+1}^{-H}(c_j)\,v_j \,/\, \|\mathcal{B}_{N:j+1}^{-H}(c_j)\,v_j\|_2$$

Since $-\bar{c}_j$ is a pole of $\mathcal{B}(s)$ it is a zero of $\mathcal{B}^{-1}(s)$ with input zero direction equal to the output pole direction and output zero direction equal to the input pole direction. Inverting (A.23) gives

$$\mathcal{B}^{-1}(s) = \mathcal{B}_{j-1:1}^{-1}(s)\mathcal{B}_j^{-1}(s)\mathcal{B}_{N:j+1}^{-1}(s)$$

We then have

$$u^H \mathcal{B}_{j-1:1}^{-1}(-\bar{c}_j) = v_j^H \quad \text{and} \quad \mathcal{B}_{N:j+1}^{-1}(-\bar{c}_j)y = v_j$$

Which gives the *normalized* input and output pole directions for $-\bar{c}_j$

$$u_{p=-\bar{c}_j} = \mathcal{B}_{j-1:1}^H(-\bar{c}_j)\,v_j \quad \text{and} \quad y_{p=-\bar{c}_j} = \mathcal{B}_{N:j+1}(-\bar{c}_j)\,v_j$$

$\square$

Proof of Theorem A.1. The proof is only given for $N_z = 1$ (in this case $\hat{u}_z = u_z$ and $\hat{x}_z = x_{zi}$). The proof for $N_z > 1$ is to apply the proof of $N_z = 1$ repeatedly. To see that the minimum phase representation G_{mi} can be written as given in (A.29) with the matrix B' given by (A.31) one has to use the generalized eigenvalue problem (A.5). For $G(s)$, $s = z$ is a zero so (A.5) becomes

$$\begin{bmatrix} A - zI & B \\ C & D \end{bmatrix} \begin{bmatrix} \hat{x}_z \\ \hat{u}_z \end{bmatrix} = \begin{bmatrix} 0 \\ 0 \end{bmatrix} \tag{A.101}$$

For the minimum phase system, $G_{mi}(s)$, the zero $s = -\bar{z} = -\text{Re}(z) + \text{Im}(z)j$ has the same input direction and the same state direction as $G(s)$ for $s = z$. The generalized eigenvalue problem becomes

$$\begin{bmatrix} A + \bar{z}I & B' \\ C & D \end{bmatrix} \begin{bmatrix} \hat{x}_z \\ \hat{u}_z \end{bmatrix} = \begin{bmatrix} 0 \\ 0 \end{bmatrix} \tag{A.102}$$

By subtracting (A.102) from (A.101) one obtains

$$\begin{bmatrix} A - A - zI - \bar{z}I & B - B' \\ 0 & 0 \end{bmatrix} \begin{bmatrix} \hat{x}_z \\ \hat{u}_z \end{bmatrix} = \begin{bmatrix} 0 \\ 0 \end{bmatrix} \tag{A.103}$$

from the first equation one gets

$$-zI\hat{x}_z - \bar{z}I\hat{x}_z + B\hat{u}_z - B'\hat{u}_z = 0$$

By extracting $\hat{u}_z$ on the right and solving for B' one obtains

$$B' = B - 2\text{Re}(z)\hat{x}_z\hat{u}_z^H$$

which proves (A.29) and (A.31). The all-pass filter with RHP-zero for $s = z$ with input and output zero directions $\hat{u}_z$, and LHP-pole for $s = -\bar{z}$ with input and output pole directions $\hat{u}_z$ is given by Lemma A.1, (A.13) and (A.14) with $N_z = 1$, $v_i = \hat{u}_z$ and $c_i = z$. From the construction of $G_{mi}(s)$ we know there is a zero for $s = -\bar{z}$ with input direction $\hat{u}_z$. We may therefore cancel the pole for $s = -\bar{z}$ in $\mathcal{B}_{zi}(G)$ with the zero in same location in $G_{mi}(s)$ and it follows that $G_{mi}\mathcal{B}_{zi}(G) = G$. $\quad\square$

Proof of Theorem A.2. Since z_i is a RHP-zero for $G(s)$ it follows that z_i is a RHP-zero for

$$G^T = \left[\begin{array}{c|c} A^T & C^T \\ \hline B^T & D^T \end{array} \right]$$

From Theorem A.1 we have

$$G^T = (G^T)_{mi}\,\mathcal{B}_{zi}(G^T) \quad \Leftrightarrow \quad G = \mathcal{B}_{zi}^T(G^T)\,(G^T)_{mi}^T$$

We get

$$G_{mo} = (G^T)_{mi}^T = \left[\begin{array}{c|c} A^T & C'^T \\ \hline B^T & D^T \end{array} \right]^T = \left[\begin{array}{c|c} A & B \\ \hline C' & D \end{array} \right]$$

The relation between modified zero-input directions y_i and the modified zero-input-state vector x_i for the transposed system G^T and the corresponding output directions for G, follows from

$$\begin{bmatrix} A^T - z_iI & C_{i-1}^T \\ B^T & D^T \end{bmatrix} \begin{bmatrix} x_i \\ y_i \end{bmatrix} = 0 \quad \Leftrightarrow \quad [\, x_i^T \;\; y_i^T \,] \begin{bmatrix} A - z_iI & B \\ C_{i-1} & D \end{bmatrix} = 0$$

which implies

$$\hat{y}_{z_i} = \bar{y}_i \quad \text{and} \quad \hat{x}_{z_i} = \bar{x}_i$$

The modified input matrix C' can be calculated by applying the following formula repeatedly for $i = 1\ldots, N_z$

$$C_i = (C_{i-1}^T - 2\text{Re}(z_i)x_iy_i^H)^T = C_{i-1} - 2\text{Re}(z_i)\bar{y}_ix_i^T = C_{i-1} - 2\text{Re}(z_i)\hat{y}_{z_i}\hat{x}_{z_i}^H$$

with $C_0 = C$ and $C' = C_{N_z}$. The all-pass filter becomes

$$\mathcal{B}_{zo}(G) = \mathcal{B}_{zi}^T(G^T) = \prod_{i=1}^{N_z} \mathcal{B}_i(s) \quad \text{with} \quad \mathcal{B}_i = I - \frac{2\text{Re}(z_i)}{s + \bar{z}_i}\bar{y}_iy_i^T = I - \frac{2\text{Re}(z_i)}{s + \bar{z}_i}\hat{y}_{z_i}\hat{y}_{z_i}^H$$

$\square$

Proof of Theorem A.3. Assume without loss of generality (see discussion below) that G is square and that the state space matrix D is non-singular. Then D^{-1} exists and G^{-1} is given by (2.33)

$$G^{-1} = \left[\begin{array}{c|c} A - BD^{-1}C & -BD^{-1} \\ \hline D^{-1}C & D^{-1} \end{array}\right]$$

Furthermore, p_i is a RHP-zero of G^{-1} which can be factorized in an "input" factorization (Theorem A.1)

$$G^{-1} = (G^{-1})_{mi}\mathcal{B}_{zi}(G^{-1}) \quad \Leftrightarrow \quad G = \mathcal{B}_{zi}^{-1}(G^{-1})(G^{-1})_{mi}^{-1}$$

The relations between the input zero direction y_i, the input zero state vector x_i for G^{-1} (due to RHP-pole p_i in G) and the output pole direction $\hat{y}_{p_i}$, the output pole state vector $\hat{x}_{p_i}$ are (2.37)

$$x_i = -\hat{x}_{p_i} \quad \text{and} \quad y_i = \hat{y}_{p_i}$$

We then have that

$$\mathcal{B}_{po}(G) = \mathcal{B}_{zi}(G^{-1}) \quad \text{and} \quad G_{po} = (G^{-1})_{mi}^{-1}$$

where

$$\mathcal{B}_{po}(G) = \mathcal{B}_{zi}(G^{-1}) = \prod_{i=0}^{N_p-1} \mathcal{B}_{N_p-i}(s) \quad \text{with} \quad \mathcal{B}_i(s) = I - \frac{2\mathrm{Re}(p)}{s+\bar{p}}y_i y_i^H = I - \frac{2\mathrm{Re}(p)}{s+\bar{p}}\hat{y}_{p_i}\hat{y}_{p_i}^H$$

$$(G^{-1})_{mi} = \left[\begin{array}{c|c} A - BD^{-1}C & -BD^{-1} + \Delta \\ \hline D^{-1}C & D^{-1} \end{array}\right]$$

where Δ is the change in the input matrix due to the factorization of RHP-zeros in G^{-1}. We obtain

$$\begin{aligned} G_{po} &= (G^{-1})_{mi}^{-1} = \left[\begin{array}{c|c} A - BD^{-1}C - (-BD^{-1}+\Delta)DD^{-1}C & -B + \Delta D \\ \hline C & D \end{array}\right] \\ &= \left[\begin{array}{c|c} A - \Delta C & -B + \Delta D \\ \hline C & D \end{array}\right] = \left[\begin{array}{c|c} A' & B' \\ \hline C & D \end{array}\right] \end{aligned}$$

The change Δ becomes

$$\Delta = -BD - \sum_{i=1}^{N_p} 2\mathrm{Re}(p_i)x_i y_i^H + BD = \sum_{i=1}^{N_p} 2\mathrm{Re}(p_i)\hat{x}_{p_i}\hat{y}_{p_i}^H$$

the modified matrices A' and B' can be found by applying the following formulas repeatedly

$$(A_{i-1} - p_i I)\hat{x}_{p_i} = 0, \qquad \hat{y}_{p_i} = C\hat{x}_{p_i}$$
$$A_i = A_{i-1} - 2\mathrm{Re}(p_i)\hat{x}_{p_i}\hat{y}_{p_i}^H C \quad \text{and} \quad B_i = B_{i-1} - 2\mathrm{Re}(p_i)\hat{x}_{p_i}\hat{y}_{p_i}^H D$$

for $i = 1, \ldots, N_p$ with $A_0 = A$, $B_0 = B$, $A' = A_{N_p}$ and $B' = B_{N_p}$. Note that the vector $[\,\hat{x}_{p_i}^T \quad \hat{y}_{p_i}^T\,]$ is scaled such that $\hat{y}_{p_i}^H \hat{y}_{p_i} = 1$.

Non-square and strictly proper systems G (singular D matrix). The output pole directions are independent of the matrix D in the state space description. Also the relation between output pole directions of G and the input zero directions of G^{-1} is independent of D, this means that we can add non-zero elements to D without affecting the the pole directions. So, if D is singular we add non-zero elements along the diagonal of D so that it becomes non-singular. Consider next the case where G has more outputs than inputs. Then fictitious inputs with zero effect on y can be included by adding columns

with zeros in B and D so that D becomes square. The next step is then to add non-zero elements to D, so that D becomes non-singular. Similarly if G has more inputs than outputs one can add rows with zeros to the C and D matrices. Note, that adding columns with zeros to the B matrix and rows with zeros to the C matrix do not change the direction of the pole, it only expands the dimension. $\qquad\square$

Proof of Theorem A.4. Since p_i are RHP-poles of $G(s)$ it follows that p_i also are RHP-poles of

$$G^T = \left[\begin{array}{c|c} A^T & C^T \\ \hline B^T & D^T \end{array}\right]$$

From Theorem A.3 we have

$$G^T = \mathcal{B}_{po}^{-1}(G^T)(G^T)_{so} \quad \Leftrightarrow \quad G = (G^T)_{so}^T \mathcal{B}_{po}^{-T}(G^T)$$

We get

$$G_{si} = (G^T)_{so}^T = \left[\begin{array}{c|c} A'^T & C'^T \\ \hline B^T & D^T \end{array}\right]^T = \left[\begin{array}{c|c} A' & B \\ \hline C' & D \end{array}\right]$$

The output pole direction u_i and the output pole state vector x_i for the transposed system G^T are related to the input pole direction $\hat{u}_{p_i}$ and the the input pole state direction $\hat{x}_{p_i}$, (2.31) and (2.29)

$$\bar{u}_i = \hat{u}_{p_i} \quad \text{and} \quad \bar{x}_i = \hat{x}_{p_i}$$

The modified matrices A' and C' can be computed by applying the following formula repeatedly for $i = 1, \ldots, N_z$

$$A_i = (A_{i-1}^T - 2\mathrm{Re}(p)x_i u_i^H B^T)^T = A_{i-1} - 2\mathrm{Re}(p)B\bar{u}_i x_i^T = A_{i-1} - 2\mathrm{Re}(p)B\hat{u}_{p_i}\hat{x}_{p_i}^H$$
$$C_i = (C_{i-1}^T - 2\mathrm{Re}(p)x_i u_i^H D^T)^T = C_{i-1} - 2\mathrm{Re}(p)D\bar{u}_i x_i^T = C_{i-1} - 2\mathrm{Re}(p)D\hat{u}_{p_i}\hat{x}_{p_i}^H$$

with $A_0 = A$, $C_0 = C$, $A' = A_{N_p}$ and $C' = C_{N_p}$. The all-pass filter becomes

$$\mathcal{B}_{pi}(G) = \mathcal{B}_{po}^T(G) = \prod_{i=1}^{N_p} \mathcal{B}_i(s)$$

with

$$\mathcal{B}_i(s) = (I - \frac{2\mathrm{Re}(p_i)}{s + \bar{p}_i} u_i u_i^H)^T = I - \frac{2\mathrm{Re}(p_i)}{s + \bar{p}_i} \bar{u}_i u_i^T = I - \frac{2\mathrm{Re}(p_i)}{s + \bar{p}_i} \hat{u}_{p_i}\hat{u}_{p_i}^H$$

$\qquad\square$

Appendix B

Eigenvalue problems and Jordan form

B.1 Left and right eigenvalue problems

Assume in the following that the dimensions of A is $n \times n$. The standard eigenvalue problem (referred to in this context as the right eigenvalue problem) is to find the eigenvalue λ and the eigenvector (referred to as the right eigenvector) x_R which satisfy

$$Ax_R = \lambda x_R \tag{B.1}$$

In a similar way, the left eigenvector problem is to find eigenvalue λ and the left eigenvector x_L which satisfy

$$x_L^H A = x_L^H \lambda \tag{B.2}$$

It is well known that any scalar $s \in \mathbb{C}$ times an eigenvector also is an eigenvector and that eigenvectors $x_1, \ldots, x_k$ corresponding to *different eigenvalues* $\lambda_1, \ldots, \lambda_k$, then those eigenvectors are linearly independent. These properties are of course valid for both types of eigenvalue problems.

The following property relates the right eigenvector $x_{R,1}$, corresponding to an eigenvalue λ_1, to the left eigenvector $x_{L,2}$, corresponding to an eigenvalue λ_2, when $\lambda_1 \neq \lambda_2$.

PROPERTY B.1 *Left and right eigenvectors which corresponds to different eigenvalues, are orthogonal to one another.*

Proof. Let $x_{R,1}$ be a right eigenvector corresponding to the eigenvalue λ_1 and $x_{L,2}$ be a left eigenvector corresponding to the eigenvalue λ_2 we then have

$$Ax_{R,1} = \lambda_1 x_{R,1} \quad \text{and} \quad x_{L,2}^H A = \lambda_2 x_{L,2}^H$$

Multiplying the latter on the right by $x_{R,1}$ gives

$$\lambda_2 x_{L,2}^H x_{R,1} = x_{L,2}^H A x_{R,1} = x_{L,2}^H \lambda_1 x_{R,1}$$

which implies $x_{L,2}^H x_{R,1} = 0$ since $\lambda_2 \neq \lambda_1$. $\qquad \square$

The eigenvalue problems (B.1) and (B.2) can be written on matrix form by arranging $x_{R,i}$ and $x_{L,i}$ so that they both correspond to eigenvalue λ_i. We then form the matrices

$$X_R = [\, x_{R,1} \quad x_{R,2} \quad \cdots \quad x_{R,n} \,]$$

$$X_L = [\, x_{L,1} \quad x_{L,2} \quad \cdots \quad x_{L,n} \,]$$

and the diagonal matrix $\Lambda = \mathrm{diag}\{\lambda_i\}$. Then we have the following relationships

$$AX_R = X_R\Lambda \quad \text{and} \quad X_L^H A = \Lambda X_L^H \tag{B.3}$$

The right eigenvalue problem of the transpose of A becomes

$$A^T X = X\Lambda \tag{B.4}$$

Taking the transpose of (B.4) gives

$$X^T A = \Lambda X^T \tag{B.5}$$

Comparing (B.5) and the last equation in (B.3) gives that $X_L = \bar{X}$. That is, the left eigenvectors are equal to the conjugate of the right eigenvectors to A^T. In MATLAB the left eigenvectors can therefore be computed as the conjugate of the right eigenvectors of A^T.

B.1.1   Scaling

Since any scalar times an eigenvector is an eigenvector, the eigenvectors can be scaled independently. It is usual to scale the eigenvectors so that the norm of the vectors are equal to one. Note that the eigenvectors are still not unique they can be multiplied with a complex number with magnitude one and arbitrary phase. In this work we assume that both left and right eigenvalues are scaled so that their norm are one. Consider next a pair of left and right eigenvectors $(x_{L,i}, x_{R,i})$ corresponding to the eigenvalue λ_i, define the scalar $s_i = x_{L,i}^H x_{R,i}$ and the diagonal matrix $S = \mathrm{diag}\{s_i\}$. In the case of n linearly independent eigenvectors we can write the diagonalization of A in terms of X_R, X_L and S as given in (B.9).

B.1.2 n linearly independent eigenvectors

It is well known that a matrix A with n linearly independent eigenvectors $x_{R,i}$ can be diagonalized by the matrix X_R

$$X_R^{-1} A X_R = \Lambda \quad \text{or} \quad A = X_R \Lambda X_R^{-1} \tag{B.6}$$

In a similar way A can be diagonalized by X_L if A has n linearly independent left eigenvectors.

$$X_L^H A X_L^{-H} = \Lambda \quad \text{or} \quad A = X_L^{-H} \Lambda X_L^H \tag{B.7}$$

From (B.6) and (B.7) we have

$$X_L' = X_R^{-H} \tag{B.8}$$

when A has n linearly independent right eigenvectors. When computing the left eigenvectors according to (B.8) it follows that the left eigenvectors are scaled so that $x_{R,i}^H x_{L,i} = 1$. To see this multiply X_L' on the left with X_R^H to obtain $X_R^H X_L' = X_R^H X_R^{-H} = I$. It is therefore necessary to normalize the left eigenvectors, $X_L = X_L' S$, where S contains the inverse of the norm of the columns in X_L' on the diagonal. Multiplying X_L on the left by X_R^H reveals

$$X_R^H X_L = X_R^H X_L' S = X_R^H X_R^{-H} S = S$$

which is desired. Multiplying (B.3) on the left by X_L^H, using (B.8) and $X_L = X_L' S$ we obtain

$$\boxed{X_L^H A X_R = S^H \Lambda = \Lambda S^H} \tag{B.9}$$

The last identity follows since two diagonal matrices commute. In a similar way we can multiply (B.3) on the right with $X_R^{-1} = S^{-H} X_L^H$ to obtain

$$\boxed{A = X_R \Lambda S^{-H} X_L^H = X_R S^{-H} \Lambda X_L^H} \tag{B.10}$$

B.1.3 n distinct eigenvalues

In the case of n distinct eigenvalues there exists n linearly independent eigenvectors and we have

$$X_L^H X_R = X_R^H X_L = S = \operatorname{diag}\{x_{L,i}^H x_{R,i}\}$$

B.2 Jordan form

It is not our intention to show how to compute the Jordan form or to derive it. However, the intention is to show how we can use the Jordan form to obtain both left and right generalized vectors which can be used to describe the directionality of those poles or eigenvalues which do not have sufficient number of linearly independent eigenvectors.

A defective matrix A is a matrix which does not possess n linearly independent eigenvectors and can therefore not be diagonalized. Those matrices which cannot be diagonalized can be brought into Jordan form.

If a matrix has v linearly independent eigenvectors, then it is similar to a matrix which is in Jordan form with v square blocks on the diagonal:

$$J = M^{-1} A M = \begin{bmatrix} J_1 & & & & \\ & \ddots & & & \\ & & J_\ell & & \\ & & & \ddots & \\ & & & & J_v \end{bmatrix}$$

Each block has one eigenvector, one eigenvalue, and 1's just above the diagonal:

$$J_\ell = \begin{bmatrix} \lambda_\ell & 1 & & \\ & \ddots & \ddots & \\ & & \lambda_\ell & 1 \\ & & & \lambda_\ell \end{bmatrix}$$

It follows that $AM = MJ$, the single eigenvector for each block satisfy $Aw_i = \lambda_i w_i$, and for each block J_ℓ of size greater than one there exists $\nu - 1$, where ν is the size of J_ℓ, additional vectors w_i which satisfy $Aw_i = \lambda_i w_i + w_{i-1}$. These additional vectors are called *generalized vectors*. The eigenvectors together with the generalized vectors form the matrix M which has rank equal to n. Since M has rank equal to n, M^{-1} exists and $J = M^{-1}AM$.

From this point we change notation and use M_R in the meaning of M above, since M multiplies A on the right in $AM_R = M_R J$. Following the same arguments for constructions of M_R and J (see Strang, 1986) it follows that there also exists a M_L such that

$$M_L^H A = JM_L^H \tag{B.11}$$

Since both M_R and M_L are nonsingular we can write

$$J = M_R^{-1}AM_R \quad \text{or} \quad A = M_R J M_R^{-1} \tag{B.12}$$

$$J = M_L^H A M_L^{-H} \quad \text{or} \quad A = M_L^{-H} J M_L^H \tag{B.13}$$

From (B.12) and (B.13) it follows that

$$M_L' = M_R^{-H} \tag{B.14}$$

REMARK 1. We can split up both $AM_R = M_R J$ and $M_L^H A = JM_L^H$. To do this let $M_{R,\ell}$ and $M_{L,\ell}$ denote the the columns in M_R and M_L corresponding to J_ℓ. From the right Jordan form we get

$$A\,[\,M_{R,1} \;\; \cdots \;\; M_{R,\ell} \;\; \cdots \;\; M_{R,v}\,] = [\,M_{R,1} \;\; \cdots \;\; M_{R,\ell} \;\; \cdots \;\; M_{R,v}\,]\begin{bmatrix} J_1 & & & & \\ & \ddots & & & \\ & & J_\ell & & \\ & & & \cdots & \\ & & & & J_v \end{bmatrix}$$

which gives $AM_{R,\ell} = M_{R,\ell}J_\ell$, and from the left Jordan form we get

$$\begin{bmatrix} M_{L,1}^H \\ \vdots \\ M_{L,\ell}^H \\ \vdots \\ M_{L,v}^H \end{bmatrix} A = \begin{bmatrix} J_1 & & & & \\ & \ddots & & & \\ & & J_\ell & & \\ & & & \ddots & \\ & & & & J_v \end{bmatrix}\begin{bmatrix} M_{L,1}^H \\ \vdots \\ M_{L,\ell}^H \\ \vdots \\ M_{L,v}^H \end{bmatrix}$$

which gives $M_{L,\ell}^H A = J_\ell M_{L,\ell}^H$.

REMARK 2. From $AM_R = M_R J$ and for Jordan block number ℓ, $AM_{R,\ell} = M_{R,\ell} J_\ell$ it follows that the first column $m_{R,i}$ in $M_{R,\ell}$ is the eigenvector and the remaining columns in $M_{R,\ell}$ are the generalized vectors. Let $m_{R,i}$ be the first column in $M_{R,\ell}$ and assume that the size of the Jordan block is three, we get

$$A \begin{bmatrix} m_{R,i} & m_{R,i+1} & m_{R,i+2} \end{bmatrix} = \begin{bmatrix} m_{R,i} & m_{R,i+1} & m_{R,i+2} \end{bmatrix} \begin{bmatrix} \lambda_\ell & 1 & 0 \\ 0 & \lambda_\ell & 1 \\ 0 & 0 & \lambda_\ell \end{bmatrix}$$

or $Am_{R,i} = \lambda_\ell m_{R,i}$, $Am_{R,i+1} = \lambda_\ell m_{R,i+1} + m_{R,i}$ and $Am_{R,i+2} = \lambda_\ell m_{R,i+2} + m_{R,i+1}$.

REMARK 3. *Importantly*, for the left Jordan problem the ordering of the vectors in M_L are reversed compared to that of the right Jordan problem. That is, the last column in $M_{L,\ell}$ is the eigenvector and the remaining columns are the generalized vectors. We have $M_L^H A = J M_L^H$ and for Jordan block ℓ, $M_{L,\ell}^H A = J_\ell M_{L,\ell}^H$. Let $m_{L,i}$ be the first column in $M_{L,\ell}$ and assume that the size of the Jordan block is three, we get

$$\begin{bmatrix} m_{L,i}^H \\ m_{L,i+1}^H \\ m_{L,i+2}^H \end{bmatrix} A = \begin{bmatrix} \lambda_\ell & 1 & 0 \\ 0 & \lambda_\ell & 1 \\ 0 & 0 & \lambda_\ell \end{bmatrix} \begin{bmatrix} m_{L,i}^H \\ m_{L,i+1}^H \\ m_{L,i+2}^H \end{bmatrix}$$

or $m_{L,i}^H A = \lambda_\ell m_{L,i}^H + m_{L,i+1}^H$, $m_{L,i+1}^H A = \lambda_\ell m_{L,i+1}^H + m_{L,i+2}^H$ and $m_{L,i+2}^H A = \lambda_\ell m_{L,i+2}^H$

B.2.1 Scaling

We know that each eigenvector can be scaled independently, however, the generalized vectors described by $Aw_i = \lambda_\ell w_i + w_{i-1}$ must be scaled with the same scalar as the eigenvector which starts or ends the chain. As an example, suppose that we have found an eigenvector w_1 and two generalized vectors w_2 and w_3 so that $Aw_1 = \lambda w_1$, $Aw_2 = \lambda w_2 + w_1$ and $Aw_3 = \lambda w_3 + w_2$ are all satisfied. Next, assume that we scale the eigenvector w_1 to become $w_1' = sw_1$ where $s \in \mathbb{C}$. In order to satisfy $Aw_2 = \lambda w_2 + w_1'$ we must scale w_2 with the same scalar s to obtain $w_2' = sw_2$ and $Aw_2' = \lambda w_2' + w_1'$ which again imply that we must scale w_3 with s. So, for each Jordan block we have *one degree of freedom* for scaling. The structure of the scaling matrix for a matrix A with v linearly independent eigenvectors

$$S = \begin{bmatrix} s_1 I_{\nu_1} & & & & \\ & \ddots & & & \\ & & s_\ell I_{\nu_\ell} & & \\ & & & \ddots & \\ & & & & s_v I_{\nu_v} \end{bmatrix} \tag{B.15}$$

where $s_\ell \in \mathbb{C}$ and the sizes of the identity matrices $I_{\nu_1}, \ldots, I_{\nu_v}$ are equal to the sizes of the corresponding Jordan blocks $J_1, \ldots, J_v$, i.e. $\nu_1, \ldots, \nu_v$. It follows from (B.14) that selecting $M_L = M_L' S$,

$$M_R^H M_L = M_R^H M_L' S = M_R^H M_R^{-H} = S \tag{B.16}$$

Usually, we select the scalings $s_1, \ldots, s_v$ to be real and equal to the inverse of the norms of the columns in M_L' corresponding to the left eigenvectors. This implies that all $s_1, \ldots, s_v$ are real, and by taking the complex conjugate transpose of (B.16) we obtain

$$M_L^H M_R = S^H = S = M_R^H M_L \quad \text{when } s_\ell \in \mathbb{R}, \ \forall \ell \in \{1, \ldots, v\} \tag{B.17}$$

Multiplying (B.11) on the right with M_R gives

$$M_L^H A M_R = J M_L^H M_R = J S^H \tag{B.18}$$

which is valid for all diagonal scaling matrices S with the predescribed structure given in (B.15). In a similar way we can multiply $A M_R = M_R J$ on the left by M_L^H to get

$$\boxed{M_L^H A M_R = S^H J = J S^H} \tag{B.19}$$

So, S and J commute, which can also be seen from

$$
\begin{aligned}
JS &= \begin{bmatrix} J_1 & & \\ & \ddots & \\ & & J_v \end{bmatrix} \begin{bmatrix} s_1 I_{\nu_1} & & \\ & \ddots & \\ & & s_v I_{\nu_v} \end{bmatrix} = \begin{bmatrix} J_1 s_1 I_{\nu_1} & & \\ & \ddots & \\ & & J_v s_v I_{\nu_v} \end{bmatrix} \\
&= \begin{bmatrix} s_1 I_{\nu_1} J_1 & & \\ & \ddots & \\ & & s_v I_{\nu_v} J_v \end{bmatrix} = \begin{bmatrix} s_1 I_1 & & \\ & \ddots & \\ & & s_v I_{\nu_v} \end{bmatrix} \begin{bmatrix} J_1 & & \\ & \ddots & \\ & & J_v \end{bmatrix} = SJ
\end{aligned}
$$

Multiplying $A M_R = M_R J$ on the left with $M_R^{-1} = M_L'^H = S^{-H} M_L^H$ gives

$$\boxed{A = M_R J S^{-H} M_L^H = M_R S^{-H} J M_L^H} \tag{B.20}$$

B.2.2   Inverse of Jordan block J

The inverse of J consisting of v square blocks along the main diagonal is the matrix

$$
J^{-1} = \begin{bmatrix} J_1^{-1} & & & & \\ & \ddots & & & \\ & & J_\ell^{-1} & & \\ & & & \ddots & \\ & & & & J_v^{-1} \end{bmatrix}
$$

and the inverse of a Jordan J_ℓ block of size ν with $p = \lambda_\ell$

$$
J_\ell = \left. \begin{bmatrix} p & 1 & \cdots & 0 & 0 \\ 0 & p & \cdots & 0 & 0 \\ \vdots & \vdots & \ddots & \vdots & \vdots \\ 0 & 0 & \cdots & p & 1 \\ 0 & 0 & \cdots & 0 & p \end{bmatrix} \right\} \nu \tag{B.21}
$$

is

$$
J_\ell^{-1} = \begin{bmatrix} 1/p & -1/p^2 & \cdots & (-1)^{\nu-2}/p^{\nu-1} & (-1)^{\nu-1}/p^\nu \\ 0 & 1/p & \cdots & (-1)^{\nu-3}/p^{\nu-2} & (-1)^{\nu-2}/p^{\nu-1} \\ \vdots & \vdots & \ddots & \vdots & \vdots \\ 0 & 0 & \cdots & 1/p & -1/p^2 \\ 0 & 0 & \cdots & 0 & 1/p \end{bmatrix} \tag{B.22}
$$

References

Strang, G. (1986). *Linear Algebra and Its Applications*, Harcourt Brace Jovanovich, Orlando, Florida.